

Maynooth University
National University of Ireland Maynooth

Investigating the role of *miR-223* in Ulcerative colitis and Colitis-associated colorectal cancer

A thesis submitted to Maynooth University for the degree of Doctor of Philosophy

Ciara Flynn, MSc

Biology Department

September 2024

Supervisor: Dr. Eóin N. McNamee

Head of Department: Prof. Paul Moynagh

This thesis has been prepared in accordance with the PhD regulations of Maynooth University and is subject to copyright.

TABLE OF CONTENTS

List of Figures ..... *viii*

List of Appendix Figures ..... *xiii*

List of Tables ..... *xiv*

List of Appendix Tables ..... *xvi*

Declaration ..... *xvii*

Acknowledgements ..... *xviii*

Abbreviations ..... *xx*

Publications and Presentations ..... *xxiv*

Abstract ..... *xxvi*

Chapter 1 Introduction **1**

Introduction *2*

1.1.1 Ulcerative colitis 2

1.1.2 Physiology of the large intestine 2

1.1.3 Epidemiology of Ulcerative colitis 4

1.1.3.1 Genetics of Ulcerative colitis 5

1.1.3.2 Environmental factors implicated in the development of Ulcerative colitis 5

1.1.3.3 Microbial factors implicated in the development of Ulcerative colitis 6

1.1.4 Pathophysiology of Ulcerative colitis 8

1.1.4.1 Role of the innate immune system in Ulcerative colitis 8

1.1.4.2 Role of the adaptive immune system in Ulcerative colitis 11

1.1.5 Diagnosis of Ulcerative colitis 12

1.1.6 Treatment of Ulcerative colitis 15

1.1.7 Colitis associated colorectal cancer 16

1.1.8 Risk factors for the development of Colitis associated colorectal cancer 17

1.1.9 Detection of Colitis associated colorectal cancer 19

1.1.10 Treatment of Colitis associated colorectal cancer 19

1.1.11 The inflammatory microenvironment of Colitis associated colorectal cancer 20

1.1.12 MicroRNAs 21
1.1.13 Biogenesis of miRNAs 21
1.1.14 Diagnostic and therapeutic potential of miRNAs 23
1.1.15 miRNAs in Ulcerative colitis and Colitis associated colorectal cancer 23
1.1.16 *miR-223* a critical regulator of myeloid cells 25
1.1.17 Models to investigate the role of *miR-223* in Ulcerative colitis and Colitis associated colorectal cancer 27

Thesis hypothesis and aims *28*

Chapter 2 Materials and methods 29

Materials *30*

Methods *40*
2.1.1 IBD patient biopsies or samples 40
2.1.2 Mouse strains 40
2.1.3 Induction of Colitis-associated colorectal cancer 41
2.1.4 Generation of bone marrow chimeric mice 42
2.1.5 Cell Culture 43
2.1.5.1 Cell counting 43
2.1.5.2 In vitro culture of Raw 264.7 macrophage 44
2.1.5.3 Lentiviral transduction of RAW 264.7 macrophage 44
2.1.5.4 Experiments using Raw macrophage cell lines 45
2.1.5.5 Protein translation using a SUNSET assay 46
2.1.5.6 Generation of murine colon organoids 46
2.1.5.7 In vitro maintenance of murine colonic organoids 47
2.1.5.8 Experiments using murine colonic organoids 47
2.1.6 Immunohistochemistry 48
2.1.6.1 Haematoxylin and Eosin (H&E) staining 48
2.1.6.2 Immunohistochemistry 48
2.1.6.3 Quantification of immunohistochemistry 50
2.1.6.4 Histology Scoring 50
2.1.7 Analysis of protein expression 53
2.1.7.1 Protein extraction 53
2.1.7.2 Bicinchoninic acid (BCA) assay 54

2.1.7.3 Sodium dodecyl sulphate polyacrylamide gel electrophoresis 54
2.1.7.4 Western Blot 55
2.1.7.5 Analysis of protein expression 60
2.1.8 RNA Analysis 60
2.1.8.1 Purification of total RNA from cells 60
2.1.8.2 Purification of total RNA from organoids 61
2.1.8.3 Purification of total RNA from tissue samples 61
2.1.8.4 Purification of miRNA from tissue samples 61
2.1.8.5 Purification of miRNA from blood samples 62
2.1.8.6 RNA Quantification 63
2.1.8.7 cDNA synthesis from mRNA 63
2.1.8.8 TaqMan Real-time polymerase chain reaction 64
2.1.8.9 cDNA synthesis from miRNA 65
2.1.8.10 SyberGreen PCRs 65
2.1.9 Identification of *miR-223-3p* mRNA targets 66
2.1.10 RNA Sequencing 67
2.1.10.1 Bioinformatic pipeline for the analysis of a treatment-naïve paediatric IBD RNA sequencing dataset 67
2.1.10.2 Sample preparation for RNA Sequencing 68
2.1.10.3 Library Construction, Quality Control and Sequencing 68
2.1.10.4 Mapping to the reference Genome and gene expression quantification . 68
2.1.10.5 Differential expression analysis 69
2.1.10.6 Enrichment analysis of differentially expressed genes 69

Chapter 3 Investigating The Expression Of *miR-223* In Paediatric Patients With Ulcerative Colitis 71

Introduction 72

Aims of this chapter 75

Results 76

3.1.1 Characteristics of treatment-naïve paediatric patients with Ulcerative colitis 76
3.1.2 Identification of differentially expressed genes between control and treatment-naïve paediatric patients with Ulcerative colitis 77

3.1.3 Myeloid inflammatory pathways are upregulated in treatment non-responsive paediatric patients with Ulcerative colitis 77
3.1.4 *miR-223-3p* target genes are differentially expressed genes between control and treatment-naïve paediatric patients with Ulcerative colitis 78
3.1.5 Myeloid cell activity is increased in treatment non-responsive paediatric patients with Ulcerative colitis 83
3.1.6 Characteristics of an Irish treatment naïve paediatric Ulcerative Colitis cohort 88
3.1.7 Inflammatory markers associated with treatment non-responsiveness are upregulated in treatment-naïve paediatric patients with pancolitis 91
3.1.8 Inflammatory markers associated with treatment non-responsiveness are increased in treatment-naïve paediatric patients with Ulcerative colitis 92
3.1.9 *miR-223-3p* expression is increased in Irish treatment-naïve paediatric patients with pancolitis 95
3.1.10 *miR-223-3p* expression correlates with the expression of inflammatory markers in biopsies from pancolitis patients 96
3.1.11 Pathways associated with cytokine signalling are enriched in genes used to identify treatment non-responsive patients with Ulcerative colitis 105
Discussion *107*

Chapter 4 *miR-223* is critical for constraining inflammatory driven tumorigenesis in the AOM/DSS model of Colitis associated colorectal cancer 112

Introduction *113*

Aims of this chapter *117*

Results *118*
4.1.1 Increased tumour size in *miR-223*$^{-/y}$ mice treated with chronic AOM/DSS .. 118
4.1.2 Increased proliferation in colonic tissue of *miR-223*$^{-/y}$ mice treated with chronic AOM/DSS 118
4.1.3 *miR-223*$^{-/y}$ regulates the infiltration of CCR2+ monocytes following AOM-DSS 119
4.1.4 *miR-223*$^{-/y}$ regulates the infiltration of CCR2+ monocytes and its associated inflammatory cytokine profile 120

4.1.5 Hematopoietic deficiency of *miR-223* enhances susceptibility to AOM-DSS 126

4.1.6 Hematopoietic deficiency of *miR-223* increases macrophages infiltrating into colonic tissue of *miR-223*$^{-/y}$ → WT following AOM/DSS 126

4.1.7 Hematopoietic deficiency of *miR-223* increases inflammatory markers after AOM/DSS treatment in chimeric mice 130

Discussion *133*

Chapter 5 Investigating the role of *miR-223* on IL-6/STAT3 signaling during Colitis associated colorectal cancer 136

Introduction *137*

Aims of this chapter *141*

Results *142*

5.1.1 *miR-223* deficiency results in altered gene expression following AOM/DSS 142

5.1.2 *miR-223* deficiency results in the upregulation of pathways associated with poor prognosis in the AOM/DSS model of CAC 142

5.1.3 *miR-223*$^{-/y}$ mice treated with AOM/DSS have increased cytokine signalling 145

5.1.4 Increased IL-6 cytokine family and STAT3 signalling in *miR-223*$^{-/y}$ mice following AOM/DSS modelling of CAC 146

5.1.5 Antibody-mediated depletion of infiltrating Ly6G^{+} myeloid cells with RB6-8C5 reduced early tumorigenesis in *miR-223*$^{-/y}$ mice using an acute model of AOM-DSS 153

Discussion *155*

Chapter 6 Investigating the role of *miR-223* deficiency on nitric oxide signalling and its impact on the development of colitis associated colorectal cancer 159

Introduction *160*

Aims of this chapter *165*

Results *166*

6.1.1 *miR-223* deficiency results in the upregulation of pathways associated with nitric oxide production in the AOM/DSS model of CAC 166
6.1.2 Increased production of NOS2 and s-nitrotyrosine in *miR-223*$^{-/y}$ mice following AOM/DSS modelling of CAC 166
6.1.3 Antibody depletion of infiltrating Ly6G^{+} myeloid cells reduced early expression of NOS2 and s-nitrotyrosine in *miR-223*$^{-/y}$ mice following acute AOM/DSS 167
6.1.4 NOS2 expression is modulated in *miR223KD* RAWs by inhibiting pathways contributing to the production of NO 174
6.1.5 IFN-γ signalling is increased in *miR-223*$^{-/y}$ mice treated with AOM/DSS 174
6.1.6 Stimulation with IFN-γ does not alter the expression of markers implicated in nitric oxide production in *miR-223KD* RAW 264.7 cells 178
6.1.7 *miR-223KD* RAW 264.7 cells have increased protein translation 179
6.1.8 Stem cell markers are altered by the pharmacologic inhibition or activation of NOS2 +/- IFN-γ for 48 hours 181
6.1.9 IFN-γ induced alterations in the stem cell marker Ly6a is regulated by NOS signalling 181

Discussion *187*

Chapter 7 Discussion and future directions 192

Discussion *193*

Future directions *199*

Appendix *201*

References *229*

LIST OF FIGURES

Figure 1. *Overview of the gastrointestinal tract and the large intestine.* 3
Figure 2. *Global incidence of Ulcerative colitis.* 4
Figure 3. *Factors that contribute to the development of Ulcerative colitis.* 7
Figure 4. *Overview of the differentiation of monocytes into macrophage under steady-state and Ulcerative colitis.* 10
Figure 5. *Hallmark endoscopic and histological changes associated with Ulcerative colitis.* 13
Figure 6. *The Montreal classification system for disease extent in Ulcerative colitis.* 14
Figure 7. *Differences in the progression of Sporadic colorectal cancer and Colitis associated colorectal cancer.* 18
Figure 8. *Canonical biogenesis of miRNAs.* 22
Figure 9. *miRNAs implicated in the hallmarks of cancer.* 25
Figure 10. *Induction of Colitis-associated colorectal cancer in mice using chronic AOM/DSS.* 41
Figure 11. *Generation of bone marrow chimeric mice and subsequent timeline of treatment with chronic AOM/DSS .* 43
Figure 12. *Illustration of immunostaining performed on FFPE tissue generated from a chronic mouse model of CAC.* 52
Figure 13. *Overview of protein analysis via western blotting.* 59
Figure 14. *Workflow for the identification of miR-223-3p targets in humans and mice.* 67
Figure 15. *Overview of RNA sequencing from sample preparation to bioinformatic analysis.* 70
Figure 16. *Overview of bioinformatic workflow performed on the mucosal transcriptome of treatment-naïve paediatric patients with Ulcerative colitis.* 79
Figure 17. Genes are differentially expressed between control and paediatric patients with Ulcerative colitis. 80
Figure 18. *Hallmark pathways associated with inflammation and poor prognosis in are upregulated in treatment non-responsive paediatric patients with Ulcerative colitis.* 81
Figure 19. *Pathways associated with chemokine and cytokine signalling are upregulated in treatment non-responsive paediatric patients with Ulcerative colitis.* 82
Figure 20. *miR-223-3p target genes are differentially expressed among control and treatment non-responsive paediatric patients with Ulcerative colitis.* 84

Figure 21. *Neutrophil recruitment is upregulated in treatment non-responsive paediatric patients with Ulcerative colitis.* 85
Figure 22. *Monocyte activity is upregulated in treatment non-responsive paediatric patients with Ulcerative colitis.* 86
Figure 23. *Macrophage activation is upregulated in treatment non-responsive paediatric patients with Ulcerative colitis.* 87
Figure 24. *Overview of workflow performed on caecum and rectum pinch biopsies from an Irish treatment naïve paediatric Ulcerative Colitis cohort.* 89
Figure 25. *Paris classification for phenotyping paediatric patients with Ulcerative colitis.* 90
Figure 26. *Inflammatory markers are upregulated in caecum biopsies from patients with pancolitis.* 93
Figure 27. *Inflammatory markers are upregulated in rectal biopsies from patients with pancolitis.* 94
Figure 28. miR-223-3p is increased in caecum and rectum biopsies from patients with pancolitis. 95
Figure 29. *The inflammatory markers OSM, MMP3 and IL-6 positively correlate with miR-223-3p expression in caecum biopsies from patients with pancolitis.* 97
Figure 30. *miR-223-3p expression does not correlate with the inflammatory markers MUC2, IL-1β, CCL2, IL-11, REG3G, LCN2 or CSF1 in caecum biopsies from patients with pancolitis.* 98
Figure 31. *miR-223-3p expression does not correlate with the expression of inflammatory markers in caecum biopsies taken from patients with Ulcerative colitis (Rectosigmoid).* ..99
Figure 32. *miR-223-3p expression does not correlate with the inflammatory markers MUC2, IL-1β, CCL2, IL-11, REG3G, LCN2, S100A8 or CSF1 in caecum biopsies from patients with Ulcerative colitis (Rectosigmoid).* 100
Figure 33. *The inflammatory markers NOS2 and LCN2 negatively correlate with miR-223-3p expression in rectal biopsies from patients with pancolitis.* 101
Figure 34. *The inflammatory markers IL-6, CCL2, Col4A1, S100A8, IL-1β, REG3G and MUC2 do not correlate with miR-223-3p expression in rectal biopsies from patients with pancolitis.* 102
Figure 35. *miR-223-3p negatively correlates with IL-6 expression in rectal biopsies from patients with Ulcerative colitis (Rectosigmoid).* 103

Figure 36. *The inflammatory markers CCL2, IL-1β, NOS2, CSF1, REG3G, S100A8 and TREM2 do not correlate with miR-223-3p expression in rectal biopsies from patients with Ulcerative colitis (Rectosigmoid).* 104
Figure 37. *Cytokine signalling pathways are enriched in genes that can be used to identify treatment non-responsive patients with Ulcerative colitis.* 106
Figure 38. *Tumour microenvironment is diverse in Colitis associated colorectal cancer.* 114
Figure 39. *Pro-inflammatory and anti- inflammatory functions of tumour associated macrophages.* 115
Figure 40. *Clinical readouts from chronic AOM/DSS study performed in mice.* 119
Figure 41. *miR-223$^{-/y}$ mice have increased tumour size following chronic AOM/DSS.* ... 121
Figure 42. *miR-223$^{-/y}$ mice have enhanced proliferation following chronic AOM/DSS.* . 122
Figure 43. Macrophage, neutrophils and monocytes infiltrate into the colon of miR-223$^{-/y}$ following chronic AOM/DSS. 123
Figure 44. *Colonic tissue from miR-223$^{-/y}$ mice show an increased chemokine signature for monocytes and neutrophils following chronic AOM/DSS.* 124
Figure 45. *Colonic tissue from miR-223$^{-/y}$ mice have increased expression of myeloid associated growth factors.* 125
Figure 46. *Bone marrow chimera shows that hematopoietic deficiency of miR-223 enhances susceptibility to AOM/DSS.* 127
Figure 47. *Bone marrow chimera study shows there is increased macrophage infiltrating into unaffected colonic tissue of miR-223$^{-/y}$ → WT following AOM/DSS.* 128
Figure 48. *Bone marrow chimera showed that there is increased macrophage infiltrating into tumour tissue of miR-223$^{-/y}$ → WT following AOM/DSS.* 129
Figure 49. *Hematopoietic deficiency of miR-223 increases inflammatory markers after chronic AOM/DSS treatment in chimeric mice.* 131
Figure 50. *Hematopoietic deficiency of miR-223 does not alter growth factors following chronic AOM/DSS treatment in chimeric mice.* 132
Figure 51. *Overview of IL-6/STAT3 signalling in humans.* 138
Figure 52. *Gene expression is altered in WT and miR-223$^{-/y}$ mice following chronic AOM/DSS.* 143
Figure 53. *miR-223$^{-/y}$ mice present with an upregulation of pathways associated with Inflammatory Bowel Disease and Colorectal Cancer following chronic AOM/DSS.* 144

Figure 54. *miR-223$^{-/y}$ mice present with an upregulation of pathways associated with poor prognosis in CAC when treated with chronic AOM/DSS.* 145
Figure 55. *miR-223$^{-/y}$ mice present with an upregulation of chemokine and cytokine activity after chronic AOM/DSS.* 147
Figure 56. *miR-223$^{-/y}$ mice present with increased expression of cytokine and IL-6 family signalling following chronic AOM/DSS.* 148
Figure 57. *miR-223$^{-/y}$ mice present with increased expression of hematopoietic cells after chronic AOM/DSS.* 149
Figure 58. *Illustration of the binding sites in LIF, IL-6ST and STAT3 that are miR-223-3p targets.* 150
Figure 59. *IL-6 family members and cytokines that signal via STAT3 are increased in miR-223$^{-/y}$ mice following chronic AOM/DSS.* 151
Figure 60. *miR-223$^{-/y}$ mice have increased p-stat3 and stat3 expression following treatment with chronic AOM/DSS.* 152
Figure 61. *Depletion of infiltrating Ly6G^{+}myeloid cells reduces early tumorigenesis in miR-223$^{-/y}$ mice following acute AOM/DSS.* 154
Figure 62. *Overview of the induction, synthesis and post-translation modifications of nitric oxide.* 162
Figure 63. *Hallmarks of cancer regulated that are regulated by nitric oxide.* 164
Figure 64. *Bulk RNA sequencing on colonic tissues revealed that pathways associated with nitic oxide expression are differentially expressed between miR-223$^{-/y}$ and WT mice following chronic AOM/DSS.* 168
Figure 65. *Pathways associated with nitrosylation are differentially expressed in colonic tissue from miR-223$^{-/y}$ and WT mice after treatment with chronic AOM/DSS.* 169
Figure 66. *Colonic NOS2 expression is increased in colonic tissue from miR-223$^{-/y}$ mice in the AOM/DSS model of CAC.* 169
Figure 67. *Expression of s-nitrotyrosine is increased in colonic tissue from miR-223$^{-/y}$ mice in the AOM/DSS model of CAC.* 170
Figure 68. *miR-223$^{-/y}$ mice have increased NOS2 and s-nitrotyrosine in unaffected tissue following AOM/DSS.* 171
Figure 69. *miR-223$^{-/y}$ mice have increased s-nitrotyrosine in tumour tissue following AOM/DSS.* 172

Figure 70. *Antibody depletion of infiltrating Ly6G^{+} myeloid cells reduced NOS2 and s-nitrotyrosine expression in unaffected tissue of miR-223$^{-/y}$ mice following acute AOM/DSS.* 173
Figure 71. *NOS2 expression is altered in miR-223KD RAW 264.7 cells by pharmacologically inhibiting pathways implicated in its production.* 175
Figure 72. *Pharmacologic inhibition of pan-JNK, ERK or JAK1/2 prior to LPS stimulation reduces NOS2 expression in miR-223KD RAW 264.7 cells.* 176
Figure 73. *Pharmacologic inhibition of pathways implicated in nitric oxide production alter the production of NOS2 following stimulation with IFN-γ in miR-223KD RAW 264.7 cells.* 177
Figure 74. *Type II interferon signalling is increased in colonic tissue from miR-223$^{-/y}$ mice treated with AOM/DSS.* 178
Figure 75. *Expression of markers implicated in nitric oxide signaling are unchanged overtime following stimulation with IFN-γ in miR-223KD RAW 264.7.* 179
Figure 76. *miR-223KD RAW 264.7 cells have higher protein translation than RAW 264.7 cells.* 180
Figure 77. *Pharmacologic inhibition or activation of NOS2 +/- IFN-γ for 48 hours alters the growth of mouse colonic organoids.* 183
Figure 78. *Pharmacologic inhibition or activation of NOS2 +/- IFN-γ for 48 hours alters the expression of stem cell markers in mouse colonic organoids.* 184
Figure 79. *Early pharmacologic inhibition or activation of NOS2 +/- IFN-γ, followed by a recovery period alters the growth of mouse colonic organoids.* 185
Figure 80. *Early pharmacologic inhibition or activation of NOS2 +/- IFN-γ, followed by a recovery period alters the expression of ly6a in mouse colonic organoids.* 186
Figure 81. *Overview of key findings from investigating the role of miR-223-3p Ulcerative colitis and Colitis-associated colorectal cancer.* 198

LIST OF APPENDIX FIGURES

Appendix Figure 1. β-catenin expression is unchanged between WT and *miR-223*$^{-/y}$ mice in the AOM/DSS model of CAC. 211

Appendix Figure 2. WT and *miR-223*$^{-/y}$ have similar expression of Ly6G, CD68, CD206 and CCR2. 212

Appendix Figure 3. Paper "The MicroRNA *miR-223* constrains colitis-associated tumorigenesis by limiting myeloid cell infiltration and chemokine expression"..... 213

LIST OF TABLES

Table 1. *Animals and cell lines.* 30
Table 2. *TaqMan Primers.* 30
Table 3. *SyberGreen Primers.* 32
Table 4. *Antibodies.* 33
Table 5. *Commercial kits.* 34
Table 6. *Reagents.* 34
Table 7. *Consumables.* 37
Table 8. *Equipment.* 37
Table 9. *Software.* 38
Table 10. *Ulcerative colitis disease activity index.* 42
Table 11. *Inhibitors used in cell culture.* 45
Table 12. *Sequential immersions for deparaffinizing FFPE slides.* 49
Table 13. *Primary antibodies used for immunohistochemistry.* 49
Table 14. *Sequential immersions for dehydrating FFPE slides.* 50
Table 15. *Classification of tumours following AOM/DSS mouse model of CAC.* 51
Table 16. *Components used for protein extraction from tissue samples.* 53
Table 17. *Components used for protein extraction from cells.* 54
Table 18. *Reagents used for western blotting.* 56
Table 19. *Antibodies used for western blots.* 56
Table 20. *Components used to make reverse transcription master mix for use with mRNA.* 63
Table 21. *Thermocycler conditions used for cDNA synthesis from mRNA.* 64
Table 22. *Components of TaqMan RT-PCR master mix.* 64
Table 23. *TaqMan RT-PCR cycling conditions.* 64
Table 24. *Components used to make reverse transcription master mix for use with miRNA.* 65
Table 25. *Thermocycler conditions used for cDNA synthesis from miRNA.* 65
Table 26. *Components of SyberGreen PCR master mix.* 66
Table 27. *SyberGreen RT-PCR cycling conditions.* 66
Table 28. *Differentially expressed miRNAs in Ulcerative colitis.* 74
Table 29. *Characteristics of control and patients with Ulcerative colitis from GSE109142 cohort.* 76

Table 30. *Characterisation of an Irish treatment naïve paediatric Ulcerative Colitis cohort.* 90
Table 31. *Summary of clinical information provided for Irish treatment naïve paediatric Ulcerative Colitis cohort.* 91
Table 32. *miRNAs implicated in colitis associated colorectal cancer.* 116

LIST OF APPENDIX TABLES

Appendix Table 1. Mayo scoring system for classifying disease activity in Ulcerative colitis. 202
Appendix Table 2. Paediatric Ulcerative Colitis Activity Index. 203
Appendix Table 3. *miR-223-3p* target genes in mice identified using Target Scan. 204
Appendix Table 4. *miR-223-3p* target genes in humans identified using Target Scan.... 205
Appendix Table 5. *miR-223-3p* target genes in mice identified using miRTarBase. 207
Appendix Table 6. *miR-223-3p* target genes in humans identified using miRTarBase... 208
Appendix Table 7. *miR-223-3p* target genes are differentially expressed between control and paediatric patients with Ulcerative colitis from GSE109142 cohort. 209
Appendix Table 8. *miR-223* target genes are differentially expressed between control and treatment non-responsive patients with Ulcerative colitis from GSE109142 cohort. 210

DECLARATION

This thesis has not been submitted whole or in part to this, or any other university for any other degree and is the original work of the author except where stated otherwise.

Signed: _____

Ciara Flynn, MSc

Date: 16th September 2024

ACKNOWLEDGEMENTS

First and foremost, I would like to thank my supervisor Dr. Eóin McNamee. From when I first started in the lab as a research assistant, yet to learn how important adding BME is to lamelli, and throughout every step of my PhD your support has been unwavering. I will always be extremely grateful for the opportunity to pursue this PhD. Thank you for your kindness, patience, guidance and for always letting me "follow the science".

To Dr. Joanne Masterson, thank you for all your support, advice and encouragement over the years. Also, a decent chunk of this thesis wouldn't have been possible without access to your ChemiDoc, which saved me from the dark room and for that I am extremely grateful.

To everyone in the Biology Department, thank you. To Áine and Michelle, for sorting everything order related and to Noel, for fixing a lot of equipment. To Dr. Paul Dowling and Dr. Emmanuelle Graciet, thank you for all your feedback and suggestions during my advisor/assessor meetings.

To all the members of the MiR/AIRR lab, past and present: We might be like a dysfunctional family at times but thank you all for making the last four years so enjoyable. Georgia, I'm glad the morning crew is getting a new member, and I'm excited for you as you start your PhD journey. Olga, thank you for your medical advice and always having a story to tell. Lauren, I don't think I have ever been asked so much if I'm related to someone. We started together, and I'm glad we get to finish together as well. Sofia, your singing has brightened up the lab. Dafne, thank you for our morning conversations and for giving me all the Italian tips and tricks.

Taylor, you may have left the lab, but you're certainly not forgotten. Thank you for always being willing to try whatever Irish treat I had brought in and for our late-night chats during my 12-hour days. Gary, as the other founding member of the morning crew, we have spent many mornings together gossiping/ranting over a cup of coffee. Thank you for always finding my phone and returning it, often before I've even realized it's missing.

Sinéad you have listened and offered advice at different stages when I needed it, and for that, I will always be grateful. Louise, we started as RAs together and have gone through every step since then together. I've thoroughly enjoyed our planning of the Christmas door each year, even if it did typically start in the middle of summer. Megan, thank you for all your advice and guidance over the last year. Your "it'll be grand, it'll all work out" attitude

has helped me more than you know. Thank you for always listening, even if you might forget.

Shauna and Caoimhe, thank you both for endless laughs, chats, voice notes, coffee runs and trips to McDonald's. You have both gotten me through some bad days and provided hope when I didn't have any. Shauna, there is no one else I would rather share pancakes with, and I hope it continues - even if it means my Nutella isn't always safe. Thank you for always having a funny story, providing endless entertainment and I'm glad we got to write together. Caoimhe "Quava", thank you for all your advice and support over the years. From checking my calculations (and assuming excel is wrong), you have always been there for me. I'm also going to miss your singing in TC. I'm excited to see what the future holds for both of you, and I'm glad this PhD brought us together.

To my Family, thank you for putting up with me over the last few months. Willow, who has never left my side. My brothers Conor and Dáire, Dáire for providing the late-night snacks while I was writing and Conor for listening to my latest rant, thank you both. To my parents, I can't thank you enough for everything. You have both always supported and encouraged me, even when you didn't fully understand what the next step would entail.

To my boyfriend Niall, from undergraduate through to PhD, you never left my side. Thank you for listening to my presentations and for putting up with me when I was stressed. You have helped more than you will ever know and I'm forever grateful for your continued support.

ABBREVIATIONS

223KD	*miR-223* Knockdown
223OE	*miR-223* Overexpression
3′ UTR	3′ untranslated region
5-ASA	5-aminosalicyclic acid
ACK	Ammonium-Chloride-Potassium
AGO	Argonaute
AMPs	Anti-microbial peptides
AOM	Azoxymethane
APS	Ammonium persulfate
ARDS	Acute respiratory distress syndrome
AtRA	All-trans retinoic acid
BCA	Bicinchoninic acid assay
BM	Bone marrow
BMDM	Bone marrow derived macrophage
BSA	Bovine serum albumin
C/EBP	CCAAT-enhancer-binding proteins
CAC	Colitis-associated colorectal cancer
CD	Crohns disease
cDNA	Complementry DNA
cGMP	Cyclic guanosine monophosphate
CRC	Colorectal cancer
DAI	Disease activity index

DAMPs	Damage-associated molecular pattern molecules
DNA	Deoxyribonucleic acid
DOCHAS	Determinants and Outcomes of Children and Adolescents
DSS	Dextran sodium sulphate
EDTA	Ethylenediaminetetraacetic acid
ESR	Erythrocyte sedimentation rate
FBS	Fetal bovine serum
FFPE	Formalin-fixed and paraffin embedded
FPKM	Fragments per kilobase of transcript per millions base pairs sequenced
G-MCSF	Granulocyte-monocyte colony stimulating factor
GEO	Gene expression omnibus
GP130	Glycoprotein 130
GSEA	Gene Set Enrichment Analysis
GTP	Guanosine triphosphate
GWAS	Genome-wide association studies
H&E	Haematoxylin and Eosin
HCC	Hepatocellular carcinoma
HCV	Hepatitis C virus
HLA	Human Leukocyte Antigen
IBD	Inflammatory bowel diseases
IV	Intravenous
KEGG	Kyoto Encyclopaedia of genes and genomes
KLF6	Kruppel-like factor 6

M-CSF	Macrophage stimulating factor
Mefc	Myocyte enhancer factor 2C
miRNA	Micro RNA
mRNA	Messenger RNA
NCRC	National Children's Research Centre
NFIA	Nuclear factor 1A
NO	Nitric oxide
NOS	Nitric oxide synthase enzymes
NOS1	Neuronal NOS
NOS2	Inducible NOS
NOS3	Endothelial NOS
NSCLC	Non-small cell lung cancer
PAMPS	Pathogen associated molecular patterns
PBS	Phosphate buffered saline
PCNA	Proliferating cell nuclear antigen
PKG	Protein kinase G
Pre-miRNA	Precursor miRNA
Pri-miRNA	Primary miRNA
PRRs	Pattern recognition receptors
PUCAI	Paediatric Ulcerative Colitis Activity Index
RCF	Relative centrifugal force
Rhob	Ras homolog gene family member B
RIPA	Radioimmunoprecipitation assay

RISC	RNA-induced silencing complex
RNA	Ribonucleic acid
RT	Reverse transcription
RT-PCR	Real-time polymerase chain reaction
SDS	Sodium dodecyl sulphate
SDS-PAGE	Sodium dodecyl sulphate polyacrylamide gel electrophoresis
sGC	Soluble guanylyl cyclase
STAT	Signal transducer and activator of transcription
T-PER	Tissue protein extraction reagent
TAMs	Tumour associated macrophage
TEMED	Tetramethylethylenediamine
TME	Tumour microenvironment
TRAF6	TNF receptor-associated Factor 6
TRBP	Trans-activator RNA binding protein
UC	Ulcerative colitis
UNT	Untranslated region
WT	Wild Type

PUBLICATIONS AND PRESENTATIONS

Publications

- **Flynn CL**, Markey GE, Neudecker V, Farrelly C, Furuta GT, Eltzschig HK, Masterson JC, McNamee EN. The MicroRNA *miR-223* Constrains Colitis-associated Tumorigenesis by Limiting Myeloid Cell Infiltration and Chemokine Expression. J Immunol. 2024 Dec 15;213(12):1869-1883. doi: 10.4049/jimmunol.2400129. PMID: 39485006; PMCID: PMC11611642.
- **In preparation** – '*miR-223* regulates differentiation of reparative macrophage and the inflammatory tone of CCR2+ monocytes to influence mucosal healing following colitis' *Lindsey Gumer, ***Ciara L. Flynn,** Gary Markey, Kathleen M. Scullion, Paul Jedlicka, Mack Matthias, Glenn T. Furuta, Séamus Hussey, Joanne Masterson, Eóin N. McNamee **(* joint first-author)**
- **In preparation** - 'CXCR3+ T-cells shape the intestinal stem cell niche and Paneth cell anti- microbial responses in experimental Crohn's disease via IFNy' Caroline P. Nguyen, Caoimhe Cadden, Megan O'Brien, **Ciara Flynn**, Tom T. Nguyen, Owen Jensen, Lauren Flynn, Paul Jedlicka, Edwin F. de Zoeten, Jesus Rivera-Nieves, Eóin N. McNamee

Oral presentations

- **The International Congress of Mucosal Immunology (ICMI) 2024** - 'The MicroRNA *miR-223* constrains Colitis-associated Tumorigenesis by limiting myeloid cell infiltration and chemokine expression'.
- **SFI Annual Progress Meeting 2023** - 'The MicroRNA *miR-223* constrains Colitis-associated Tumorigenesis by limiting myeloid cell infiltration and Chemokine expression'.
- **Biology research day 2023 in Maynooth University** - 'The MicroRNA *miR-223* constrains Colitis-associated Tumorigenesis by limiting myeloid cell infiltration and Chemokine expression'.

Poster presentations

- **Biology research day 2024 –** "Investigating the link between *miR-223* deficiency and increased nitric oxide signaling, what is the impact on the development of colitis associated colorectal cancer?" **Ciara Flynn** and Eóin N. McNamee.
- **Irish Society for Immunology Conference 2022 -** "The microRNA *mir-223* constrains colitis-associated tumorigenesis by limiting myeloid cell infiltration and chemokine expression" **Ciara Flynn** and Eóin N. McNamee.
- **Biology Department Research Day 2022 -** 'Immune-Epithelial cross talk in Colitis-Associated Colon Cancer' **Ciara Flynn** and Eóin N. McNamee**.**

ABSTRACT

Aberrant intestinal inflammation is a pathological feature of Ulcerative colitis (UC), and plays a crucial role in the development of Colitis-associated colorectal cancer (CAC). However, the mechanisms behind the role of the myeloid immune compartment in this inflammatory process are not fully understood. miRNA-mediated gene expression regulates numerous biological processes, with altered miRNA expression identified in both UC and CAC. Despite this, the role of myeloid-specific microRNA's in the inflammatory process that underpins the continuum from UC to tumorigenesis remains unresolved.

Here, gene set enrichment analysis (GSEA) on a discovery RNA seq data set from treatment-naïve paediatric patients with UC, revealed that there was a positively enriched signature for myeloid inflammation among patients who were non-responsive to therapeutics. Confirmatory analysis on an Irish validation cohort of treatment-naïve paediatric patients with UC showed a similar inflammatory profile in mucosal biopsies via RT-PCR. Expression of *miR-223* was increased in patients with pancolitis and correlated with the expression disease relevant inflammatory gene sets including OSM, MMP3 and IL-6.

An Azoxymethane-Dextran Sodium Sulfate (AOM/DSS) mouse model of CAC showed that *miR-223* is critical limit myeloid-driven inflammation. In this model, *miR-223*$^{-/y}$ mice presented with significantly larger tumours and an enhanced proliferative signature. Immunoprofiling showed that *miR-223*$^{-/y}$ mice have significantly increased colonic myeloid immune infiltrate (neutrophils, monocytes and macrophage) following AOM/DSS. This was accompanied by an increased inflammatory chemokine and cytokine signature for monocytes and neutrophils. Bone marrow chimera studies demonstrated that myeloid-expressed *miR-223* is responsible for the enhanced tumor proliferation and inflammatory response. RNA sequencing on chronic AOM/DSS samples identified several pathways that could be contributing to the development of CAC in *miR-223*$^{-/y}$ mice, including the IL-6-IL-17a cytokine family/STAT3 signalling.

Finally, to mechanistically understand how *miR-223* regulates epithelial tumorigenesis following myeloid inflammation, Nitric oxide signalling was identified as a major pathway of interest. Pharmacologic inhibition, lentiviral gene knock down and colonic mouse organoids were utilized to understand how *miR-223* regulated type II interferon-NOS signalling and its impact on epithelial stem cell function.

CHAPTER 1 INTRODUCTION

1.1.1 Ulcerative colitis

Ulcerative colitis (UC) is a major global health burden (Kaplan, 2015, Le Berre et al., 2023). This is an inflammatory bowel disease (IBD) characterised by chronic mucosal inflammation in the large intestine that starts in the rectum and extends continuously towards the caecum (Kobayashi et al., 2020). For patients, a diagnosis with UC can alter their life and lead to long-term complications. The most severe consequence for patients is the potential to develop colitis-associated colorectal cancer (CAC) (Nardone et al., 2023). The mechanisms that underpin this progression remain poorly understood. To address this, an improved understanding of the inflammatory process that drives both UC and CAC is needed for the development of therapeutics, to improve quality of life for patients.

1.1.2 Physiology of the large intestine

The large intestine is part of the gastrointestinal system, which includes the mouth, esophagus, stomach and small intestine (**Figure 1**). The large intestine consists of the anal canal, rectum, colon and the caecum. The colon can be further divided into the sigmoid colon, descending colon, transverse colon and the ascending colon (**Figure 1**) (Greenwood-Van Meerveld et al., 2017). The mucosa of the colon is covered by a single layer of epithelial cells that are organised into crypts. Amongst these epithelial cells, are intestinal stem cells that reside in the base of the crypt and are critical for the continuous renewal of the intestinal epithelium. These stem cells can differentiate into goblet cells, tuft cells and enteroendocrine cells (Mowat and Agace, 2014, Walsh and Zemper, 2019). Goblet cells are necessary to produce mucin, which creates a protective mucus layer over the epithelial cells. Additionally, Tuft cells are protective as they recognise helminth infections. Furthermore, enteroendocrine cells are essential for the secretion of hormones and the regulation of intestinal homeostasis (Hendel et al., 2022, Zeve et al., 2022, Gologorsky et al., 2023) Collectively, these cells are critical for maintaining homeostasis and act as a protective barrier against pathogens. However, if this process is altered or the intestinal epithelial barrier is defective, chronic intestinal inflammation can occur.

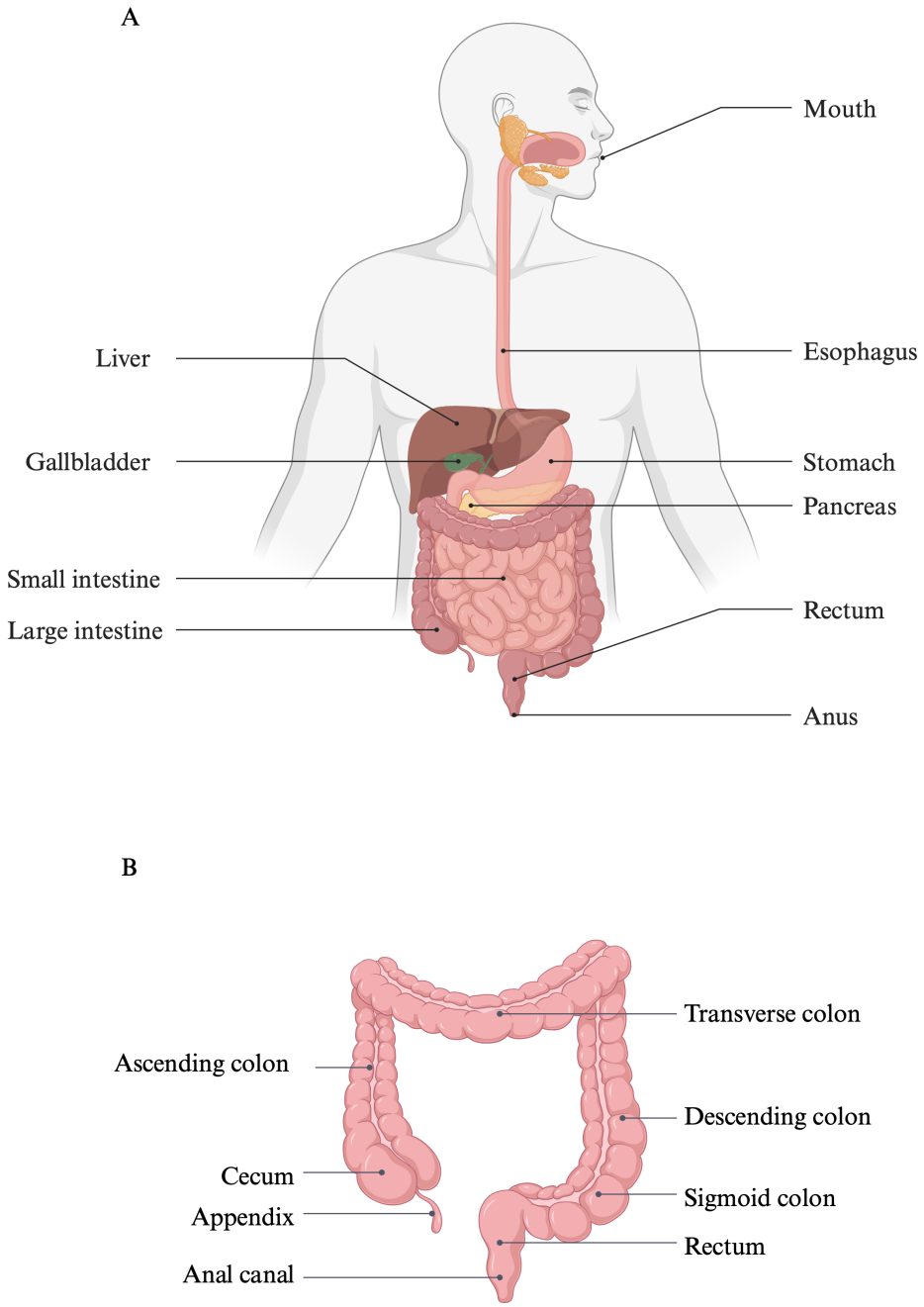


Figure 1. *Overview of the gastrointestinal tract and the large intestine.*

A. The gastrointestinal tract consists of the mouth, esophagus, stomach, small intestine, large intestine, rectum and anus. The liver, pancreas and gallbladder are also involved. **B.** The large intestine consists of the anal canal, rectum, sigmoid colon, descending colon, transverse colon, ascending colon, cecum and appendix. **A.** Adapted from 'Digestive system' on BioRender.com (2024). **B.** Created on BioRender.com.

1.1.3 Epidemiology of Ulcerative colitis

UC was previously believed to be a disease confined to the western world, but its incidence and prevalence are continuing to rise internationally (**Figure 2**) (Le Berre et al., 2023). Globally, the incidence rate of UC is between 9 to 20 cases per 100,000 people per year and the prevalence rate is between 156 to 291 cases per 100,000 people per year (Randall et al., 2020). Research into the prevalence of UC has shown the disease occurs equally among men and women. While UC can be diagnosed at any age, disease onset predominantly occurs between the second and fourth decades of life (Molodecky et al., 2012). Despite significant research into UC, the exact cause of the disease remains unknown. It has been proposed that UC is multifactorial in nature, with environmental factors eliciting an altered immune response in genetically susceptible individuals.

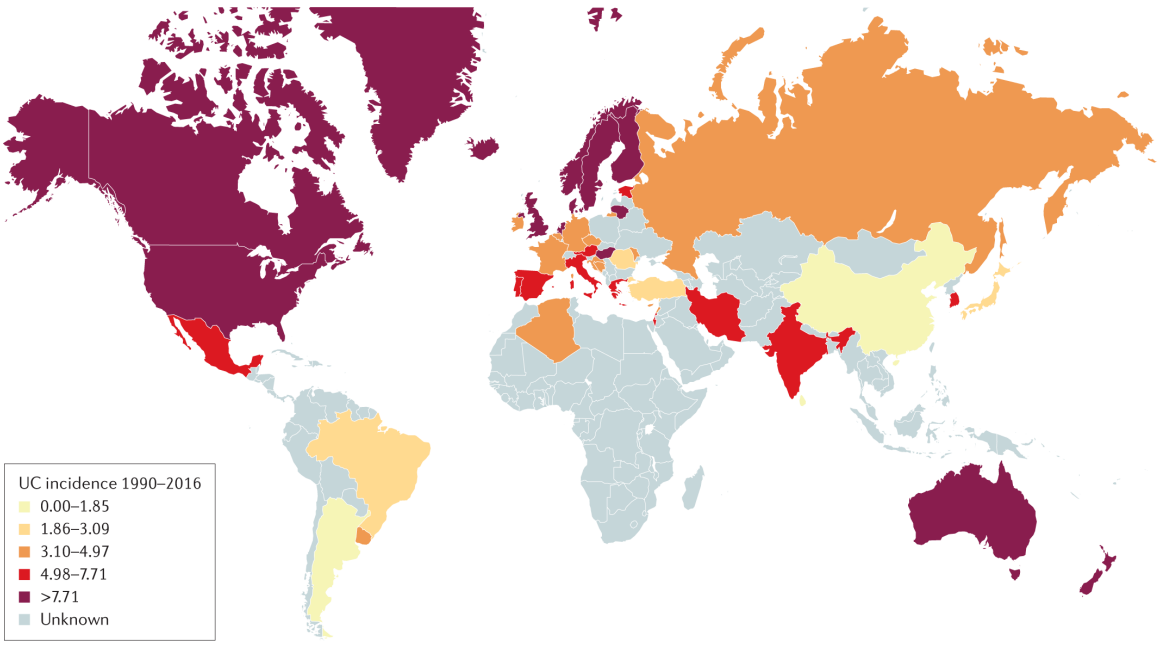


Figure 2. *Global incidence of Ulcerative colitis.*

Globally, the incidence of UC increased from 1990 to 2016. Image taken from (Kobayashi et al., 2020).

1.1.3.1 Genetics of Ulcerative colitis

Arguably the biggest risk factor for the development of UC is a family history of IBD. First degree relatives have a four-fold higher risk of developing the disease, but extended family members are also at increased risk (Moller et al., 2015). A maternal or a sibling diagnosis of IBD significantly increases the likelihood of a sibling or offspring developing IBD (Bernstein et al., 2019, Halfvarson et al., 2022). Advancements in technology have led to improved understanding of the genetic basis of UC. Since its development, genome-wide association studies (GWAS) have identified over 133 susceptibility loci for UC, with the functions of many still to be determined (Wang et al., 2014a). Of these the Human Leukocyte Antigen (HLA) region is among the most extensively studied in UC, with its expression being identified in 7-11% of patients with pancolitis (Thompson and Lees, 2010). Additional genes have been linked with increased susceptibility to UC including, MDR1, ECM1, LAMB1 and CDH1 are all associated with ensuring the epithelial barrier is maintained. Whilst STAT3, IL-23R, TNFα and IL10R are expressed as part of the immune response (Sarlos et al., 2014). However, due to the nature and varying clinical presentation of patients with UC, the presence or absence of these genes is not sufficient for its diagnosis.

1.1.3.2 Environmental factors implicated in the development of Ulcerative colitis

As cases of UC continue to rise globally, it suggests that environmental factors could be contributing to the development of UC. It has been proposed that smoking is protective in UC as those who actively smoke are less likely to develop the disease, whilst those that cease smoking are at increased risk (Higuchi et al., 2012, Berkowitz et al., 2018). Similarly, research has shown that undergoing an appendectomy at an early age is protective against UC. It has been suggested that this could be due to bacteria that reside in the appendix or the immunological activities that this organ controls. However, performing an appendectomy after a diagnosis of UC has been shown to increase the risk of a colectomy (Agrawal et al., 2023, Arjomand Fard et al., 2023, Parian et al., 2017).

In 1989 the hygiene hypothesis was proposed as a potential risk factor for the development of UC (Strachan, 1989). This hypnosis is based on improvements in hygiene coinciding with the rising incidence of UC internationally. It has been proposed that smaller families, overuse of antibiotics, urbanisation, processed foods and over sanitisation are collectively

contributing to UC through a lack of microbial exposure, particularly early in life (Cholapranee and Ananthakrishnan, 2016, Panelli et al., 2020). Additionally, breast feeding decreases the risk of developing UC, whilst living in an industrialised area increasing the risk (Soon et al., 2012, Xu et al., 2017). Collectively this demonstrates that events throughout a patient's life, all contribute to the development of UC (**Figure 3**).

1.1.3.3 Microbial factors implicated in the development of Ulcerative colitis

Huge numbers of microorganisms reside in the human body. These are predominately found in the gastrointestinal tract, with over 100 trillion microbes identified in the gut. Collectively, these microorganisms are referred to as the gut microbiome (Nishida et al., 2018). While the species of bacteria and their abundance varies among individuals, majority of bacteria are from four phyla, Firmicutes, Bacteroidetes, Proteobacteria and Actinobacteria. In healthy individuals these bacteria are important for nutrient processing, preventing the invasion of pathogens and regulating the hosts immune system (Leslie et al., 2019, Lopetuso et al., 2014). However, dysbiosis can result in adverse effects for the host.

Dysbiosis of the gut microbiome has been proposed as contributing factor in the development of many diseases including UC (Pittayanon et al., 2020). While this isn't associated with a specific bacteria, a reduction in the diversity of microbes present has been shown in patients with UC. Additionally, there is a decreased abundance of Firmicutes and Bacteroidetes, coinciding with an increase in Proteobacteria (Sheehan et al., 2015, Sjöberg et al., 2017). This dysbiosis affects the functions of the gut microbiome. In particular, the production of metabolites is altered. This affects the repair of epithelial cells and the differentiation of Treg cells. These are both critical for ensuring that homeostasis in the colon is maintained (Atarashi et al., 2013, Den Besten et al., 2013). Furthermore, patients with UC have an increased abundance of sulfate reducing bacteria such as *Desulfovibrio* species. These species contribute to intestinal damage via the production of hydrogen sulfate, which subsequently promotes colonic inflammation (Kushkevych et al., 2019, Xie et al., 2024, Singh et al., 2023).

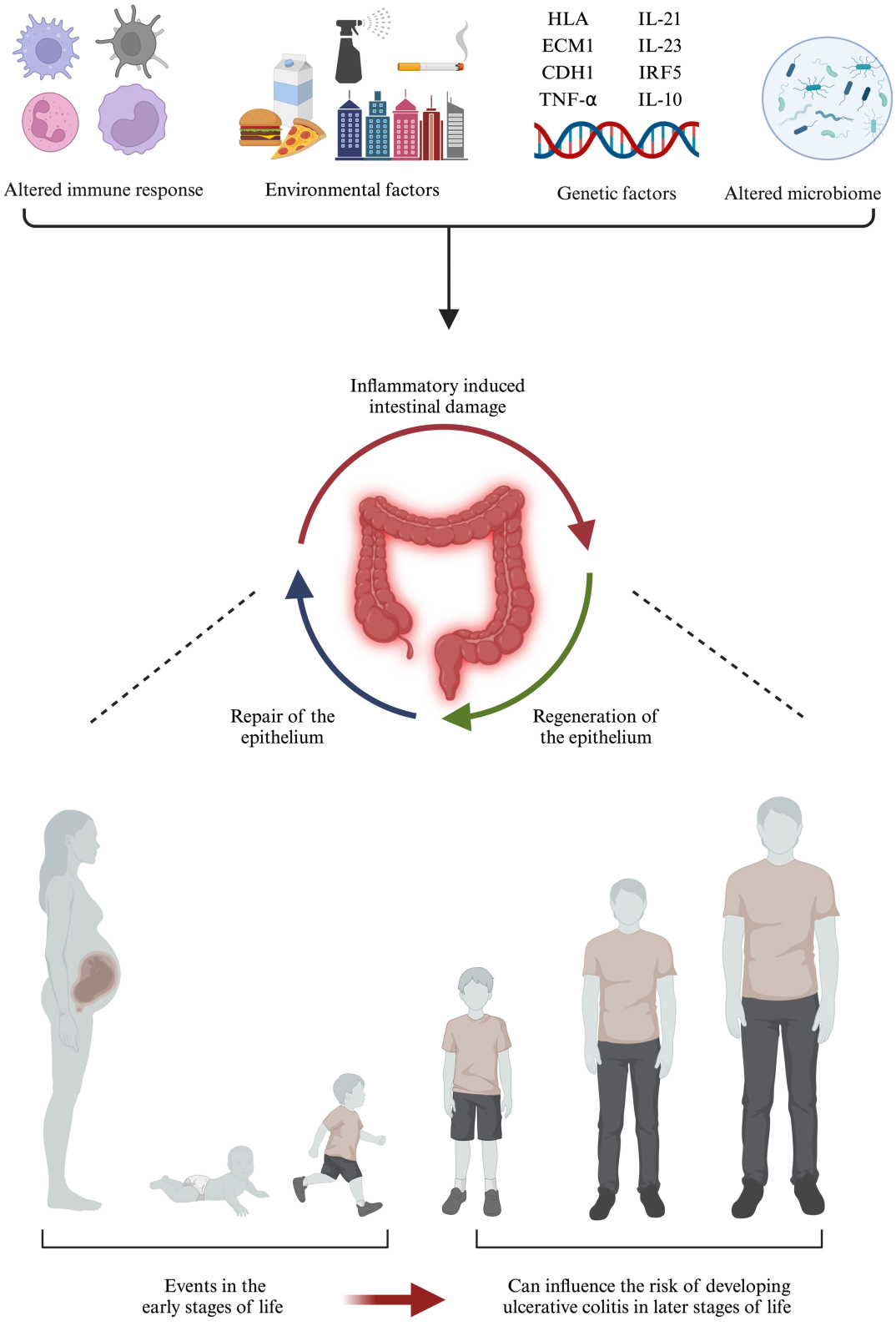


Figure 3. *Factors that contribute to the development of Ulcerative colitis.*

UC is a multifactorial disease that involves interplay between environmental, microbial and genetic factors, which elicit an altered immune response. Early life events and exposures can also affect the lifetime risk of developing UC. Created with BioRender.com.

1.1.4 Pathophysiology of Ulcerative colitis

As previously mentioned, UC is a multifactorial disease that occurs in genetically susceptible individuals, who have an altered immune response to environmental or bacterial triggers. This altered immune response results in excessive inflammation in the mucosa and sub-mucosa of the colon and rectum. In UC this inflammation is uncontrollable, which leads to increased intestinal permeability and impaired barrier function as a consequence. Both the innate and adaptive immune systems are dysregulated in UC.

1.1.4.1 Role of the innate immune system in Ulcerative colitis

The innate immune system is the first line of defence to protect against invading pathogens. While it is non-specific and does not have an immunological memory, its response is rapid. The innate immune system consists of physical barriers, effector cells, physiological responses and inflammatory responses. These responses enable cytokine production and antigen presentation, which are critical for the initiation of the adaptive immune response. However, dysregulation of the innate immune system is central to UC pathogenies.

In UC, defects in both the mucosal and epithelial barrier contribute to disease. This is demonstrated by MUC2 knockout mice spontaneously developing colitis and the identification of the altered expression of epithelial barrier genes in patients with UC (Zhang et al., 2024a, Sæterstad et al., 2022). Defects in either, or both protective mechanisms increases exposure to antigens and initiates an immune response. The initially invading microorganisms are detected through pathogen associated molecular patterns (PAMPs). In response to invading pathogens, epithelial cells secrete anti-microbial peptides (AMPs). However, in UC this protective mechanism is often ineffective and microorganisms are still able to penetrate the intestinal barrier (Cardoso et al., 2022). This infiltration of pathogens can further damage epithelial cells, causing inflammation and the expression of damage-associated molecular pattern molecules (DAMPs). Both PAMPs and DAMPs further activate the innate immune system through their interaction with pattern recognition receptors (PRRs). PRRs include NOD-like receptors and toll-like receptors (Boyapati et al., 2016). These PRRs are recognised by various innate immune cells including monocytes, neutrophils, macrophage and dendritic cells.

In response to intestinal damage, circulating neutrophils are recruited to the site of inflammation via the production of various cytokines including TNF-α, IL-1β and IL-17. Once at the site of inflammation, neutrophils remove invading microorganisms through phagocytosis. Once complete, neutrophils undergo apoptosis to enable tissue repair and a return to homoeostasis (Danne et al., 2024). However, excessive neutrophil activity can contribute to mucosal damage and the progression of UC. This is primarily through the secretion of proteases and pro-inflammatory cytokines, which recruits circulating monocytes to the site of inflammation. Patients with UC have increased neutrophil activity compared to healthy controls (Wéra et al., 2016, Dinallo et al., 2019).

Following the secretion of PAMPs, DAMPs and chemokines from neutrophils, circulating Ly6C^{hi} monocytes are recruited into the site of inflammation via CCR2 (Bain et al., 2014). Once in the colon, monocytes migrate to the lamina propria where they are the most abundant cell type present. Under steady state conditions, the expression of Ly6C is downregulated in monocytes, whilst MHC-II, CX3CR1 and CD64 are upregulated to enable their differentiation into mature macrophage (De Calisto et al., 2012, Bain et al., 2013). These macrophages are either pro- or anti-inflammatory based on environmental ques. In the early stages of inflammation, monocytes differentiate into a pro-inflammatory phenotype to eliminate pathogens and recruit additional immune cells to the site of inflammation. Following pathogen removal, an anti-inflammatory macrophage phenotype is promoted to initiate tissue repair and resolve inflammation (Liao et al., 2024). However, in UC this process is dysregulated and the ability for macrophages to differentiate into an anti-inflammatory phenotype is limited. This results in an accumulation of pro-inflammatory macrophage that secrete inducible nitric oxide synthase, IL-6, TNF-α and IL-1β. This collectively contributes to excessive inflammation which damages intestinal tissue. Patients with UC have increased expression of pro-inflammatory macrophage compared to controls (Zhang et al., 2023a, Zigmond et al., 2012).

In the presence of GM-CSF, monocytes differentiate into dendritic cells in mucosal tissue. Their primary role is antigen presentation and the secretion of cytokines to enhance the immune response to invading pathogens, by activating the adaptive immune system. In UC, the function of dendritic cells is altered, demonstrated by the increased secretion of IL-6 and TNF-α, along with the recruitment of immune cells (Jiménez-Cortegana et al., 2024). Additionally, patients with UC have an increased abundance of dendritic cells, which further drives the inflammatory process resulting in tissue destruction (Yang et al., 2021b).

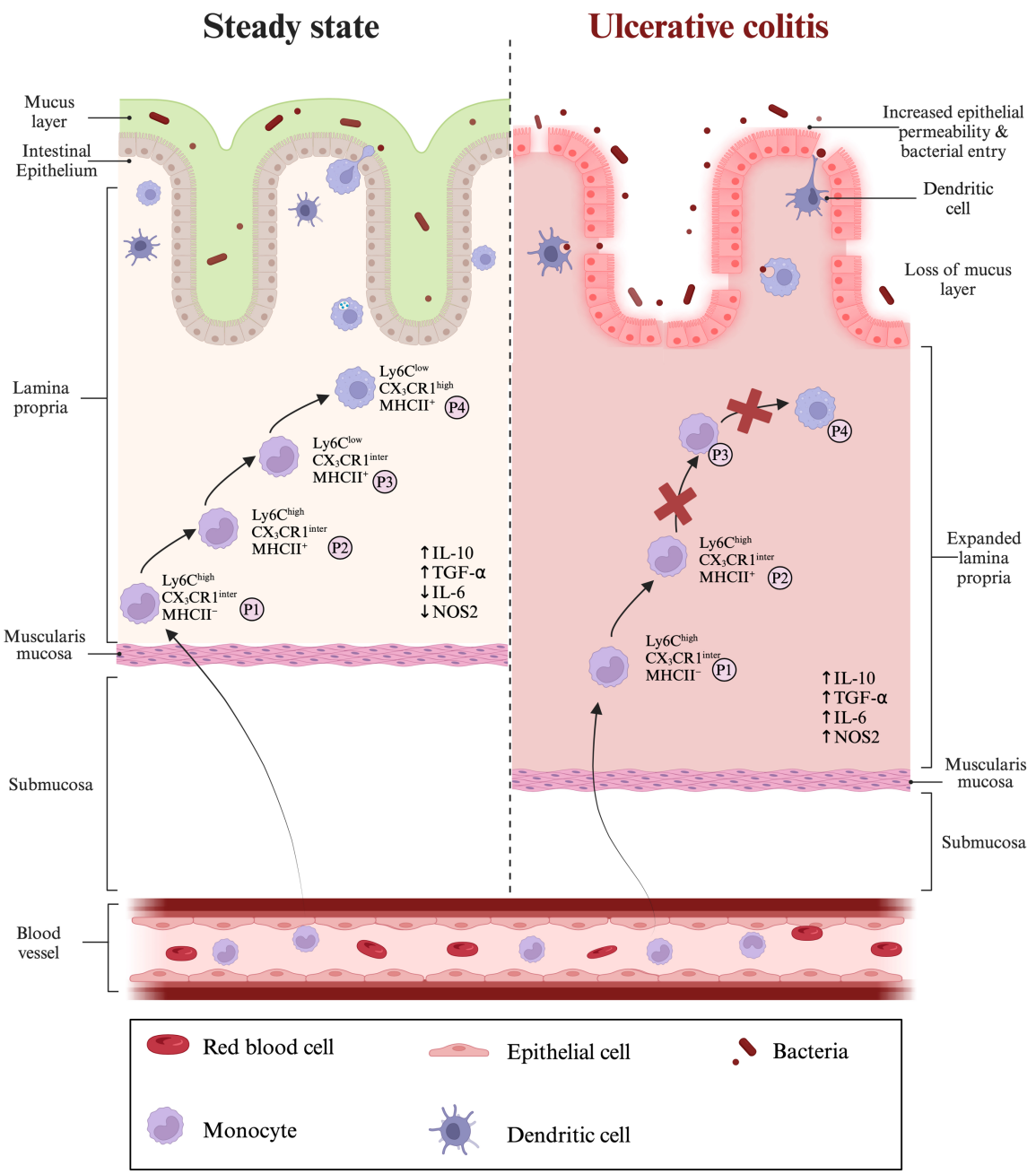


Figure 4. *Overview of the differentiation of monocytes into macrophage under steady-state and Ulcerative colitis.*

In the lamina propria, monocytes undergo differentiation into macrophage. Under steady state conditions, circulating Ly6C^{high} CX3CR1^{intermediate} MHCII^{-} monocytes (P1) infiltrate into the lamina propria and differentiate into macrophages through various stages including: (P2) Express MHCII, (P3) downregulation of Ly6C and (P4) upregulation of CX_3CR1. In UC this process is dysregulated, and monocyte differentiation does not progress passed (P2), resulting an abundance of pro-inflammatory macrophage as a consequence. Created on BioRender.com.

1.1.4.2 Role of the adaptive immune system in Ulcerative colitis

The adaptive immune response is much slower than the innate immune systems. However, due to its immunological memory, it can respond more specifically to antigens presented to B-cells and T-cells. Nevertheless, the dysregulated expression of T-cells and B-cells is associated with several diseases including UC, as they can promote inflammation through the secretion of cytokines and chemokines.

Upon activation, T-cells proliferate and differentiate into Th1, Th2, Th17 or Treg cells, with each sub-set having a specific function. Th1 cells are primarily involved in the removal of intracellular pathogens and the secretion of the pro-inflammatory cytokines IL-1, IL-6, IL-12, TNF-α and IFN-γ. Excessive production of these Th1 cytokines and their transcription factors has been identified in patients with UC compared to health controls (Nakase et al., 2022).

IL-4 and IL-13 promotes the differentiation of Th2 cells, which ensures protection against helminth infections and under homeostatic conditions, promotes tissue repair. Additionally, Th2 cells are responsible for the production of IL-4, IL-5, IL-9 and IL-13. Collectively, this enables the differentiation and activation of B-cells (Zeng, 2013). The activation of Th2 cells increases the production of IL-5 and IL-13 at the site of inflammation in UC patients. This can have adverse effects on the epithelial barrier and inhibit the regeneration of epithelial cells. Furthermore, excessive activation of Th2 cells can contribute a chronic inflammatory microenvironment, which is central to UC progression (Heller et al., 2008, Bamias and Cominelli, 2015).

Th17 cells are protective against infiltrating bacterial and fungal pathogens. They elicit their functions and promote inflammation through the production of IL-17, IL-21 and IL-22. Patients with UC have higher expression of IL-17 in their serum and lamina propria during active inflammation (Ordás et al., 2012, Kmieć et al., 2017). Additionally, the presence of Th17 cells and their associated cytokines recruits neutrophils to the site of inflammation, which further contributes to mucosal damage and sustains inflammation (Chen et al., 2021a).

Treg cells are critical for maintaining homeostasis and preventing abnormal immune responses to the hosts intestinal microbiome. This is primarily achieved through the expression of Foxp3 and the secretion of IL-10, IL-15 and TGF-β. However, their

dysregulation is associated with many autoimmune diseases, including UC. Defects in the production of IL-10 is associated with UC and in DSS models IL-10 knockout mice develop spontaneous colitis (Kiesler et al., 2015). Furthermore, patients with UC have increased expression of IL-10. It has been identified that during active UC, Tregs undergo increased apoptosis which can be reversed through anti-TNFα treatment (Veltkamp et al., 2011, Kałużna et al., 2022b).

B-cells are a critical component of the adaptive immune response. Under steady state conditions they are essential for the synthesis of antibodies, production of cytokines, modulating the inflammatory response and presenting antigens to T-cells. Patients with UC have reduced numbers of Breg cells compared to healthy controls, which leads to decreased production of the anti-inflammatory cytokine IL-10. This reduced abundance of Breg cells correlates with disease severity for patients (Wang et al., 2016c, Spencer and Bemark, 2023). Additionally, in UC the secretion of IgG is promoted over IgA. This results in the synthesis of antibodies against commensal microorganisms in the hosts microbiome. Consequently, there is increased production of cytokines which boosts the recruitment of infiltrating neutrophils and macrophage to the site of inflammation (Castro-Dopico et al., 2019).

1.1.5 Diagnosis of Ulcerative colitis

Early diagnosis of UC is critical for the initiation of treatment, to improve the patient's quality of life and limit disease progression. As there is currently no gold standard for the diagnosis of UC, this is achieved by evaluating a patient's medical history, a clinical evaluation, laboratory tests, histological findings and the absence of an alternative diagnosis.

The predominant symptom patients with UC present with is blood in their stools. This may be accompanied by symptoms such as diarrhoea, abdominal pain, mucus discharge, fatigue, weight loss, nausea and vomiting. However, the severity of these symptoms can vary based on the extent of disease. Additionally, symptoms may be intermittent initially, but increase in duration overtime as the disease progresses (Gajendran et al., 2019).

When patients present with the above symptoms, preliminary tests may include a full blood count, liver tests, along with screening for markers associated with inflammation including erythrocyte sedimentation rate (ESR) and C-reactive protein. Additionally, a stool sample is

typically obtained, to rule out infectious diseases and parasitic infections. Stool samples can also be used to measure faecal levels of calprotectin, which is a marker of colonic inflammation (Ungaro et al., 2017). However, these tests alone are not sufficient to diagnose a patient with UC, as many patients will present within the normal range.

For patients with suspected UC, a colonoscopy is needed to confirm the diagnosis and establish disease extent. Hallmark features of UC include bleeding, erythema, oedema, ulceration and loss of normal vascular pattern, with inflammation that begins in the rectum extending continuously proximally (**Figure 5)** (Gajendran et al., 2019). A colonoscopy also allows mucosal biopsies to be taken for histological analysis. These can be used to verify diagnosis and aid in determining the extent of disease. Histological changes associated with UC include mucosal inflammation, crypt architectural distortion and irregular mucosal layers (**Figure 5 E - H)** (Kellermann and Riis, 2021).

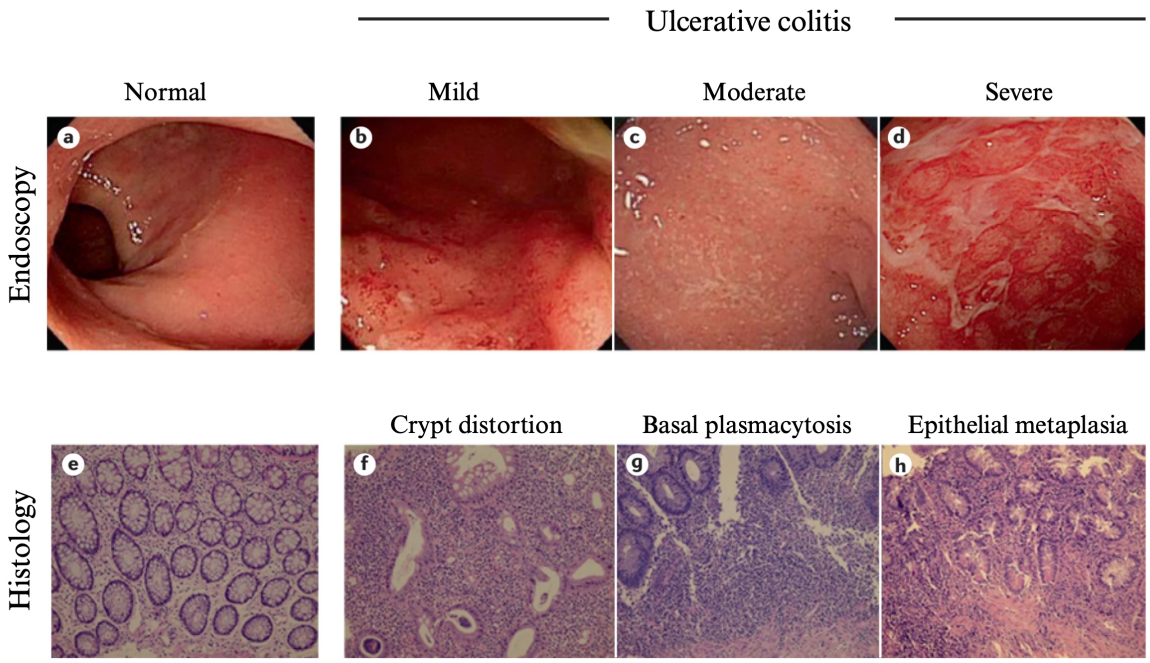


Figure 5. *Hallmark endoscopic and histological changes associated with Ulcerative colitis.*

An endoscope and histological analysis of colonic biopsies are critical for the diagnosis of UC. Endoscopic images of **A.** normal colon, **B.** mild UC, **C.** moderate UC and **D.** severe UC. Histological H&E images of **E.** normal colon, **F.** crypt distortion, **G.** basal plasmacytosis and **H.** epithelial metaplasia. Images and labelling taken from (Kobayashi et al., 2020).

Following colonoscopy and histological analysis, patients with UC are classified based on disease extent and disease activity. For the defining disease extent, the Montreal classification system is currently the most frequently used. This system classifies UC into ulcerative proctitis, rectosigmoid colitis or extensive colitis (**Figure 6**). In ulcerative proctitis, involvement is limited to the rectum. Rectosigmoid colitis, inflammation is confined to the colorectum distal to the splenic flexure. Whilst extensive colitis, often referred to as pancolitis, is defined as involvement that extends proximally to the splenic flexure (De Deo et al., 2024).

Once patients have been diagnosed with UC, it is important that their disease activity is classified. This is critical as it can affect the treatment approach, and it can also be used as an indicator for response to therapeutics or disease progression. The Mayo Score is currently the most widely used disease activity index, with modified non-invasive versions also routinely used (Naegeli et al., 2021). This scoring system allows disease activity to be determined more frequently, without the reliance on colonoscopies. In this method, each section is scored between 0-3 with a maximum score of 12. These sections include stool frequently, rectal bleeding, physician rating of disease severity and mucosal appearance if a colonoscopy has been performed. A total score of < 2 indicates the patient is in remission, 2-4 indicates mild disease activity, 5-7 suggests moderate disease activity and a score <7 indicates the patient has severe disease (Naegeli et al., 2021). This scoring system is shown in **Appendix Table 1**.

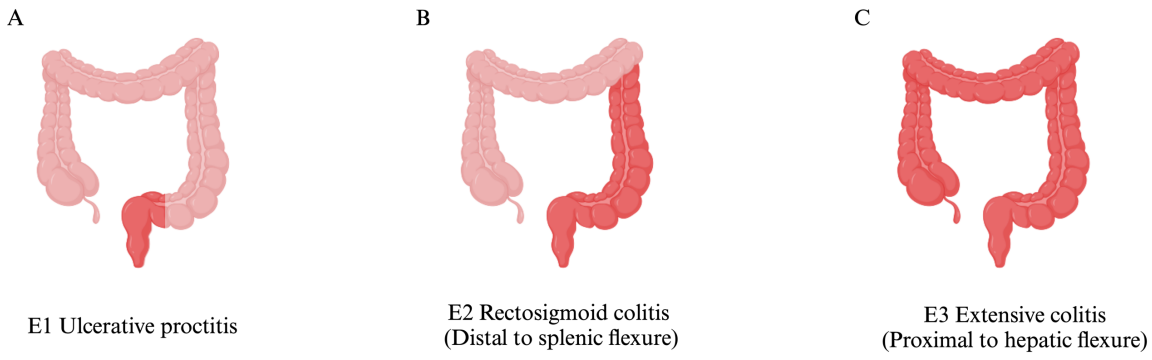


Figure 6. *The Montreal classification system for disease extent in Ulcerative colitis.*

Disease extent in UC is classified into **A.** Ulcerative proctitis, where involvement is confined to the rectum; **B.** Rectosigmoid colitis, involvement is limited to the colorectum distal to the splenic flexure and **C.** extensive colitis, where involvement extents proximally to the splenic flexure. Created on BioRender.com.

1.1.6 Treatment of Ulcerative colitis

Treatment options for patients diagnosed with UC vary based on the patients age, disease duration, disease activity and extent of disease. Regardless of the treatment chosen, the overall aim is to induce and maintain remission, to improve each patient's quality of life and minimise their risk of developing CAC.

For patients with proctitis, 5-aminosalicyclic acid (5-ASA) is currently used as the initial treatment. It is recommended that patients are prescribed topical 5-ASA suppositories as it has been shown to be more effective in this cohort of patients, due to its ability to reach higher concentrations in the rectum than oral 5-ASA (Gionchetti et al., 1998, Pimpo et al., 2010). If patients achieve remission on this treatment, it is recommended that they continue with topical 5-ASA suppositories to maintain remission.

In patients with rectosigmoid colitis, a combination of 5-ASA enemas and oral 5-ASA is initially prescribed. This treatment has previously been shown to be more effective than topical or oral 5-ASA alone in this cohort (Bressler et al., 2015, Marteau et al., 2005). While majority of patients typically respond to treatment within two weeks, it can take up to eight weeks to achieve symptomatic remission in some patients (Bressler et al., 2015). In patients that achieve remission, it is recommended that patients continue on the same treatment to maintain remission. For patients that are treatment non-responsive, it is recommended that they are prescribed oral corticosteroids, such as prednisolone, to induce remission. Patients should see a reduction in symptoms within two weeks. Once a response has been observed, the dosage of corticosteroids is tapered down as they are unsuitable for long-term use (Kornbluth et al., 2010, Dignass et al., 2012). In patients that achieve remission, 5-ASA can be prescribed to those that have not previously been treated with 5-ASA. In patients that have poor prognosis or did not achieve remission, it is recommended that they are treated with biologics such as anti-TNF-α or anti-integrin (Bressler et al., 2015).

Patients with either moderate to severe disease, or extensive colitis should be treated initially with corticosteroids. If the patient is treatment non-responsive then they should be treated with biologics, either anti-TNF-α or anti-integrin. Anti-TNF-α drugs include infliximab and adalimumab and are effective for both inducing and maintaining remission in patients with extensive colitis (Rutgeerts et al., 2005). Additionally, anti-integrin drugs include vedolizumab and have been shown to be effective in this cohort of patients (Colombel et al.,

2017). Once remission has been achieved, it is recommended that patients continue on the same medication to maintain remission (Dignass et al., 2012).

While improved in therapeutic options has reduced the number of patients with UC requiring surgery, is still recommended for patients that are treatment non-responsive. Indications that surgery is required include extreme side-effects to biologics, perforation, uncontrollable haemorrhage and CAC. Approximately 10% of patients will undergo surgery within a year post-diagnosis, and 30% will undergo surgery in their lifetime (Gallo et al., 2018). For majority of patients, a restorative proctocolectomy with ileal pouch-anal anastomosis is recommended.

Regardless of treatment, it is essential that patients with UC are monitored frequently to ensure treatment is still effective. Once patients are in remission, their disease activity should be monitored through non-invasive biomarkers such as faecal calprotectin, to allow early therapeutic intervention if necessary. Additionally, eight years post-diagnosis patients should start have regular colonoscopies every one – two years to monitor for the progression to CAC (Kornbluth et al., 2010).

1.1.7 Colitis associated colorectal cancer

Patients with UC are at increased risk of developing colitis associated colorectal cancer (CAC). While CAC only accounts for 1-2% of colorectal cancer (CRC) cases annually, it is the cause of death in approximately 10-15% of patients with UC (Maryńczak et al., 2022). The risk of developing CAC has been linked to a previous family history of CRC, along with increased duration, extent and severity of inflammation associated with UC (Kameyama et al., 2018) (Bocchetti et al., 2021). As the incidence and prevalence of UC is rising globally, it is expected that CAC cases will also increase (Le Berre et al., 2023).

In UC, the colonic epithelium is persistently exposed to cycles of chronic inflammation, followed by the regeneration of the epithelium and then its subsequent repair. Over a prolonged period of time, this can cause irreparable tissue damage and DNA mutations. In CAC, inflammation is the primary driver of disease progression. This is further propelled by the genetic, environmental and immunological factors that contribute to UC (Zhou et al., 2023b). This enables CAC to develop through a multistep process that differs significantly

from sporadic CRC. In CAC, the colonic epithelium undergoes numerous molecular and histological changes as the disease progresses through advancing stages of dysplasia and eventually the development of a carcinoma. However, CRC follows an adenoma to adenocarcinoma process (**Figure 7 A + B**) (Nguyen et al., 2020, Low et al., 2014).

Whilst similar genetic changes are found in both sporadic CRC and CAC, the stage at which they occur differs. For instance, the loss of the *APC* gene occurs early in sporadic CRC due to the continuous activation of WNT/ β-Catenin signalling. However, the loss of function for *APC* occurs late in CAC progression (Zhao et al., 2022a). In contrast, the opposite has been reported for *p53* mutations, which occur early in the inflammatory driven CAC process but late in the progression of CRC. It has also been reported that KRAS mutations occur less frequently in CAC than CRC (**Figure 7 A + B**) (Robles et al., 2016).

CAC and sporadic CRC further differ in their clinical presentation. Sporadic CRC is typically visible as a polyp during a colonoscopy. In contrast, dysplastic areas in CAC are normally flat with indistinct margins, which makes them difficult to detect. CAC is normally diagnosed at a later stage than CRC, which is potentially due to difficulties in identifying dysplastic regions (**Figure 7 C - E**) (Baker et al., 2019).

1.1.8 Risk factors for the development of Colitis associated colorectal cancer

Among UC patients, increased duration and extent of disease are the biggest risk factors for the development of CAC. Following UC diagnosis, the risk of developing CAC increases by 2% after ten years, 8% after twenty years and 18% after thirty years compared to the general population (Bocchetti et al., 2021). Additionally, patients diagnosed with pancolitis have a high risk of developing CAC and those diagnosed with left-sided colitis are moderately at risk (Zhou et al., 2019). In patients with UC, a previous family history of CRC also increases the risk of developing CAC. This is approximately an 8-fold increase if a first degree relative (Samadder et al., 2019). Treatment options for UC can also impact the development of CAC, with patients who received 5-ASA at reduced risk. Furthermore, patients that had regular colonoscopies were less likely to be diagnosed at a later stage of disease (Wijnands et al., 2021).

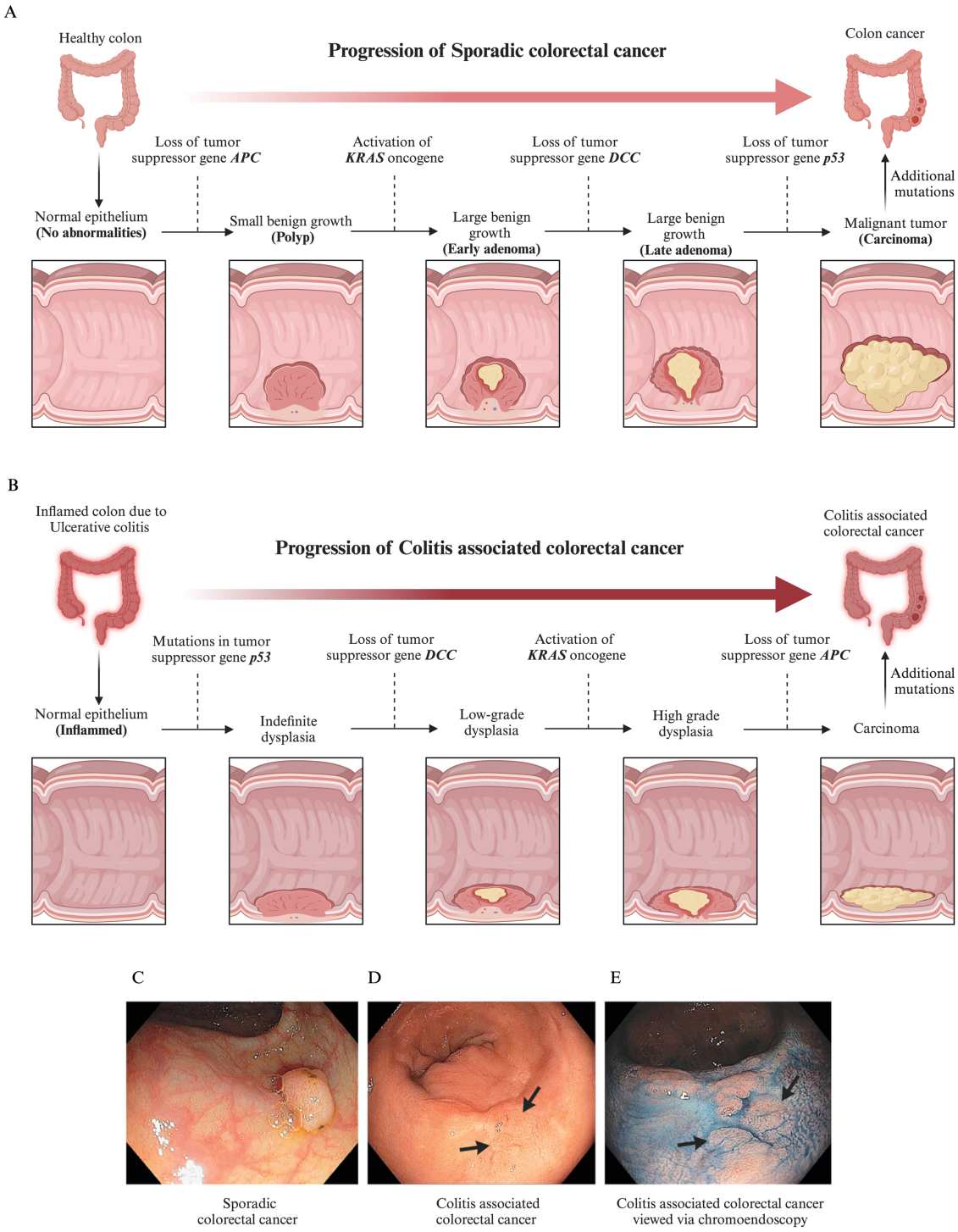


Figure 7. *Differences in the progression of Sporadic colorectal cancer and Colitis associated colorectal cancer.*

The sequence of events leading to the development of CRC and CAC are different. **A.** Sporadic CRC follows and adenoma to adenocarcinoma sequence. **B.** CAC develops in a multistep process from UC associated inflammation to dysplasia to carcinoma. Endoscopic image of **C.** Sporadic CRC; **D.** CAC and **E.** CAC viewed via chromoendoscopy. **A + B** Adapted from 'The Multi-Hit Model of Colorectal Cancer' on BioRender.com, originally published in (Campbell et al., 2017); **C - E** Images taken from (Beaugerie and Itzkowitz, 2015).

1.1.9 Detection of Colitis associated colorectal cancer

To ensure early detection of CAC, it is recommended that patients with UC undergo regular colonoscopy. While guidelines differ between countries, it is generally recommended that regular colonoscopies are initiated 8 – 10 years post UC diagnosis to determine the extent of disease (Gu et al., 2016, Cairns et al., 2010). Following this, it is recommended that a colonoscopy is performed every 1-2 years, until 30 years post-UC diagnosis when it should be performed yearly (Guagnozzi, 2012).

Due to technological advancements, the technology used for the detection of CAC is continuously improving. Previously, detection relied on white-light technologies, with biopsies being taken every 10cm (Zhen et al., 2018). Due to the flat nature of CAC dysplasia, detection can be difficult. Recently, high-definition white light endoscopy and chromoendoscopy technologies have been developed. These have since been shown to have a better detection rate of dysplasia than previous methods and are currently recommended for the surveillance of CAC (Choi et al., 2015, Zhen et al., 2018).

1.1.10 Treatment of Colitis associated colorectal cancer

If dysplasia is detected via colonoscopy, it is recommended that the sample is analysed by a second pathologist. This is due to the difficultly in distinguishing between indefinitive dysplasia and low-grade dysplasia, in chronically inflamed tissues (Wijnands et al., 2021). If low-grade dysplasia has been detected there is a 9-fold risk of developing CAC (Thomas et al., 2007).

Whilst it was previously recommended that a proctocolectomy should be performed if dysplasia at any grade was detected, endoscopic resection is now performed when possible. This decision is made on the basis of the modified Montreal classification system (Laine et al., 2015). If the affected area can be removed, the method chosen depends on the area affected, the surrounding mucosal tissue, the size of the area affected, the shape of the area and its surface (Adamina et al., 2021). However, for patients that have high-grade dysplasia and additional risk factors for CAC, a total proctocolectomy can also be considered based on the patient's preference.

As CAC is an inflammatory driven disease, constraining inflammation and promoting mucosal healing is key to preventing the progression of CAC and the need for a colectomy. This is achieved through the same treatments used in the treatment of UC, as discussed in section 1.1.6. Of these, 5-ASA has been shown to reduce the risk of developing CAC (Qiu et al., 2017, Clapper et al., 2008). This is achieved through reduced inflammation, oxidative stress and proliferation. Additionally, 5-ASA targets Wnt/β-catenin, NF-κB, p38 and EGF signalling pathways, which are all involved in the development of CAC (Qu et al., 2017, Dixon et al., 2021, Nardone et al., 2023). Similarly, anti-TNF-α treatment for UC is associated with decreased risk of developing CAC, by limiting inflammation and promoting mucosal healing (Alkhayyat et al., 2021).

1.1.11 The inflammatory microenvironment of Colitis associated colorectal cancer

The chronic inflammation associated with UC gives rise to an inflammatory microenvironment consisting of an abundance of immune cells and inflammatory mediators. These collectively contribute to DNA damage, tissue destruction and dysregulation of the immune system, that aids the initiation of CAC. However, as CAC progresses it can give rise to an immunosuppressive tumour microenvironment (TME) that limits protective anti-tumour immune responses (Yin et al., 2023, Wang et al., 2020b).

Myeloid cells are among the most abundant cells that infiltrate into the colon during UC and are key to the progression to CAC (Yang et al., 2021a). During UC, infiltrating monocytes differentiate into pro-inflammatory macrophage, creating a chronic inflammatory microenvironment (Liao et al., 2024). However, prolonged exposure to excessive inflammation enables the differentiation of macrophage into tumour associated macrophage (TAM). These TAMs have the ability to create an immunosuppressive TME, that limits the detection and removal of cancerous cells whilst promoting tumour progression and metastasis (Lin et al., 2019). TAMs promote tumour growth through the production of anti-inflammatory cytokines including IL-10, TGF-β, IL-13 and EGF. Collectively, these regulate the recruitment of monocytes and there subsequent differentiation, promoting an anti-inflammatory macrophage phenotype to sustain an immunosuppressive TME (Pan et al., 2020). EGF is central to this process, and disruption of its signalling reduces the abundance of TAMs and improved prognosis in a mouse model of CAC (Zhang et al., 2016).

TAMs also modulate the TME by altering the function T-cells. TAMs promote the recruitment of $CD4^+$ Tregs via the secretion of CCL22 (Curiel et al., 2004). This is immunosuppressive as $CD4^+$ Treg cells produce IL-10 and TGF-β, which alters the function of $CD8^+$ T-cells, natural killer cells and dentric cells (Workman et al., 2009). Treg cells also express the programmed cell death protein 1(PD-1). TAMs also modulate T-cell function through expression of the programmed cell death ligands (PDL), PD-L1 and PD-L2. These bind to the programmed cell death protein 1(PD-1), which results in further expression of PD-1 from T-cells eventually resulting in T-cell exhaustion (Quaranta and Schmid, 2019). Targeting the PD-L1/PD-L2 is currently under investigation as prognostic markers and for the treatment of disease. In UC, CRC and CAC, the expression of PD-L1/PD-L2 correlates with poor prognosis and severe disease (Rajabian et al., 2019, Zengin et al., 2021, Yassin et al., 2019). Recently, microRNAs (miRNAs) have been proposed as a method to alter the expression of TAMs and the expression of PD-L1/PD-L2 to promote anti-tumour immune responses (Zhou et al., 2022, Skafi et al., 2020).

1.1.12 MicroRNAs

miRNAs were initially discovered in 1993 (Lee et al., 1993, Wightman et al., 1993). Since then, over 2300 miRNAs have been identified in humans, accounting for approximately 1-5% of the human genome (Macfarlane and Murphy, 2010, Alles et al., 2019). These are small non-coding RNAs that are approximately 22 nucleotides in length. They are critical for the regulation of numerous biological processes and are estimated to target 30% of the human genome (Kilic et al., 2018). Furthermore, their aberrant expression is associated with many diseases including UC and CAC (Yarani et al., 2022). Due to their diverse functions, the restoration of dysregulated miRNA circuits is of interest clinically.

1.1.13 Biogenesis of miRNAs

The biogenesis of miRNA is a multistep process that can be further divided into the canonical and non-canonical pathways. miRNAs are predominantly synthesised and elect their functions through the canonical pathway. In this method, primary miRNA (pri-miRNA) transcripts are first transcribed from their genes. These transcripts are processed

by a microprocessor complex that consists of Drosha, a ribonuclease III enzyme that is bound to DGCR8. This releases a precursor miRNA (pre-miRNA) that is exported from the nucleus to the cytoplasm by exportin 5 (XPO5). Here, the pre-miRNA is processed by another ribonuclease III enzyme, Dicer, and a trans-activator RNA binding protein (TRBP) which produces a mature miRNA duplex. This duplex interacts with members of the argonaute (AGO) family to form an RNA-induced silencing complex (RISC) complex. Based on environmental ques, the miRNA duplex is unwound, and one strand is retained, the other passenger strand is degraded. The retained, mature miRNA strand has the ability to regulate gene expression by binding to the 3′ untranslated region (3′ UTR) of target messenger RNAs (mRNA). When this binding is complementary the mRNA is degraded, whereas imperfect pairing suppresses the expression of the target mRNA (**Figure 8**). Non-canonical pathways of miRNA synthesis have also been identified, including drosha/DGCR8-independent or dicer-independent pathways (Yang and Lai, 2011).

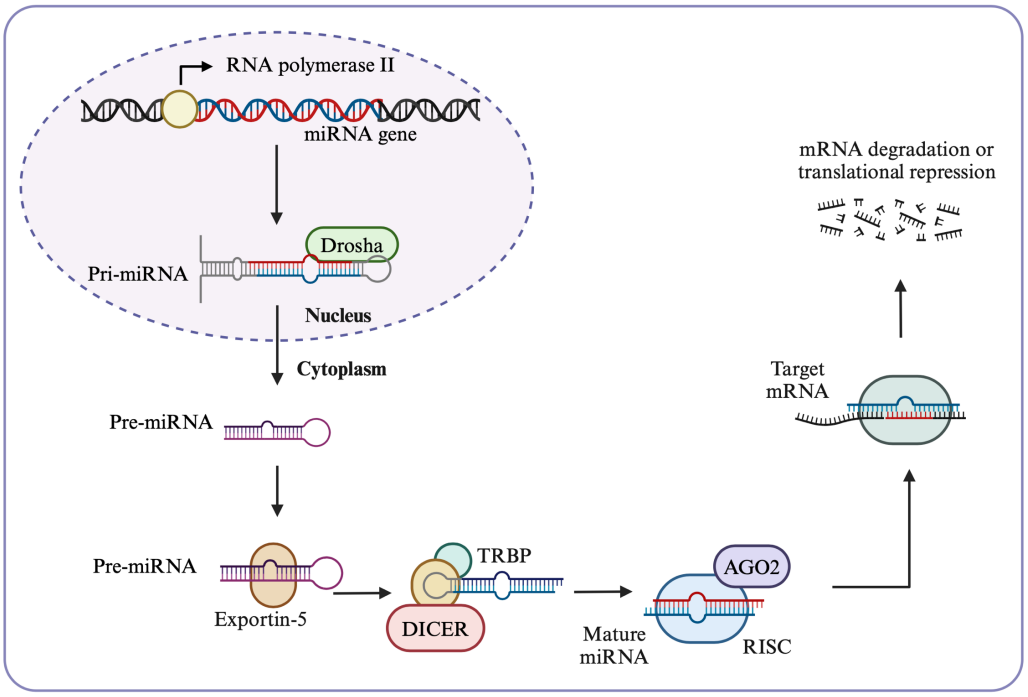


Figure 8. *Canonical biogenesis of miRNAs.*

Pri-miRNA is transcribed. This is then processed by drosha, to produce pre-miRNA. Pri-miRNA is exported into the cytoplasm by exportin-5. Pri-miRNA is further processed by dicer to produce a mature miRNA duplex. The miRNA duplex binds with argonaute to form the RISC complex. One strand of the miRNA duplex is retained and then subsequently targets mRNAs. Complementry binding to mRNAs results in mRNA degradation, partial binding suppresses its expression. Created on BioRender.com.

1.1.14 Diagnostic and therapeutic potential of miRNAs

miRNAs have been proposed as diagnostic and prognostic markers for many diseases, including UC and CAC (Zhou et al., 2021, Bocchetti et al., 2021). This is primarily due to their key role in the regulation of many biological processes. Additionally, miRNAs can be detected from various bodily fluids including serum, plasma, urine and saliva. This is beneficial as miRNA biomarkers could be used as non-invasive alternatives for the diagnosis of disease or as a marker of disease activity (Lamprou et al., 2023). Furthermore, miRNAs have a high stability which further aids their detection (Ye et al., 2019).

As they are key regulators of gene expression, the modulation of miRNA expression has recently been proposed as an alternative therapeutic approach for the treatment of UC and CAC (Innocenti et al., 2023, Grillo et al., 2021). This method is based on the use of synthetic molecules that mimic a specific miRNA in both sequence and function. This enables a targeted approach for the treatment of disease by either restoring the function of a miRNA or inhibiting abnormally expressed miRNAs (Menon et al., 2022). Using this approach, systemic addition of *miR-26a* in a mouse model of hepatocellular carcinoma reduced proliferation and provided protection against the disease (Kota et al., 2009). Other miRNA mimics have been developed for the *let-7* miRNA, which reduced tumour formation *in vivo* in a lung cancer model (Esquela-Kerscher et al., 2008). Similar results were seen with the application of a *miR-34* mimic (Trang et al., 2011). In the context of UC, the suppression of *miR-115, miR-31* and *miR-423* have all reduced disease in a DSS model (Shi et al., 2017, Wang et al., 2020a, Zhu et al., 2020a). Furthermore, the use of antagomirs to suppress *miR-214* reduced the development of UC and CAC (Polytarchou et al., 2015). However, miRNA therapeutics are still in the early stages of development. The delivery to the target tissue, with minimal toxicity and high efficiency remains a problem.

1.1.15 miRNAs in Ulcerative colitis and Colitis associated colorectal cancer

UC and CAC both develop due to the presence of chronic inflammation an altered immune response and the upregulation of pro-inflammatory signalling pathways (Suszynska et al., 2024, Ungaro et al., 2017). miRNAs regulate each of these processes and their dysregulation has been identified in both UC and CAC.

In UC, *miR-146a* is down regulated and negatively correlates with disease severity in patients (Feng et al., 2020b). However, the restoration of its expression via a miRNA mimic improved colonic inflammation by increasing NF-κB expression (Nata et al., 2013). In contrast, the overexpression of *miR-155* is associated with severe epithelial damage in the colon through the IL-23/IL-17/IL-6 signalling axis. Additional miRNAs implicated in UC include *miR-182-5p, miR-29, miR-124, miR-141* and *miR-21* (Tang et al., 2021b, Guo et al., 2021)

miRNAs also have the ability to regulate the hallmarks of cancer (**Figure 9**) (Larrea et al., 2016, Peng and Croce, 2016). Dysregulated miRNAs are classified into either oncomiRs or tumour suppressors. When a oncomiR is upregulated, its downstream targets are suppressed. In contrast, if a miRNA is suppressed, its targets which are often oncogenes are overexpressed (Zhang et al., 2007). However, due to the complexity of miRNAs, their function as either a tumour promotor or suppressor varieties between different tissues (Otmani and Lewalle, 2021).

In CAC, several miRNAs have been identified as being dysregulated. For instance, *miR-21* expression correlates with enhanced proliferation and migration. This effect was reduced in an AOM/DSS model using *miR-21*$^{-/-}$ mice, associated with a reduced expression of pro-inflammatory cytokines and decreased tumour burden (Shi et al., 2016). *miR-214* is also upregulated in mucosal biopsies from patients with CAC and its expression correlated with disease severity (Polytarchou et al., 2015). Similarly, *miR-222* is overexpressed in the AOM/DSS model of CAC, and its downregulation reduced inflammation and oxidative stress that damages the epithelial barrier (Wang et al., 2023).

In comparison, miRNAs that act as suppressors in CAC include *miR-320*, *miR-34* and *miR-146a* (Zhu et al., 2020a, Rokavec et al., 2014, Garo et al., 2021). *miR-320* is decreased in AOM/DSS mice, but delivery of a miRNA mimic for *miR-320* reduced colonic inflammation and tumour burden. Furthermore, proliferation and migration were also inhibited (Wu et al., 2022b). *miR-34* is also protective in CAC as prevents epithelial-to-mesenchymal transition (Rokavec et al., 2014). Finally, *miR-146a* inhibits chronic inflammation and tumorigenesis by altering IL-17 signalling (Garo et al., 2021).

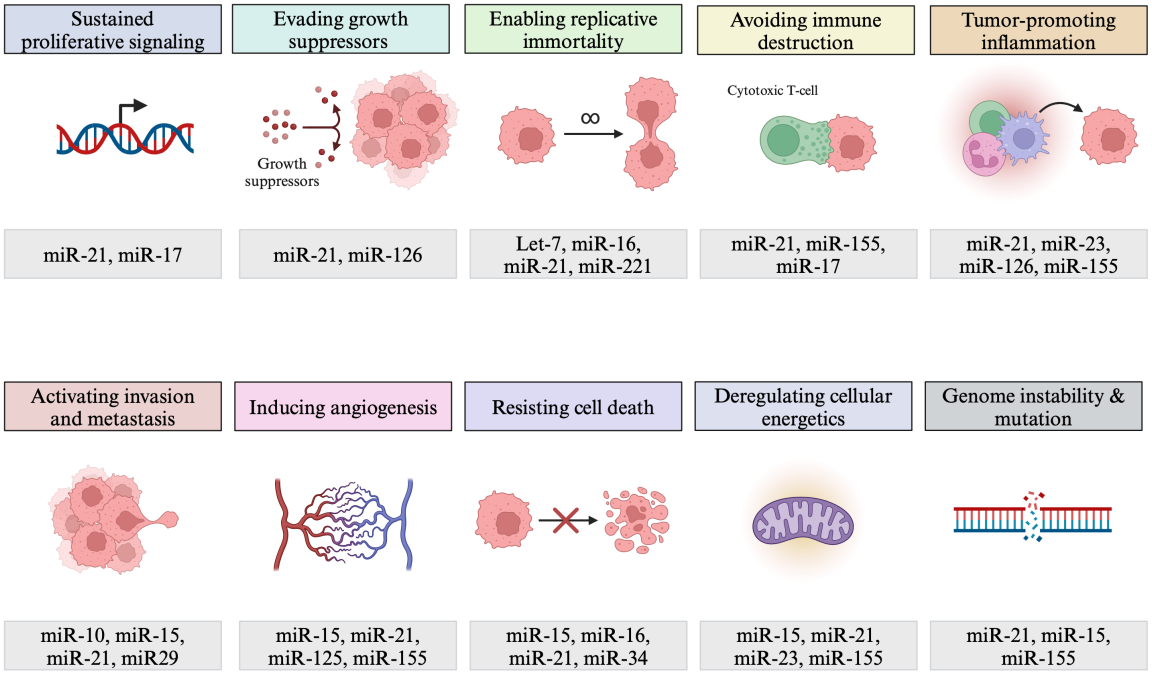


Figure 9. *miRNAs implicated in the hallmarks of cancer.*

miRNAs have the ability regulate the hallmarks of cancer. Some of these miRNA include l*et-7, miR-21, miR-17, miR-126, miR-16, miR221, miR-155, miR-10, miR-29, miR-15* and *miR-34.* Diagram adapted from 'Hallmarks of Cancer' on BioRender.com which was originally published in (Hanahan and Weinberg, 2011b) and information relating to the involvement of miRNAs in the hallmarks of cancer was obtained from (Larrea et al., 2016).

1.1.16 *miR-223* a critical regulator of myeloid cells

miR-223, is a highly conserved hematopoietic miRNA that is critical for the development and function of myeloid cells. This miRNA was first identified in 2003 and is located on the X chromosome (Johnnidis et al., 2008, Fukao et al., 2007). Among its many biological functions is immune regulation and hematopoiesis. The expression of *miR-223* is promoted by myeloid transcription factors that bind to its promotor including PU.1, CCAAT-enhancer-binding proteins (C/EBP)-α and C/EBP-ß to increase *miR-223* expression. In contrast, myocyte enhancer factor 2C (Mefc), nuclear factor I A (NFIA) and Kruppel-like factor 6 (KLF6) inhibit *miR-223* expression through binding to its promotor region (Yuan et al., 2021). Of these transcription factors NFIA and C/EBPβ are targets of *miR-223*, which creates a negative feedback loop between the expression of *miR-223* and its transcription factors (Sun et al., 2010, Fazi et al., 2005). *miR-223* is highly expressed in the myeloid

compartment and its expression is induced during myeloid differentiation (Yuan et al., 2018). As an anti-inflammatory miRNA, *miR-223* is critical in the activation and regulation of immune cells in order to direct the immune response.

miR-223 is a key regulator of neutrophil chemotaxis and activation. This is particularly important as neutrophils are essential regulators of the innate immune system during the early stages of inflammation (Johnnidis et al., 2008). Through targeting the NLRP3 inflammasome, *miR-223* reduced the expression of IL-1β and inflammation (Neudecker et al., 2017b, Bauernfeind et al., 2012). Additionally, *miR-223*$^{-/y}$ have an increased abundance of neutrophils, which promote a pro-inflammatory response that contributes to tissue damage (Johnnidis et al., 2008, Yuan et al., 2018).

To further regulate the immune response, *miR-223* has the ability to regulate the polarization and activation of macrophage. *miR-223* has the ability to promote the production of anti-inflammatory macrophage. This is primarily achieved through its binding targets. For example, *miR-223* binding to TNF receptor-associated Factor 6 (TRAF 6) limits inflammation through NF-κB signalling (Wang et al., 2023). Similarly, binding to STAT3 reduces the production of pro-inflammatory cytokines downstream of its signalling pathway (Zhang et al., 2021a). In contrast, *miR-223* has also been linked to the production of pro-inflammatory macrophage. In this process, STAT3 binds to the promotor region of *miR-223* to down regulate its expression. As a consequence, there is increased expression of the pro-inflammatory marker IL-6 and IL-1β (Chen et al., 2012). Furthermore, low expression of *miR-223* enables the synthesis of the Ras homolog gene family member B (RhoB). Downstream this increases NF-κB and MAPK signalling pathways, promoting a pro-inflammatory macrophage phenotype and the secretion of their associated cytokines (Yan et al., 2019).

However, the altered expression of *miR-223* has been identified in multiple inflammatory diseases including UC, Rheumatoid arthritis, Acute lung injury and Enteritis (Neudecker et al., 2017b, Zhang et al., 2021c, He et al., 2022, Huang et al., 2022). Further highlighting its role as a critical regulator, the downregulation of *miR-223* is associated with increased disease severity and poor patient prognosis in many cancers including lung, hepatocellular, colorectal and breast cancer (Gong et al., 2013, Nian et al., 2013, Dong et al., 2017, Li et al., 2014).

1.1.17 Models to investigate the role of *miR-223* in Ulcerative colitis and Colitis associated colorectal cancer

Several models have been developed to investigate the pathogenesis of both UC and CAC. UC is primarily mimicked in mice through the administration of dextran sulfate sodium (DSS), this damages epithelial cells in the colon which results in inflammation and the formation of ulcers (Wen et al., 2024). Repeated cycles of DSS, followed by a recovery period, where DSS is withdrawn mimics the inflammatory cycle that is typically seen in patients with UC (Gelmez et al., 2022). This model has been modified to investigate CAC, this includes an injection of azoxymethane (AOM) three days prior to the administration of DSS. AOM is a carcinogen that induces O^6 methylguanine adducts in DNA which causes G→A transitions. The administration of AOM/DSS to mice is currently the most frequently used and accurate method of modelling CAC (Sun et al., 2023, Parang et al., 2016).

To investigate the role of *miR-223* in diseases, *miR-223* knockout mice have been developed. In this strain, the 110 base pair coding region for *miR-223* on the X chromosome has been replaced with *frt*-flanked neomycin (neo) resistance cassette that prevents the function of the *miR-223* gene (Johnnidis et al., 2008). Thus, these mice have previously been used to investigate the role of *miR-223* in both UC and CAC (Neudecker et al., 2017b, Flynn et al., 2024). While the use of DSS and AOM/DSS in mice remains the most frequently used method to mimic UC and CAC, the primary limitation of both models is the human immune system cannot be fully recapitulated.

While cell lines are commercially available for studying the development of sporadic CRC, these are not always suitable for studying CAC due to key differences in the development of the diseases as previously discussed in section 1.1.7. To address this, colonic organoids are increasingly being utilised to model CAC. Organoids have the ability to self-assemble from stem cells into three dimensional structures that are similar in both structure and function to the organ the stem cells originated from (Liu et al., 2024). As such, the use of organoids to investigate the pathogenesis of disease is increase, including UC and CAC (Liu et al., 2024, DeHaan et al., 2020).

THESIS HYPOTHESIS AND AIMS

The hypothesis of this thesis is that *miR-223* is critical for limiting myeloid driven inflammation in Ulcerative colitis and the continuum to Colitis-associated colorectal cancer.

Specific aims of the project are:

Aim 1: Define the expression profile of *miR-223* and its correlation to inflammatory-clinical phenotypes in samples from patients with Ulcerative Colitis.

Aim 2: Elucidate the mechanisms of how *miR-223* regulates the development of CAC, using samples generated from *in vivo* models of colitis-associated colon cancer (AOM-DSS) in *miR-223*$^{-/y}$ mice.

Aim 3: Identify how *miR-223* in macrophage regulates intestinal epithelial stemness versus DNA-damage responses *in vitro* using 3D colonic organoids.

CHAPTER 2 MATERIALS AND METHODS

MATERIALS

Table 1. *Animals and cell lines.*

Product	Catalog Number	Company
264.7 RAWs	91062702	Sigma
Lentiviral miR-223KD 264.7 RAWs	N/A	N/A
Lentiviral miR-223OE 264.7 RAWs	N/A	N/A
Lentiviral negative control 264.7 RAWs	N/A	N/A
Mouse colon organoids	N/A	N/A
C57BL/6J mice (male and female)	000664	The Jackson Laboratory
CD45.1 Congenic CD57BL/6J (male and female)	Strain #:002014	The Jackson Laboratory
miR-223-/y mice on a C57BL/6J background (male and female)	N/A	Provided by V. Dawson (Johns Hopkins University, Baltimore, MD)

Table 2. *TaqMan Primers.*

TaqMan primers		
Target	**Catalog number**	**Company**
18S	Hs99999901_a1	Applied Biosystems by Thermo FisherScientific
Acida (AID)	Mm01184115_m1	Applied Biosystems by Thermo FisherScientific
Arg1	Mm00475988_m1	Applied Biosystems by Thermo FisherScientific
CCL17	Mm01244826_m1	Applied Biosystems by Thermo FisherScientific
Ccl2	Mm00441242_m1	Applied Biosystems by Thermo FisherScientific
CCL22	Mm00436439_m1	Applied Biosystems by Thermo FisherScientific
Ccl7	Mm00443113_m1	Applied Biosystems by Thermo FisherScientific
Chil3	Mm00657889_m1	Applied Biosystems by Thermo FisherScientific
Csf1	Mm00432686_m1	Applied Biosystems by Thermo FisherScientific
Csf2	Mm01290062_m1	Applied Biosystems by Thermo FisherScientific
Cxcl1	Mm04207460_m1	Applied Biosystems by Thermo FisherScientific

Cxcl2	Mm00436450_m1	Applied Biosystems by Thermo FisherScientific
Il-11	Mm00434162_m1	Applied Biosystems by Thermo FisherScientific
IL-13	Mm00434204_m1	Applied Biosystems by Thermo FisherScientific
Il-17a	Mm00439618_m1	Applied Biosystems by Thermo FisherScientific
Il-17f	Mm00521423_m1	Applied Biosystems by Thermo FisherScientific
Il-1b	Mm00434228_m1	Applied Biosystems by Thermo FisherScientific
Il-1rn	Mm00446186_m1	Applied Biosystems by Thermo FisherScientific
IL-21	Mm00517640_m1	Applied Biosystems by Thermo FisherScientific
IL-22	Mm01226722_m1	Applied Biosystems by Thermo FisherScientific
Il-4	Mm00445259_m1	Applied Biosystems by Thermo FisherScientific
Il-6	Mm00446190_m1	Applied Biosystems by Thermo FisherScientific
Irf4	Mm00516431_m1	Applied Biosystems by Thermo FisherScientific
Irf5	Mm00496477_m1	Applied Biosystems by Thermo FisherScientific
Lgr5	Mm00448890_m1	Applied Biosystems by Thermo FisherScientific
Lif	Mm00434762_m1	Applied Biosystems by Thermo FisherScientific
Ly6A	Mm00726565_m1	Applied Biosystems by Thermo FisherScientific
Nos2	Mm00440502_m1	Applied Biosystems by Thermo FisherScientific
H2a.x	Mm00515990_m1	Applied Biosystems by Thermo FisherScientific
Olfm4	Mm01320260_m1	Applied Biosystems by Thermo FisherScientific
Relna	Mm00445109_m1	Applied Biosystems by Thermo FisherScientific
S100A8	Mm00496696_g1	Applied Biosystems by Thermo FisherScientific
Sprr1a	Mm01962902_s1	Applied Biosystems by Thermo FisherScientific
Tacstd2	Mm00498401_s1	Applied Biosystems by Thermo FisherScientific
Tgf-b1	Mm00441727_m1	Applied Biosystems by Thermo FisherScientific
Tnf	Mm00443258_m1	Applied Biosystems by Thermo FisherScientific
Vegfa	Mm00437306_m1	Applied Biosystems by Thermo FisherScientific
Vegfc	Mm00437310_m1	Applied Biosystems by Thermo FisherScientific

Table 3. *SyberGreen Primers.*

SyberGreen primers		
Target	**Catalog Number**	**Company**
Has-miR-223-3p	YP00205986	miRCURY miRNA Assay by Qiagen
U6 snRNA	YP00203907	miRCURY miRNA Assay by Qiagen
Hs_IL6_1_SG	QT00083720	QuantiTect Primer Assay by Qiagen
HS_IL11_1_SG	QT00074088	QuantiTect Primer Assay by Qiagen
HS_CCL2_1_SG	QT00212730	QuantiTect Primer Assay by Qiagen
HS_CXCL8_1_SG	QT00000322	QuantiTect Primer Assay by Qiagen
Hs_IL1B_1_SG	QT00021385	QuantiTect Primer Assay by Qiagen
Hs_TNF_1_SG	QT00029162	QuantiTect Primer Assay by Qiagen
Hs_NOS2_1_SG	QT00068740	QuantiTect Primer Assay by Qiagen
Hs_OSM_1_SG	QT00209286	QuantiTect Primer Assay by Qiagen
Hs_MUC2_2_SG	QT01004675	QuantiTect Primer Assay by Qiagen
Hs_TREM1_1_SG	QT00046284	QuantiTect Primer Assay by Qiagen
Hs_LCN2_1_SG	QT00028098	QuantiTect Primer Assay by Qiagen
Hs_CSF1_1_SG	QT00035224	QuantiTect Primer Assay by Qiagen
Hs_MMP3_1_SG	QT00060025	QuantiTect Primer Assay by Qiagen
Hs_REG3G_1_SG	QT01030596	QuantiTect Primer Assay by Qiagen
Hs_S100A8_1_SG	QT00226121	QuantiTect Primer Assay by Qiagen
Hs_Col4A1_1_SG	QT00005250	QuantiTect Primer Assay by Qiagen
Hs_RRN18S_1_SG	QT00199367	QuantiTect Primer Assay by Qiagen
Hs_HPRT1_1_SG	QT00059066	QuantiTect Primer Assay by Qiagen

Table 4. *Antibodies.*

Target	Catalog Number	Company
Anti-puromycin (12D10)	MABE343	Sigma
β-Actin (AC-15)	A1978	Sigma
β-Actin (C4)	Sc-1616	Santa Cruz
β-Catenin (Clone 14)	610154	BD Biosciences
C-myc (E5Q6W)	17583	Cell Signalling
CD68 (E307V)	97778	Cell Signalling
CCR2	Ab273050	Abcam
Cyclin D1 (E3p5S)	55506	Cell Signalling
E-Cadherin (Clone 36)	610182	BD Biosciences
Goat anti-rabbit IgG	Ab205718	Abcam
Goat anti-mouse IgG	AP308P	Millipore
IRF5 (E9I4Z)	96527	Cell Signalling
Ly6G (E6Z1T)	87048	Cell Signalling
N-Cadherin (D4R1H)	13116	Cell Signalling
NF-kB p65 (D14E12)	8242	Cell Signalling
NOS2 (D6B6S)	13120	Cell Signalling
Phospho-akt (Ser473) (D9E)	4060	Cell Signalling
Phospho-β-Catenin (S33/37/T41)	9561	Cell Signalling
Phospho-β-Catenin (S552) (D8E11)	5651	Cell Signalling
Phospho-histone H2A.X (Ser139) (20E3)	9718	Cell Signalling
Phospho-Jak 2 (Tyr1008) (D4A8)	8082	Cell Signalling
Phospho-JNK (Thr183/Tyr185)	9255	Cell Signalling
Phospho-p38 (Thr180/Tyr182) (D3F9)	4511	Cell signalling
Phospho-S6 ribosomal protein (Ser235/236)	4858	Cell Signalling
Phospho-stat1 (Tyr701) (58D6)	9167	Cell Signalling
Phospho-p44/42 MAPK (Erk1/2) (Thr202/Tyr204)	9101	Cell Signalling

Phospho-stat3 (Tyr705) (D3A7)	9145	Cell Signalling
Total-STAT3 antibody (EPR787Y)	Ab68153	Abcam
PCNA (D3H8P)	13110	Cell Signalling
s-nitrotyrosine (39B6)	ab61392	Abcam
TGF-alpha	ab9585	Abcam
TGF-alpha (MF9)	nbp2-34296	Novus
Tubulin	T2200	Sigma

Table 5. *Commercial kits.*

Name	Catalog Number	Company
EasyPure RNA kit	ER101-01	TransGen Biotech
Elite ABC Kit	PK-7200	Vector Laboratories
ImmPact NovaRed Substrate Kit	SK-4805	Vector Laboratories
PaxGene Blood RNA Kit	763134	PreAnalyticX
Pierce BCA protein assay kit	23227	Thermo scientific
RNeasy Kit	74034	Qiagen

Table 6. *Reagents.*

Name	Catalog Number	Company
1400W	HY-18731	MedChemExpress
2-Mercaptoethanol	M3148	Sigma
4x Laemmelli sample buffer	1610747	BioRad
2-Propanol	I9516	Sigma
Ammonium persulfate (APS)	A3678	Sigma Aldrich
AMG 548	3920	Tocris
ACK Lysing Buffer	A1049201	ThermoFisher
Antigen unmasking solution	H-3300	Vector Laboratories
Bay 11-7085	1743	Tocris
Bovine serum albumin	A3733	Sigma
Blockall blocking solution	SP-6000	Sigma

Chloroform	J67241	Alfa Aesar
Cyrostor	7959	Stemcell
Cycloheximide	C4859	Sigma
DEA/NO	D184	Sigma
DPX Mounting Media	06522	Sigma
DMEM Media	41965039	Fisher Scientific
DMEM/F12 with 15mM HEPES	36254	StemCell
DMSO	D2650	Sigma
D-PBS	37350	Stem Cell
Ethanol	32221	Honeywell
Fetal Bovine Serum (FBS)	F9665	Sigma
FR180204	HY-12275	MedChemExpress
Glycine	G8898	Sigma Aldrich
Gentle cell dissociation reagent	7174	Stem Cell
Greiss Reagent	AB234044	Abcam
Halt Protease Inhibitor Cocktail	87786	ThermoFisher
Hydrochloric Acid	H1758	Sigma
IFN-γ	AF-315-05	PeproTech
LPS	L5293	Sigma
ImmEdge Pen	H-4000	Vector Laboratories
Intesticult Organoid Growth Media	6000	Stem Cell
Intesticult Organoid Growth Media Supplement 1	6002	Stem Cell
Intesticult Organoid Growth Media Supplement 2	6003	Stem Cell
JSH-23	J4455	Sigma
Mayers Haematoxylin Solution	MHS32	Sigma
Matrigel	356231	Corning
Methanol	34860	Sigma
N, N, N', N'-Tetramethyl-ethylenediamine	T9281	Sigma

Non-fat-dried milk bovine	3033922	Marvel
Nuclease-free water	129114	Qiagen
PageRuler Prestained Ladder	26619	ThermoFisher
Phosphate Buffered Saline Tablets	BR0014G	Oxoid
Ponceau solution	P7170	Sigma
Protease inhibitor cocktail	Ab271306	Abcam
Protein ladder	26618	Thermo scientific
Puromycin	Sigma	P9620
Sp600125	HY-12041	MecChem Express
Protogel 30% acrylamide	EC-890	National Diagnostics
Penicillin-Streptomycin	P43333	Sigma
RIPA buffer	R0278	Sigma
RNaseZap	R2020	Sigma
Ruxolitinib	S1378	MecChem Express
Sodium chloride	S9888	Sigma Aldrich
Sodium dodecyl sulfate (SDS)	L3771	Sigma Aldrich
SuperSignal west femto maximum sensitivity substrate	34096	ThermoFisher
Syber Green PCR Kit	HB-0169	Qiagen
T-PER tissue protein extraction reagent	78510	Thermo scientific
Trition X 100	X100	Sigma
Trizma base	T1503	Sigma
TaqMan Fast Advanced Master Mix	00849407	ThermoFisher
Tween 20	P1379	Sigma
Tris-EDTA	BP2473-100	Fisher
Tris buffered saline	T5030	Sigma
Trizol reagent	15596018	ThermoFisher
Trypan Blue	93595	Sigma
Vectastain Elite, R.T.U (Horse anti-mouse/rabbit IgG)	PK-7200	Vector Laboratories
Xylene	CRTSX0021612	Lennox

Table 7. *Consumables.*

Name	Catalog Number	Company
0.5ml tubes	72.735.002	Sarstedt
1000ul pipet tips	02-707-400	Fisherbrand
10ml stripettes	4488	Costar
10ul pipette tips	70.3010	Sarstedt
200ul pipette tips	70.3030	Sarstedt
25ml stripettes	4489	Costar
500ul tubes	3745	Corning
Cover glass 22x 50 mm	631-0137	VWR
Kimberly Clark Dry Cleaning Wipes	7552	KimTech Science
Nuc-immunoplate	475094	Thermofisher
Pasteur pipettes	2600135	Ratiolab
SuperFrost Plus Slides	631-0108	VWR

Table 8. *Equipment.*

Name	Catalog Number	Company
Beaded water bath	JB Nova	Grant
Cell culture Incubator	300508314	Biosciences
Centrifuge	5427R	Eppendorf
Centrifuge	5702	Eppendorf
ChemiDoc MP Imaging System	12003154	BioRad
Decloaking Chamber NxGen	DC2012	BioCare Medical
Gyro-Rocker	SSL3	Stuart
Heating Block	RH B 2 S2	Laboratory Instruments
Histocore Biocut	N/A	Leica
Microcentrifuge	6770	Corning
Microplate centrifuge	C2000-E	Benchmark Scientific
Microscope	AE2000	Motic
Microscope	Evos M5000	ThermoFisher Scientific
MiniAmpPlus Thermal Cycler	A37835	Applied Biosystems
Monair Recirculating Fume Cabinet	1250 plus	Astec

Motic Microscope	Panthera L Series	Motic
Nanophotometer N60	T61688	Implen
Orbital Incubator	SI500	Stuart
Paraffin Section Flotation Bath	MH8517	Electrothermal
Ph Meter	Orion Star A211	ThermoScientifc
PolarStar Omega	POLARstar Omega	BMG LabTech
Roller Mixer	SRT9	Stuart
StepOne Plus PCR Machine	4376600	Applied Biosystems
TissueLyser LT	85600	Qiagen
Vortex	SLS1620	SLS Lab Basics
Vortex-Genie 2	SI-0236	Scientific Industries
Water bath	11459509	Clifton
Weighing Scales	SI-402	Denver Instrument
Weighing Scales	SI-114	Denver Instrument

Table 9. *Software.*

Name	Version	Company
Biorender	BioRender 2024	Biorender
clusterProfiler	3.8.1	Bioconductor
DESeq2	1.20.0	Illumina
Diamond	0.9.14	N/a
edgeR	3.22.5	Bioconductor
Excel	16.80	Microsoft
featureCounts	1.5.0-p3	N/a
GATK	4.1.4.1	Broad Institute
GraphPad Prism	10.1.1	GraphPad (USA)
GSEA	V4.3.1 Mac	Broad Institute
hisat2	2.0.5	N/a
ImageLab	6.1	Bio-Rad
Mienturnet	3.17	N/a
miRTarBase	9.0	N/a
Motic Images Plus	3.0.19 (124)	Motic
Nanodrop	NPOS 4.2h build 14900	Implen
PowerPoint	16.80	Microsoft

QuPath	0.05	N/a
rMATS	4.1.0	Children's Hospital of Philadelphia
snpEff	4.3q	N/a
StepOne Plus Real-time Software	Version 2.3	Applied Biosystems
TargetScanHuman	8.0	N/a
TargetScanMouse	8.0	N/a
Word	16.80	Microsoft

2.1.1 IBD patient biopsies or samples

Pinch biopsies were taken from the caecum and rectum of paediatric patients diagnosed with Ulcerative Colitis as part of the DOCHAS study (Determinants and Outcomes of Children and Adolescents with IBD) by Dr. Seamus Hussey in National Children's Research Centre (NCRC) in Dublin. Blood samples were also obtained from these patients. UC diagnosis was made based on histological, clinical and endoscopic findings, and patients were phenotyped based on the Paris classification (Levine et al., 2011). Additional data was collected at diagnosis including gender, age, extent of disease, previous medications and family history of IBD. Patients were assigned a PUCAI score at diagnosis, as previously defined (Turner et al., 2009), with ≤10 remission, 11–34 mild, 35-64 moderate, and ≥65 severe. Follow-up data was also provided for these patients which included failure of first line therapeutics and if a relapse had occurred since initial treatment. Following treatment, Patients were classified as either treatment responsive, or treatment non-responsive, on the basis of an improvement in symptoms and a PUCAI score of <10. This work was done in according with Maynooth Universities code of ethics 2441279.

2.1.2 Mouse strains

miR-223$^{-/y}$ mice on a C57BL/6J background were obtained and bred in-house at the University of Colorado Anschutz Medical Campus as previously described(Neudecker et al., 2017b). C57BL/6J mice (CD45.2) and CD45.1 congenic C57BL6 mice (B6.SJL-*Ptprc*^{a} *Pepc*^{b}/BoyJ) were purchased from The Jackson Laboratory (Maine, USA). Following weaning at 21 days, mice were co-housed and experimental colitis was induced at 8 weeks old. All mice were bred under specific pathogen-free conditions, and their faecal samples tested negative for Helminth, Protozoa and Heliobacter species. All animal procedures were approved by the Institutional Animal Care and Use Committees at the University of Colorado Denver. All animal procedures were carried out by staff at the University of Colorado Denver.

2.1.3 Induction of Colitis-associated colorectal cancer

8-week-old mice were injected intraperitoneally with 10mg/kg of azoxymethane (AOM) (Sigma Aldrich). After three days, dextran sodium sulphate (DSS) (2% w/v, 36–50,000 kDa; MP Biomedicals) was administered in drinking water *ad libitum* for six days. DSS was then removed, and mice were given two weeks to recover. For chronic AOM/DSS the cycle of DSS, followed by a recovery period was repeated three times in total, to mimic the inflammatory cycle typically seen in IBD patients. A schematic of this protocol is shown in **Figure 10.**

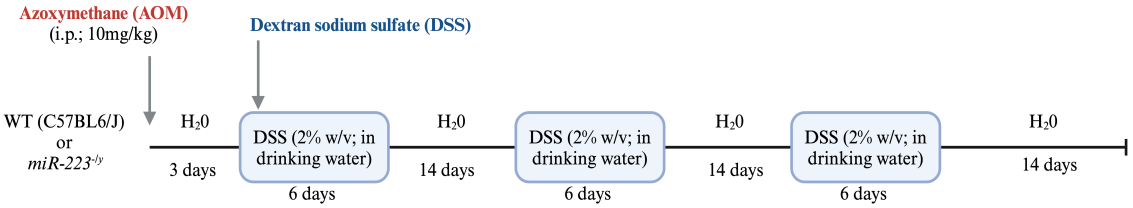


Figure 10. *Induction of Colitis-associated colorectal cancer in mice using chronic AOM/DSS.*

Mice were injected intraperitoneally with AOM. After three, days DSS was added to drinking water. After six days, DSS was removed, and mice were given two weeks to remover. This cycle was repeated three times in total. Created on BioRender.com

In another series of studies, the impact of $Ly6G^{+}$ neutrophils and myeloid-derived suppressor cells on CAC development was assessed in an acute model of AOM/DSS. Initially, 8-week-old mice were injected intraperitoneally with 10mg/kg of AOM. After three days recovery, 2% DSS (w/v) was given in drinking water *ad libitum* for six days. DSS was then withdrawn, and mice were given two weeks to recover. *miR-223*$^{-/y}$ mice were randomly assigned into two groups: one receiving IgG control and the other receiving treatment with 20µg of anti-GR1 (Lyg6/Ly6C: RB6-8C5 clone, BioXcell, USA) via intraperitoneal injection every three days for a total of three weeks (8 injections in total). Euthanasia of all mice occurred 24 hours after the last injection.

In all studies mice were monitored daily for clinical signs of CAC such as weight loss, faecal blood, and stool consistency. Based on this data, a UC disease activity index (DAI) was

calculated for each mouse. Each parameter in the DAI was given a score of 1-4, with a maximum potential score of 12. The DAI was defined as per **Table 10**. Upon necropsy colons were removed and flushed with ice-cold PBS. The length and weight of each colon was also recorded. Colons were then snap-frozen or fixed in 10% buffered formalin. All procedures relating to the induction of CAC in mouse models was performed by staff at the University of Colorado-Anschutz Medical Campus, Aurora, Colorado USA.

Table 10. *Ulcerative colitis disease activity index.*

Ulcerative colitis disease activity index	
Score 0	No weight loss, normal stool, no blood
Score 1	1–3% weight loss
Score 2	3–6% weight loss, loose stool, blood visible in stool
Score 3	6–9% weight loss
Score 4	>9% weight loss, diarrhoea, gross bleeding

*Loose stool was defined as a stool pellet that easily loses its consistency when handled. Diarrhoea was defined as no pellet formation. Gross bleeding was defined as perianal blood with haematochezia.

2.1.4 Generation of bone marrow chimeric mice

Bone marrow (BM) chimeric mice were generated by staff at the University of Colorado Denver as previously described(Neudecker et al., 2017b), and illustrated in **Figure 11**. Briefly, femurs and tibias from WT (CD45.2) and *miR-223*$^{-/y}$ (CD45.1) donor mice were removed. BM was removed using 25-gauge needle containing ice-cold RPMI, BM cells were subsequently flushed through a 70µm cell strainer. Recipient mice (8-12 weeks old) were irradiated with 500 rads, this was repeated 4 hours later (1000 rads total). Following irradiation, 1×10^7 donor BM cells/mouse (either *miR223*$^{-/y}$ CD45.2 or WT CD45.1) were intravenously injected via the retro-orbital route in 0.1ml 0.9% sodium chloride. Mice were housed in microisolator cages for 8 weeks to recover before the onset of chronic AOM/DSS protocol as per in section 2.1.3. To evaluate BM reconstitution, spleens were excised at necropsy, red blood cells were lysed, and flow cytometry was performed for CD45+ leukocytes expressing either CD45.1 (clone A20) or CD45.2 (clone 104; eBioscience).

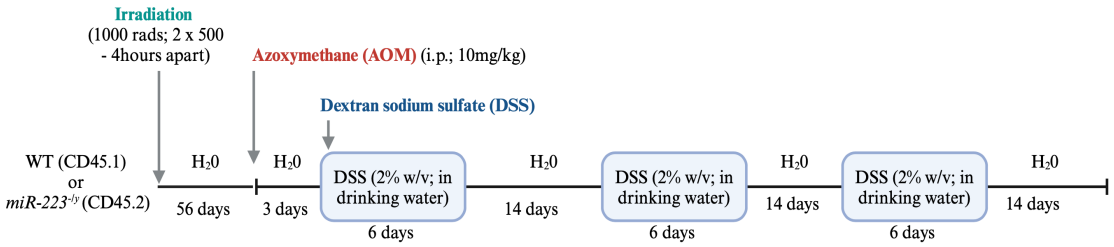


Figure 11. *Generation of bone marrow chimeric mice and subsequent timeline of treatment with chronic AOM/DSS.*

Recipient mice where irradiated with 500 rads twice, 4 hours apart. After 56 days, chronic AOM/DSS was induced. Created on BioRender.com.

2.1.5 Cell Culture

All cell culture was performed in a class II biological safety cabinet (ThermoScientifc) using aseptic technique. The safety cabinet was wiped down with 70% ethanol before/after each use, and all items brought into the cabinet were sprayed with 70% ethanol. UV sterilisation was also used after each use, with only one cell line being used at a time. All cells were grown in a humidified incubator (ThermoScientifc) at 37°C with 5% CO_2, which was regularly checked to ensure readings were correct.

2.1.5.1 Cell counting

Briefly, after subculturing cells were resuspended with 4ml of cell culture media. Next, 15µl of resuspended cells were transferred to a 1.5ml tube, 15µl trypan blue (Sigma) was added, sample was mixed and 20µl was loaded onto a haemocytometer. Using light microscope (Motic), viable cells were identified by their bright appearance, while apoptotic cells appeared blue. Viable cells were counted across 4 quadrants, the average was determined and multiplied by two. This was then multiplied by 10^4 to determine cells per ml.

2.1.5.2 In vitro culture of Raw 264.7 macrophage

Raw 264.7 cells were purchased from ATCC. This macrophage cell line was originally established from a tumour of a male BALB/c mouse induced via intraperitoneal injection of the Abelson leukemia virus (Ng et al., 2018). Cells were grown in DMEM (Fisher) supplemented with 10% fetal bovine serum (FBS; Sigma), media was changed every 2-3 days as per manufactures recommendations. Cells were grown until they were 70% confluent, cells were then removed mechanistically by scrapping and placed into a 50ml tube. Tubes were centrifuged at 400 *rcf* for 5 minutes at room temperature. Supernatant was removed, pellet was resuspended with media. For sub-culturing, a 1:5 split was performed. If seeding for an experiment, cells were plated at 200,000 cells/well on a 6-well plate with 2mls of media. For all experiments media was changed prior to treatment.

2.1.5.3 Lentiviral transduction of RAW 264.7 macrophage

To produce an experimental tool system to assess *miR-223* biology in macrophage, RAW 264.7 cells were generated with lentivirus by a member of the Mucosal Immunology Research lab at Maynooth University. Specifically, RAW 264.7 macrophage cells were lentivirally transduced to generate *miR-223* knockdown (*223KD*), *miR-223* over-expressing (223OE) and a negative control cell lines. Briefly, 264.7 RAW macrophage were plated at 200,000 cells per well and grown until they were 70% confluent. Once confluent, cells were rinsed with pre-warmed PBS to remove serum and 2ml of DMEM media was added. Polybrene (10mg/ml; Sigma) was added to each well and the plate was swirled to ensure sure even distribution. Pre-made lentiviral transduction nanoparticles (MISSION® Lenti-miRs; Sigma) were then added to corresponding wells, plate was swirled and left to incubate overnight at 37°C. After 24 hours media was changed and cells where placed back into the incubator. Cells that had been successfully transduced contained a vector for puromycin resistance, thus the following day media was changed and puromycin (2µg/ml) was added to select transduced cells. After 48 hours, transduced cells were split into a T25 flask containing DMEM media supplemented with 10% FBS and were then used for experiments. Once generated cells where used for experimentation.

2.1.5.4 Experiments using Raw macrophage cell lines

Raw cells where cultured as described in section 2.1.5.2. For treatments, cells where plated at 200,000 cells per well on a 6-well plate. Cells were used for treatment when they were 70% confluent, with media being changed prior to treatment.

To identify intracellular signalling pathways that may identify how *miR-223* is controlling macrophage activation, lenti-transduced RAW cell lines were pre-treated with small molecule inhibitors 30 mins prior to stimulation. Doses were identified from literature review, with final concentrations as indicated in **Table 11**, cells where harvested for mRNA after 12 hours. This study was repeated with the addition of either LPS (100ng/ml) or IFN-γ (20ng/ml) 30 minutes after inhibitors were added, cells where harvested after 12 hours for mRNA.

To define how *miR-223* regulates the kinetics of inflammatory signalling in macrophage, RAW's and 223KD RAW's where treated with IFN-γ (20ng/ml) and harvested at either 15 minutes, 30 minutes, 1 hour, 2 hours, 6 hours or 12 hours for protein as described in section 2.1.7.1. All treatments were performed in cell culture media and inhibitors were reconstituted as per manufactures instructions in DMSO.

Table 11. *Inhibitors used in cell culture.*

Inhibitors	Target	Concentration (per ml)
AMG538	Selective p38α inhibitor	20μM
Sp600125	Pan-JNK inhibitor	40μM
F418024	Selective ERK1 and ERK2 inhibitor	50μM
Ruxolitinib	Selective JAK1 and JAK2 inhibitor	5μM
JSH-23	Selective inhibitor of NF-κB transcriptional activity	10μM
BAY-11	Selective inhibitor of NF-κB activation	1μM

2.1.5.5 Protein translation using a SUNSET assay

To access protein synthesis a SUNSET assay was utilized. In this method puromycin, a structural analog of aminoacyl-transfer RNA, is incorporated into growing peptide chains. The rate puromycin-peptide chains are formed is reflective of the overall rate of protein translation and is detectable in whole cell lysates via western blotting.

RAW 264.7 and 223KD RAW cells where cultured as described in section 2.1.5.2. Once 70% confluent, cells where treated with IFN-γ (20ng/ml; PeproTech) for 50 minutes. As a negative control to block translation cycloheximide (100µg/ml) was then added to designated wells for ten minutes. Puromycin (10µg/ml) was then added for a further 10 minutes, which is incorporated into elongating peptide chains, and allows the translation in the cells to be assessed through the use of an anti-puromycin antibody. Samples were harvested for western blotting as described in section 2.1.7.1.

2.1.5.6 Generation of murine colon organoids

C57BL/6J mice were euthanized and the colon was extracted, taking care to cut 5mm above the rectum and below the caecum. Colon were flushed with 1ml ice-cold PBS, cut open using a scissors and subsequently washed again with cold PBS. Colon were then cut into 2mm pieces using a scalpel, and they were placed into a 50ml conical tube containing 15ml cold PBS. Colon pieces were pipetted up and down three times, then left to settle and the supernatant removed. This step was then repeated 15 times in total. Colon pieces were resuspended in 25ml of gentle cell dissociation reagent (Stem Cell) and put on a rocker (Stuart) at 20 rpm for 20 minutes at 25°C. Samples were left to settle and supernatant was removed. Colon pieces were resuspended in 10ml PBS with 0.1% BSA and mixed three times. The supernatant was filtered through a 70µm filter into a 50ml tube to generate fraction 1. The generation of fractions was repeated 3 times. All fractions were centrifuged at 300 *rcf* for 5 minutes at 5°C. Supernatant was removed from and pellets were resuspended in 10ml PBS with 0.1% BSA. Samples were centrifuged at 200 *rcf* for 3 minutes at 5°C to pellet the colonic crypts. Each pellet was resuspended in 1ml PBS and colon organoid fractions enriched for intestinal crypts, as indicated by smooth edges and either circular or rectangular in shape, were used for organoid culture. The number of crypts in each fraction was determined by placing 10µL of each fraction onto a hemocytometer and counting the number of crypts. This number was multiplied by 100 to determine the

number of crypts per ml, this was repeated for each fraction. Samples were centrifuged at 200 *rcf* for 5 minutes at 5°C, supernatant was removed, and the pellets were resuspended in 150µL IntestiCult organoids growth media (Stem Cell). 150µL of matrigel (Stem Cell) was added to each tube, a pre-wetted tip was then used to mix samples. 50µL of the suspension was loaded onto a pre-heated 24-well plate to form domes. Plates were then put into an incubator for 20 minutes at 37°C. Once the domes had solidified, 750µL of IntestiCult organoids growth media was added to each well. Plates were then placed in an incubator at 37°C and 5% CO_2. Media was changed three times per week.

2.1.5.7 In vitro maintenance of murine colonic organoids

Media was removed from all wells. 1ml of ice-cold gentle cell dissociation reagent (Stem Cell) was added on top of each well for 1 minute. A pre-wetted tip was then used to pipette the liquid in each well up and down 20 times to ensure the dome was fully broken up. The liquid was then transferred to a 15ml tube, with each well being placed into a separate tube. Each well was further washed with 1ml of gentle cell dissociation reagent, and this was transferred to the corresponding tube. All tubes were placed on a rocker for 10 minutes at room temperature. Tubes where centrifuged at 300 *rcf* for 5 minutes at 5°C. Supernatant was then carefully removed, pellet was resuspended with 10ml of cold DMEM/F12 with 0.1% FBS (Sigma). Samples were centrifuged for 5 minutes at 200 *rcf* at 5°C and the supernatant removed via pipetting. Each pellet was resuspended in a 1:1 mix of media and matrigel (Stem cell). 50µL of this suspension was loaded onto a pre-heated 24-well plate to form domes. Plates were put into an incubator for 20 minutes at 37°C. Once the domes had solidified, 750µL of IntestiCult organoid growth media (Stem Cell) was added to each well. Plates were placed in an incubator at 37°C and 5% CO_2.

2.1.5.8 Experiments using murine colonic organoids

Murine colonic organoids where cultured as previously described. In one series of experiments, organoids where again pre-treated for 5 days post-split with either DEA/NO (25µM/ml) or 1400W (100µM/ml) for 30 minutes followed by stimulation with recombinant IFN-γ (10ng/ml) for 48 hours. Samples were harvested for mRNA as per section 2.1.8.2.

In another study, to assess organoid recovery, 24 hours following a split organoids were pre-treated with either DEA/NO (25µM/ml) or 1400W (100µM/ml), IFN-γ (10ng/ml) was added after 30 minutes. Media was changed 24 hours post-treatment. Organoids where grown for a further 72 hours and where then harvested for mRNA as per section 2.1.8.2.

2.1.6 Immunohistochemistry

2.1.6.1 Haematoxylin and Eosin (H&E) staining

Formalin-fixed and paraffin embedded (FFPE) tissue was cut into 0.7µm sections using a microtome (Lecia) and baked at 60°C for 24hrs. Following this slides were deparaffinized using xylene and rehydrated using an ethanol gradient (100 – 70%). Slides were then placed in hematoxylin for 4 minutes, followed by washing with water for 1 minute. Slides were immersed in an acid wash for 1 minute and rinsed with water for 1 minute. Slides where placed in eosin for 15 seconds and then washed in water until clear. Slides were then dehydrated via sequential immersion in ethanol (70 - 100%) and xylene. 10µl of mounting media (Sigma) was added to each sample, a coverslip was added. All H&E stains were performed by staff at the University of Colorado Denver. H&E samples were subsequently imaged using a Motic Panthera L Series or Invitrogen Evos M5000 microscope.

2.1.6.2 Immunohistochemistry

Using a microtome (Leica) 7µm sections were taken from FFPE blocks, sections were placed onto polarised slides (VWR) and baked overnight at 60°C. Slides were deparaffinized via sequential immersions, as outlined in **Table 12.** Samples were heated in a 1% citrate-based antigen retrieval buffer in a pressure cooker (BioCare Medical) at 110°C, 6p.si. for 10 minutes. Slides were then rinsed for 5 minutes with dH_2O, placed in PBS for 5 minutes and then put into a humidified camber. Sections where then covered in 200µl Trition X (Sigma) for 10 minutes, if permeabilization was needed for target antibody, and blocked for 20 minutes with 200µl 5% BSA/PBS. Blocking agent was removed, 200µl primary antibody was added and left to incubate overnight at 4°C. Primary antibodies were prepared as per **Table 13**. Slides were washed with PBS for 5 minutes, 200µl secondary antibody (Vector ABC kit) was added for an hour at room temperature. Slides washed in PBS for 5 minutes. 200µl NovaRed detection

reagent (Vector Labs) was added and development was monitored using a microscope (Motic). Slides then placed in dH_2O before counterstaining with Mayer's hematoxylin (Sigma) for 1 minute. Slides were washed with tap water for 5 minutes and subsequently dehydrated by sequential immersion, as per **Table 14**. Slides where left to dry overnight in a fumehood (Astec). 10µl of mounting media was added to each slide and a coverslip applied. Slides where imaged using a microscope (Motic). An overview of this technique is shown in **Figure 12.**

Table 12. *Sequential immersions for deparaffinizing FFPE slides.*

Component	Repetitions	Duration
Xylene	2	5 minutes
100% Ethanol	2	1 minute
90% Ethanol	2	1 minute
70% Ethanol	2	1 minute
dH_2O	1	3 minutes

Table 13. *Primary antibodies used for immunohistochemistry.*

Antibody Name	Company	Catalog Number	Dilution used
β-Catenin	BD Biosciences	610154	1 in 500 in PBS
CCR2	Abcam	AB273050	1 in 500 in PBS
CD68	Cell Signalling	97778	1 in 300 in PBS
Ly6G	Cell Signalling	87048	1 in 150 in PBS
NOS2	Cell Signalling	68186	1 in 500 in PBS
PCNA	Cell Signalling	13110	1 in 4000 PBS
Phosphop-STAT3	Cell signalling	9145	1 in 500 in PBS
Total STAT3	Abcam	Ab68153	1 in 500 in PBS
S-nitrotyrosine	Abcam	ab61392	1 in 300 in PBS

Table 14. *Sequential immersions for dehydrating FFPE slides.*

Component	Duration
70% Ethanol	2 minutes
90% Ethanol	2 minutes
100% Ethanol	1 minutes
Xylene	5 minutes

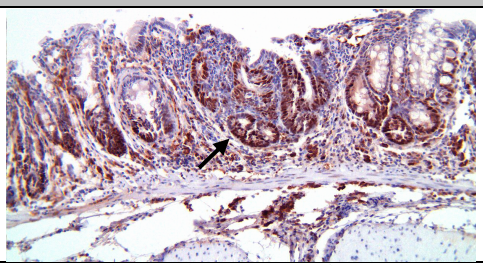
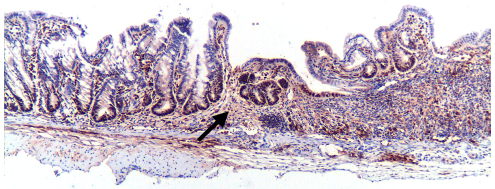
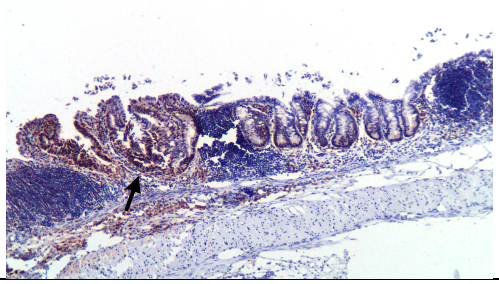
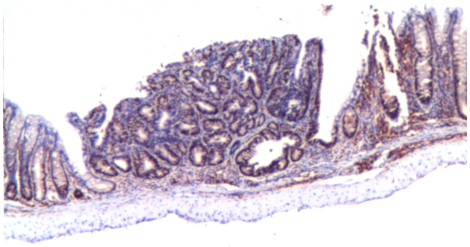
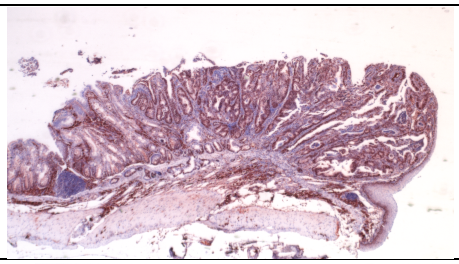
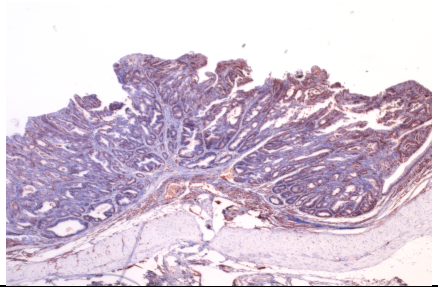
2.1.6.3 Quantification of immunohistochemistry

Stained slides where imaged using a microscope (Motic). Images where then analysed using QuPath software. Briefly, tiff images were imported, image type was set to brightfield (H-DAB), and the area being analysed for each image was selected. Stain vectors for DAB and haematoxylin was set for each experiment using the auto detect function. Cells were detected using the cell detection function based on the optical density sum. Positive cells were identified using the positive cell detection function, based on the optical density sum. For each image the number of positive was recorded, which was subsequently analysed using GraphPad Prism.

2.1.6.4 Histology Scoring

To determine the number of tumours and dysplasic regions present in each sample, H&E and PCNA stained FFPE samples were analysed, and the number present was counted. An image of each tumour was taken using a Motic Panthera L Series microscope. These images where then analysed using Motic Images Plus Software to determine the area of each tumour. This was utilized to classify tumours into either: dysplastic, <100,000µm^2, small 100,000-300,000µm^2, medium 300,000 - 500,000µm^2, large 500,000 - 1,000,000µm^2 or very large tumour >1,000,000µm^2. Representative images from PCNA stained AOM/DSS treated *miR-223*$^{-/y}$ mice for each group are shown in **Table 15**.

Table 15. *Classification of tumours following AOM/DSS mouse model of CAC.*

Classification	Representative Image
Dysplastic	
<100,000µm^2	
Small 100,000 – 300,000µm^2	
Medium 300,000–500,000µm^2	
Large 500,000–1,000,000µm^2	
Very large tumour >1,000,000µm^2	

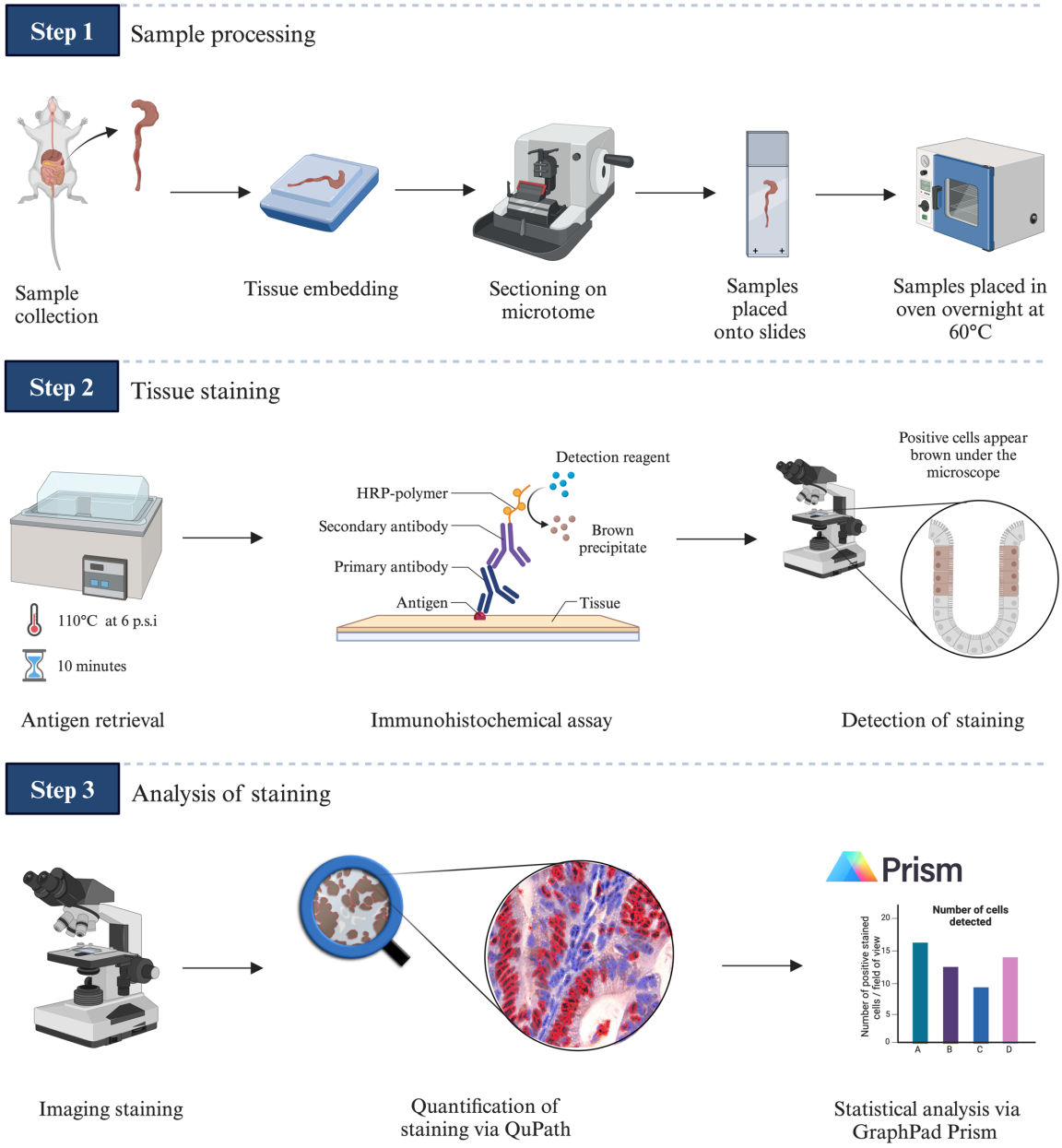


Figure 12. *Illustration of immunostaining performed on FFPE tissue generated from a chronic mouse model of CAC.*

Colons from mice where FFPE. These samples where sectioned and then subsequently baked overnight. Samples where deparaffinized and antigen retrieval was performed for 10 minutes at 6 p.s.i. Immunohistochemistry assay was performed, and staining was detected. Samples where imaged and staining was quantified using QuPath. Statistical analysis was performed using GraphPad Prism. Diagram was created on BioRender.com.

2.1.7 Analysis of protein expression

2.1.7.1 Protein extraction

Protein was extracted from tissues using a Tissue Lyser LT (Qiagen). Briefly, tissue was placed into a round bottomed tube containing a metal bead and 600µl of TPER buffer containing Ethylenediaminetetraacetic acid (EDTA), protease and phosphatase inhibitors, as per **Table 16**. TPER buffer is a mild detergent that is used for the extraction of total protein from tissue samples without affecting protein function. The addition of protease and phosphatase inhibitors was to prevent protease and enzymatic degradation respectively. Samples were placed in the tissue lyser for 5 minutes at 50Hz. After lysis the bead was removed and samples where centrifuged at 10,000 x g for 3 minutes at 4°C. The supernatants were transferred into new tube.

Protein was extracted from cells by removing media, rinsing cells with PBS and adding 200µl of RIPA buffer containing EDTA, protease and phosphatase inhibitors as per **Table 17**.

For both cell and tissue samples, the protein concentration was determined using the bicinchoninic acid (BCA) assay, as described in section 2.1.7.2.

Table 16. *Components used for protein extraction from tissue samples.*

Component	Volume added
TPER buffer	564 µl
Protease inhibitor	6 µl
Phosphatase inhibitor	6 µl
EDTA	6 µl

Table 17. *Components used for protein extraction from cells.*

Component	Volume added
RIPA buffer	291 µl
Protease inhibitor	3 µl
Phosphatase inhibitor	3 µl
EDTA	3 µl

2.1.7.2 Bicinchoninic acid (BCA) assay

The BCA assay was performed to determine the protein concentration of all samples. This protein assay is based on the reduction of Cu^{2+} to Cu^{1+} when there are proteins present in an alkaline solution. When bicinchoninic acid reacts with the reduced cation it produces a purple colour that is used for protein quantification. The BCA protein assay kit (Pierce BCA protein assay kit, Thermo Scientific) was used as per manufactures guidelines. Briefly, 10µl of each protein sample was loaded in duplicate onto a 96 well plate (Thermofisher), along with 10µl of bovine serum albumin (BSA) protein standards ranging from 2000µg to 125µg. The BCA reagents were mixed in a 1:50 dilution and 200uL was added to each sample. The plate was then covered and incubated at 37°C for 30 minutes. The absorbance values where then read at 562nm using a PolarStar Omega plate reader (BMG LabTech). A standard curve was generated using the average absorbances from the protein standards, this was used to generate an equation of the line from which the protein concentration of the protein samples was determined.

2.1.7.3 Sodium dodecyl sulphate polyacrylamide gel electrophoresis

Sodium dodecyl sulphate polyacrylamide gel electrophoresis (SDS-PAGE) was carried out to separate proteins based on their molecular weight. This method uses Sodium dodecyl sulphate (SDS), an anionic detergent, to both denature the proteins and provide them with a negative charge. As this negative charge is proportional to the molecular weight, it allows the proteins to be separated on a gel based on this basis. SDS-PAGE gels where prepared as per **Table 18** for the resolving and stacking gels, ensuring that tetramethylethylenediamine (TEMED) and ammonium persulfate (APS) where added last as they interact to solidify the gel. The resolving

gel is prepared first, once poured it was covered with 70% ethanol. When it had polymerized, the ethanol was removed, and the stacking gel was prepared. The stacking gel was then poured on top of the resolving gel, and a comb was inserted. Once the gel had polymerized, the gels were placed in an electrophoresis chamber (Bio-Rad) filled with running buffer, prepared as per **Table 18**, and the comb was removed. Protein samples were prepared with 4x lamelli to give a final concentration of 10µg, samples were then placed in a thermocycler (Applied Biosystems) at 95°C for 10 minutes to ensure the protein is denatured. Samples and a molecular weight ladder (Thermo Scientific) were loaded onto the gel and electrophoresis was run at 80V for 15 minutes, followed by 110V for an hour. Once finished, the gels were removed from the electrophoresis chamber and the stacking gel was removed.

2.1.7.4 Western Blot

Protein samples that had been run on an SDS-PAGE gel were transferred to a nitrocellulose membrane. Briefly, filter paper and nitrocellulose membranes that where pre-soaked in transfer buffer, prepared as per **Table 18,** for 10 minutes and where then arranged as follows: two pieces of filter paper, nitrocellulose membrane, polyacrylamide gel and two pieces of filter paper. This was then placed on a Trans-blot semi-dry transfer rig (Bio-Rad) and run for 80 minutes at 0.2mA. The membrane was washed once in TBT-T for 5 minutes and blocked in 5% skimmed milk in TBS for 20 minutes to block any non-specific binding. Membrane was then washed three times in TBT-T for 5 minute each and incubated overnight at 4°C in primary antibody, as per **Table 19**. Membrane was washed another three times in TBT-T for 5 minutes each before corresponding secondary antibody was added for an hour at room temperature. Membrane was washed a further three times. Membrane was then covered in 1mL of a 1:1 solution of WesternBright ECL and WesternBright Peroxide for 1-5 minutes. This was then drained off and the membrane was placed in a ChemiDoc MP Imaging System (Bio-Rad). Blots where imaged using the auto-exposure feature. This method is illustrated in **Figure 13**.

Table 18. *Reagents used for western blotting.*

10% Resolving gel	Volume added	Stacking gel	Volume added
dH_2O	5.2 mL	dH_2O	5.8 mL
4X 1.5M Tris-HCL (pH 8.8)	3.1 mL	4X 1.5M Tris-HCL	2.5 mL
Acrylamide	4.2 mL	Acrylamide	1.7 mL
15% APS	75 µL	15% APS	30 µL
TEMED	7 µL	TEMED	10 µL
Running buffer	**Volume added**	**Transfer buffer**	**Volume added**
Tris	3 g	Tris	3 g
Glycine	14.4 g	Glycine	14.4 g
SDS	1 g	Methanol	200ml
dH_2O	1000 mL	dH_2O	800 mL

Table 19. *Antibodies used for western blots.*

Antibody Name	Blocking Reagent	Working Dilution	Secondary antibody Used	Secondary Antibody Concentration
Anti-puromycin	5% Milk/TBS	1:1000 in 5% Milk/TBS	Goat anti-mouse IgG	1:2000 in 5% BSA/TBS
β-Actin	5% Milk/TBS	1:500 in 5% Milk/TBS	Donkey anti-Goat IgG	1:1000 in 5% Milk/TBS
C-myc	5% BSA/TBS	1:500 in 5% BSA/TBS	Goat anti-rabbit IgG	1:2000 in 5% BSA/TBS
Cyclin D1	5% BSA/TBS	1:500 in 5% BSA/TBS	Goat anti-rabbit IgG	1:1000 in 5% BSA/TBS
E-Cadherin	5% BSA/TBS	1:500 in 5% BSA/TBS	Goat anti-mouse IgG	1:2000 in 5% BSA/TBS
IRF5	5% Milk/TBS	1:1000 in 5% BSA	Goat anti-rabbit IgG	1:5000 in 5% BSA/TBS

N-Cadherin (D4R1H)	5% BSA/TBS	1:500 in 5% BSA/TBS	Goat anti-rabbit IgG	1:2000 in 5% BSA/TBS
NF-kB p65	5% BSA/TBS	1:500 in 5% BSA/TBS	Goat anti-rabbit IgG	1:1000 in 5% BSA/TBS
NOS2	5% BSA/TBS	1:500 in 5% BSA/TBS	G Goat anti-rabbit IgG	1:1000 in 5% BSA/TBS
PCNA	5% BSA/TBS	1:500 in 5% BSA/TBS	Goat anti-rabbit IgG	1:2000 in 5% BSA/TBS
Phospho-AKT	5% BSA/TBS	1:2000 in 5% BSA/TBS	Goat anti-rabbit IgG	1:1000 in 5% BSA/TBS
Phospho-β-Catenin (S33/37/T41)	5% BSA/TBS	1:500 in 5% BSA/TBS	Goat anti-rabbit IgG	1:2000 in 5% BSA/TBS
Phospho-β-Catenin (S552)(D8E11)	5% BSA/TBS	1:500 in 5% BSA/TBS	Goat anti-rabbit IgG	1:2000 in 5% BSA/TBS
Phospho-ERK	5% BSA/TBS	1:1000 in 5% BSA/TBS	Goat anti-rabbit IgG	1:1000 in 5% BSA/TBS
Phospho-histone H2A.X	5% BSA/TBS	1:500 in 5% BSA/TBS	Goat anti-rabbit IgG	1:2000 in 5% BSA/TBS
Phospho-Jak 2	5% BSA/TBS	1:500 in 5% BSA/TBS	Goat anti-rabbit IgG	1:2000 in 5% BSA/TBS
Phospho-JAK2	5% BSA/TBS	1:500 in 5% BSA/TBS	Goat anti-rabbit IgG	1:2000 in 5% BSA/TBS
Phospho-JNK	5% BSA/TBS	1:1000 in 5% BSA/TBS	Goat anti-mouse IgG	1:2000 in 5% BSA/TBS
Phospho-p38	5% Milk/TBS	1:1000 in 5% BSA/TBS	Goat anti-rabbit IgG	1:2000 in 5% BSA/TBS
Phospho-S6 ribosomal protein	5% BSA/TBS	1:2000 in 5% BSA/TBS	Goat anti-rabbit IgG	1:1000 in 5% BSA/TBS

Phospho-stat1	5% Milk/TBS	1:1000 in 5% BSA/TBS	Goat anti-rabbit IgG	1:2000 in 5% BSA/TBS
Phospho-stat3	5% BSA/TBS	1:500 in 5% BSA/TBS	Goat anti-rabbit IgG	1:2000 in 5% BSA/TBS
Total STAT3	5% BSA/TBS	1:500 in 5% BSA/TBS	Goat anti-rabbit IgG	1:1000 in 5% BSA/TBS
s-nitrotyrosine	5% Milk/TBS	1:500 in 5% Milk/TBS	Goat anti-mouse IgG	1:1000 in 5% Milk/TBS
TGF-alpha	5% BSA/TBS	1:2000 in 5% BSA/TBS	Goat anti-rabbit IgG	1:1000 in 5% BSA/TBS
Tubulin	5% Milk/TBS	1:500 in 5% Milk/TBS	Goat anti-rabbit IgG	1:1000 in 5% milk/TBS

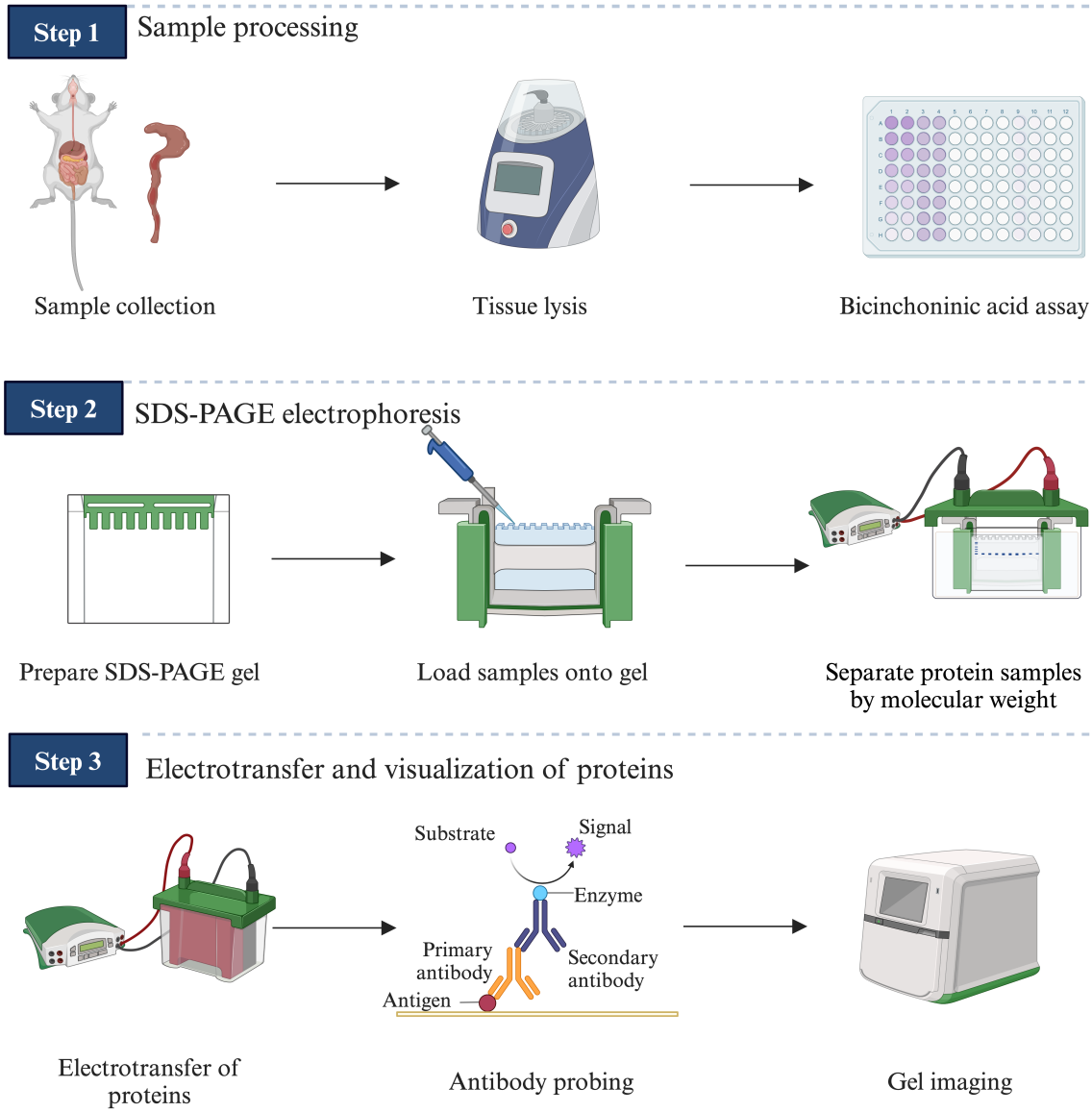


Figure 13. *Overview of protein analysis via western blotting.*

Mouse colons were lysed and protein concentration was determined via BCA assay. Samples where ran on an SDS-PAGE gel. Once samples has separated, proteins where transferred onto a nitrocellulose membrane. Samples where probed with antibody of interest which was imaged using a ChemiDoc MP Imaging System. Diagram created on BioRender.com.

2.1.7.5 Analysis of protein expression

To analyse protein expression the MSCN image for each target was imported into Image lab software (BioRad). Lanes and bands were identified manually. The adj. volume for each well was divided by the corresponding well in the control blot (β-actin), the resulting figure is referred to as the normalised value. The fold change was calculated by dividing the normalised value by the control well ran for that target. GraphPad Prism was then used to perform statistical analysis on the fold change values for each blot.

2.1.8 RNA Analysis

2.1.8.1 Purification of total RNA from cells

Total RNA was extracted from cells using the EasyPure kit (TransGen Biotech) as per manufactures instructions. Briefly, media was removed from cell culture plates, 1ml of PBS was added gently to wash the cells which was then subsequently removed. 200µl binding buffer (TransGen Biotech) was added per sample, each sample was then scrapped and liquid was placed into a 1.5ml Eppendorf. 200ul of 70% molecular grade ethanol was added to each sample and samples were mixed via pipetting. The liquid was then loaded onto a silica membrane 12,000 *rcf* for 30 seconds and the flow through was discarded. 500µl of clean buffer (TransGen Biotech) was added, samples centrifuged for 30 seconds at 12,000 *rcf* and flow through discarded. 500µl of wash buffer (TransGen Biotech) added samples centrifuged for 30 seconds at 12,000 *rcf* and flow through discarded. This step was repeated once. To remove ethanol residues the silica membranes were placed into new collection tubes and spun for two minutes at 12,000 *rcf.* Tubes were then left to air dry for two minutes. Membranes were placed into new 1.5ml tubes, 30µl of nuclease free H_2O was loaded directly onto each membrane. Samples where then spun for 1 minute at 12,000 *rcf*. Samples were quantified as per section 2.1.8.6.

2.1.8.2 Purification of total RNA from organoids

RNA was extracted using a modified protocol from Stem Cell Technologies. Briefly, media was removed from the wells and 1ml of cold PBS with 1% FBS was added directly on top of each dome. Each well was mixed up and down twenty times to break up the domes, after this liquid was placed into a 15ml tube and centrifuged for 5 minutes at 300 *rcf.* The supernatant was removed and pellet was resuspended in 200µl binding buffer (EasyPure). RNA was quantified as per section 2.1.8.6.

2.1.8.3 Purification of total RNA from tissue samples

Total RNA was extracted from mouse or human tissue samples using the Qiagen RNeasy kit (Qiagen). Briefly, tissue was placed into a tube containing a metal bead and 700µl RLT, and was then put in a Tissue Lyser (Qiagen) for 5 minutes at 30Hz or until the tissue was broken up. The bead was then removed and the sample centrifuged for 3 minutes at 10,000 *rcf* . The supernatant was removed into a new tube, 70% molecular grade ethanol was added in a 1:1 ratio and the sample was mixed by pipetting. 700µl of this mixture was then loaded onto silica membrane and spun at 10,000 *rcf* for 20 seconds, miRNA is enriched in the flow through, so it was retained and further processed as described in section 2.1.8.4. The membrane is then washed with 700µl of RW1 buffer and spun at 10,000 *rcf* for 20 seconds. 500µl is added to the column and sample is centrifuged at 10,000 *rcf* for 20 seconds and flow through discarded, this step is then repeated. Column is then spun for a further 2 minutes at 10,000 *rcf*. Finally, 50µl nuclease free H_2O is loaded onto the column and sample is spun at 10,000 *rcf* for 1 minute at 4°C to elute total RNA. Sample was then quantified as per section 2.1.8.6.

2.1.8.4 Purification of miRNA from tissue samples

miRNA was extracted from mouse or human tissue samples using the Qiagen RNeasy kit (Qiagen). The miRNA enriched flow through from mRNA extraction was added to 500µl of 100% molecular grade ethanol, loaded onto a new column and spun for 1 minute at 10,000 *rcf*. Flow through was discarded. 500µl RPE buffer (Qiagen) was pipetted onto the column, sample

was spun at 10,000 *rcf* for 20 seconds and flow through was discarded. 80% ethanol was added, sample was spun at 10,000 *rcf* for 2 minutes and flow through was discarded. Filter column was placed into a new 1.5ml collection tube and spun at 10,000 *rcf* for 2 minutes to remove excess ethanol. Filter columns were placed into a new collection tube, 30µl nuclease free H_2O was loaded onto the filter column. Sample was then quantified as per section 2.1.8.6.

2.1.8.5 Purification of miRNA from blood samples

miRNA was extracted from human blood samples using the PaxGene Blood RNA kit (Qiagen). Briefly, blood was collected directly into PaxGene blood RNA tubes which contained an additive to prevent RNA degradation. Samples were inverted 10 times and left at room temperature for 2 hours, then stored at -80°C until processing. On day of processing, samples where defrosted, brought to room temperature and centrifuged for 10 minutes at 5000 *rcf*. Supernatant was removed, 4ml RNase free H_2O was added and sample was vortexed until the pellet was dissolved. Samples were centrifuged for another 10 minutes at 5000 *rcf,* supernatant was then removed. 350µl of resuspension buffer (Qiagen) was added to each pellet, samples were subsequently vortexed until the pellet was dissolved. Samples were transferred to new 1.5ml tubes, 300µl binding buffer (Qiagen) was added and 40µl of proteinase K (Qiagen). Samples were vortexed for 5 seconds and incubated at 55°C for 10 minutes in a shaker at 300 *rpm*. Samples were transferred into a PAX gene shredder spin column and centrifuged for 10 minutes at 18,000 *rcf*. The flow through was transferred into a new 1.5ml tube, 350µl of 100% molecular grade ethanol was added and samples mixed by pipetting. Samples were loaded onto a PAXgene RNA spin column and centrifuged for 1 minute at 18,000 *rcf*. 350µl of wash buffer (Qiagen) was added to each sample, centrifuged for 1 minute at 18,000 *rcf*. 80µl of DNase I incubation mix (Qiagen)was added to all samples, which were then incubated at room temperature for 15 minutes. 350µl of wash buffer was added to each sample and they were subsequently centrifuged for 1 minute at 18,000 *rcf*. 500µl of wash buffer 2 (Qiagen) was added to samples and they were then centrifuged for 1 minute at 18,000 *rcf*, this step was repeated once. Samples were placed into a new collection tube, 40µl elution buffer (Qiagen) added to each sample and centrifuged at 18,000 *rcf* for 1 minute. Samples placed in a shaker for 5 minutes at 60°C. Samples were quantified as per section 2.1.8.6.

2.1.8.6 RNA Quantification

The concentration and purity of the RNA was determined by using a Nanophotometer N60 (Implen). Nucleic acids was selected on the home screen and either miRNA or mRNA was chosen. The volume of sample being loaded was set to 2µl. Prior to use the sample window and the mirror were cleaned using a kimwipe. 2µl of nuclease free H_2O was loaded onto the sample window and a blank reading was taken. A kimwipe was used to clean the sample window and the mirror, 2µl of the next sample was loaded and measured, this step was repeated for all samples. The concentration of each sample was determined by measuring the absorbance at 260nm and applying the Beer-Lambert law equation. For miRNA this was absorbance at 260nm * 33 = concentration of sample in ng/µl and for mRNA it was absorbance at 260nm * 40 = concentration of sample in ng/µl. The purity of samples was also determined, a 260/280 ratio ≥ 1.80 was considered pure miRNA or RNA. Samples were then equalised to either 100ng/µl for mRNA or 5ng/µl for miRNA using nuclease free H_2O and stored at -80°C.

2.1.8.7 cDNA synthesis from mRNA

cDNA was synthesised using the High-capacity cDNA reverse transcription kit (Applied Biosystems). 10µl of reverse transcription (RT) master mix, prepared as per **Table 22**, was added to 10µl of equalised RNA and mixed via pipetting. Sample was then placed in a thermocycler (Applied Biosystems) and run as per **Table 23**. cDNA was then diluted 1:10 with nuclease free water and stored at -80°C.

Table 20. *Components used to make reverse transcription master mix for use with mRNA.*

Component	Volume added
10X RT buffer	2 µl
25X dNTP mix (100mM)	0.8µl
10X RT Random primers	2 µl
MultiScribe reverse transcriptase	1 µl
Nuclease free water	4.2 µl

Table 21. *Thermocycler conditions used for cDNA synthesis from mRNA.*

Setting	Step 1	Step 2	Step 3	Step 4
Temperature	25°C	37°C	85°C	4°C
Time	10 minutes	120 minutes	5 minutes	Hold

2.1.8.8 TaqMan Real-time polymerase chain reaction

For real-time polymerase chain reactions (RT-PCR) 5.5 µl of 1:10 cDNA was added to predetermined wells on a 96-well PCR plate (Applied Biosystems). A master mix was prepared, as per **Table 22**, with commercially bought TaqMan primers. 5.5 µl of mater mix was added to each well. Plate was sealed and centrifuged at 1000 x g for 1 minute at 4°C. Plate was inserted into a StepOne RT-PCR machine (Applied Biosystem), and run as per **Table 23**.

Table 22. *Components of TaqMan RT-PCR master mix.*

Component	Volume added
TaqMan master mix	5 µl
Primer	0.5 µl

Table 23. *TaqMan RT-PCR cycling conditions.*

Setting	Step 1	Step 2	Step 3	Step 4
Temperature	50°C	95°C	95°C	60°C
Time	2 minutes	2 minutes	1 second	20 seconds
Number of cycles	40			

2.1.8.9 cDNA synthesis from miRNA

cDNA was synthesised using the miRCURY LNA RT kit (Qiagen). 6µl of RT master mix was prepared as per **Table 24**. 2µl of equalised miRNA was added to RT master mix, sample was vortexed briefly. Sample was then placed in a thermocycler (Applied Biosystems) and ran as per **Table 25**. cDNA was then diluted 1:60 with nuclease free water and stored at -80°C.

Table 24. *Components used to make reverse transcription master mix for use with miRNA.*

Component	Volume added
5X miRCURY Syber green RT buffer	2 µl
Nuclease free water	5µl
10X miRCURY RT enzyme	1µl
Equalised miRNA (5ng/µl)	2µl

Table 25. *Thermocycler conditions used for cDNA synthesis from miRNA.*

Setting	Step 1	Step 2	Step 3
Temperature	42°C	95°C	4°C
Time	60 minutes	5 minutes	Hold

2.1.8.10 SyberGreen PCRs

For SyberGreen PCRs 3µl of 1:60 cDNA was added to predetermined wells on a 96-well PCR plate (Applied Biosystems). A master mix was prepared, as per **Table 26**, with commercially bought SyberGreen primers. 7µl of master mix was added to each well. Plate was sealed and centrifuged at 1000 x g for 1 minute at 4°C. Plate was inserted into a StepOne RT-PCR machine (Applied Biosystem), and run as **Table 27**.

Table 26. *Components of SyberGreen PCR master mix.*

Component	Volume added
2X miRCURY Syber Green master mix	5µl
Rox reference dye	0.5µl
Target specific primer	1µl
Nuclease free water	0.5µl

Table 27. *SyberGreen RT-PCR cycling conditions.*

Setting	Step 1	Step 2	Step 3	Step 4
Temperature	95°C	95°C	56°C	4°C
Time	2 minutes	10 seconds	1 minute	Hold
Number of cycles	40			

2.1.9 Identification of *miR-223-3p* mRNA targets

In order for miRNAs to elicit their functional effects they have to bind to specific target mRNAs. The most common method of identifying these target mRNAs utilises computational prediction methods which are based on the 3' UTR of mRNAs and the sequence of the seed region for the miRNA of interest. Using this workflow, as illustrated in **Figure 14**, TargetScan was initially used to identify targets of *miR-223-3p*. This algorithm uses comparative sequence analysis to predict potential mRNA targets of specific miRNAs, based on conserved sites in the 6mer, 7mer and 8mer sites that match the seed region of *miR-223-3p.* A second database, miRTarBase, was also utilised as it identifies targets that have previously been experimentally validated. Finally, miRNA targets from both if these databases were combined and visualized using mienturnet. These lists were combined and used for further bioinformatic analysis.



Figure 14. *Workflow for the identification of miR-223-3p targets in humans and mice.*

miR-223-3p targets where identified using target identification software. These lists where combined to generate a list of miRNA targets.

2.1.10 RNA Sequencing

2.1.10.1 Bioinformatic pipeline for the analysis of a treatment-naïve paediatric IBD RNA sequencing dataset

Bioinformatic analysis was performed on the Gene Expression Omnibus (GEO) dataset GSE109142. This dataset was chosen for further analysis as it phenocopied the treatment-naïve paediatric biopsies provided by Dr. Hussey from the NCRC in Dublin. The dataset contained the transcriptomic profiles from 226 rectal mucosal biopsies, taken from 206 treatment-naïve, paediatric UC patients and 20 control patients. Additionally, data was also available on the gender, age, severity of disease and responsiveness to treatment for each patient.

Initially, transcriptomic data for each patient was categorised as either control, responding to treatment and non-responders to treatment. Gene Set Enrichment Analysis (GSEA) was performed as described in section 2.1.10.6 to identify genes that were differentially expressed among the different patient cohorts. Further GSEA analysis, was performed at the GO, KEGG and Reactome levels to identify pathways were upregulated or down-regulated in each sub-group of patients. For analyse weighted enrichment analysis was performed and genes were ranked based on Signal2Noise. This method used to identify differentially expressed genes in patients based on the treatment they received; either 5-ASA oral or intravenous (IV) steroids, along with the corresponding outcome for each treatment; responders or non-responders.

A separate analysis was performed on this dataset to investigate the expression of *miR-223* target genes this patient cohort. *miR-223* target genes that had previously been identified as per section 2.1.9 were extracted and analysed as described above via GSEA analysis.

2.1.10.2 Sample preparation for RNA Sequencing

Total RNA was extracted from colon samples of mice treated with chronic AOM/DSS, as described in section 2.1.8.3, using the RNeasy kit (Qiagen). Total RNA was quantified as per section 2.1.8.6. Samples were then sent to Novogene were mRNA was purified using poly-T oligo-attached magnetic beads and was then used for sequencing.

2.1.10.3 Library Construction, Quality Control and Sequencing

Following fragmentation, first strand cDNA was synthesized using random hexamer primers. Second strand cDNA was synthesized using dTTP to create a non-directional library. The library underwent quality control checks using Qubit, qPCR and bioanalyzer for size distribution. Once quantified, the libraries were pooled and Illumina PE150 sequencing was performed. To obtain clean reads, the raw data in fastq format was processed to remove any reads that contained adapter, ploy-N or were of low quality. Following this, the Q20, Q30 and GC content was determined for the clean reads. All subsequent analysis was performed using the clean reads.

2.1.10.4 Mapping to the reference Genome and gene expression quantification

In order to map the clean reads, the reference genome and gene model annotation files were downloaded from genome website. An index of the reference genome was created using Histat2 v2.0.5 and paired-end clean reads were aligned to the reference genome using Hisat2 v2.0.5 mapping tool. To quantify gene expression levels, the counts of read numbers mapped to each gene was determined using FeatureCounts v1.5.0-p3. Following this, the FPKM (fragments Per Kilobase of transcript sequence per Millions base pairs sequenced) of each gene was determined based on the length of the gene and the read counts for that gene.

2.1.10.5 Differential expression analysis

To determine the differential expression, DESeq2 R package (1.20.0) was utilized. This method determines differential expression using a negative binominal distribution model. The generated p-values were adjusted using the Benjamini and Hochberg method for controlling the false discovery rate. Genes with an adjusted P-value <=0.05 were considered differentially expressed.

2.1.10.6 Enrichment analysis of differentially expressed genes

Genes that were differentially expressed were further analysed by NovoGene using the ClusterProfiler R package to perform Gene Ontology (GO) enrichment, KEGG and Reactome analysis. Terms that had an adjusted p value of <=0.05 were classified as being significantly enriched by genes that were differentially expressed. Further independent Gene Set Enrichment Analysis (GSEA) (http://www.broadinstitute.org/gsea/index.jsp) was performed to investigate GO, KEGG and Reactome pathways. For GSEA analysis weight enrichment analysis was performed and genes were ranked based on Signal2Noise. A schematic illustrating the process from sample preparation through to bioinformatic analysis is shown in **Figure 15.**

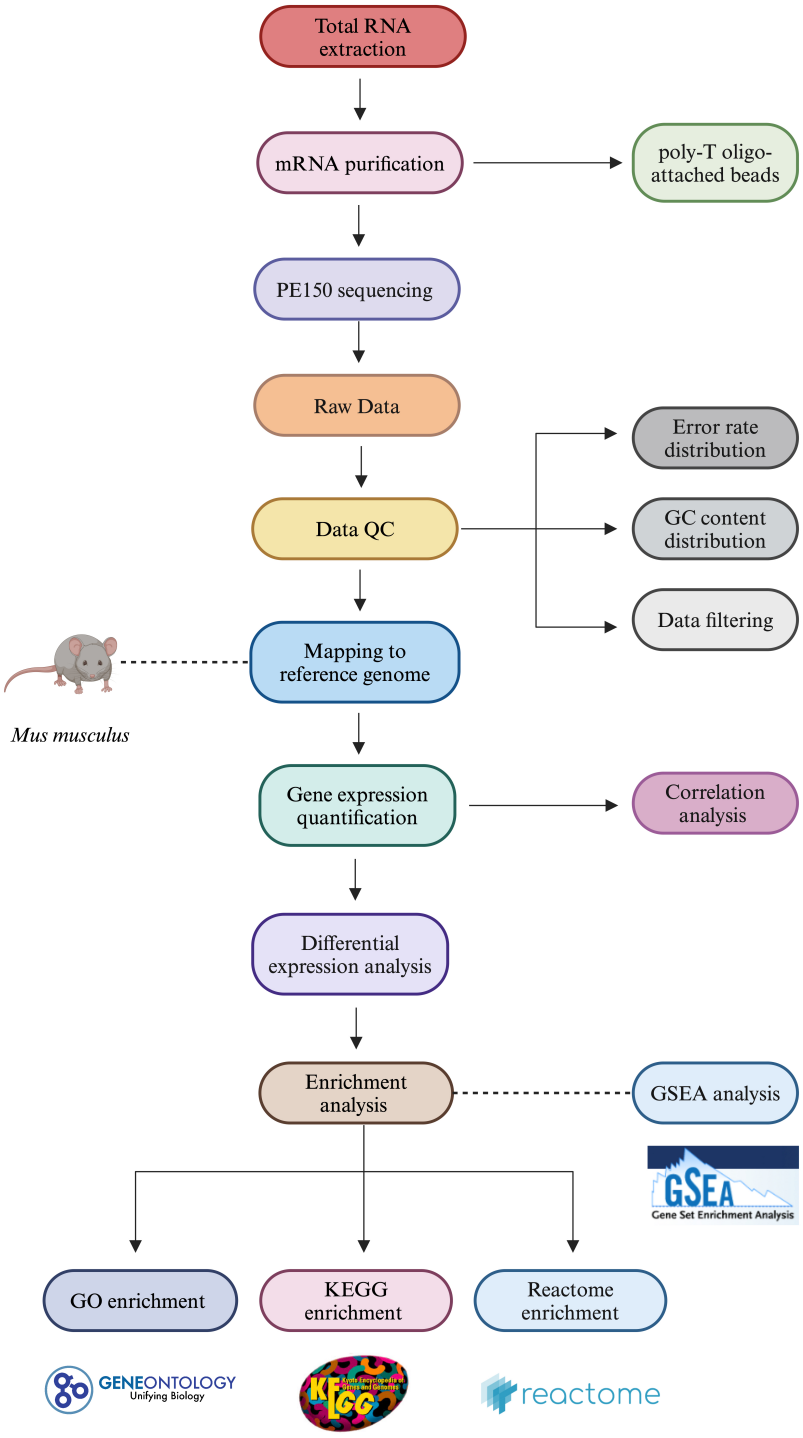


Figure 15. *Overview of RNA sequencing from sample preparation to bioinformatic analysis.*

RNA was extracted from whole colonic mouse tissue. This was then sequenced by Novogene which involved various quality control checks. Sequences where then mapped to the reference genome, expression was determined and analysis was performed.

CHAPTER 3 INVESTIGATING THE EXPRESSION OF *MIR-223* IN PAEDIATRIC PATIENTS WITH ULCERATIVE COLITIS

INTRODUCTION

Inflammatory bowel diseases (IBD) are chronic relapsing inflammatory diseases of the gastrointestinal tract. IBD encompasses Crohns disease (CD) and Ulcerative colitis (UC). These are both multifactorial diseases that stem from interplay between the hosts microbiome, immune system, genetics along with their environment. Collectively, this results in a dysregulation of the hosts immune system potentially leading to the initiation and progression of disease. Globally, IBD among paediatric patients is increasing (Pivac et al., 2023, Benchimol et al., 2011a).

UC is a chronic inflammatory disease of the colon, characterised by mucosal inflammation that initially begins in the rectum and extends proximally to the caecum (Segal et al., 2021). In Ireland, the incidence of IBD among children has been reported as increasing from 2.5 cases per 100,000 in 2001 to 5.2 cases per 100,000 in 2010 (Hope et al., 2012, Skafi et al., 2020). Similar findings have been reported globally, with the incidence and prevalence of paediatric patients being diagnosed with UC increasing (Benchimol et al., 2011a).

Paediatric patients with UC present with similar clinical symptoms to adults, including abdominal pain, weight loss, tiredness and bloody diarrhoea. However, paediatric patients typically present with more severe and extensive disease at diagnosis than adults. Due to the severity of disease, 34% of paediatric patients living with UC are steroid refractory within a year of diagnosis (Turner et al., 2018). Additionally, 50-75% of paediatric patients have extended or pancolitis (Schechter et al., 2015, Van Limbergen et al., 2008). In comparison, adults are predominantly diagnosed with left-sided UC, with 14–35% being diagnosed with pancolitis (Ungaro et al., 2017).

Paediatric patients with UC are at increased risk of disease progression due to duration and extent of disease. Multiple studies investigating the long-term progression of the disease have highlighted that of those diagnosed with left-sided UC, 60-80% had progressed to pancolitis within 5 years (Malaty et al., 2013, Gower-Rousseau et al., 2009). Additionally, one follow-up study showed that 52% of paediatric patients required hospitalization within 5 years of their initial UC diagnosis. Similarly, 16.4% and 20.6% of patients from this cohort underwent colectomy within 5 and 10 years respectively (Benchimol et al., 2011b). Rapid diagnosis, combined with a minimally invasive method to monitor disease progression and response to therapeutics, will play a central role in improving long-term outlook for paediatric patients with

UC. Additionally, there is a need for new therapeutics and improved understanding of the disease mechanisms that drive UC. One potential is to identify critical regulatory check points of the immune responses, that might identify therapeutic targets, such as microRNAs.

miRNAs are small non-coding RNAs that are critical for controlling gene expression. In the colon, miRNAs have a variety of functions including the regulation of intestinal immunity and inflammation. Additionally, they have the ability to alter the production, differentiation and function of immune cells in response to environmental ques (Hirschberger et al., 2018). Furthermore, there dysregulation is associated with many diseases, and numerous miRNAs are implicated in UC as shown in **Table 28**.

Of these miRNAs, *miR-223* has been identified as a critical regulator of the innate immune response during active UC (Yuan et al., 2018). *miR-223* is highly expressed in the myeloid compartment and can control myeloid differentiation and function. Depletion studies have demonstrated that in an acute DSS model of UC, infiltrating neutrophils and monocytes are the initial source of *miR-223*. Furthermore, studies on irradiated WT mice receiving bone marrow from *miR-223*$^{-/y}$ mice, have shown that hematopoietic deficiency of *miR-223* aggravates DSS induced colitis (Neudecker et al., 2017b). This indicates that increased *miR-223* expression in the early inflammatory stages of UC is from infiltrating myeloid cells.

The expression of *miR-223* has previously been shown to be upregulated in patients with active UC. Its role was demonstrated to be anti-inflammatory as *miR-223*$^{-/y}$ mice had exacerbated colitis and nanoparticle delivery impaired DSS induced colitis, by limiting cytokine mediated dysregulation (Neudecker et al., 2017b). Further studies have verified this finding with delivery of a *miR-223* agomir limiting DSS induced colitis and delivery of its antagomir exacerbating disease. Additionally, expression of pro-inflammatory cytokines IL-6, IL-17 and TNF-α were all reduced upon treatment with a *miR-223* agomir and expression of the anti-inflammatory cytokine IL-10 was increased. It was also hypothesized that *miR-223* is involved in the regulation of IL-6/STAT3 signalling, as overexpression of *miR-223* leads to reduced expression of IL-6, gp130 and p-STAT3 (Zhang et al., 2021a). As *miR-223* overexpression reduces DSS induced UC, it is currently being proposed as a therapeutic target to constrain disease progression.

In patients with UC, early diagnosis and treatment of disease is central to improving patient outcomes. Currently, the most accurate method of diagnosing UC is via colonoscopy.

However, this method is invasive, particularly for paediatric patients (Dilillo et al., 2019). To address this miRNAs have been proposed as non-invasive biomarkers for the detection of disease, monitoring its progression and individual response to therapeutics (Salla et al., 2023). miRNAs are detectable and stable in tissue and a variety of bodily fluids including urine, blood, saliva and faeces (Weber et al., 2010). As previously mentioned, *miR-223* expression is increased in colonic biopsies from patients with active UC (Zhou et al., 2021). Separate studies have shown that expression of *miR-223* is also upregulated in blood, serum and faecal samples from patients with active UC (Yarani et al., 2022, Schönauen et al., 2018). While further research is needed, miRNAs are viable biomarkers for both diagnosing disease and as indicators of disease progression.

Table 28. *Differentially expressed miRNAs in Ulcerative colitis.*

miRNA	Expression	Reference
miR-126	Upregulated in patients with active UC and contributes to disease by targeting an inhibitor of the NF-κB pathway	(Feng et al., 2012)
miR-142	Increased expression in patients with active UC	(Han et al., 2018)
miR-155; miR-122; miR-146a	Increased colonic expression in paediatric patients with UC	(Béres et al., 2016)
miR-20b; miR-93; miR-125b	Upregulated in patients with UC	(Coskun et al., 2013)
miR-21	Increased in patients with UC and contributes to inflammation; promotes TNF- α expression	(Bakirtzi et al., 2016) (Ke et al., 2024)
miR-214	Increased in patients with active UC and correlates with disease activity	(Polytarchou et al., 2015)
miR-223	Upregulated in patients with active UC and regulates intestinal inflammation	(Neudecker et al., 2017b) (Wang et al., 2016a)
miR-143; miR-145	Decreased during in patients with chronic UC	(Pekow et al., 2012)
miR-146a	Downregulated in UC patients and expression negatively correlated with expression of inflammatory markers	(Feng et al., 2020a)
miR-192	Decreased expression in colonic epithelial cells during active UC	(Wu et al., 2008)

AIMS OF THIS CHAPTER

The overall aim of this chapter was to evaluate two cohorts of treatment-naïve paediatric patients with UC. Specific aims where to:

1. Evaluate a large treatment-naïve paediatric UC RNA seq data set, identify potential pathways implicated in non-responsiveness to therapeutics and their potential link to *miR-223.*
2. Assess an Irish treatment-naïve paediatric UC cohort for the expression of *miR-223-3p* and inflammatory genes associated with treatment non-responsiveness in UC. Compare this validation cohort to the RNA seq analysis from the discovery cohort in aim 1.
3. Determine if *miR-223-3p* correlates with the expression of disease-associated inflammatory markers in an Irish UC paediatric cohort.

3.1.1 Characteristics of treatment-naïve paediatric patients with Ulcerative colitis

The publicly available dataset, GSE109142, contained the mucosal transcriptome 206 treatment-naïve paediatric patients with UC and 20 controls from Cincinnati children's hospital in the US. Patient characteristics are shown in **Table 29**. The average age of patients with UC at biopsy was 12.9 years and 54% of the cohort were male. The control group were age and sex matched to the UC cohort. At diagnosis patients were assessed using the Paediatric Ulcerative Colitis Activity Index (PUCAI) scoring system (**Appendix Table 2**). On this basis, 34% of patients had severe disease, 41% moderate disease and 26% mild. Mayo endoscopic scoring had comparable results, with 13%, 52% and 34% of patients being classified as having mild, moderate or severe disease respectively. 81% of patients had pancolitis at diagnosis and 19% had left-sided colitis. In this cohort of patients, 34% were initially given oral steroids, 34% IV steroids and 26% were treated with 5-ASA. Four weeks after initial treatment 51% of patients were in remission (**Table 29**).

Table 29. *Characteristics of control and patients with Ulcerative colitis from GSE109142 cohort.*

Characteristic	Control (n=20)	Paediatric patients with Ulcerative Colitis (n=206)
Average age at biopsy (+/- SD)	13.9 years (+/- 3.3)	12.9 years (+/- 3.2)
Sex	Male: 45% Female: 55%	Male: 54% Female: 46%
PUCAI score	_	<34 Mild: 26% <35-64 Moderate: 41% ≥65 Severe: 33%
Mayo endoscopy score	_	Mild: 13% Moderate: 52% Severe: 34%
Disease location	_	Rectosigmoid colitis: 19% Pancolitis: 81%
Initial treatment	-	Mesalamine(5-ASA): 26% Oral steroids: 40% IV steroids: 34%
Week 4 remission (PUCAI <10)	-	Yes: 51% No: 49%
Week 4 faecal calprotectin (<250µg/mg)	-	26%

3.1.2 Identification of differentially expressed genes between control and treatment-naïve paediatric patients with Ulcerative colitis

To identify genes that are differentially expressed in paediatric patients with UC, the RNAseq data from GSE109142 discovery cohort was analysed (**Figure 16**). In patients diagnosed with UC, differential expression analysis showed 19,256 genes were upregulated and 11,323 were downregulated compared to controls (**Figure 17 A**). To determine if gene expression was altered among patients who were treatment responsive or non-responsive, patients were stratified based on their 4-week remission following treatment, with those having a PUCAI <10 classified as treatment responsive. In treatment non-responsive patients, 24,118 genes were upregulated and 8,088 downregulated compared to controls (**Figure 17 B**). In analysis of patients that responded to treatment vs control, 24,323 genes were identified as upregulated and 7,601 were downregulated (**Figure 17 C**). This analysis was performed on treatment responsive vs non-responsive patients, which showed no genes were differentially expressed between the two groups (**Figure 17 D**). As treatment non-responsiveness is associated with poor prognosis, early identification of these patients is critical. Thus, all further analysis was performed on treatment non-responsive patient's vs control.

3.1.3 Myeloid inflammatory pathways are upregulated in treatment non-responsive paediatric patients with Ulcerative colitis

To assess the impact of disease in treatment non-responsive patients, unbiased GSEA analysis was performed on the discovery cohort. Analysis of hallmark pathways revealed that patients had an enriched signature for 'inflammation', 'epithelial mesenchymal transition', interferon gamma and 'IL-6/STAT3 signalling' compared to controls (**Figure 18 A - D)**. GO enrichment analysis also showed that pathways associated with poor clinical outcome in UC were significantly positively enriched in treatment non-responsive patients, including 'acute inflammatory response', 'macrophage cytokine production', 'chemokine production' and 'interleukin 6 production' (**Figure 19 A**). KEGG analysis showed that 'cytokine-cytokine receptor interactions', 'chemokine signalling', 'hematopoietic cell lineage' and 'JAK/STAT' signalling were all significantly increased in treatment non-responders (**Figure 19 B**). Following Reactome analysis, 'chemokine receptors bind chemokine receptors', 'signalling by interleukins', 'interleukin 6 signalling' and 'interferon signalling', were significantly positively

enriched in treatment non-responsive patients (**Figure 19 C**). Collectively, these data show that early myeloid inflammation, chemokine and myeloid associated pathways could be contributing to treatment non-responsiveness in patients with UC.

3.1.4 *miR-223-3p* target genes are differentially expressed genes between control and treatment-naïve paediatric patients with Ulcerative colitis

miR-223 has previously been shown to be critical for regulating the innate immune response during UC and its expression is increased in mucosal biopsies from patients with active inflammation. Furthermore, *miR-223* has been implicated in the regulation of several pathways identified as significant in the discovery cohort (**Figure 18** + **Figure 19**). However, little is known about the expression of *miR-223* targets in patients who are treatment non-responsive following diagnosis. To address this, *miR-223-3p* target genes in both mouse and humans were first identified using Target Scan and miRTarBase (**Appendix Table 3-6**). These targets where identified in the discovery cohort GSE109142 (**Figure 16)** and differentially expressed target genes were identified. In patients diagnosed with UC, differential expression analysis showed 179 genes were upregulated and 137 were downregulated compared to controls (**Figure 20 A + Appendix Table 7**). In treatment non-responsive patients, 181 genes were upregulated and 158 were downregulated compared to controls (**Figure 20 B + Appendix Table 8**). These data shows that *miR-223* targets are differentially expressed in treatment non-responsive paediatric patients with UC vs controls.

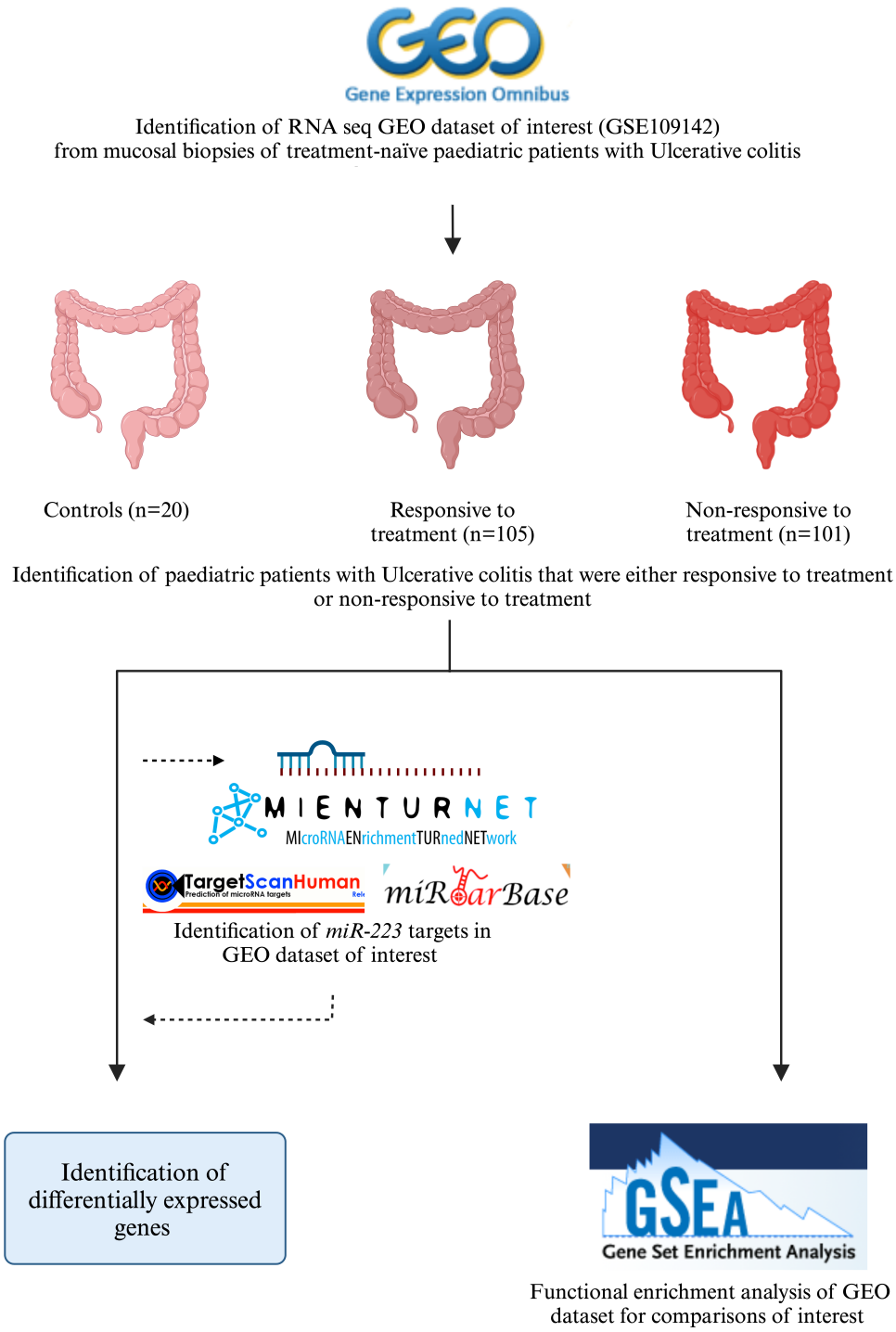


Figure 16. *Overview of bioinformatic workflow performed on the mucosal transcriptome of treatment-naïve paediatric patients with Ulcerative colitis.*

The GEO dataset, GSE109142, containing the mucosal transcriptome from rectal biopsies of treatment-naïve paediatric patients with Ulcerative colitis was identified. Patients were separated based on their response to treatment. RNA seq data was used to identify differentially expressed genes or perform GSEA analysis. Separately, *miR-223-3p* targets were identified in this dataset and differentially expressed targets were determined. Diagram created on BioRender.com.

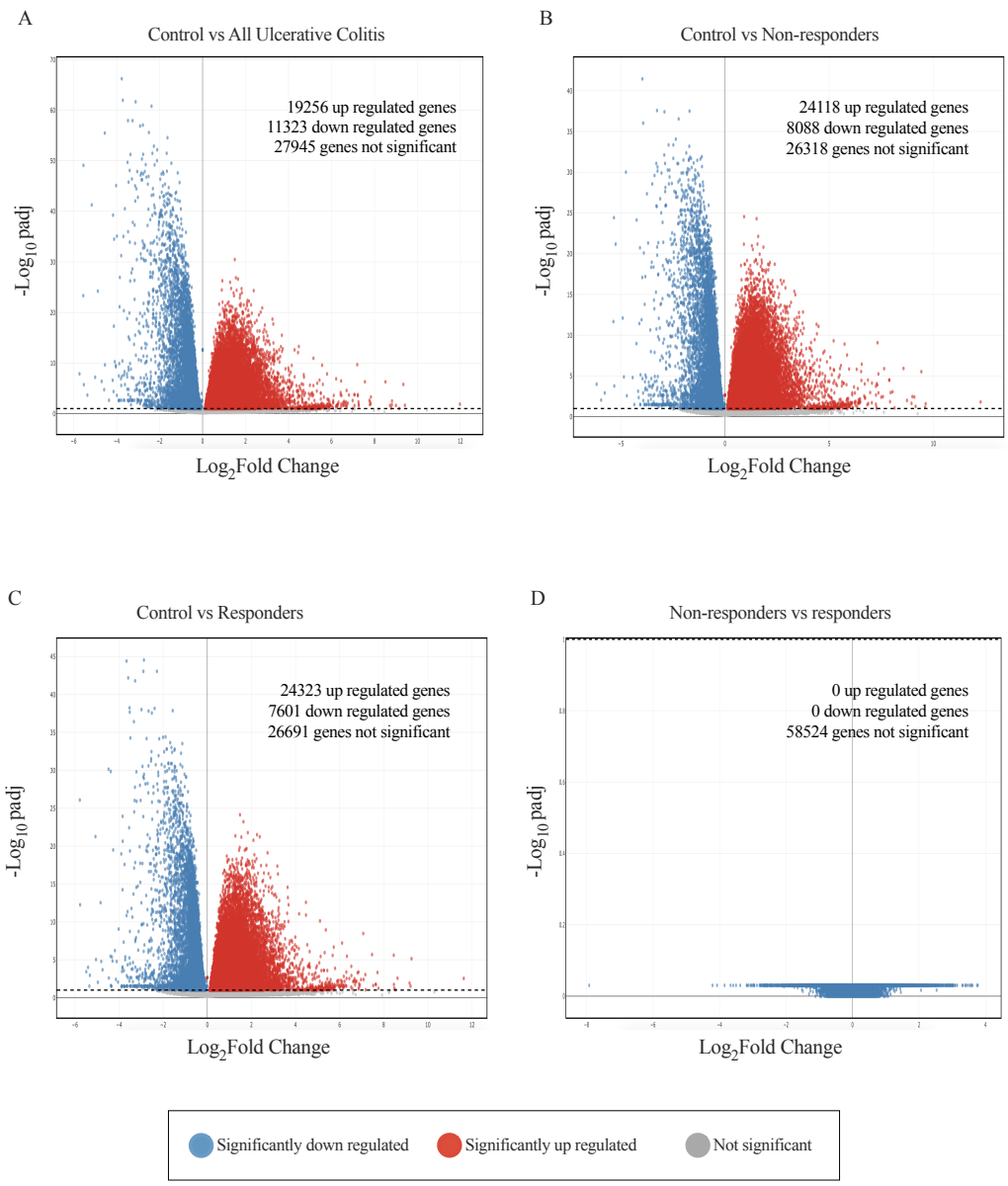


Figure 17. *Genes are differentially expressed between control and paediatric patients with Ulcerative colitis.*

Control and paediatric patients with UC from GSE109142 cohort were analysed to identify genes that were differentially expressed. Patients with UC were also divided into responders and non-responders of treatment to determine what genes were differentially expressed. Volcano plot of differentially expressed genes between **A.** Control and all with UC, **B.** Control and non-responders. **C.** Control and responders. **D.** non-responders and non-responders. Genes with a padj value of ≤0.1 were identified as significant, this yielded: **A.** 19256 up regulated genes; 11323 down regulated genes and 27945 genes that weren't significant **B.** 24118 up regulated genes; 8088 down regulated genes and 26318 genes that weren't significant. **C.** 24323 up regulated genes; 7601 down regulated genes and 26691 genes that weren't significant. **D.** 0 up regulated genes; 0 down regulated genes and 58524 genes that weren't significant **A.** Control n=20; All Ulcerative colitis n=206 **B.** Control n=20; non-responders n=101 **C.** Control n=20; Responders n=105 **D.** Responders n=105; non-responders n=101.

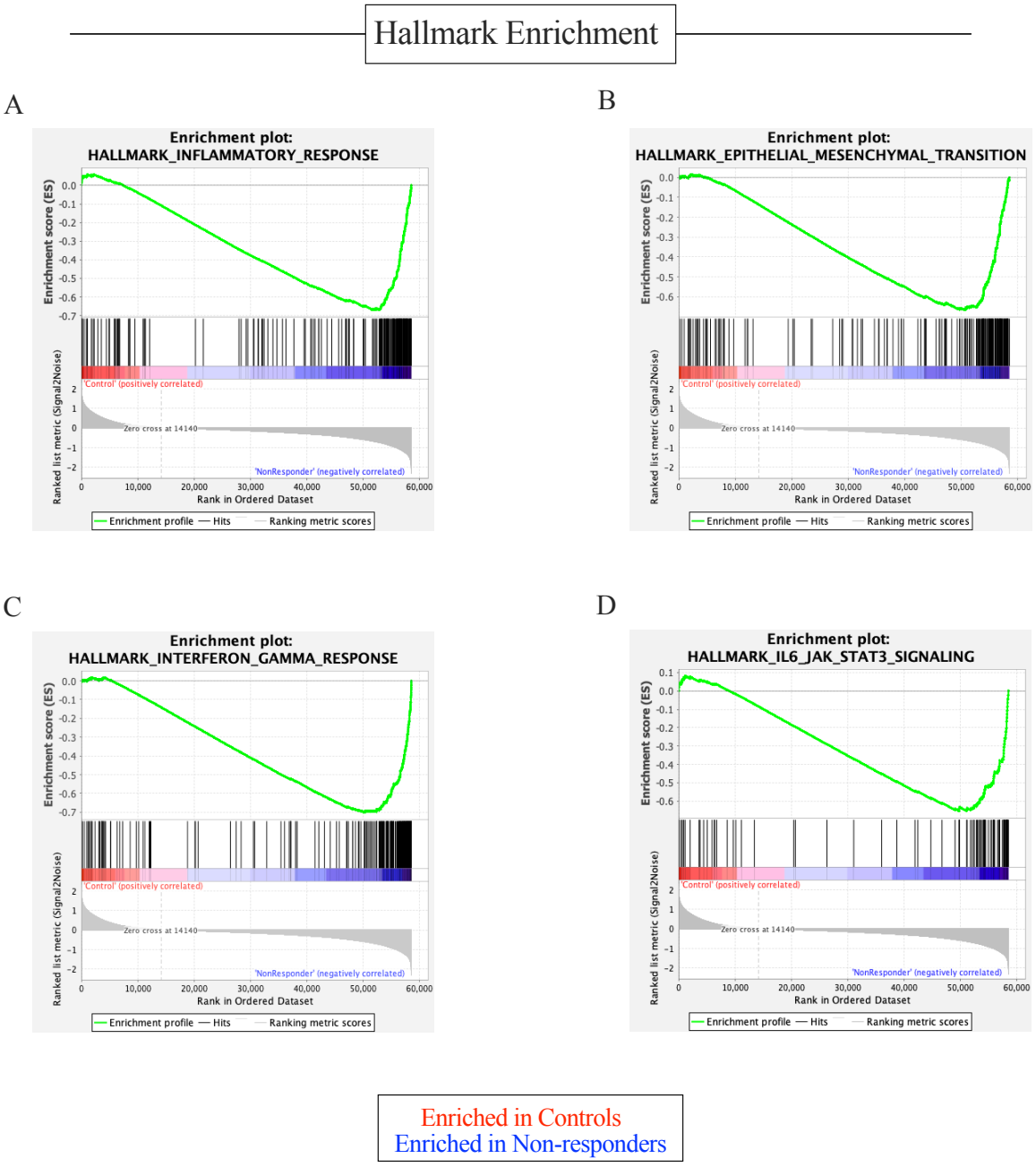


Figure 18. *Hallmark pathways associated with inflammation and poor prognosis in are upregulated in treatment non-responsive paediatric patients with Ulcerative colitis.*

GSEA analysis of Hallmark pathways was performed on RNA sequencing data from Control and paediatric patients with UC that where treatment non-responsive from GSE109142 cohort. **A.** Enrichment plot for Inflammatory Response (M5932) (NES: -1.9; FDR 0.015) **B.** Enrichment plot for Epithelial Mesenchymal Transition (M5930) (NES: -1.87; FDR q-val: 0.011) **C.** Enrichment plot for Interferon Gamma Response (M5913) (NES: -1.89; FDR q-val: 0.01) and **D.** Enrichment plot for IL-6/STAT3 signalling (M5897) (NES: -1.87; FDR q-val: 0.01). Controls n=20; non-responders n=101.

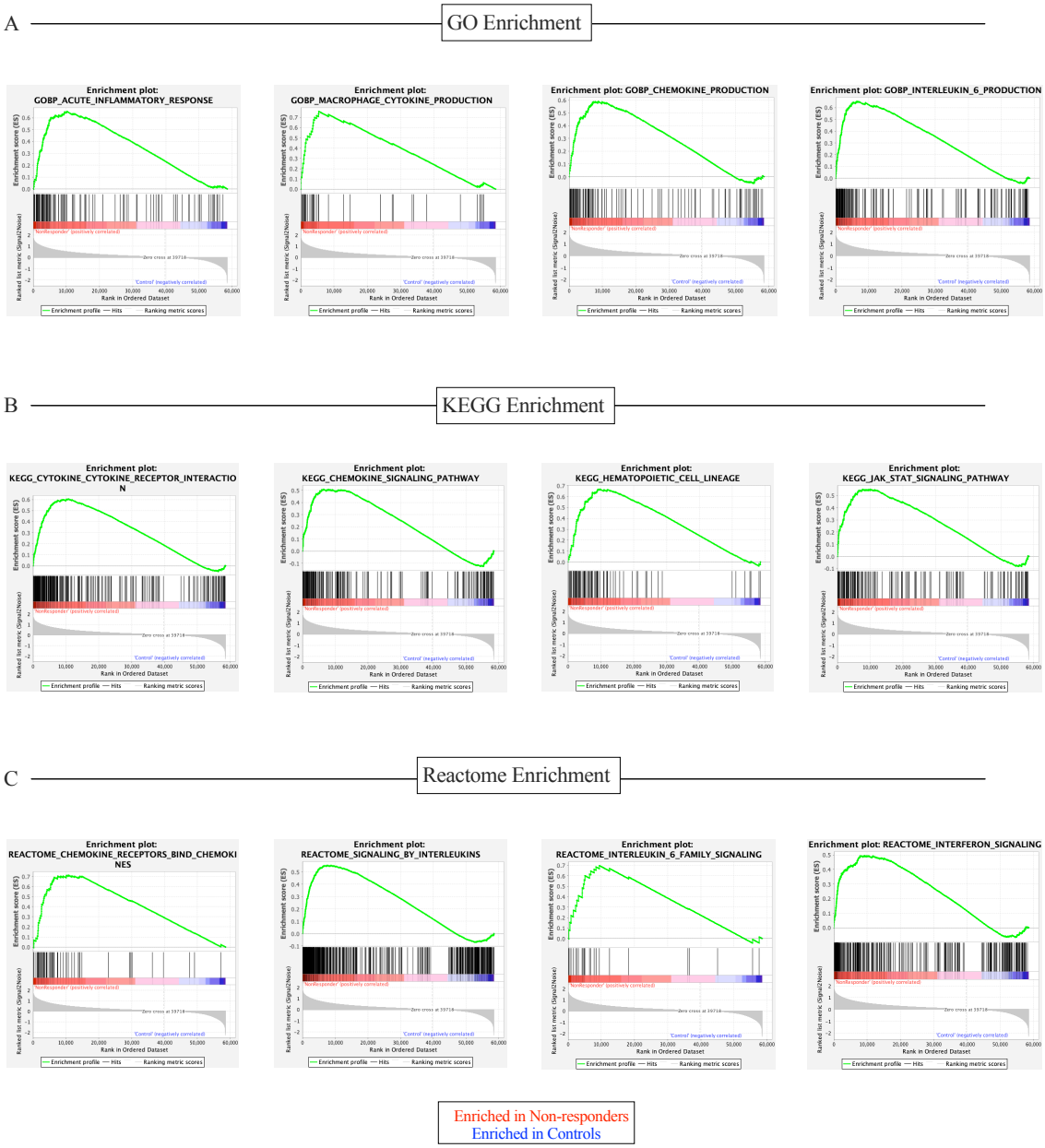


Figure 19. *Pathways associated with chemokine and cytokine signalling are upregulated in treatment non-responsive paediatric patients with Ulcerative colitis.*

Following GSEA analysis on RNA sequencing data from Control and paediatric patients with UC that where treatment non-responsive from the GSE109142 cohort, enrichment plots for **A.** Acute Inflammatory Response (M6557) (NES: -1.9; FDR 0.015); Macrophage Cytokine Production (M22703) (NES: 2.03; FDR 0.007); Chemokine Production (M23107) (NES: 1.87; FDR 0.01) and Interleukin 6 Production (M23123) (NES: 2.07; FDR 0.009); **B.** Cytokine-Cytokine Receptor Interaction (M9809) (NES: 2.05; FDR q-val: 0.001); Chemokine signalling (M4844) (NES: 1.64; FDR q-val: 0.07); Hematopoietic Cell lineage (M6856) (NES: 1.85; FDR q-val: 0.01) and JAK STAT Signalling (M17411) (NES: 1.88; FDR q-val: 0.01) **C.** Chemokine Receptors Bind Chemokines (M625) (NES: 1.83; FDR q-val: 0.03); Signalling By Interleukins (M874) (NES: 1.7; FDR q-val: 0.08; Interleukin 6 Family Signalling (M27604) (NES: 1.72; FDR q-val: 0.08) and Interferon Signalling (M983) (NES 1.522; FDR q-val: 0.24). Controls n=20; non-responders n=101.

3.1.5 Myeloid cell activity is increased in treatment non-responsive paediatric patients with Ulcerative colitis

The discovery cohort highlighted showed enhanced myeloid inflammation, and targets of the myeloid associated miRNA, *miR-223* where differentially expressed in treatment non-responsive patient's vs controls. Thus, to assess if myeloid activity was altered, unbiased GSEA analysis was performed. Analysis of myeloid associated pathways revealed these patients had an enriched signature for neutrophil recruitment including 'neutrophil migration' (M25402), 'neutrophil chemotaxis' (M34121) and 'neutrophil activation involved in immune response' (M42597) (**Figure 21 A - D**). Similarly, pathways associated with monocyte activity were increased such as 'regulation of monocyte differentiation' (M14623), 'monocyte activation' (M23505), 'monocyte aggregation' (M24392) and 'monocyte chemotaxis' (M15503) (**Figure 22 A - D**). Furthermore, treatment non-responsive patients had increased macrophage activation with pathways including 'macrophage cytokine production' (M22703), 'macrophage chemotaxis' (M14291), 'macrophage activation involved in the immune response' (M10789) and 'macrophage activation' (M42597) all significantly enriched (**Figure 23 A - D**). Collectively, this suggests that the early myeloid immune response is an important indicator of patient response to treatment.

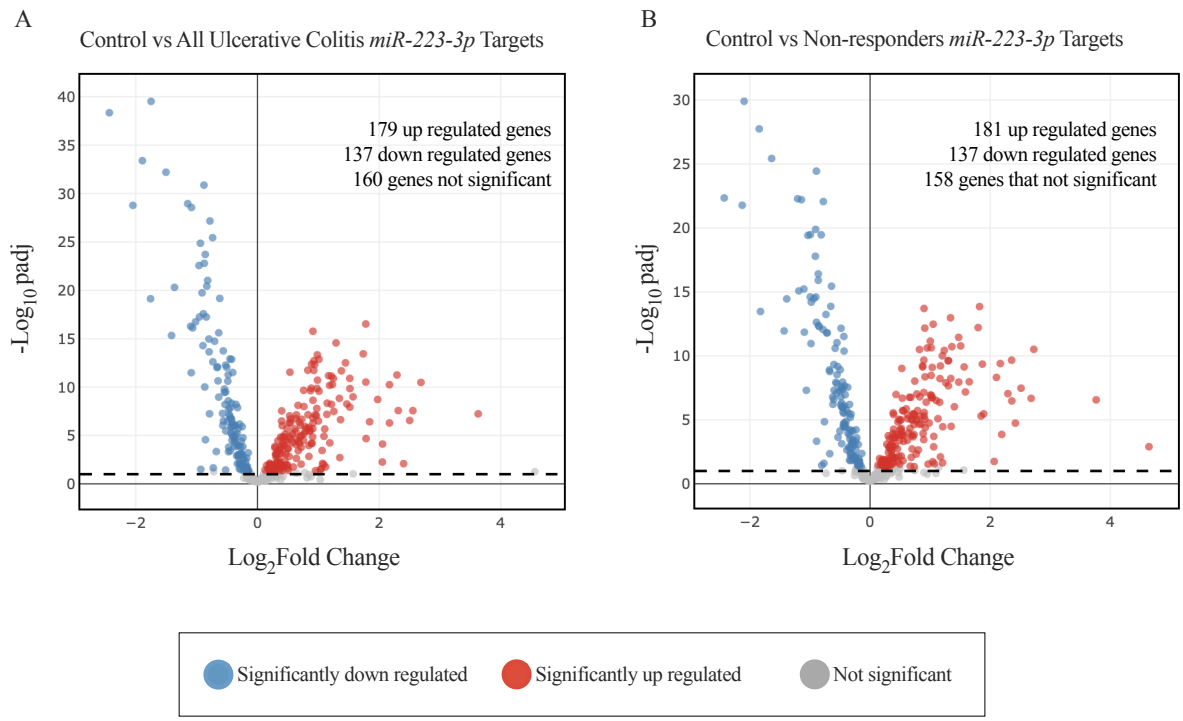


Figure 20. *miR-223-3p target genes are differentially expressed among control and treatment non-responsive paediatric patients with Ulcerative colitis.*

Due to its role in the regulation of the innate immune response during intestinal inflammation in patients with UC, *miR-223-3p* targets were identified in both control vs all paediatric patients with UC, and control vs treatment non-responsive patients with UC, from GSE109142 cohort. Targets were then analysed to identify differentially expressed genes. Volcano plot of differentially expressed *miR-223-3p* genes for **A.** Control vs all patients with UC and **B.** Control vs non-responders. Genes with a padj value of ≤0.1 were identified as significant, this yielded: **A.** 179 up regulated genes; 137 down regulated genes and 160 genes that weren't significant **B.** 181 up regulated genes; 137 down regulated genes and 158 genes that weren't significant. **A.** Control n=20; All Ulcerative colitis n=206 **B.** Control n=20; non-responders n=101.

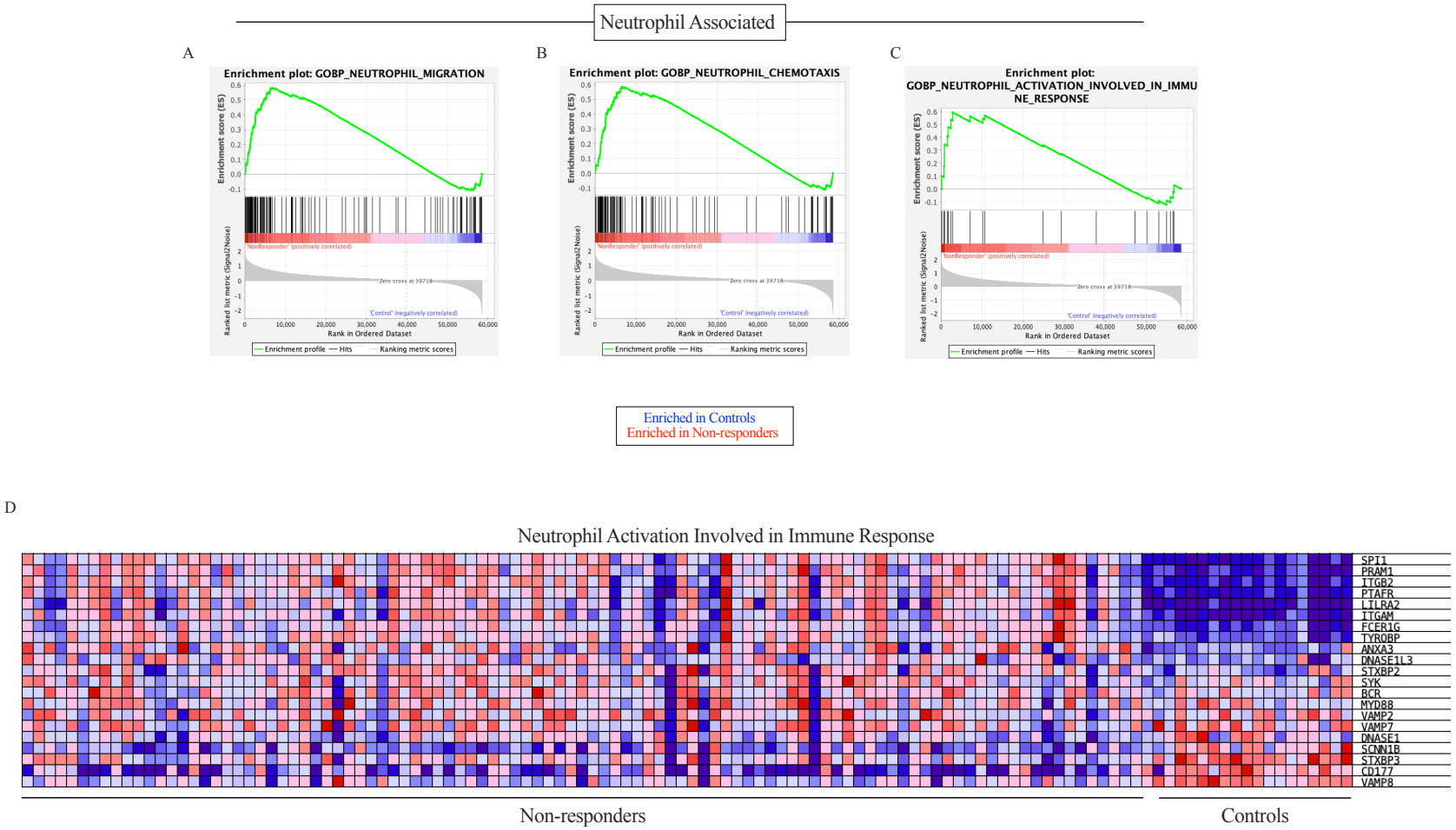


Figure 21. *Neutrophil recruitment is upregulated in treatment non-responsive paediatric patients with Ulcerative colitis.*

Following GSEA analysis on Control vs treatment non-responsive UC patients from the GSE109142 cohort, enrichment plots for **A.** Neutrophil Migration (M25402) (NES: 1.82; FDR q-val: 0.01) B. Neutrophil Chemotaxis (M34121) (NES: 1.82; FDR q-val: 0.01) **C.** Neutrophil Activation Involved in Immune Response (M42597) (NES: 1.52; FDR: 0.08) **D.** Heat map for Neutrophil Activation Involved in Immune Response (M42597) (NES: 1.52; FDR: 0.08). Controls n=20; non-responders n=101.

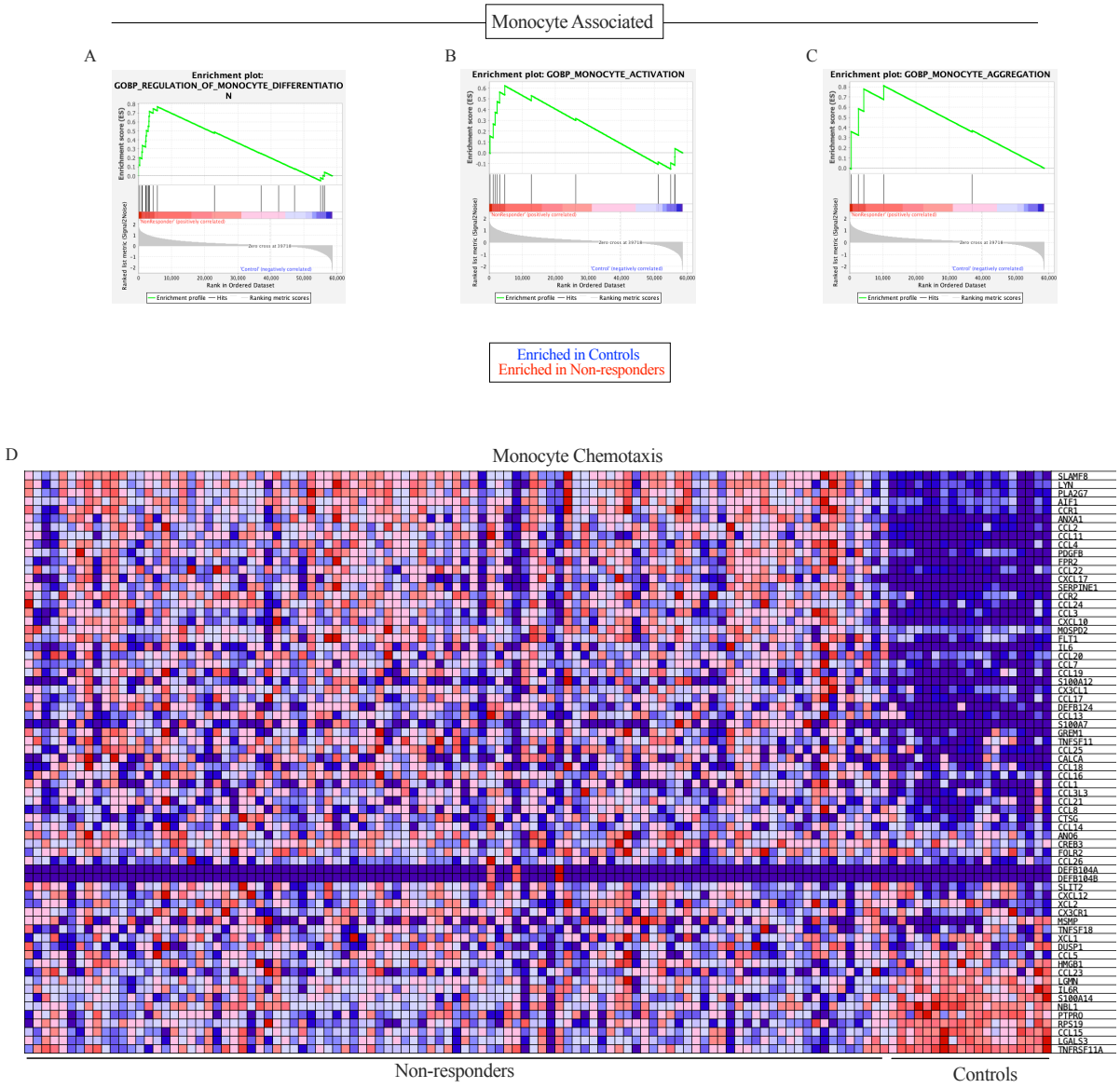


Figure 22. *Monocyte activity is upregulated in treatment non-responsive paediatric patients with Ulcerative colitis.*

Following GSEA analysis on control vs treatment non-responsive patients with UC, enrichment plots where generated for **A.** Regulation of Monocyte Differentiation (M14623) (NES: 1.87; FDR q-val: 0.009) **B.** Monocyte Activation (M23505) (NES: 1.55; FDR q-val: 0.03) **C.** Monocyte Aggregation (M24392) (NES: 1.45; FDR: 0.05) **D.** Heat map for Monocyte Chemotaxis (M15503) (NES: 1.70; FDR: 0.009). Controls n=20; non-responders n=101.

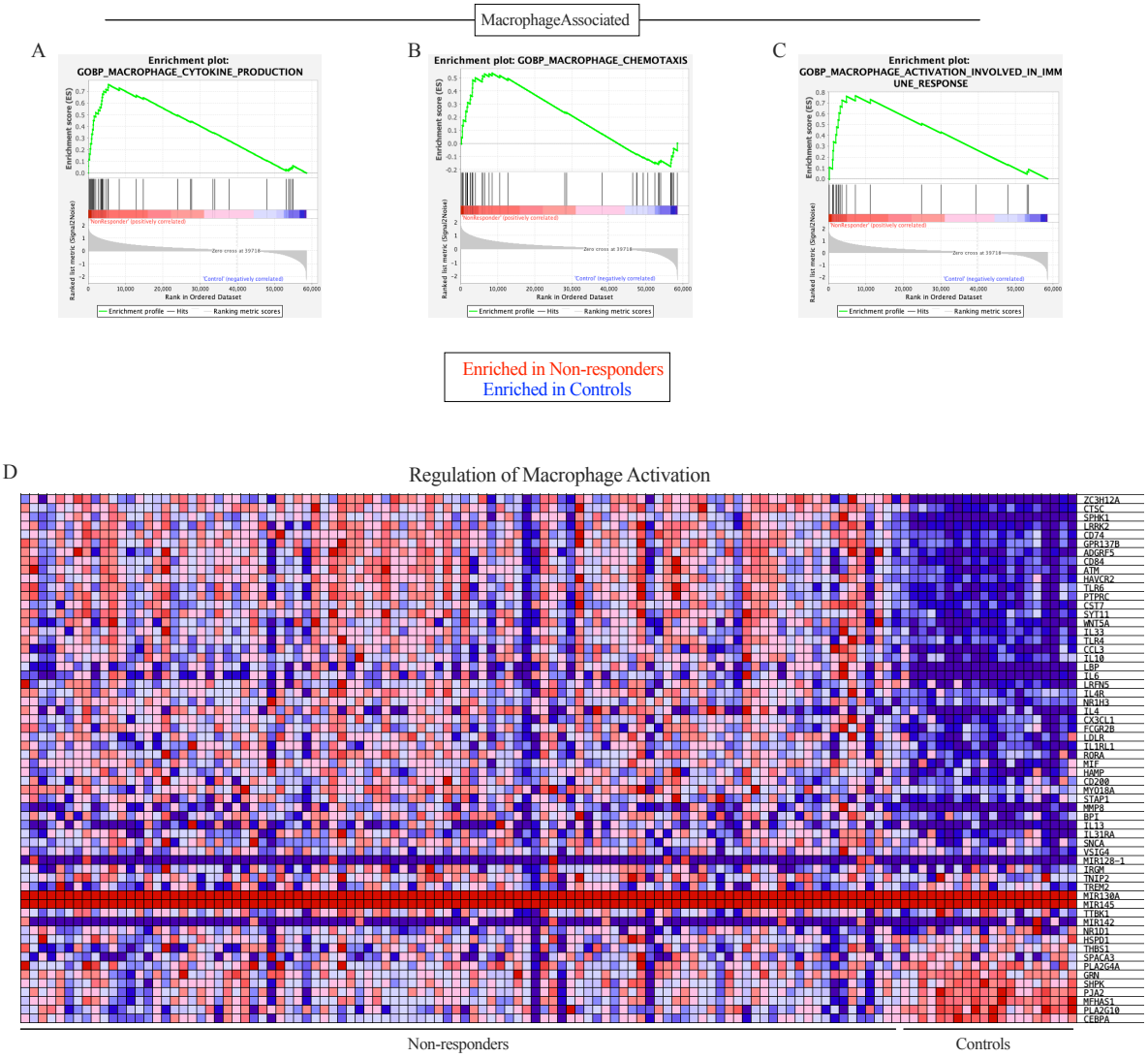


Figure 23. *Macrophage activation is upregulated in treatment non-responsive paediatric patients with Ulcerative colitis.*

Following GSEA analysis on control vs treatment non-responsive patients with UC, enrichment plots where generated for **A.** Macrophage Cytokine Production (M22703) (NES: 1.97; FDR q-val: 0.001) B. Macrophage Chemotaxis (M14291) (NES: 1.69; FDR q-val: 0.01) **C.** Macrophage Activation Involved in The Immune Response (M10789) (NES: 1.82; FDR: 0.002) **D.** Heat map for Macrophage Activation (M42597) (NES: 1.82; FDR: 0.003). Controls n=20; non-responders n=101.

3.1.6 Characteristics of an Irish treatment naïve paediatric Ulcerative Colitis cohort

In the previous cohort, GSE109142, treatment non-responsive paediatric patients had increased expression of pathways associated with poor prognosis in UC such as inflammation, cytokine signalling and myeloid infiltration. Furthermore, gene expression analysis stratifying patients with UC based on treatment responsiveness has recently been performed. This research identified inflammatory genes that can be used to distinguish between patients that will be treatment non-responsive (UC 1) vs those that will respond (UC 2) (Czarnewski et al., 2019). Samples from an Irish validation cohort, of treatment-naïve paediatric patients, where stratified into pancolitis or rectosigmoid colitis. This enabled the analysis and correlation of genes associated with treatment non-responsive patients (UC 1) as illustrated in **Figure 24**.

The Irish cohort contained samples from 18 treatment naïve paediatric patients with UC and 10 controls. Patient characteristics are shown in **Table 30**.The average age of patients with UC was 12.4 years and for controls it was 9.9 years. Males accounted for 66.6% of patients with UC and 60% of controls. 83.3% of the UC cohort were treatment naïve when biopsies were taken. On average patients has symptoms for 4.5 months prior to diagnosis. Of those diagnosed with UC, 50% had no prior family history of IBD. 77.7% had a previous history of atopy.

Clinical information was also recorded for these patients (**Table 31**). At diagnosis patients were assessed using the PUCAI scoring system (**Appendix Table 2)**, from this 27.7% of patients had severe disease, 44.44% moderate disease and 27.7% had mild disease. Extent of disease was determined using the Paris classification system (**Figure 25**), with patients being diagnosed with either ulcerative proctitis (11.11%), left-sided colitis (33.33%) and pancolitis (55.55%). Within a year of diagnosis 50% of patients has relapsed and 44% had severe disease. Two years post-diagnosis a further 5% of patients has relapsed. Initial treatment with 1st line therapeutics failed in 44.44% of patients. Furthermore, 38.8% of patients in this cohort were reliant on anti-TNF treatment within two years of diagnosis.

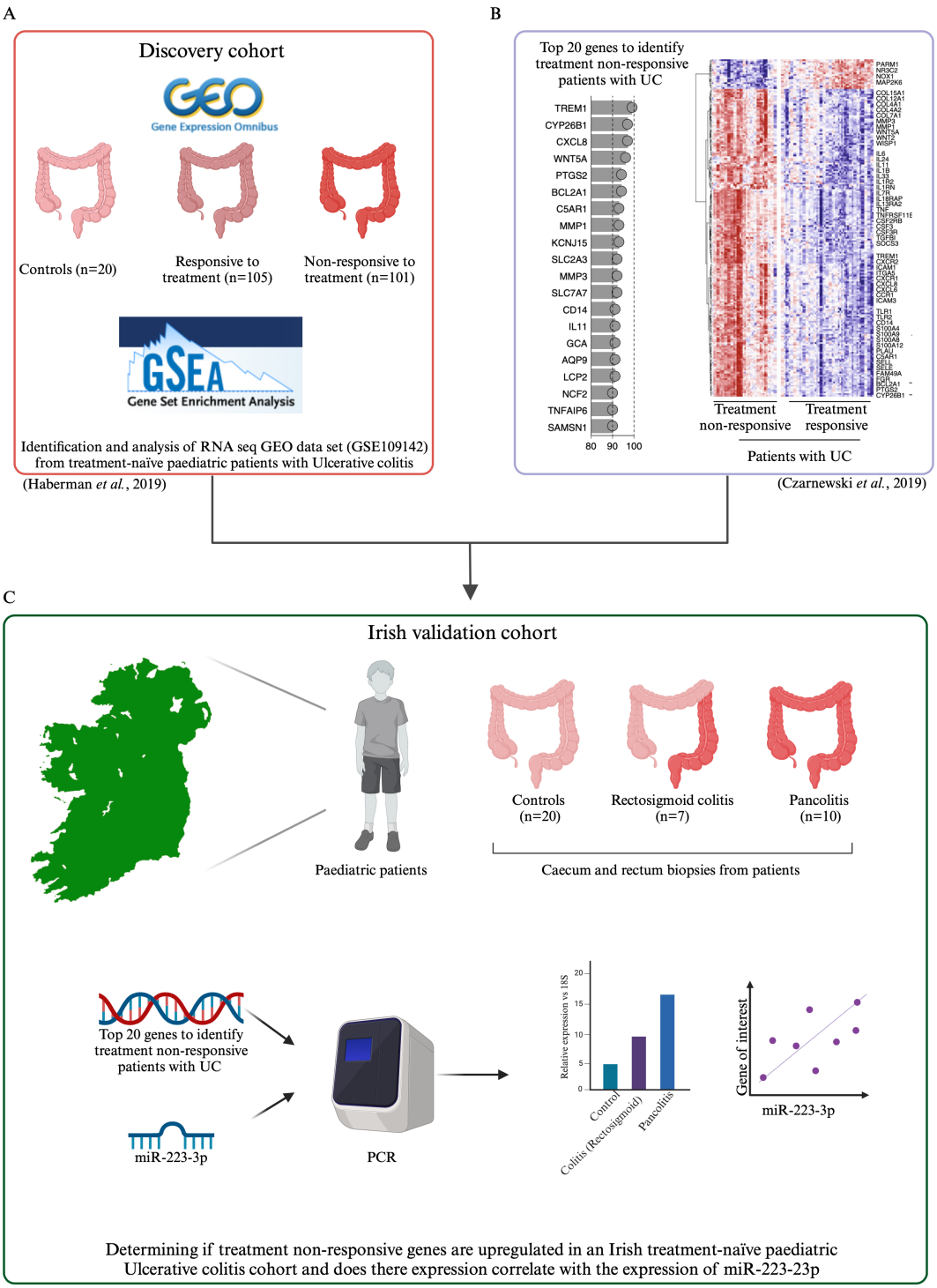


Figure 24. *Overview of workflow performed on caecum and rectum pinch biopsies from an Irish treatment naïve paediatric Ulcerative Colitis cohort.*

A. An RNA Seq dataset, GSE109142 (Haberman et al., 2019), of treatment-naïve paediatric patients with UC was identified and analysed. **B.** Top genes used for distinguishing treatment responsive vs treatment non-responsive patients was published (Czarnewski et al., 2019) **C.** Biopsies from Irish treatment-naïve paediatric patients with UC were analysed via RT-PCR for the expression of the top twenty genes used to identify treatment non-responsive patients. *miR-223* expression was analysed and correlated with the expression of the identified genes. Diagram created on BioRender.com.

Table 30. *Characterisation of an Irish treatment naïve paediatric Ulcerative Colitis cohort.*

Characteristic	Control (n=10)	Treatment naïve paediatric patients with Ulcerative colitis (n=18)
Total patient number	10	18
Gender	Male: 60% Female: 40%	Male: 66.6% Female: 33.33%
Average age at biopsy	9.957 years (SD +/- 3.730)	12.39 years (SD +/- 2.761)
Treatment naïve at biopsy	Yes: 90% No: 10%	Yes: 83.3% No: 16.6%
Family history of Inflammatory Bowel Disease	No: 60% Yes: 10% 2° Relative: 30%	No: 50% Yes: 22.22 % 2° Relative: 5.55% >2° Relative: 22.22%
Duration of symptoms prior to diagnosis	-	4.5 months (SD +/- 3.871)
Previous history of Atopy	-	No: 22.22% Yes: 77.7%
Family history of Atopy	-	No: 33.3% Yes: 66.66%
Household smoking pre-diagnosis	-	Yes: 66.66% No: 33.33%

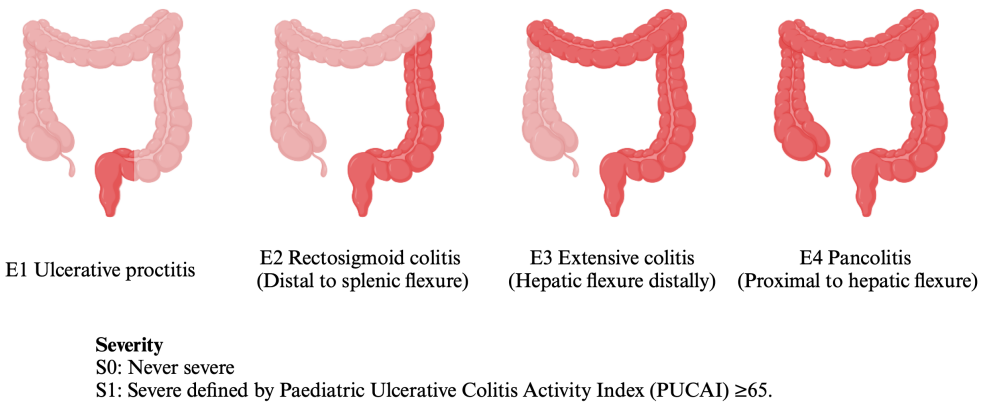


Figure 25. *Paris classification for phenotyping paediatric patients with Ulcerative colitis.*

Paris classification system is used to stratify patients based on extent of disease as being either 'E1 Ulcerative proctitis', 'E2 Rectosigmoid colitis, 'E3 extensive colitis' or 'E4 pancolitis'. Diagram created on BioRender.com.

Table 31. *Summary of clinical information provided for Irish treatment naïve paediatric Ulcerative Colitis cohort.*

Characteristic	Treatment naïve paediatric patients with Ulcerative colitis (n=17)
PUCAI Score	<34 Mild: 27.77% <35-64 Moderate: 44.44% ≥65 Severe: 27.77%
Verified phenotype at diagnosis	Ulcerative proctitis: 11.11% Rectosigmoid colitis: 33.33% Pancolitis: 55.55%
Relapsed within a year post-diagnosis	Yes: 50% No: 44.44% Unknown: 5.55%
Severe disease within a year post-diagnosis	Yes: 44.44% No: 50% Unknown: 5.55%
Relapsed within two years post-diagnosis	Yes: 55.55% No: 27.77% Unknown: 16.66%
Failed 1st line agents	Yes: 44.44% No: 50% Unknown: 5.55%
Anti-TNF treatment required by 2 years post-diagnosis	Yes: 38.88% No: 55.55% Unknown: 5.55%

3.1.7 Inflammatory markers associated with treatment non-responsiveness are upregulated in treatment-naïve paediatric patients with pancolitis

As previously mentioned, inflammatory genes have recently been identified that can differentiate between patients with UC that are treatment responsive vs non-responsive (Czarnewski et al., 2019). However, the expression of these markers has yet to be determined in a treatment-naïve paediatric UC cohort. To address this, caecum biopsies were analysed from an Irish paediatric UC cohort via RT-PCR for the expression of these genes.

Caecum biopsies from healthy patients were used as controls. For all markers there was no differential expression between control and patients with rectosigmoid colitis. However,

patients with pancolitis presented with a significantly increased expression profile for genes associated with treatment non-responsiveness compared to the other groups assessed. Of these, there was an increase in pro-inflammatory and colitis-associated cytokines (IL-1β, MMP3 and NOS2, **Figure 26 A, D + K**). Interestingly, there was also a marked increase in the expression of IL-6/STAT3 signalling markers (IL-11, IL-6 and REG3G, **Figure 26 B, C + J**). Patients with pancolitis also had increased expression of neutrophil (CXCL8 and COL4A, **Figure 26 F + G)** and monocyte markers (CSF1, TREM2 and CCL2, **Figure 26 I, L + O)**. Furthermore, many biomarkers used for the diagnosis of UC were also increased in patients with pancolitis (TNF, S100A8, OSM and LCN2, **Figure 26 E, H, M + N)**. Interestingly, the protective marker MUC2 was the only marker that had increased expression in patients with rectosigmoid colitis vs patients with pancolitis (**Figure 26 P)**. Collectively, these data suggest that early myeloid driven inflammation is increased in patients with pancolitis.

3.1.8 Inflammatory markers associated with treatment non-responsiveness are increased in treatment-naïve paediatric patients with Ulcerative colitis

As inflammation is confined to the rectum in patients with rectosigmoid colitis, the expression of inflammatory genes was also assessed in rectum biopsies from treatment-naïve paediatric patients with UC. Rectum biopsies from healthy patients were used as controls. For all markers there was increased expression in patients diagnosed with UC vs controls (**Figure 27**). In both groups, there was an increase pro-inflammatory and colitis-associated markers (IL-1β, IL-11, IL-6, MMP3 and NOS2, **Figure 27 A – D + K).** Interestingly, there was a significant increase in the neutrophil markers (CXCL8 and COL4A, **Figure 27 F + G**) in patients with rectosigmoid colitis compared to controls. There was mixed expression of monocyte markers with similar expression of CSF1 across patient's groups but an increased expression of TREM2 and CCL2 in patients with UC vs controls (**Figure 27 I, L and O**). While non-significance trends of increased expression in was seen in patients with rectosigmoid colitis vs pancolitis patients for some markers (IL-1β, IL-6, MMP3, TNF, CXCL3, COL4A1, S100A8, REG3G, OSM, CCL2, **Figure 27**). There was similar expression of the protective marker MUC2 between all groups (**Figure 27 P**). Collectively, this data suggests that some inflammatory markers associated with treatment non-responsiveness are increased in rectum biopsies from both rectosigmoid colitis and pancolitis patients.

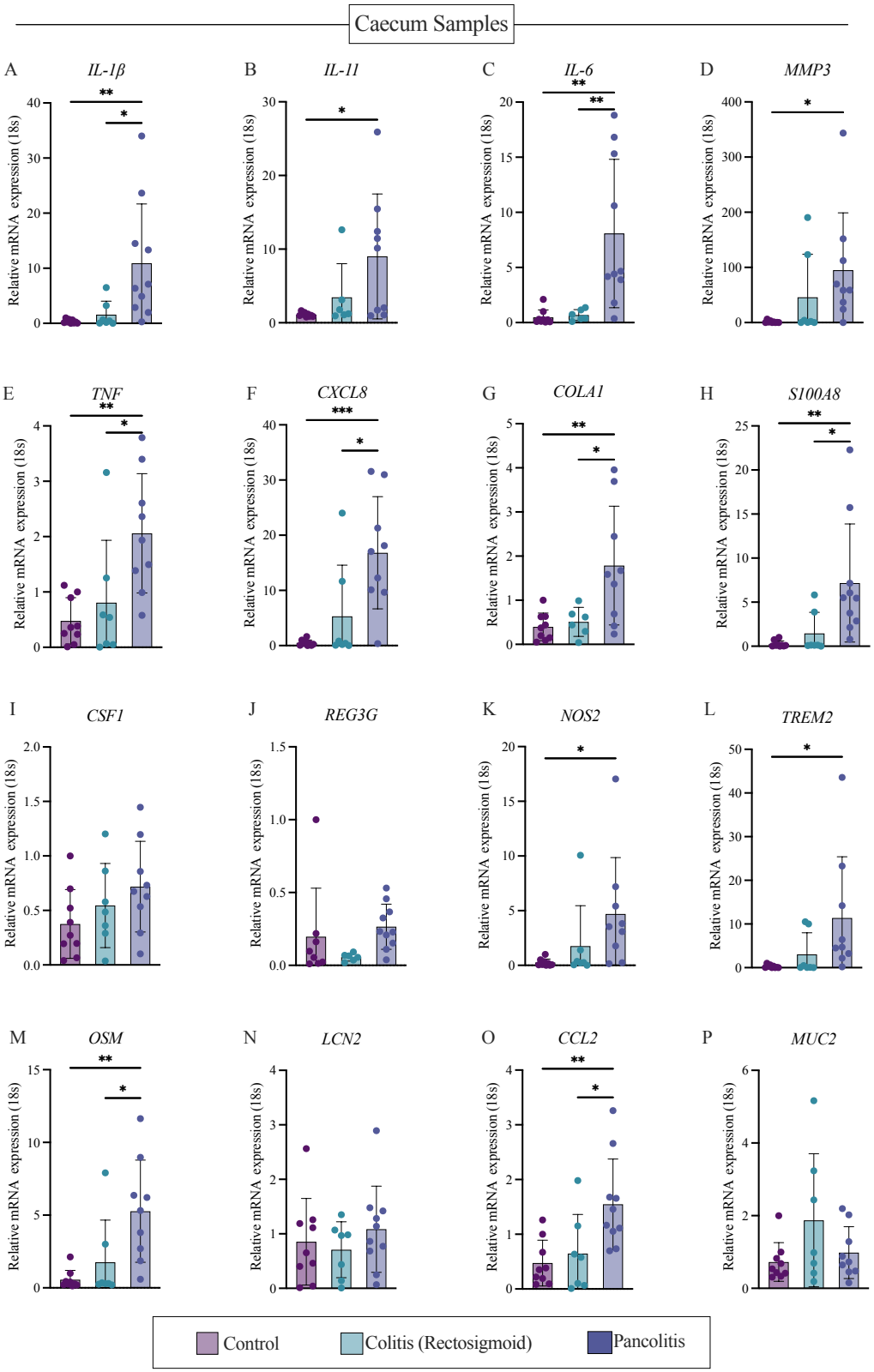


Figure 26. *Inflammatory markers are upregulated in caecum biopsies from patients with pancolitis.*

Relative mRNA expression in caecum biopsies from patients with pancolitis for **A.** IL-1β, **B.** IL-11, **C.** IL-6, **D.** MMP3, **E.** TNF, **F.** CXCL8, **G.** COL4A1 **H.** S100A8 **I.** CSF1 **J.** REG3G **K.** NOS2 **L.** TREM2, **M.** OSM, **N.** LCN2, **O.** CCL2 and **P.** MUC2. All data is expressed as mean ± SD *, P<0.05; **, P<0.01; ***, P<0.001, versus the indicated counterpart (One-way anova). **A-P** n=7-10 patients/group.

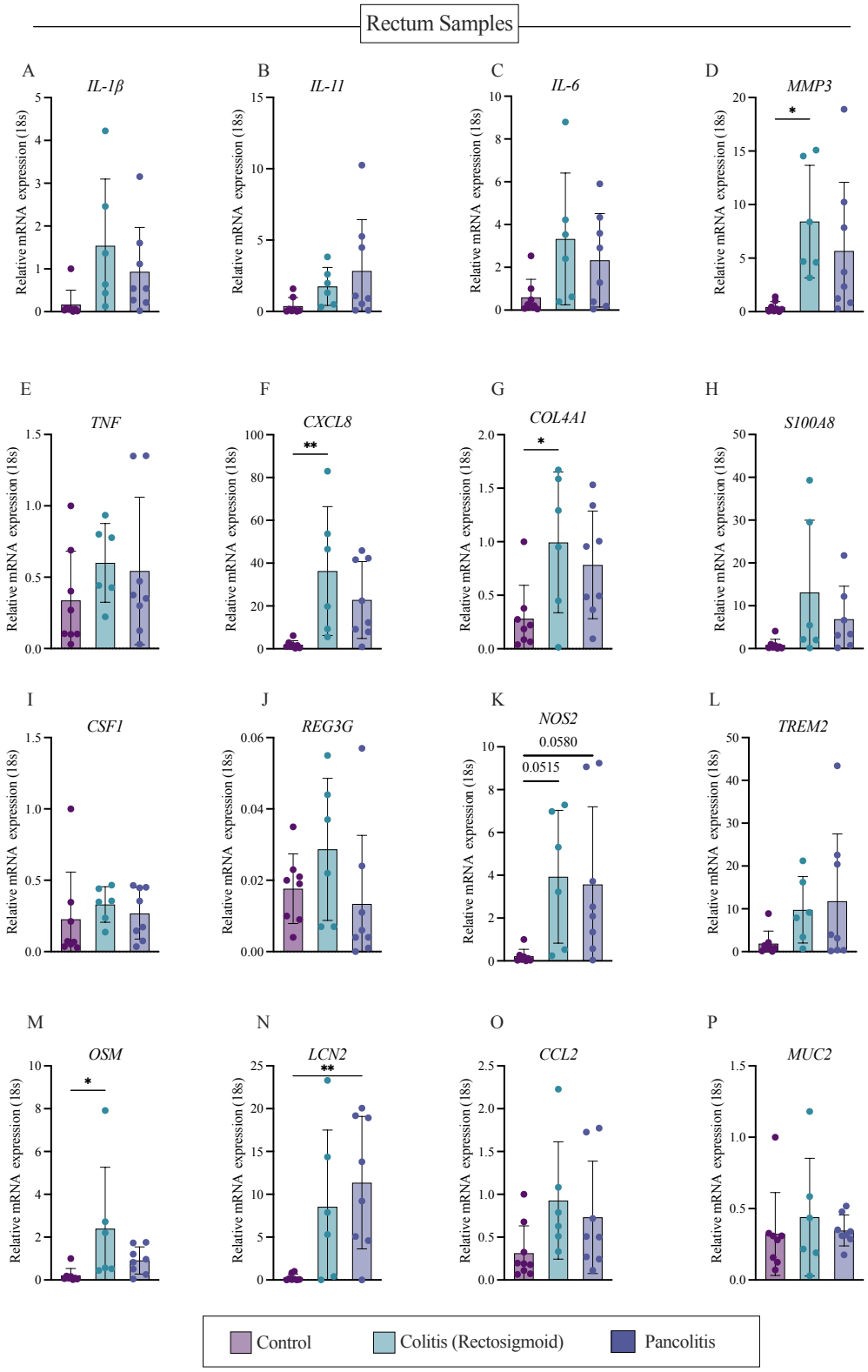


Figure 27. *Inflammatory markers are upregulated in rectal biopsies from patients with pancolitis.*

Relative mRNA expression in rectal biopsies from patients with pancolitis for **A.** IL-1β, **B.** IL-11, **C.** IL-6, **D.** MMP3, **E.** TNF, **F.** CXCL8, **G.** COL4A1 **H.** S100A8 **I.** CSF1 **J.** REG3G **K.** NOS2 **L.** TREM2, **M.** OSM, **N.** LCN2, **O.** CCL2 and **P.** MUC2. All data is expressed as mean ± SD; *, P<0.05; **, P<0.01; ***, P<0.001, versus the indicated counterpart (One-way anova). **A-P** n=6-9 patients/group.

3.1.9 *miR-223-3p* expression is increased in Irish treatment-naïve paediatric patients with pancolitis

miR-223-3p expression is known to be increased in patients with active colitis. As its expression is stable in various tissue and bodily fluids, it is also of interest as a non-invasive biomarker for the detection and progression of UC. However, its expression in treatment-naïve patients has yet to be determined. In caecum samples, *miR-223-3p* expression was comparable in control and patients with rectosigmoid colitis. However, pancolitis patients showed increased expression of *miR-223-3p* (**Figure 28 A**). Similar results were seen when *miR-223-3p* was measured in rectal samples, with pancolitis patients having enhanced expression compared to control and patients with rectosigmoid colitis (**Figure 28 B**). In contrast, blood samples obtained from control patients had higher expression of *miR-223* than those diagnosed with UC (**Figure 28 C**). This demonstrates that *miR-223-3p* expression is increased in colonic biopsies taken from treatment-naïve paediatric patients with diagnosed with pancolitis.

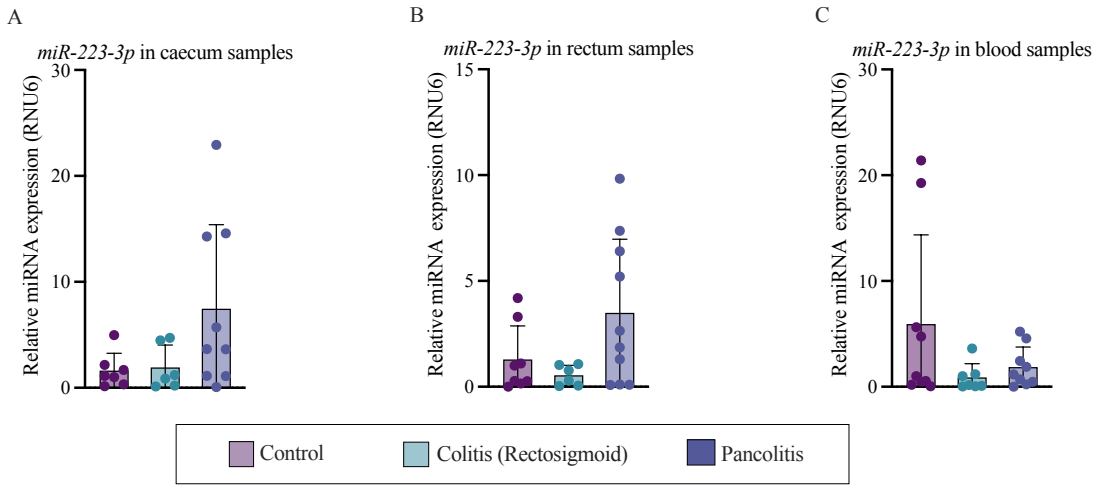


Figure 28. *miR-223-3p is increased in caecum and rectum biopsies from patients with pancolitis.*

A. Relative expression of *miR-223-3p* in caecum samples **B.** Relative expression of *miR-223-3p* in rectum samples **C.** Relative expression of *miR-223-3p* in blood samples. All data is expressed as mean ± SD; *, P<0.05; **, P<0.01; ***, P<0.001, ****, P<0.0001 versus the indicated counterpart (One-way anova). **A-C** n=6-10 patients/group.

3.1.10 *miR-223-3p* expression correlates with the expression of inflammatory markers in biopsies from pancolitis patients

To assess if *miR-223* expression correlated with the expression of inflammatory markers in the validation Irish cohort, pearson correlation analysis was performed on RT-PCR data generated from caecum and rectum samples of patients with rectosigmoid colitis and pancolitis. In caecum biopsies, *miR-223* expression positively correlated with the inflammatory markers OSM, MMP3 and IL-6 in patients with pancolitis (**Figure 29 A - C**). Furthermore, the neutrophil markers CXCL8 and COL4A1 were also positively trending (**Figure 29 D + E**). *miR-223* expression did not correlate with any other genes in patients with pancolitis (NOS2, TNF, S100A8, CCL2, MUC2, IL-1β, CCL2, IL-11, REG3G, LCN2 and CSF1 **Figure 29 F – I** + **Figure 30 A – G**). In caecum biopsies taken from patients with rectosigmoid colitis, there was no correlation between *miR-223* expression and the inflammatory markers assessed (**Figure 31 A – I** + **Figure 32 A – G**).

In rectum biopsies from patients with pancolitis, the inflammatory marker NOS2 and the UC biomarker LCN2 both negatively correlated with *miR-223-3p* expression (**Figure 33 A** + **D)**. Additionally, the expression of TNF which is a biomarker for UC and MMP3 a pro-inflammatory gene, were also negatively trending with *miR-223-3p* expression (**Figure 33 B** + **F)**. The monocyte and neutrophil markers, TREM2 and CXCL8, we also trending negatively with *miR-223-3p* expression (**Figure 33 C** + **E)**. For all other markers there was no correlation with *miR-223-3p* in rectum biopsies from patients with pancolitis (CSF1, OSM and IL-11 **Figure 33 G – I** + IL-6, CCL2, COL4A, S100A8, IL-1β, REG3G and MUC2 **Figure 34 A - G)**. In biopsies taken from patients with Rectosigmoid colitis, IL-6 negatively correlated with *miR-223-3p* expression, IL-11 showed the same trend. (**Figure 35 A + B**). There was no correlation with *miR-223-3p* for the other genes analysed (CXCL8, MMP3, OSM, LCN2, TNF, MUC2 and COL4A1 (**Figure 35 C – I** and CCL2, IL-1β, NOS2, CSF1, REG3G, S100A8 and TREM2; **Figure 36 A – G)**. Collectively, these data show that *miR-223-3p* expression correlates with several inflammatory markers that are used to identify treatment non-responsive patients with UC.

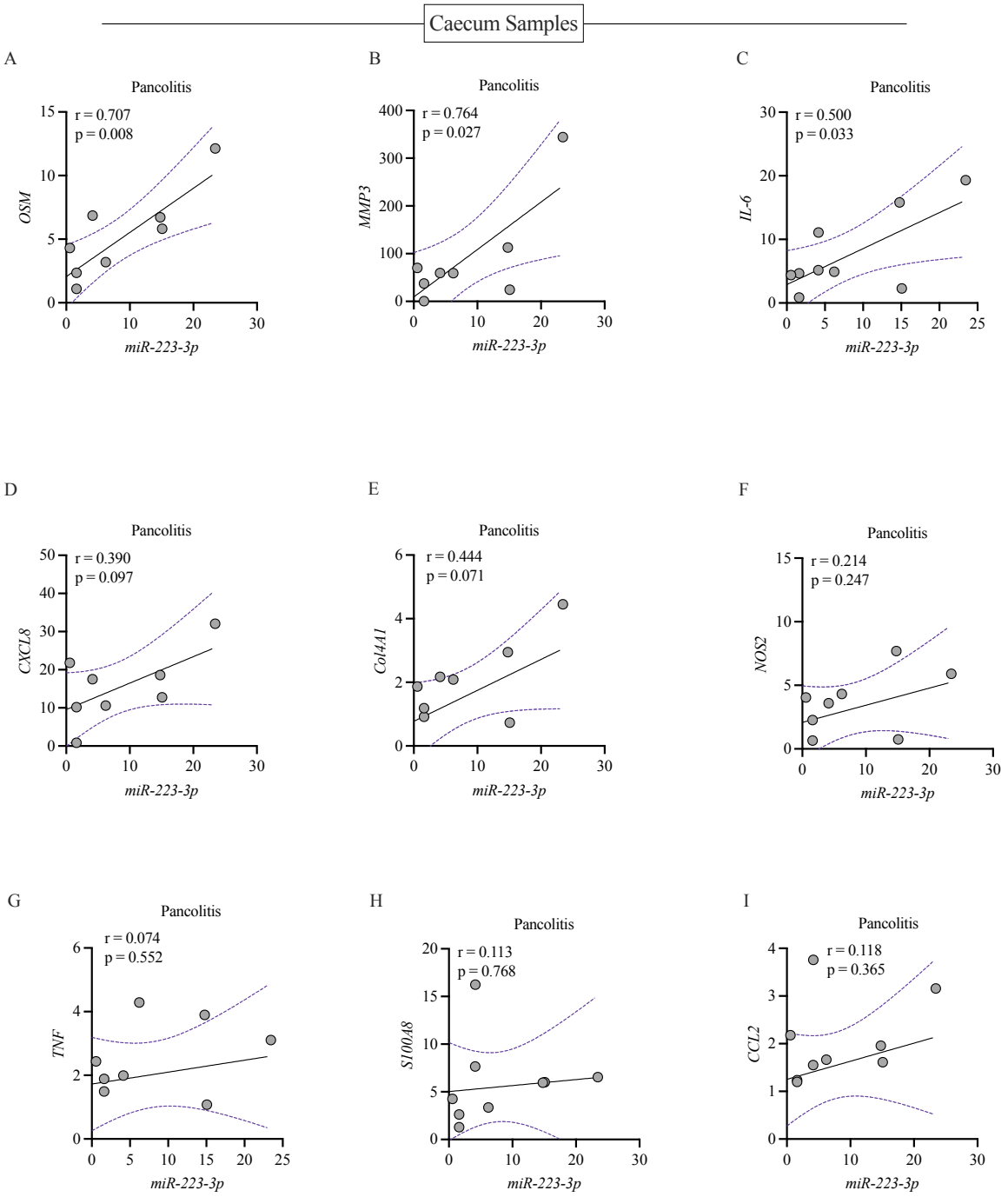


Figure 29. *The inflammatory markers OSM, MMP3 and IL-6 positively correlate with miR-223-3p expression in caecum biopsies from patients with pancolitis.*

Pearson correlation analysis of *miR-223-3p* expression in caecum biopsies with **A.** OSM, **B.** MMP3, **C.** IL-6, **D.** CXCL8, **E.** Col4A1, **F.** NOS2, **G.** TNF, **H.** S100A8 and **I.** CCL2. **A-I** n=9 patients/group; p-value of ≤ 0.05 was identified as a significant correlation.

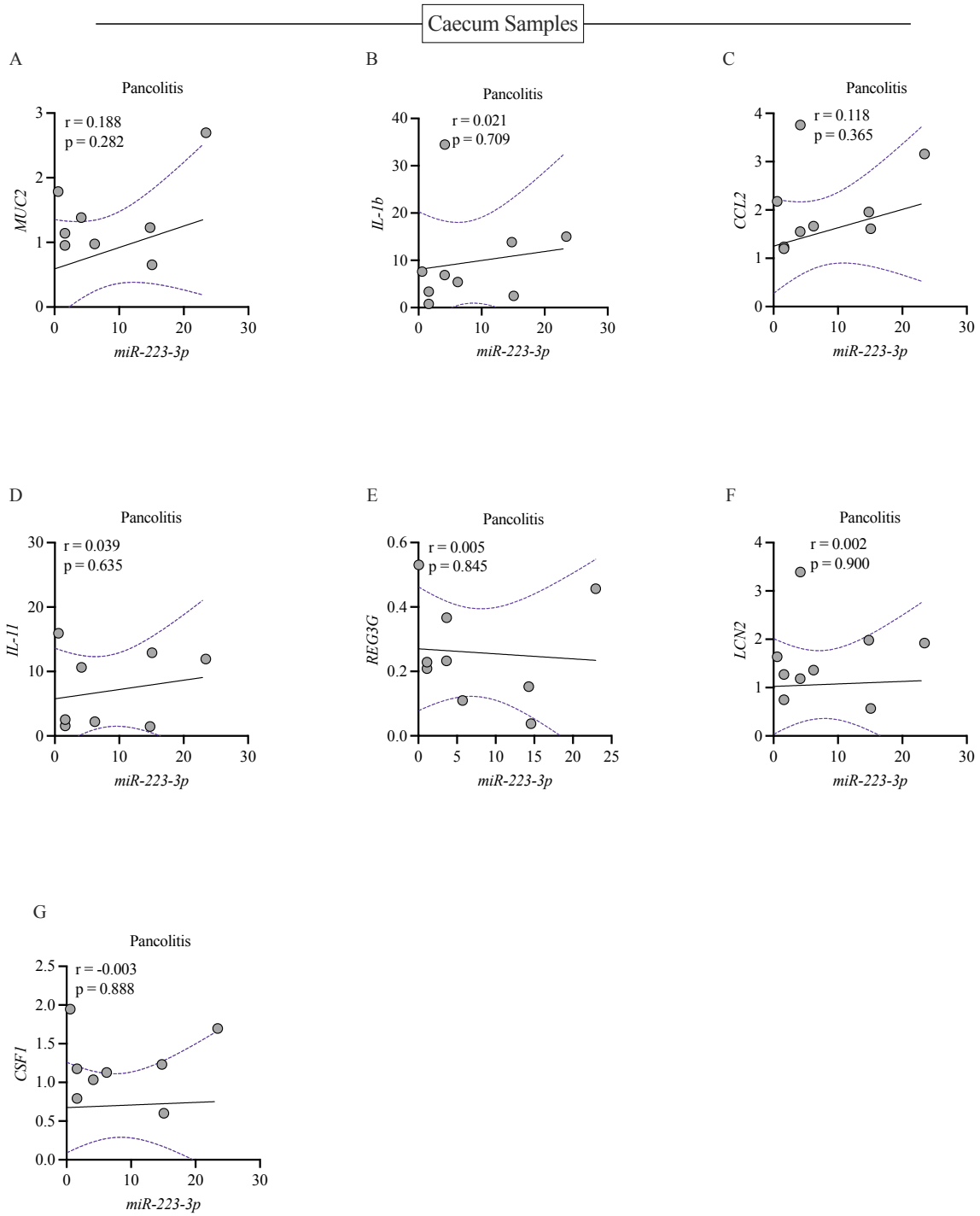


Figure 30. *miR-223-3p expression does not correlate with the inflammatory markers MUC2, IL-1β, CCL2, IL-11, REG3G, LCN2 or CSF1 in caecum biopsies from patients with pancolitis.*

Pearson correlation analysis of *miR-223-3p* expression in caecum biopsies with **A.** MUC2, **B.** IL-1β, **C.** CCL2, **D.** IL-11, **E.** REG3G, **F.** LCN2 and **G.** CSF1. **A-H** n=9 patients/group; p-value of ≤ 0.05 was identified as a significant correlation.

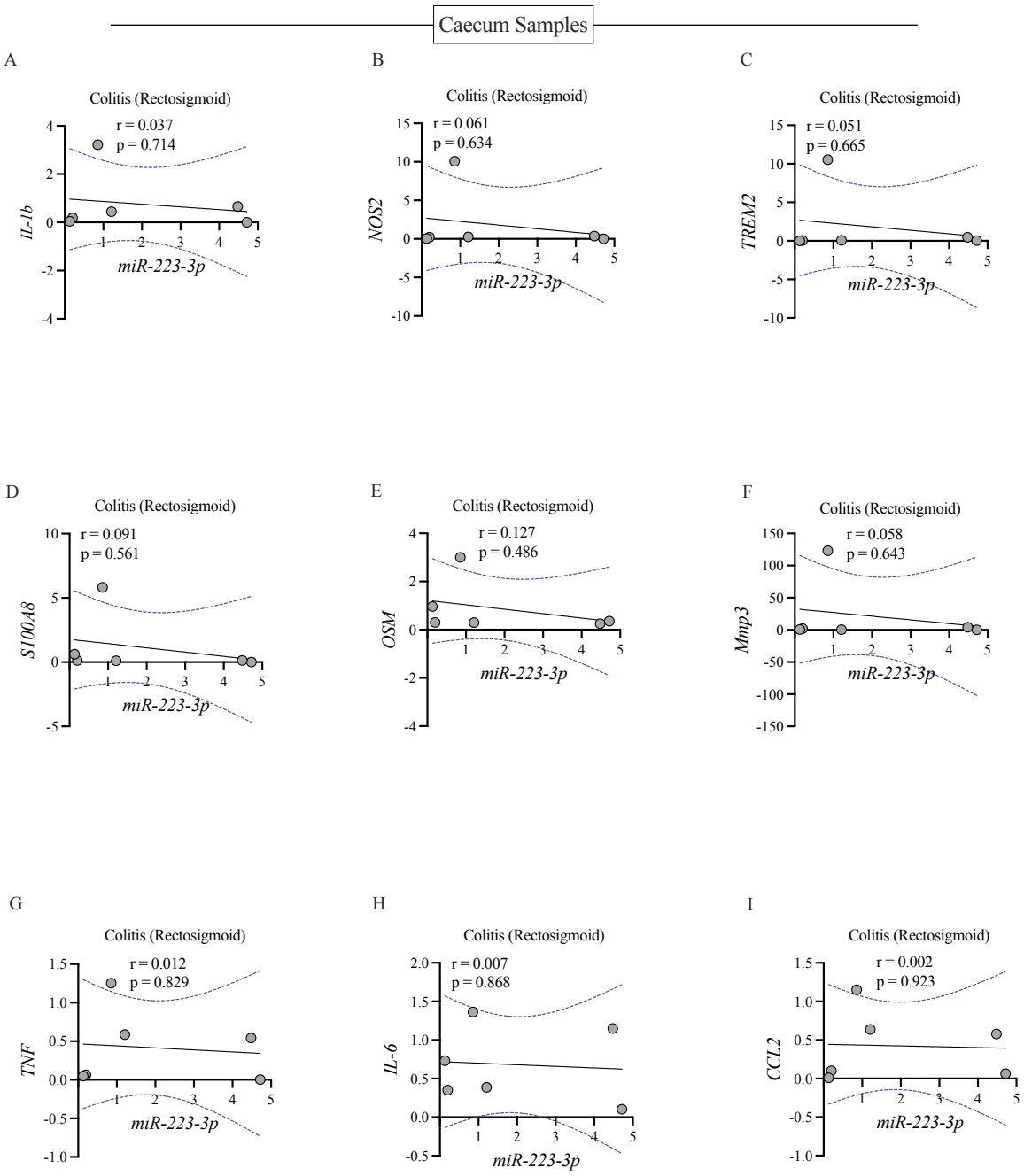


Figure 31. *miR-223-3p expression does not correlate with the expression of inflammatory markers in caecum biopsies taken from patients with Ulcerative colitis (Rectosigmoid).*

Pearson correlation analysis of *miR-223-3p* expression in caecum biopsies with **A.** IL-1β, **B.** NOS2, **C.** TREM2, **D.** S100A8, **E.** OSM, **F.** MMP3, **G.** TNF, **H.** IL-6 and **I.** CCL2. **A-I** n=6 patients/group; p-value of ≤ 0.05 was identified as a significant correlation.

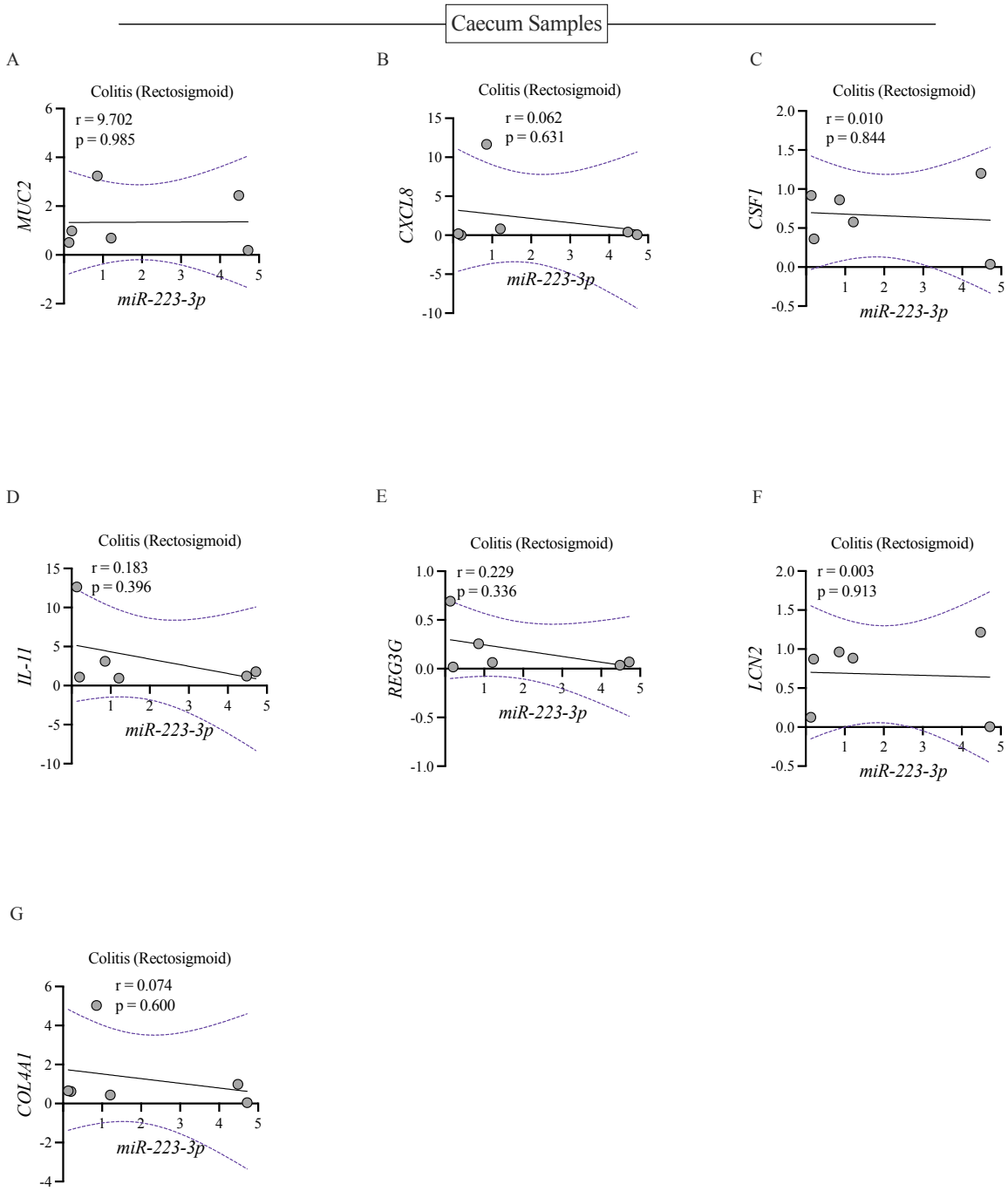


Figure 32. *miR-223-3p expression does not correlate with the inflammatory markers MUC2, IL-1β, CCL2, IL-11, REG3G, LCN2, S100A8 or CSF1 in caecum biopsies from patients with Ulcerative colitis (Rectosigmoid).*

Pearson correlation analysis of *miR-223-3p* expression in caecum biopsies with **A.** MUC2, **B.** CXCL8, **C.** CSF1, **D.** IL-11, **E.** REG3G, **F.** LCN2 and **G.** Col4A1. **A-H** n=6 patients/group; p-value of ≤ 0.05 was identified as a significant correlation.

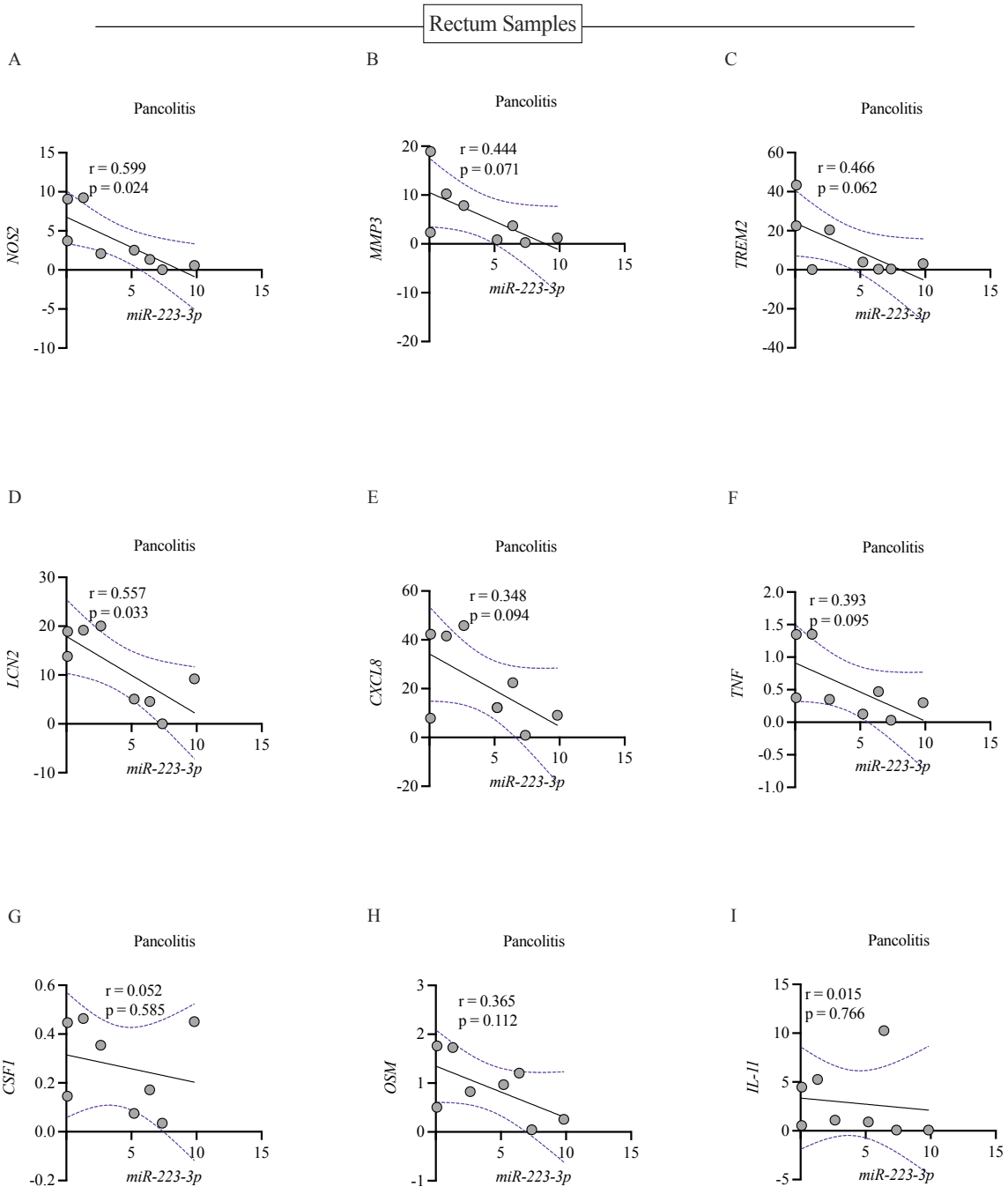


Figure 33. *The inflammatory markers NOS2 and LCN2 negatively correlate with miR-223-3p expression in rectal biopsies from patients with pancolitis.*

Pearson correlation analysis of *miR-223-3p* expression in rectal biopsies with **A.** NOS2, **B.** MMP3, **C.** TREM2 **D.** LCN2, **E.** CXCL8, **F.** TNF, **G.** CSF1, **H.** OSM and **I.** IL-11. **A-I** n=8 patients/group; p-value of ≤ 0.05 was identified as a significant correlation.

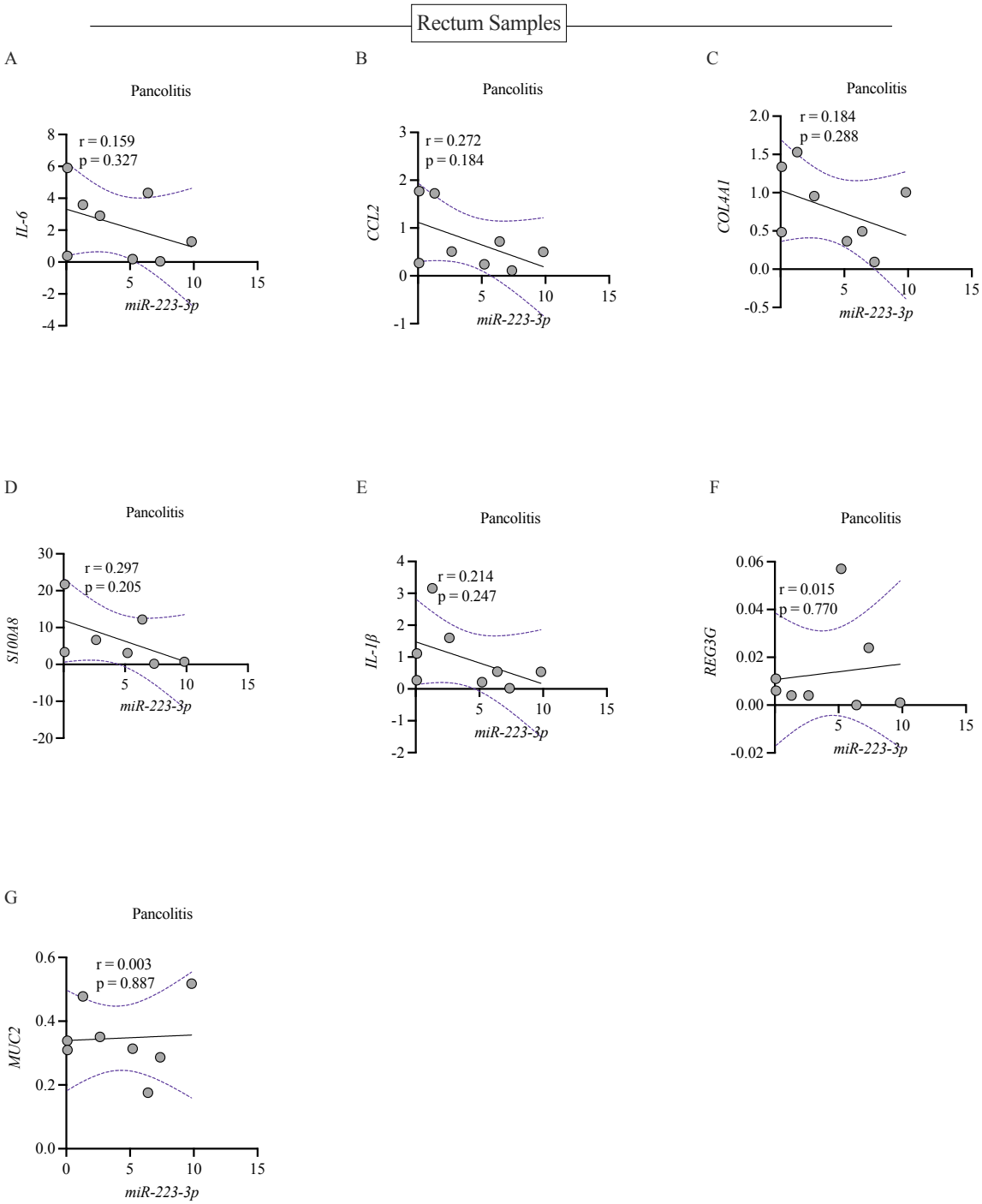


Figure 34. *The inflammatory markers IL-6, CCL2, Col4A1, S100A8, IL-1β, REG3G and MUC2 do not correlate with miR-223-3p expression in rectal biopsies from patients with pancolitis.*

Pearson correlation analysis of *miR-223-3p* expression in rectal biopsies with **A.** IL-6, **B.** CCL2, **C.** Col4A1, **D.** S100A8, **E.** IL-1β, **F.** REG3G and **G.** MUC2. **A-I** n=8 patients/group; p-value of ≤ 0.05 was identified as a significant correlation.

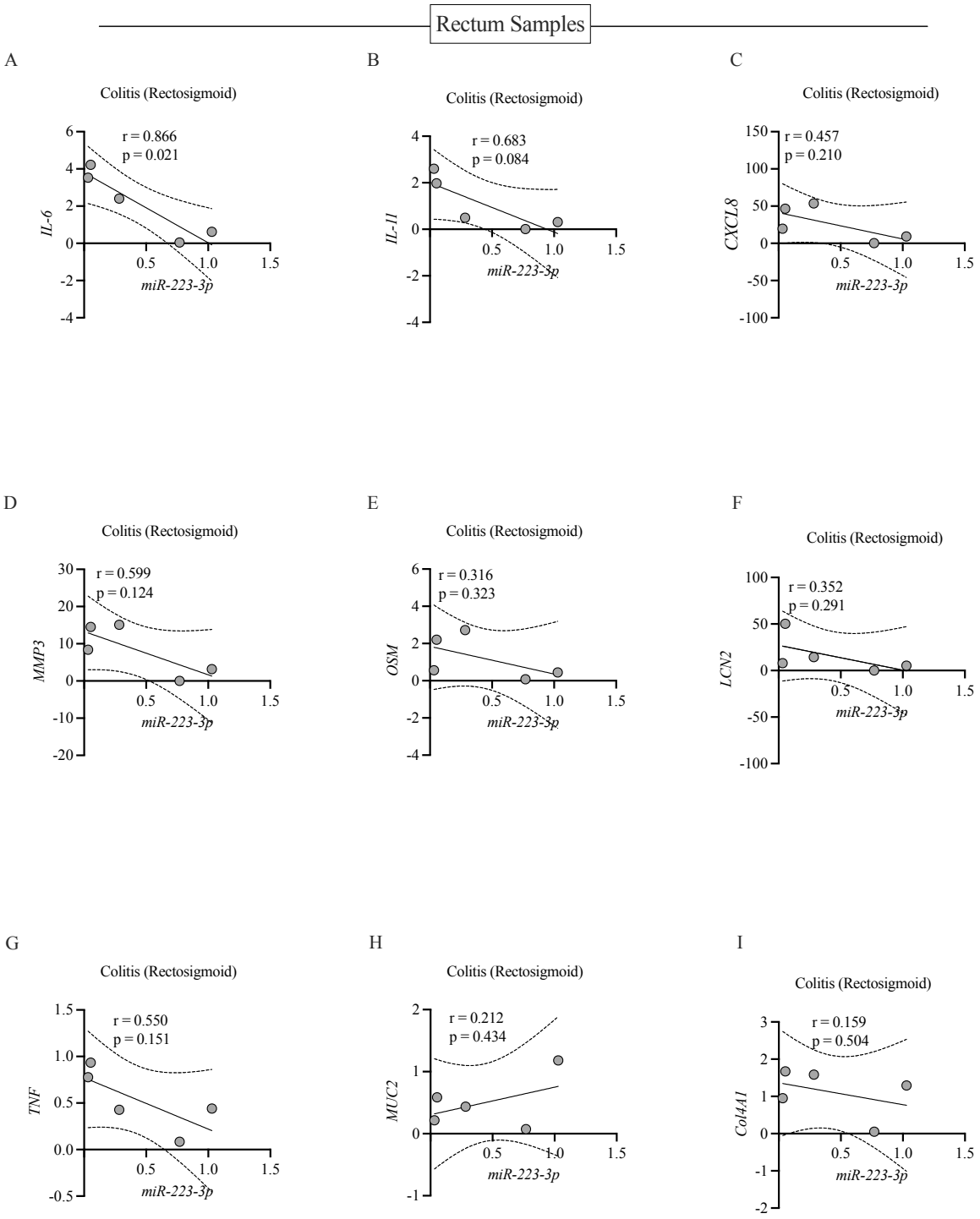


Figure 35. *miR-223-3p negatively correlates with IL-6 expression in rectal biopsies from patients with Ulcerative colitis (Rectosigmoid).*

Pearson correlation analysis of *miR-223-3p* expression in rectal biopsies with **A.** IL-6, **B.** IL-11, **C.** CXCL8, **D.** MMP3, **E.** OSM, **F.** LCN2, **G.** TNF, **H.** MUC2 and **I.** Col4A1. **A-I** n=5 patients/group; p-value of ≤ 0.05 was identified as a significant correlation.

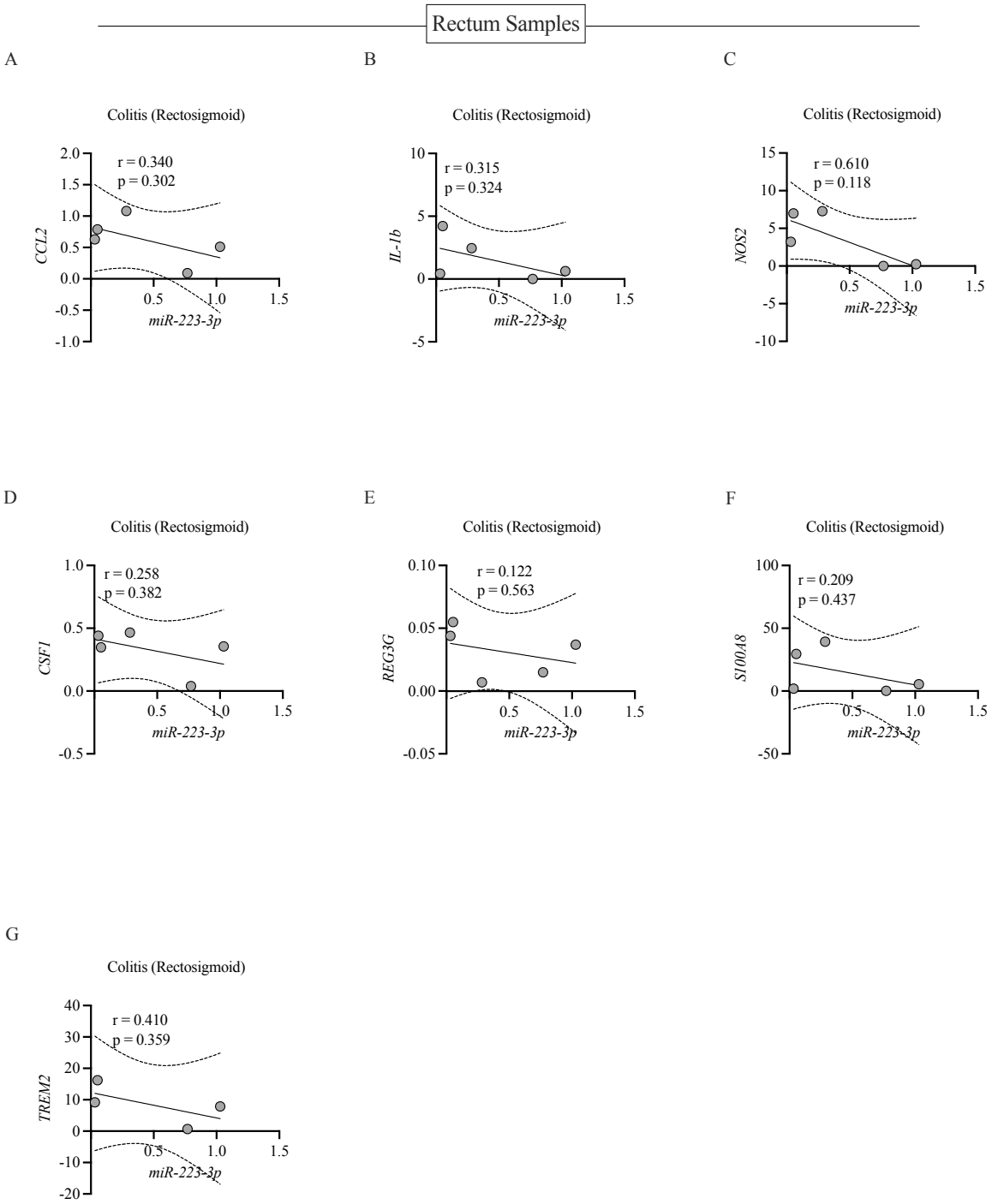


Figure 36. *The inflammatory markers CCL2, IL-1β, NOS2, CSF1, REG3G, S100A8 and TREM2 do not correlate with miR-223-3p expression in rectal biopsies from patients with Ulcerative colitis (Rectosigmoid).*

Pearson correlation analysis of *miR-223-3p* expression in rectal biopsies with **A.** CCL2, **B.** IL-1β, **C.** NOS2, **D.** CSF1, **E.** REG3G, **F.** S100A8 and **G.** TREM2. **A-I** n=4/5 patients/group.

3.1.11 Pathways associated with cytokine signalling are enriched in genes used to identify treatment non-responsive patients with Ulcerative colitis

Enricher analysis was performed on the genes previously identified for the stratification of patients into treatment responsive vs treatment non-responsive. Analysis on GO biological processes revealed that these genes are involved in pathways that were previously shown to be upregulated in the GSE109142 cohort, including, 'cellular response to cytokine stimulus', 'neutrophil chemotaxis' and 'inflammatory response' (**Figure 37 A)**. Further GO analysis of molecular function also confirmed this, with the genes being involved in 'cytokine activity', 'chemokine activity', 'chemokine receptor binding' and 'cytokine receptor binding' at a molecular level (**Figure 37 E**). These genes are also involved in critical cellular functioning including 'collagen-containing extracellular matrix' and 'endoplasmic reticulum lumen' (**Figure 37 C**). Enricher analysis of KEGG pathways also demonstrated cytokine involvement for these genes for 'IL-17 signalling', 'TNF signalling' and 'cytokine-cytokine receptor interactions' (**Figure 37 B**). Finally, the genes are also involved in the Reactome pathways 'signalling by interleukins', 'IL-10 signalling' and 'immune systems' (**Figure 37 D**). Collectively this analysis shows that the top twenty genes used to distinguish between treatment responsive vs non-responsive patients with UC, are involved in a variety of pathways that are upregulated in the GSE109142 cohort and have previously been shown to be altered by *miR-223* expression.

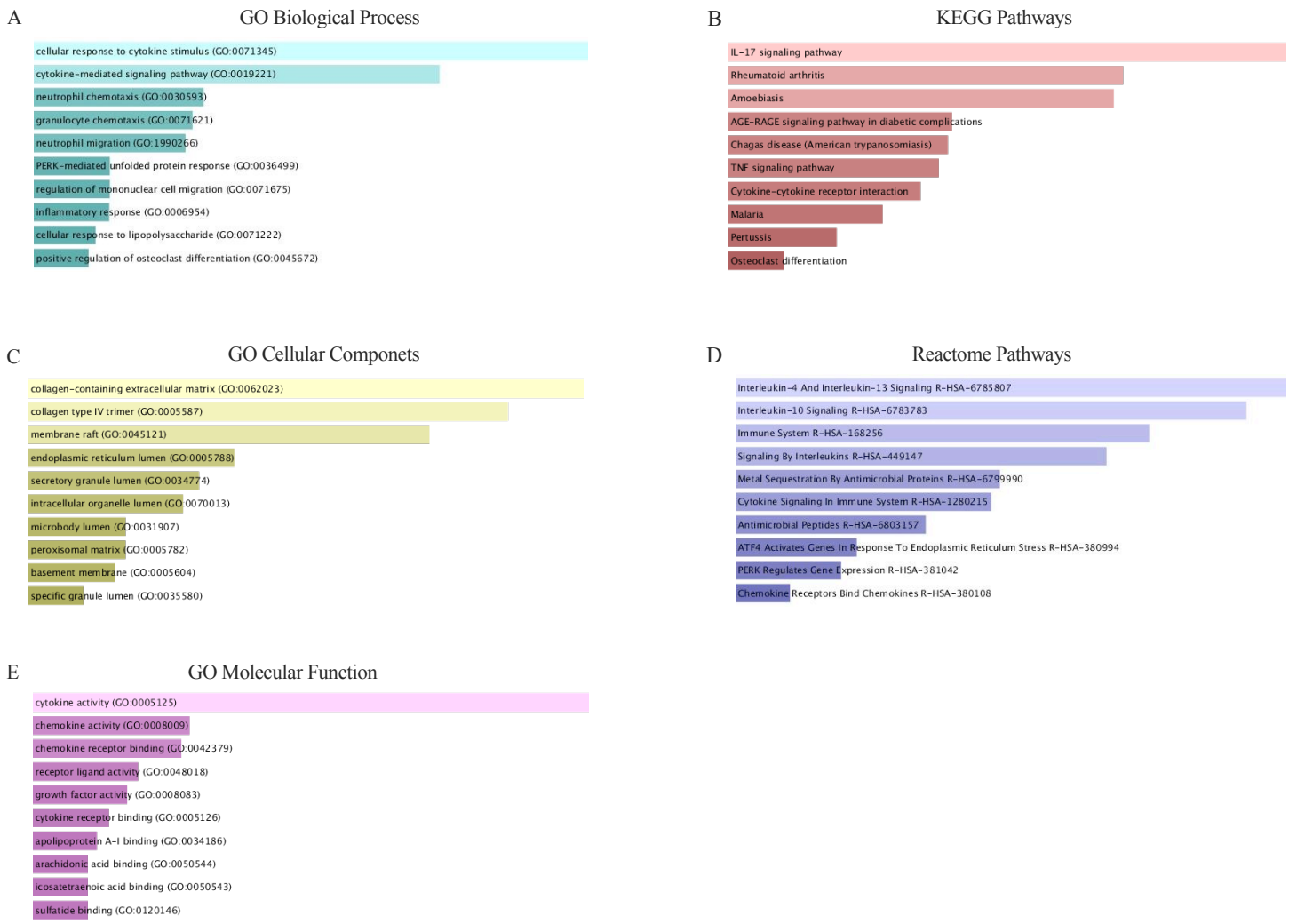


Figure 37. *Cytokine signalling pathways are enriched in genes that can be used to identify treatment non-responsive patients with Ulcerative colitis.*

Enricher analysis of PCR target genes ran on Irish treatment naïve paediatric Ulcerative Colitis cohort. Top pathways associated with **A.** GO Biological Processes, **B.** KEGG Pathways, **C.** GO Cellular Processes, **D.** Reactome Pathways and **E.** GO Molecular Function.

DISCUSSION

UC is a major global health burden. Despite this, our understanding of the initiation and progression of the disease remains incomplete. Internationally, the number of paediatric patients being diagnosed with UC is increasing (Benchimol et al., 2011a). As these patients are typically diagnosed with extended and severe disease, its rapid detection and treatment is critical to improving patient outcomes. Currently, this is hindered by invasive methods used for diagnosis and existing therapeutics being ineffective for a significant sub-set of patients. Recently, the stratification of patients based on treatment responsiveness, defined by a PUCAI score of <10, has been proposed to gain a better understanding of key pathways and regulatory processes that are altered. Furthermore, bioinformatic analysis of these patients could identify new therapeutic targets or improve existing therapeutics, potentially enabling personalised treatment in the future. Due to their ability to modulate gene expression, miRNAs are emerging as potential therapeutic targets.

Bioinformatic analysis was performed on the largest treatment-naïve paediatric transcriptomic data set currently available (GSE109142), with patients being stratified based on their 4-week remission (Haberman et al., 2019). This discovery cohort revealed that patients with UC have a different expression profile compared to controls. Unexpectedly, there was no significant difference in the expression profile of treatment responder's vs treatment non-responders. This was due to a cut off of $P \leq 0.05$ to be deemed as significantly different expression between the two groups. As *miR-223* is upregulated in patients with active UC, and the importance of identifying why patients don't respond to therapeutics, all further analysis was performed on treatment non-responsive patient's vs control.

GSEA analysis performed on the discovery cohort demonstrated that treatment non-responsive paediatric patients had an enriched signature for IL-6/STAT3 signalling and cytokine production. Members of this signalling pathway have been identified as targets of *miR-223-3p.* Thus, identifying *miR-223* regulated circuits has the potential to identify therapeutic targets which would be beneficial for the treatment of UC through the suppression of inflammation in the colon. Current therapeutics, such as 5-ASA and infliximab, act to suppress colonic inflammation by limiting the production of pro-inflammatory cytokines (Muth et al., 2023, Peppercorn and Doherty, 2009). Due to their success, additional anti-cytokine treatments are currently under investigation including IL-

6 blockade, which is increased in patients with active UC (Chen et al., 2021a). This finding indicates that these could potentially be viable treatment options for patients that are non-responsive to currently available therapeutics. As aberrant IL-6 signalling is increasingly being recognised as a contributor to the progression of many cancers, including the progression from UC to CAC, investigation into its use as a therapeutic are ongoing. These include Siltuximab, an IL-6 inhibitor which is currently in clinical trials (Angevin et al., 2014).

Treatment non-responsive patients in the discovery cohort also had an increased myeloid inflammatory signature compared to control patients. Myeloid inflammation is a hallmark of UC and promotes the secretion of pro-inflammatory cytokines such as IL-6 and TNF-α (Reinecker et al., 2008). This creates an inflammatory feedback loop that ensures inflammation is maintained but consequently causes DNA damage and insufficient tissue repair (Ungaro et al., 2017). Under normal homeostatic conditions myeloid cells interact with intestinal epithelial cells to ensure the integrity of the epithelial barrier is maintained (Bai et al., 2020). However, in patients with UC this process is dysregulated and has previously been shown to contribute to both the initiation and progression of disease. Additionally, myeloid driven inflammation is emerging as a central contributor to the progression from UC to CAC (Balandran et al., 2023). Furthermore, *miR-223* is critical for limiting myeloid driven inflammation during UC.

The myeloid associated miRNA, *miR-223* is a key regulator of intestinal inflammation and its expression has previously been shown to be increased in patients with active UC (Neudecker et al., 2017b, Yuan et al., 2018). However, the expression of its targets has not previously identified in treatment-naïve paediatric patients with UC. Here it is shown that targets of the active strand of *miR-223*, *miR-223-3p,* are differentially expressed in treatment non-responsive patient's vs control in the discovery cohort. *miR-223* expression is highest among circulating neutrophils and monocytes, and its expression is induced following myeloid differentiation (Johnnidis et al., 2008). GSEA analysis revealed that myeloid signalling is enhanced in treatment non-responsive paediatric patients, in particular neutrophil recruitment, monocyte activity and macrophage activation. Collectively, inflammation, the secretion of pro-inflammatory cytokines and enhanced myeloid signalling are all increased in treatment non-responsive paediatric patients from the discovery cohort. As *miR-223* is involved in the regulation of these pathways its modulation could be a

potential therapeutic target. However, early identification of these patient still remains an issue.

Recently, gene expression profiles from patients with UC, classified as either treatment non-responsive (UC 1) or treatment responsive (UC 2) where analysed (Czarnewski et al., 2019). This revealed different inflammatory signatures between treatment responsive vs treatment non-responsive patients, that have similar clinical readouts. This study also identified 20 inflammatory genes that can be used to distinguish between patients that will respond to treatment and those that will be treatment non-responsive (Czarnewski et al., 2019). The expression of these genes was assessed in the Irish validation cohort, to determine if there expression was increased in either patients with rectosigmoid colitis or pancolitis. Furthermore, their correlation with *miR-223-3p* could also be determined. RT-PCR analysis on caecum samples from these patients showed that majority of the markers were increased in patients with pancolitis. In particular, IL-6, IL-11 and REG3G where all increased which corresponds to increased IL-6/STAT3 signalling observed in the GSE109142 cohort. Furthermore, patients with pancolitis also had increased expression of neutrophil and monocyte markers, which corresponds to the enhanced myeloid activity shown bioinformatically in the GSE109142 discovery cohort. Additionally, the enhanced inflammatory profile identified in the GSE109142 discovery cohort was also shown in the Irish validation cohort, with inflammatory markers all increased. These inflammatory markers were all genes identified as being increased in treatment non-responsive patients. Patients with rectosigmoid colitis showed comparable, or slightly increased expression levels to controls for majority of genes analysed. This was expected as disease and inflammation in these patients had not extended to the caecum. The exception to this was MUC2, which was increased compared to both control and patients with pancolitis. This is perhaps indicative of reduced inflammation and less severe disease as MUC2 has a protective role in UC (Yao et al., 2021).

Rectum samples were also analysed to determine if the genes used for distinguishing between treatment responsive (UC 2) vs treatment non-responsive (UC 1) patients were changed. If so, it would be beneficial for the early detection of UC and patients with less severe disease. This showed that patients with rectosigmoid colitis and pancolitis both had increased expression of the genes assessed via RT-PCR vs controls. In particular, neutrophil inflammatory markers were increased in patients with rectosigmoid colitis and pancolitis. This potentially represents the early innate immune response in UC (Kałużna et al., 2022a).

As targets of the myeloid associated *miR-223-3p* were shown to be differentially expressed in the GSE109142 discovery cohort, the expression of *miR-223-3p* was determined in the Irish validation cohort. This showed that *miR-223-3p* expression is increased in caecum and rectum biopsies from patients with pancolitis. In blood samples collected from the Irish validation cohort, *miR-223-3p* expression was highest in control patients. However, it has previously been reported that in UC *miR-223* detection in blood is dependent on disease activity. This showed that patients with active UC express less *miR-223* than those in remission (Schönauen et al., 2018). If this was further verified it could potentially enable *miR-223* to be used as a non-invasive biomarker to monitor treatment response in patients.

As *miR-223* expression was increased in patients with UC, it was hypothesized that *miR-223* expression could correlate with genes used to identified treatment non-responsive patients (UC 1). To determine this, pearson correlation analysis was performed. This indicated that in patients with pancolitis, three markers correlated with *miR-223-3p* expression OSM, IL-6 and MMP3. These are all involved in IL-6/STAT3 signalling or its downstream effector pathways (Cutler et al., 2017). Additionally, these markers have previously been shown to positively correlate with disease severity in UC patients (Von Lampe, 2000, Feng et al., 2023, Zhang et al., 2021d). It is also important to note that *miR-223-3p* expression did not correlate with the majority of genes analysed in caecum biopsies from patients with pancolitis. In caecum samples from patients with rectosigmoid colitis *miR-223* did not correlate with any genes. This is potentially as inflammation has not extended to the caecum in these patients.

In rectal biopsies, *miR-223-3p* negatively correlated with the inflammatory markers NOS2 and MMP3. Additional markers were also trending negatively including TREM2, LCN2 and CXCL3. Conversely, in rectum biopsies from patients with rectosigmoid colitis IL-6 and IL-11 negatively correlated with *miR-223-3p* expression. This is potentially representative of different inflammatory processes in rectosigmoid colitis compared to pancolitis (Bjerrum et al., 2014). Furthermore, GSEA analysis revealed that genes upregulated in pancolitis patients from the validation cohort, are involved in inflammatory response and cytokine signalling. These were also enriched in the GSE109142 paediatric discovery cohort.

Collectively, inflammatory, cytokine and myeloid pathways were shown to be upregulated in treatment non-responsive paediatric patients from the GSE109142 discovery cohort. Analysis on an Irish paediatric validation cohort showed that patients with pancolitis had a

similar inflammatory profile to the discovery cohort. Additionally, genes associated with treatment non-responsiveness were also upregulated in pancolitis patients, with the expression of some markers positively correlating with *miR-223-3p* expression. Whilst further research is needed, these markers could be used in conjunction with biomarkers currently used for UC diagnosis, to aid the early identification of patients with extended and severe inflammation.

CHAPTER 4 *MIR-223* IS CRITICAL FOR CONSTRAINING INFLAMMATORY DRIVEN TUMORIGENESIS IN THE AOM/DSS MODEL OF COLITIS ASSOCIATED COLORECTAL CANCER

INTRODUCTION

CRC is the third most frequently diagnosed cancer worldwide, with approximately 1.9 million new cases diagnosed annually, with incidence rates continuing to rise. Globally, CRC is also the second leading cause of cancer related deaths (Sung et al., 2021). UC is a major risk factor for the development of colon cancer. Aberrant intestinal inflammation, a central progressor of the disease, results in epithelial cells becoming damaged and can eventually contribute to the development of CAC. In particular, patients with UC that have extended duration and severity of disease are at increased risk of developing CAC (Bopanna et al., 2017, Zhou et al., 2019). Collectively, this highlights the central role of inflammation in the development and progression of this disease.

Inflammation has been conserved throughout evolution to prevent tissue damage, but its dysregulation is associated with many diseases and is recognised as a hallmark of cancer (Hanahan, 2022). Furthermore, inflammation can also affect other hallmarks of cancer including metastasises, angiogenesis and DNA damage. In the tumour microenvironment (TME), immune cells predominantly secrete pro-inflammatory mediators to promote cancer development (Atsumi et al., 2014).

Chronic inflammation is a major contributor to the TME in CAC. This microenvironment consists of many different cell types that collectively act to promote tumour development (Wang et al., 2017b). Myeloid cells are a major component of the TME and are increasingly being recognised as critical drivers of inflammatory driven tumorigenesis. Under homeostatic conditions, myeloid cells interact with intestinal epithelial cells to ensure the integrity of the epithelial barrier is maintained (Balandran et al., 2023). However, chronic inflammation disrupts this process. As a consequence, the epithelial barrier can be irreparably damaged creating a pro-tumourigenic microenvironment (Balandran et al., 2023, Lechuga et al., 2023).

Amongst myeloid cells present in the TME, TAMs are the largest myeloid cell type present. These are derived from circulating monocytes that are constantly being recruited due to chemoattractants produced by the TME. Once in the TME, monocytes differentiate into macrophage via either M-CSF or GM-CSF.

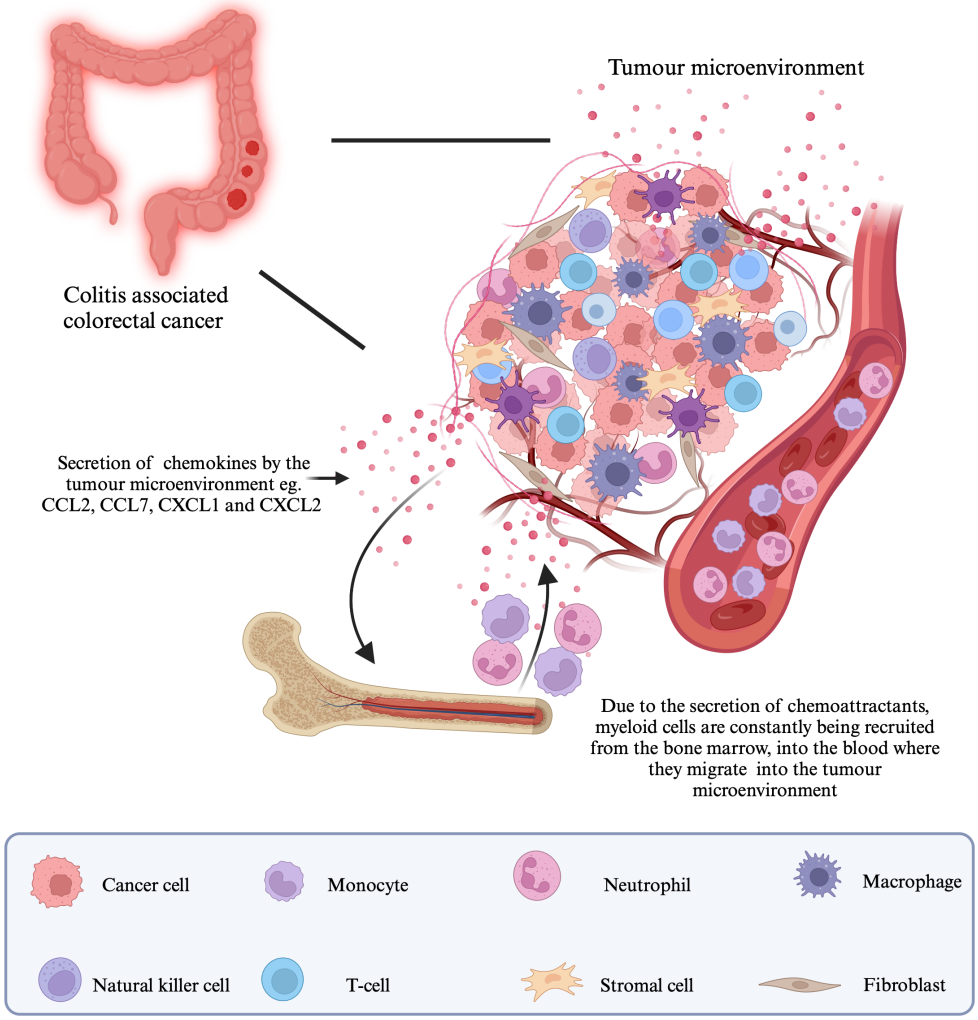


Figure 38. *Tumour microenvironment is diverse in Colitis associated colorectal cancer.*

The TME consist of a variety of different cell types. Myeloid cells are constantly being recruited into the TME through the secretion of chemoattractants such as CCL2, CCL7, CXCL1 and CXCL2. Once in the TME, monocytes differentiate into TAMs. Adapted from "Tumor Extracellular Matrix Reduces Therapeutic Efficiency in Solid Tumors", by BioRender.com (2024), originally published in (Henke et al., 2020).

TAMs have two differentiation states, pro-inflammatory TAMS or anti-inflammatory TAMs. The phenotype a TAM takes on is based on environmental ques from the TME. Pro-inflammatory TAMs are associated with anti-tumour activity, whereas anti-inflammatory TAMs are associated with promoting tumour growth (**Figure 39**). In the TME, evidence has suggested that majority of TAMs have an anti-inflammatory phenotype (Yahaya et al., 2019, Schmitt and Greten, 2021). Thus, gaining a better understanding of how chronic myeloid inflammation is driven and how TAMs function is controlled, is of interest for the development of therapeutics for inflammatory driven diseases and cancers.

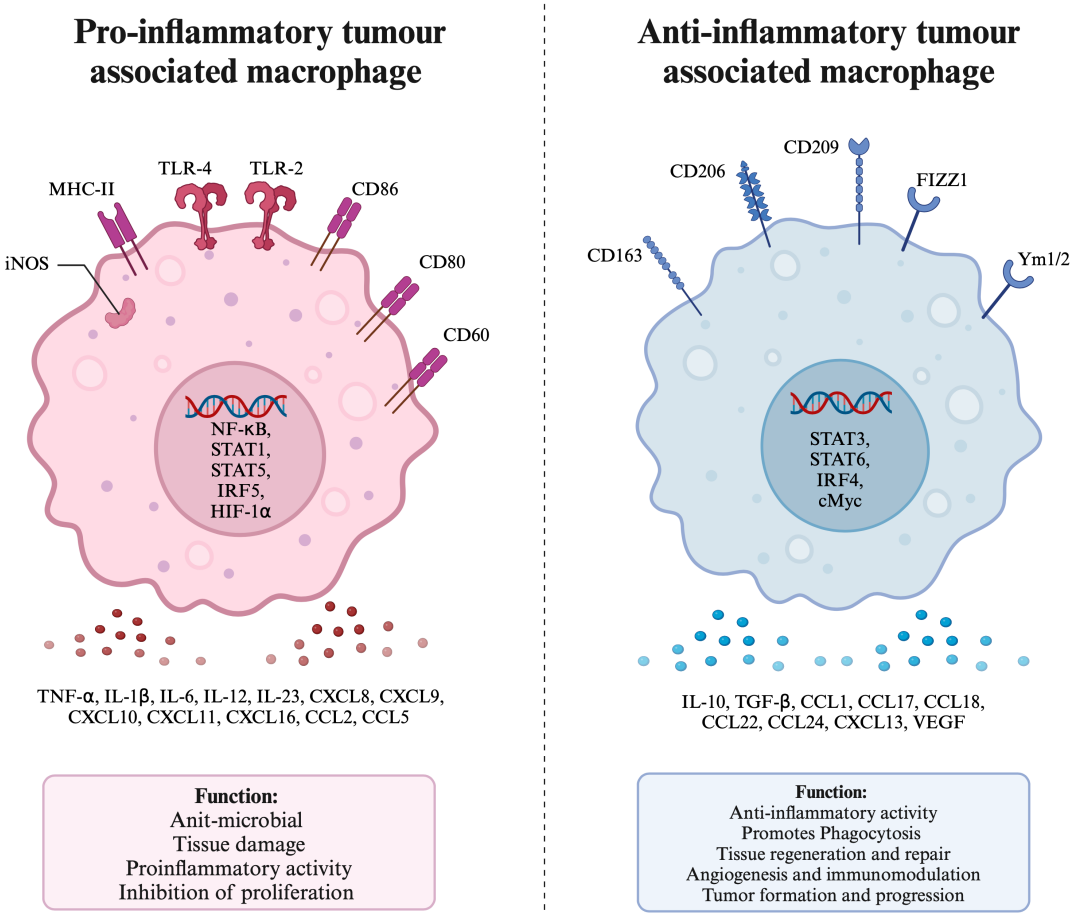


Figure 39. *Pro-inflammatory and anti- inflammatory functions of tumour associated macrophages.*

Pro-inflammatory macrophage promotes inflammation and the secretion of inflammatory cytokines. They cause function effects such as tissue damage, inhibit proliferation and anti-microbial activity. This TAM phenotype acts to limit tumour formation. In contrast, anti-inflammatory have the ability to promote tumour formation. This is done through the promotion of angiogenesis and suppressing inflammation. Adapted from "Macrophage Polarization: M1 and M2 Subtypes", by BioRender.com (2024), originally published in (Yao et al., 2019b).

miRNAs are critical for the post-transcriptional regulation of gene expression, mediating their effects through complementary base pairing of the 3' UTRs of the target mRNAs (Berindan-Neagoe et al., 2014). Among their many regulatory functions, miRNAs are essential for controlling inflammation. Furthermore, aberrant expression of miRNAs has previously been reported in many diseases, including UC (Zhu et al., 2017, Chen et al., 2019, Colangelo et al., 2017). Altered miRNA expression has been identified in nearly all types of cancer and emerging evidence suggests that they have the capability to alter many of the

hallmarks of cancer (Peng and Croce, 2016). Furthermore, several miRNAs have been shown to be implicated in CAC (**Table 32**).

miR-223 has recently emerged as a crucial regulator of the innate immune response during intestinal inflammation. This miRNA is specifically expressed in the myeloid compartment, is induced during myeloid differentiation and among its many roles is the regulation of myeloid cell activity (Johnnidis et al., 2008). Additionally, patients with active UC have increased expression of *miR-223* and *miR-223*$^{-/y}$ mice have exacerbated colitis following DSS, that is driven by inflammatory monocytes and neutrophils (Neudecker et al., 2017b). In the context of CRC*, miR-223* expression is increased in patients biopsies and correlated with disease severity (Zhang et al., 2014). However, the role of this myeloid associated *miR-223* has yet to be characterized in the progression from UC to CAC.

Table 32. *miRNAs implicated in colitis associated colorectal cancer.*

miRNA	Expression	References
miR-21	Increased in patients with CAC; upregulation associated with increased proliferation	(Shi et al., 2016)
miR-449a	Expression is decreased during the progression from UC to CAC; inhibits the growth and metastasis of colon cancer cells	(Feng et al., 2018b)
miR-123	Regulates the expression of STAT3; downregulation leads to increased inflammation via STAT3	(Koukos et al., 2013)
miR-155	Promotes CAC via Wnt/β-catenin signalling pathway	(Li et al., 2021)
miR-19a	Promotes CAC via upregulation of NF-κB signaling	(Wang et al., 2017c)
miR-301a	Promotes inflammation in CAC	(He et al., 2017)
miR-26	Suppresses intestinal inflammation	(Zhang et al., 2021f)
miR-146a	Limits inflammation via IL-17 signalling	(Garo et al., 2021)
miR-148a	Limits the progression from UC to CAC by suppressing NF-κB	(Zhu et al., 2017)

AIMS OF THIS CHAPTER

The overall aim of this chapter was to investigate the role of *miR-223* on the development of CAC, using in the AOM/DSS mouse model. Specific aims of the chapter where to:

1. Determine if *miR-223* deficiency results in more severe disease following chronic AOM/DSS modelling of CAC.
2. Identify what cell types are implicated in the inflammatory-driven progression to tumorigenesis in *miR-223*$^{-/y}$ mice following chronic AOM/DSS.
3. Determine if the stromal or hematopoietic compartment is responsible for the development of carcinoma in the chronic AOM/DSS model by using bone marrow chimeric mice.

4.1.1 Increased tumour size in *miR-223*$^{-/y}$ mice treated with chronic AOM/DSS

miR-223 expression is increased in patients with active UC and correlates with severe disease in CAC. However, the role of *miR-223* in the inflammatory driven progression from UC to CAC has yet to be determined. To investigate this, a chronic AOM/DSS model of CAC was utilised, which mimics the reoccurring periods of inflammation, recovery and repair observed in patients with UC.

An initial model using 3% DSS resulted in 66% of *miR-223*$^{-/y}$ mice dying over the course of the study, highlighting the critical role of *miR-223* in constraining excessive inflammation (**Figure 40 A**). Consequently, in all further experiments DSS was reduced to 2%. Following necropsy, colon weight, colon length and spleen weight were measured. As they are markers of gross tumour burden, physiologic side effects of colitis and systemic inflammation respectively. There were minimal differences recorded between *miR-223*$^{-/y}$ and WT treated mice (**Figure 40 B – D).** The number of macroscopic polyps and tumours per section was also evaluated, which showed that *miR-223*$^{-/y}$ mice developed more tumours than WT counterparts (**Figure 41 A – C**). Furthermore, when dysplasia and tumour area were calculated by microscopy, it revealed that *miR-223*$^{-/y}$ mice developed larger tumours than WT when treated with AOM/DSS (**Figure 41 D – H**). Collectively, these data suggest that in the AOM/DSS model, *miR-223* is critical for constraining inflammation that drives the progression from UC to CAC.

4.1.2 Increased proliferation in colonic tissue of *miR-223*$^{-/y}$ mice treated with chronic AOM/DSS

As *miR-223*$^{-/y}$ mice presented with more frequent and significantly larger tumours compared to WT counterparts, potentially proliferation was also enhanced. To assess this, colonic tissue from *miR-223*$^{-/y}$ and WT mice treated with chronic AOM/DSS were analysed via western blot for the expression of proliferation markers. *miR-223*$^{-/y}$ mice had significantly more expression of the proliferating cell nuclear antigen (PCNA) and cyclin-D1 compared to all other groups assessed (**Figure 42 A - C**). Confirmatory immunohistochemical staining also showed significantly more expression of PCNA in *miR-223*$^{-/y}$ mice, in both unaffected

and tumour tissue (**Figure 42 G – H**). This appeared to be specific as additional markers for proliferation and tumour growth were unchanged between AOM/DSS treated groups, in particular phospho-AKT (Ser473), phospho-ERK (Thr202/Tyr204) and phospho-ribosomal S6 (Ser235/236) (**Figure 42 D – F**) . This was also shown in β-catenin isoforms which showed no significant differences across genotypes (**Appendix Figure 1 A + B**). Collectively, these data suggests that *miR-223* is involved in controlling proliferation.

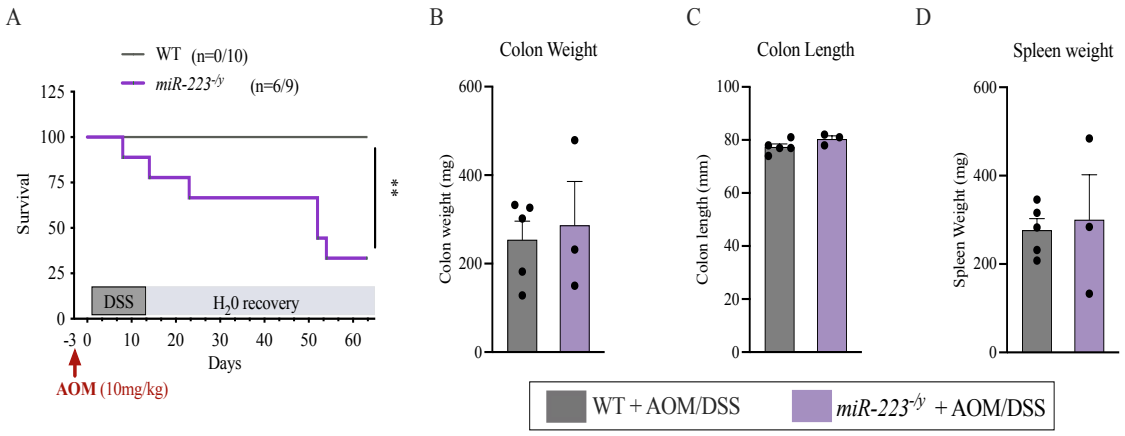


Figure 40. *Clinical readouts from chronic AOM/DSS study performed in mice.*

A. After administration of AOM and 1 round of DSS (3% w/v), mice were allowed to recover, and survival scores were recorded over a 62-day period. While 0 out of 10 WT mice died (C57BL6/J), 6 out of 9 died from the *miR-223*$^{-/y}$ group. Following this a revised treatment regime of chronic AOM/DSS (2% w/v) was performed on WT or *miR-223*$^{-/y}$ mice, at necropsy mice were assessed for **B.** Colon weight **C.** Colon length and **D.** Spleen weight. All data is expressed as mean ± SEM; *, P<0.05, **, P<0.01; versus the indicated counterpart (A; Log rank test, B- D unpaired students t-test). A. n=9-10 mice/group, B-D. n=3-5 mice/group.

4.1.3 *miR-223*$^{-/y}$ regulates the infiltration of CCR2+ monocytes following AOM-DSS

To identify what cells are potentially implicated in the increased tumourigenic and proliferative signature seen in the *miR-223*$^{-/y}$ mice, colonic tissue from chronically treated AOM/DSS mice was initially analysed via immunohistochemical staining. Quantification of immunohistochemical staining on unaffected colonic tissue revealed that there is significantly more Ly6G^{+} neutrophils, CD68^{+}macrophage, CD206^{+} macrophage and CCR2^{+} monocytes infiltrating into the colon of *miR-223*$^{-/y}$ mice following AOM/DSS compared to WT counterparts (**Figure 43 A – H**). Comparable numbers of Ly6G^{+} neutrophils and CD68^{+}

macrophage were seen in both WT and *miR-223*$^{-/y}$ AOM/DSS treated (**Figure 43 A, B, E + F**). There was a slightly reduced numbers of CD206^{+} macrophage in *miR-223*$^{-/y}$ vs WT AOM/DSS treated (**Figure 43 C + G**). However, there was significantly more CCR2^{+} monocytes detected in the tumours of *miR-223*$^{-/y}$ mice following AOM/DSS compared to WT counterparts (**Figure 43 D – H**). Furthermore, untreated WT and *miR-223*$^{-/y}$ had similar expression of Ly6G, CD68, CCR2 and CD206 (**Appendix Figure 2)**.As miR-223 is primarily expressed by myeloid cells, these data indicate that this increased expression is from new myeloid cells infiltrating into the colon.

4.1.4 *miR-223*$^{-/y}$ regulates the infiltration of CCR2+ monocytes and its associated inflammatory cytokine profile

To gain a better understanding of how *miR-223* is regulating inflammation in the AOM/DSS model, RT-PCR was performed on colonic tissue from chronically treated AOM/DSS mice. Gene expression was determined for markers associated with macrophage, neutrophil and monocyte functional responses to inflammation. At baseline there was no significant difference between untreated WT and *miR-223*$^{-/y}$ mice (**Figure 44** + **Figure 45**). Consistent with increased tumour burden previously reported, chronically treated *miR-223*$^{-/y}$ mice had a significantly increased cytokine and chemokine expression profile, compared to all other groups assessed. In particular, there was an enhanced expression of colitis associated, pro-inflammatory cytokines (*nos2, tnf-α, il-1b and s100a8;* **Figure 44 A)** and anti-inflammatory TAM associated cytokines (*arg1, chi3l3* and *irf4* **Figure 44 B).** Chemokines associated with monocytes (*ccl2* and *ccl7;* **Figure 44 C)** and neutrophils (*cxcl1 and cxcl2;* **Figure 44 C)** were also increased in *miR-223*$^{-/y}$ AOM/DSS mice. Furthermore, myeloid associated growth factors were also increased (*csf1, IL-34* and *gm-csf;* **Figure 45 A)**. However, there was no difference in expression seen between genotypes for vascular growth factors that are implicated in tumour survival (*vegfa* and *vegfc;* **Figure 45 A)**. Genes associated with the immunoregulation of tumours were also unchanged (*tgfb1* and *il-1rn;* **Figure 45 B)**. *miR-223-3p* expression was also shown to be increased in WT AOM/DSS mice vs WT controls (**Figure 45 C)**. Collectively, these data indicate that *miR-223* is critical for limiting the recruitment of monocytes and neutrophils into the colon, along with the secretion of their associated cytokines, which as implications for the progression from UC to CAC.

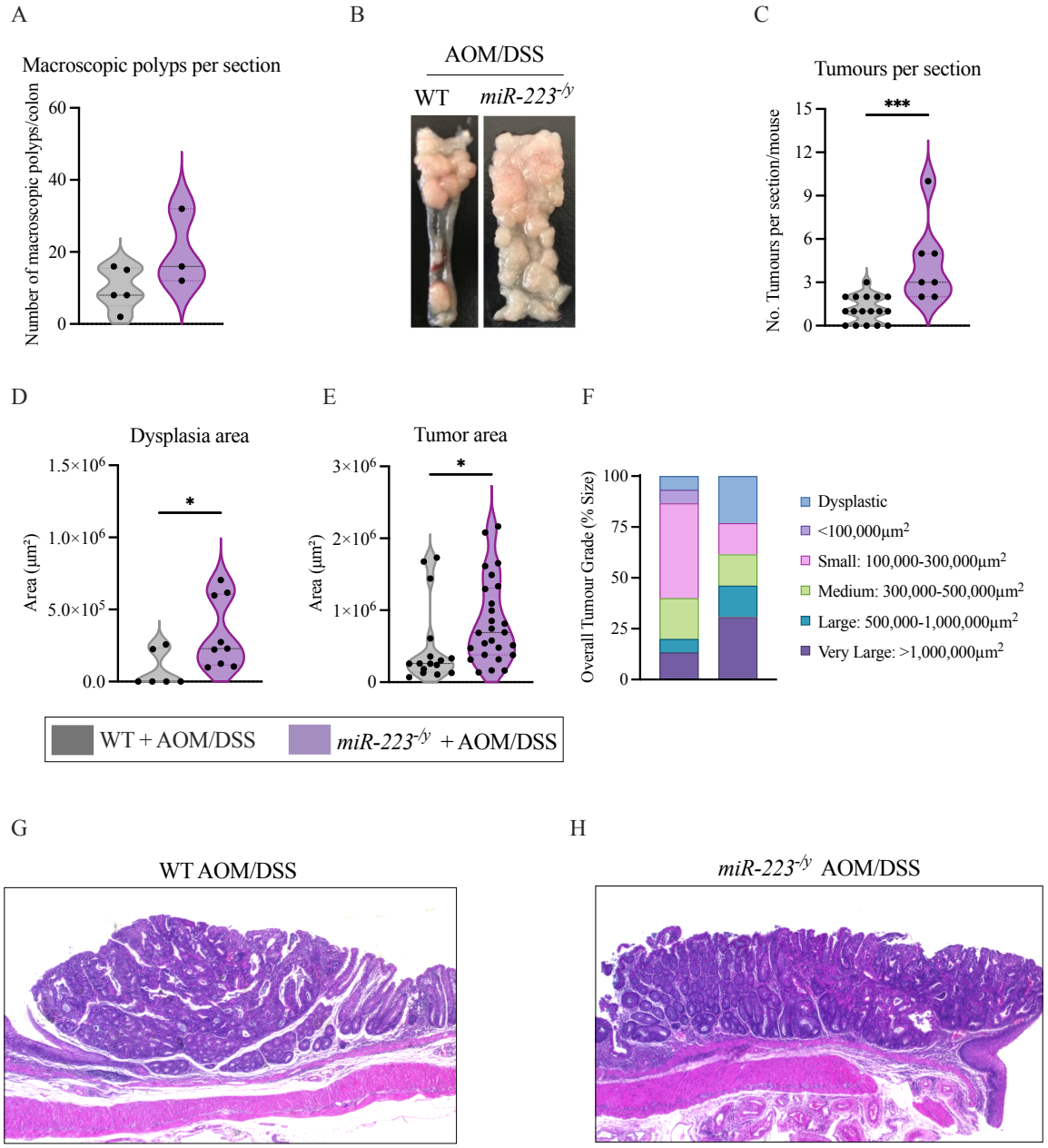


Figure 41. *miR-223$^{-/y}$ mice have increased tumour size following chronic AOM/DSS.*

A. After treatment with chronic AOM/DSS (2% w/v) WT (C57BL6/J) and *miR-223$^{-/y}$* counterparts were assessed for the number of macroscopic tumours per colon **B.** Representative images from the distal colons of WT and *miR-223$^{-/y}$* mice following chronic AOM/DSS (2% w/v). Following H&E staining the **C.** Number of tumours per section, **D.** dysplasia size (µm^2) and **E.** tumour size (µm^2) was determined following chronic AOM/DSS (2% w/v). **F.** Tumour grading based size from H&E micrographs for WT and *miR-223$^{-/y}$* mice following chronic AOM/DSS (2% w/v). Representative 10x micrographs from **G**. WT and **H.** *miR-223$^{-/y}$* mice following chronic AOM/DSS. All data is expressed as mean ± SEM; *, P<0.05; **, P<0.01; ***, P<0.001 versus the indicated counterpart (Unpaired, one-tailed students t-test). **D+E**. WT AOM-DSS: 16 tumours and 2 dysplastic regions counted from 17 mice; *miR-223$^{-/y}$* AOM-DSS: 27 tumours and counted across 7 mice. Data is presented from 2 independent experiments.

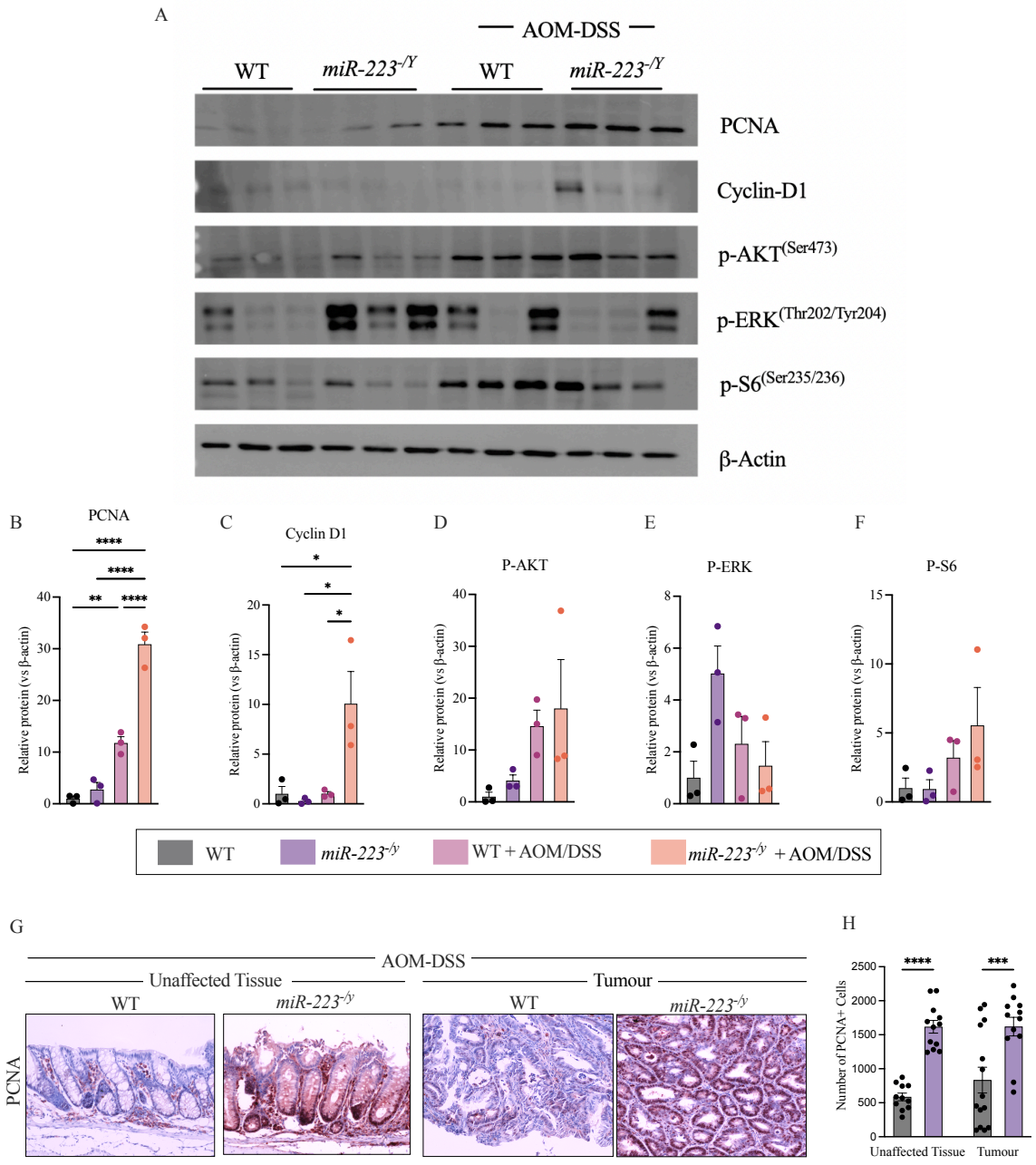


Figure 42. *miR-223$^{-/y}$ mice have enhanced proliferation following chronic AOM/DSS.*

A. Western immunoblot assessment of PCNA, cyclin-D1, phospho-AKT, phospho-S6, phospho-ERK and β-actin on WT (C57BL6/J) and *miR-223$^{-/y}$* chronic AOM/DSS treated mice. Quantification of western immunoblots for **B.** PCNA, **C**. Cyclin-D1, **D.** Phospho-AKT, **E.** phospho-ERK and **F.** Phospho-S6. **G.** Representative 10x micrographs of unaffected and tumours from WT and *miR-223$^{-/y}$* mice treated with chronic AOM/DSS after immunohistochemical staining for PCNA. **H.** Quantification of PCNA immunostaining. All data is expressed as mean ± SEM; *, P<0.05; **, P < 0.01; ***, P<0.001; ****, P<0.0001 versus the indicated counterpart (One-way ANOVA). **A – F** n=3 mice/group; **G + H** n=4 mice/group with 3 fields of view presented per animal).

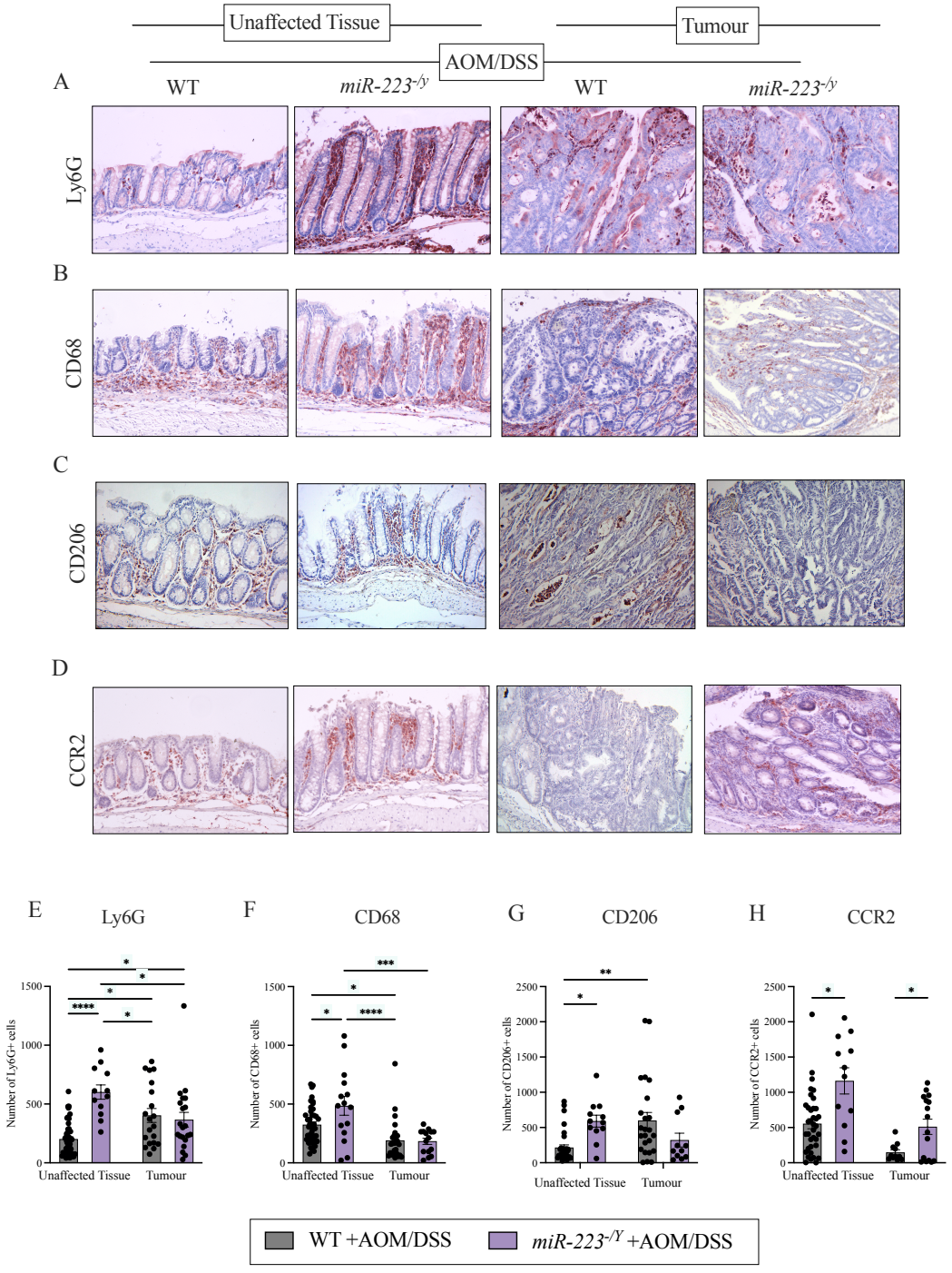


Figure 43. *Macrophage, neutrophils and monocytes infiltrate into the colon of miR-223$^{-/y}$ following chronic AOM/DSS.*

Representative 20x micrographs of unaffected tissue and tumor of WT (C57BL6/J) and *miR-223$^{-/y}$* counterparts after immunohistochemical staining for **A**. Ly6G, **B**. CD68, **C.** CD206 and **D.** CCR2. Staining was then quantified for E. Ly6G, **F.** CD68, **G.** CD206 and **H.** CCR2. All data is expressed as mean ± SEM; *, P<0.05; **, P<0.01; ***, P<0.001; ****, P<0.0001 versus the indicated counterpart (One-way ANOVA). **A+E** WT AOM/DSS n=16; *miR-223$^{-/y}$* AOM/DSS n=4; **B+F** WT AOM/DSS n=14; *miR-223$^{-/y}$* AOM/DSS n=4; **C+G** WT AOM/DSS n=11; *miR-223$^{-/y}$* AOM/DSS n=4; and **D+H** WT AOM/DSS n=12; *miR-223$^{-/y}$* AOM/DSS n=4; with 3 fields of view quantified per animal.

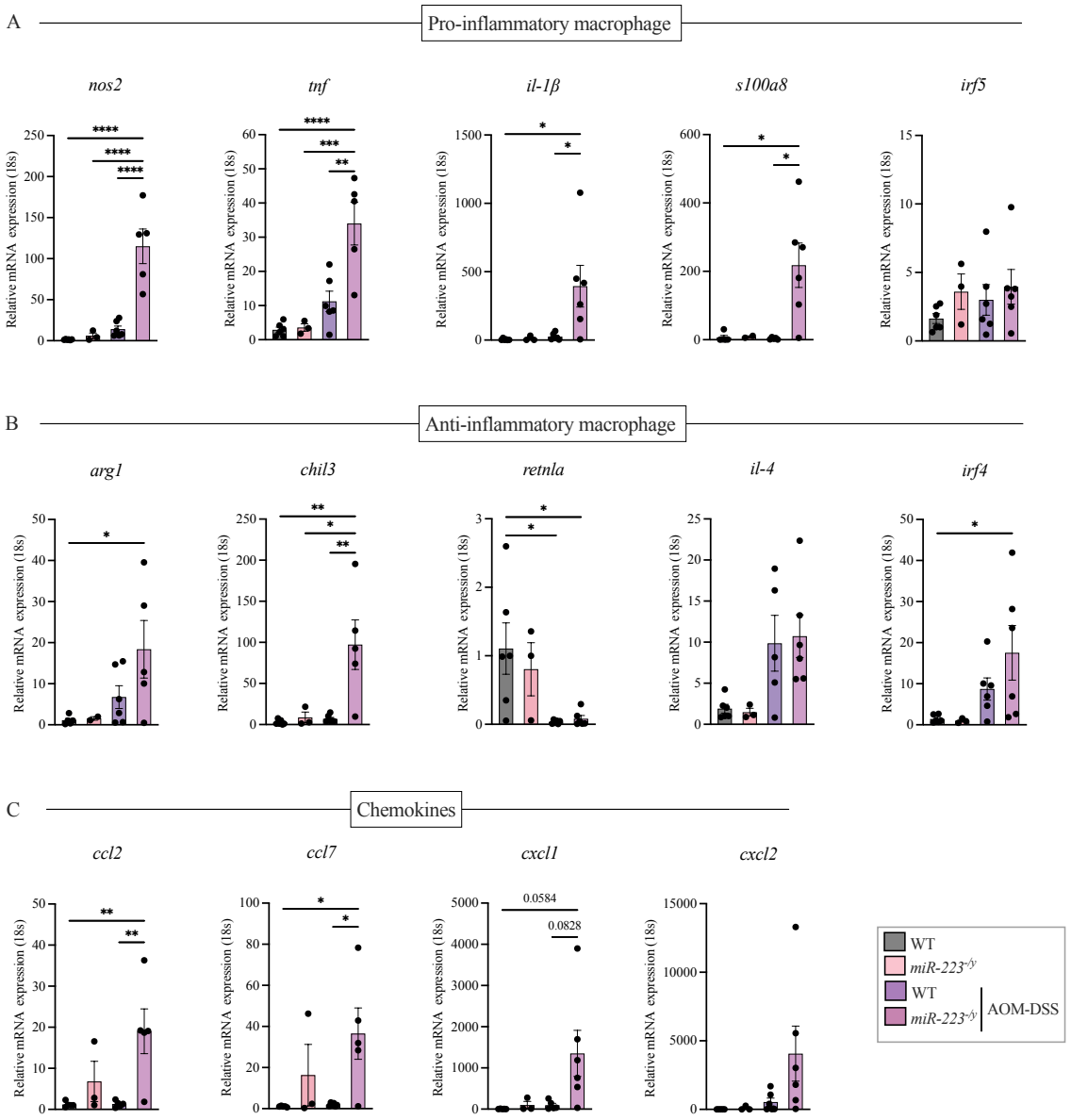


Figure 44. *Colonic tissue from miR-223$^{-/y}$ mice show an increased chemokine signature for monocytes and neutrophils following chronic AOM/DSS.*

A. Relative mRNA expression of the pro-inflammatory macrophage markers nos2, tnf, il-1β, S100a8 and irf5. **B.** Relative mRNA expression of the anti-inflammatory macrophage markers arg1, chi3l3, retnla, il-4, and irf4. **C.** Relative mRNA expression of the monocyte chemokines ccl2 and ccl7; neutrophil chemokines cxcl1 and cxcl2. All data is expressed as mean ± SEM; *, P<0.05; **, P<0.01; ***, P<0.001, ****, P<0.0001 versus the indicated counterpart (One-way anova). **A-C** n=3-6 mice/group.

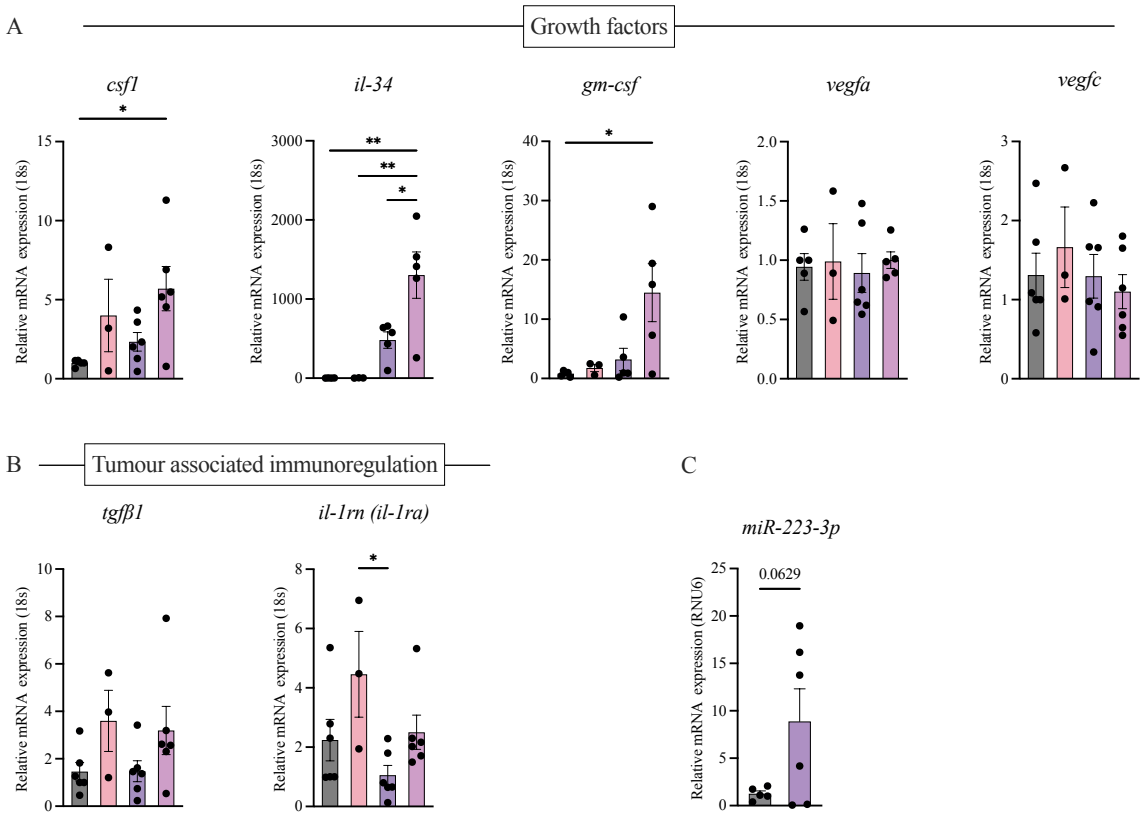


Figure 45. *Colonic tissue from miR-223$^{-/y}$ mice have increased expression of myeloid associated growth factors.*

A. Relative mRNA expression of the myeloid growth factors m-csf1, il-34, gm-csf, vegfa and vegfc. **B**. Relative expression of the tumor associated immunoregulation markers tgf-β1 and il-1rn. **C.** Relative expression of *miR-223-3p.* All data is expressed as mean ± SEM; *, P<0.05; **, P<0.01; ***, P<0.001, ****, P<0.0001 versus the indicated counterpart (One-way anova). **A-C** n=3-6 mice/group.

4.1.5 Hematopoietic deficiency of *miR-223* enhances susceptibility to AOM-DSS

As all previous studies were performed on a germline hemizygous knockout strain of *miR-223*$^{-/y}$ mice, samples generated from a bone marrow chimera study were used to determine if the stromal or hematopoietic compartment was responsible for the inflammatory driven progression to tumorigenesis. After necropsy, spleen weight, colon weight and colon length were measured. There was minimal differences spleen weight between genotypes (**Figure 46 A**). Differences were observed in colon weight, with *miR-223*$^{-/y}$ → WT and *miR-223*$^{-/y}$→ *miR-223*$^{-/y}$ colons being significantly heavier than WT → *miR-223*$^{-/y}$ recipients (**Figure 46 B**). Conversely, WT → *miR-223*$^{-/y}$ recipients had significantly longer colons compared to *miR-223*$^{-/y}$ → WT (**Figure 46 C**). The number of macroscopic polyps and tumours per section was also determined and found to be increased in *miR-223*$^{-/y}$ → WT recipients (**Figure 46 D - F**). Further confirming that hematopoietic derived *miR-223* exacerbates disease in this model, dysplasia and tumour area were also increased in *miR-223*$^{-/y}$ → WT recipients compared to WT → *miR-223*$^{-/y}$ recipients (**Figure 46 G + I**).

4.1.6 Hematopoietic deficiency of *miR-223* increases macrophages infiltrating into colonic tissue of *miR-223*$^{-/y}$ → WT following AOM/DSS

To identify what cells are potentially implicated in the increased tumourigenic signature seen in the in *miR-223*$^{-/y}$ → WT recipients, colonic tissue from bone marrow chimera mice chronically treated AOM/DSS mice was analysed via immunohistochemical staining. Quantification of immunohistochemical staining on unaffected colonic tissue revealed that there is significantly more CD68^{+}macrophage infiltrating into the colon of *miR-223*$^{-/y}$ → WT and *miR-223*$^{-/y}$ → *miR-223*$^{-/y}$ recipients following chronic AOM/DSS compared to WT → *miR-223*$^{-/y}$ recipients (**Figure 47 A + C**). Whilst there was significantly less infiltrating Ly6G^{+} neutrophils into the colon of *miR-223*$^{-/y}$ → WT recipients compared to both WT → *miR-223*$^{-/y}$ and *miR-223*$^{-/y}$ → *miR-223*$^{-/y}$ recipients (**Figure 47 B + D**). Quantification of immunohistochemical staining on tumour tissue also showed significantly more CD68^{+}macrophage infiltrating into the colon of *miR-223*$^{-/y}$ → WT recipients compared to other chimera treatment groups (**Figure 48 A + C**). In contrast, similar numbers of Ly6G^{+} neutrophils were detected in the numbers across all chimera recipient groups (**Figure 48 B + D**).

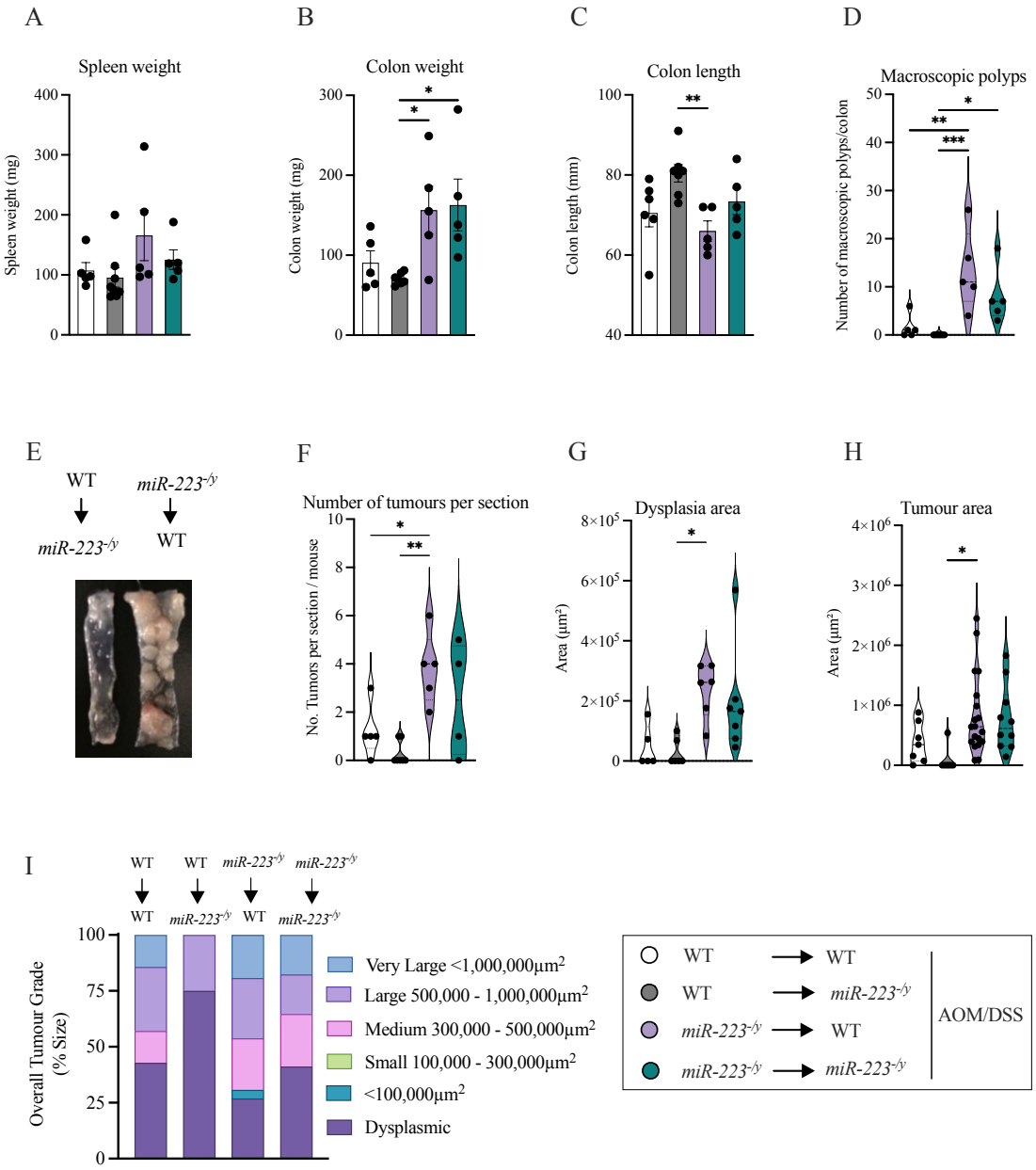


Figure 46. *Bone marrow chimera shows that hematopoietic deficiency of miR-223 enhances susceptibility to AOM/DSS.*

Following irradiation and bone marrow transplantation, chimeric mice were chronically treated with AOM/DSS (2% w/v). At necropsy mice were assessed for: **A.** Spleen weight, **B.** Colon weight, **C.** Colon length and the **D.** number of macroscopic polyps per colon. **E.** Representative images of colon polyps F. Number of tumours per section **G.** Quantification of dysplasia area (µm^2) per section **H**. Quantification of tumour area (µm^2) per section **I**. Tumour grading based size from H&E micrographs following chronic AOM/DSS (2% w/v). All data is expressed as mean ± SEM; *, P<0.05; **, P<0.01; versus the indicated counterpart (one-way ANOVA). **A-D**. n=5-8 mice / group F-I. WT → WT: 4 tumours and 3 dysplastic regions from 5 mice; WT → *miR-223*$^{-/y}$: 1 tumor and 3 dysplastic regions from 7 mice; *miR-223*$^{-/y}$ → WT: 19 tumours and 7 dysplastic regions from 5 mice; *miR-223*$^{-/y}$ → *miR-223*$^{-/y}$: 10 tumours and 7 dysplastic regions from 4 mice.

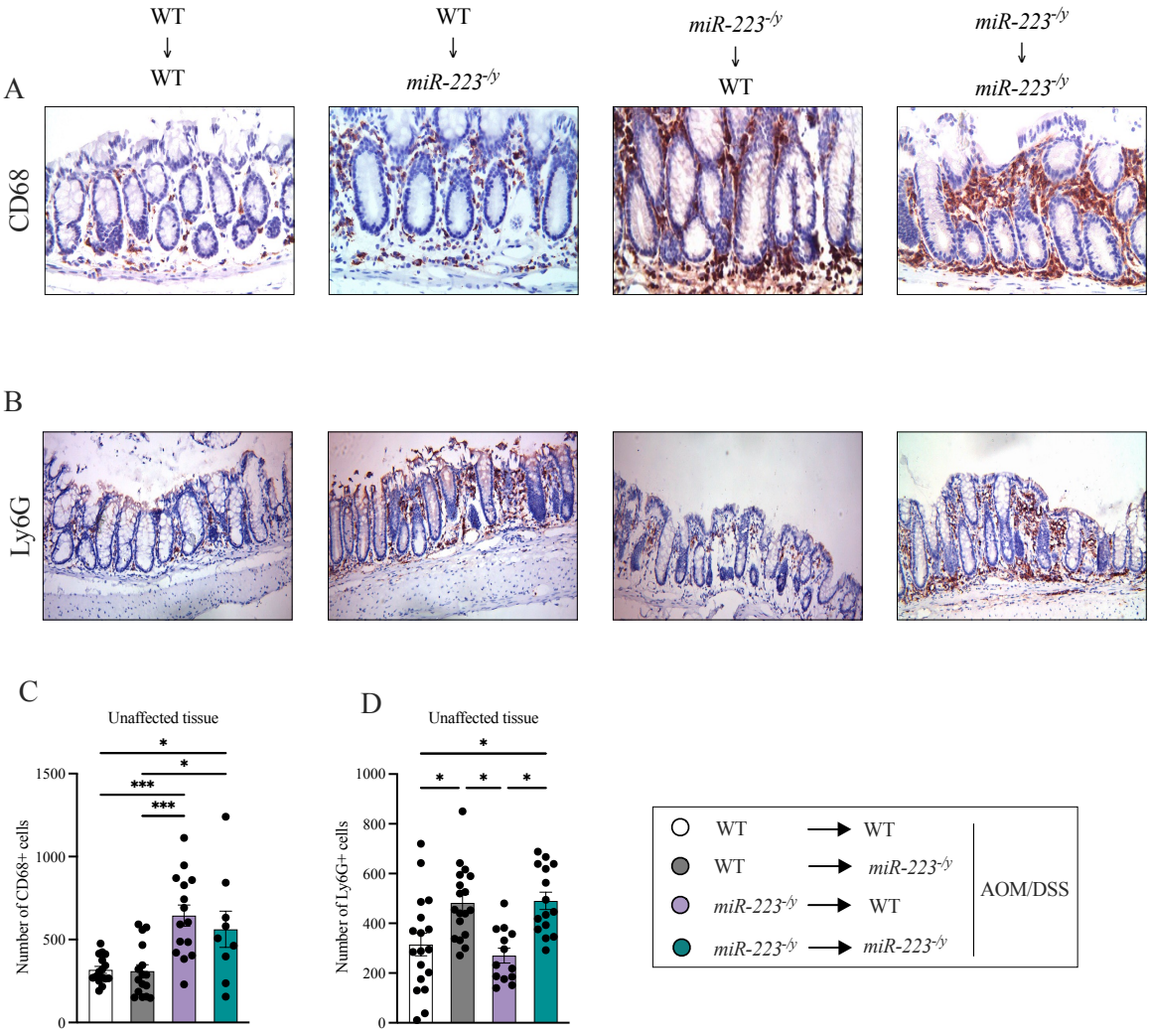


Figure 47. *Bone marrow chimera study shows there is increased macrophage infiltrating into unaffected colonic tissue of miR-223$^{-/y}$ → WT following AOM/DSS.*

Representative 40x (CD68) and 20x (Ly6G) micrographs of unaffected tissue and tumor of WT (CD45.1) and *miR-223$^{-/y}$* (CD45.2) counterparts after immunohistochemical staining for **A**. CD68 and **B**. Ly6G Staining was then quantified for **C.** CD68 and **F**. Ly6G. All data is expressed as mean ± SEM; *, P<0.05; **, P<0.01; ***, P<0.001; versus the indicated counterpart (One-way ANOVA). **A+C** WT → WT n=5; WT → miR-223$^{-/y}$ n=6; *miR-223$^{-/y}$* → WT n=5; and *miR-223$^{-/y}$* → *miR-223$^{-/y}$* n=3. **B+D** WT → WT n=6; WT → *miR-223$^{-/y}$* n=6; *miR-223$^{-/y}$* → WT n=4; and miR-223$^{-/y}$ → *miR-223$^{-/y}$* n=3; with 2/3 fields of view quantified per animal.

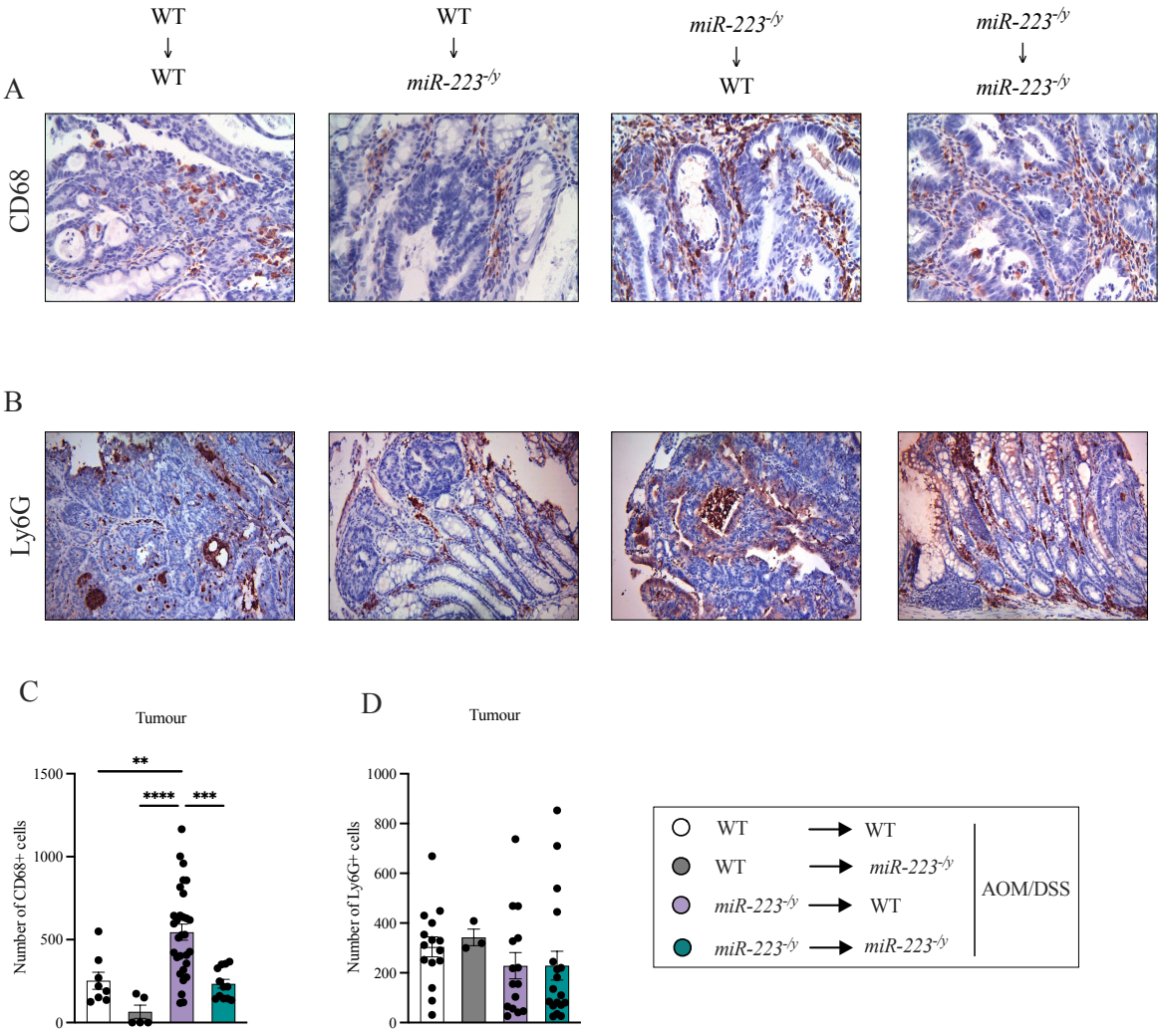


Figure 48. *Bone marrow chimera showed that there is increased macrophage infiltrating into tumour tissue of miR-223$^{-/y}$ → WT following AOM/DSS.*

Representative 40x (CD68) and 20x (Ly6G) micrographs of unaffected tissue and tumor of WT (CD45.1) and *miR-223$^{-/y}$* (CD45.2) counterparts after immunohistochemical staining for **A.** CD68 and **B**. Ly6G Staining was then quantified for **C**. CD68 and **E**. Ly6G. All data is expressed as mean ± SEM; *, P<0.05; **, P<0.01; ***, P<0.001; versus the indicated counterpart (One-way ANOVA). **A+C** WT → WT n=3; WT → *miR-223$^{-/y}$* n=6; *miR-223$^{-/y}$* → WT n=5; and *miR-223$^{-/y}$* → *miR-223$^{-/y}$* n=3. **B+D** WT → WT n=3; WT → *miR-223$^{-/y}$* n=1; *miR-223$^{-/y}$* → WT n=4; and *miR-223$^{-/y}$* → *miR-223$^{-/y}$* n=3; with 1-3 fields of view quantified per tumour.

4.1.7 Hematopoietic deficiency of *miR-223* increases inflammatory markers after AOM/DSS treatment in chimeric mice

To further confirm the consequence of *miR-223* derived from the hematopoietic compartment versus the stromal compartment, RT-PCR analysis was performed on colonic tissue from bone marrow chimera mice. Relative mRNA expression of pro- and anti-inflammatory macrophage, neutrophil and monocyte markers was determined. Expression of *tnf*, *nos2* and *chi3l3* were increased in *miR-223*$^{-/y}$ → WT compared to the stomal chimera (WT → *miR-223*$^{-/y}$ **Figure 49 A + B**). This was accompanied by increases in the neutrophil chemokines *cxcl1* and *cxcl2* (**Figure 49 C**) and non-significant trends towards increased expression of the monocyte chemokines *ccl2* and *ccl7* (**Figure 49 C**). As previously seen in chronic AOM/DSS model, markers associated with vascular growth (*vegfa* and *vegfc)*, macrophage activation (*irf5*) and tumour immunoregulation (*tgfb1* and *il-1rn*) (**Figure 49 A** and **Figure 50 A + B**). Collectively, these data suggest that *miR-223* constrains the inflammatory tone of infiltrating myeloid cells to limit the progression towards tumorigenesis in the AOM/DSS model of CAC.

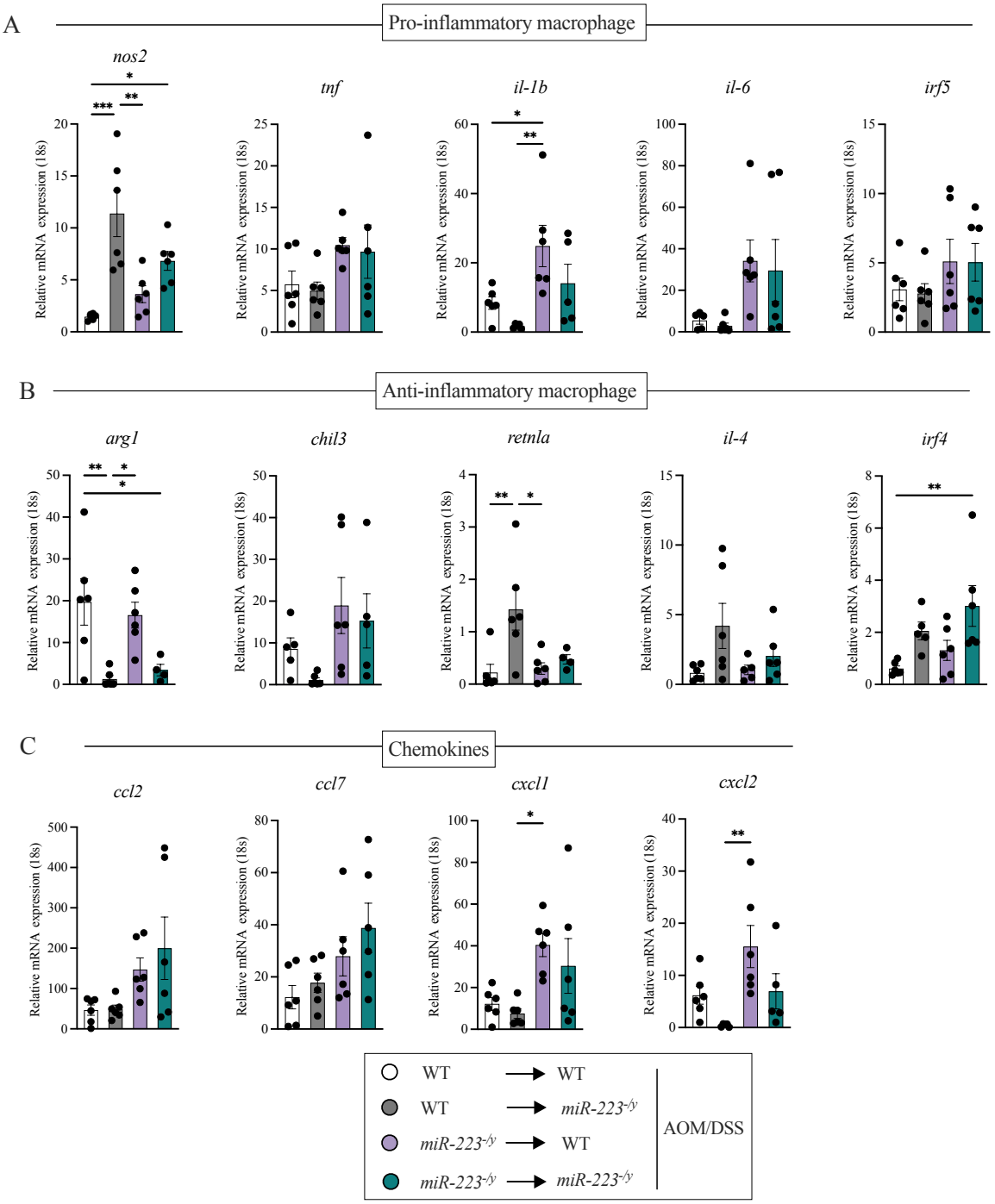


Figure 49. *Hematopoietic deficiency of miR-223 increases inflammatory markers after chronic AOM/DSS treatment in chimeric mice.*

A. Relative mRNA expression of the pro-inflammatory macrophage markers nos2, tnf, il-1β, il-6 and irf5. **B.** Relative mRNA expression of the anti-inflammatory macrophage markers arg1, chi3l3, retnla, il-4, and irf4**. C.** Relative mRNA expression of the monocyte chemokines ccl2 and ccl7; neutrophil chemokines cxcl1 and cxcl2. All data is expressed as mean ± SEM; *, P<0.05; **, P<0.01; ***, P<0.001, versus the indicated counterpart (One-way anova). **A-C** n=5-6 mice/group.

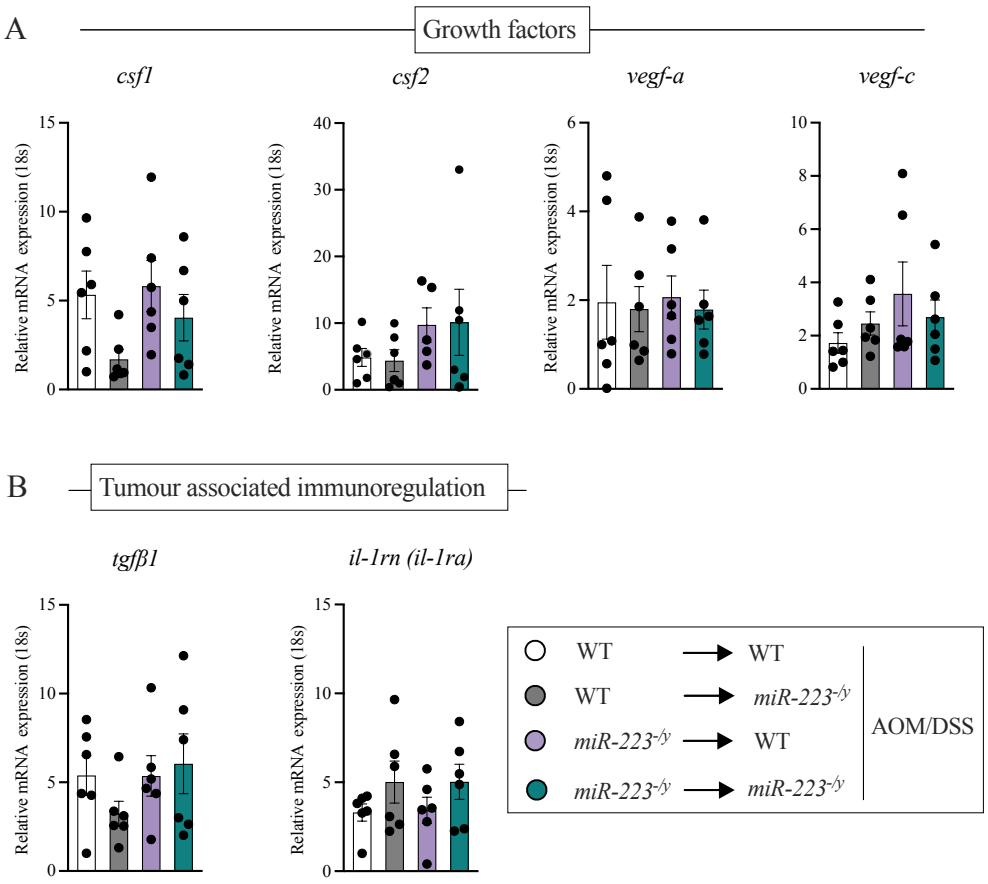


Figure 50. *Hematopoietic deficiency of miR-223 does not alter growth factors following chronic AOM/DSS treatment in chimeric mice.*

A. Relative mRNA expression of the tumour associated growth factors csf1, csf2, vegf-a, and vegf-c. **B.** Relative mRNA expression of markers associated with tumour immunoregulation TGF-β1 and il-1rn. All data is expressed as mean ± SEM; *, P<0.05; **, P<0.01; ***, P<0.001, versus the indicated counterpart (One-way anova). **A-C.** n=5-6 mice/group.

DISCUSSION

Globally the incidence of colorectal cancer, including CAC, continue to rise (Hossain et al., 2022). However, our understanding of the underlying mechanisms behind the progression from UC to the development of CAC remains incomplete. The myeloid associated miRNA, *miR-223* has been identified as a critical regulator of the innate immune system during intestinal inflammation and its expression is increased in patients with active UC. However, to date little research has investigated its role in CAC.

Chronic inflammation is a well-established contributor to both the initiation and progression of cancer (Multhoff et al., 2012). It has previously been implicated in gastric (O'Reilly et al., 2018), esophageal (Muthupalani et al., 2023) and cervical cancers (Fernandes et al., 2015). In CAC, chronic inflammation associated with UC, is the primary contributor to the development and progression of disease. In a chronic mouse model of CAC, *miR-223* was shown to be critical for controlling excessive inflammation, as its deficiency resulted in 66% of mice dying. This model also indicated that *miR-223* is important for limiting tumour development as *miR-223*$^{-/y}$ mice presented with more frequent and larger tumours compared to WT counterparts. This indicates that *miR-223* is a critical regulator in inflammation in CAC.

miRNAs have previously been reported as having the ability to modulate several hallmarks of cancer including apoptosis (Beilankouhi et al., 2024), angiogenesis (Annese et al., 2020), metastasis (Kim et al., 2018), regulation of immune response (Hirschberger et al., 2018) and evasion of tumour suppressors (Yi et al., 2020). Data generated from the chronic AOM/DSS model of CAC, indicates that *miR-223* is a potential regulator of proliferation as its absence resulted in excessive expression of the proliferation markers PCNA and Cyclin D1. This increased tumourigenic and proliferative signature corresponded with increased CCR2^{+} monocytes, CD68^{+} macrophage and Ly6G^{+} neutrophils infiltrating into the colons and increased monocytes migrating into tumours of *miR-223*$^{-/y}$ mice following chronic AOM/DSS. This suggests that in the AOM/DSS model of CAC, the absence of *miR-223* enables the development excessive myeloid driven inflammation, which contributes to the development of a pro-tumourigenic and proliferative microenvironment.

In CAC, the inflammatory microenvironment promotes the release of cytokines, such as IL-6, IL-1β, TNF- α and TGF-β, to promote tumor growth (Bhat et al., 2022). This results in

excessive production of NOS2, along with increased reactive nitrogen and oxidative species, which further boosts the production of pro-inflammatory cytokines (Gochman et al., 2012). This creates a cycle that ensures inflammation is maintained. This leads to DNA damage and ineffective tissue repair. In the model presented, *miR-223*$^{-/y}$ AOM/DSS mice had significantly enhanced cytokine and chemokine expression profile. In particular, there was a mixed expression of both pro-inflammatory and anti-inflammatory cytokines which collectively act to further promote tumour growth. Additionally, NOS2 was significantly increased in the AOM/DSS treated *miR-223*$^{-/y}$ mice. Monocyte and neutrophil chemokines were also increased, with a marked increase seen in myeloid associated growth factors. Collectively, suggesting that *miR-223* is critical for limiting the recruitment of neutrophils and monocytes into the colon during chronic inflammation, along with the secretion of their associated cytokines. Additionally, it indicates that suppression of myeloid driven inflammation by *miR-223* is necessary to prevent the progression from UC to CAC.

The role of *miR-223* in controlling myeloid driven inflammation was further confirmed from samples generated in a bone chimera study. This showed that hematopoietic-derived *miR-223* (*miR-223*$^{-/y}$ → WT recipients) exacerbated AOM-DSS, as indicated by increased macroscopic polyps, dysplasia and tumor numbers compared with controls (WT → *miR-223*$^{-/y}$ recipients). Similar to the chronic AOM/DSS model, this corresponded with increased infiltration of $CD68^{+}$ macrophage, along with the expression of pro-inflammatory and anti-inflammatory macrophage markers (*miR-223*$^{-/y}$ → WT recipients). Furthermore, this was accompanied by significantly increased expression of neutrophil chemokines and trending increase of monocyte markers. This further demonstrates that *miR-223* regulates infiltrating myeloid cells from the hematopoietic compartment to prevent excessive inflammation and limit the progression to CAC.

Persistent inflammation in CAC has also been shown to increases the number of immune cells infiltrating into the colon, with neutrophils and monocytes among the most abundant (Yang et al., 2021a). In the AOM/DSS model of CAC, there was significantly more myeloid cells infiltrating into the colons of *miR-223*$^{-/y}$ mice. As monocytes have the ability to further differentiate into TAMs, this further contributes to a sustained inflammatory cycle through the production of inflammatory cytokines and growth factors. In particular, CCL2, CCL7, TNF, TGF-β and M-CSF1 are critical in this process (Yahaya et al., 2019) . These were all increased in *miR-223*$^{-/y}$ mice in the AOM/DSS model of CAC. This creates a pro-

tumourigenic, immunosuppressive microenvironment that limits the detection and elimination of cancerous cells. As such, TAMs are associated with poor prognosis in many cancers (Wang et al., 2021a). Additionally, TAMs can modulate their microenvironment, they are currently being investigated as a potential therapeutic target for CAC and other cancers. Studies to date have focused on either reducing the presence of TAMs or altering their functions, with current research in CRC showing promising results (Liu et al., 2020, Halama et al., 2016).

TAMs and tissue resident macrophage in the colon, have previously been linked to the recruitment of neutrophils and myeloid-derived suppressor cells via the expression of CXCL1 and CXCL2, which where both increased in *miR-223*$^{-/y}$ mice following AOM/DSS (De Filippo et al., 2013, Cai et al., 2023). Recently, neutrophils have been associated with tumour growth and tumour vascularization (Bui et al., 2024). Whilst further research still needs to be done to fully elucidate the various roles of myeloid cells on the development of CAC, it is critical in order to fully understand the disease, particularly as a subset of patients are non-responsive therapeutics that are currently available. However, CAC is particularly challenging for the development of therapeutics. This is primarily due to the heterogeneity of the disease and its development from UC. For instance, while there is increased expression of the T-cell derived PDl and the PD1 ligands, PD-L1 and PD-L2 in AOM/DSS models, PD1 blockade was shown to have no therapeutic effect in the model (Yassin et al., 2019). As check-point inhibitor blockers are insufficient for the treatment of gastrointestinal tumours, improved understanding of myeloid driven inflammation will be critical.

In conclusion, these data show that *miR-223* is essential for controlling myeloid driven inflammation in the progression from UC to CAC. This is done by suppressing the production of proinflammatory cytokines, limiting tumor growth and controlling proliferation.

CHAPTER 5 INVESTIGATING THE ROLE OF *MIR-223* ON IL-6/STAT3 SIGNALING DURING COLITIS ASSOCIATED COLORECTAL CANCER

INTRODUCTION

CAC is a disease that both develops and progresses due to the presence of chronic colonic inflammation. Due to this persistent inflammation many pathways are dysregulated, including the IL-6/STAT3 signalling pathway. IL-6 is a pro-inflammatory cytokine that is increased in UC and CAC patient biopsies (Atreya and Neurath, 2005, Chung and Chang, 2003). This expression correlates with disease severity, poor patient outcomes and the increased activation of STAT3 (Grivennikov et al., 2009b, Chung and Chang, 2003).

IL-6 family members form one of the largest cytokine families and are classified by their shared use of the ubiquitously expressed signalling receptor glycoprotein 130 (gp130) (Diveu et al., 2003). These cytokines are produced in a variety of cell types but are predominantly secreted from monocytes, macrophages, and intestinal epithelial cells (Grivennikov and Karin, 2011). Members have many functions including the regulation of the innate immune system, proliferation and directing inflammatory responses. As such, their dysregulated expression is associated with many diseases. To elicit their effects, this family of cytokines use two different mechanisms for signalling, classical and trans-signalling as illustrated in **Figure 51** (Hunter and Jones, 2015).

The majority of IL-6 cytokine signalling is via the classical signalling family. In this mechanism, cytokines bind to their membrane bound receptor, which then associates with either a homodimer or heterodimer of gp130. This signalling method has previously been linked to immune activation during the acute stages of inflammation (Baran et al., 2018). Alternatively, some family members, such as IL-6 and IL-11, can also generate soluble receptors through proteolytic processing. This allows cells that do not express membrane bound receptors to be activated, in a process referred to as trans-signalling. This signalling method has previously been linked to chronic inflammation in IBD (Schreiber et al., 2021). Regardless of the signalling mechanism, once an IL-6 family member has formed a complex with gp130, kinases such as JAK enzymes are activated. This results in the phosphorylation of tyrosine residues in gp130, to which proteins critical for the initiation of signalling pathways can bind (Bowman et al., 2000).

STAT3 is a member of the signal transducer and activator of transcription (STAT) protein family. While this family of cytokines has many members, STAT3 is most commonly

associated with inflammation and tumour development (Hu et al., 2024a). Once JAK enzymes have been activated, cytosolic STAT3 monomers are stabilised by dimerization. The STAT3 dimer then translocates into the nucleus where it binds to its corresponding promoter in DNA (Bowman et al., 2000). Following activation, STAT3 induces the expression of genes associated with the regulation of differentiation, angiogenesis, proliferation, and apoptosis. While STAT3 dimerization can be induced by many cytokines and growth factors, JAK/STAT3 signalling is most commonly associated with the hyperactivation of STAT3. Consequently, inflammatory responses are dysregulated enabling tumour progression through the promotion of angiogenesis and proliferation (Wang et al., 2018b, Bollrath et al., 2009).

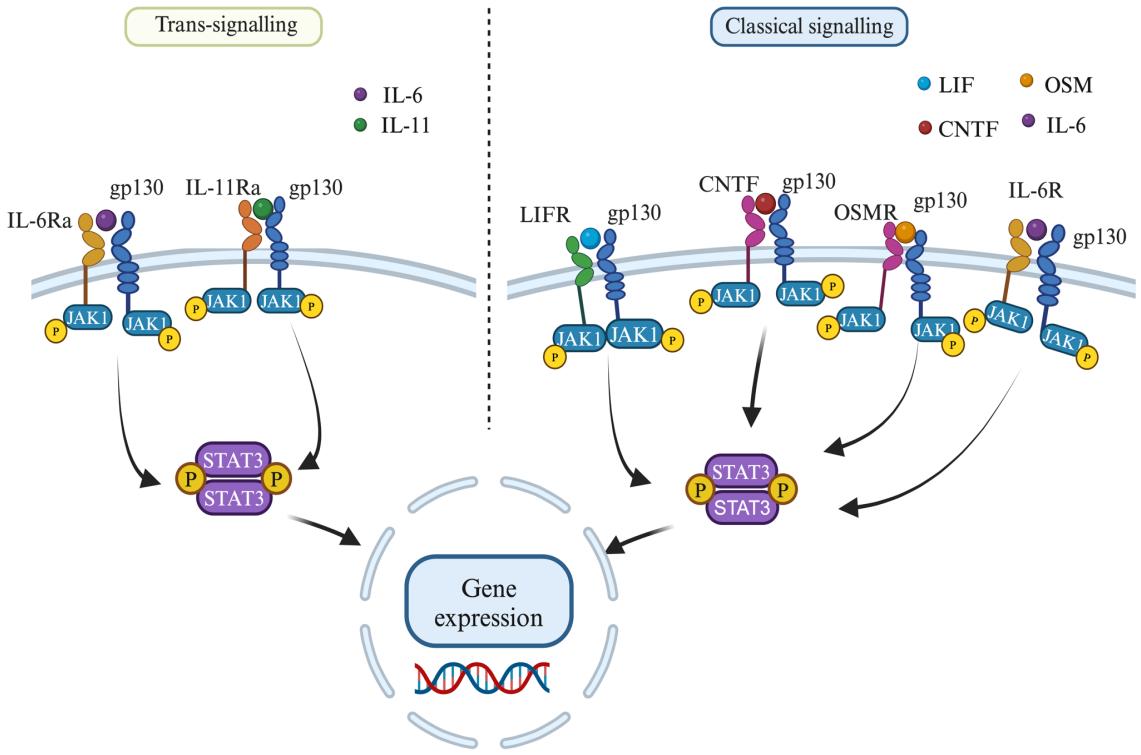


Figure 51. *Overview of IL-6/STAT3 signalling in humans.*

Members of the IL-6 cytokine family signal via trans- or classical signalling. Receptors bind to gp130 resulting in STAT3 stabilization and translocation to the nucleus. After binding to its corresponding promotor STAT3 is activated and can induce its regulatory effects. Created with BioRender.com.

Altered IL-6/STAT3 signalling has been shown to contribute to the development of several types of cancers including breast (Wang et al., 2018a), lung (Hu et al., 2024b), ovarian (Zhang et al., 2023c), liver (Zhang et al., 2021b) and colon (Zhang et al., 2018, Jin, 2020). In IBD and CAC, IL6/STAT3 signalling is often dysregulated. Additionally, patients present with increased IL-6 expression that correlates with disease severity (Akanda et al., 2018, Schreiber et al., 2021, Zhang et al., 2020, Grivennikov et al., 2009b). AOM/DSS models of CAC have demonstrated that infiltrating myeloid cells are a major producer of IL-6. Additionally, when IL-6/STAT3$^{-/-}$ mice were treated with AOM/DSS they had less infiltrating myeloid cells and developed reduced tumours compared to WT controls (Grivennikov et al., 2009a). Furthermore, activated macrophages have the ability to promote CAC via the IL-6/STAT3 pathway (Zhang et al., 2023b, Sheng et al., 2022). As a result of increased IL-6/STAT3 signalling, STAT3 target genes are upregulated. These include cyclin d1, which promotes a proliferative microenvironment (Leslie et al., 2006). Thus, as the importance of IL-6/STAT3 signalling becomes increasingly clear, targeting networks that are implicated in its expression could be beneficial.

miRNAs are involved in many biological processes including proliferation, apoptosis, cell signalling and differentiation. They also play a critical role in regulating immune responses and can act to either promote or supress tumour development. Several miRNAs have been implicated in IL-6/STAT3 signalling in CAC. For instance, *miR-218* and *miR-124* reduce the expression of IL-6 and STAT3, respectively (Yang et al., 2017) . In contrast, *miR-21* and *miR-551b* upregulate IL-6/STAT3 signalling (Chaluvally-Raghavan et al., 2016). In UC patients and AOM/DSS treated mice, *miR-320* expression is decreased (Pierdomenico et al., 2016). However, its overexpression in mice reduced inflammation, proliferation, and tumour formation. This was mediated through the downregulation of IL-6/STAT3 signalling (Wu et al., 2022a). Comparable results were seen in with overexpression of *miR-26* suppressing IL-6 production in macrophage (Zhang et al., 2021f).

It has previously been demonstrated that *miR-223* plays a key role in regulating the innate immune response during intestinal inflammation in UC patients. However, its role has yet to be elucidated in CAC. In the context of IL-6/STAT3 signalling, this miRNA is potentially important due to its role in UC progression and the production of pro-inflammatory cytokines, such as IL-6. Additionally, this is a myeloid associated miRNA, and myeloid cells are one of the largest producers of IL-6. Thus, further research investigating the role of

miR-223 in IL-6/STAT3 signalling during CAC could potentially be of interest as a therapeutic target.

AIMS OF THIS CHAPTER

The overall aim of this chapter was to perform bioinformatic analysis on an RNA seq dataset generated from the AOM/DSS model of CAC. Specific aims of this chapter where:

1. To determine if pathways associated with poor prognosis in CAC are upregulated in *miR-223*$^{-/y}$ mice following chronic AOM/DSS.
2. Identify pathways that are potentially implicated in the inflammatory-driven progression to tumorigenesis in *miR-223*$^{-/y}$ mice following chronic AOM/DSS.
3. Investigate the role of IL-6/STAT3 signalling using acute and chronic AOM/DSS models of CAC.

5.1.1 *miR-223* deficiency results in altered gene expression following AOM/DSS

To determine why *miR-223*$^{-/y}$ mice develop more a severe tumorigenic and proliferative signature following AOM/DSS compared to WT counterparts, RNA sequencing was initially performed on whole colon samples. Pearsons's correlation analysis showed that within each treatment group, the samples were similar (**Figure 52 A**). Co-expression analysis revealed that there was overlap in expression between the three treatment groups, but also highlighted mRNAs that were only expressed by individual groups (**Figure 52 B**). Differential expression analysis showed that mRNA expression varied between each of the different treatment groups, WT AOM/DSS vs WT, *miR-223*$^{-/y}$ AOM/DSS vs WT and *miR-223*$^{-/y}$ AOM/DSS vs WT AOM/DSS (**Figure 52 C – E**). These data show that *miR-223* deficiency alters gene expression in the AOM/DSS model of CAC.

5.1.2 *miR-223* deficiency results in the upregulation of pathways associated with poor prognosis in the AOM/DSS model of CAC

Bioinformatic analysis using unbiased gene set enrichment (GSEA), showed that KEGG pathways for Inflammatory Bowel Disease (MMU05321) and Colorectal Cancer (MMU05210) were positively enriched in *miR-223*$^{-/y}$ AOM/DSS mice compared to WT AOM/DSS controls (**Figure 53 A – D**). Additional GSEA analysis showed that multiple pathways associated with poor clinical prognosis in CAC and CRC were positively enriched in the *miR-223*$^{-/y}$ AOM/DSS mice including ‘apoptosis’, ‘cytosolic DNA sensing’, ‘p53 signalling’ ‘DNA damage bypass’, ‘cellular response to stress’ and ‘regulation of PTEN regulation’ (**Figure 54 A - F**). These data suggest that *miR-223* is involved in the regulation of key pathways that are essential for limiting the development of tumorigenesis.

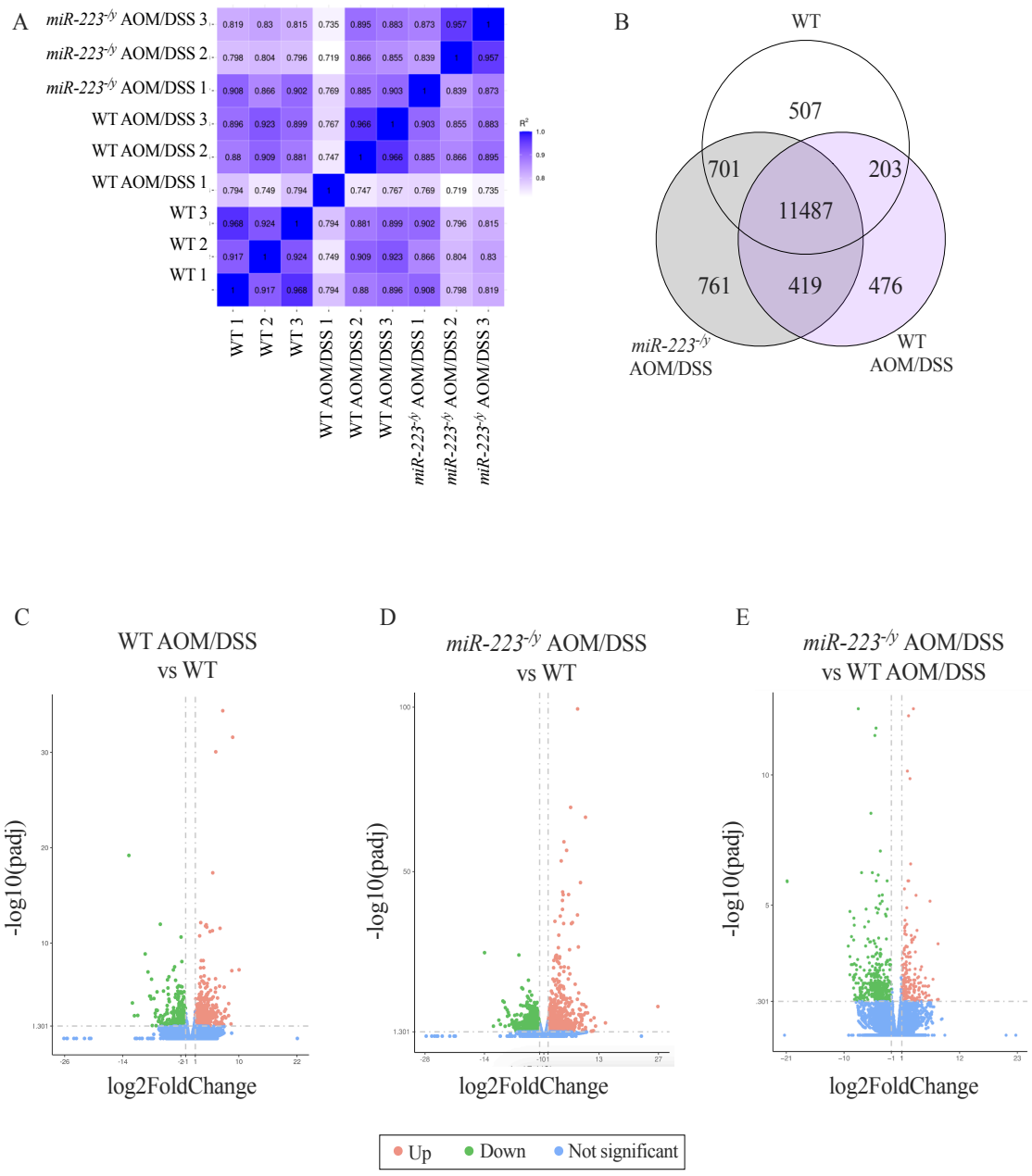


Figure 52. *Gene expression is altered in WT and miR-223$^{-/y}$ mice following chronic AOM/DSS.*

WT and *miR-223$^{-/y}$* mice were treated with chronic AOM/DSS. Following necropsy colonic samples were analysed via RNA sequencing. This was used to generate **A.** Heatmap using Pearson coefficient between all samples analysed. **B**. Venn diagram illustrating the overlap of mRNA expression between all treatment groups. Volcano plot of differentially expressed mRNA between **C.** WT AOM/DSS and WT, **D.** *miR-223$^{-/y}$* AOM/DSS vs WT, and **E.** *miR-223$^{-/y}$* AOM/DSS vs WT AOM/DSS. N=3 mice/group.

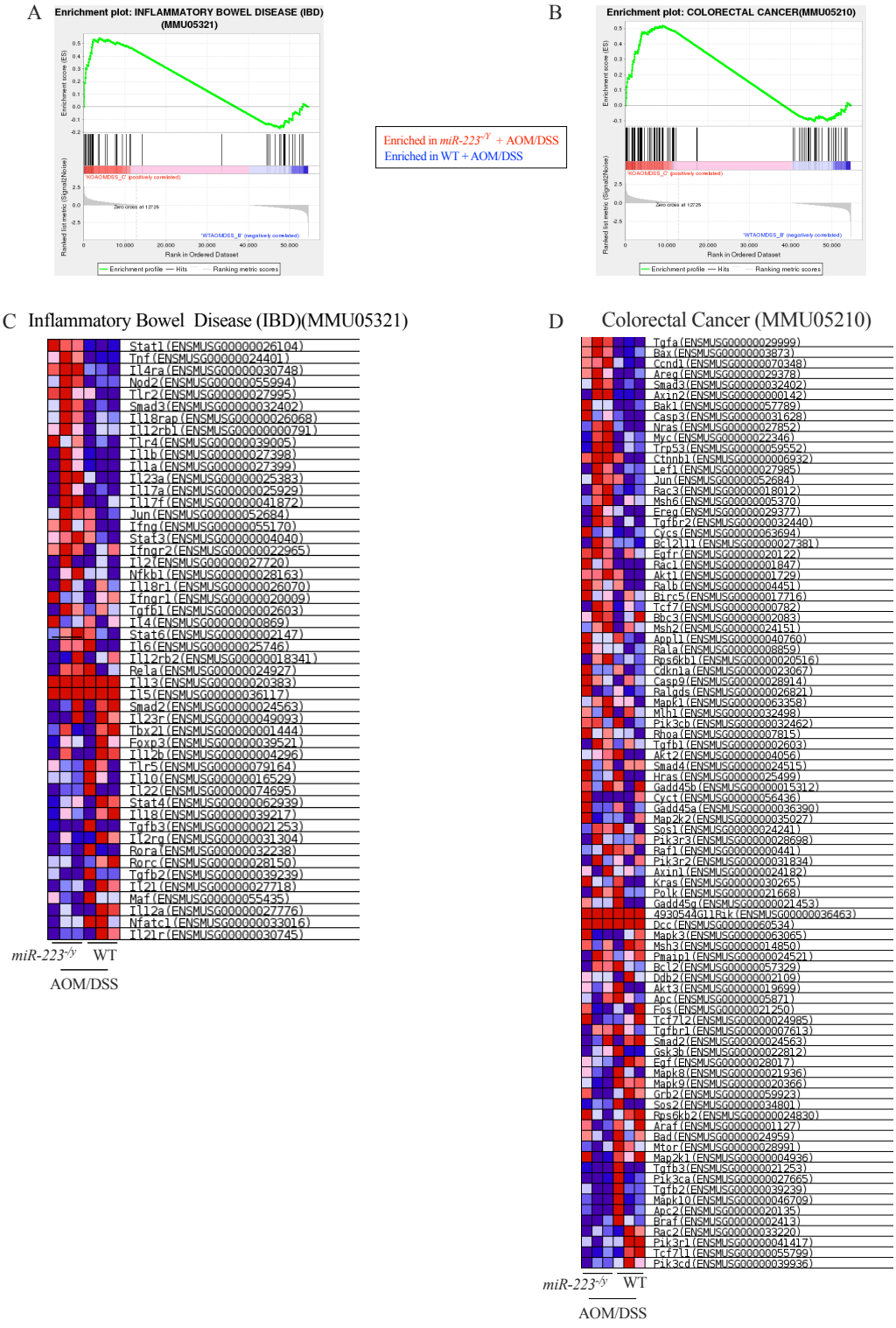


Figure 53. *miR-223$^{-/y}$ mice present with an upregulation of pathways associated with Inflammatory Bowel Disease and Colorectal Cancer following chronic AOM/DSS.*

A. Enrichment plot for Inflammatory Bowel Disease (MMU05321) (NES: 1.209; FDR q-val: 0.473). **B.** Enrichment plot for Colorectal Cancer (MMU05210) (NES: 1.343; FDR q- val: 0.281). **C.** Heat map for Inflammatory Bowel Disease (MMU05321) **D.** Heat map for Colorectal Cancer (MMU05210). N=3 mice/group.

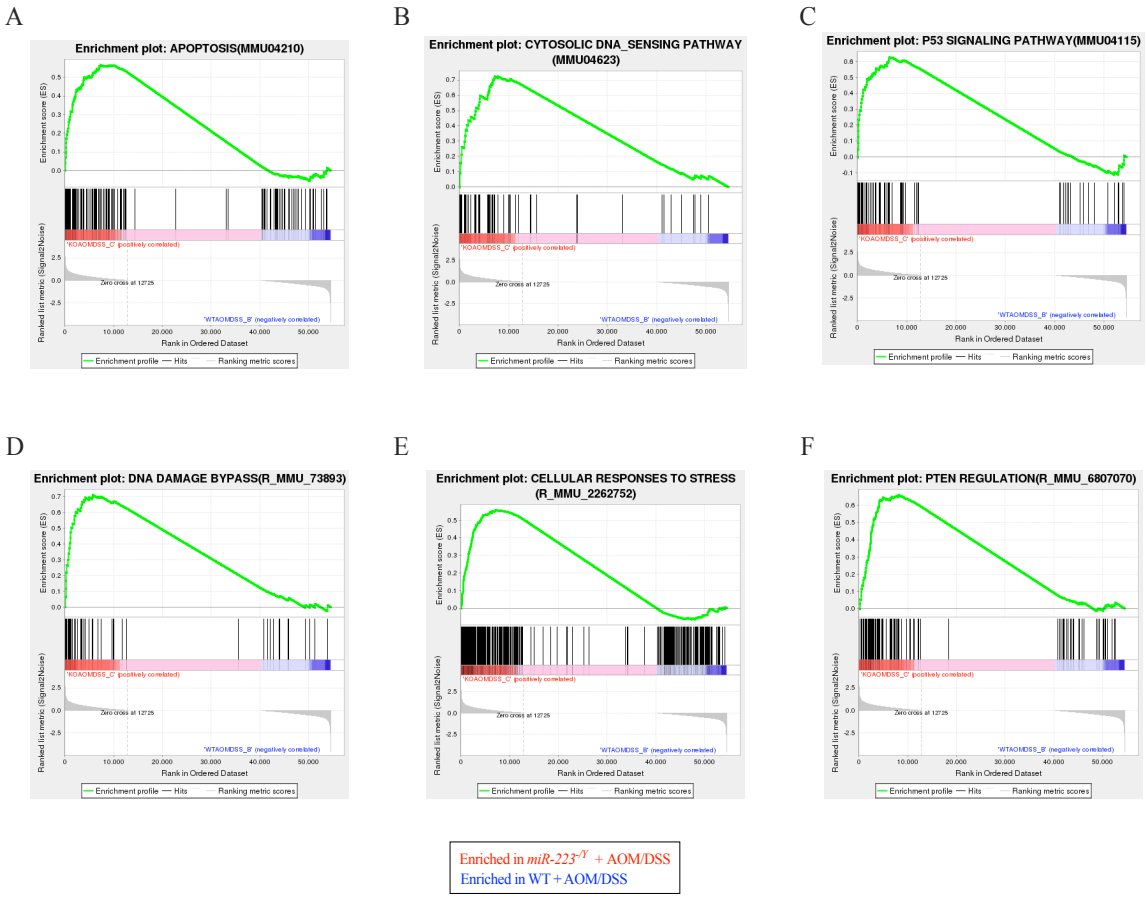


Figure 54. *miR-223$^{-/y}$ mice present with an upregulation of pathways associated with poor prognosis in CAC when treated with chronic AOM/DSS.*

Following GSEA analysis **A.** Enrichment plot for Apoptosis (MMU04210) (NES: 1.404; FDR q-val: 0.212). **B.** Enrichment plot for Cytosolic DNA Sensing Pathway(MMU04623) (NES: 1.438; FDR q-val: 0.285) **C.** Enrichment plot for p53 signalling (MMU04115) (NES: 1.404; FDR q-val: 0.239), **D.** Enrichment plot for DNA damage bypass (R_MMU_73893) (NES: 1.368; FDR q-val: 0.308) **E.** Enrichment plot for Cellular response to stress (R_MMU_2262752) (NES:1.365; FDR q-val: 0.292) **F.** Enrichment plot for PTEN regulation (R_MMU_8948751) (NES: 1.391; FDR q-val: 0.402). N=3 mice/group.

5.1.3 *miR-223$^{-/y}$* mice treated with AOM/DSS have increased cytokine signalling

RNA-sequencing analysis of GO pathways highlighted a consistent pattern of increased cytokine signalling in AOM/DSS treated *miR-223$^{-/y}$* mice including 'cytokine receptor binding', 'cytokine activity', 'cellular response to interferon gamma' and 'response to lipopolysaccharide' (**Figure 55**). This was also observed following Reactome GSEA analysis where 'IL-6 family members', 'cytokine signalling in the immune system', 'regulation of Interferon gamma signalling' and 'signalling by interleukins' were all

upregulated in *miR-223*$^{-/y}$ mice compared to WT following AOM/DSS (**Figure 56**). GSEA analysis on KEGG pathways showed that there is increased expression of cells from the hematopoietic compartment (**Figure 57**), which based on bone marrow chimera data (Chapter 4), is the primary source of *miR-223* that is crucial for constraining the inflammatory driven progression of CAC. Collectively, this analysis shows that there is increased cytokine signalling in *miR-223*$^{-/y}$ mice in the AOM/DSS model of CAC.

5.1.4 Increased IL-6 cytokine family and STAT3 signalling in *miR-223*$^{-/y}$ mice following AOM/DSS modelling of CAC

As *miR-223*$^{-/y}$ mice had an enriched signature for increased cytokine signalling and IL-6 family members (**Figure 56**), and these are both of interest clinically for the treatment of CAC, they were investigated further. miRNA target identification was performed to identify binding partners involved in these processes. This revealed that some IL-6 family members and its downstream targets are binding partners for *miR-223-3p* including LIF, IL6ST and STAT3 (**Figure 58 A – C**). Further analysis on whole colonic tissue via RT-PCR showed that expression of IL-6 family members are significantly upregulated in *miR-223*$^{-/y}$ mice compared to WT controls, such as *il-6, il-11* and *lif (***Figure 59 A**). Additionally, cytokines that signal via STAT3, *il-22* and *il-17a,* were also significantly increased in *miR-223*$^{-/y}$ mice (**Figure 59 B**).

Expression and localisation of active p-STAT3 and total STAT3 proteins were assessed by immunoblot and immunohistochemistry. There was an increase in p-STAT3 observed via western blot (**Figure 60 A**). This was also shown via immunohistochemistry where there was significantly more p-STAT3 infiltrating into the unaffected tissue of *miR-223*$^{-/y}$ mice compared to WT controls following AOM/DSS (**Figure 60 B + D**). There was also significantly more total STAT3 detected in the unaffected tissue of *miR-223*$^{-/y}$ mice (**Figure 60 C + E**). When taken collectively, these findings suggests that IL-6 and p-STAT3 signalling are contributing to the development of CAC in *miR-223*$^{-/y}$ mice.

A

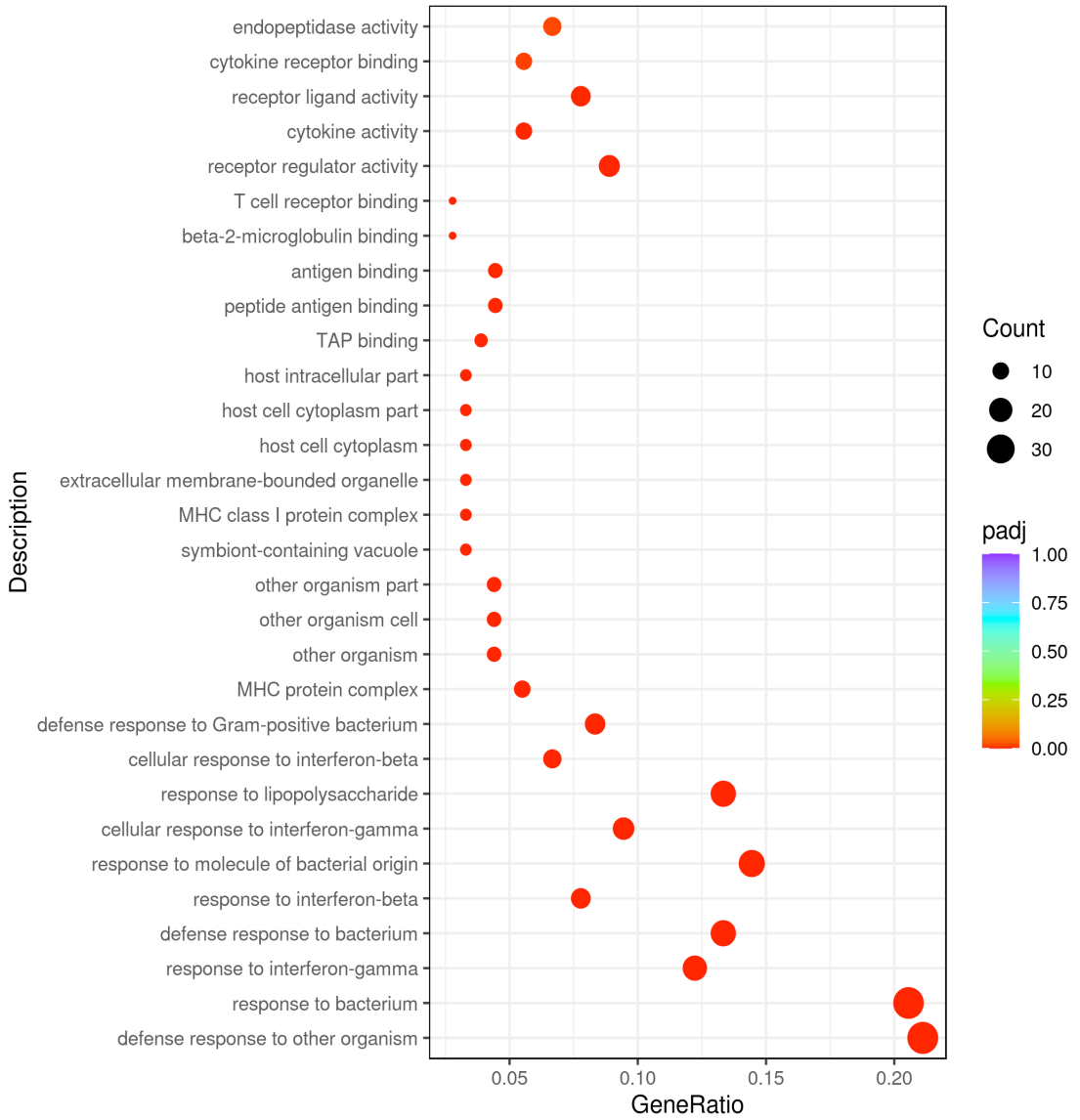


Figure 55. *miR-223$^{-/y}$ mice present with an upregulation of chemokine and cytokine activity after chronic AOM/DSS.*

A. GO Enrichment Analysis Scatter Plot for GO terms upregulated in *miR-223$^{-/y}$* AOM/DSS vs WT AOM/DSS. N=3 mice/group.

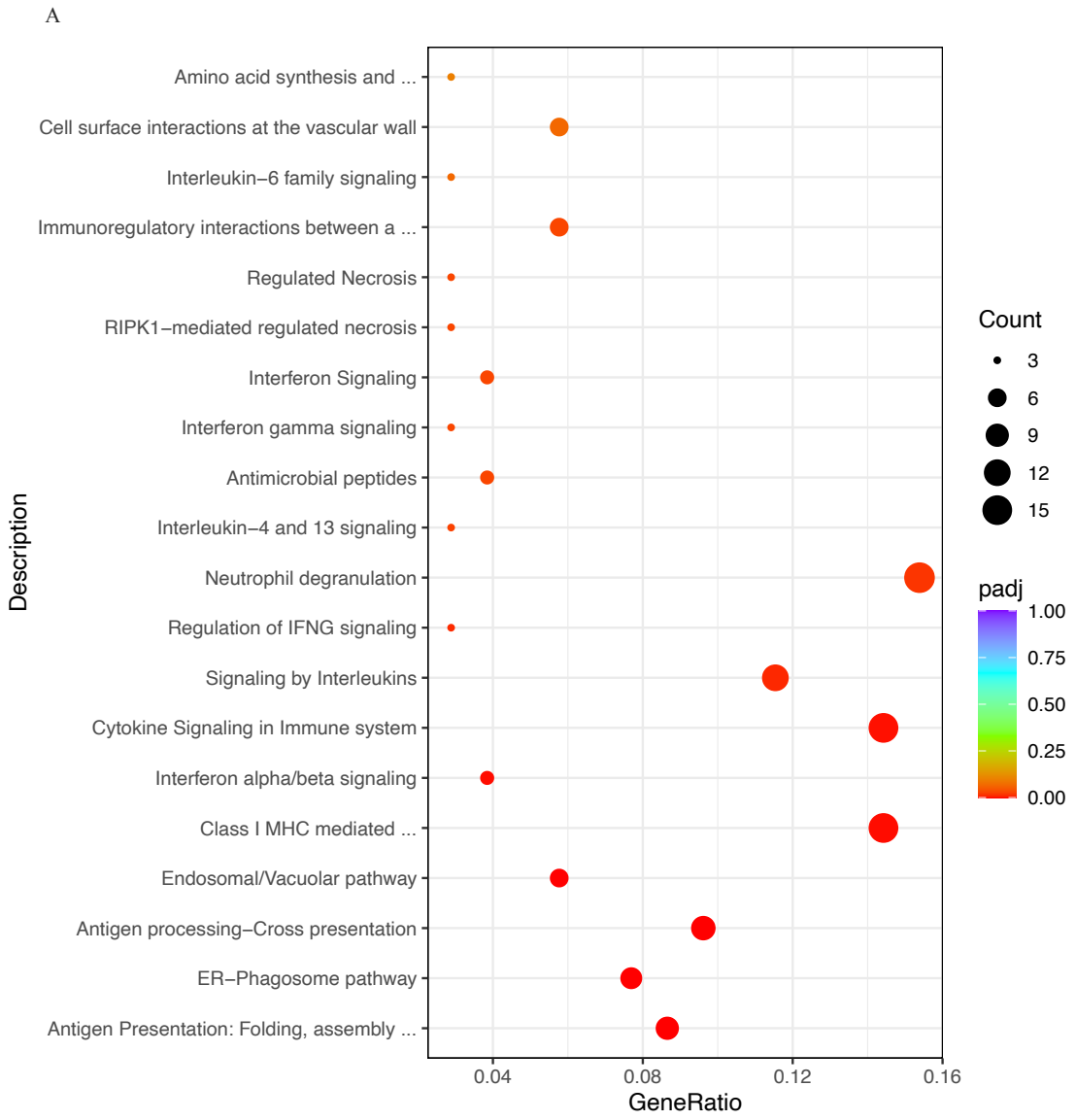


Figure 56. *miR-223$^{-/y}$ mice present with increased expression of cytokine and IL-6 family signalling following chronic AOM/DSS.*

A. Reactome Enrichment Analysis Scatter Plot for Reactome terms upregulated in *miR-223$^{-/y}$* AOM/DSS vs WT AOM/DSS. N=3 mice/group.

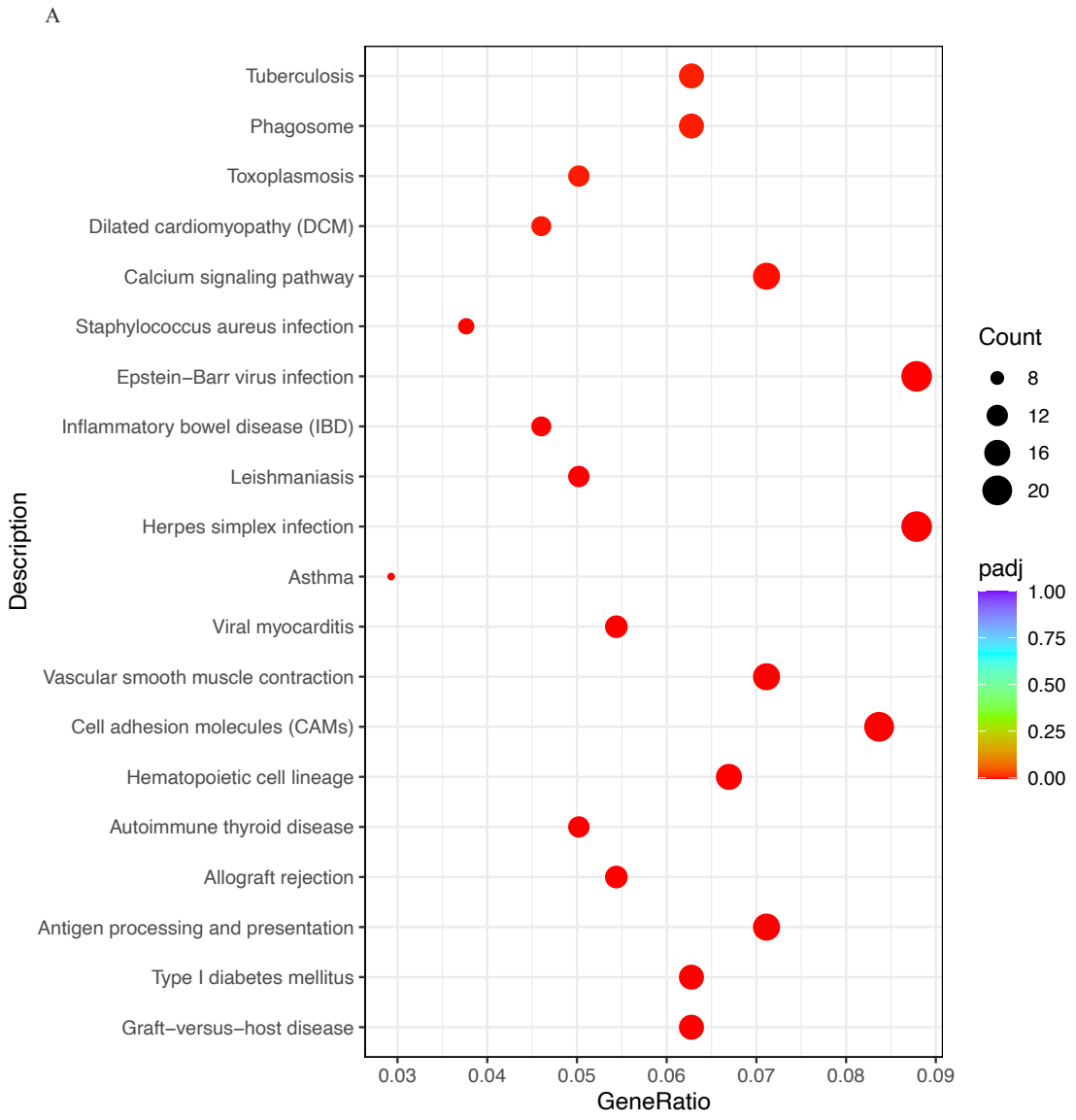


Figure 57. *miR-223$^{-/y}$ mice present with increased expression of hematopoietic cells after chronic AOM/DSS.*

A. KEGG Enrichment Analysis Scatter Plot for KEGG terms upregulated in *miR-223$^{-/y}$* AOM/DSS vs WT AOM/DSS. N=3 mice/group.

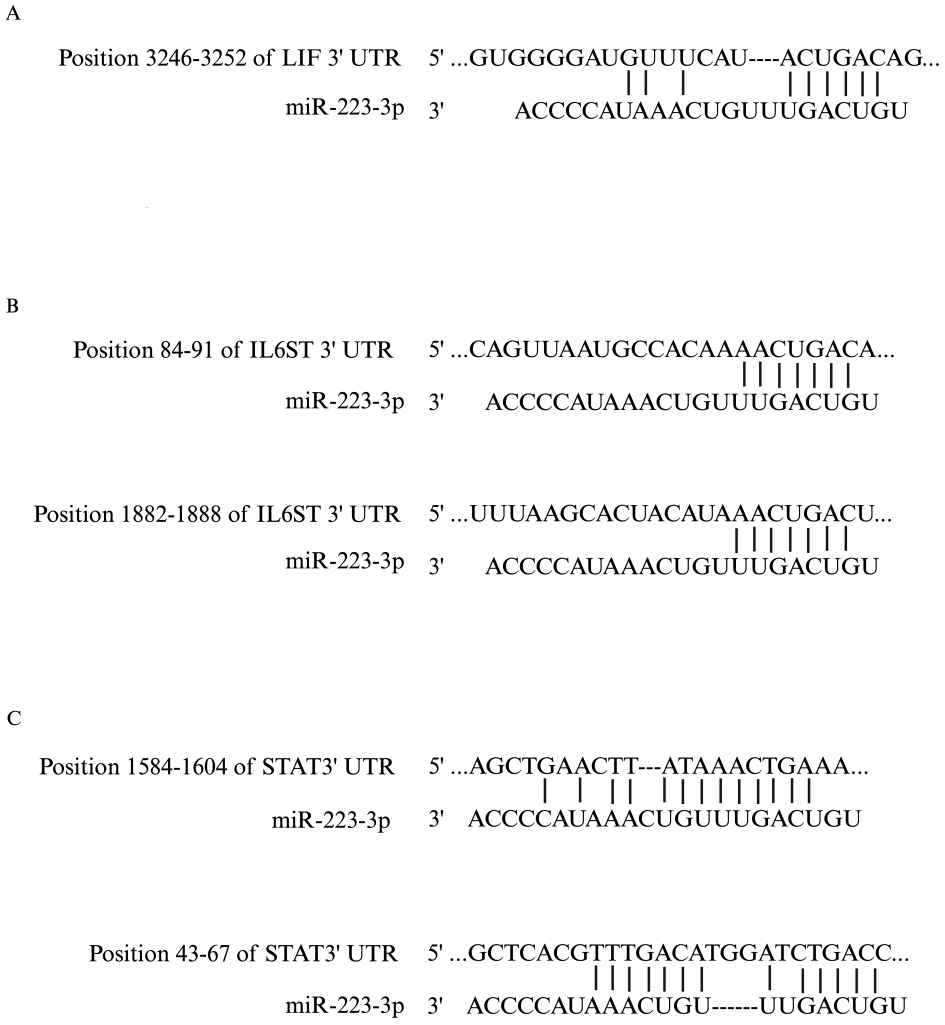


Figure 58. *Illustration of the binding sites in LIF, IL-6ST and STAT3 that are miR-223-3p targets.*

Following miRNA target identification, binding sites for *miR-223-3p* were identified on **A.** LIF, **B.** IL6ST and **C.** STAT3. Diagram created on BioRender.com.

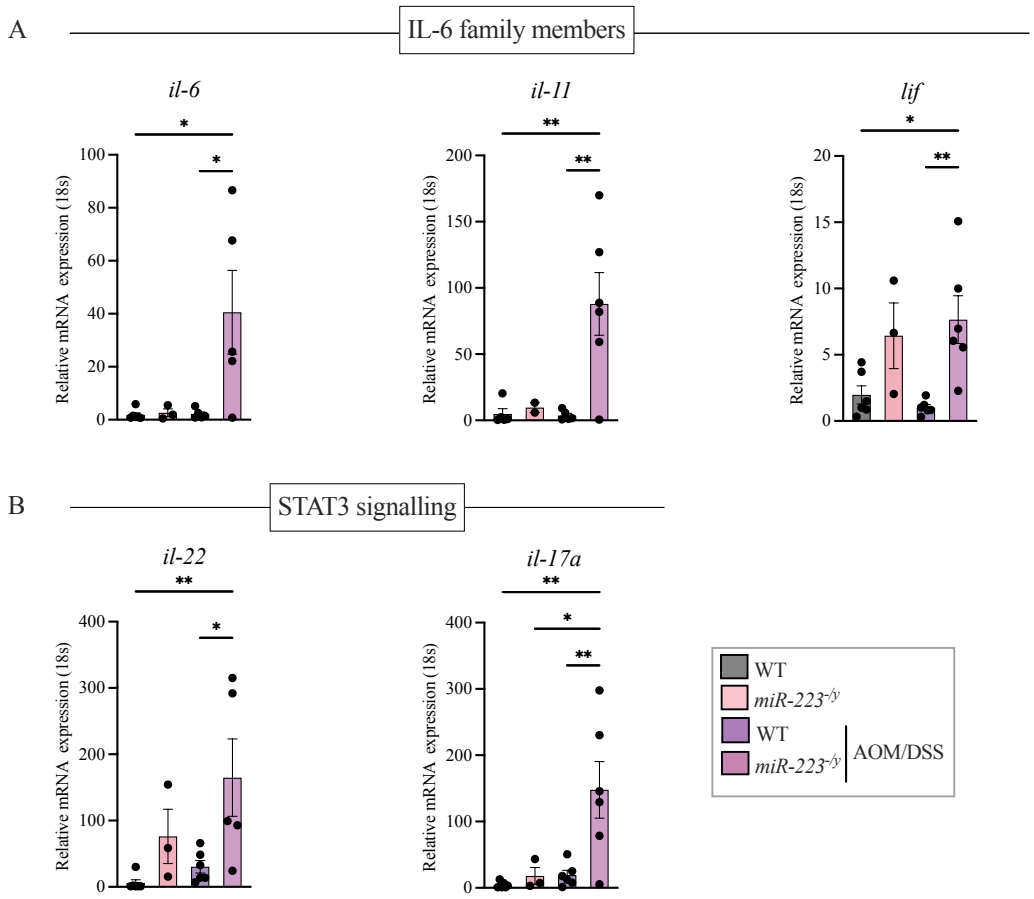


Figure 59. *IL-6 family members and cytokines that signal via STAT3 are increased in miR-223$^{-/y}$ mice following chronic AOM/DSS.*

WT and *miR-223$^{-/y}$* mice were treated with chronic AOM/DSS. Following necropsy colonic samples were used to measure **A.** Relative mRNA expression of the IL-6 family members IL-6, IL-11 and LIF. **B.** Relative mRNA expression of IL-22 and IL-17a which signalling via STAT3. All data is expressed as mean ± SEM; *, P<0.05; **, P<0.01; ***, P<0.001 versus the indicated counterpart (One-way ANOVA). N=3-6 mice/group.

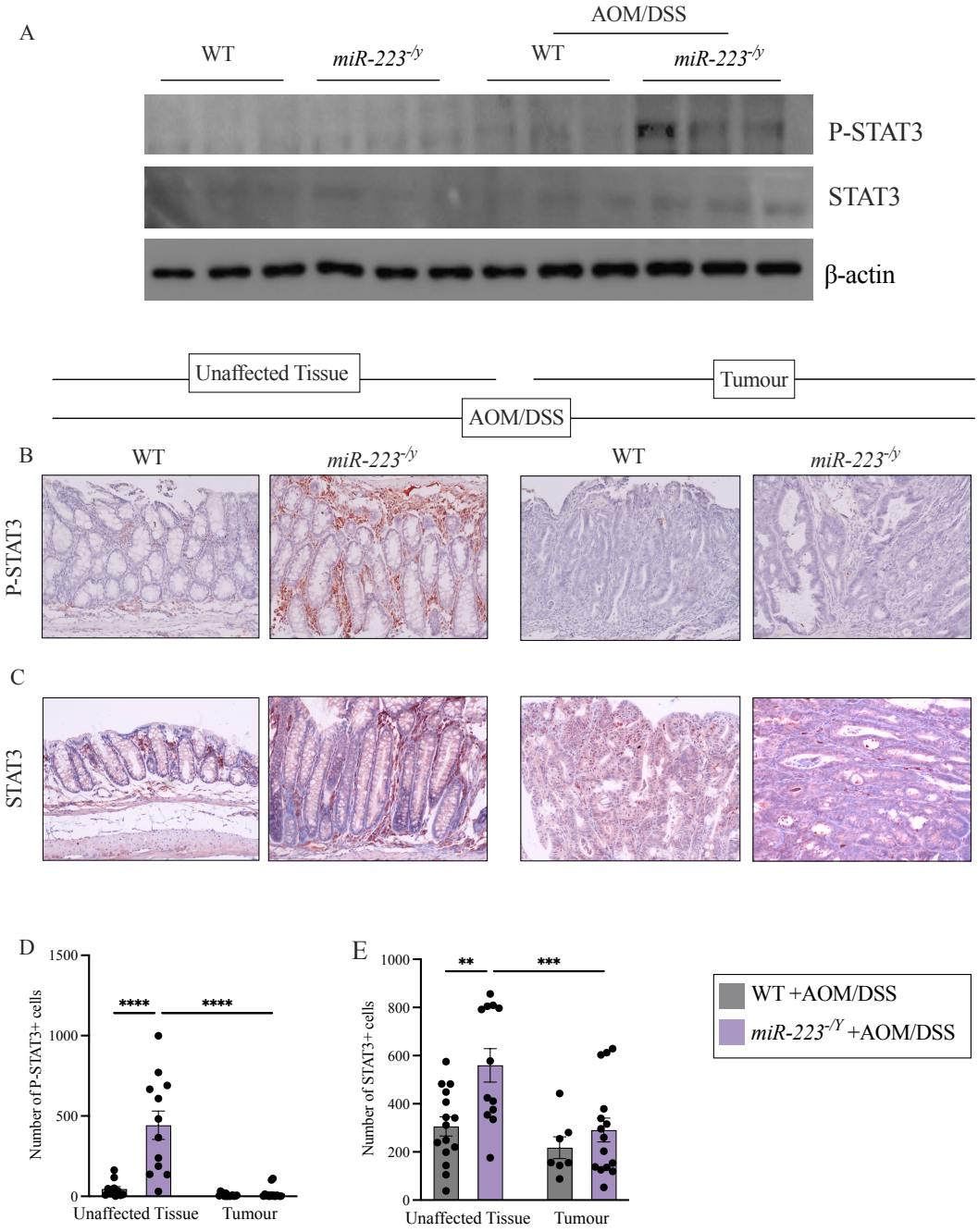


Figure 60. *miR-223$^{-/y}$ mice have increased p-stat3 and stat3 expression following treatment with chronic AOM/DSS.*

WT and *miR-223$^{-/y}$* mice were treated with chronic AOM/DSS. Following necropsy colonic samples were used for **A.** Western immunoblot assessment of P-STAT3, STAT3 and β-actin. Representative 20x micrographs of unaffected and tumour tissue of immunohistochemical staining of WT and *miR-223$^{-/y}$* mice after chronic AOM/DSS for **B.** p-STAT3 and **C.** STAT3. Quantification of immunohistochemical staining of **D.** p-STAT3 and **E.** STAT3. All data is expressed as mean ± SEM; *, P<0.05; **, P<0.01; ***, P<0.001 versus the indicated counterpart (One-way ANOVA). **A.** N=3-6 mice/group. **B+D** WT AOM/DSS n=5; *miR-223$^{-/y}$* AOM/DSS n=4; **C+E** WT AOM/DSS n=5; *miR-223$^{-/y}$* AOM/DSS n=4 with 3 fields of view presented per animal.

5.1.5 Antibody-mediated depletion of infiltrating Ly6G^{+} myeloid cells with RB6-8C5 reduced early tumorigenesis in *miR-223*$^{-/y}$ mice using an acute model of AOM-DSS

As shown in chapter 4, bone marrow chimera data suggests that haematopoietic derived *miR-223* is critical for constraining tumour development in the AOM/DSS model of CAC. Additionally, *miR-223*$^{-/y}$ mice have increased expression of haematopoietic cells. However, the sub-type of immune cells involved in this regulation of inflammation is still unknown. Due to increased IL-6/STAT3 signalling infiltrating neutrophils could potentially be responsible as this signalling pathway is critical for their recruitment into mucosal tissues. To investigate if *miR-223* controlled neutrophil recruitment was responsible for the increased tumorigenic and proliferative signature observed in *miR-223*$^{-/y}$ mice, samples generated from a shortened AOM/DSS model were used (AOM + 1 round of DSS and 5 weeks recovery with water). This showed that in *miR-223*$^{-/y}$ mice treated with an anti-GR1 (clone RB6-8C5) antibody there was significantly fewer tumours per section compared to IgG controls (**Figure 61 A**). Furthermore, anti-GR1 treated *miR-223*$^{-/y}$ mice had significantly smaller areas of dysplasia than those treated with IgG control (**Figure 61 B**). Finally, tumour area was also significantly lower in the anti-GR1 treated corresponding to the development of lower grade tumours (**Figure 61 C - E**).

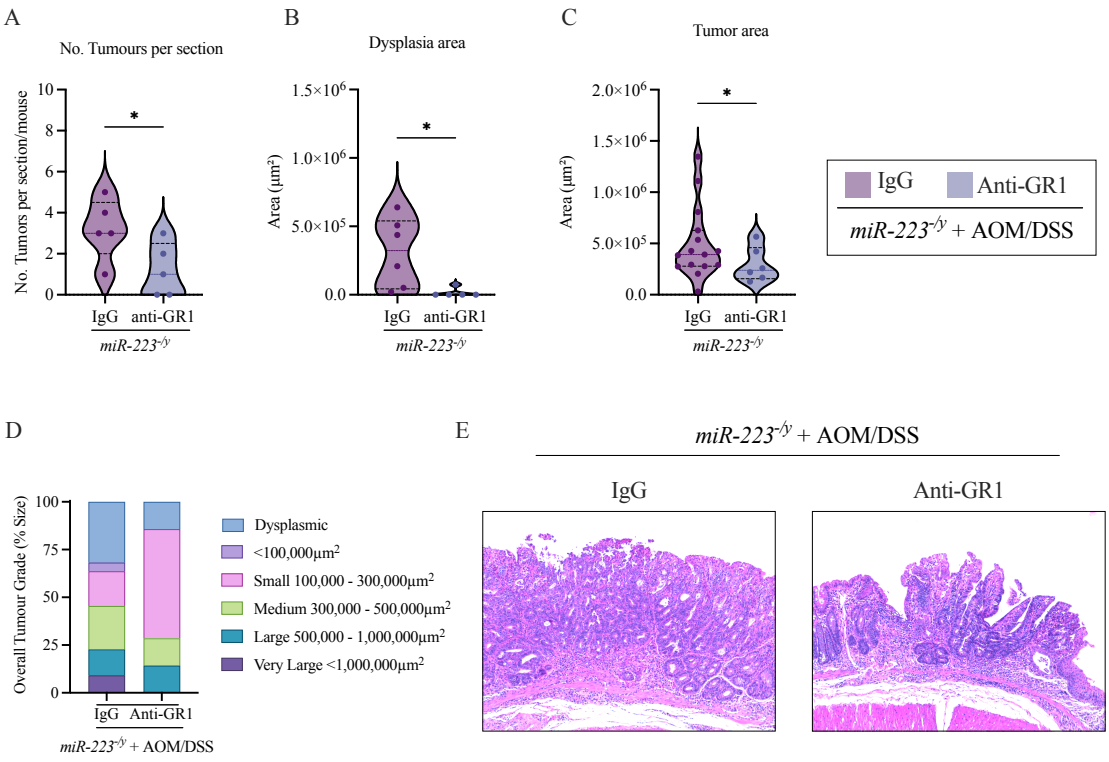


Figure 61. *Depletion of infiltrating Ly6G^{+} myeloid cells reduces early tumorigenesis in miR-223$^{-/y}$ mice following acute AOM/DSS.*

miR-223$^{-/y}$ mice were treated with either 20µg (i.p) anti-GR1 (Lyg6/Ly6C: RB6-8C5 clone) or an isotype control were treated with acute AOM/DSS. Following H&E staining the **A.** Number of tumours per section **B.** Dysplasia area (µm²) per section **C.** Tumour area (µm²) per section and **D.** Tumour grading based on size (µm²) per section was determined, based on H&E staining of IgG or Anti-GR1 treated *miR-223$^{-/y}$* treated with acute AOM/DSS. **E.** Representative micrographs of IgG and anti-GR1 treated *miR-223$^{-/y}$* mice. **A-D.** IgG n=6 mice; anti-GR1 n=5 mice.

DISCUSSION

Due to the continued increase in CAC cases annually, improved understanding of the regulatory pathways that contribute to the development and progression of this disease is critical. This would contribute to the development of new therapeutic options for patients, leading to improved patient outcomes and reducing the associated global health burden of the disease. Collectively, these data indicate that in the AOM/DSS model of CAC, *miR-223* is involved in the regulation of several pathways that that are essential for the control of proliferation, inflammation and prevent the development of cancer.

While many inflammatory pathways have been previously been linked to tumour development in CAC, the increased production of pro-inflammatory cytokines is associated with poor prognosis for patients (Landskron et al., 2014). In this CAC model, *miR-223*$^{-/y}$ mice had increased cytokine signalling, suggesting that *miR-223* has a key role in preventing aberrant cytokine production during chronic inflammation. In particular, IL-6 family signalling was shown to be increased in *miR-223*$^{-/y}$ mice compared to WT controls and several IL-6 family members have been identified as binding partners of *miR-223.*

The IL-6 family of cytokines are increasingly being recognized for their role in intestinal carcinogenesis. A variety of different cell types have the ability to produce IL-6 family members. However, during chronic intestinal inflammation the primary producers of IL-6, IL-11 and LIF are monocytes and macrophage following activation from NF-κB (Naugler and Karin, 2008). These markers where all significantly increased in *miR-223*$^{-/y}$ mice compared to WT controls in the chronic AOM/DSS model. Furthermore, in CRC increased expression of IL-6 correlates with larger tumours, metastasis, and poor prognosis (Chung and Chang, 2003, Zeng et al., 2017). IL-6 also correlates with more severe inflammation in patients with active UC, which precedes the development of CAC (Feng et al., 2023).

IL-6 has previously been shown to be upregulated in CAC (Li *et al.*, 2010) and is associted with increased infiltration of neutrophils (Li et al., 2010, Wang et al., 2014b). Furthermore, samples analysed from a chronic AOM/DSS model showed that there are significantly more neutrophils infiltrating into the colons of *miR-223*$^{-/y}$ mice and a marked increase in their associated chemokines, *cxcl1* and *cxcl2.* Increased IL-6 and infiltrating neutrophils result in the activation of STAT3, along with the upregulation of its target gene Cyclin-D1, which promotes a proliferative pro-inflammatory microenvironment (Leslie et al., 2006).

There are few studies investigating the role of other IL-6 family members in CAC. STAT3 activation via IL-11 has also been shown to contribute to the progression of CAC and correlates with poor prognosis in CRC patient's (Wang et al., 2021b, Heichler et al., 2020). Similarly, OSM is associated with poor patient prognosis and its elevated expression has been identified in CAC patients that are non-responsive to anti- TNF-α (Nardone et al., 2023). In CRC, LIF has previously been shown to contribute to disease through the downregulation of p53 expression, in a process mediated by the activation of STAT3. This promotes chemoresistance, consequently enhanced LIF expression correlated with poor prognosis for CRC patients (Yu et al., 2014). Additionally, LIF expression has been shown to correlate with infiltrating TAMs in the TME in glioblastoma, ovarian and thyroid cancers, impairing anti-PD1 therapy (Pascual-García et al., 2019). In UC, LIF expression is upregulated in patients with UC (Guo et al., 2021, Guimbaud et al., 1998). In a DSS model the increased expression of LIF resulted in the activation of STAT3 and prevented Th17-cell differentiation (Zhang et al., 2019b). Thus, while further research is needed into the role of LIF, IL-11 and OSM in CAC, they could potentially play a critical role in its progression. As there expression is elevated in *miR-223*$^{-/y}$ mice in the AOM/DSS model of CAC, further research is warranted to fully elucidate their role.

In CAC, the upregulation of IL-22 and IL-17 have previously been reported, which are both upregulated in *miR-223*$^{-/y}$ mice following AOM/DSS (Yuksel et al., 2019). Specifically, excessive production of IL-22 in UC contributes to tumour growth and promotes metastasis through the activation of STAT3 (Jiang et al., 2013). IL-17a also contributes to cancer by increasing the expression of PD-L1, which promotes resistance to anti-PD-L1 therapy in CRC (Liu et al., 2021). In CAC, IL-17A-deficient mice developed less tumours, had less proliferation and inflammation than WT counterparts following AOM/DSS. This was associated with decreased production of inflammatory cytokines and expression of STAT-3 (Hyun et al., 2012).

Haematopoietic derived *miR-223* was shown to be critical for constraining chronic colonic inflammation, with knockout mice having increased expression of haematopoietic cells following treatment with AOM/DSS. However, the immune cells responsible have yet to be fully elucidated. Due to the importance of IL-6/STAT3 signalling in the recruitment of neutrophils, samples generated from a shorted AOM/DSS model that mimics the development phase of CAC were analysed. This was to assess if *miR-223* controlled

neutrophil recruitment was responsible for the increased tumorigenesis in *miR-223*$^{-/y}$ mice. This showed that early depletion of neutrophils and myeloid-derived suppressor cells, reduced the development of colonic dysplasia and tumour development in *miR-223*$^{-/y}$ mice compared to the IgG counterparts. This suggest that neutrophils and myeloid-derived suppressor cells are contributing to the progression from UC to CAC. These cells have been shown to contribute to the production of pro-inflammatory cytokines such as TNF-α, IL-1, TGF-β and IL-6, further activating inflammatory pathways in CAC (Li et al., 2023). Additionally, myeloid-derived suppressor cells are critical in the development of CAC, and this has recently been shown to be primarily through the production of IL-19 and subsequent activation of STAT3 (Zhang et al., 2024b, Wang et al., 2024, Ibrahim et al., 2018). As there is increasing evidence that aberrant IL-6/STAT3 signalling is contributing to the progression of CAC, research has focused on its role as a potential therapeutic target. Currently, the IL-6 inhibitor, Siltuximab is in clinical trials and the STAT3 inhibitor Bruceantinol is in development (Angevin et al., 2014, Wei et al., 2019). Thus, mining selective non-coding RNA networks to identify important therapeutic opportunities, such as *miR-223* regulated mRNA circuits, could be beneficial in identifying druggable targets.

Besides being used as potential biomarkers for disease detection, using microRNAs to identify critical signalling pathways, such as IL-6/STAT3, could potentially give rise to more personalized treatment options for patients due to their ability to bind to hundreds of mRNA sequences (Landskron et al., 2014). While these data indicate that *miR-223* is a tumour suppressor in CAC, its role in other cancers varies. In gastric cancer the overexpression of *miR-223* is associated with increased proliferation, migration, and poor prognosis for patients (Zhu et al., 2020b, Li et al., 2011). In contrast, the overexpression of *miR-223* in lung cancer has been linked to tumour suppression via a *miR-223-3p*-mutant p53 feedback loop that acts to inhibit proliferation (Luo et al., 2019). Additionally, *miR-223* also targets its binding partners in the IGF-1R pathway which results in cancer cells being more sensitive to chemotherapy (Nian et al., 2013). In breast cancer, the role of *miR-223* is complex, primarily due to the heterogenicity of the disease. Some research has suggested that the upregulation of *miR-223* limits the progression of cancer cells through the suppression of the EGF pathways, this was associated with improved prognosis in patients with triple negative breast cancer (Fabris et al., 2016, Chen et al., 2021b). However, other research has proposed that *miR-223* promotes the development of breast cancer via the upregulation of pro-tumorigenic pathways such as Mef2c-β-catenin, EGF and Hippo/YAP

signalling pathways (Du et al., 2021, Wang et al., 2022, Pinatel et al., 2014). *miR-223* has also been shown to contribute to tumour development in sporadic CRC (Chai et al., 2019, Sun et al., 2015, Wang et al., 2017a), with its expression correlating with poor patient prognosis and metastasis (Li et al., 2014).

While CAC is also a cancer that develops in the colon, the pathogenic sequence that precedes the development of disease differs significantly. These data show that *miR-223* is protective during the inflammatory driven tumorigenesis that leads to CAC development. Thus, as *miR-223* has a dual role in cancer, having the ability to both promote and suppress disease, its use as a therapeutic target needs to be investigated in a disease specific manner. These data collectively indicate that restoring the expression of *miR-223,* or its regulated mRNA binding partners and associated protein circuits, could potentially lead to reduced tumour growth and prevent the development of CAC. However, this has yet to be investigated in mouse models or in a clinical setting in the context of CAC. Recent research into *miR-233* as a therapeutic target has focused on hepatocellular carcinoma, where delivery of *miR-223* through adenovirus inhibited angiogenesis and prevented disease progression (Fu et al., 2023).

In conclusion, *miR-223* is essential for controlling myeloid driven inflammation in the progression from UC to CAC by suppressing the production of pro-inflammatory cytokines and carcinogenic pathways.

CHAPTER 6 INVESTIGATING THE ROLE OF *MIR-223* DEFICIENCY ON NITRIC OXIDE SIGNALLING AND ITS IMPACT ON THE DEVELOPMENT OF COLITIS ASSOCIATED COLORECTAL CANCER

INTRODUCTION

Nitric oxide (NO) is a short-lived signaling molecule that is critical in various biochemical and physiological processes. Chief among these in the colon is ensuring that intestinal integrity is maintained (Mu et al., 2019), along with eliciting appropriate immune responses (Wink et al., 2011). Dysregulated NO production is associated with many diseases including UC. UC patients have increased production of NO, which has been shown to contribute to the secretion of pro-inflammatory cytokines, further driving the inflammatory process and disease progression (Rafa et al., 2013, Soufli et al., 2016, Krzystek-Korpacka et al., 2020). However, the involvement of NO on the development of CAC is yet to be fully elucidated.

NO is predominately synthesized via the enzymatic conversion of L-arginine to L-citrulline by nitric oxide synthase (NOS) enzymes in the presence of oxygen. This family of enzymes consists of three isoforms, neuronal NOS (NOS1), endothelial NOS (NOS3) and inducible NOS (NOS2). NOS1 and NOS3 are constitutively expressed by neuronal and endothelial cells respectively. To produce NO these isoforms require high levels of intracellular calcium (200 - 400nM), followed by its subsequent binding to calmodulin. Due to the transient nature of intracellular calcium levels, NOS1 and NOS3 are associated with low levels of NO production in the picomolar to nanomolar range (Piazza et al., 2015). In contrast, NOS2 expression by immune cells, particulary macrophage, is often referred to as calcium independent due to its high affinity for calmodulin at extremely low levels of intracellular calcium (< 40nM) (Cho et al., 1992). This enables NOS2 to produce higher levels of NO, typically in the micromolar range, for much longer periods of time.

Another mechanism of nitric oxide production is through the nitrate-nitrite-nitric oxide pathway. In this pathway commensal bacteria in the oral cavity reduce dietary nitrate to nitrite, which this is then swallowed. Once in the stomach, nitrite undergoes protonation to form nitrous oxide that eventually decomposes into NO. While this pathway produces considerably lower amounts of NO, its production is not reliant on the bioavailability of oxygen. This ensures that NO is still produced under hypoxic conditions when NOS enzymes aren’t fully functional (Lundberg et al., 2008). An overview of nitric oxide

synthesis is shown in

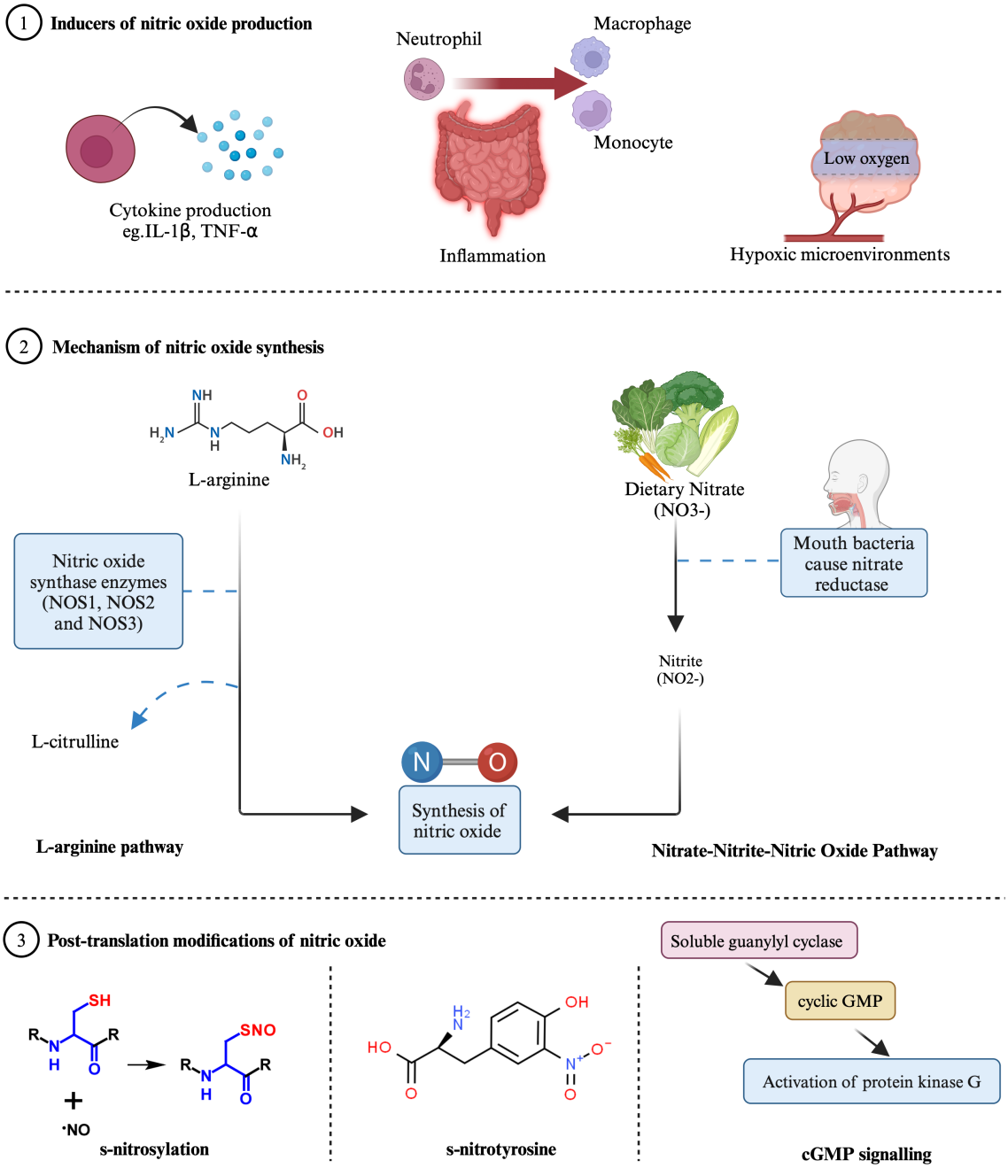


Figure 62.

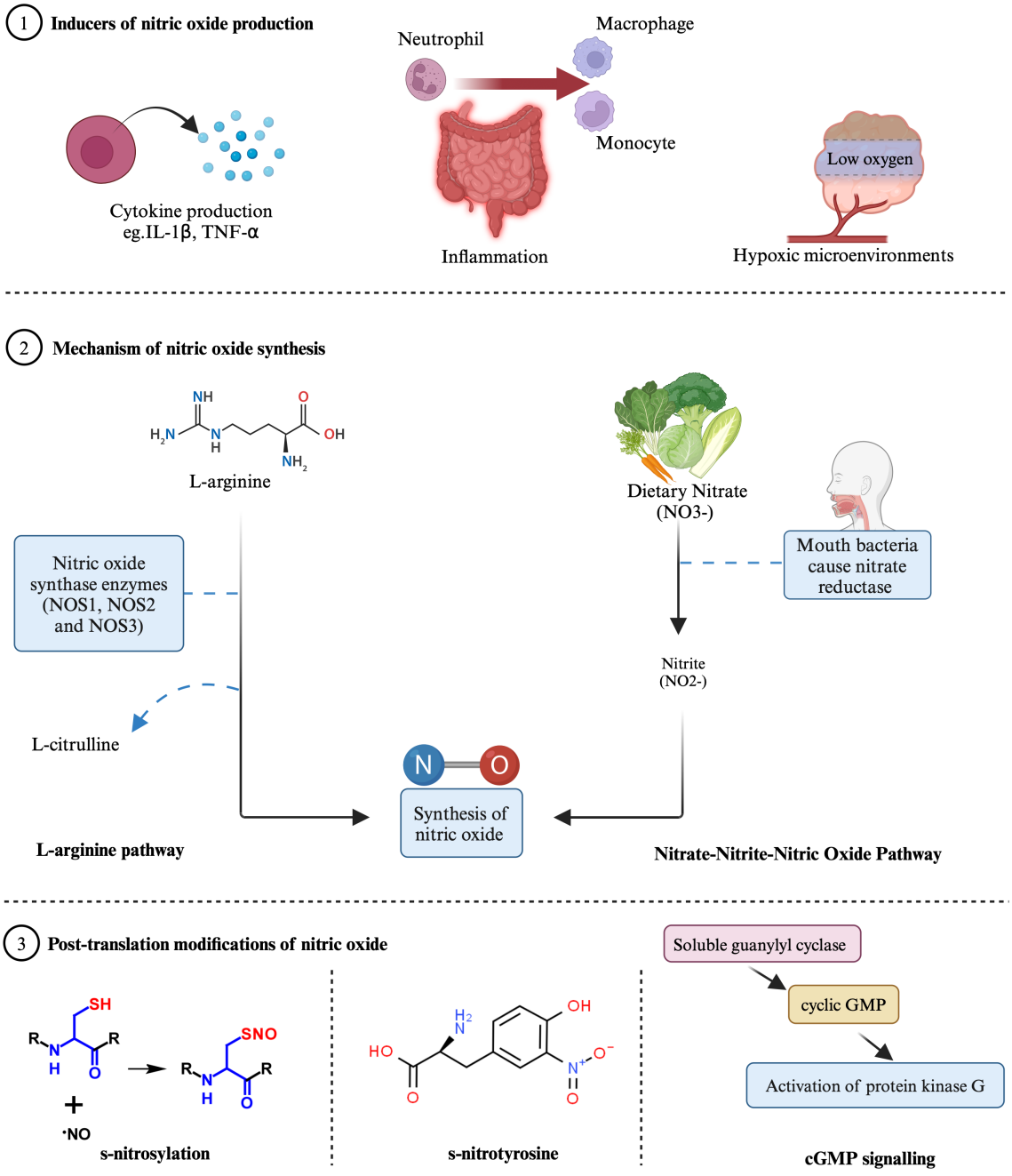


Figure 62. *Overview of the induction, synthesis and post-translation modifications of nitric oxide.*

Nitric oxide synthesis is induced due to the presence of inflammation, increased cytokine production or low oxygen concentrations. Nitric oxide is produced either by NOS enzymes or via the conversion of dietary nitrate. Nitric oxide then causes post-translational modifications. Created with BioRender.com.

NO carries out its functional effects through either cyclic guanosine monophosphate (cGMP) signaling or the post-translational modification of proteins. In cGMP signalling, the heme group in soluble guanylyl cyclase (sGC) binds to NO, leading to guanosine triphosphate (GTP) being converted to cGMP. This activates protein kinase G (PKG) and ion channels, and is essential for NO's roles in the regulation of vasodilation and neurotransmission (Xiong et al., 2011).

In the post-translational modification of proteins, NO can either alter their structure, function or how proteins interact with other proteins. The primary mechanism is referred to as s-nitrosylation, which involves the formation of a covalent bond between NO and the thiol side chain of a cysteine residue (Sun et al., 2006). In a similar modification, s-glutathionylation is the ability of NO to form disulfide bonds between cysteine and glutathione residues (Grek et al., 2013). Finally, NO can also cause functional effects via tyrosine nitration. This modification incorporates NO into a tyrosine residue to form 3-nitrotyrosine (Ischiropoulos, 2003).

In cancer, NO has a complex multifaceted role that varies depending on the type of tissue, the stage of tumour development and the concentration of NO. The contrasting role of NO stems from its ability to alter many of the hallmarks of cancer as summarised in **Figure 63.** At low concentrations NO promotes proliferation and metastasis. In contrast, while high NO is associated with DNA damage in the early stages of disease, it has also been shown to activate immune cells in developed tumours (Korde Choudhari et al., 2013). As such, NO been implicated in the progression of various carcinomas including breast (Basudhar et al., 2017), cervical (Dong et al., 2014), lung (Saisongkorh et al., 2016), pancreatic (Wang et al., 2016b) and colon (Puglisi et al., 2015a).

In colorectal cancer, enhanced expression of NOS2 has been identified in 60% of colon adenomas (Yagihashi et al., 2000, Ambs et al., 1998) and has since been found to correlate with poor patient outcome (Gochman et al., 2012, Zafirellis et al., 2010). UC is a known risk factor for the development of colon cancer. NOS2 expression is upregulated in biopsies from UC and colon cancer patients, while low expression was detected in non-cancerous tissue (Gochman et al., 2012). This suggests that NO expression, via the production of NOS2, is enhanced in inflamed tissues.

miRNAs are critical regulators of inflammation and the production of nitric oxide production, with their aberrant expression contributing to excessive NO, these include *miR-939, miR-146a* and *miR-369* (Guo et al., 2012, Li et al., 2016, Scalavino et al., 2020). *miR-223* is essential for directing the innate immune response during intestinal inflammation and its expression is increased in patients with active UC (Zhang *et al.*, 2014;(Neudecker et al., 2017b). However, the impact of *miR-223* deficiency in CAC and its role in the regulation of nitric oxide production has yet to be determined. As the progression from UC to CAC is inflammatory driven, further research into the role of NOS2 could be beneficial both as a biomarker and a potential therapeutic for UC and CAC patients.

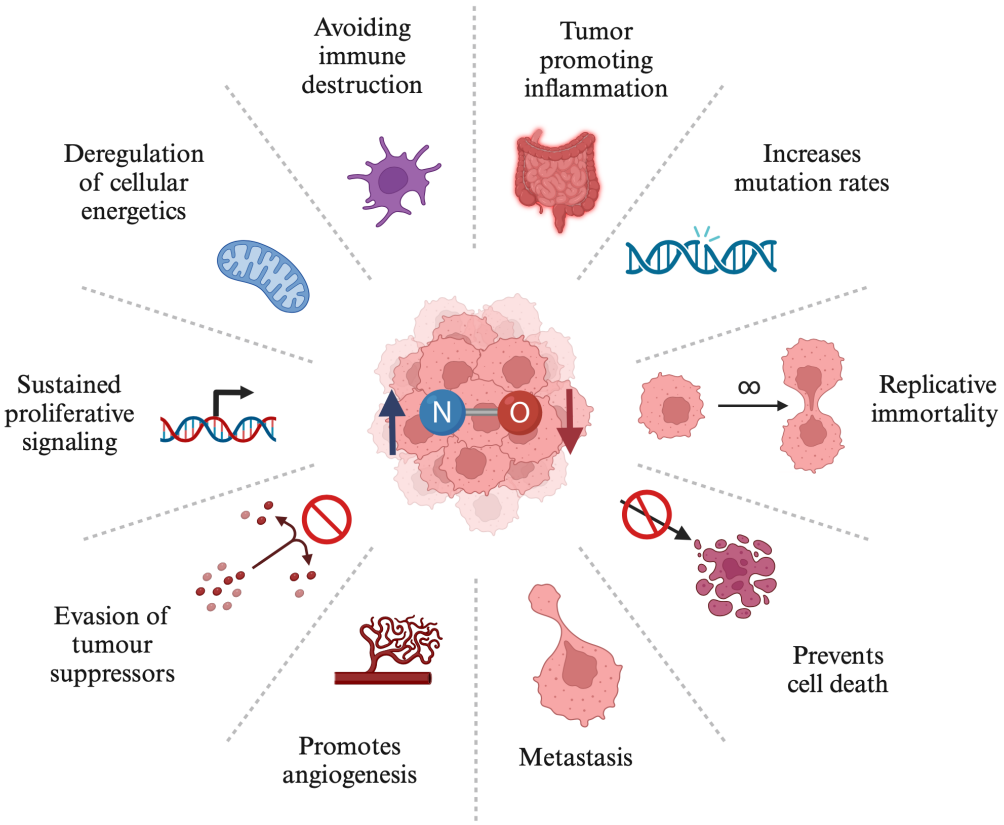


Figure 63. *Hallmarks of cancer regulated that are regulated by nitric oxide.*

Nitric oxide regulated varies processes that contribute to tumorigenesis. Some of these include promoting metastasis, angiogenesis, mutations and a sustained proliferation capacity. Nitric oxide also has the capacity to enable the evasion of tumour suppressors, prevent cell death and dysregulate cellular metabolism. Adapted from "Hallmarks of Cancer", by BioRender.com (2024), originally published in (Hanahan and Weinberg, 2011a).

AIMS OF THIS CHAPTER

The overall aim of this chapter was to investigate the role of nitric oxide signalling in the AOM/DSS model of CAC. Specific aims of this chapter where:

1. To determine if nitric oxide signalling is altered in *miR-223*$^{-/y}$ mice following chronic AOM/DSS and to assess if NO contributes to heightened disease in *miR-223*$^{-/y}$ mice in this model.
2. To investigate if pathways implicated in nitric oxide signalling are altered in *miR-223*$^{-/y}$ mice following chronic AOM/DSS.
3. Assess if nitric oxide contributes to intestinal epithelial stemness using colonic mouse organoids.

6.1.1 *miR-223* deficiency results in the upregulation of pathways associated with nitric oxide production in the AOM/DSS model of CAC

Differential gene expression analysis revealed that the NOS enzyme, NOS2, was among the top 25 genes differentially expressed between *miR-223*$^{-/y}$ and WT mice treated with AOM/DSS (**Figure 64 A**). Unbiased GSEA analysis showed that KEGG pathways 'nitric oxide stimulants guanylate cyclase' (MM15015) and 'citrulline metabolic process' (MM3920) where upregulated in *miR-223*$^{-/y}$ mice following AOM/DSS (**Figure 64 B + C**). Further analysis showed that pathways associated with the post-translation modification, nitrosylation, induced by the presence of NOS enzymes where also upregulated in *miR-223*$^{-/y}$ in the AOM/DSS model of CAC, including 'nitric oxide biosynthetic process' (MM8841), 'protein nitrosylation' (MM5882) and 'response to nitrosative stress' (MM8757) (**Figure 65 A - C**). Collectively, this suggests that *miR-223* is involved in the regulation of NO production, which could have implications for the progression from UC to CAC.

6.1.2 Increased production of NOS2 and s-nitrotyrosine in *miR-223*$^{-/y}$ mice following AOM/DSS modelling of CAC

As *miR-223*$^{-/y}$ mice had an enriched signature for NO production, and this is of interest clinically for the treatment of CRC and CAC, this was investigated further. Analysis on whole colonic tissue via RT-PCR revealed that *NOS2* expression is significantly increased in *miR-223*$^{-/y}$ mice in the AOM/DSS model of CAC (**Figure 66 A**). This was specific as the expression of *NOS3* was comparable between treatment groups, while *NOS1* expression was lower in AOM/DSS treated groups it wasn't significant (**Figure 66 B + C**).

Expression and localisation of NOS2 and its associated post-translation modification, s-nitrotyrosine, was assessed in whole colonic tissue by immunoblot and immunohistochemistry. There was a trending increase in NOS2 expression in *miR-223*$^{-/y}$ AOM/DSS mice seen via western blot (**Figure 67 A + B**). The expression of s-nitrotyrosine varied between treatment groups at different molecular weights. For instance, at 70kDa there was significantly higher expression in WT mice compared to AOM/DSS treated WT and *miR-223*$^{-/y}$ mice. In contrast, *miR-223*$^{-/y}$ and *miR-223*$^{-/y}$ AOM/DSS had higher expression of

s-nitrotyrosine at 55kDa and 25kDA compared to WT (**Figure 67 A + C**). These results were also shown via immunohistochemistry were there was significantly more NOS2 and s-nitrotyrosine expression in unaffected tissue of *miR-223*$^{-/y}$ AOM/DSS mice (**Figure 68 A - D**). There was also significantly more s-nitrotyrosine expressed in the tumours of *miR-223*$^{-/y}$ mice treated with AOM/DSS vs WT counterparts (**Figure 69 B + D**). These data indicate that excessive NO production via NOS2, and its subsequent post-translational modification of proteins via s-nitrotyrosine are contributing to the progression of CAC in *miR-223*$^{-/y}$ mice treated with AOM/DSS.

6.1.3 Antibody depletion of infiltrating Ly6G^{+} myeloid cells reduced early expression of NOS2 and s-nitrotyrosine in *miR-223*$^{-/y}$ mice following acute AOM/DSS

To assess if excessive NOS2 and s-nitrotyrosine were being produced early in the progression from UC to CAC, samples generated from an acute AOM/DSS model were analysed via immunohistochemistry. This showed that both markers were significantly increased expression in *miR-223*$^{-/y}$ mice following acute AOM/DSS. Furthermore, depletion of Ly6G^{+} myeloid cells reduced this expression (**Figure 70 A – D**). This indicates that enhanced NO production via NOS2 occurs early in the progression from UC to CAC with potential implications for the development of tumorigenesis.

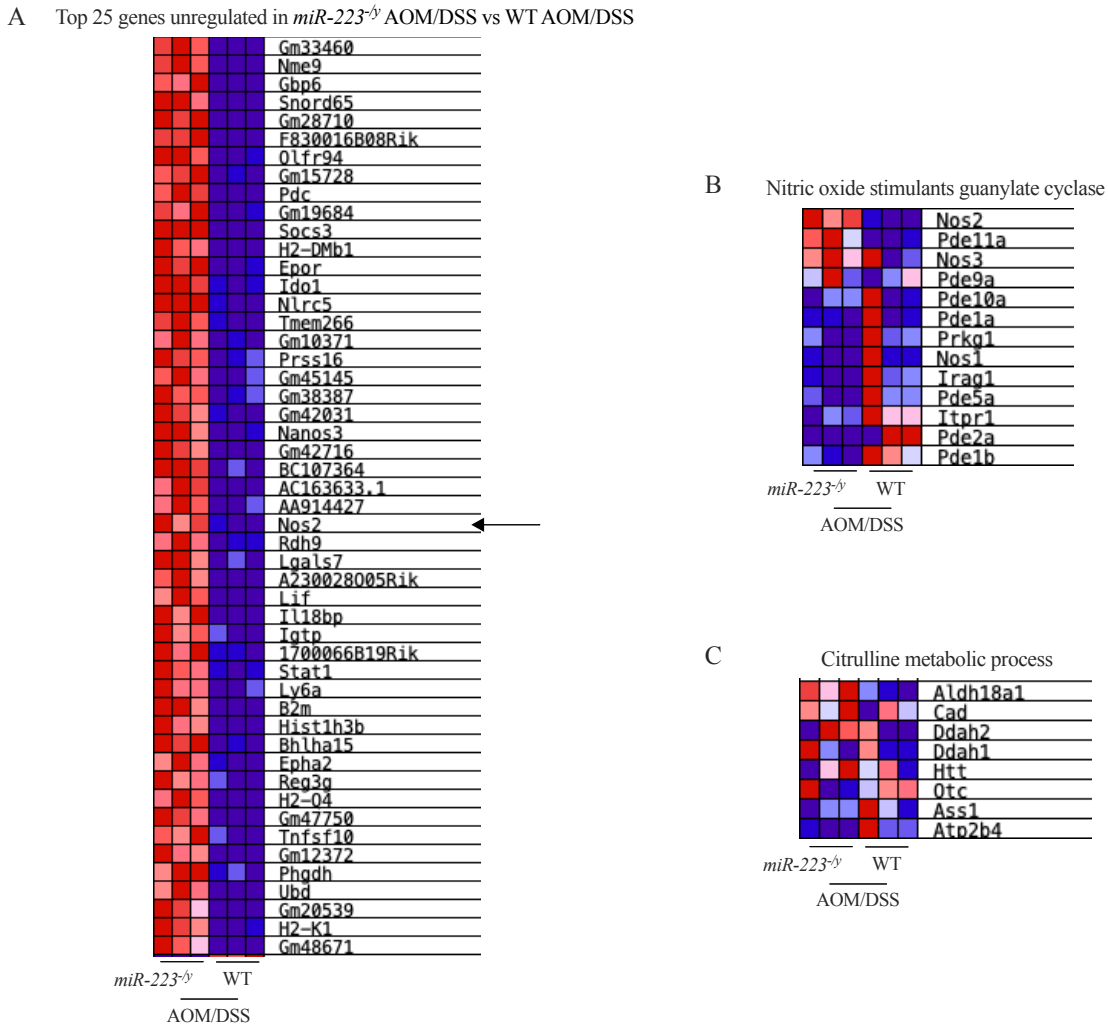


Figure 64. *Bulk RNA sequencing on colonic tissues revealed that pathways associated with nitic oxide expression are differentially expressed between miR-223$^{-/y}$ and WT mice following chronic AOM/DSS.*

Following chronic AOM/DSS colonic tissue was harvested from WT and *miR-223$^{-/y}$* mice, and bulk RNA sequencing was performed **A.** Heatmap of top 25 upregulated genes in *miR-223$^{-/y}$* AOM/DSS vs WT AOM/DSS. **B**. Heat map of 'Nitric oxide stimulants guanylate cyclase' (MM15015) (NES: -0.721; FDR: 1.0) **C.** Heat map of 'Citrulline metabolic process' (MM3920) (NES: 0.794; FDR: 0.807). n=3 mice/group.

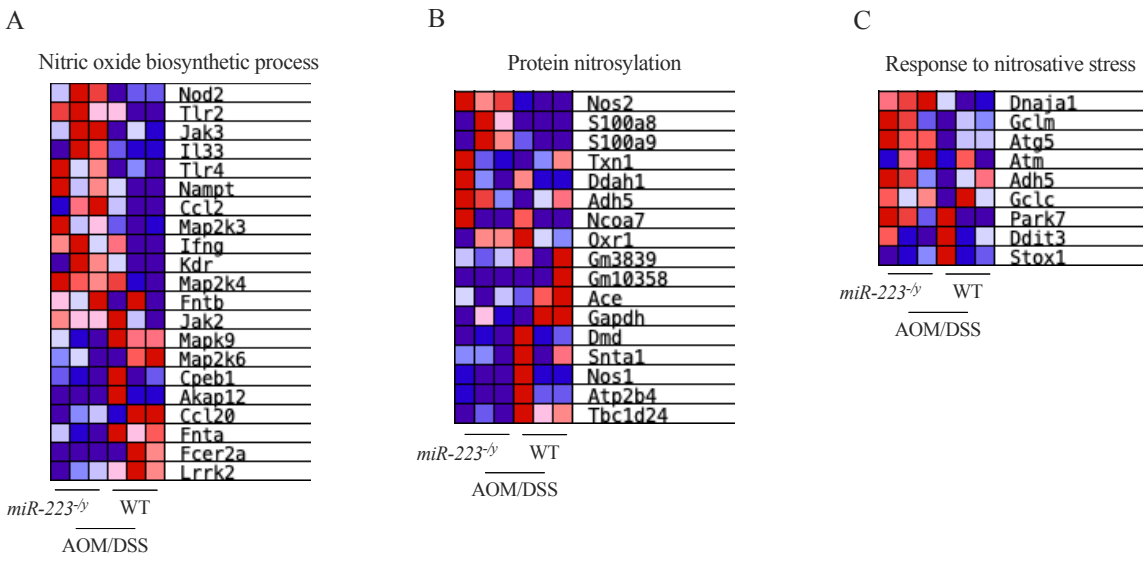


Figure 65. *Pathways associated with nitrosylation are differentially expressed in colonic tissue from miR-223$^{-/y}$ and WT mice after treatment with chronic AOM/DSS.*

Following RNA sequencing of colonic tissue from WT vs *miR-223$^{-/y}$* mice, GSEA analysis was performed A. Heat map of 'Nitric oxide biosynthetic process' (MM8841) (NES: 1.348; FDR: 0.425). **B**. Heat map of 'Protein nitrosylation' (MM5882) (NES: 0.876; FDR: 0.822) **C.** Heat map of 'Response to nitrosative stress' (MM8757) (NES: 1.135; FDR: 0.539). n=3 mice/group.

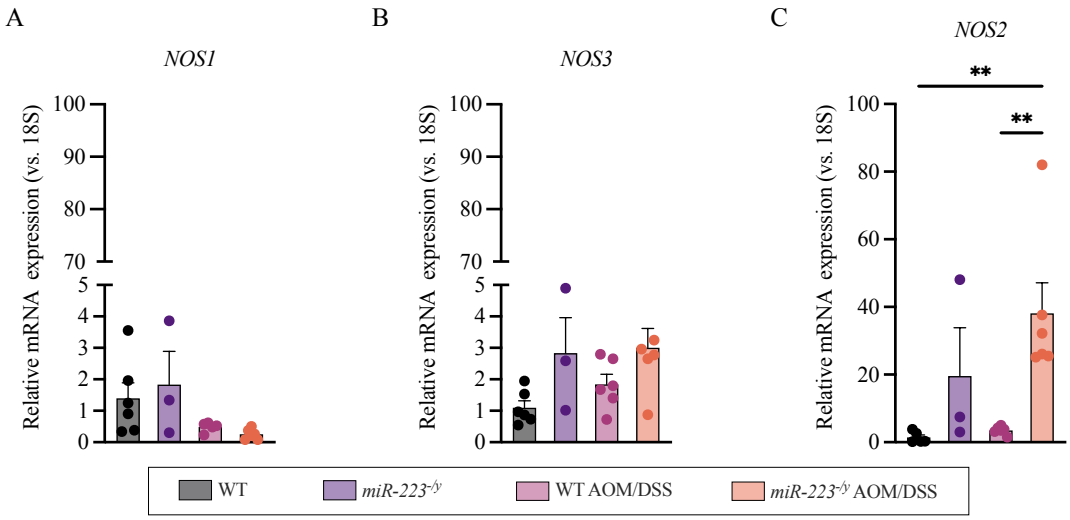


Figure 66. *Colonic NOS2 expression is increased in colonic tissue from miR-223$^{-/y}$ mice in the AOM/DSS model of CAC.*

Following chronic AOM/DSS colonic tissue was harvested from WT and *miR-223$^{-/y}$* mice. This was processed and analysed via PCR for **A.** NOS1, **B**. NOS3 and **C.** NOS2. All data is expressed as mean ± SEM; *, P<0.05; **, P<0.01; versus the indicated counterpart (One-way ANOVA). **A-C** n=3-6 mice/group.

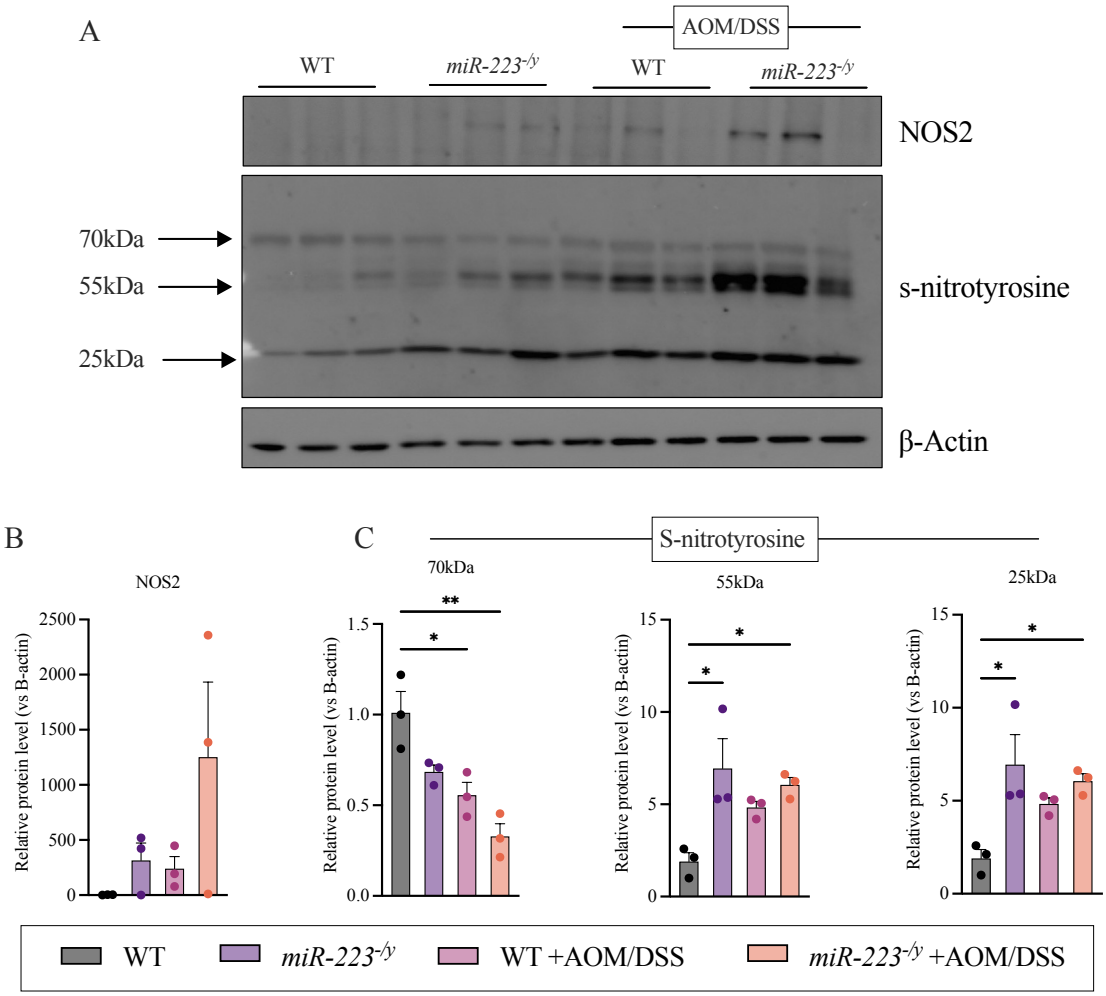


Figure 67. *Expression of s-nitrotyrosine is increased in colonic tissue from miR-223$^{-/y}$ mice in the AOM/DSS model of CAC.*

WT and *miR-223$^{-/y}$* mice were treated with chronic AOM/DSS. Following necropsy colonic samples were used for **A.** Western immunoblot assessment of NOS2 and s-nitrotyrosine. Western immunoblots were analysed via densitometry for **B.** NOS2 and **C.** S-nitrotyrosine. All data is expressed as mean ± SEM; *, P<0.05; **, P<0.01; versus the indicated counterpart (One-way ANOVA). **A-C** n=3 biological replicates/group.

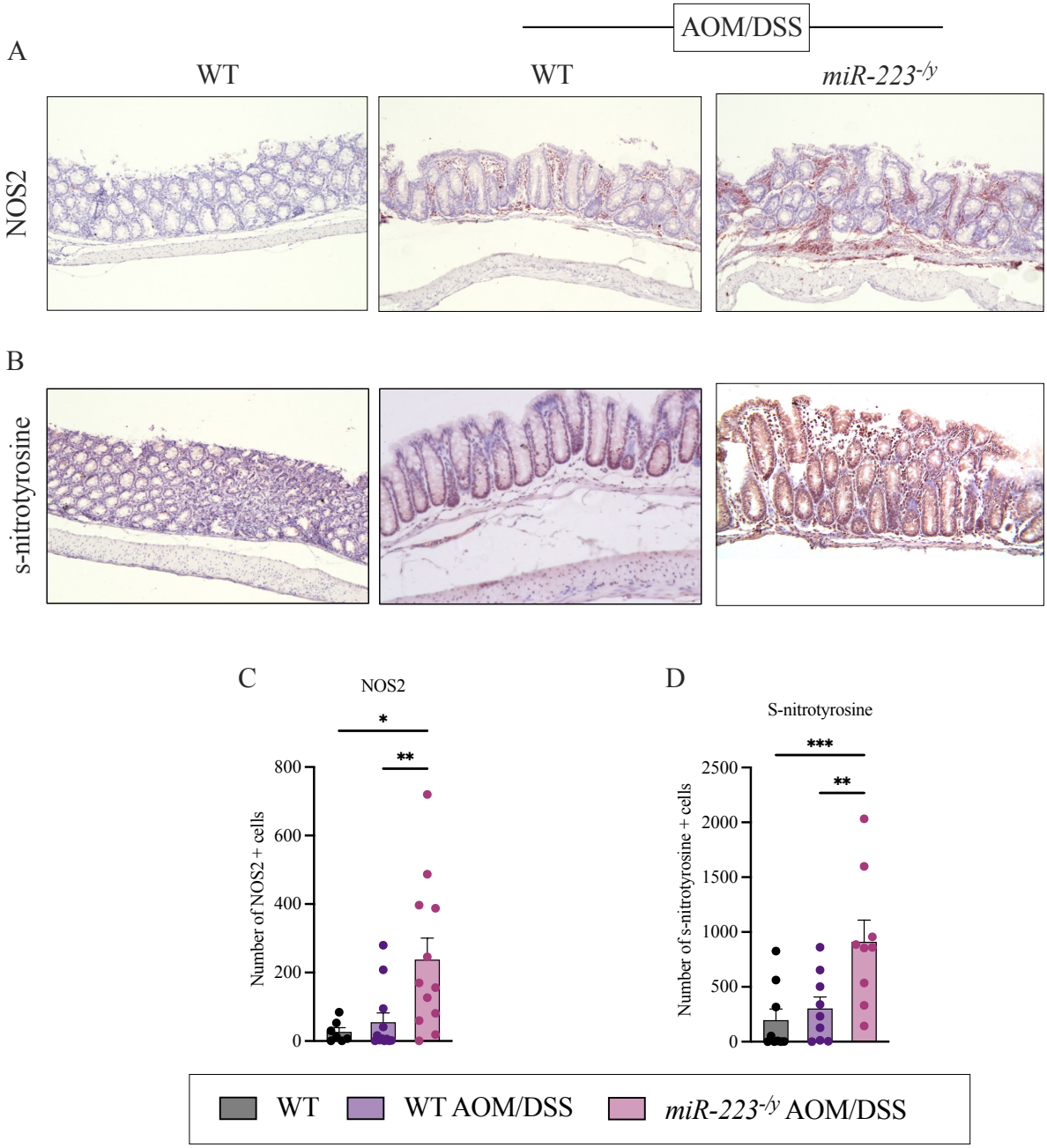


Figure 68. *miR-223$^{-/y}$ mice have increased NOS2 and s-nitrotyrosine in unaffected tissue following AOM/DSS.*

Representative 10x micrographs of unaffected tissue after immunohistochemical staining of colonic samples harvested from WT and *miR-223$^{-/y}$* AOM/DSS treated mice for **A.** NOS2 and **B**. s-nitrotyrosine. Quantification of immunohistochemical staining of **C.** NOS2 and **D.** S-nitrotyrosine. All data is expressed as mean ± SEM; *, P<0.05; **, P<0.01; ***, P<0.001, versus the indicated counterpart (One-way ANOVA). **A-D** n=3-4 mice/group with three fields of view presented per animal.

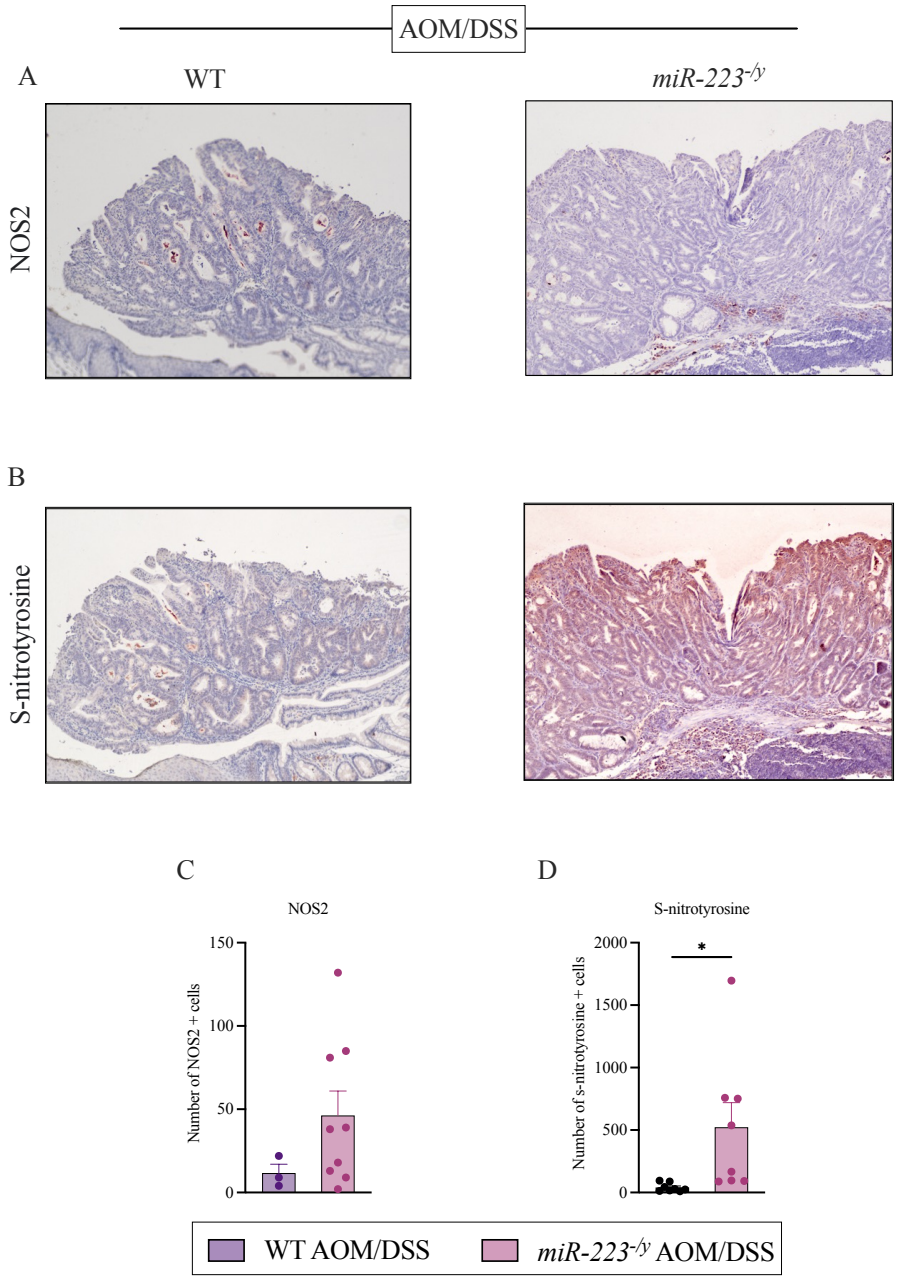


Figure 69. *miR-223$^{-/y}$ mice have increased s-nitrotyrosine in tumour tissue following AOM/DSS.*

Representative 10x micrographs of tumour tissue of immunohistochemical staining of WT and *miR-223$^{-/y}$* mice treated with chronic AOM/DSS for **A.** NOS2 and **B**. s-nitrotyrosine. Quantification of immunohistochemical staining of **C.** NOS2 and **D.** S-nitrotyrosine. All data is expressed as mean ± SEM; *, P<0.05; versus the indicated counterpart (One-way ANOVA). **A-D** n=3-4 mice/group with 1-3 fields of view quantified per animal.

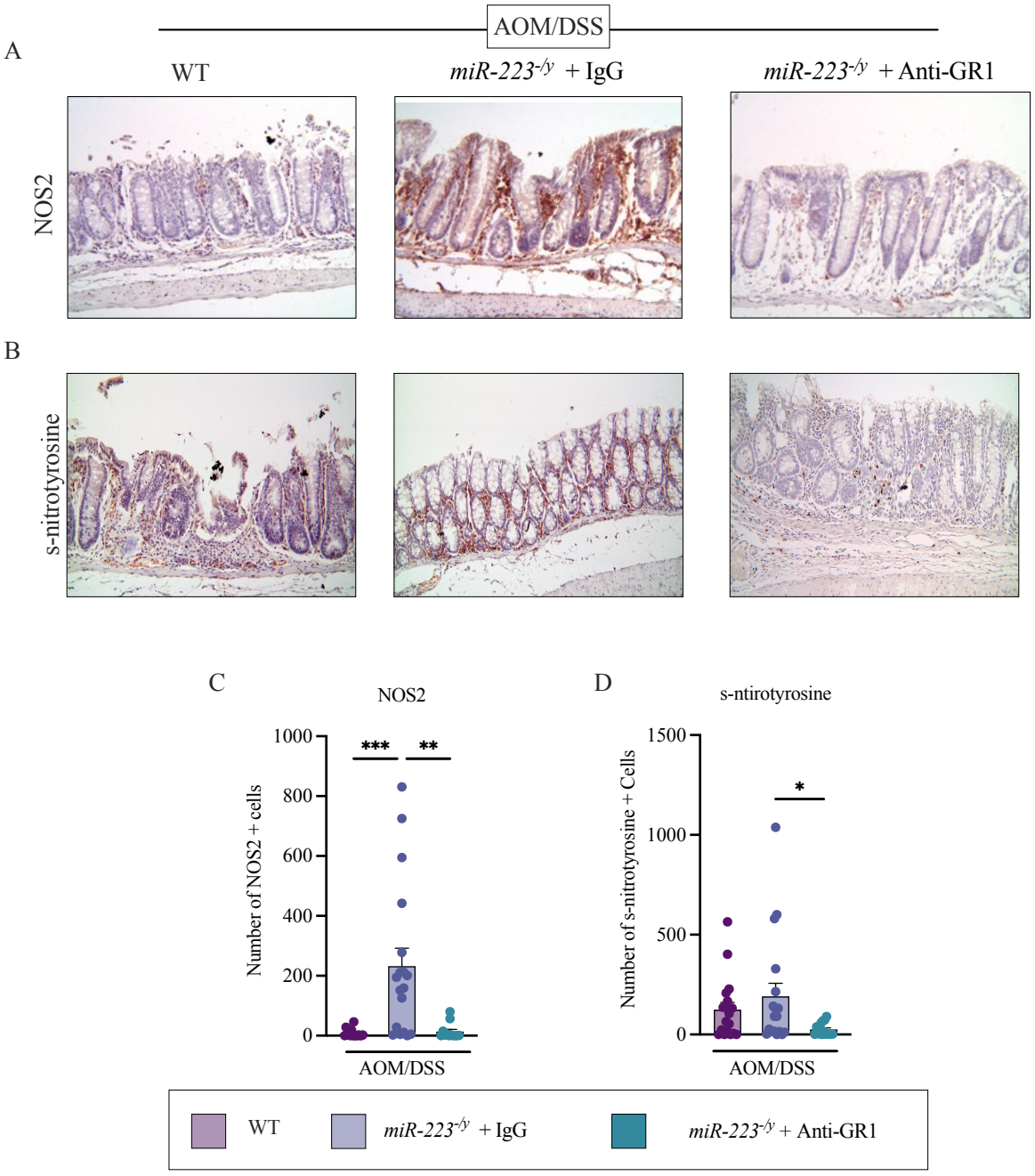


Figure 70. *Antibody depletion of infiltrating Ly6G^{+} myeloid cells reduced NOS2 and s-nitrotyrosine expression in unaffected tissue of miR-223$^{-/y}$ mice following acute AOM/DSS.*

Representative 10x micrographs of unaffected tissue of immunohistochemical staining of WT, *miR-223$^{-/y}$* + IgG and *miR-223$^{-/y}$* + Anti-GR1 mice after acute AOM/DSS for **A.** NOS2 and **B**. s-nitrotyrosine. Quantification of immunohistochemical staining of **C.** NOS2 and **D.** S-nitrotyrosine. All data is expressed as mean ± SEM; *, P<0.05; **, P<0.01; ***, P<0.001, versus the indicated counterpart (One-way ANOVA). **A-D** n=4-6 mice/group with 3 fields of view quantified per animal.

6.1.4 NOS2 expression is modulated in *miR223KD* RAWs by inhibiting pathways contributing to the production of NO

As *miR-223*$^{-/y}$ mice treated with AOM/DSS had increased expression of NOS2 and s-nitrotyrosine, pathways involved in the production of NO are potentially implicated. To test this, various pathways involved in NO production were inhibited in RAW 264.7 and *miR-223KD* RAW 264.7 cells. This showed that inhibition of p38α (AMG548) in RAW 264.7 cells lead to increased *nos2* production. Conversely, inhibition of ERK (FR180204) leads to significantly decreased *nos2* production. While *nos2* expression was comparable to control when JAK (Ruxolitinib) and NF-κB (JSH-23 and BAY-11) where inhibited in RAW 264.7 cells (**Figure 71 A**). However, in *miR-223KD* RAW 264.7 cells *nos2* expression was not altered by p38α inhibition (AMG548). Additionally, its expression was significantly decreased by the inhibition of JNK (Sp600125), ERK (FR180204), JAK (Ruxolitinib) and NF-κB's transcriptional activity (JSH-23) (**Figure 71 A**).

To assess if this was altered by inflammatory stimulation, the same experiment was performed followed by the addition of either LPS or IFN-γ. In LPS stimulated cells, similar trends were observed between *miR-223KD* RAW 264.7 and RAW 264.7 cells (**Figure 72 B – E**). In contrast, the addition of IFN-γ following inhibition of various pathways altered *nos2* expression in *miR-223KD* RAWs (**Figure 73**). For instance, the addition of IFN-γ after inhibition of ERK (FR180204) lead to increased *nos2* expression in *miR-223KD* RAW 264.7 cells, whereas it reduced *nos2* expression in RAW 264.7 cells (**Figure 73 C**). Additionally, inhibition of JNK (SP600125) and JAK (Ruxolitinib) significantly reduced the expression of *nos2* in *miR-223KD* RAW 264.7 cells (**Figure 73 B + D**). These data suggest that the presence of IFN-γ can alter NOS2 production in the absence of *miR-223*.

6.1.5 IFN-γ signalling is increased in *miR-223*$^{-/y}$ mice treated with AOM/DSS

As stimulation with IFN-γ and inhibition of various pathways altered NOS2 production in *miR-223KD* RAW 264.7 cells (**Figure 73**), potentially its expression is altered in *miR-223*$^{-/y}$ mice. To test this, GSEA analysis was performed on RNA sequencing data from whole colonic tissue of AOM/DSS treated WT and *miR-223*$^{-/y}$ mice. This showed that in *miR-223*$^{-/y}$ mice 'cellular response to type II interferon' (MM16298) was upregulated. Similarly, 'Type II Interferon Mediated Signalling Pathway' (MM16280) and 'Interferon Gamma

Signalling' (MM15473) were also upregulated in *miR-223*$^{-/y}$ mice treated with AOM/DSS vs WT counterparts. Collectively, these data suggest that in the AOM/DSS model of CAC, IFN-γ signalling is altered in the absence of *miR-223*.

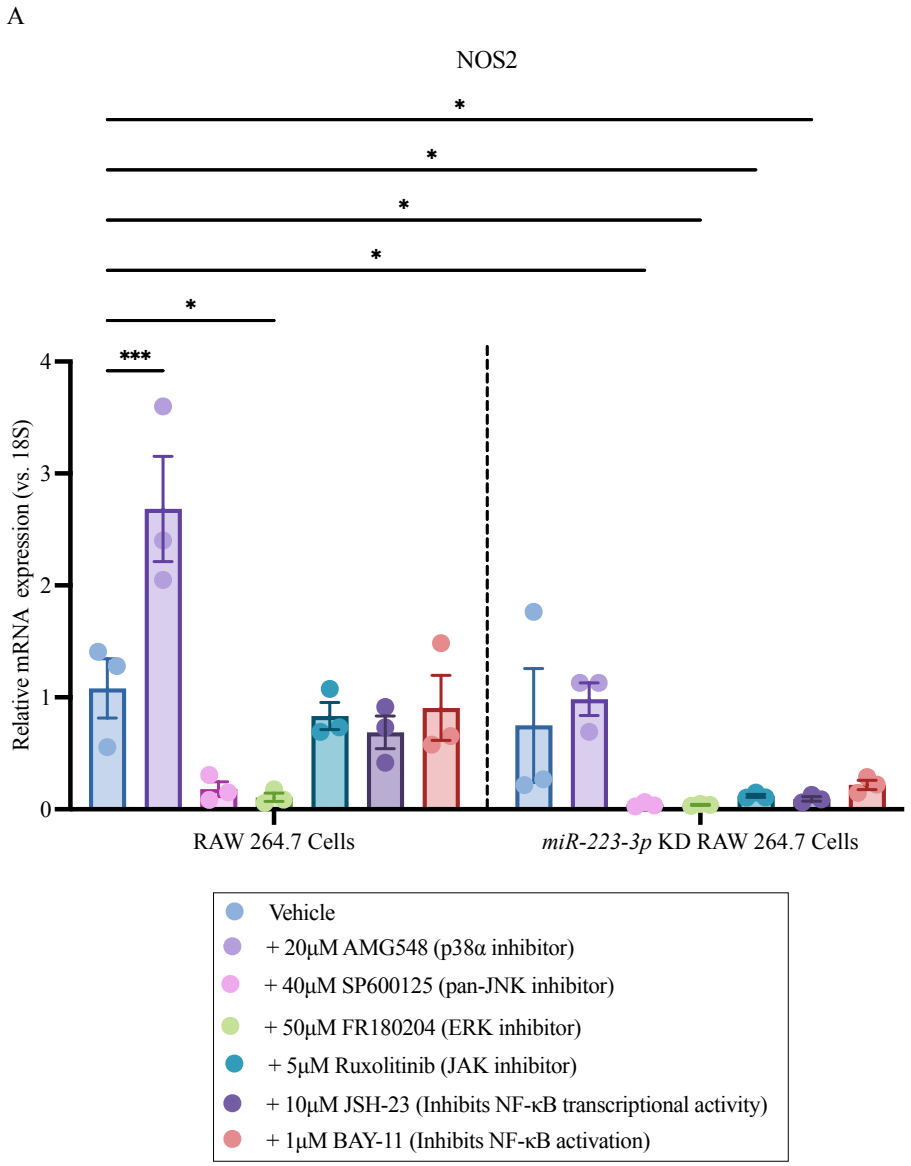


Figure 71. *NOS2 expression is altered in miR-223KD RAW 264.7 cells by pharmacologically inhibiting pathways implicated in its production.*

A. NOS2 expression was measured in RAW 264.7 and *miR-223KD* RAW 264.7 cells following treatment with either 20μM AMG548 (p38α inhibitor), 40μM Sp600125 (pan-JNK inhibitor), 50μM FR180204 (ERK inhibitor), 5μM Ruxolitinib (JAK inhibitor), 10μM JSH-23 (Inhibits NF-κB transcriptional activity) and 1μM BAY-11 (Inhibits NF-κB activation). All data is expressed as mean ± SEM; *, P<0.05; **, P<0.01; ***, P<0.001, the indicated counterpart (Two-way ANOVA). n=3 technical replicates/group.

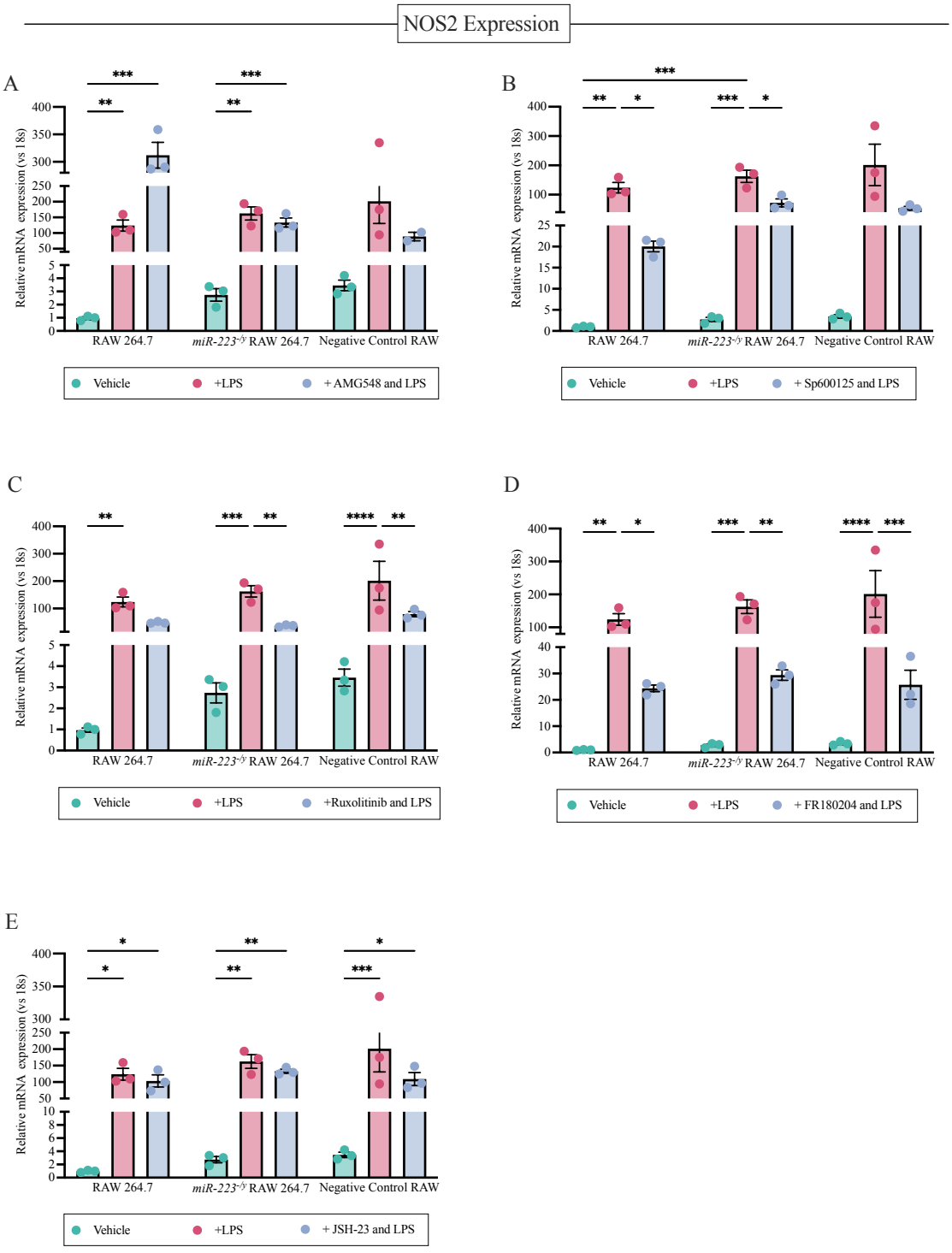


Figure 72. *Pharmacologic inhibition of pan-JNK, ERK or JAK1/2 prior to LPS stimulation reduces NOS2 expression in miR-223KD RAW 264.7 cells.*

NOS2 expression was measured in RAW 264.7, *miR-223KD* RAW 264.7 and Negative control RAW 264.7 cells following stimulation with LPS and inhibition of: **A.** AMG548 (p38α inhibitor), **B.** Sp600125 (pan-JNK inhibitor), **C.** FR180204 (ERK inhibitor), **D.** Ruxolitinib (JAK inhibitor) and **E.** JSH-23 (NF-κB transcriptional activity inhibitor). All data is expressed as mean ± SEM; *, P<0.05; **, P<0.01; ***, P<0.001, ****, P<0.0001 the indicated counterpart (Two-way ANOVA). **A-E** n=3 technical replicates/group.

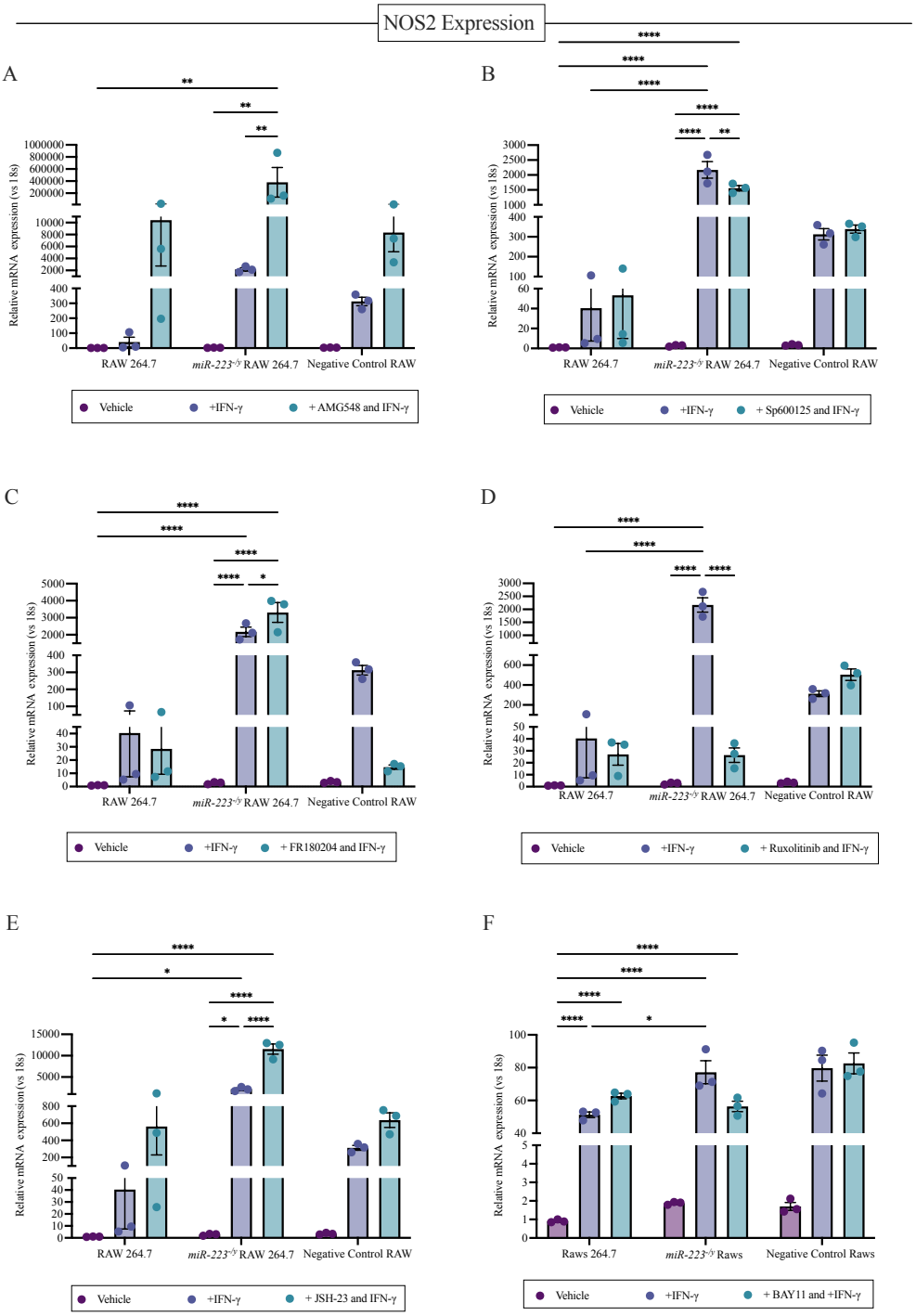


Figure 73. *Pharmacologic inhibition of pathways implicated in nitric oxide production alter the production of NOS2 following stimulation with IFN-γ in miR-223KD RAW 264.7 cells.*

NOS2 expression was measured in RAW 264.7, *miR-223KD* RAW 264.7 and Negative control RAW cells following stimulation with IFN-γ and inhibition of: **A.** AMG548 (p38α inhibitor), **B.** Sp600125 (pan-JNK inhibitor), **C.** FR180204 (ERK inhibitor), **D.** Ruxolitinib (JAK inhibitor), **E.** JSH-23 (NF-κB transcriptional activity inhibitor) and **F.** Bay-11 (Inhibits NF-κB activation). All data is expressed as mean ± SEM; *, P<0.05; **, P<0.01; ***, P<0.001, ****, P<0.0001 the indicated counterpart (Two-way ANOVA). **A-F.** n=3 technical replicates/group.

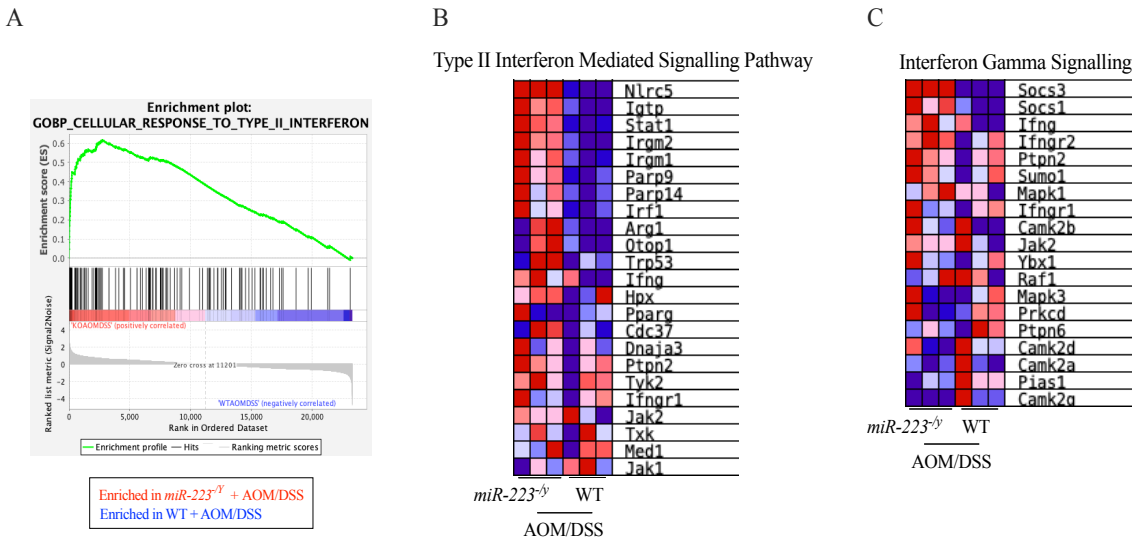


Figure 74. *Type II interferon signalling is increased in colonic tissue from miR-223$^{-/y}$ mice treated with AOM/DSS.*

GSEA analysis was performed on RNA sequencing data from colonic tissue of *miR-223$^{-/y}$* and WT mice treated with AOM/DSS. A. Enrichment plot of 'Cellular Response to Type II Interferon (MM16298) (NES: 2.044; FDR: 0.0782) **B**. Heatmap of 'Type II Interferon Mediated Signalling Pathway' (MM16280) (NES: 1.541; FDR: 0.09). **C.** Heat map of 'Interferon Gamma Signalling' (MM15473) (NES: 1.408; FDR: 0.094). n=3 mice/group.

6.1.6 Stimulation with IFN-γ does not alter the expression of markers implicated in nitric oxide production in *miR-223KD* RAW 264.7 cells

As NOS2 expression was altered by IFN-γ stimulation following the inhibition of pathways involved in the production of nitric oxide, potentially the expression of these pathways is altered due to the presence of IFN-γ. To test this, RAW 264.7 and *miR-223KD* RAW 264.7 cells were stimulated with IFN-γ and harvested at various timepoints to assess if early signalling events are altered. Following extraction, markers inhibited in previous experiments (**Figure 71**) and are involved in the induction of NO synthesis, were assessed via western immunoblot (**Figure 75 A**). This showed that NF-κB expression is increased in 223KD RAW 264.7 cells compared to RAW 264.7 cells, regardless of stimulation with IFN-γ. Comparable expression in RAW 264.7 and *miR-223KD* RAW 264.7 cells was observed for all other markers assessed with or without IFN-γ (**Figure 75 A**).

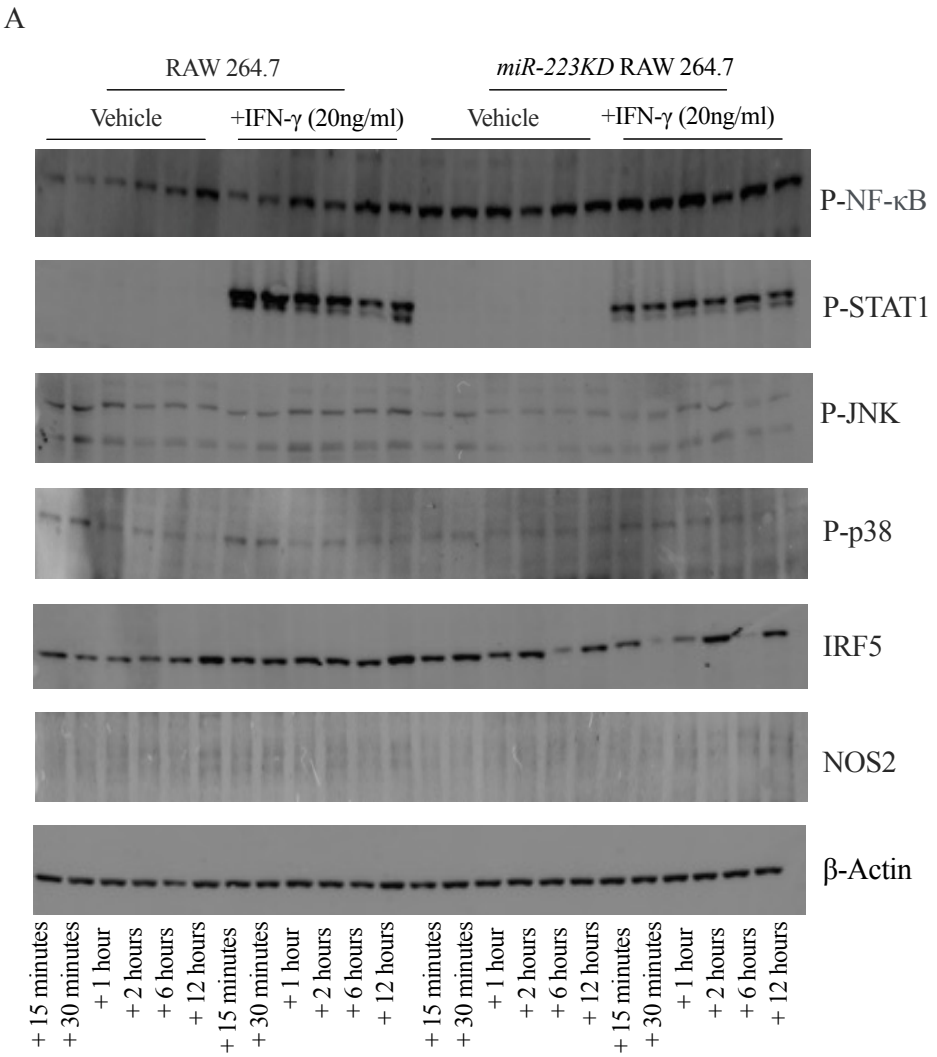


Figure 75. *Expression of markers implicated in nitric oxide signaling are unchanged overtime following stimulation with IFN-γ in miR-223KD RAW 264.7.*

A. Western immunoblot assessment of p-NF-κB p65, P-STAT1, P-JNK-P-p38, IRF5, NOS2 and β-actin in 20ng/ml IFN-γ stimulated RAW 264.7 and *miR-223KD* RAW 264.7 at various time points (15minutes, 30 minutes, 1 hour, 2 hours, 6 hours or 12 hours). **A** Representative n1 of an n=3 biological replicates/group.

6.1.7 *miR-223KD* RAW 264.7 cells have increased protein translation

As IFN-γ signalling is altered in *miR-223*$^{-/y}$ mice, potentiality deficiency of *miR-223* combined with the presence of IFN-γ alters the protein translation rate. This would have consequences both to produce NO and the progression from UC to CAC. To investigate this, a SUNSET assay was performed on RAW 264.7 and *223KD* RAW 264.7 cells that were

stimulated with IFN-γ for 50 minutes. This revealed that *miR-223KD* RAW 264.7 cells had higher protein translation compared to RAW 264.7 counterparts. Additionally, stimulation with IFN-γ further enhanced protein translation in *223KD* RAW 264.7 cells (**Figure 76 A**). This indicates that protein translation is altered by *miR-223* deficiency and the presence of IFN-γ.

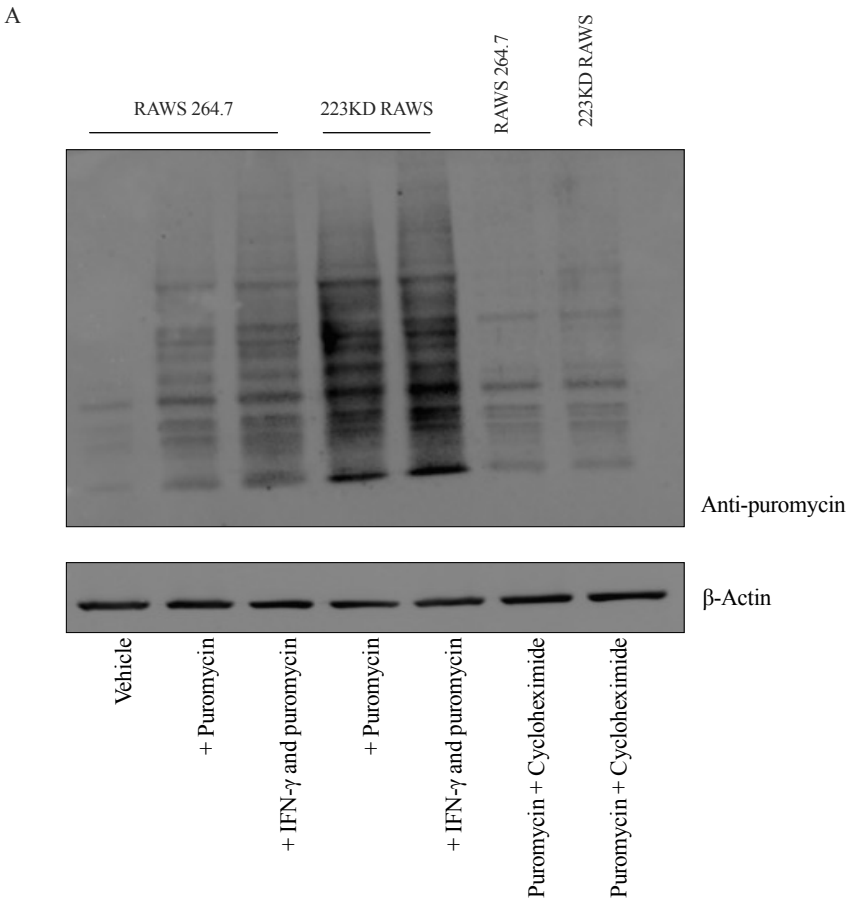


Figure 76. *miR-223KD RAW 264.7 cells have higher protein translation than RAW 264.7 cells.*

A. Western immunoblot assessment of SUNSET assay to assess protein translation following stimulation with 20ng/ml IFN-γ in *223KD* RAW 264.7 and RAW 264.7 cells for 50 minutes. Representative n1 of an n=3 biological replicates/group.

6.1.8 Stem cell markers are altered by the pharmacologic inhibition or activation of NOS2 +/- IFN-γ for 48 hours

In the absence of *miR-223,* NOS2 and IFN-γ expression are both enhanced and could potentially be contributing to the progression from UC to CAC. To limit inflammation, the identification of stem cell markers that might be altered in the early stages of disease could potentially be of use in a clinical setting. To assess this, mouse colonic organoids were treated with either a pharmacologic inhibitor, or activator of NOS2 +/- IFN-γ for 48 hours and then the expression of stem cell markers was determined via RT-PCR. These treatments did alter the growth and appearance of the colonic organoids compared to vehicle control (**Figure 77 A - C**). RT-PCR showed that treatment with IFN-γ significantly increased the expression of the fetal like stem-cell markers *tacstd2* and *sprr1a*, whilst *lgr5* expression was decreased (**Figure 78 C, F, D**). Furthermore, when IFN-γ was used in combination with the NOS donor (DEA/NO*), tacstd2*, *ly6a* and *sprr1a* expression were all significantly increased compared to control with IFN-γ +/- DEA/NO but not significantly (**Figure 78 A**). However, treatment with the NOS inhibitor (1400W) and IFN-γ significantly reduced the expression of *lgr5* (**Figure 78 D**). The expression of *h2a.x*, a marker of DNA damage, was unchanged regardless of treatment (**Figure 78 A**). Collectively, these data indicates that early production of NOS, in the presence of IFN-γ alters the expression of stem cell markers.

6.1.9 IFN-γ induced alterations in the stem cell marker Ly6a is regulated by NOS signalling

The previous organoid experiment showed that the expression of fetal stem cell markers is altered by the pharmacologic inhibition or activation of NOS2 +/- IFN-γ (**Figure 78**). However, this experiment was performed when organoid growth had been established. As the early intervention in progression from UC to CAC is critical to improving patient outcomes, this experiment was repeated with an earlier pharmacologic inhibition or activation of NOS2 +/- IFN-γ. This was followed by a recovery period, to determine if the expression of the stem cell markers could be restored or if they were irreparably altered. This showed that organoid growth was altered by the inhibition or activation of NOS2 +/- IFN-γ (**Figure 79 B**). However, regardless of treatment organoids did visuality appear to

start to recover by 72 hours in fresh media, indicated either by new organoid formation or growth comparable to either vehicle (**Figure 79 E**).

Once treatment was completed, organoids were extracted, and the expression of stem cell markers was analysed via RT-PCR. This showed that the expression of *ly6a* was significantly increased by IFN-γ alone and when it was added in combination with either a NOS donor or inhibitor, *tacstd2* showed a comparable trend but differences in expression were not significant (**Figure 80 E**). *Olfm4* expression was slightly reduced compared to vehicle with the addition of IFN-γ to various treatment groups (**Figure 80 A**). Additionally, *lgr5* and *sprr1a* expression was comparable to vehicle regardless of treatment (**Figure 80 D + F**). These data suggest that *ly6a* expression is altered by early pharmacologic inhibition or activation of NOS2 +/- IFN-γ, whilst other stem cell markers are unchanged suggesting that their expression is an acute response.

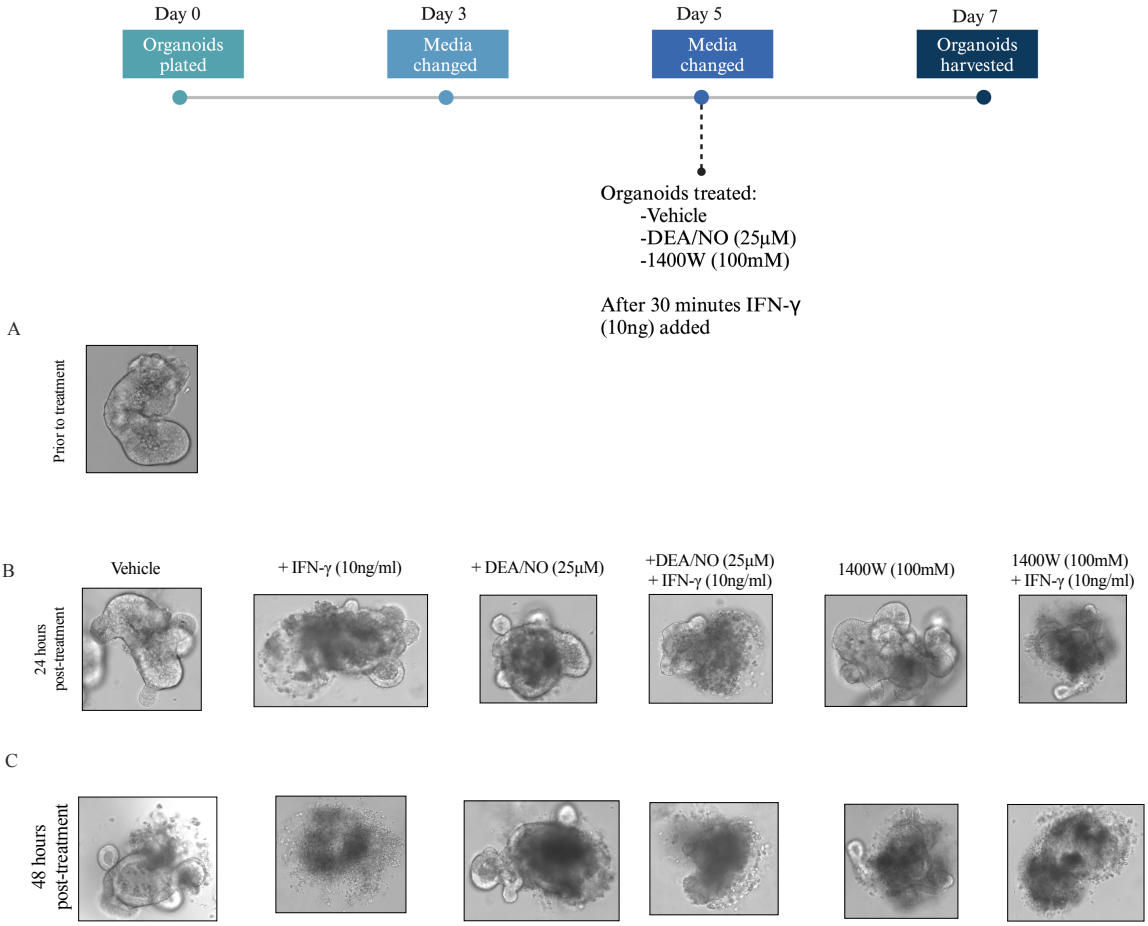


Figure 77. *Pharmacologic inhibition or activation of NOS2 +/- IFN-γ for 48 hours alters the growth of mouse colonic organoids.*

Schematic of organoid treatment. Mouse colonic organoids were treated with either IFN-γ (10ng/ml), DEA/NO +/- IFN-γ (25µM; NOS donor) or 1400W +/- IFN-γ (100mM; NOS inhibitor) **A.** Colonic organoids prior to treatment **B**. Colonic organoids 24 hours after treatment **C.** Colonic organoids 48 hours after treatment. **A-C.** Representative images taken at 20x of n=3-7 biological replicates/group.

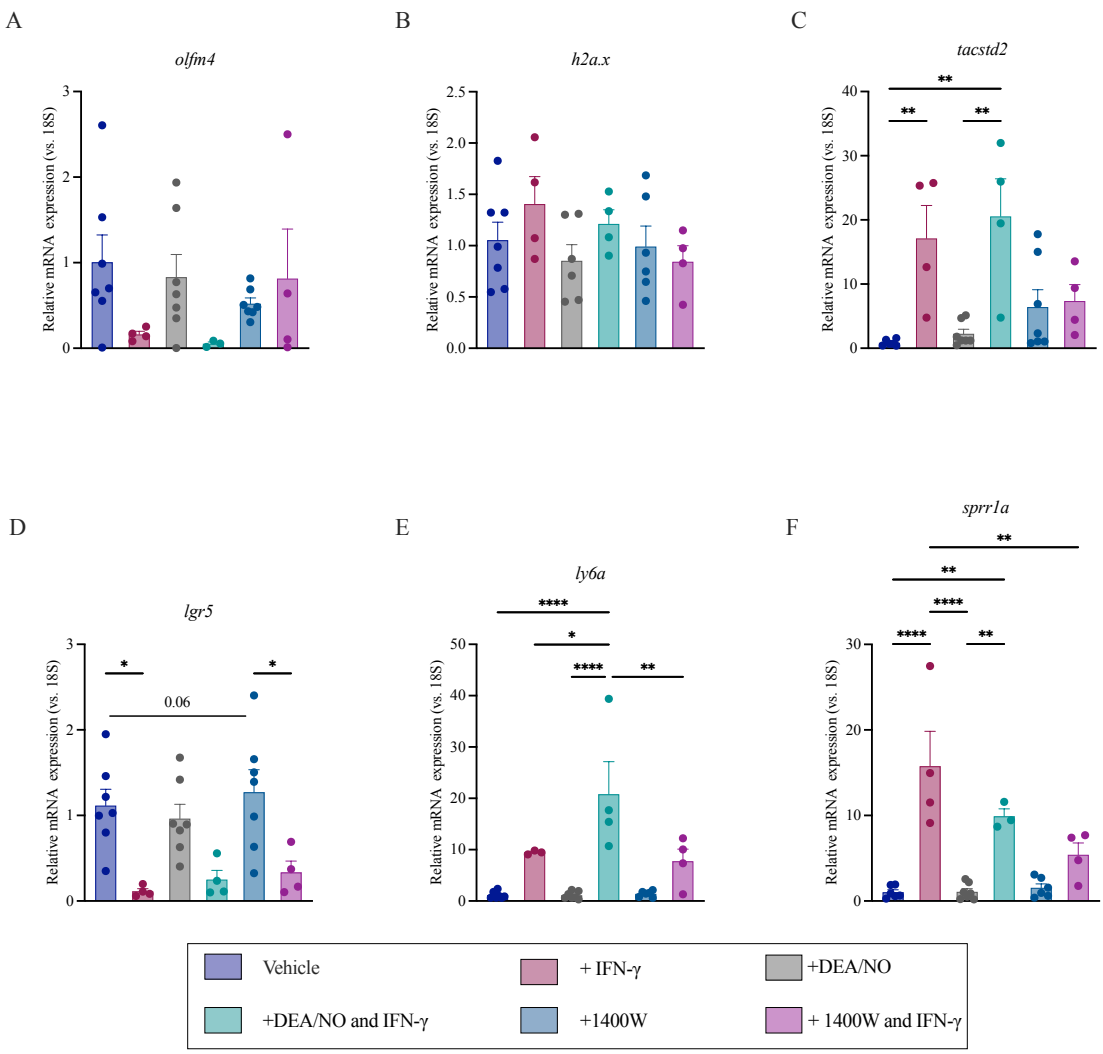


Figure 78. *Pharmacologic inhibition or activation of NOS2 +/- IFN-γ for 48 hours alters the expression of stem cell markers in mouse colonic organoids.*

Following treatment with either IFN-γ (10ng/ml), DEA/NO +/- IFN-γ (25μM; NOS donor) or 1400W +/- IFN-γ (100mM; NOS inhibitor), colonic organoids were harvested and analysed via PCR for **A.** Olmf4, **B**. H2a.x, **C.** Tacstd2, **D.** Lgr5, **E.** Ly6a and **F.** Sprr1a. **A-F.** All data is expressed as mean ± SEM; *, P<0.05; **, P<0.01; ***, P<0.001, ****, P<0.0001 the indicated counterpart (One-way ANOVA). n=3-7 biological replicates/group.

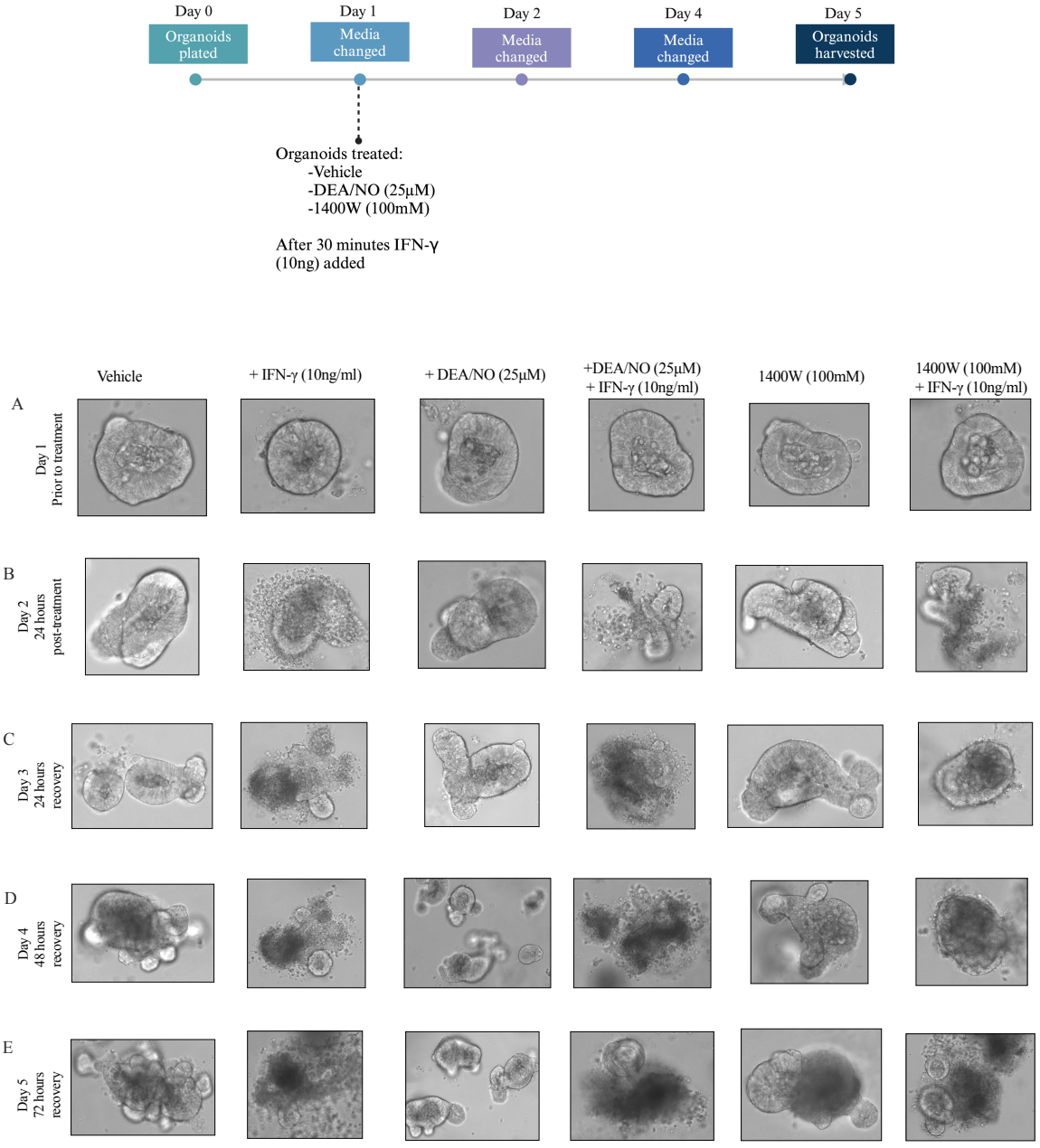


Figure 79. *Early pharmacologic inhibition or activation of NOS2 +/- IFN-γ, followed by a recovery period alters the growth of mouse colonic organoids.*

Schematic of organoid treatment. Mouse colonic organoids were treated with either + IFN-γ (10ng/ml), DEA/NO +/- IFN-γ (25µM; NOS donor) or 1400W +/- IFN-γ (100mM; NOS inhibitor) 24 hours post-split. After 24 hours media was changed, and organoids were left to recover for 72 hours. Representative images taken at 20x for **A.** Colonic organoids prior to treatment **B**. Colonic organoids 24 hours after treatment **C.** Colonic organoids 48 hours after treatment. **A-C** Representative images taken at 20x of n=3 biological replicates/group.

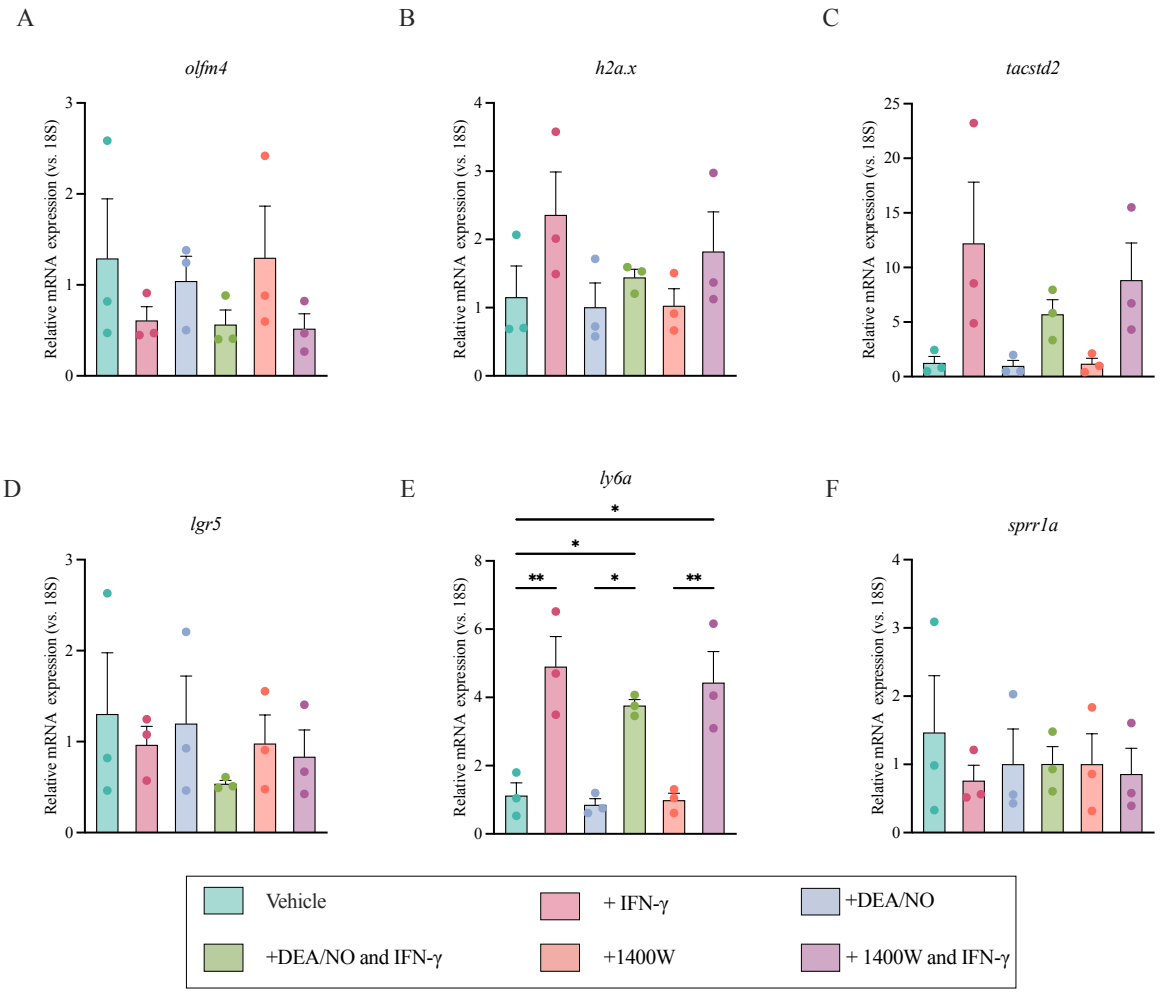


Figure 80. *Early pharmacologic inhibition or activation of NOS2 +/- IFN-γ, followed by a recovery period alters the expression of ly6a in mouse colonic organoids.*

Following treatment with either + IFN-γ (10ng/ml), DEA/NO +/- IFN-γ (25µM; NOS donor) or 1400W +/- IFN-γ (100mM; NOS inhibitor), colonic organoids were harvested and analysed via PCR for **A.** Olmf4, **B**. H2a.x, **C.** Tacstd2, **D.** Lgr5, **E.** Ly6a and **F.** Sprr1a. **A-F.** All data is expressed as mean ± SEM; *, P<0.05; **, P<0.01; ***, P<0.001, ****, P<0.0001 the indicated counterpart (One-way ANOVA). n=3 biological replicates/group.

DISCUSSION

CAC develops in UC patients due to the presence of chronic inflammation. However, the mechanisms that promote this progression are still poorly understood. NO is a critical signaling molecule and its dysregulation is increasingly being recognised in many diseases. In UC, CRC and CAC, excessive NO is associated with poor clinical outcomes for patients and production correlates with disease severity (Gochman et al., 2012, Mandal, 2018, Zafirellis et al., 2010). Improved understanding of the consequences of this aberrant NO expression could contribute to the development of new treatment options, with the restoration of miRNA circuits emerging as potential therapeutic targets.

Bioinformatic analysis performed on AOM/DSS samples, showed that *miR-223*$^{-/y}$ mice have an enriched signature for pathways critical to the production of NO. Additionally, NO induced post-translational modifications were also upregulated in these mice, in particular 'protein nitrosylation' and 'response to nitrosative stress'. The post-translation modification of proteins by nitrosylation has previously been shown to correlate with inflammation and the progression of tumorigenesis in CRC (Liang et al., 2023, Dorf et al., 2022). Furthermore, nitrosylation has been identified as an important regulator of inflammation in the DSS model of UC (Kao et al., 2016). This nitrosylation of proteins also corresponds with enhanced production of pro-inflammatory cytokines in UC and CRC (Dorf et al., 2022, Sharma et al., 2021). An enhanced cytokine signature in *miR-223*$^{-/y}$ mice has previously been demonstrated in the AOM/DSS model of CAC. This collectively indicates that the absence of *miR-223* has implications for the production and signalling of NO.

NO is predominantly produced by NOS enzymes via the L-arginine pathway. NOS2 has previously been identified as the primary producer of NO in patients with UC and has been reported to contribute to the inflammatory process in many cancers (Soufli et al., 2016, Thomas and Wink, 2017). In the AOM/DSS model of CAC, *miR-223*$^{-/y}$ mice had higher colonic expression of *nos2* compared to WT counterparts. This indicates that *miR-223* is essential for limiting excessive production of *nos2.* Both *miR-223* and NOS2 are predominantly produced by myeloid cells, which are increasingly being recognised as critical drivers of inflammatory driven tumorigenesis (Deng and Fleming, 2022).

To further verify this increased NOS2 expression, AOM/DSS samples were analysed by immunohistochemistry. This revealed that *miR-223*$^{-/y}$ mice had significantly increased

expression of NOS2, that corresponded to increased expression of s-nitrotyrosine. This suggest that in this model, *miR-223*$^{-/y}$ mice have excessive activation of NOS2 and as a consequence proteins are undergoing nitrosation. This post-translational modification is considered a marker of nitrosative stress, that is upregulated in patients with CRC and CAC (Dorf et al., 2022, Gochman et al., 2012). This increased expression of NOS2 and s-nitrotyrosine was shown to occur early in the development of CAC using an acute AOM/DSS model. Furthermore, antibody depletion of infiltrating Ly6G^{+} myeloid cells reduced the expression of NOS2 and s-nitrotyrosine significantly, suggesting that they are being expressed by myeloid cells. Collectively, elevated NOS2 and s-nitrotyrosine induce DNA damage and reduce the efficiency of DNA repair (Griswold-Prenner et al., 2023, Lala and Chakraborty, 2001). This could overtime be contributing to the progression from UC to CAC. Thus, restoring the expression of *miR-223* in myeloid cells to limit excessive NO production, and the subsequent nitrosation of proteins, could be a therapeutic target for the treatment of CAC.

Several signalling pathways are involved in the production of NO including JNK/p38 mitogen activated protein kinase (MAPK), NF-κB and JAK/STAT signalling pathways (Wang et al., 2016d, Gochman et al., 2012, Temby et al., 2023). Previous studies have shown that these signalling pathways are dysregulated in CAC. JAK/STAT signalling is important for the secretion of cytokines, along with the regulation of proliferation and apoptosis. Furthermore, IL-6/STAT3 signaling is believed to contribute to the progression from UC to CAC as shown in chapter 3 (Li et al., 2010). p38 MAPK signalling mediated inflammation is also important for the progression to tumorigenesis in patients with UC (Yin et al., 2016). Additionally, upregulation of NF-κB corresponds to increased expression of pro-inflammatory cytokines that contribute to colitis-associated carcinogenesis (Zhang et al., 2021e, Viennois et al., 2013). When these pathways were pharmacologically inhibited in *miR-223KD* RAW 264.7 cells, *nos2* expression was significantly decreased compared to RAW 264.7 cells.

To further assess the importance of these pathways in relation to *miR-223*, they were inhibited, and inflammatory stimulants were added to mimic the inflammatory process associated with CAC. Inhibition of pathways involved in the production of NO followed by LPS stimulation showed comparable trends, and expression of *nos2* between *miR-223KD* RAW 264.7 and RAW 264.7 cells. Potentially indicating that *miR-223* is not critical for

NOS2 production following stimulation with LPS. However, *in vitro* inhibition of JNK and ERK pathways that were subsequently stimulated with IFN-γ, had altered *nos2* expression in *miR-223KD* RAW 264.7 cells compared to RAW 264.7 counterparts. IFN-γ is a key mediator of inflammation that is upregulated in patients with UC (Langer et al., 2019). In the context of cancer, IFN-γ has been associated with apoptosis, metastasis and the promotion of PD-L1 expression (Zhao et al., 2020, Kobelt et al., 2020). Bioinformatic analysis on samples generated from a chronic AOM/DSS model of CAC, also showed that *miR-223*$^{-/y}$ mice have an enriched signature for IFN-γ signalling. Additionally, it has previously been shown that in the TME, IFN-γ is necessary to activate myeloid cells to promote excessive production of NOS2 (Cheng et al., 2023).

To further investigate the effects of IFN-γ on NO production, the early signalling events were assessed following IFN-γ stimulation. For the majority of markers assessed, there was similar expression between *miR-223KD* RAW 264.7 cells and RAW 264.7 cells, regardless of stimulation with IFN-γ. In both cell lines, p-STAT1 was only expressed following stimulation with its activator IFN-γ (Hu and Ivashkiv, 2009). However, there was slightly more expression of NF-κB in *miR-223KD* RAW 264.7 cells compared to RAW 264.7 cells. Extended activation of NF-κB has been shown in several cancers including CAC and promotes a pro-inflammatory macrophage phenotype (Cooks et al., 2013, Kashfi et al., 2021). *miR-223* has previously been shown to suppress the activation of the NF-κB pathway through its binding partners (Jeffries et al., 2019, Zhou et al., 2018). Thus, if stimulation with IFN-γ alters the functionality or expression of *miR-223,* NF-κB expression could be affected, which would have implications for the production of NO.

In the TME, it has previously been shown that NO produced from NOS2 in myeloid cells has the ability to suppress pro-inflammatory macrophage polarisation. This was restored through the inhibition of NOS2 production, which lead to reduced tumour size (Lu et al., 2015). Additionally, IFN-γ also has the ability to alter the mRNA translation rate to further promote inflammation (Su et al., 2015). SUnSET assay analysis showed that *miR-223KD* RAW 264.7 cells had more translation compared to RAW 264.7 cells. The addition of IFN-γ also appeared to speed up translation in *miR-223KD* RAW 264.7 cells. This could potentially have implications for the development of colitis-associated carcinogenesis as faster mRNA translation has been shown to promote an anti-inflammatory phenotype in

TAMs to promote tumour growth (Bartish et al., 2020). Indicating that potentially *miR-223* has a protective role in the limiting the rate of mRNA translation.

Both NO and IFN-γ, have been shown individually be involved in the regulation of intestinal stem cells (Puglisi et al., 2015b, Takashima et al., 2019b). However, previous experiments have not investigated their combined impact on the development of CAC through the regulation of epithelial stemness. If critical, they could be targeted in order to reduce the inflammation that is associated with the progression to CAC. Several stem cell markers have been identified in the colon including *olfm4, lgr5, ly6A, tacstd2* and *sprr1a* (Meyer et al., 2022, Kim et al., 2017). *Olfm4* is upregulated in patients with active UC and its expression has been identified in precancerous lesions (Liu and Rodgers, 2022). In CRC $Olfm4^{+}$ and $LGR5^{+}$ cells have the ability to rapidly regenerate following DNA damage to ensure the intestinal barrier is maintained (Sheahan et al., 2021, Meyer et al., 2022). If $LGR5^{+}$ cells have been lost due to tissue injury, the expression of $ly6a^{+}$ cells is increased. This is an IFN-γ responsive fetal stem cell marker that is upregulated in UC (Girish et al., 2021, Duckworth, 2021). Additional fetal stem cell markers TACSTD2 and SPRR1A are upregulated in CRC (Deng et al., 2020, Morgenstern-Kaplan et al., 2024).

When colonic organoids were treated pharmacologically for either the inhibition or activation of NOS2 +/- IFN-γ for 48 hours, there was a visible difference in their growth. In particular, those stimulated with IFN-γ looked visibly stressed, and their morphology extremely different to treatment groups not stimulated with IFN-γ. When these organoids where assessed for the expression of stem cell markers via RT-PCR, several where altered. In particular, activation of NOS2 and stimulation with IFN-γ, significantly increased the expression of the fetal stem cell markers *tacstd2, ly6a* and *sprr1a* compared to vehicle control. This suggests that these organoids have been exposed to cytokine-mediated injury. In particular, IFN-γ has been shown to induce apoptosis in epithelial stem cells (Takashima et al., 2019a, Omrani et al., 2023). Of note, none of the markers assessed were significantly changed with NOS2 inhibition and stimulation with IFN-γ compared to vehicle. This indicates that excessive NOS2, as observed in *miR-223*$^{-/y}$ mice, is more detrimental to formed organoids than its absence.

The same study with a shortened exposure to IFN-γ, at an earlier stage in organoid formation was also performed. This enabled the effects of the inhibition or activation of NOS2 +/- IFN-γ on organoid growth to be determined. Additionally, it allowed the recovery ability of

stem cell markers to be assessed or highlighted if there their expression was irreversibly altered. For all treatment groups, organoids did visibly start to recover, as indicated my new organoid formation by 72 hours. When analysed via RT-PCR, *ly6a* was significantly increased in IFN-γ treated groups. This suggests that short term exposure of colonic organoids to IFN-γ, alters the expression of this IFN-γ responsive marker. A similar trend was observed in *tacstd2*, however the difference wasn't significant. All other markers analysed showed no significant difference compared to vehicle. This indicates that short term exposure to either the inhibition or activation of NOS2 +/- IFN-γ does not alter the expression of these stem cell markers. However, further experiments need to be performed to investigate if *miR-223* deficiency alters the expression of these stem cell markers.

As aberrant concentrations of NO contribute to the development of many diseases, it is currently under investigation as a therapeutic target. L-NAME, a pan-NOS inhibitor, has previously been shown to reduce invasion and migration in CRC and breast cancer cell lines (Granados-Principal et al., 2015, Yu, 2005). Selective NOS inhibitors have also been developed, particularly for NOS2 due to its association with inflammation. One example is 1400W which reduces proliferation and migration in CRC (Thomsen et al., 1997). Additionally, when it is used in combination with 5-FU, these effects are further boosted (Gao et al., 2019). In CAC recent research has focused on all-trans retinoic acid (AtRA) as a treatment option. AtRA inhibits the expression of NOS2 and TNFα by modulating the expression of the NF-κB signalling pathway, which is increased in CAC (Rafa et al., 2017).

The role of miRNAs in the regulation of NO signalling still needs to be fully elucidated. *miR-24* has been shown to be involved in the regulation of NOS3 which affects the proliferation of endothelial cells (Zhang et al., 2015). Similarly, *miR-195* and *miR-582* also control the release of NO from endothelial cells through binding to their target NOS3 (Qin et al., 2018). NO can also decrease the expression of p53 dependent miRNAs in particular *miR-34, miR-203* and *miR-131* to further CRC (Li et al., 2015). The interplay between *miR-223* expression and NO signalling has not previously been reported. As *miR-223*$^{-/y}$ mice have excessive NOS2 production, the restoration of *miR-223* could be a potential therapeutic target in a particular subset of patients to limit the excessive production of NOS2 but further research is needed.

CHAPTER 7 DISCUSSION AND FUTURE DIRECTIONS

DISCUSSION

UC is lifelong disease that severely impacts a patient's quality of life. Globally, 0.3% of the world's population are affected by UC but treatment options remain limited (Caviglia et al., 2023). Therapeutics currently available focus on reducing inflammation, which is primarily achieved through targeting inflammatory mediators such as TNF-α (Muth et al., 2023). However, a large subset of patients respond poorly to these treatments and still experience debilitating symptoms, reflecting the complexity of the disease (Pakpoor and Travis, 2023). As a continuum from UC, CAC is the most harmful consequence of the disease accounting for approximately 10 – 15% of deaths in patients with UC (Kameyama et al., 2018). Thus, there is currently an unmet need for improved therapeutic options for both UC and CAC. These data suggest that targeting miRNA circuits, could be used as a therapeutic target for the treatment of UC and CAC, specifically the myeloid associated miRNA *miR-223*, to reduce myeloid driven inflammation.

Paediatric patients with UC are more likely to be diagnosed with severe, extensive disease, requiring intensive pharmacological treatments and often surgery (Assa et al., 2017). It is well documented that the excessive inflammation associated with UC leads to adverse side effects such as the development of CAC (Saez et al., 2023, Shah and Itzkowitz, 2022). As such, its increasingly being recognised that the early identification of patients who are likely to exhibit a poor response to therapeutics is necessary. This would allow early intervention and adjustment of treatment if needed, with an overall aim of improving the long-term prognosis for each patient (Solitano et al., 2020, Revés et al., 2021). These data show that in a discovery cohort of treatment-naïve paediatric patients, who were treatment non-responsive, had increased myeloid activity and enhanced expression of myeloid inflammatory pathways. Myeloid inflammation has previously been shown to be critical in the development of UC, through the secretion of inflammatory mediators (Zhou et al., 2023a). Furthermore, increased myeloid activity is associated with severe disease and poor response to TNF-α treatment (Jha et al., 2023).

Recently, transcriptomic profiling has identified molecular profiles for the identification of patients that are treatment non-responsive and present with enhanced cytokine signalling (Czarnewski et al., 2019). By analysing genes identified from this study, these data show that treatment-naïve paediatric patients with pancolitis, from an Irish validation cohort, have

increased expression of these markers. Additionally, they also had a similar inflammatory profile to treatment non-responsive patients in the discovery cohort, with both presenting with enhanced cytokine signalling. Increased cytokine signalling has been shown to be implicated in the progression of UC and the development of CAC (Yao et al., 2019a, Nakase et al., 2022). *miR-223* has previously been shown to regulate the function of macrophages through the production of inflammatory cytokines (Liu et al., 2015). In the validation cohort, two of these cytokines positively correlated with *miR-223* expression, OSM and IL-6 which are both members of the IL-6 signalling family. Increased OSM has previously been shown to be predictive of resistance to TNF-α treatment in patients with UC and has been suggested as a driver of disease through the secretion of cytokines (West et al., 2017, Verstockt et al., 2021). Furthermore, OSM expression in inflamed mucosal tissue has been shown to predominantly be from macrophage (Yang et al., 2024).

While previous work has shown that *miR-223* is involved in the immune response and the production of cytokines during UC, its role in the context of CAC was previously unreported (Neudecker et al., 2017b). Here, *miR-223* has been shown to be a critical regulator of the myeloid immune response. The deficiency of *miR-223* lead to increased proliferation, larger tumours and an increased myeloid chemokine signature. Collectively this indicates that *miR-223* is critical for preventing the progression of CAC. This is potentially due to *miR-223* having the ability to target multiple members of the IL-6/STAT3 signalling pathway, as demonstrated by target identification, and the increased expression of LIF, IL-6 and IL-11 in *miR-223*$^{-/y}$ mice following AOM/DSS. Furthermore, as patients with pancolitis also had increased IL-6 that correlated with *miR-223* expression, potentially targeting the IL-6/STAT3 signalling pathway via *miR-223* could be of use as a therapeutic target.

Investigations into the viability of miRNAs as therapeutics are currently underway. The first miRNA therapeutic to be developed was for hepatitis C virus (HCV) using the drug miravirsen (Janssen et al., 2013). This drug targets *miR-122*, which has multiple binding sites on the HCV genome and acts protects the HCV genome from innate immune responses and nucleolytic degradation during infection. By inhibiting the 5'UTR of *miR-122*, HCV proliferation was blocked and infected chimpanzees had long lasting protection without any adverse side effects (Ottosen et al., 2015, Janssen et al., 2013). While this drug has completed a phase 2 clinical trial, the results have not yet been published. At present, there

is no miRNA therapeutics for either UC or CAC, that is currently in a clinical trial or approved for the clinical use.

In experimental UC, nanoparticle delivery of *miR-223* reduced disease severity in mice. This study also showed that with this treatment there was a significant reduction in the mRNA expression of IL-1β, IL-6, TNF, and CXCL1 compared to controls, with protein expression of IL-1β also reduced (Neudecker et al., 2017b). This further demonstrates that *miR-223* is crucial for limiting dysregulation of the inflammatory responses in the DSS model of UC. However, in this study the effects of nanoparticle delivery of *miR-223* was only assessed in an acute DSS model (Neudecker et al., 2017b). IL-1β, IL-6 and TNF were increased in mucosal biopsies from treatment-naïve paediatric patients with pancolitis and in whole colonic tissue from *miR-223*$^{-/y}$ mice following AOM/DSS modelling of CAC. As these cytokines are major contributors to the inflammatory pathogenesis of UC and CAC, it would be beneficial to assess the effects of this nanoparticle in more chronic models (Aggeletopoulou et al., 2024). If this successfully reduced disease severity in these models, it could potentially be investigated further for the treatment of UC and CAC, in clinical trials.

Further highlighting the crucial role of *miR-223* in controlling inflammation, nanoparticle delivery of *miR-223* has been investigated for the treatment of acute respiratory distress syndrome (ARDS). In this inflammatory disease, *miR-223* deficiency is associated with severe lung infections (Aggeletopoulou et al., 2024). Studies in this disease have shown that nanoparticle of *miR-223* provided protection from acute disease in an experimental mouse model (Neudecker et al., 2017a). Additionally, nanoparticle delivery of *miR-223* has been shown to re-polarize pro-inflammatory macrophage to be anti-inflammatory *in vitro*. This was associated with decreased expression of NOS2 and increased expression of Arg1. Following this re-polarization, there was decreased expression of IL-6, TNF and IL-1β (Tran et al., 2016). In a model of sepsis, this repolarisation was shown to be mediated through the alteration of glycolysis via downregulation of HIF-1α which is a target for *miR-223* (Dang and Leelahavanichkul, 2020).

The modulation of *miR-223* as a therapeutic has also been investigated in cancer. In particular, in hepatocellular carcinoma (HCC) the expression of *miR-223* is repressed leading to an upregulation of the oncoprotein stathmin1 (Ye et al., 2018). Transfection of *miR-223* into HCC cell lines inhibited migration and invasion *in vitro*, with a reduction in

proliferation and expression of stathmin1 also observed (Li et al., 2020, Wong et al., 2008). The overexpression of *miR-223* has also been shown to increase the chemosensitivity of non-small cell lung cancer (NSCLC) cell lines and the radiosensitivity of glioblastoma *in vitro* (Liang et al., 2014, Zhao et al., 2016, Han et al., 2016).

Inhibition of *miR-223* has also been investigated as a therapeutic in cancers where its overexpression contributes to tumorigenesis. In prostate cancer, the suppression of *miR-223 in vitro* via transfection, increased apoptosis and chemosensitivity. This was further confirmed in *in vivo* models (Feng et al., 2018a). Similarly, the inhibition of *miR-223* in thyroid cancer inhibited proliferation and colony formation *in vitro* (Zhang et al., 2019a).

As the myeloid immune response is central in the progression from UC to CAC, coupled with *miR-223* expression predominantly occurring in myeloid cells, it is essential to consider how they respond to immunotherapy. In a model of metastatic CRC, the number of myeloid cells decreased following treatment with 5-FU (Yagiz et al., 2018). In head and neck squamous cell carcinoma , treatment with a PI3Kγ inhibitor induced the re-polarization of macrophage and increased the infiltration of CD8+ T-cells (Kaneda et al., 2016). Additionally, this treatment also increased the sensitivity to docetaxel in a murine model of breast cancer (De Henau et al., 2016). In CAC, treatment with OTSSP167 prevented the infiltration of macrophage which prevented tumorigenesis (Tang et al., 2021a). Thus, the repolarization or targeting of myeloid cells is a viable treatment option. However, further research needs to be carryout to determine how the restoration of *miR-223* would affect myeloid cells in the context of UC and CAC.

While the treatment of UC and CAC is crucial at any stage, its early detection often provides patients with more treatment options and can limit the progression of disease. miRNAs are emerging as potential biomarkers for the detection of numerous diseases. In particular, the number of miRNAs being identified for the diagnosis of inflammatory diseases including UC, Rheumatoid arthritis, Asthma and ARDs is increasing (Zhou et al., 2021, Kmiołek and Paradowska-Gorycka, 2022, Gil-Martínez et al., 2023, Martucci et al., 2020). Similarly, the potential application of miRNAs as a diagnostic tool is increasingly being recognised in cancer, in particular for CAC, breast cancer, ovarian cancer and lung cancer (James et al., 2020, Jordan-Alejandre et al., 2023, Zhao et al., 2022b, Ying et al., 2020). Ideally, biomarkers should be easily detected with high sensitivity and specificity for the disease being detected. Additionally, non-invasive biomarkers are particulary of interest for ease of

sampling and the lower cost associated (Ahmad et al., 2023). miRNAs have these characteristics, are detectable in various bodily fluids and are stable at various conditions. As such, several miRNA based diagnostic technologies have already been developed with CohniMIR currently in a clinical trial for the early diagnosis of Alzheimer's disease, ThrombomiR for determining a patients platelet function and ThyraMir for the detection of thyroid cancer (Yang et al., 2023, Kunwar et al., 2023, Krammer et al., 2022). As the use of miRNAs for diagnosis increases *miR-223* could be included in a panel of miRNAs for the diagnosis of UC and CAC.

In summary, this thesis has demonstrated that *miR-223,* is a key regulator of myeloid inflammation that underpins the continuum from UC to CAC (**Figure 81**). In the future this miRNA could potentially be used as therapeutic target for the treatment of these chronic diseases.

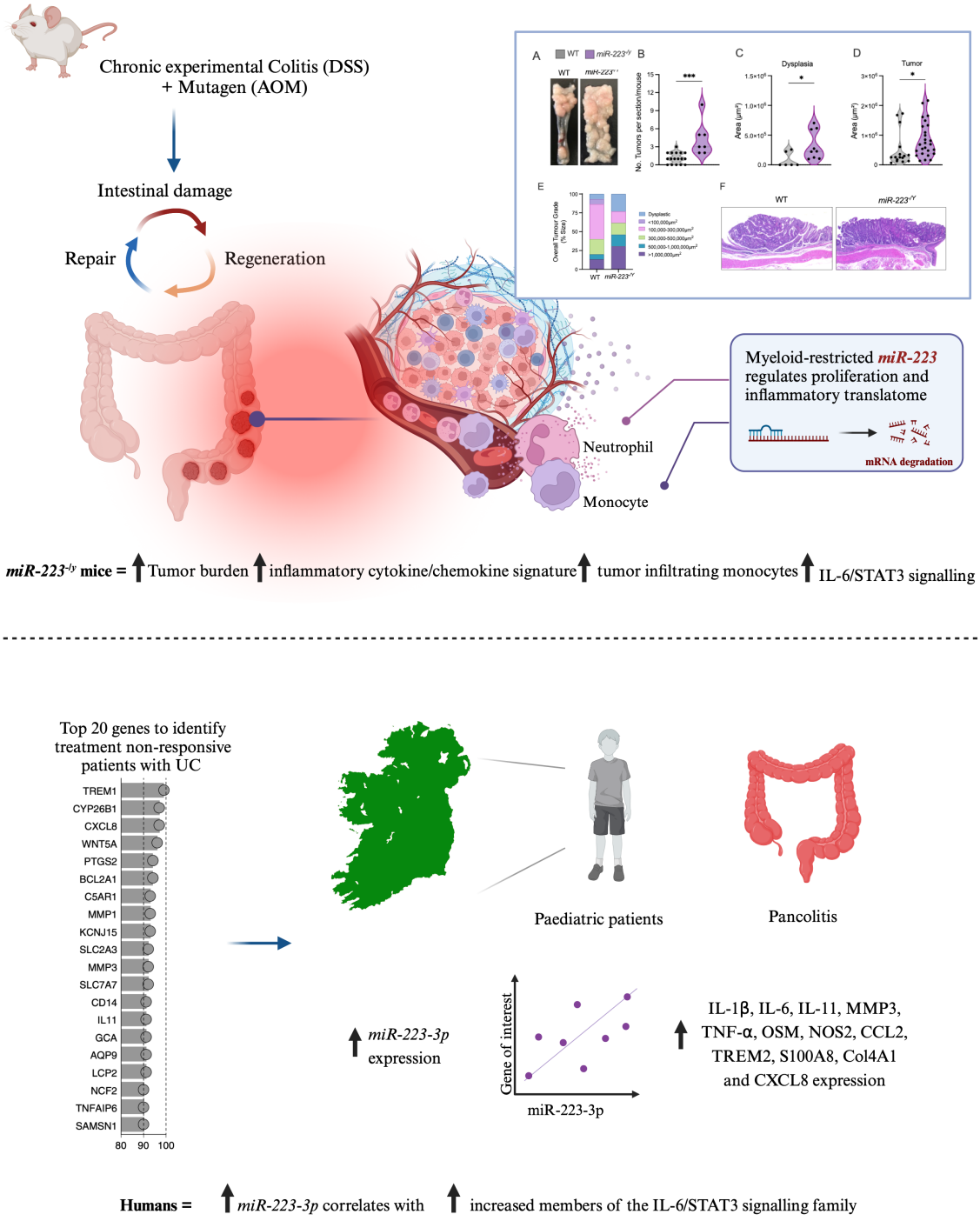


Figure 81. *Overview of key findings from investigating the role of miR-223-3p Ulcerative colitis and Colitis-associated colorectal cancer.*

FUTURE DIRECTIONS

miRNAs play a crucial role in the regulation of many biological processes, including immune responses and controlling inflammation. Dysregulation of these processes is a hallmark feature in both UC and CAC. This thesis aimed to improve the understanding of role of *miR-223* in UC and CAC. The data presented indicates that *miR-223* is essential for controlling myeloid driven inflammation, through the suppression of pro-inflammatory cytokines, limiting tumour growth, controlling proliferation and carcinogenic pathways. However, additional work still needs to be done if *miR-223* is to be used in a clinical setting for UC or CAC.

Further work could focus on identifying how different aspects of the IL-6/STAT3 signalling pathway are affected by either the overexpression or inhibition of *miR-223.* This would be useful as it could identify what *miR-223* is targeting and its subsequent downstream effects. Colonic organoids could also be grown in conditioned media from *223KD* RAW 264.7 cells, to determine the effect of *miR-223* deficiency on the expression of stem cells. Different aspects of the IL-6/STAT3 pathway could then be recombinantly added or inhibited, to assess if they alter the expression of stem cell markers. This would improve the understanding of a pathway that is critical to the development of UC and the progression to CAC. It could also allow a more targeted approach to be taken for the development of a therapeutic for this pathway.

Given that *miR-223KD* RAW 264.7 cells presented with increased translation, additional work could use a SUnSET assay to determine if the translation efficiency of RAW 264.7 cells is also altered when *miR-223* is over-expressed. This would be informative as the polarisation of macrophages is altered by the rate of translation. Thus, if the rate of translation could be slowed down to enable the polarization into anti-inflammatory macrophage during the early stages of UC, it could aid in resolving inflammation.

As *miR-223*$^{-/y}$ mice presented with increased NOS2, as shown in IHC and PCR, it would be interesting to perform a double immunofluorescence staining of NOS2 and immune markers such as CD68, Ly6G and CD11b. This would determine what cells are the primary producers of NOS2 in this model. Furthermore, if biopsies could be obtained from patients with CAC, it could provide valuable insights into whether NOS2 expression is increased with disease severity via PCR and IHC.

If biopsies could be obtained from patients with UC and CAC from different stages of disease, it would be useful to generate colonic organoids to have as a system to investigate pathways of interest such as NO and IL-6/STAT3 signalling. Furthermore, these samples could also be analysed by spatial transcriptomics to identify at what stage molecular changes occur, which could enable a more targeted approach to treatment.

APPENDIX

Appendix Table 1. *Mayo scoring system for classifying disease activity in Ulcerative colitis.*

Mayo Scoring System	
Stool Frequency	0 = Normal 1 = 1–2 stools/day more than normal 2 = 3–4 stools/day more than normal 3 = >4 stools/day more than normal
Rectal bleeding	0 = None 1 = Visible blood with stool less than half the time 2 = Visible blood with stool half the time or more 3 = Passing blood alone
Mucosal appearance at colonoscopy (*If performed)	0 = Normal or inactive disease 1 = Mild disease (mild friability, erythema and decreased vascular pattern) 2 = Moderate disease (friability, marked erythema, absent vascular pattern and erosions) 3 = Sever disease (ulceration and spontaneous bleeding)
Physician rating of disease activity	0 = Normal 1 = Mild 2 = Moderate 3 = Severe

* Scoring system from (Naegeli et al., 2021).

Appendix Table 2. *Paediatric Ulcerative Colitis Activity Index.*

Item	Points
Abdominal Pain	No pain = 0 Pain can be ignored = 5 Pain cannot be ignored = 10
Rectal bleeding	None = 0 Small amount only, in less than 50% of stools = 10 Small amount with most stools = 20 Large amount, more than 50% of stools = 30
Stool consistency	Formed = 0 Partially formed = 5 Completely unformed = 10
Number of stools in 24 hours	0–2 = 0 3–5 = 5 6–8 = 10 More than 8 = 15
Nocturnal stools (any episode that causes wakening)	No = 0 Yes = 10
Activity level	No limitation of activity = 0 Occasional limitation of activity = 5 Severe restricted activity = 10
Total =	Disease not present = Less than 10 Mild disease = 10-34 Moderate disease = 35-64 Severe disease = 65 or more

Appendix Table 3. *miR-223-3p target genes in mice identified using Target Scan.*

***miR-223-3p* targets in mice**
2210018m11rik, 2310035c23rik, 4732440d04rik, 5031414d18rik, 5830473c10rik, Abhd13, Aco1, Acsl3, Actr1a, Acvr2a, Adamts18, Adcy7, Aebp2, Agmo, Ago3, Alcam, Ankrd17, Ankrd40, Anks1b, Apool, Arfip1, Arhgap5, Arid1a, Armc1, Armcx1, Arpp19, Arvcf, Atp1b1, Atp2b1, Atp5s, Atp7a, Atxn1, Atxn10, Bai3, Baz1a, Bet1l, Brinp3, Brpf3, Btbd1, Calb1, Calml4, Carm1, Casq2, Cbfb, Cbx5, Ccne1, Ccnt2, Cd2ap, Cdh12, Cdk17, Cdyl, Celf1, Celf2, Cenpm, Cep68, Cers6, Clvs1, Cnep1r1, Cnot2, Cops2, Cpeb3, Cpne4, Crebzf, Crim1, Csnk1g1, Ctsl, Cux1, Cyb5rl, Dcn, Dennd5b, Dennd6a, Dera, Derl1, Dlgap1, Dmrt2, Dnaja1, Dpf3, Dusp2, Ebf3, Edc3, Efna1, Eif1ad, Eif5b, Elk1, Elp4, Eva1a, F3, Fa2h, Fam120c, Fam168a, Fam199x, Fam46a, Fam46d, Fam96b, Fat1, Fbxo25, Fbxo46, Fbxo8, Fbxw7, Fgf6, Fgfr2, Fignl2, Flrt1, Fnbp1l, Foxo3, Foxp1, Frk, Frmd4a, Fubp3, G0s2, G3bp1, Gm10300, Gm9887, Gm9938, Gmpr, Gna13, Golga1, Gpm6b, Gpr126, Gpr155, Gpr22, Gpr62, Gstz1, Gtpbp8, Hhex, Hipk2, Hist1h1a, Hlf, Hs3st1, Hsp90b1, Hspa1b, Igf1r, Inip, Inpp4a, Inpp5b, Itgb1, Jmy, Kat6a, Kcnq1, Kdm1b, Kif21b, Kmt2c, Kpna3, Lcor, Lelp1, Lif, Lmln, Lmo2, Maf, Mafb, Mamld1, Map1b, Map2k6, Map4, March3, Mbnl1, Mboat2, Mcmbp, Mef2c, Mga, Mkln1, Mmp16, Mon2, Mpv17l2, Mpz, Msi2, Mtpn, Mybl1, Myh10, Myo5b, Naa30, Naa50, Napepld, Ndnf, Nefh, Nelfa, Neto1, Nfat5, Nfia, Nfib, Nlrp3, Olfm1, Orc4, Otud4, Pag1, Pak3, Papolg, Pde4d, Pds5b, Pdzd8, Phactr4, Phf20l1, Phip, Phlpp1, Pik3c2a, Pkn2, Pknox1, Pkp4, Plagl2, Plce1, Plekhh1, Polr3e, Pou2f1, Pou2f1, Ppp1r12b, Ppp1r3a, Ppp2r3a, Prdm1, Prdx2, Prpf38a, Prpf39, Ptbp2, Pura, Purb, Rab22a, Rab8b, Rabep1, Rabgap1, Ralgps2, Rap2a, Rasa1, Rbm20, Rc3h1, Rcn2, Rdh10, Rhob, Rnf145, Rnf34, Rnpc3, Rorb, Rprd1b, Rps6kb1, Rras2, Sacs, Scaf8, Scn1a, Scn2a1, Scn3a, Sept11, Sept6, Sept8, Sft2d2, Sgms2, Sh3pxd2b, Siah1a, Slain2, Slc23a2, Slc24a2, Slc26a7, Slc35f1, Slc37a3, Slc39a8, Slc4a4, Slc8a1, Slco1a1, Smarcd1, Smlr1, Smoc1, Smurf2, Snai2, Snx12, Sox11, Sox6, Sp3, Spata13, Spred1, Srek1, Srgap3, Srp19, Srpk2, Ss18, St3gal6, Stam, Stk39, Styx, Syncrip, Tbx5, Tcerg1, Tet3, Tgfbr3, Tmc3, Tmem170, Tmem229a, Tmem47, Tmem64, Tmprss11e, Tnfrsf19, Tnfsf15, Tnni3k, Tnrc6b, Treml2, Trim3, Trmt5, Trpm4, Trpv2, Tshz3, Tspan7, Ttc9, Ube2a, Ube2q2, Uhmk1, Ulk2, Uqcc1, Usp40, Usp6nl, Vamp2, Vmp1, Vti1a, Wasl, Wbp1l, Wdr26, Wdr62, Wwtr1, Xcr1, Xpo4, Ypel1, Zbtb10, Zbtb18, Zbtb9, Zc3h14, Zcchc14, Zeb1, Zfand5, Zfhx3, Zfx.

Appendix Table 4. *miR-223-3p target genes in humans identified using Target Scan.*

***miR-223-3p* targets in humans**
ABCG4, ABHD13, ABI2, ACSL3, ACTRT3, ACVR2A, ADCYAP1, AEBP2, AGMO, AGO3, AIFM1, AKAP1, ANKFY1, ANKRD17, APC, APOBEC4, ARID1A, ARMC1, ARMCX1, ARPC5L, ARPP19, ATG7, ATL2, ATP10D, ATP1B1, ATP2B1, ATP7A, ATXN7L1, BAI3, BRINP3, BRMS1L, BRPF3, C10orf11, C11orf30, C14orf142, C17orf75, C18orf54, C8orf46, CALML4, CAND1, CARM1, CBLB, CBX5, CCDC149, CCDC85C, CCNT2, CCT3, CDK17, CDYL, CEP41, CHUK, CLPB, CLSTN1, CNDP1, CNOT1, CNOT2, COPS2, COPS8, CPEB3, CREBZF, CRIM1, CSNK1G1, CSPG5, CTNNA2, CTSV, CYTIP, DCUN1D3, DENND5B, DESI2, DLEU1, DNAJB13, DNAJC6, DOCK2, E2F1, EBF3, ECT2, EIF4E3, EIF5B, ELF2, ELK4, ELL2, ELP4, ENPP5, EPOR, EPSTI1, ERC1, ERO1LB, EYA3, F3, FAM160B1, FAM168A, FAM199X, FAM46A, FAM46C, FAM83D, FAM98A, FAT1, FBXL4, FBXO28, FBXO30, FBXO8, FBXW7, FDX1L, FGFR2, FNBP1L, FOXO1, FOXO3, FOXP1, FPGT-TNNI3K, FRMD4A, FUBP3, FZD4, G3BP1, GABPB2, GALNT18, GFPT1, GLIPR1, GLUL, GNA13, GPM6B, GPR155, GPR22, GRAMD4, GRHPR, GTDC1, GTPBP8, GTSF1, HDAC4, HEY2, HHEX, HIPK2, HLF, HMGCS1, HNMT, HSP90B1, IFNLR1, IGF1R, IL6ST, INPP4A, INPP5B, ITPR3, JMY, KANSL1L, KAT6A, KBTBD6, KCNMB4, KIAA0226, KIAA0226L, KIAA0355, KIAA1468, KIAA1755, KIF4A, KLF12, KLF7, KLK15, KMT2C, KPNA3, LACC1, LAYN, LELP1, LHX8, LIF, LMO2, LONP2, LRP12, LRRC19, LRRC40, LYPD6, MAFB, MAP1B, MAP2K6, MAP4, MARCH3, MAT2B, MBNL1, MBNL3, MBOAT2, MCMBP, MEF2C, MEF2D, METAP1, MFSD6, MGA, MID1IP1, MMP16, MMP19, MOSPD1, MPZ, MSI2, MSMO1, MTMR2, MTSS1, MYBL1, MYCBP, MYH10, NAA50, NCOA1, NDNF, NDP, NF2, NFASC, NFIA, NFIB, NFIC, NLE1, NLRP3, NOVA2, NRF1, NRXN3, NUCKS1, NUDT3, NUP210, NUTF2, NXF1, OPCML, OTUD4, PA2G4, PAPD5, PAX5, PAX6, PCDH12, PDE3B, PDE4D, PDPK1, PDS5A, PDS5B, PDZD11, PEX16, PFKFB3, PFN2, PHF19, PHF20L1, PHIP, PHKG2, PHLPP1, PIK3C2A, PKNOX1, PKP4, PLAGL2, PLCE1, PLEKHA3, PLEKHH1, POLR1C, POLR3E, POMP, POU2F1, PPP1R15A, PRDM1, PRKACB, PRKCE, PROKR2, PRR14L, PSD3, PSMA5, PTBP2, PTS, PURA, PURB, RAB10, RAB8B, RALGPS2, RAP2A, RASA1, RASSF4, RBBP4, RBM20, RBMS2, RBPJ, RC3H1, RCN2, RERG, RFTN2, RGS1, RGS9BP, RHOB, RIMS3, RNF145, RNF217, RNF34, RNF4, RORB, RP11-10A14.4, RP11-192H23.4, RP11-315D16.2, RPS15A, RPS6KB1, RRAS2, RSBN1L, RWDD1, RYBP, SCAF8, SCARB1, SCN1A, SCN2A, SCN3A, SDC2, SECISBP2L, SELT, SEPT4, SEPT6, SEPT8, SESN3, SETBP1, SGMS2, SH2B3, SH3D19, SHOX2, SIAH1, SLC23A2, SLC24A2, SLC25A32, SLC35F1, SLC37A3, SLC39A1, SLC4A4, SLC8A1, SLCO1A2, SMARCD1, SMOC1, SNCA, SNX24, SORBS1, SOX11, SOX6, SP1, SP3, SPATA13, SPPL2A, SPRED1, SPTLC2, SREK1, SRGAP3, SRP19, SRPK2, SRSF10, SSRP1, ST3GAL1, ST8SIA3, STIM1, STK39, STYX, SYAP1, SYNCRIP, TAOK3, TBC1D15, TBC1D17, TBC1D4, TCERG1, TET3, TGFBR2, TGFBR3, TIAL1, TMC5, TMED7, TMEM170A, TMEM178B, TMEM47, TMEM64, TNNI3K, TNRC6B, TOP2B, TRMT2B, TRPV2, TSC22D1, TSHZ3, TSPAN5, TWIST1, TXLNG, U2SURP, UBE2A, UBE2W, UBXN1, UCP3, UHMK1, ULK2, UQCC1, USP16, USP42, USP6NL, VAMP2, VAV3, VHL, VMP1, VPS39, VTI1A, WASL, WBP1L, WDR26, WDR43, WDR62, WDR7, WDR77, XKR6, XPR1, ZBTB10, ZBTB18, ZBTB4, ZBTB40, ZBTB41, ZC3H6, ZCCHC14, ZEB1,

ZFHX3, ZFP3, ZFX, ZIC1, ZNF207, ZNF395, ZNF507, ZNF706, ZSCAN12, ZSWIM7, ZXDA, ZXDB, ZZZ3.

Appendix Table 5. *miR-223-3p target genes in mice identified using miRTarBase.*

***miR-223-3p* targets in mice**
1190002N15Rik, 1700012B15Rik, 3110043O21Rik, 4932438A13Rik, 4933426M11Rik, Abca1, Abhd13, Acap2, Adcy1, Afap1, Ago1, Ak3, Akt3, Akap9, Amot, Ank2, Ank3, Ankrd17, Ankra2, Antxr2, Apc2, Aplp2, Ap2b1, Arglu1, Arl5a, Arrdc3, Atg16l1, Atg4d, Atp2b1, Atp9a, Atrn, B3galt1, B3galnt1, Bbs4, Bdp1, Cadm3, Camk1d, Camsap2, Caskin1, Casp9, Car12, Cblb, Ccdc42bpa, Cckbr, Ccnt2, Cdc42bpa, Cd99l2, Cdkn1b, Celf1, Cep120, Cpeb3, Clasp2, Cxcl2, Dag1, Daam1, Dbn1, Ddn, Ddx17, Dennd6a, Derl2, Dgcr8, Dlc37a3, Dmn3, Dock1, Dnacj6, Dnajc9, Draxin, Dusp8, Dusp11, Eml6, Enc1, Enpp1, Eps15, Ercc3, Epdr1, Ets1, Eva1a, Exlt2, F2r, F3, Fam13a, Fam57a, Fam73b, Fam78b, Fbxl20, Fbxw7, Fmnl2, Fmn1, Foxo3, Foxp1, Fut9, Gabra6, Gabrg1, Gcc2, Glcci1, Gm16515, Golga1, Golgb1, Gopc, Gnpda1, Gnptg, Gpatch2, Gpr158, Gprc5b, Gria2, Gria3, Grin2b, Grm7, Gzmb, Hlcs, Hlf, Hpcal4, Igf1r, Il17rd, Ino80d, Inpp5f, Itgb1, Jmjd1c, Jph3, Kat6a, Kbtbd2, Kidins220, Kif1b, Klhl5, Klf12, Kmt2a, Kras, Kpn1a, Ksr2, Ktn1, L3mbtl2, Ldlr, Lgi2, Lonrf2, Lonrf3, Lrrc55, Luzp1, Luzp2, Lsamp, Macf1, Map1b, Mapk10, Mar-08, Mb21d2, Mbnl1, Mef2c, Mecp2, Mfhas1, Mical3, Mlc1, Mllt6, Mob1a, Mga, Mvp, Myh10, Myo1c, Napb, Nceh1, Ndnf, Nefh, Nfib, Nnext2, Nf1, Nltrk2, Nmtmr4, Npeg3, Nprc, Nptx2, Nrep, Nsmarcd2, Nsyn1, Nsyn3, Pacs2, Paqr4, Pard6g, Pcdh15, Pcdh17, Pcdhac1, Pea15a, Peg3, Phf20l1, Phf21a, Phka1, Pik3r3, Pitpnm3, Pk1a, Plod1, Plxna2, Podn, Polr3g, Ppdfr1, Ppp4r2, Prdx6, Prkar2b, Prkcb, Prnp, Prrt3, Prpf8, Prtpu, Psd3, Ptbp2, Ptpn9, Pvt1, Rasa1, Rap2a, Rbm33, Rbm45, Rest, Rhbdl1, Rgs2, Robo2, Rnf11, Rnf14, Rnf220, Rnf467, Rragc, Rsrc2, Rtn3, Sdpr, Scd1, Scn8a, Sec62, Sep-08, Serf1, Sestd1, Shroom2, Slc25a46, Slc33a1, Slc37a3, Slc5a6, Smad5, Smarcd2, Smpb1, Smpb2, Socs5, Sox6, Spag9, Spata13, Srgap2, Srek1, Stard13, Stat3, Stk39, Syn1, Syn3, Syp, Syt4, Tbc1d14, Tgm57, Tgm67, Tm9sf3, Tmod2, Tom1l2, Tmx4, Tnik, Tnfaip1, Tnrc18, Tnxt2, Tnxt32, Tppp, Trappc6b, Trim9, Trip12, Trp53bp1, Tspyl3, Ttx4, Ube3b, Ubfd1, Usp14, Usp32, Usp36, Usp42, Vim, Vangl2, Vezt, Vopp1, Vti1a, Wasf2, Xkr6, Xpc, Xpr1, Ypel1, Ywhaz, Yipf6, Znrf3, Zbtb39, Zbtb7a, Zcchc24, Zfp26, Zfp467, Zfp619, Zfp704, Zfp91, Zhx3, Zmynd8.

Appendix Table 6. *miR-223-3p target genes in humans identified using miRTarBase.*

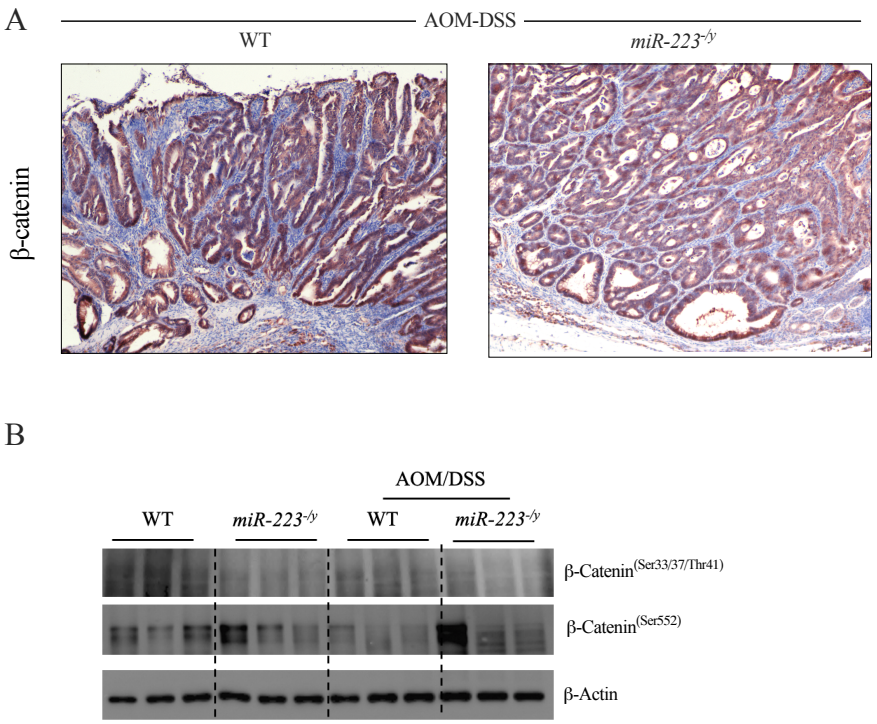
***miR-223-3p* targets in humans**
AIMP1, ABI2, ABHD13, ABCB1, ACBD5, ADAMTS9, ADD2, ADH1B, ADAT2, AGO2, AKAP2, AKT3, ALG1, AMD1, AMER1, ANG, APOL6, AR, ARID4B, ARL8B, ARTN, ARRB1, ASB11, ASH1L, ATM, ATP2A2, ATP5S, ATP7A, BAG2, BMPR1A, BMP2, BNC2, BRCC3, BRI3BP, BTBD19, BVES, C12orf60, C15orf41, C4orf29, CACNG8, CABP4, CALML4, CAPRIN1, CARM1, CCDC137, CBX1, CCND1, CD226, CDC27, CDH6, CDK2, CDK4, CDK6, CDS1, CFL2, CHAF1B, CHIC1, CHMP2B, CHORDC1, CHUK, COL19A1, CNTNAP5, CREBRF, CRIM1, CRP, CSRNP3, CYB5A, CYGB, CYP4F11, CYP4V2, DCUN1D3, DENND4C, DGKH, DMXL1, DOCK7, DMD, DUSP7, DYM, E2F1, E2F8, EDA2R, EFCAB11, EHD3, EPB41L3, EPHA1, EPHA5, EPOR, ERG, ERMP1, ESCO2, ETV3, ETV6, FABP7, FAM127A, FAM127B, FAM177A1, FAM26E, FAM60A, FBXW7, FGL2, FGFR1, FGFR2, FNIP1, FOXC1, FOXO1, FOXO3, FOXP1, FREM2, FHL2, FLVCR1, F2RL1, F3, G6PC, GALNT3, GIMAP7, GLRA2, GLRX2, GPATCH8, GPBP1L1, GPR173, GRIN2B, GTF2H1, GXYLT2, H3F3B, HACE1, HEPHL1, HEXIM1, HHIP, HMGB2, HNRNPA0, HSP90B1, IFFO2, IGLON5, ICAM1, ID4, IGF1, IGF1R, IL6, IL6ST, INSIG2, INPP5B, IRS1, ITGA1, ITGB1, KANSL1L, KATNAL1, KCNJ3, KCNK12, KCNQ5, KAT6A, KIAA1671, KIAA2018, KIAA2022, KLHL15, KLHL23, KLF6, LATS2, LDLR, LDHAL6A, LHFPL2, LHFPL5, LIF, LIFR, LIPN2, LMNB2, LMOD3, LMO2, LRRC31, MBD6, MBNL2, MDM2, MEF2C, MGRN1, MKLN1, MKNK2, MLLT3, MMADHC, MON1B, MSMO1, MSANTD4, MTRF1L, MX2, MYL9, MYLK3, NAMPT, NAA25, NDFIP2, NECAB1, NELL2, NFAT5, NFIA, NFIC, NFIX, NRF1, NLGN4X, NLRP3, NMNAT2, NOTCH2, NOVA2, NSUN3, NT5C1B, NT5C1B-RDH14, NT5DC1, OBFC1, OSBPL9, OTX1, PALM2-AKAP2, PAPSS2, PARD6G, PCGF3, PCDH10, PCDH11Y, PDE10A, PEAK1, PFN1, PHF19, PHF7, PLA2G16, PLAG1, PLCB1, PLP1, PLXDC2, POLR3G, POT1, POTEM, PPID, PPP1CC, PPP1R16B, PRDM1, PROX1, PTBP2, PTEN, RAB11FIP3, RANGAP1, RARS2, RBM22, RBBP9, RGS2, RGS4, RGS5, RIF1, RNF115, RNF152, RRAGC, RRAS2, RUNX1T1, SATB1, SCARB1, SEC23IP, SECISBP2L, SFT2D3, SHH, SIGMAR1, SKIL, SLC2A4, SLC2A12, SLC7A5, SLC7A11, SLC24A2, SLC35E3, SLC35F6, SMAD9, SMARCD1, SNX2, SNX24, SP1, SP3, SPATA6, SPPL2A, SPRY4, SPTAN1, SSPL1, SLC2A4, STARD8, STAT1, STAT5A, STIM1, STMN1, SUV420H1, SV2B, SYNPO, TSC22D3, TAL1, TAOK1, TMEM64, TMEM67, TMEM106B, TMEM133, TMEM47, TMTC3, TNFAIP8, TOX, TP53, TRIM13, TRIM2, TRIM42, TRPV2, TXNIP, TWF1, UBFD1, UBN2, UGCG, UGT2B4, USP5, USP14, USP25, VAMP4, VDR, VENTX, VIM, WASL, WDR3, WDR72, XRCC3, YWHAB, ZBTB18, ZBTB39, ZBTB7A, ZCCHC24, ZFHX2, ZHX3, ZKSCAN4, ZNF134, ZNF268, ZNF365, ZNF449, ZNF460, ZNF529, ZNF562, ZNF655, ZNF704, ZNF850, ZNF860, ZNFR3.

Appendix Table 7. *miR-223-3p target genes are differentially expressed between control and paediatric patients with Ulcerative colitis from GSE109142 cohort.*

miR-223-3p **target genes upregulated in patients with Ulcerative colitis from GSE109142 cohort vs controls**
ABCG4, ABI2, ADCYAP1, AGO3, ARMCX1, ARPC5L, ATG7, ATM, ATP10D, BAG2, BRMS1L, C11orf30, C18orf54, C8orf46, CACNG8, CARM1, CBLB, CCL3, CCNT2, CDC27, CDK17, CDK2, CEP41, CLPB, CNDP1, CNOT2, COPS8, CREBZF, CXCL2, CYTIP, DNAJB13, DNAJC6, DOCK2, E2F1, EBF3, ECT2, ELK4, ELL2, EPOR, EPSTI1, ERC1, EYA3, F3, FAM160B1, FAM168A, FAM46C, FAM83D, FAM98A, FAT1, FBXW7, FGFR1, FRMD4A, FZD4, GALNT18, GLIPR1, GLUL, GPR155, GRIN2B, GTSF1, HDAC10, HDAC4, HEY2, HHEX, HMGCS1, HSP90B1, ICAM1, IL6, IL6ST, INPP4A, INPP5B, ITPR3, JMY, KANSL1L, KIAA0226L, KIAA1755, KIF4A, KLF7, KMT2C, LATS2, LAYN, LIF, LMO2, LONP2, MAFB, MAP1B, MAP4, MDM2, MEF2C, MEF2D, MID1IP1, MMP19, MSI2, MYBL1, MYH10, NAMPT, NDP, NFASC, NFAT5, NFIB, NFIC, NLRP3, NMNAT2, NOTCH2, NOVA2, NRXN3, NUP210, NXF1, OTUD4, PARP1, PAX5, PCDH12, PFKFB3, PHF19, PHF20L1, PHIP, PHKG2, PKNOX1, PKP4, POLR3E, POLR3G, PRDM1, PTBP2, PTS, RAB8B, RALGPS2, RANGAP1, RASSF4, RBPJ, RERG, RFTN2, RGS1, RIF1, RIMS3, RNF145, RNF217, RNF34, RP11-192H23.4, RP11-315D16.2, RPS6KB1, S1PR1, SCN2A, SCN3A, SDC2, SETBP1, SH2B3, SKIL, SLC23A2, SLC24A2, SLC25A32, SLC7A5, SLC8A1, SLCO1A2, SMARCD1, SMOC1, SNCA, SOX11, SOX6, SP1, SREK1, SRGAP3, SRP19, SRSF10, ST3GAL1, STAT1, STAT5A, SYNE1, TAL1, TBC1D15, TBC1D17, TBC1D4, TCERG1, TGFBR2, TIAL1, TMC5, TMEM178B, TMEM64, TMEM67, TNRC6B, TRPV2, TSHZ3, TSPAN5, TWIST1, U2SURP, UCP3, ULK2, VMP1, VPS39, WDR26, WDR62, WDR77, XKR6, ZBTB40, ZEB1, ZNF207, ZNF365, ZNF460
miR-223-3p **target genes down regulated in patients with Ulcerative colitis from GSE109142 cohort vs controls**
ABCB1, ABHD13, ACVR2A, AGMO, AIFM1, AKAP1, APOBEC4, ARMC1, ATL2, ATP2B1, ATXN7L1, BMP2, BRINP3, BRPF3, C14orf142, C9orf40, CALML4, CCDC85C, CDK6, CDS1, CDYL, CFTR, CHMP2B, CLSTN1, CNOT1, COPS2, CPEB3, CRIM1, CSPG5, CTSV, CYB5A, DESI2, DLEU1, EIF4E3, ELP4, ENPP5, EPB41L3, FAM199X, FAM46A, FAM60A, FBXL4, FBXO28, FBXO8, FGFR2, FNBP1L, FOXO3, FOXP1, GFPT1, GNA13, GRAMD4, GRHPR, GTPBP8, HEXIM1, HLF, HNMT, IFNLR1, IGF1R, KLK15, KPNA3, LRRC19, LYPD6, MAT2B, MBNL3, MBOAT2, MCMBP, METAP1, MFSD6, MKNK2, MOSPD1, MTRF1L, NCOA1, NDNF, NFIX, NLE1, NSUN3, NUCKS1, OPCML, PAX6, PDE4D, PDPK1, PDS5A, PDZD11, PDZD8, PFN2, PHLPP1, PLAGL2, PLCE1, PRKACB, PRKCE, PRR14L, PSD3, PURA, RAB10, RASA1, RBBP4, RBMS2, RGS9BP, RPS15A, RRAS2, RWDD1, RYBP, SCAF8, SCARB1, SELT, SH3D19, SIAH1, SLC37A3, SLC4A4, SNX24, SORBS1, SP3, SPPL2A, SPTLC2, ST8SIA3, STIM1, STK39, SUV420H1, SYAP1, TET3, TMED7, TMEM170A, TNNI3K, TOP2B, TOX, TP53, TRMT2B, TSC22D1, TWF1, TXNIP, UBE2A, UBXN1, UHMK1, VAV3, WASL, WBP1L, XPR1, ZBTB10, ZBTB41, ZCCHC14, ZFHX3, ZFP3, ZNF395, ZNF706, ZZZ3.

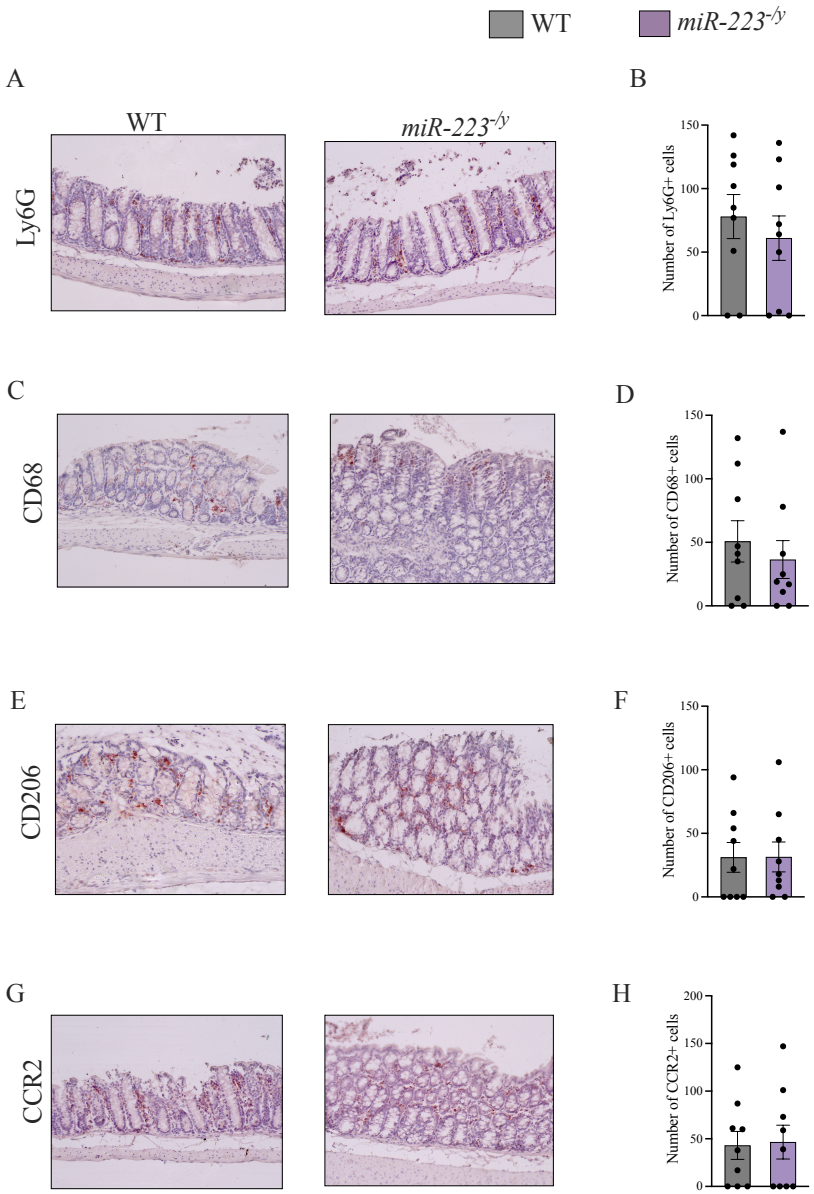
Appendix Table 8. *miR-223 target genes are differentially expressed between control and treatment non-responsive patients with Ulcerative colitis from GSE109142 cohort.*

miR-223-3p **target genes upregulated in treatment non-responsive patients with Ulcerative colitis from GSE109142 cohort vs controls**
ABCG4, ABI2, ADCYAP1, AGO3, ARMCX1, ARPC5L, ATG7, ATM, ATP10D, BAG2, BRMS1L, C11orf30, C18orf54, C8orf46, CACNG8, CBLB, CCL3, CCNT2, CDC27, CDK17, CDK2, CEP41, CLPB, CNDP1, CNOT2, COPS8, CREBZF, CXCL2, CYTIP, DNAJB13, DNAJC6, DOCK2, E2F1, EBF3, ECT2, ELK4, ELL2, EPOR, EPSTI1, ERC1, EYA3, F3, FAM160B1, FAM168A, FAM46C, FAM83D, FAM98A, FAT1, FBXW7, FGFR1, FRMD4A, FZD4, GALNT18, GLIPR1, GLUL, GPR155, GRIN2B, GTSF1, HDAC10, HDAC4, HEY2, HHEX, HMGCS1, HSP90B1, ICAM1, IL6, IL6ST, INPP4A, INPP5B, ITPR3, JMY, KANSL1L, KIAA0226L, KIAA1755, KIF4A, KLF7, KMT2C, LATS2, LAYN, LIF, LMO2, LONP2, MAFB, MAP1B, MAP4, MDM2, MEF2C, MEF2D, MID1IP1, MMP19, MSI2, MYBL1, MYH10, MYL9, NAMPT, NDP, NFASC, NFAT5, NFIB, NFIC, NLRP3, NMNAT2, NOTCH2, NOVA2, NRXN3, NUP210, NXF1, OTUD4, PARP1, PAX5, PCDH12, PFKFB3, PHF19, PHF20L1, PHIP, PHKG2, PIK3C2A, PKNOX1, PKP4, POLR3E, POLR3G, PRDM1, PTBP2, PTS, RAB8B, RALGPS2, RANGAP1, RASSF4, RBPJ, RERG, RFTN2, RGS1, RIF1, RIMS3, RNF145, RNF217, RNF34, RP11-192H23.4, RP11-315D16.2, RPS6KB1, S1PR1, SCN2A, SCN3A, SDC2, SETBP1, SH2B3, SHOX2, SKIL, SLC23A2, SLC24A2, SLC25A32, SLC35F1, SLC7A5, SLC8A1, SLCO1A2, SMARCD1, SMOC1, SNCA, SOX11, SOX6, SP1, SPRED1, SREK1, SRGAP3, SRP19, SRSF10, ST3GAL1, STAT1, STAT5A, SYNE1, TAL1, TBC1D17, TBC1D4, TCERG1, TGFBR2, TIAL1, TMC5, TMEM178B, TMEM64, TMEM67, TNRC6B, TRPV2, TSHZ3, TSPAN5, TWIST1, U2SURP, UCP3, ULK2, VMP1, VPS39, WDR26, WDR62, WDR77, XKR6, ZBTB40, ZEB1, ZNF207, ZNF365, ZNF460
miR-223-3p **target genes down regulated in treatment non-responsive patients with Ulcerative colitis from GSE109142 cohort vs controls**
ABCB1, ABHD13, ACVR2A, AGMO, AIFM1, AKAP1, APOBEC4, ARL8B, ARMC1, ATL2, ATP2B1, ATP7A, ATXN7L1, BMP2, BRINP3, BRPF3, C14orf142, C9orf40, CALML4, CCDC85C, CDK6, CDS1, CDYL, CFTR, CHMP2B, CLSTN1, CNOT1, COPS2, CPEB3, CRIM1, CSPG5, CTSV, CYB5A, DESI2, DLEU1, EIF4E3, ELP4, ENPP5, EPB41L3, FAM199X, FAM46A, FAM60A, FBXL4, FBXO28, FBXO8, FGFR2, FNBP1L, FOXO1, FOXO3, FOXP1, GFPT1, GNA13, GRAMD4, GRHPR, GTPBP8, HEXIM1, HLF, HNMT, IFNLR1, IGF1R, KLK15, KPNA3, LRRC19, LRRC40, LYPD6, MAT2B, MBNL3, MBOAT2, MCMBP, METAP1, MFSD6, MKNK2, MOSPD1, MTRF1L, NCOA1, NDNF, NFIX, NLE1, NSUN3, NUCKS1, OPCML, PAPD5, PAX6, PDE3B, PDE4D, PDPK1, PDS5A, PDZD11, PDZD8, PFN2, PHLPP1, PLAGL2, PLCE1, PRKACB, PRKCE, PRR14L, PSD3, PTEN, PURA, RAB10, RASA1, RBBP4, RBMS2, RGS9BP, RPS15A, RRAS2, RWDD1, RYBP, SCAF8, SCARB1, SELT, SH3D19, SIAH1, SLC37A3, SLC4A4, SNX24, SORBS1, SP3, SPPL2A, SPTLC2, STIM1, STK39, SUV420H1, SYAP1, TET3, TMED7, TMEM170A, TNNI3K, TOP2B, TOX, TP53, TRMT2B, TSC22D1, TWF1, TXNIP, UBE2A, UBXN1, UHMK1, UQCC1, VAV3, WASL, WBP1L, XPR1, ZBTB10, ZBTB41, ZCCHC14, ZFHX3, ZFP3, ZNF395, ZNF706, ZZZ3



Appendix Figure 1. *β-catenin expression is unchanged between WT and miR-223$^{-/y}$ mice in the AOM/DSS model of CAC.*

A. Representative micrographs of tumours from immunostaining for β-catenin. **B.** Western blot immunoblot assessment of β-catenin $^{(ser33/37/Thr41)}$ and β-catenin $^{(ser552)}$. **B.** n=3 mice/group.



Appendix Figure 2. *WT and miR-223$^{-/y}$ have similar expression of Ly6G, CD68, CD206 and CCR2.*

Representative 20x micrographs of colonic tissue from immunostaining and corresponding quantification for ***A+B*** *Ly6A,* ***C+D*** *CD68,* ***E+F*** *CD206 and* ***G+H*** *CCR2.* n=3 mice/group, 3 fields of view quantified per tumour.

Appendix Figure 3. *Paper "The MicroRNA miR-223 constrains colitis-associated tumorigenesis by limiting myeloid cell infiltration and chemokine expression"*



The Journal of Immunology

RESEARCH ARTICLE | NOVEMBER 01 2024

The MicroRNA *miR-223* Constrains Colitis-associated Tumorigenesis by Limiting Myeloid Cell Infiltration and Chemokine Expression FREE

Ciara L. Flynn; ... et. al

J Immunol (2024) 213 (12): 1869–1883.
https://doi.org/10.4049/jimmunol.2400129

Related Content

Targeting Pim2 improves effector function and longevity of T cells in cancer immunotherapy through regulating autophagy
J Immunol (May,2024)

Immunoprofiling determines survival and guides therapy in sepsis
J Immunol (May,2016)

Multiparameter cellular and humoral immunoprofiling to differentiate progressive from nonprogressive non-tuberculous mycobacterial lung disease (NTM-LD)
J Immunol (May,2023)

Downloaded from http://journals.aai.org/jimmunol/article-pdf/213/12/1869/1671867/jimmunol.2400129.pdf by guest on 02 February 2025

The MicroRNA *miR-223* Constrains Colitis-associated Tumorigenesis by Limiting Myeloid Cell Infiltration and Chemokine Expression

Ciara L. Flynn,* Gary E. Markey,† Viola Neudecker,‡ Charlotte Farrelly,* Glenn T. Furuta,§ Holger K. Eltzschig,¶ Joanne C. Masterson,†,§ and Eóin N. McNamee*

Aberrant intestinal inflammation plays a critical role in the development of colitis-associated colorectal cancer (CAC), yet the mechanisms controlling tumor development by the myeloid immune compartment are not fully understood. Although altered microRNA expression is observed in CAC, it is also unclear how myeloid-specific microRNAs impact the inflammatory process that underpins the continuum from ulcerative colitis to tumorigenesis. In this study, we report that *miR-223* acts to limit myeloid-driven inflammation in the azoxymethane (AOM)–dextran sodium sulfate (DSS) model of CAC in mice. In this model, *miR-223*$^{-/y}$ mice present with significantly larger tumors with an enhanced proliferative signature. Immunoprofiling showed that *miR-223*$^{-/y}$ mice have significantly increased colonic myeloid immune infiltrate (neutrophils, monocytes, and macrophages) following AOM-DSS. This was accompanied by an increased inflammatory chemokine and cytokine signature for monocytes and neutrophils. Bone marrow chimera studies demonstrate that myeloid-expressed *miR-223* is responsible for the enhanced tumor proliferation and inflammatory response. RNA sequencing identified several pathways that could be contributing to the development of CAC in *miR-223*$^{-/y}$ mice, including the IL-6/IL-17a cytokine family and STAT3 signaling. Lastly, neutrophil depletion with an anti-GR1 Ab (Ly6G/Ly6C) during the initial phase of the AOM-DSS model reduced the tumor burden in *miR-223*$^{-/y}$ mice. Collectively, our data indicate that *miR-223* is an important regulator of mucosal inflammation and acts to constrain the progression from ulcerative colitis to CAC by limiting myeloid-associated inflammation. ***The Journal of Immunology*****, 2024, 213: 1869–1883.**

Colorectal cancer (CRC) is the third most frequently diagnosed cancer worldwide, with ~1.9 million new cases diagnosed annually, and incidence rates are continuing to increase. Globally, CRC is also the second leading cause of cancer-related deaths (1). A major risk factor for the development of CRC is a diagnosis of an inflammatory bowel disease, in particular ulcerative colitis (UC). This disease is characterized by aberrant intestinal inflammation, which results in colonic epithelial cells becoming damaged over time, and can eventually lead to colitis-associated CRC (CAC). Additionally, UC patients with increased duration and extent of disease have a heightened risk for developing CAC (2, 3). This further highlights the critical role of inflammation in both the initiation and the progression of CAC.

Myeloid-associated inflammation is emerging as a critical driver of tumorigenesis (4). Under normal physiological conditions the crosstalk between myeloid and intestinal epithelial cells acts to maintain the integrity of the epithelial barrier (5). However, during chronic inflammation this process is disrupted, and the epithelial barrier is often irreparably damaged. Consequently, this further promotes a protumorigenic environment (4, 6). In CAC, chronic inflammation is also a major contributor to the tumor microenvironment (TME) once a tumor has been established. The TME consists of a host of different cell types, which, together with their associated cytokines, metabolites (i.e., lactic acid), and growth factors, interact with the surrounding tissue to enhance tumor growth (7). Among these cells are tumor-associated macrophages (TAMs) and neutrophils. TAMs are the largest myeloid cell type in the TME (8), where they can be polarized by environmental cues to differentiate into mature macrophages that can be broadly characterized as either proinflammatory or anti-inflammatory. Proinflammatory macrophages have traditionally been associated with antitumor activity, whereas anti-inflammatory macrophages have been shown to promote tumor

*Mucosal Immunology Research Laboratory, Kathleen Lonsdale Institute for Human Health Research, Department of Biology, Maynooth University, Maynooth, Ireland; †Allergy, Inflammation & Remodelling Research Laboratory, Kathleen Lonsdale Institute for Human Health Research, Department of Biology, Maynooth University, Maynooth, Ireland; ‡Department of Anesthesiology, Columbia University Medical Center, New York, NY; §Gastrointestinal Eosinophilic Diseases Program, Digestive Health Institute, Children's Hospital Colorado, Department of Paediatrics, University of Colorado School of Medicine, Aurora, CO; and ¶Department of Anaesthesiology, Critical Care and Pain Medicine, McGovern Medical School, University of Texas Health Science Center at Houston, Houston, TX

ORCIDs: 0000-0001-7319-086X (C.L.F.); 0000-0002-0698-3824 (G.E.M.); 0000-0003-3021-5523 (V.N.); 0009-0005-3307-430X (C.F.); 0000-0003-3262-3571 (G.T.F.); 0000-0002-3331-3148 (E.N.M.).

Received for publication March 8, 2024. Accepted for publication October 3, 2024.

This work was supported in part by Crohn's and Colitis Foundation Grant 409992 (to E.N.M.), National Institute of Diabetes and Digestive and Kidney Diseases Grant R01DK111856 (to E.N.M.), and by Science Foundation Ireland Grants 17/FRL/4863 (to J.C.M.) and 18/FRL/6201 (to E.N.M.).

E.N.M., study concept and design; C.L.F., G.E.M., V.N., C.F., and E.N.M. acquisition of data or critical resources; C.L.F., G.E.M., V.N., C.F., J.C.M., and E.N.M., analysis and interpretation of data; H.K.E. and G.T.F., provision of critical resources; C.L.F. and E.N.M., drafting of the manuscript; C.L.F., G.E.M., V.N., C.F., H.K.E., G.T.F., J.C.M., and E.N.M., critical revision of the manuscript for important intellectual content; and J.C.M. and E.N.M., obtained funding.

The Bulk RNA-seq data presented in this article have been submitted to the Gene Expression Omnibus (https://www.ncbi.nlm.nih.gov/geo/query/acc.cgi?acc=GSE245724) under accession number GSE245724.

Address correspondence and reprint requests to Dr. Eóin N. McNamee, Department of Biology, Maynooth University | NUIM, Room 2.19 Bioscience Building, Maynooth, Co Kildare, Ireland. E-mail address: eoin.n.mcnamee@mu.ie

The online version of this article contains supplemental material.

Abbreviations used in this article: AOM, azoxymethane; BM, bone marrow; CAC, colitis-associated CRC; CRC, colorectal cancer; DSS, dextran sodium sulfate; miRNA, microRNA; PCNA, proliferating cell nuclear Ag; RNA-seq, RNA sequencing; TAM, tumor-associated macrophage; TME, tumor microenvironment; UC, ulcerative colitis; WT, wild-type.

Copyright © 2024 by The American Association of Immunologists, Inc. 0022-1767/24/$37.50

https://doi.org/10.4049/jimmunol.2400129

Downloaded from http://journals.aai.org/jimmunol/article-pdf/213/12/1869/1671867/jji2400129.pdf by guest on 02 February 2025

growth (9). Recent evidence has suggested that while macrophages can alter their phenotype in response to signals from their local environment, most TAMs within the TME act to promote tumorigenesis (9, 10). Thus, identifying mechanisms that both control excessive myeloid inflammation and the regulation of TAM function are of therapeutic interest.

MicroRNAs (miRNAs) are small noncoding RNA molecules, ~18–22 nt in length, that are essential for the posttranscriptional regulation of gene expression. This regulation is primarily executed via complementary base pairing to the 3′ untranslated region of their target mRNA (11). As such, miRNAs can be critical for the regulation of several biological processes, including inflammation. Additionally, the aberrant expression of miRNAs has previously been reported separately in UC, CAC, and TAMs (12–14).

miR-223 has emerged as a key regulator of the innate immune system during intestinal inflammation. This miRNA is specifically expressed in the myeloid compartment, is induced during myeloid differentiation, and is essential for regulating myeloid cell activity (15). Additionally, *miR-223-3p* expression is increased in patients with active UC, and *miR-223*$^{-/y}$ mice have exacerbated colitis that is driven by inflammatory monocytes and neutrophils (16). In CRC, *miR-223* in increased in patient biopsies and correlates with more advanced disease (17). However, despite this correlation, a direct role for myeloid-expressed *miR-223* in the progression from UC to CAC remains to be characterized.

In this study, we investigated the role of *miR-223* in the development of CAC, using the chronic azoxymethane (AOM)–dextran sodium sulfate (DSS) mouse model of CAC. We show that *miR-223*$^{-/y}$ mice have increased susceptibility to CAC, with an increased proliferative signature, larger tumor burden, and a significant infiltration of monocytes and mixed cytokine profiles. RNA sequencing (RNA-seq) on *miR-223*$^{-/y}$ colonic tissue also showed that there is enhanced expression of several pathways previously identified to be central to the progression from UC to CAC, particularly expression of IL-6 and IL-17a cytokine family members and STAT3 signaling. Collectively, these data implicate that enhanced early myeloid inflammation plays a key role in the onset of experimental CAC and that *miR-223* constrains the progression to CAC.

Materials and Methods

Mouse strains

miR-223$^{-/y}$ mice on a C57BL/6J background were previously described (16) and bred in-house at the University of Colorado Anschutz Medical Campus. C57BL/6J mice were purchased from The Jackson Laboratory. After weaning (21 d), mice were cohoused and experimental colitis was induced at 8 wk of age. All mice were bred under specific pathogen-free conditions, and fecal samples tested negative for helminth, protozoa, and *Heliobacter* species. Animal procedures were approved by the Institutional Animal Care and Use Committees at the University of Colorado Denver.

Bone marrow chimera

Bone marrow (BM) chimeric mice were generated as previously described (16, 18). Briefly, femurs and tibias from C57BL/6J (wild-type [WT]) and *miR-223*$^{-/y}$ donor mice were removed and flushed through a 70-μm cell strainer with cold RPMI 1640 to harvest BM cells. Recipient mice (8–12 wk of age) were irradiated with a total dose of 1000 rad (500 rad twice, 4 h apart). Immediately after irradiation, 1×10^7 BM cells/mouse were i.v. injected via the retro-orbital route in 0.1 ml of 0.9% sodium chloride. Mice were housed in microisolator cages for 8 wk to recover before induction of the AOM-DSS colitis-associated tumorigenesis. To assess BM reconstitution, spleens were excised at necropsy, and RBCs were lysed, followed by flow cytometry for $CD45^+$ leukocytes expressing either CD45.1 (clone A20) or CD45.2 (clone 104; eBioscience).

Induction of experimental CAC (AOM-DSS) and Ab depletion studies

Eight-week-old mice from indicated genotypes were injected i.p. with 10 mg/kg AOM (Sigma-Aldrich). Three days later and to assess survival in one study (Supplemental Fig. 1A), mice were administered DSS (3% w/v, 36–50,000 kDa; MP Biomedicals) in drinking water ad libitum for 6 d. All mice were then returned to drinking water ad libitum and monitored for 50 d for survival. For all remaining in vivo studies, mice received DSS (2% w/v, 36–50,000 kDa; MP Biomedicals), administered in drinking water ad libitum for 6 d. This was followed by a 2-wk recovery period where DSS was removed (drinking water only). This cycle of DSS was performed three times (chronic AOM-DSS). Upon necropsy, colons were removed and flushed with cold PBS. Their length and weight were recorded. Colon tissue was either snap-frozen or fixed in 10% buffered formalin.

To assess the effects of neutrophils and myeloid-derived suppressor cells on the development of CAC, an acute phase model of AOM-DSS was performed where both cell types were depleted. In this study, one round of AOM (i.p.; 10 mg/kg) was administered and followed 3 d later by DSS (2% w/v) for 6 d, as above. This was then followed by a 2-wk recovery period where DSS was removed (drinking water only). Next, *miR-223*$^{-/y}$ mice were randomly assigned to two groups of either IgG control or a treatment group with 20 μg (i.p.) of anti-GR1 (Lyg6/Ly6C: RB6-8C5 clone, Bio X Cell, Lebanon, NH) every 3 d for 3 wk (eight total injections). All mice were euthanized 24 h following the last injection.

Colon pathology and immunohistochemistry

Formalin-fixed, paraffin-embedded tissue was cut into 7-μm sections and baked at 60°C for 24 h. Slides were deparaffinized by xylene and rehydrated using an ethanol gradient (100–70%). Samples were placed in hematoxylin for 4 min, followed by washing with water for 1 min. Slides were immersed in an acid wash for 1 min and then rinsed with water for 1 min. A bluing reagent was added to slides for 1 min before rinsing for 30 s with water. Slides where placed in eosin for 15 s and then washed in water until clear. Slides were dehydrated via sequential immersion in ethanol (70–100%) and xylene, after which a coverslip was added. Samples were imaged using a Motic Panthera L series microscope.

Immunohistochemistry

Formalin-fixed, paraffin-embedded tissues were paraffin embedded, cut into 7-μm sections, and deparaffinized as above. Ag retrieval was performed using a citrate-based solution in a pressure cooker for 10 min at 6 psi, slides were cooled with water and then washed with PBS for 5 min, after which 0.2% Triton X-100 was added to slides for 10 min, followed by 5% BSA/PBS for 20 min. Samples were then incubated overnight at 4°C with the following primary Abs; rabbit anti-mouse β-catenin (610154, BD Biosciences), rabbit anti-mouse STAT3 (ab68153, Abcam), rabbit anti-mouse CD68 (97778, Cell Signaling Technology), rabbit anti-mouse Ly6G (87048, Cell Signaling Technology), rabbit anti-mouse proliferating cell nuclear Ag (PCNA; 13110, Cell Signaling Technology), and rabbit anti-mouse CCR2 (ab27305, Abcam). Slides were washed in PBS and secondary Ab (Vector ABC kit) was added as per the manufacturer's instructions (Vector Laboratories). Staining was detected using ImmPACT NovaRED as per the manufacturer's instructions (Vector Laboratories). Slides were washed in PBS and then counterstained with hematoxylin for 1 min. Slides were dehydrated via sequential immersion in ethanol (70–100%) and xylene. Samples were imaged using either a Motic Panthera L series or Invitrogen Evos M5000 microscope.

Histology scoring and quantification

H&E images were used to determine the number of tumors present in each sample. Motic Images Plus software was also used to determine the area of each tumor, which was used to classify tumors into either dysplastic ($<100{,}000$ μm^2), small (100,000–300,000 μm^2), medium (300,000–500,000 μm^2), large (500,000–1,000,000 μm^2), or very large tumors ($>1{,}000{,}000$ μm^2). Immunostaining was quantified using QuPath software (version 0.3.1). Images were imported, image type was set to brightfield (H-DAB), and stain vectors were set using the automatic detection function. Staining was detected based on OD sum. The number of positive cells was recorded for each image. Statistical analysis was performed using GraphPad Prism.

Intestinal lamina propria cell isolation and flow cytometry

Resected colon tissues were washed with cold PBS, mesenteric fat was excised, and the tissue was opened longitudinally. Intestines were then cut into 2-cm pieces, washed with cold PBS, and vortexed in IEL solution (PBS/15 mmol/l HEPES/1 mmol/l EDTA) to remove epithelial cells. Following a PBS wash, tissues were enzymatically digested (RPMI 1640, 5% FBS,

Downloaded from http://journals.aai.org/jimmunol/article-pdf/213/12/1869/1671867/jji400129.pdf by guest on 02 February 2025

10 mmol/l HEPES, 0.07 mg/ml Liberase [Roche], 10 μg/ml DNase I [Roche]) at 37°C with gentle agitation for ~45 min. Debris was extracted using a 100-μm filter and the cell suspension was washed with cold RPMI 1640/10% FBS twice. Single-cell suspensions of lamina propria mononuclear cells were blocked with 1 μg/μl Fc block (CD16/32; eBioscience, San Diego, CA) and then stained for 2 h at 4°C with anti-mouse Abs, including Ly6G (1A8), Ly6C (AL-21), Siglec-F (E50-2440) (BD Biosciences, Franklin Lakes, NJ), MHC class II (M5/114.15.2), CD19 (6D5), CD103 (3E7), Foxp3 (FJK-16 s), CX3CR1 (SA011F11) (BioLegend, San Diego, CA), and CD4 (RM4-5), CD8 (53-6.7), CD11b (M1/70), CD11c (N418), CD45 (30-f11), and CD64 (X54-5/7.1) (eBioscience, San Diego, CA). Viable cells were gated up using AquaVi Live/Dead staining (Invitrogen, Grand Island, NY). Flow cytometric analysis was performed using a BD FACSCanto II (BD Biosciences, San Jose, CA). Data files were further analyzed using FlowJo software (Tree Star, Ashland, OR).

miRNA and mRNA transcriptional analysis by RT-PCR

Total RNA or separated fractions of miRNA and mRNA were isolated from snap-frozen colonic tissue using QIAzol reagent and an RNeasy kit following the manufacturer's instructions (Qiagen). Concentration of extracted RNA was determined using a NanoPhotometer N60 and then samples were equalized. RNA was then transcribed into cDNA using the a high-capacity cDNA reverse transcription kit (Thermo Fisher Scientific) or miRCURY LNA RT kit (Qiagen) as per the manufacturer's instructions. Transcript levels were determined by real-time RT-PCR using specific primer sets (Table I; miRNA: SYBR Green, Qiagen; mRNA: TaqMan, Applied Biosystems). Expression levels of mRNA were normalized to endogenous 18S, while RNU-6 was used to normalize miRNA expression profiles.

Western immunoblot analysis

To measure protein content, colonic biopsies were freeze-thawed in T-PER tissue protein extraction reagent with phosphatase and protease inhibitors (Abcam). Samples were then processed using TissueLyser LT as per the manufacturer's instructions (Qiagen). Supernatant protein concentrations were quantified using a Pierce BCA protein assay kit (Thermo Scientific), resuspended in reducing 4× Laemmli sample buffer (Bio-Rad), and heated to 98°C for 10 min. Samples were resolved on an 8, 10, or 12% polyacrylamide gel and semidry transferred to nitrocellulose membranes. The membranes were blocked for 30 min at room temperature in TBST supplemented with 5% nonfat milk or 5% BSA. Membranes were subsequently incubated with rabbit anti-mouse NF-κB p65 (8242), rabbit anti-mouse cyclin D1 (55506), rabbit anti–p-STAT3 (Tyr^{705}) (9145), rabbit anti–c-Myc (18583), rabbit anti-PCNA (13110), rabbit anti–phospho-S6 ribosomal protein ($Ser^{235/236}$) (4858), rabbit anti–phospho-AKT (Ser^{473}) (4060), rabbit anti–B-catenin $Ser^{33/37}$/Thr^{41} (9561), and rabbit anti–B-catenin Ser^{552} (5651) from Cell Signaling Technology; rabbit anti-STAT3 (AB68153) from Abcam; or anti–TGF-α (nbp2-34296) from Novus Biologicals. All primary Abs were incubated overnight at 4°C. Membranes were then washed three times in TBST for 15 min. Secondary Abs including goat anti-rabbit IgG-HRP (AP307), goat anti-mouse IgG-HRP (AP308), or donkey anti-goat IgG-HRP (AP180) from Sigma-Aldrich were incubated for 1 h at room temperature. Membranes were washed three times in TBST for 15 min, and proteins were then detected by ECL (Thermo Fisher Scientific). β-Actin was used as a loading control with anti-mouse β-actin (sc-1616) from Santa Cruz Biotechnology and donkey anti-goat IgG-HRP (AP180) from Sigma-Aldrich.

Bulk mRNA sequencing and bioinformatics analysis

Colon samples were stored in RNAlater (Ambion) at −80°C, and total RNA was isolated using an RNeasy kit (Qiagen). Poly(A) mRNA sequencing was performed by Novogene. mRNA was purified from total RNA using poly-T oligo-attached magnetic beads. First-strand cDNA was synthesized using random hexamer primers, and second-strand cDNA was synthesized using either dUTP for a directional library or dTTP for a nondirectional library. The library was checked with Qubit and real-time PCR for quantification and Bioanalyzer for size distribution detection. Quantified libraries were pooled and sequenced on the Illumina platform (poly(A) mRNA sequencing, with 40M PE150 reads).

Quality control. Raw data in the fastq format were processed by removing reads containing adapter, poly(N), and low-quality reads from raw data. Q20, Q30 and GC content of the clean data were determined. Clean data with high quality were used for all downstream analyses. featureCounts v1.5.0-p3 was used to calculate the read numbers mapped to each gene.

Reads mapping to the reference genome. Reference genome and gene model annotation files were downloaded from a genome Web site directly. Index of the reference genome was built using HISAT2 v2.0.5, and paired-end clean reads were aligned to the reference genome using the HISAT2 v2.0.5 mapping tool.

Quantification of gene expression level. featureCounts v1.5.0-p3 was used to count the reads numbers mapped to each gene, after which FPKM (fragments per kilobase of transcript per million mapped reads) of each gene were calculated based on the length of the gene and reads count mapped to the gene.

Differential expression and enrichment analysis. The DESeq2 R package (1.20.0) was used to determine the differential expression of two conditions/groups using a model based on the negative binomial distribution. The *p* values that were generated were adjusted using the Benjamini and Hochberg approach for controlling the false discovery rate. Genes with an adjusted *p* value ≤0.05 were classified as being differentially expressed. To further analyze differently expressed genes, the clusterProfiler R package was used to perform Gene Ontology enrichment, with correction for gene length bias. The KEGG database (http://www.genome.jp/kegg/) was used to identify the biological system involved, and the clusterProfiler R package tested the statistical enrichment of differential expression of genes in KEGG pathways. The DO (Disease Ontology) database was used to identify disease association, and the DisGeNET database integrated human disease-related genes. clusterProfiler software was used to test the statistical enrichment of differentially expressed genes in the Reactome pathway, the DO pathway, and the DisGeNET pathway. Gene Ontology, KEGG, Reactome, DO, and DisGeNET datasets were used for independent gene set enrichment analysis (GSEA) (http://www.broadinstitute.org/gsea/index.jsp).

Statistical analysis

Outside of RNA-seq analysis, all other statistical analyses were performed using ANOVA or a two-tailed Student *t* test using GraphPad Prism 10.1 software. Data are expressed as mean ± SEM. Statistical significance was set at $p < 0.05$ or $p_{adj} < 0.05$.

Data availability

Bulk RNA-seq data generated for this study is available through the Gene Expression Omnibus with accession number GSE245724.

Results

Increased tumor size in miR-223$^{-/y}$ *mice following experimental CAC*

The miRNA *miR-223* is increased in biopsies from patients with UC during active inflammation and correlates with more severe disease in CAC patients (16), but its role in the progression from UC to CAC is yet to be elucidated. To determine the role of *miR-223* in the development of intestinal tumorigenesis associated with UC, an AOM-DSS model of CAC was used. Notably, our initial studies using a higher percentage of DSS (3% w/v) highlighted a central role for miR-223 in constraining excessive inflammation and tissue destruction during the treatment course, with 66% of mice dying over the length of the protocol in *miR-223*$^{-/y}$ mice (Supplemental Fig. 1A). Tapering this dosing regimen to a lower DSS insult (2% w/v) for further chronic studies, we performed a series of experiments with three repeated rounds of DSS and recovery following an initial AOM insult. This model mimics the recurring periods of active colitic flare and then recovery and remodeling in patients with UC. We assessed spleen weight, colon weight, and colon length (Supplemental Fig. 1B–D). These serve as markers of systemic inflammation, gross tumor burden, and lingering physiologic implications of colitis induced by DSS, respectively. Differences between treatment groups with this initial analysis were negligible. Notably, when the number of macroscopically visible tumors was also assessed (Fig. 1A) and dysplasia and tumor size were determined by microscopy, our data indicate that *miR-223*$^{-/y}$ mice developed more frequent and larger tumors when compared with WT counterparts (Fig. 1C–F). This suggests that *miR-223* acts to constrain inflammatory-driven progression from UC to CAC in the AOM-DSS model.

Enhanced proliferation in colon tissues of miR-223$^{-/y}$ *mice following AOM-DSS*

As *miR-223*$^{-/y}$ mice had significantly larger tumors compared with WT mice when treated with chronic AOM/DSS, we hypothesized

Downloaded from http://journals.aai.org/jimmunol/article-pdf/213/12/1869/1671867/jji400129.pdf by guest on 02 February 2025

Table I. Primer probe list

Target	Catalog No.
TaqMan primers (Applied Biosystems by Thermo Fisher Scientific)	
Acida (AID)	Mm01184115_m1
Arg1	Mm00475988_m1
CD274 (pdl1)	Mm03048248_m1
CD273 (pdl2)	Mm00451734_m1
Ccl2	Mm00441242_m1
Ccl7	Mm00443113_m1
Chi3l3	Mm00657889_m1
Csf1	Mm00432686_m1
Csf2	Mm01290062_m1
Cxcl1	Mm04207460_m1
Cxcl2	Mm00436450_m1
Ifny	Mm01168134_m1
Il-11	Mm00434162_m1
Il-17a	Mm00439618_m1
Il-17f	Mm00521423_m1
Il-1b	Mm00434228_m1
Il-1rn	Mm00446186_m1
IL-21	Mm00517640_m1
IL-22	Mm01226722_m1
Il-4	Mm00445259_m1
Il-6	Mm00446190_m1
Irf4	Mm00516431_m1
Irf5	Mm00496477_m1
Lif	Mm00434762_m1
Nos2	Mm00440502_m1
Relna	Mm00445109_m1
Tgf-b1	Mm00441727_m1
Tnf	Mm00443258_m1
18S	Hs99999901_a1
SYBR Green primers (miRCURY miRNA Assay by Qiagen)	
Has-miR-223-3p	YP00205986
U6 snRNA	YP00203907

that *miR-223* deficiency results in enhanced proliferation. To test this, colonic tissues from AOM-DSS–treated mice were analyzed for the expression of proliferation markers via Western immunoblotting. First, WT and *miR-223*$^{-/y}$ mice did not express a marked increase in the proliferation markers assessed at baseline. In contrast, *miR-223*$^{-/y}$ mice presented with significantly higher expression of PCNA and cyclin D1 and c-Myc compared with WT controls (Fig. 1G, 1H). An increase in other proliferative markers such as p-AKT (Ser^{473}) was replicated in the tumors of both genotypes compared with nontreated controls (Fig. 1G, 1H). Of note, this increased proliferative signature appears to be selective, as other markers associated with tumor growth, nutrient sensing, and proliferation were unchanged across AOM-DSS genotypes, namely the mTOR signaling p-ribosomal S6 (Ser$^{235/236}$) (Fig. 1G) or NF-κB (Supplemental Fig. 3B). This was also evident for β-catenin isoforms, which failed to show differences in expression across genotypes (as measured by Western immunoblot and immunohistochemistry) (Supplemental Fig. 3A, 3B). Collectively, these data indicate that *miR-223* plays a role in controlling the proliferation capacity of the AOM-DSS–derived tumors.

miR-223$^{-/y}$ *regulates the infiltration of CCR2*$^{+}$ *monocytes and associated inflammatory cytokine profile following AOM-DSS*

To identify what cells are potentially implicated in the increased tumorigenic and proliferative signature observed in the *miR-223*$^{-/y}$ mice, we performed immunohistochemical and RT-PCR analysis on colon samples from AOM-DSS–treated mice. Immunostaining of CCR2^{+} monocytes, CD68^{+} macrophages, CD206^{+} "M2-like" macrophages, and Ly6G^{+} neutrophils were equivalent in noninflamed WT and *miR-223*$^{-/y}$ colons at baseline (Supplemental Fig. 2). Following a chronic AOM-DSS protocol, quantification of immunostaining on unaffected tissue showed that significantly more CCR2^{+} monocytes, CD68^{+} macrophages, and Ly6G^{+} neutrophils infiltrate into the colons of *miR-223*$^{-/y}$ mice compared with WT mice (Fig. 2). Similar numbers of CD68^{+} macrophages and Ly6G^{+} neutrophils were observed in the tumors across groups (Fig. 2A–D). However, there were significantly more CCR2^{+} monocytes detected within the tumors of the *miR-223*$^{-/y}$ mice compared with the WT when treated with AOM-DSS (Fig. 2E, 2F). Of note, we observed an increase in *miR-223* expression in the colons of WT mice following AOM-DSS (Fig. 3A). Although not conclusive, given that *miR-223* was described by our work and others as predominantly expressed from myeloid progenitors in the BM (15, 16, 19, 20), we hypothesized that this expression represents the influx of new myeloid cells (e.g., neutrophils and monocytes) into the colon.

Next, to better understand the inflammatory microenvironment that *miR-223* might regulate in the context of CAC progression, we performed a series of RT-PCR experiments on colon tissue from WT and *miR-223*$^{-/y}$ mice following an AOM-DSS course. Untreated uninflamed WT and *miR-223*$^{-/y}$ mice served as controls. We assessed gene expression for markers associated with both proinflammatory and anti-inflammatory macrophage, neutrophil, and monocyte functional responses, in addition to cytokines and chemokines for these respective cell types, given the differential tissue numbers. For all markers assessed, there was no differential expression between untreated WT and *miR-223*$^{-/y}$ mice at baseline, while nonsignificant trends of increased expression were observed for some proinflammatory mediators and cytokines such as NOS2 and GM-CSF compared with untreated WT controls (Fig. 3B, 3E). Consistent with the increase in tumor burden, *miR-223*$^{-/y}$ mice present with a significantly increased cytokine and chemokine expression profile following AOM-DSS challenge compared with all other groups assessed. Interestingly, there was a mixed profile of both classical proinflammatory and colitis-associated cytokines (*nos2*, *tnf*, *il-1b*, and *s100a8*; Fig. 3B) and TAM-associated markers (*arg1*, *chi3l3*, and *irf4*; Fig. 3C). *miR-223*$^{-/y}$ mice further demonstrated a marked increase in chemokine expression for both monocytes (*ccl2* and *ccl7*; Fig. 3D) and neutrophils (*cxcl1* and *cxcl2*; Fig. 3D) and, interestingly, myeloid growth factors (*m-csf1*, *IL-34*, and *gm-CSF*) (Fig. 3E). These later data indicate that in a *miR-223*–deficient intestine under AOM-DSS conditions, the recruitment, maturation, and survival factors for monocytes and neutrophils are significantly enhanced. This phenocopies the previously described cytokine profile of *miR-223*$^{-/y}$ during the initial phase of DSS colitis in mice and collectively with the data presented in this study indicate that *miR-223* maintains a consistent or enhanced myeloid cell recruitment to the colon following AOM-DSS challenge (16). Of note, not all tumor-associated cytokines or growth factors assessed were altered by *miR-223* deficiency; for example, vascular growth factors that are implicated in tumor survival, namely *vegfa* and *vegfc*, were unchanged in whole-tissue analysis (Supplemental Fig. 1E, 1F), as were genes for macrophage activation (*irf5*) and tumor-associated immunoregulation (*tgfb1 and il-1rn*) (Supplemental Fig. G–I). Collectively, these data suggest that *miR-223* acts as an important break to limit monocyte and neutrophil recruitment and their associated cytokine responses in the colon, with implications for the progression from UC to CAC.

miR-223 *deficiency results in the upregulation of pathways associated with poor prognosis in AOM-DSS*

To further elucidate why induction of CAC with chronic AOM-DSS results in *miR-223*$^{-/y}$ mice exhibiting more severe disease and increased proliferation, we performed RNA-seq on whole-colon samples. Pearson's correlation matrix analysis showed that all samples within each group were similar (Fig. 5A). Coexpression analysis showed that there was overlap between the three treatment groups, but also identified unique mRNAs that were only expressed by individual groups (Fig. 5B). Analysis of the differentially expressed genes

Downloaded from http://journals.aai.org/jimmunol/article-pdf/213/12/1869/1671867/jji2400129.pdf by guest on 02 February 2025

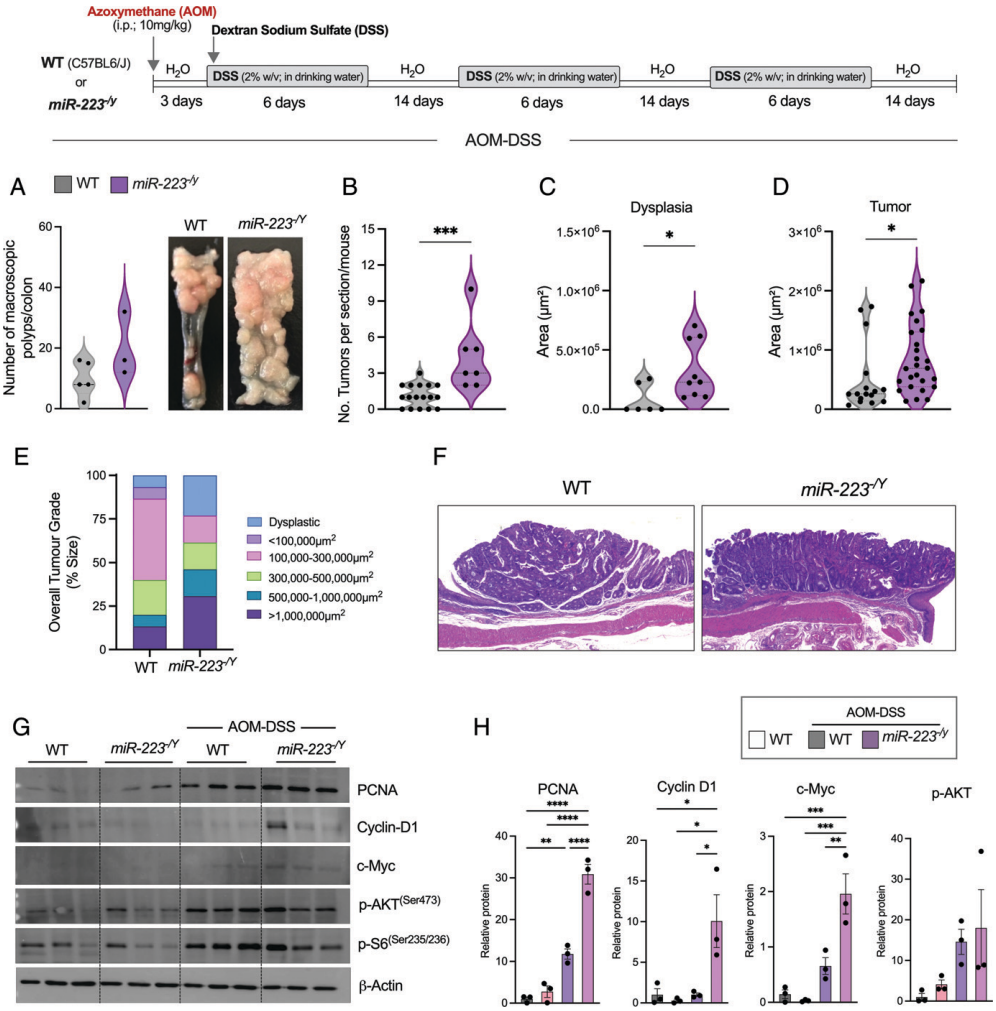


FIGURE 1. Increased tumor size and proliferative capacity in *miR-223*$^{-/y}$ mice following AOM-DSS. Schematic overview and timeline of the AOM-DSS study are shown. (**A**) Number of macroscopic polyps per colon (following H&E staining). (**B**) Number of tumors per section. (**C**) Quantification of dysplasia (µm^2) per section. (**D**) Quantification of tumor size (µm^2) per section was determined at the time of necropsy following treatment with AOM-DSS. (**E**) Tumor grading according to size from H&E micrographs in WT or *miR-223*$^{-/y}$ mice treated with chronic AOM/DSS. (**F**) Representative H&E micrograph of a tumor from WT or *miR-223*$^{-/y}$ mice treated with chronic AOM/DSS. Original magnification, ×20. All data are expressed as mean ± SEM. $*p < 0.05$, $***p < 0.001$ versus the indicated counterpart (unpaired, one-tailed students *t* test). (A) $n = 3$ mice/group, (C and D) WT AOM-DSS: 16 tumors and two dysplastic regions counted from 17 mice; *miR-223*$^{-/y}$ AOM-DSS: 27 tumors and nine dysplastic regions counted across 7 mice. Data are presented from two independent experiments. (**G**) Western immunoblot assessment of PCNA, cyclin D1, c-Myc, p-AKT$^{(Ser473)}$, p-S6$^{(Ser235/236)}$, and β-actin in colon biopsies ($n = 3$ mice/group). (**H**) Quantification of Western immunoblots for PCNA, cyclin D1, c-Myc, and p-AKT. All data are expressed as mean ± SEM. $*p < 0.05$, $**p < 0.01$, $***p < 0.001$, $****p < 0.0001$ versus the indicated counterpart (one-way ANOVA).

between *miR-223*$^{-/y}$ AOM-DSS and WT AOM-DSS showed that mRNA expression varied between the two groups (Fig. 5C, 5D). Additionally, application of unbiased GSEA KEGG pathway analysis showed that both the inflammatory bowel disease pathways (mmu05321) (Fig. 5D–F) and CRC pathways (mmu05210) (Fig. 5G–1) were significantly altered between genotypes with positive enrichment in the *miR-223*$^{-/y}$ AOM-DSS mice compared with WT AOM-DSS controls. Further GSEA revealed that selected pathways associated with poor clinical prognosis in CRC and CAC are significantly positively enriched in the *miR-223*$^{-/y}$ AOM-DSS–treated group, including p53 signaling, apoptosis, DNA damage, and regulation of PTEN stability (Fig. 5J). It is noteworthy that the phenotype of increased proliferation and tumor burden described earlier in *miR-223*$^{-/y}$ was not representative of all CRC

Downloaded from http://journals.aai.org/jimmunol/article-pdf/213/12/1869/1671867/jji400129.pdf by guest on 02 February 2025

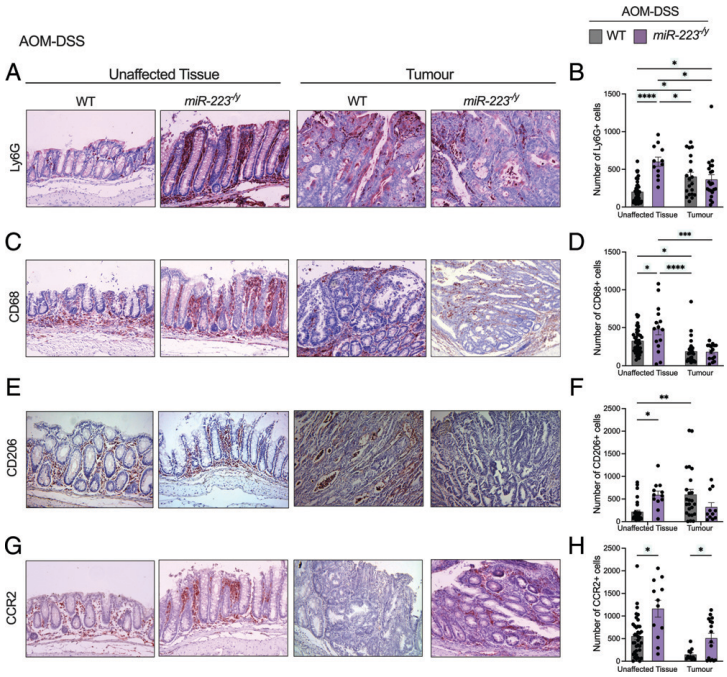


FIGURE 2. Macrophages, neutrophils, and monocytes infiltrate into the colon of *miR-223*$^{-/y}$ mice treated with chronic AOM-DSS. (**A**) Representative micrographs of unaffected tissue and tumor of WT and *miR-223*$^{-/y}$ mice treated with chronic AOM-DSS after immunohistochemical staining for Ly6G. Original magnification, ×20. (**B**) Quantification of Ly6G immunostaining. (**C**) Representative micrographs of unaffected tissue and tumor of WT and *miR-223*$^{-/y}$ mice treated with chronic AOM/DSS after immunohistochemical staining for CD68. Original magnification, ×20. (**D**) Quantification of CD68 immunostaining. (**E**) Representative micrographs of unaffected tissue and tumor of WT and *miR-223*$^{-/y}$ mice treated with chronic AOM-DSS after immunohistochemical staining for CD206. Original magnification, ×20. (**G**) Quantification of CD206 immunostaining. (E) Representative micrographs of healthy tissue and tumors WT and *miR-223*$^{-/y}$ mice treated with chronic AOM-DSS after immunohistochemical staining for CCR2. Original magnification, ×20. (**H**) Quantification of CCR2 immunostaining. All data are expressed as mean ± SEM. (A and B) WT AOM-DSS, $n = 16$; *miR-223*$^{-/y}$ AOM-DSS, $n = 4$. (C and D) WT AOM-DSS, $n = 14$; *miR-223*$^{-/y}$ AOM-DSS, $n = 4$. (E and **F**) WT AOM-DSS, $n = 11$; *miR-223*$^{-/y}$ AOM-DSS, $n = 4$. (G and H) WT AOM-DSS, $n = 12$; *miR-223*$^{-/y}$ AOM-DSS, $n = 4$. Three fields of view were quantified per animal. $^{*}p < 0.05$, $^{**}p < 0.01$, $^{***}p < 0.001$, $^{****}p < 0.0001$ versus the indicated counterpart (one-way ANOVA).

signaling pathways assessed. Although reactome analysis identifies signaling pathways that were upregulated in the *miR-223*$^{-/y}$ group with clinical relevance to CAC and CRC progression (Supplemental Fig. 4A, 4B), those of the TGF-α–EGF cytokine family were also markedly increased in *miR-223*$^{-/y}$ mice compared with WT counterparts at the protein level across groups (Supplemental Fig. 3B, 3C).

Hematopoietic deficiency of miR-223 *enhances susceptibility to AOM-DSS*

As we performed AOM-DSS studies in a germline hemizygous knockout strain of *miR-223*$^{-/y}$ mice, we generated BM chimeric animals to ascertain whether the stromal/radio-resistant or hematopoietic compartment was responsible for the effects on inflammation-driven tumorigenesis. Our data confirm hematopoietic-derived *miR-223* (*miR-223*$^{-/y}$ → WT recipients) as driving exacerbated AOM-DSS, as indicated by increased macroscopic polyps, dysplasia, and tumor numbers compared with controls (WT → *miR-223*$^{-/y}$ recipients; Fig. 5A–F). However, a significant difference for colon length and spleen weight was not observed (Supplemental Fig. 1J–L). To further confirm the effect of *miR-223* derived from the hematopoietic compartment versus the stromal compartment, we analyzed the relative mRNA expression of markers associated with proinflammatory and anti-inflammatory macrophages, monocytes, and neutrophils. Expression of *il-1β*, *nos2*, and *chi3l3* were increased in *miR-223*$^{-/y}$ → WT mice compared with the stromal chimera (WT → *miR-223*$^{-/y}$) (Fig. 5G, 5H). This was accompanied by increases in the neutrophil chemokines *cxcl1* and *cxcl2*, with non-significant trends toward increased expression of monocyte chemokines *ccl2* and *ccl7* (Fig. 5I). Similarly to gene expression analysis of AOM-DSS alone, vascular growth factors (*vegfa* and *vegfc*), macrophage activation (*irf5*), and tumor-associated immunoregulation (*tgfb1 and il-1rn*) genes were unchanged in the BM chimera study across all groups (Supplemental Fig. 1M–Q). Although the BM chimera study highlighted some genes that appeared to be regulated by stromal *miR-223* interactions (e.g., *nos2* and *arg1*), overall, our data suggest that *miR-223* constrains the inflammatory tone of infiltrating myeloid cells to limit the progression toward tumorigenesis during experimental AOM-DSS.

Increased IL-6 cytokine family and STAT3 signaling in miR-223$^{-/y}$ *mice following AOM-DSS challenge*

RNA-seq analysis highlighted a consistent pattern of increased cytokine signaling and particularly an enriched signature for IL-6 family members and STAT3 signaling in *miR-223*$^{-/y}$ following AOM-DSS

Downloaded from http://journals.aai.org/jimmunol/article-pdf/213/12/1869/1671867/jji2400129.pdf by guest on 02 February 2025

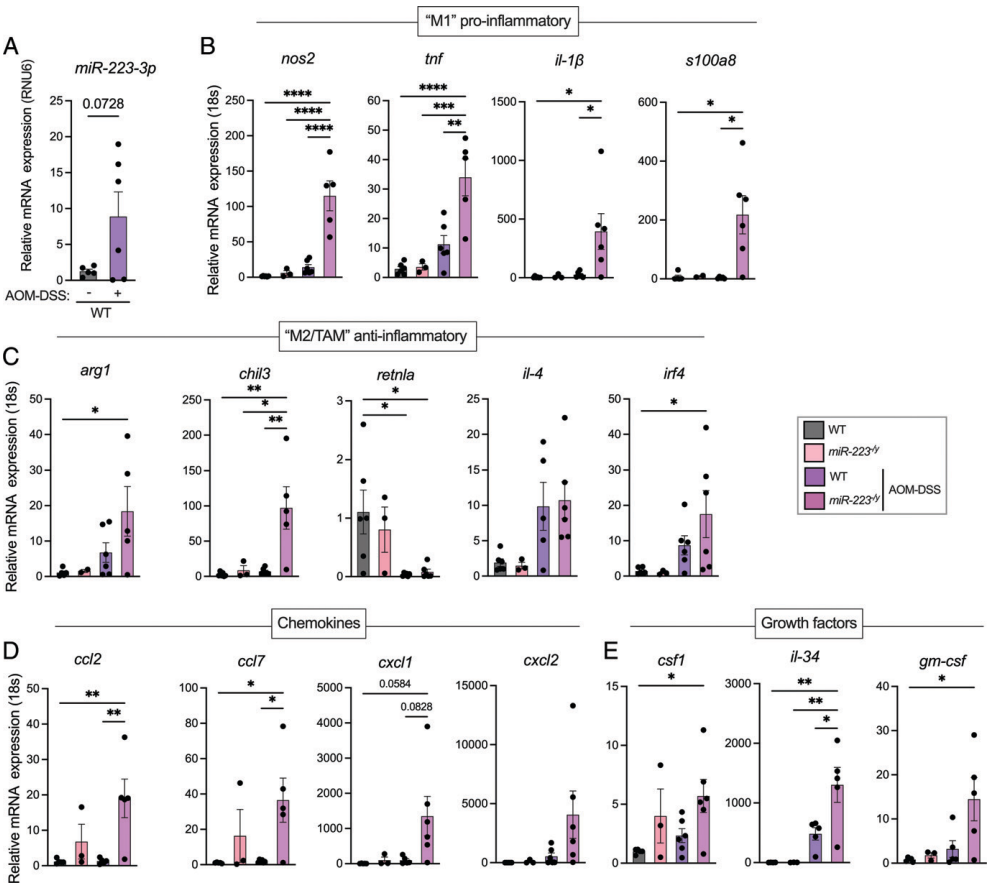


FIGURE 3. *miR-223*$^{-/y}$ mice have increased chemokine and cytokine signatures for monocytes and neutrophils following AOM-DSS. (**A**) Relative mRNA expression of *miR-223-3p.* (**B**) Relative mRNA expression of the proinflammatory macrophage markers *nos2*, *tnf*, *il-1β*, and *S100a8.* (**C**) Relative mRNA expression of the anti-inflammatory macrophage markers *arg1*, *chi3l3*, *retnla*, *il-4*, and *irf4.* (**D**) Relative mRNA expression of the monocyte chemokines *ccl2* and *ccl7* and neutrophil chemokines *cxcl1* and *cxcl2.* (**E**) Relative mRNA expression of the myeloid growth factors *m-csf1*, *il-34*, and *gm-csf.* All data are expressed as mean ± SEM. (A) $n = 5$–6 mice/group; (B–E) $n = 3$–6 mice/group. $^{*}p < 0.05$, $^{**}p < 0.01$, $^{***}p < 0.001$, $^{****}p < 0.0001$ versus the indicated counterpart (one-way ANOVA).

when compared with WT AOM-DSS (Fig. 6A–C). Given the clinical importance of STAT3 signaling to CRC progression (21), we wanted to confirm these findings further. RT-PCR analysis showed that expression of IL-6 family members and STAT3 signaling cytokines are significantly increased in *miR-223*$^{-/y}$ mice compared with WT controls, including *il-6*, *il-11*, and *lif* (Fig. 6D). We extended this analysis to include cytokines that signal via STAT3 and play a role in CRC and mucosal inflammation, namely *il-22 and il-17a*, with both also being significantly increased in *miR-223*$^{-/y}$ mice (Fig. 6D). Lastly, the expression and localization of active p-STAT3 and total STAT3 proteins were assessed by immunoblot and immunohistochemistry. A marked increase in p-STAT3 was observed in the uninvolved colon tissues of *miR-223*$^{-/y}$ mice compared with WT controls following AOM-DSS, consistent with increased tissue expression of IL-6 family cytokines and myeloid inflammatory infiltrates (Fig. 6D–I). Taken together, these findings suggests that IL-6 and p-STAT3 signaling are contributing to the development of CAC in *miR-223*$^{-/y}$ mice.

Ab-mediated depletion of infiltrating Ly6G^{+} *myeloid cells with RB6-8C5 reduced early tumorigenesis in* miR-223$^{-/y}$ *mice using an acute model of AOM-DSS*

Our previous work identified a direct role for *miR-223* in controlling the early inflammatory response to colitis and in the context of bacterial infection of the lung (16, 22). Although our BM chimeric studies indicate a role for hematopoietic-derived *miR-223* in controlling AOM-DSS pathology, we do not know which immune subsets are responsible. Given the importance of the IL-6/IL-17a/STAT3 cytokine axis in recruiting neutrophils to mucosal tissues and the role of CXCR2^{+} neutrophils in both AOM-DSS and CAC (23), we wanted to test whether *miR-223*–controlled neutrophil recruitment was responsible for the increased tumorigenesis in *miR-223*$^{-/y}$ mice.

Downloaded from http://journals.aai.org/jimmunol/article-pdf/213/12/1869/1671867/jji2400129.pdf by guest on 02 February 2025

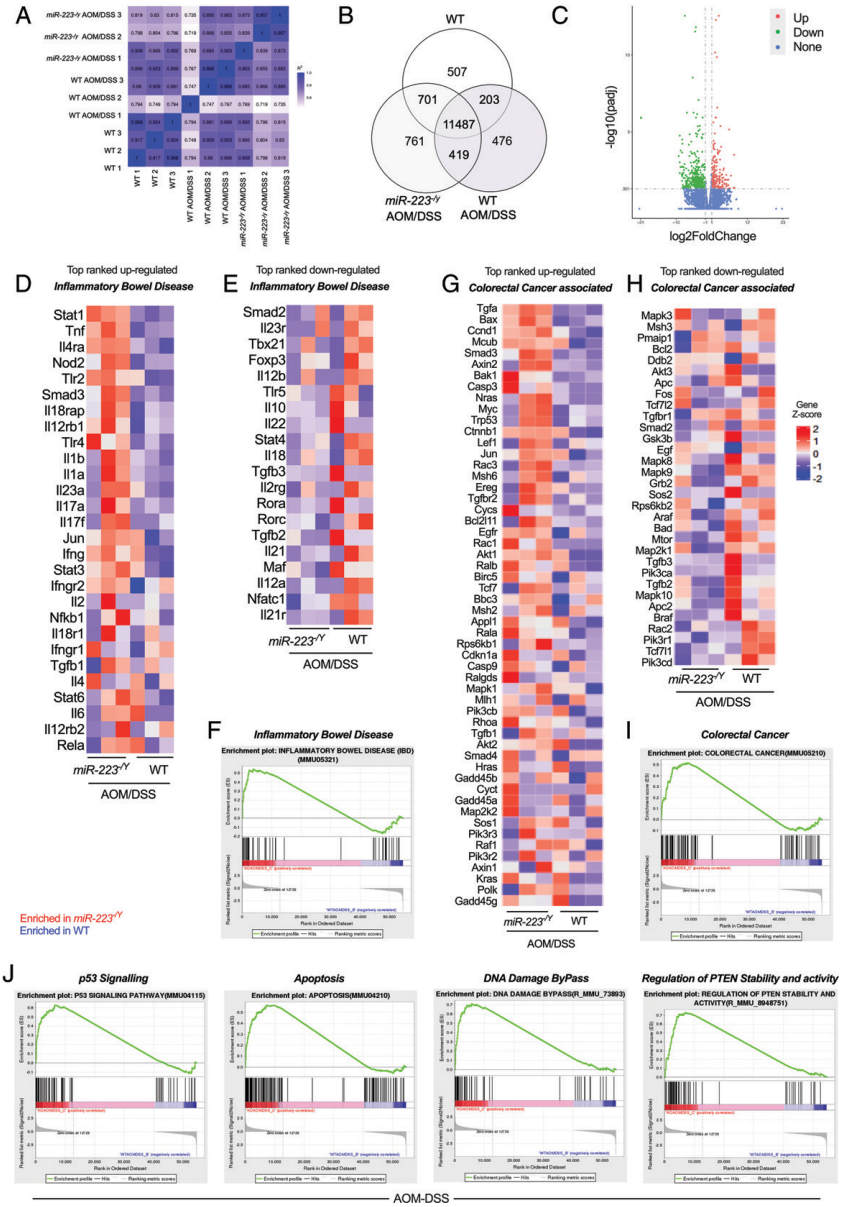


FIGURE 4. *miR-223*$^{-/y}$ mice present with an upregulation of pathways associated with poor prognosis in CAC. (**A**) Heat map of the Pearson correlation between all samples analyzed via RNA sequencing. (**B**) Venn diagram illustrating the overlap of mRNAs shared between treatment groups. (**C**) Volcano plot of differentially expressed mRNAs between *miR-223*$^{-/y}$ AOM-DSS versus WT AOM-DSS. (**D**) Heat map of the top upregulated differentially expressed mRNAs associated with inflammatory bowel disease between *miR-223*$^{-/y}$ AOM-DSS versus WT AOM-DSS. (**E**) Heat map of the most downregulated differentially expressed mRNAs associated with inflammatory bowel disease between *miR-223*$^{-/y}$ AOM-DSS versus WT AOM-DSS. (**F**) Enrichment plot for inflammatory bowel disease (MMU05321) from GSEA analysis (NES, 1.209; FDR *q* value, 0.473). (**G**) Heat map of CRC-associated mRNAs that are upregulated in *miR-223*$^{-/y}$ AOM-DSS versus WT AOM-DSS. (**H**) Heat map of CRC-associated mRNAs that are downregulated in *miR-223*$^{-/y}$ AOM-DSS versus WT AOM-DSS. (**I**) Enrichment plot for CRC (MMU05210) from GSEA analysis (NES, 1.343; FDR *q* value, 0.281). (**J**) Enrichment plots for p53 signaling (MMU04115) (NES, 1.404; FDR, *q* value 0.239), apoptosis (MMU04210) (NES, 1.404; FDR *q* value, 0.212), DNA damage *(Figure legend continues)*

Downloaded from http://journals.aai.org/jimmunol/article-pdf/213/12/1869/1671867/jji2400129.pdf by guest on 02 February 2025

To directly test this, we used a revised protocol for AOM-DSS with a shortened treatment plan (AOM + one round of DSS and 5 wk recovery with water). This allowed for modest development of inflammation-driven neoplasia and a window to target immune cell populations important during the developmental phase of CAC. We treated *miR-223*$^{-/y}$ mice with an IgG control or anti-GR1 (clone RB6-8C5) Ab every 3 d for 3 wk. This regimen selectively depleted neutrophils and myeloid-derived suppressor cells, without impacting the frequencies of other colonic myeloid cells (Fig. 7C–F). Importantly, anti-GR1 depletion studies largely blocked the development of colonic dysplasia and tumor development compared with the IgG-treated control group (Fig. 7A, 7B). Of note, neither CD4$^+$, CD8$^+$, or CD19$^+$ lymphocyte populations were significantly different in the WT versus *miR-223*$^{-/y}$ groups, nor were they altered in the anti-GR1 treatment groups (Supplemental Fig. 4A–C). In addition, we assessed the expression of tumor-promoting regulatory T cells (CD4$^+$Foxp3$^+$), and their colonic frequency was not changed at this time point (Supplemental Fig. 4F, 4G). We also show a significant increase in IFN-γ signaling in the colons of *miR-223*$^{-/y}$ mice compared with WT counterparts (bulk RNA-seq) (Supplemental Fig. 4H, 4I), whereas RT-PCR showed enhanced expression of IFN-γ and PD-L1 in *miR-223*$^{-/y}$ colons at baseline or following AOM-DSS (compared with WT counterparts) (Supplemental Fig. 4J–L). Of note, PD-L2 (thought to be expressed largely by TAMs) was not significantly altered. Collectively, these data suggest that although the frequencies of major T cells are unchanged across groups, there is a marked increase in effector T cell cytokines in the colons along with protumor checkpoint ligands. Additionally, from our original bulk RNA-seq data (Fig. 4), there is a series of protumor pathways activated that may collectively contribute to enhance tumor growth observed, which the myeloid compartment of *miR-223*$^{-/y}$ mice appears to control.

Discussion

Global incidence of CRC, including CAC, continue to rise (24). However, our understanding of the underlying mechanisms behind CAC development remains incomplete. The myeloid-associated miRNA *miR-223* is a critical regulator of innate immunity, and its expression is elevated in patients with active UC (16, 17), but little research has focused on its role in CAC. Collectively, our data suggest that this miRNA is important for controlling proliferation and limiting tumor development in the AOM-DSS model of CAC. Our data have demonstrated that deficiency in this miRNA results in increased tumor size and with increased monocytes, macrophages, and neutrophils infiltrating into the colon, in conjunction with increased monocytes migrating into tumors. This suggests that in this model of CAC, excessive myeloid inflammation is contributing to a protumorigenic microenvironment and that *miR-223* acts to limit the progression of CAC.

Chronic inflammation is a well-established contributor to both the initiation and progression of cancer (25), including gastric (26, 27), esophageal (28, 29), and cervical cancers (30, 31). In CAC, the inflammatory microenvironment promotes the release of cytokines, such as IL-6, IL-1β, TNF-α, and TGF-β, to promote tumor growth (32). Consequently, excessive NOS is produced, along with the presence of reactive oxidative species, which further boosts the production of proinflammatory cytokines (33). This creates a cycle that sustains inflammation, leading to DNA damage and ineffective tissue repair. In our model, *miR-223*$^{-/y}$ mice had significantly higher expression of proinflammatory cytokines, inducible NO synthase, and markers of proliferation (c-Myc, PCNA, and cyclin D1), suggesting that *miR-223* is critical for controlling the inflammatory response in CAC.

Persistent inflammation in CAC also increases the number of immune cells infiltrating into the colon, with neutrophils and monocytes among the most abundant (34). The ability for monocytes to subsequently differentiate into TAMs further ensures that the inflammatory cycle continues via the production of inflammatory cytokines and growth factors. Specifically, CCL2, CCL7, TNF, TGF-β, and M-CSF1 are critical for this process and are increased with *miR-223* deficiency following AOM-DSS (9). This incites a protumorigenic, immunosuppressive environment that limits the detection and elimination of cancerous cells. Accordingly, TAMs are associated with poor prognosis in many cancers (35). Due to the immunomodulatory ability of TAMs, they are currently being investigated as a potential therapeutic target for the treatment of CAC, along with many other cancers. Studies to date have focused on either reducing the presence of TAMs or altering their functionality, with research in CRC showing promising results (36, 37).

Importantly, both tissue-resident macrophages in the colon and, in particular, CD68$^+$ TAMs in the TME have been linked to the recruitment of neutrophils and myeloid-derived suppressor cells through the expression of chemokines CXCL1 and CXCL2 (38, 39). While critical for antimicrobial tissue homeostasis, neutrophils have been increasingly linked with protumor responses and tumor growth, using mechanisms such as metalloproteinases to degrade the tissue parenchyma and allow for tumor growth (23, 40, 41), and more recently being linked to tumor vascularization. Our data show that while increased neutrophil chemokines are present along with increased neutrophils in tumor-adjacent tissues, neutrophil numbers are not altered within the tumor directly. It is noteworthy that this measurement was at the end stage of CAC development in this model (three rounds of chronic AOM-DSS) and so may be indicative of the tumor stage compared with WT counterparts. The heightened cytokine and chemokine expression signature of *miR-223*$^{-/y}$ mice might also underlie the increased proliferative state of the tumors in *miR-223*$^{-/y}$ colons (possibly via pro-growth STAT3 from cytokines such as IL-6, IL-17a, and IL-22 or via TGF-EGFR signaling). There appears to be clinical discrepancies as to the scoring parameters and hallmarks of tumor-associated neutrophils, in part due to shared cellular markers to identify neutrophils with other myeloid populations (unlike mouse Ly6G) (42). However, increased neutrophils are correlated with tumor score in CAC, with location associated with altered function (e.g., angiogenesis) (43). In addition, altered neutrophil-to-lymphocyte ratios have been associated with heighted disease course and increased liver metastasis in CRC (44). While our bone marrow chimera and Ab depletion studies go some way to demonstrate that heightened myeloid inflammation (and potentially tissue damage and altered repair mechanisms) underlies the increased CAC phenotype of *miR-223*$^{-/y}$ mice, some variations are present across experiments. For example, most of the inflammatory cytokines and chemokines that were measured show similar expression profiles in AOM-DSS–treated colons, yet some important TAM-associated markers have differential expression between germline *miR-223*$^{-/y}$ mice and the bone marrow chimera studies. For example, whereas retlna, irf4, and chil3 all demonstrate similar expression patterns, arg1 shows discrepant expression profiles (increased in the chronic studies while decreased in hematopoietic

bypass (R_MMU_73893) (NES, 1.368; FDR *q* value, 0.308), and regulation of PTEN stability and activity (R_MMU_8948751) (NES, 1.391; FDR *q* value, 0.402) from GSEA analysis. $n = 3$ mice/group. FDR, false discovery rate; NES, normalized enrichment score.

Downloaded from http://journals.aai.org/jimmunol/article-pdf/213/12/1869/1671867/ji2400129.pdf by guest on 02 February 2025

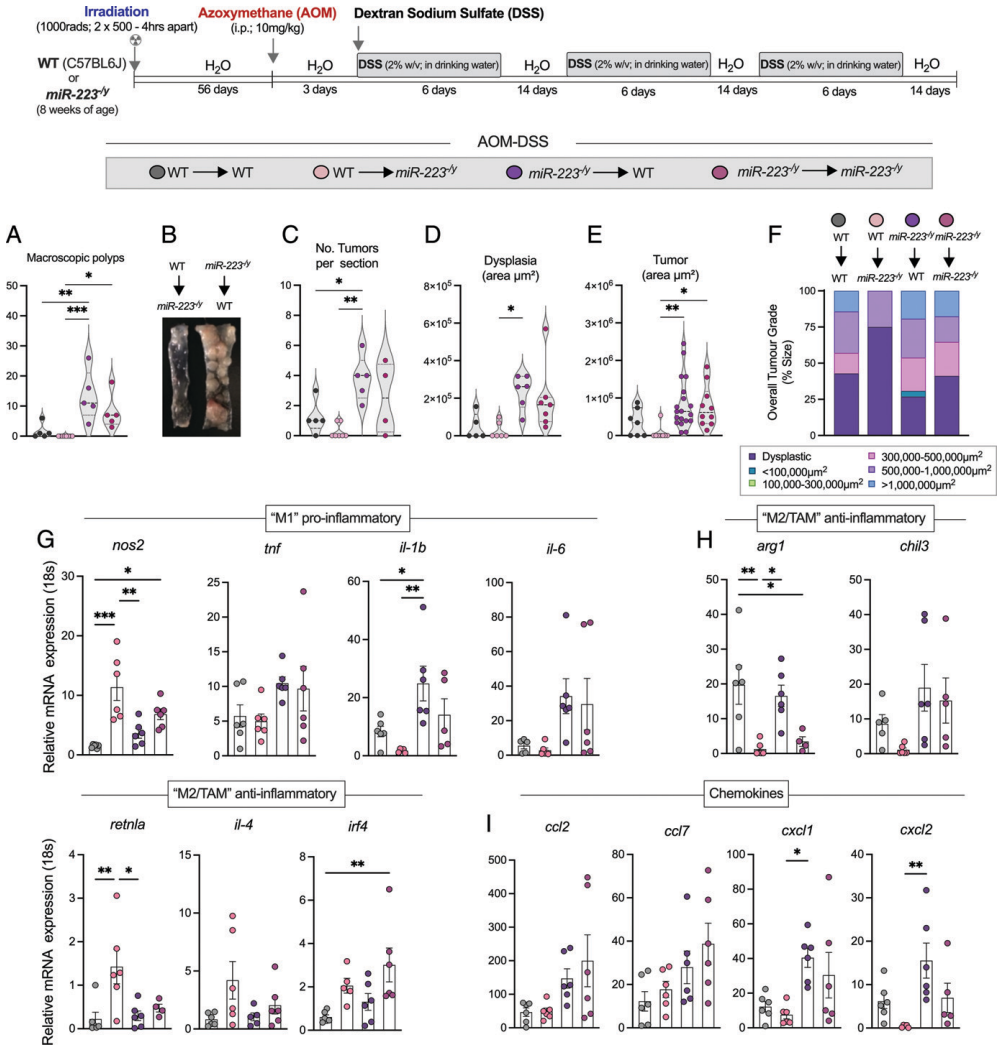


FIGURE 5. Hematopoietic deficiency of *miR-223* enhances susceptibility to AOM-DSS. Schematic overview and timeline of the bone marrow chimera AOM-DSS study are shown. (**A**) Number of macroscopic polyps per colon (following H&E staining). (**B**) Representative image of colon polyps. (**C**) Number of tumors per section. (**D**) Quantification of dysplasia (μm^2) per section. (**E**) Quantification of tumor size (μm^2) per section was determined at the time of necropsy following treatment with AOM-DSS. (**F**) Tumor grading according to size from H&E micrographs in WT or *miR-223*$^{-/y}$ mice treated with chronic AOM/DSS. RT-PCR was used to measure relative mRNA expression of the following markers from colonic tissues of indicated genotypes. (**G**) Proinflammatory markers *nos2*, *tnf*, *il-1b*, amd *il-6*. (**H**) Anti-inflammatory markers *arg1*, *chi3l3*, *retnla*, *il-4*, and *irf4*. (**I**) Monocyte chemokines *ccl2* and *ccl7* and neutrophil chemokines *cxcl1* and *cxcl2*. All data are expressed as mean ± SEM. (C–F) WT→WT: 4 tumors and 3 dysplastic regions from 5 mice; WT→*miR-223*$^{-/y}$*:* 1 tumor and 3 dysplastic regions from 7 mice; *miR-223*$^{-/y}$→WT: 19 tumors and 7 dysplastic regions from 5 mice; *miR-223*$^{-/y}$→*miR-223*$^{-/y}$*:* 10 tumors and 7 dysplastic regions from 4 mice. (G–I) n = 5–6 mice/group. $^{*}p < 0.05$, $^{**}p < 0.01$, $^{***}p < 0.001$ versus the indicated counterpart (one-way ANOVA).

groups of the bone marrow chimera). This may be reflective of altered metabolism or mixed immune cell infiltration into the colon at the time of analysis. It is noteworthy that in the case of *arg1* and arginine metabolism/the urea cycle, *nos2* remains significantly increased across all studies and correlates with tissue inflammation and progression to CAC in this model.

In addition to mixed myeloid inflammatory and TAM-associated gene expression profiles, *miR-223*$^{-/y}$ mice present with significantly increased CCR2^{+} cells within the tumors at end-stage disease. With the majority of CCR2^{+} marking inflammatory monocytes in mice, this is an interesting finding that correlates with monocyte chemokine induction (ccl2, ccl7) and growth factors (csf-1 [m-csf] and il-34).

Downloaded from http://journals.aai.org/jimmunol/article-pdf/213/12/1869/1671867/ji2400129.pdf by guest on 02 February 2025

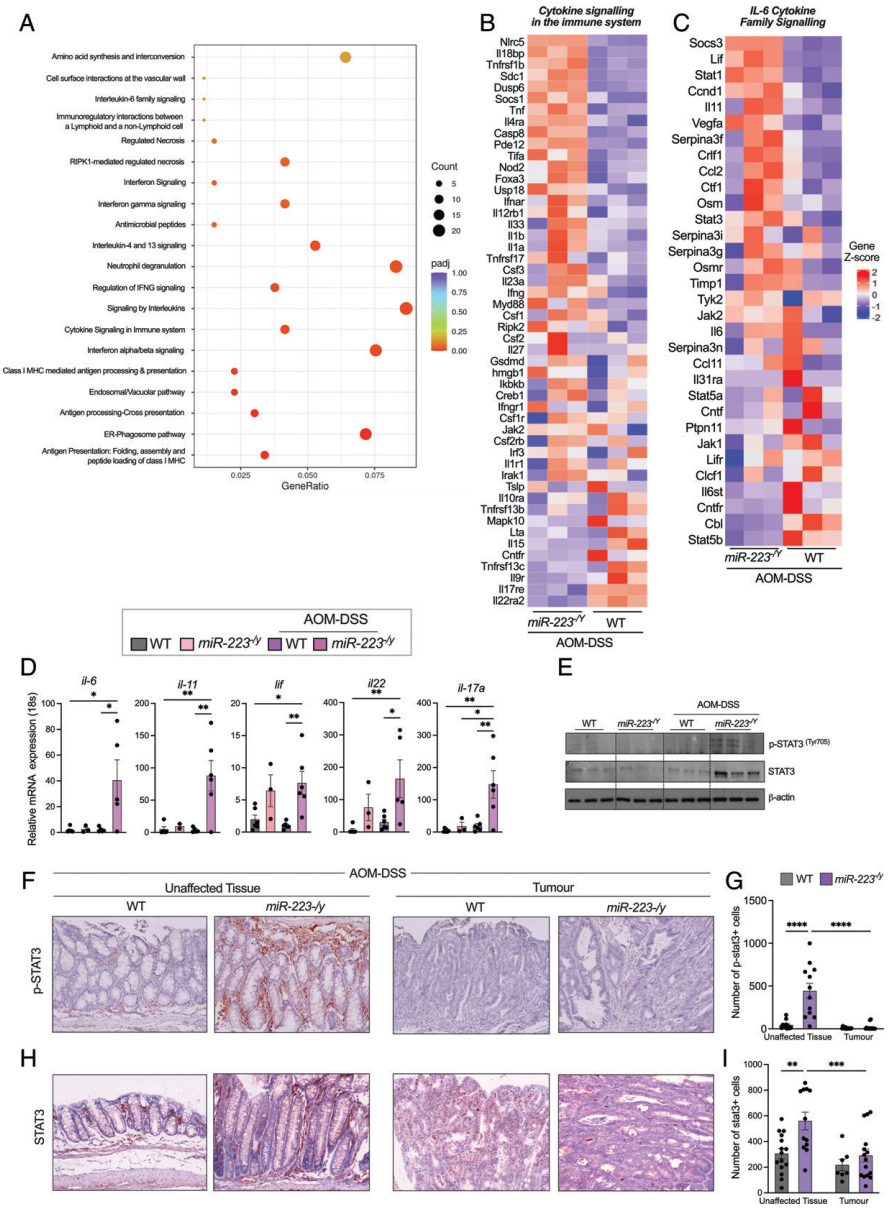


FIGURE 6. IL-6 cytokine family and p-STAT3 signaling are increased in *miR-223*$^{-/y}$ mice in the chronic AOM-DSS model of CAC. (**A**) Dot plot for Reactome pathways upregulated in *miR-223*$^{-/y}$ AOM/DSS. (**B**) Heat map of the differentially expressed mRNA in the cytokine signaling in the immune system pathway for *miR-223*$^{-/y}$ AOM-DSS versus WT AOM-DSS (n = 3/group). (**C**) Heat map of the differentially expressed mRNA in the IL-6 signaling family for *miR-223*$^{-/y}$ AOM-DSS versus WT AOM-DSS. (**D**) Gene expression was analyzed in colon tissue by RT-PCR for expression of *il-6*, *il-11*, *lif*, *il-22*, and *il-17a*. (**E**) Western immunoblot assessment of p-stat3, stat3 and β-actin in colon biopsies. (**F**) Representative micrographs of unaffected and tumor tissue from WT and *miR-223*$^{-/y}$ *mice* treated with chronic AOM-DSS after immunohistochemical staining for p-stat3. (**G**) Quantification of p-stat3 staining. Original magnification, ×20. (**H**) Representative 20 micrographs of unaffected and tumor tissue from WT and *miR-223*$^{-/y}$ mice treated with chronic AOM-DSS after immunohistochemical staining for stat3. Original magnification, ×20. (**I**) Quantification of stat3 staining. All data are expressed as mean ± SEM. (A–C, E, and F) n = 3 mice/group; (D) n = 3–6 mice/group; (F and H) WT AOM-DSS, n = 5; *miR-223*$^{-/y}$ AOM-DSS. n = 4; (G and I) WT AOM-DSS, n = 5; *miR-223*$^{-/y}$ AOM-DSS, n = 4 with three fields of view presented per animal. $^{*}p < 0.05$, $^{**}p < 0.01$, $^{***}p < 0.001$ versus the indicated counterpart (one-way ANOVA).

Downloaded from http://journals.aai.org/jimmunol/article-pdf/213/12/1869/1671867/ji2400129.pdf by guest on 02 February 2025

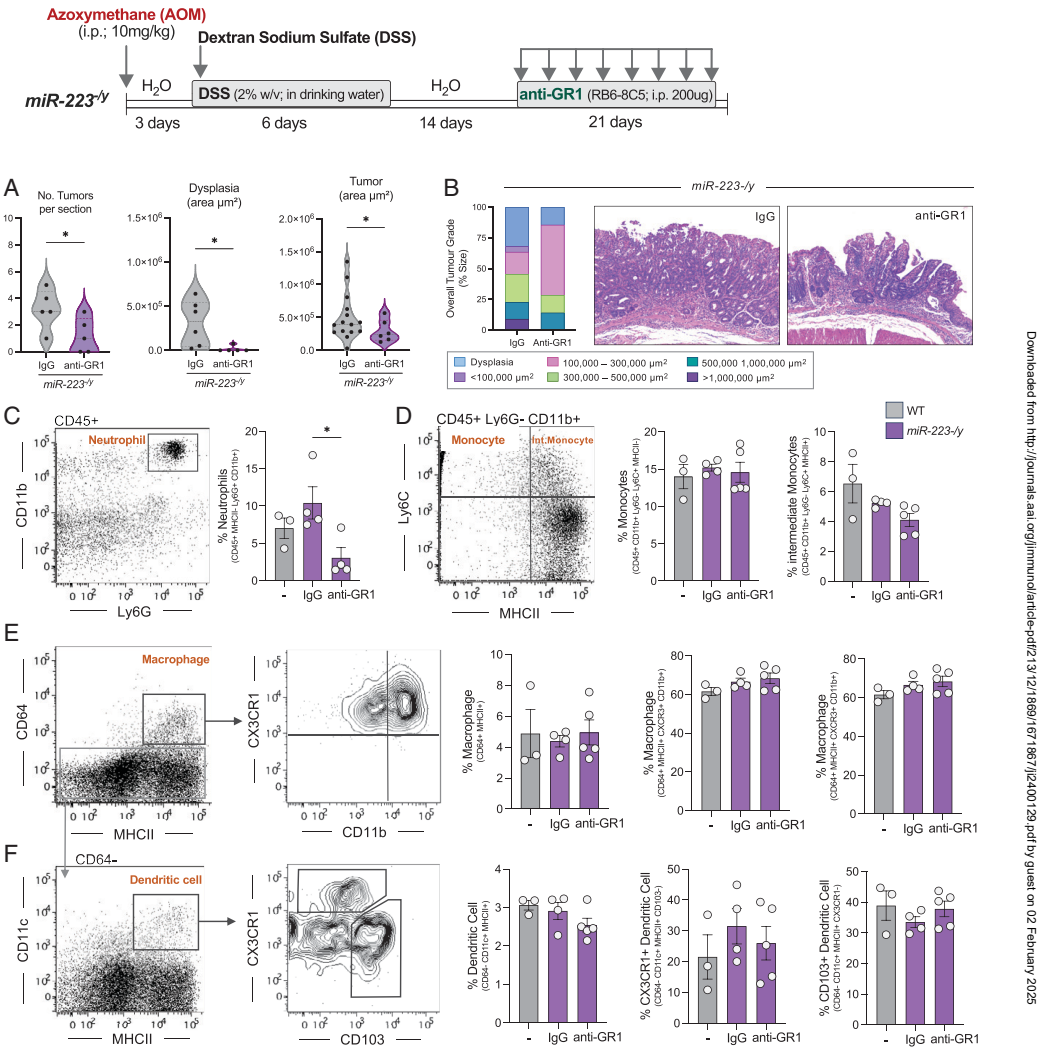


FIGURE 7. Ab-mediated depletion of infiltrating Ly6G$^+$ myeloid cells with RB6-8C5 reduced early tumorigenesis in *miR-223*$^{-/y}$ mice in an acute model of AOM-DSS. Schematic overview and timeline of the acute AOM-DSS study are shown. *miR-223*$^{-/y}$ mice were treated with either 20 µg of anti-GR1 i.p. (Lyg6/Ly6C: RB6-8C5 clone) or an isotype control every 3 d for 3 wk (eight total injections). H&E staining was used. (**A**) Number of tumors per section, quantification of dysplasia (µm^2) per section, and quantification of tumor size (µm^2) per section were determined at the time of necropsy following treatment with AOM-DSS. (**B**) Tumor grading according to size (µm^2) was determined from H&E micrographs in *miR-223*$^{-/y}$ mice treated either IgG or anti-GR1 Ab, with representative H&E micrographs shown. Flow cytometry was performed on enzyme-digested colons from WT and *miR-223*$^{-/y}$ mice after treatment to assess myeloid immune subsets. From live cells (AquaVi negative), CD45$^+$ singlets are shown. (**C**) Neutrophils were identified as Ly6G$^+$CD11b$^+$. (**D**) Monocytes were identified as Ly6G$^-$CD11b$^+$Ly6C$^+$MHCII$^-$ (inflammatory/infiltrating) or Ly6C$^+$MHCII$^+$ (intermediate/differentiating). (**E**) CD64$^+$MHCII$^+$ tissue-resident macrophages were further subdivided into CX3CR1$^+$CD11b$^-$ or CX3CR1$^+$CD11b$^+$. (**F**) Dendritic cell subsets were identified as CD64$^-$MHCII$^+$CD11c$^+$ and further subdivided into CX3CR1$^+$CD103$^-$ or CX3CR1$^-$CD103$^+$ (migratory). All data are expressed as mean ± SEM. (A and B) Effects of anti-GR1 on the volumetric size of tumors in *miR-223*$^{-/y}$ mice following an acute regimen of AOM-DSS. IgG, 15 tumors and 7 dysplastic regions from 6 mice; anti-GR1, 6 tumors and 1 dysplastic region from 5 mice. (C–F) $n = 3$–5 mice/group. *$p < 0.05$ versus the indicated counterpart (one-way ANOVA). MHCII, MHC class II.

Downloaded from http://journals.aai.org/jimmunol/article-pdf/213/12/1869/1671867/ji2400129.pdf by guest on 02 February 2025

Monocytes and monocyte-derived macrophage are found in multiple tumor types and are linked to tumor proliferation, metastasis, angiogenesis, and chemotherapy resistance (Refs. 45–47 and W. Du, B. Zhou, A. Forjaz, S. M. Shin, F. Wu, A. J. Crawford, P. R. Nair, A. C. Johnston, H. West-Foyle, A. Tang, et al., manuscript posted on bioRxiv, DOI: 10.1101/2024.07.16.603739). However, the functional or regional significance of infiltrating monocyte subsets is not clear for solid tumors such as CAC or CRC. It is noteworthy that both monocytes and TAMs are mixed cell populations with differential expression of both inflammatory and protumor markers, especially at an early stage of cancer (48). As such, early therapeutic intervention may have the capacity to reverse the inflammatory continuum of CAC and limit more chronic angiogenesis, invasion, and epithelial-to-mesenchymal progression.

Understanding the collective role of different myeloid cell subsets to the development of CAC has been challenging due to the heterogeneity of disease and varying onset of tumorigenesis. However, this avenue of research is critical to understanding CAC clinically and considering the difficulty in treating large colorectal adenocarcinomas with biologic therapeutics. For example, although there is increased expression of T cell–derived PD1 and PD1 ligands (PD-L1 and PD-L2) in AOM-DSS, PD1 Ab blockade had no therapeutic effect in this model (49). Along with clinical findings that gastrointestinal tumors are particularly refractory to checkpoint inhibitor blockade (50, 51), understanding how aberrant myeloid inflammation can control the development of solid tumors is of clinical importance going forward.

Although many inflammatory pathways have been linked to tumor development in CAC, our identification of the STAT3-inducing IL-6/IL-17a cytokine family members in *miR-223*$^{-/y}$ mice is interesting. The IL-6 family of cytokines are increasingly being recognized for their role in intestinal carcinogenesis. A variety of different cell types produce IL-6, IL-11, and LIF, but during chronic inflammation the primary producers are monocytes, macrophages, and fibroblasts following activation from NF-κB (52). Increased expression of IL-6 is correlated with metastasis, larger tumors, poor prognosis in CRC (53, 54), and with more severe inflammation in UC patients (55). Additionally, upregulation of IL-6 has also been shown in CAC (56) and is associated with neutrophilia (57). This results in increased activation of STAT3 and the upregulation of its target gene cyclin D1, promoting a proliferative microenvironment (58). Due to the evidence that aberrant IL-6 signaling is contributing to the progression of CAC, clinical investigations into its therapeutic viability are ongoing, with an IL-6 inhibitor siltuximab in clinical trials and the STAT3 inhibitor bruceantinol in development (59, 60). Thus, mining selective noncoding RNA networks to identify important therapeutic opportunities, such as miR-233–regulated mRNA circuits, may prove beneficial in elucidating druggable targets.

Aside from utility as predictive biomarkers (61), using miRNAs to identify critical signaling hubs would also provide a more selective therapeutic opportunity given their promiscuity and ability to bind hundreds of mRNA sequences (62). Although our data suggest that *miR-223* is acting as a tumor suppressor in CAC, its role in other cancers varies. In gastric cancer the overexpression of *miR-223* is associated with increased proliferation, migration, and poor prognosis for patients (63, 64). In contrast, in lung cancer upregulation of miR-223 is linked to tumor suppression and can inhibit proliferation via a *miR-223-3p*-mutant p53 feedback loop (65) and by targeting the IGF-1R pathway (66). In breast cancer some research suggests that the upregulation of *miR-223* is associated with improved patient outcomes (67), as it acts to limit cancer cells by suppressing the EGF pathway (68). This is an intriguing finding, as our data indicated that the EGFR ligand, TGF-α, is markedly increased in *miR-223*$^{-/y}$ mice compared with WT counterparts. Although we did not confirm whether this is secreted and is the processed form of TGF-α, its downstream proliferative targets (c-MYC, clyclin D1, and p-AKT) were increased in *miR-223*$^{-/y}$ mice and correlated with enhanced tumor growth. Others protumorigenic pathways associated with miR-223 translational control include Mef2c–β-catenin and Hippo/YAP signaling (69–72). miR-223 has been shown to contribute to tumor development in non-CACs (73–75); in addition, the expression of *miR-223* in CRC is an indicator of metastasis and poor patient prognosis (76). Although CAC is also a cancer of the colon, the pathogenic sequence leading to disease differs significantly, and our results show that *miR-223* plays a protective role during inflammation-driven tumorigenesis. Due to *miR-223* contribution to both the suppression and promotion of disease, its regulation for therapeutic purposes needs to be looked at in a disease-specific manner. Our data suggest that restoring the expression of *miR-223*, or its regulated mRNA and thus protein circuits, could potentially lead to reduced tumor growth and prevent the progression of CAC, but this has yet to be examined in mouse models or in a clinical setting. Most recently, research using *miR-223* as a therapeutic target has been explored in hepatocellular carcinoma, where treatment with *miR-223* inhibited angiogenesis and prevented disease progression (77).

In conclusion, we propose that *miR-223* is essential for controlling myeloid-driven inflammation in the progression from UC to CAC by suppressing the production of proinflammatory cytokines, limiting tumor growth, and controlling proliferation and tumorigenic pathways.

Disclosures

The authors have no financial conflicts of interest.

References

1. Sung, H., J. Ferlay, R. L. Siegel, M. Laversanne, I. Soerjomataram, A. Jemal, and F. Bray. 2021. Global cancer statistics 2020: GLOBOCAN estimates of incidence and mortality worldwide for 36 cancers in 185 countries. *CA Cancer J. Clin.* 71: 209–249.
2. Bopanna, S., A. N. Ananthakrishnan, S. Kedia, V. Yajnik, and V. Ahuja. 2017. Risk of colorectal cancer in Asian patients with ulcerative colitis: a systematic review and meta-analysis. *Lancet Gastroenterol. Hepatol.* 2: 269–276.
3. Zhou, Q., Z.-F. Shen, B.-S. Wu, C.-B. Xu, Z.-Q. He, T. Chen, H.-T. Shang, C.-F. Xie, S.-Y. Huang, Y.-G. Chen, et al. 2019. Risk of colorectal cancer in ulcerative colitis patients: a systematic review and meta-analysis. *Gastroenterol. Res. Pract.* 2019: 5363261.
4. Balandrán, J. C., A. Lasry, and I. Aifantis. 2023. The role of inflammation in the initiation and progression of myeloid neoplasms. *Blood Cancer Discov.* 4: 254–266.
5. Bai, R., D. Sun, M. Chen, X. Shi, L. Luo, Z. Yao, Y. Liu, X. Ge, X. Gao, G. F. Hu, et al. 2020. Myeloid cells protect intestinal epithelial barrier integrity through the angiogenin/plexin-B2 axis. *EMBO J.* 39: e103325.
6. Lechuga, S., M. B. Braga-Neto, N. G. Naydenov, F. Rieder, and A. I. Ivanov. 2023. Understanding disruption of the gut barrier during inflammation: should we abandon traditional epithelial cell lines and switch to intestinal organoids? *Front. Immunol.* 14: 1108289.
7. Wang, M., J. Zhao, L. Zhang, F. Wei, Y. Lian, Y. Wu, Z. Gong, S. Zhang, J. Zhou, K. Cao, et al. 2017. Role of tumor microenvironment in tumorigenesis. *J. Cancer* 8: 761–773.
8. Zhou, K., T. Cheng, J. Zhan, X. Peng, Zhang, Yue, J. Wen, X. Chen, and M. Ying. 2020. Targeting tumor-associated macrophages in the tumor microenvironment. *Oncol. Lett.* 20: 234.
9. Yahaya, M. A. F., M. A. M. Lila, S. Ismail, M. Zainol, and N. A. R. N. M. Afizan. 2019. Tumour-associated macrophages (TAMs) in colon cancer and how to reeducate them. *J. Immunol. Res.* 2019: 2368249.
10. Schmitt, M., and F. R. Greten. 2021. The inflammatory pathogenesis of colorectal cancer. *Nat. Rev. Immunol.* 21: 653–667.
11. Berindan-Neagoe, I., P. D. C. Monroig, B. Pasculli, and G. A. Calin. 2014. MicroRNAome genome: a treasure for cancer diagnosis and therapy. *CA Cancer J. Clin.* 64: 311–336.
12. Zhu, Y., L. Gu, Y. Li, X. Lin, H. Shen, K. Cui, L. Chen, F. Zhou, Q. Zhao, J. Zhang, et al. 2017. miR-148a inhibits colitis and colitis-associated tumorigenesis in mice. *Cell Death Differ.* 24: 2199–2209.
13. Chen, G., Y. Feng, X. Li, Z. Jiang, B. Bei, L. Zhang, Y. Han, Y. Li, and N. Li. 2019. Post-transcriptional gene regulation in colitis associated cancer. *Front. Genet.* 10: 585.
14. Colangelo, T., G. Polcaro, L. Muccillo, G. D'Agostino, V. Rosato, P. Ziccardi, A. Lupo, G. Mazzoccoli, L. Sabatino, and V. Colantuoni. 2017. Friend or foe? The tumour microenvironment dilemma in colorectal cancer. *Biochim. Biophys. Acta Rev. Cancer* 1867: 1–18.

Downloaded from http://journals.aai.org/jimmunol/article-pdf/213/12/1869/1671867/ji2400129.pdf by guest on 02 February 2025

15. Johnnidis, J. B., M. H. Harris, R. T. Wheeler, S. Stehling-Sun, M. H. Lam, O. Kirak, T. R. Brummelkamp, M. D. Fleming, and F. D. Camargo. 2008. Regulation of progenitor cell proliferation and granulocyte function by microRNA-223. *Nature* 451: 1125–1129.
16. Neudecker, V., M. Haneklaus, O. Jensen, L. Khailova, J. C. Masterson, H. Tye, K. Biette, P. Jedlicka, K. S. Brodsky, M. E. Gerich, et al. 2017. Myeloid-derived miR-223 regulates intestinal inflammation via repression of the NLRP3 inflammasome. *J. Exp. Med.* 214: 1737–1752.
17. Zhang, J., X. Luo, H. Li, X. Yue, L. Deng, Y. Cui, and Y. Lu. 2014. MicroRNA-223 functions as an oncogene in human colorectal cancer cells. *Oncol. Rep.* 32: 115–120.
18. Mcnamee, E. N., J. C. Masterson, P. Jedlicka, M. Mcmanus, A. Grenz, C. B. Collins, M. F. Nold, C. Nold-Petry, P. Bufler, C. A. Dinarello, and J. Rivera-Nieves. 2011. Interleukin 37 expression protects mice from colitis. *Proc. Natl. Acad. Sci. USA* 108: 16711–16716.
19. Bauernfeind, F., A. Rieger, F. A. Schildberg, P. A. Knolle, J. L. Schmid-Burgk, and V. Hornung. 2012. NLRP3 inflammasome activity is negatively controlled by miR-223. *J. Immunol.* 189: 4175–4181.
20. Haneklaus, M., M. Gerlic, M. Kurowska-Stolarska, A.-A. Rainey, D. Pich, I. B. McInnes, W. Hammerschmidt, L. A. J. O'Neill, and S. L. Masters. 2012. Cutting edge: miR-223 and EBV miR-BART15 regulate the NLRP3 inflammasome and IL-1β production. *J. Immunol.* 189: 3795–3799.
21. Corvinus, F. M., C. Orth, R. Moriggl, S. A. Tsareva, S. Wagner, E. B. Pfitzner, D. Baus, R. Kaufmann, L. A. Huber, K. Zatloukal, et al. 2005. Persistent STAT3 activation in colon cancer is associated with enhanced cell proliferation and tumor growth. *Neoplasia* 7: 545–555.
22. Neudecker, V., K. S. Brodsky, E. T. Clambey, E. P. Schmidt, T. A. Packard, B. Davenport, T. J. Standiford, T. Weng, A. A. Fletcher, L. Barthel, et al. 2017. Neutrophil transfer of *miR-223* to lung epithelial cells dampens acute lung injury in mice. *Sci. Transl. Med.* 9: eaah5360.
23. Katoh, H., D. Wang, T. Daikoku, H. Sun, S. K. Dey, and R. N. Dubois. 2013. CXCR2-expressing myeloid-derived suppressor cells are essential to promote colitis-associated tumorigenesis. *Cancer Cell* 24: 631–644.
24. Hossain, M. S., H. Karuniawati, A. A. Jairoun, Z. Urbi, D. J. Ooi, A. John, Y. C. Lim, K. M. K. Kibria, A. K. M. Mohiuddin, L. C. Ming, et al. 2022. Colorectal cancer: a review of carcinogenesis, global epidemiology, current challenges, risk factors, preventive and treatment strategies. *Cancers (Basel)* 14: 1732.
25. Multhoff, G., M. Molls, and J. Radons. 2012. Chronic inflammation in cancer development. *Front. Immunol.* 2: 98.
26. Sokolova, O., and M. Naumann. 2019. Crosstalk between DNA damage and inflammation in the multiple steps of gastric carcinogenesis. *Curr. Top. Microbiol. Immunol.* 421: 107–137.
27. O'Reilly, L. A., T. L. Putoczki, L. A. Mielke, J. T. Low, A. Lin, A. Preaudet, M. J. Herold, K. Yaprianto, L. Tai, A. Kueh, et al. 2018. Loss of NF-κB1 causes gastric cancer with aberrant inflammation and expression of immune checkpoint regulators in a STAT-1-dependent manner. *Immunity* 48: 570–583.e8.
28. Muthupalani, S., D. Annamalai, Y. Feng, S. M. Ganesan, Z. Ge, M. T. Whary, H. Nakagawa, A. K. Rustgi, T. C. Wang, and J. G. Fox. 2023. IL-1β transgenic mouse model of inflammation driven esophageal and oral squamous cell carcinoma. *Sci. Rep.* 13: 12732.
29. Quante, M., G. Bhagat, J. A. Abrams, F. Marache, P. Good, D. Lee, Y. Michele, R. Lee, S. Friedman, Z. Asfaha, et al. 2012. Bile acid and inflammation activate gastric cardia stem cells in a mouse model of Barrett-like metaplasia. *Cancer Cell* 21: 36–51.
30. Hemmat, N., and H. Bannazadeh Baghi. 2019. Association of human papillomavirus infection and inflammation in cervical cancer. *Pathog. Dis.* 77: ftz048.
31. Fernandes, J. V., T. A. A. De Medeiros Fernandes, J. C. V. De Azevedo, R. N. O. Cobucci, M. G. F. De Carvalho, V. S. Andrade, and J. M. G. De Araújo. 2015. Link between chronic inflammation and human papillomavirus-induced carcinogenesis (Review). *Oncol. Lett.* 9: 1015–1026.
32. Bhat, A. A., S. Nisar, M. Singh, B. Ashraf, T. Masoodi, C. P. Prasad, A. Sharma, S. Maacha, T. Karedath, S. Hashem, et al. 2022. Cytokine- and chemokine-induced inflammatory colorectal tumor microenvironment: emerging avenue for targeted therapy. *Cancer Commun. (Lond.)* 42: 689–715.
33. Gochman, E., J. Mahajna, P. Shenzer, A. Dahan, A. Blatt, R. Elyakim, and A. Z. Reznick. 2012. The expression of iNOS and nitrotyrosine in colitis and colon cancer in humans. *Acta Histochem.* 114: 827–835.
34. Yang, Y., L. Li, C. Xu, Y. Wang, Z. Wang, M. Chen, Z. Jiang, J. Pan, C. Yang, X. Li, et al. 2020. Cross-talk between the gut microbiota and monocyte-like macrophages mediates an inflammatory response to promote colitis-associated tumourigenesis. *Gut* 70: 1495–1506.
35. Wang, H., T. Tian, and J. Zhang. 2021. Tumor-associated macrophages (TAMs) in colorectal cancer (CRC): from mechanism to therapy and prognosis. *Int. J. Mol. Sci.* 22: 8470.
36. Liu, Z., Y. Xie, Y. Xiong, S. Liu, C. Qiu, Z. Zhu, H. Mao, M. Yu, and X. Wang. 2020. TLR 7/8 agonist reverses oxaliplatin resistance in colorectal cancer via directing the myeloid-derived suppressor cells to tumoricidal M1-macrophages. *Cancer Lett.* 469: 173–185.
37. Halama, N., I. Zoernig, A. Berthel, C. Kahlert, F. Klupp, M. Suarez-Carmona, T. Suetterlin, K. Brand, J. Krauss, F. Lasitschka, et al. 2016. Tumoral immune cell exploitation in colorectal cancer metastases can be targeted effectively by anti-CCR5 therapy in cancer patients. *Cancer Cell* 29: 587–601.
38. De Filippo, K., A. Dudeck, M. Hasenberg, E. Nye, N. van Rooijen, K. Hartmann, M. Gunzer, A. Roers, and N. Hogg. 2013. Mast cell and macrophage chemokines CXCL1/CXCL2 control the early stage of neutrophil recruitment during tissue inflammation. *Blood* 121: 4930–4937.
39. Cai, H., Y. Chen, X. Chen, W. Sun, and Y. Li. 2023. Tumor-associated macrophages mediate gastrointestinal stromal tumor cell metastasis through CXCL2/CXCR2. *Cell. Immunol.* 384: 104642.
40. Sheng, Y., W. Peng, Y. Huang, L. Cheng, Y. Meng, L. B. Kwantwi, J. Yang, J. Xu, H. Xiao, J. Kzhyshkowska, and Q. Wu. 2023. Tumor-activated neutrophils promote metastasis in breast cancer via the G-CSF-RLN2-MMP-9 axis. *J. Leukoc. Biol.* 113: 383–399.
41. Antuamwine, B. B., R. Bosnjakovic, F. Hofmann-Vega, X. Wang, T. Theodosiou, I. Iliopoulos, and S. Brandau. 2023. N1 versus N2 and PMN-MDSC: a critical appraisal of current concepts on tumor-associated neutrophils and new directions for human oncology. *Immunol. Rev.* 314: 250–279.
42. Zheng, W., J. Wu, Y. Peng, J. Sun, P. Cheng, and Q. Huang. 2022. Tumor-associated neutrophils in colorectal cancer development, progression and immunotherapy. *Cancers (Basel)* 14: 4755.
43. Bui, T. M., L. K. Yalom, E. Ning, J. M. Urbanczyk, X. Ren, C. J. Herrnreiter, J. A. Disario, B. Wray, M. J. Schipma, Y. S. Velichko, et al. 2024. Tissue-specific reprogramming leads to angiogenic neutrophil specialization and tumor vascularization in colorectal cancer. *J. Clin. Invest.* 134: e174545.
44. Mazaki, J., K. Katsumata, K. Kasahara, T. Tago, T. Wada, H. Kuwabara, M. Enomoto, T. Ishizaki, Y. Nagakawa, and A. Tsuchida. 2020. Neutrophil-to-lymphocyte ratio is a prognostic factor for colon cancer: a propensity score analysis. *BMC Cancer* 20: 922.
45. Ugel, S., S. Canè, F. De Sanctis, and V. Bronte. 2021. Monocytes in the tumor microenvironment. *Annu. Rev. Pathol.* 16: 93–122.
46. Soncin, I., J. Sheng, Q. Chen, S. Foo, K. Duan, J. Lum, M. Poidinger, F. Zolezzi, K. Karjalainen, and C. Ruedl. 2018. The tumour microenvironment creates a niche for the self-renewal of tumour-promoting macrophages in colon adenoma. *Nat. Commun.* 9: 582.
47. LaMarche, N. M., S. Hegde, M. D. Park, B. B. Maier, L. Troncoso, J. Le Berichel, P. Hamon, M. Belabed, R. Mattiuz, C. Hennequin, et al. 2024. An IL-4 signalling axis in bone marrow drives pro-tumorigenic myelopoiesis. *Nature* 625: 166–174.
48. Singhal, S., J. Stadanlick, M. J. Annunziata, A. S. Rao, P. S. Bhojnagarwala, S. O'Brien, E. K. Moon, E. Cantu, G. Danet-Desnoyers, H. J. Ra, et al. 2019. Human tumor-associated monocytes/macrophages and their regulation of T cell responses in early-stage lung cancer. *Sci. Transl. Med.* 11: eaat1500.
49. Yassin, M., Z. Sadowska, D. Djurhuus, B. Nielsen, P. Tougaard, J. Olsen, and A. E. Pedersen. 2019. Upregulation of PD-1 follows tumour development in the AOM/DSS model of inflammation-induced colorectal cancer in mice. *Immunology* 158: 35–46.
50. Noori, M., F. Jafari-Raddani, Z. Davoodi-Moghaddam, M. Delshad, S. Safiri, and D. Bashash. 2024. Immune checkpoint inhibitors in gastrointestinal malignancies: an umbrella review. *Cancer. Cell. Int.* 24: 10.
51. Shan, J., D. Han, C. Shen, Q. Lei, and Y. Zhang. 2022. Mechanism and strategies of immunotherapy resistance in colorectal cancer. *Front. Immunol.* 13: 1016646.
52. Naugler, W. E., and M. Karin. 2008. The wolf in sheep's clothing: the role of interleukin-6 in immunity, inflammation and cancer. *Trends Mol. Med.* 14: 109–119.
53. Chung, Y.-C., and Y.-F. Chang. 2003. Serum interleukin-6 levels reflect the disease status of colorectal cancer. *J. Surg. Oncol.* 83: 222–226.
54. Zeng, J., Z. H. Tang, S. Liu, and S. S. Guo. 2017. Clinicopathological significance of overexpression of interleukin-6 in colorectal cancer. *World J. Gastroenterol.* 23: 1780–1786.
55. Feng, W., L. Zhu, Y. Liu, L. Xu, and H. Shen. 2023. C-reactive protein/albumin ratio and IL-6 are associated with disease activity in patients with ulcerative colitis. *J. Clin. Lab. Anal.* 37: e24843.
56. Li, Y., C. de Haar, M. Chen, J. Deuring, M. M. Gerrits, R. Smits, B. Xia, E. J. Kuipers, and C. J. van der Woude. 2010. Disease-related expression of the IL6/STAT3/SOCS3 signalling pathway in ulcerative colitis and ulcerative colitis-related carcinogenesis. *Gut* 59: 227–235.
57. Wang, Y., K. Wang, G. C. Han, R. X. Wang, H. Xiao, C. M. Hou, R. F. Guo, Y. Dou, B. F. Shen, Y. Li, and G. J. Chen. 2014. Neutrophil infiltration favors colitis-associated tumorigenesis by activating the interleukin-1 (IL-1)/IL-6 axis. *Mucosal Immunol.* 7: 1106–1115.
58. Leslie, K., C. Lang, G. Devgan, J. Azare, M. Berishaj, W. Gerald, Y. B. Kim, K. Paz, J. E. Darnell, C. Albanese, et al. 2006. Cyclin D1 is transcriptionally regulated by and required for transformation by activated signal transducer and activator of transcription 3. *Cancer Res.* 66: 2544–2552.
59. Angevin, E., J. Tabernero, E. Elez, S. J. Cohen, R. Bahleda, J. L. van Laethem, C. Ottensmeier, J. A. Lopez-Martin, S. Clive, F. Joly, et al. 2014. A phase I/II, multiple-dose, dose-escalation study of siltuximab, an anti-interleukin-6 monoclonal antibody, in patients with advanced solid tumors. *Clin. Cancer Res.* 20: 2192–2204.
60. Wei, N., J. Li, C. Fang, J. Chang, V. Xirou, N. K. Syrigos, B. J. Marks, E. Chu, and J. C. Schmitz. 2019. Targeting colon cancer with the novel STAT3 inhibitor bruceantinol. *Oncogene* 38: 1676–1687.
61. Jung, G., E. Hernandez-Illán, L. Moreira, F. Balaguer, and A. Goel. 2020. Epigenetics of colorectal cancer: biomarker and therapeutic potential. *Nat. Rev. Gastroenterol. Hepatol.* 17: 111–130.
62. Mehta, A., and D. Baltimore. 2016. MicroRNAs as regulatory elements in immune system logic. *Nat. Rev. Immunol.* 16: 279–294.
63. Zhu, Y., K. Li, L. Yan, Y. He, L. Wang, and L. Sheng. 2020. miR-223-3p promotes cell proliferation and invasion by targeting *Arid1a* in gastric cancer. *Acta Biochim. Biophys. Sin. (Shanghai)* 52: 150–159.
64. Li, X., Y. Zhang, H. Zhang, X. Liu, T. Gong, M. Li, L. Sun, G. Ji, Y. Shi, Z. Han, et al. 2011. miRNA-223 promotes gastric cancer invasion and metastasis by targeting tumor suppressor EPB41L3. *Mol. Cancer Res.* 9: 824–833.
65. Luo, P., Q. Wang, Y. Ye, J. Zhang, D. Lu, L. Cheng, H. Zhou, M. Xie, and B. Wang. 2019. MiR-223-3p functions as a tumor suppressor in lung squamous cell carcinoma by miR-223-3p-mutant p53 regulatory feedback loop. *J. Exp. Clin. Cancer Res.* 38: 74.

Downloaded from http://journals.aai.org/jimmunol/article-pdf/213/12/1869/1671867/ji2400129.pdf by guest on 02 February 2025

66. Nian, W., X. Ao, Y. Wu, Y. Huang, J. Shao, Y. Wang, Z. Chen, F. Chen, and D. Wang. 2013. miR-223 functions as a potent tumor suppressor of the Lewis lung carcinoma cell line by targeting insulin-like growth factor-1 receptor and cyclin-dependent kinase 2. *Oncol. Lett.* 6: 359–366.
67. Chen, L., X. Zhu, B. Han, L. Ji, L. Yao, and Z. Wang. 2021. High expression of microRNA-223 indicates a good prognosis in triple-negative breast cancer. *Front. Oncol.* 11: 630432.
68. Fabris, L., S. Berton, F. Citron, S. D'Andrea, I. Segatto, M. S. Nicoloso, S. Massarut, J. Armenia, G. Zafarana, S. Rossi, et al. 2016. Radiotherapy-induced miR-223 prevents relapse of breast cancer by targeting the EGF pathway. *Oncogene* 35: 4914–4926.
69. Yang, M., J. Chen, F. Su, B. Yu, F. Su, L. Lin, Y. Liu, J.-D. Huang, and E. Song. 2011. Microvesicles secreted by macrophages shuttle invasion-potentiating microRNAs into breast cancer cells. *Mol. Cancer* 10: 117.
70. Du, T., D. Wang, X. Wan, J. Xu, Q. Xiao, and B. Liu. 2021. Regulatory effect of microRNA-223-3p on breast cancer cell processes via the Hippo/Yap signaling pathway. *Oncol. Lett.* 22: 516.
71. Wang, Y., S. Shi, Y. Wang, X. Zhang, X. Liu, J. Li, P. Li, L. Du, and C. Wang. 2022. miR-223-3p targets FBXW7 to promote epithelial-mesenchymal transition and metastasis in breast cancer. *Thorac. Cancer* 13: 474–482.
72. Pinatel, E. M., F. Orso, E. Penna, D. Cimino, A. R. Elia, P. Circosta, P. Dentelli, M. F. Brizzi, P. Provero, and D. Taverna. 2014. miR-223 Is a coordinator of breast cancer progression as revealed by bioinformatics predictions. *PLoS One* 9: e84859.
73. Chai, B., Y. Guo, X. Cui, J. Liu, Y. Suo, Z. Dou, and N. Li. 2019. MiR-223-3p promotes the proliferation, invasion and migration of colon cancer cells by negative regulating PRDM1. *Am. J. Transl. Res.* 11: 4516–4523.
74. Sun, D., C. Wang, S. Long, Y. Ma, Y. Guo, Z. Huang, X. Chen, C. Zhang, J. Chen, and J. Zhang. 2015. C/EBP-β-activated microRNA-223 promotes tumour growth through targeting RASA1 in human colorectal cancer. *Br. J. Cancer* 112: 1491–1500.
75. Wang, F. F., X. J. Zhang, Y. R. Yan, X. H. Zhu, J. Yu, Y. Ding, J. L. Hu, W. J. Zhou, Z. C. Zeng, W. T. Liao, et al. 2017. FBX8 is a metastasis suppressor downstream of miR-223 and targeting mTOR for degradation in colorectal carcinoma. *Cancer Lett.* 388: 85–95.
76. Li, Z.-W., Y.-M. Yang, L.-T. Du, Z. Dong, L.-L. Wang, X. Zhang, X.-J. Zhou, G.-X. Zheng, A.-L. Qu, and C.-X. Wang. 2014. Overexpression of miR-223 correlates with tumor metastasis and poor prognosis in patients with colorectal cancer. *Med. Oncol.* 31: 256.
77. Fu, Y., B. Mackowiak, D. Feng, H. Lu, Y. Guan, T. Lehner, H. Pan, X. W. Wang, Y. He, and B. Gao. 2023. MicroRNA-223 attenuates hepatocarcinogenesis by blocking hypoxia-driven angiogenesis and immunosuppression. *Gut* 72: 1942–1958.

Downloaded from http://journals.aai.org/jimmunol/article-pdf/213/12/1869/1671867/ji2400129.pdf by guest on 02 February 2025

REFERENCES

ADAMINA, M., FEAKINS, R., IACUCCI, M., SPINELLI, A., CANNATELLI, R., D'HOORE, A., DRIESSEN, A., KATSANOS, K., MOOKHOEK, A., MYRELID, P., PELLINO, G., PEROS, G., TONTINI, G. E., TRIPATHI, M., YANAI, H. & SVRCEK, M. 2021. ECCO Topical Review Optimising Reporting in Surgery, Endoscopy, and Histopathology: Collaboration Between S-ECCO, EduCom, H-ECCO. *Journal of Crohn's and Colitis,* 15**,** 1089-1105.

AGGELETOPOULOU, I., KALAFATELI, M., TSOUNIS, E. P. & TRIANTOS, C. 2024. Exploring the role of IL-1β in inflammatory bowel disease pathogenesis. *Front Med (Lausanne),* 11**,** 1307394.

AGRAWAL, M., ALLIN, K. H., MEHANDRU, S., FAITH, J., JESS, T. & COLOMBEL, J. F. 2023. The appendix and ulcerative colitis - an unsolved connection. *Nat Rev Gastroenterol Hepatol,* 20**,** 615-624.

AHMAD, A., IMRAN, M. & AHSAN, H. 2023. Biomarkers as Biomedical Bioindicators: Approaches and Techniques for the Detection, Analysis, and Validation of Novel Biomarkers of Diseases. *Pharmaceutics,* 15.

AKANDA, M. R., NAM, H.-H., TIAN, W., ISLAM, A., CHOO, B.-K. & PARK, B.-Y. 2018. Regulation of JAK2/STAT3 and NF-κB signal transduction pathways; Veronica polita alleviates dextran sulfate sodium-induced murine colitis. *Biomedicine & pharmacotherapy,* 100**,** 296-303.

ALKHAYYAT, M., ABUREESH, M., GILL, A., KHOUDARI, G., ABOU SALEH, M., MANSOOR, E. & REGUEIRO, M. 2021. Lower Rates of Colorectal Cancer in Patients With Inflammatory Bowel Disease Using Anti-TNF Therapy. *Inflammatory Bowel Diseases,* 27**,** 1052-1060.

ALLES, J., FEHLMANN, T., FISCHER, U., BACKES, C., GALATA, V., MINET, M., HART, M., ABU-HALIMA, M., GRÄSSER, F. A., LENHOF, H.-P., KELLER, A. & MEESE, E. 2019. An estimate of the total number of true human miRNAs. *Nucleic Acids Research,* 47**,** 3353-3364.

AMBS, S., MERRIAM, W. G., BENNETT, W. P., FELLEY-BOSCO, E., OGUNFUSIKA, M. O., OSER, S. M., KLEIN, S., SHIELDS, P. G., BILLIAR, T. R. & HARRIS, C. C. 1998. Frequent nitric oxide synthase-2 expression in human colon adenomas: implication for tumor angiogenesis and colon cancer progression. *Cancer Research,* 58**,** 334-341.

ANGEVIN, E., TABERNERO, J., ELEZ, E., COHEN, S. J., BAHLEDA, R., VAN LAETHEM, J. L., OTTENSMEIER, C., LOPEZ-MARTIN, J. A., CLIVE, S., JOLY, F., RAY-COQUARD, I., DIRIX, L., MACHIELS, J. P., STEVEN, N., REDDY, M., HALL, B., PUCHALSKI, T. A., BANDEKAR, R., VAN DE VELDE, H., TROMP, B., VERMEULEN, J. &

KURZROCK, R. 2014. A phase I/II, multiple-dose, dose-escalation study of siltuximab, an anti-interleukin-6 monoclonal antibody, in patients with advanced solid tumors. *Clin Cancer Res,* 20**,** 2192-204.

ANNESE, T., TAMMA, R., DE GIORGIS, M. & RIBATTI, D. 2020. microRNAs Biogenesis, Functions and Role in Tumor Angiogenesis. *Frontiers in Oncology,* 10.

ARJOMAND FARD, N., ARMSTRONG, H., PERRY, T. & WINE, E. 2023. Appendix and Ulcerative Colitis: a Key to Explaining the Pathogenesis and Directing Novel Therapies? *Inflamm Bowel Dis,* 29**,** 151-160.

ASSA, A., RINAWI, F. & SHAMIR, R. 2017. The Long-Term Predictive Properties of the Paris Classification in Paediatric Inflammatory Bowel Disease Patients. *Journal of Crohn's and Colitis,* 12**,** 39-47.

ATARASHI, K., TANOUE, T., OSHIMA, K., SUDA, W., NAGANO, Y., NISHIKAWA, H., FUKUDA, S., SAITO, T., NARUSHIMA, S., HASE, K., KIM, S., FRITZ, J. V., WILMES, P., UEHA, S., MATSUSHIMA, K., OHNO, H., OLLE, B., SAKAGUCHI, S., TANIGUCHI, T., MORITA, H., HATTORI, M. & HONDA, K. 2013. Treg induction by a rationally selected mixture of Clostridia strains from the human microbiota. *Nature,* 500**,** 232-6.

ATREYA, R. & NEURATH, M. F. 2005. Involvement of IL-6 in the pathogenesis of inflammatory bowel disease and colon cancer. *Clinical reviews in allergy & immunology,* 28**,** 187-195.

ATSUMI, T., SINGH, R., SABHARWAL, L., BANDO, H., MENG, J., ARIMA, Y., YAMADA, M., HARADA, M., JIANG, J.-J., KAMIMURA, D., OGURA, H., HIRANO, T. & MURAKAMI, M. 2014. Inflammation Amplifier, a New Paradigm in Cancer Biology. *Cancer Research,* 74**,** 8-14.

BAI, R., SUN, D., CHEN, M., SHI, X., LUO, L., YAO, Z., LIU, Y., GE, X., GAO, X., HU, G. F., ZHOU, W., SHENG, J. & XU, Z. 2020. Myeloid cells protect intestinal epithelial barrier integrity through the angiogenin/plexin-B2 axis. *EMBO J,* 39**,** e103325.

BAIN, C. C., BRAVO-BLAS, A., SCOTT, C. L., GOMEZ PERDIGUERO, E., GEISSMANN, F., HENRI, S., MALISSEN, B., OSBORNE, L. C., ARTIS, D. & MOWAT, A. M. 2014. Constant replenishment from circulating monocytes maintains the macrophage pool in the intestine of adult mice. *Nature Immunology,* 15**,** 929-937.

BAIN, C. C., SCOTT, C. L., URONEN-HANSSON, H., GUDJONSSON, S., JANSSON, O., GRIP, O., GUILLIAMS, M., MALISSEN, B., AGACE, W. W. & MOWAT, A. M. 2013. Resident and pro-inflammatory macrophages in the colon represent alternative context-dependent fates of the same Ly6Chi monocyte precursors. *Mucosal Immunol,* 6**,** 498-510.

BAKER, A.-M., CROSS, W., CURTIUS, K., AL BAKIR, I., CHOI, C.-H. R., DAVIS, H. L., TEMKO, D., BISWAS, S., MARTINEZ, P. & WILLIAMS, M. J. 2019. Evolutionary history of human colitis-associated colorectal cancer. *Gut,* 68**,** 985-995.

BAKIRTZI, K., LAW, I. K. M., XUE, X., ILIOPOULOS, D., SHAH, Y. M. & POTHOULAKIS, C. 2016. Neurotensin Promotes the Development of Colitis and Intestinal Angiogenesis via Hif-1α–miR-210 Signaling. *The Journal of Immunology,* 196**,** 4311-4321.

BALANDRAN, J. C., LASRY, A. & AIFANTIS, I. 2023. The Role of Inflammation in the Initiation and Progression of Myeloid Neoplasms. *Blood Cancer Discov,* 4**,** 254-266.

BAMIAS, G. & COMINELLI, F. 2015. Role of type 2 immunity in intestinal inflammation. *Current Opinion in Gastroenterology,* 31**,** 471-476.

BARAN, P., HANSEN, S., WAETZIG, G. H., AKBARZADEH, M., LAMERTZ, L., HUBER, H. J., AHMADIAN, M. R., MOLL, J. M. & SCHELLER, J. 2018. The balance of interleukin (IL)-6, IL-6·soluble IL-6 receptor (sIL-6R), and IL-6·sIL-6R·sgp130 complexes allows simultaneous classic and trans-signaling. *Journal of Biological Chemistry,* 293**,** 6762-6775.

BARTISH, M., TONG, D., PAN, Y., WALLERIUS, M., LIU, H., RISTAU, J., DE SOUZA FERREIRA, S., WALLMANN, T., VAN HOEF, V., MASVIDAL, L., KERZEL, T., JOLY, A.-L., GONCALVES, C., PRESTON, S. E. J., EBRAHIMIAN, T., SEITZ, C., BERGH, J., PIETRAS, K., LEHOUX, S., NALDINI, L., ANDERSSON, J., SQUADRITO, M. L., DEL RINCÓN, S. V., LARSSON, O. & ROLNY, C. 2020. MNK2 governs the macrophage antiinflammatory phenotype. *Proceedings of the National Academy of Sciences,* 117**,** 27556-27565.

BASUDHAR, D., SOMASUNDARAM, V., DE OLIVEIRA, G. A., KESARWALA, A., HEINECKE, J. L., CHENG, R. Y., GLYNN, S. A., AMBS, S., WINK, D. A. & RIDNOUR, L. A. 2017. Nitric oxide synthase-2-derived nitric oxide drives multiple pathways of breast cancer progression. *Antioxidants & redox signaling,* 26**,** 1044-1058.

BAUERNFEIND, F., RIEGER, A., SCHILDBERG, F. A., KNOLLE, P. A., SCHMID-BURGK, J. L. & HORNUNG, V. 2012. NLRP3 Inflammasome Activity Is Negatively Controlled by miR-223. *The Journal of Immunology,* 189**,** 4175-4181.

BEAUGERIE, L. & ITZKOWITZ, S. H. 2015. Cancers Complicating Inflammatory Bowel Disease. *New England Journal of Medicine,* 372**,** 1441-1452.

BEILANKOUHI, E. A. V., MAGHSOODI, M. S., SANI, M. Z., KHOSROSHAHI, N. S., ZAREZADEH, R., NARGESI, M. M., SAFARALIZADEH, R. & VALILO, M. 2024. miRNAs that regulate apoptosis in breast cancer and cervical cancer. *Cell Biochemistry and Biophysics*.

BENCHIMOL, E. I., FORTINSKY, K. J., GOZDYRA, P., VAN DEN HEUVEL, M., VAN LIMBERGEN, J. & GRIFFITHS, A. M. 2011a. Epidemiology of pediatric inflammatory bowel disease: a systematic review of international trends. *Inflammatory bowel diseases,* 17**,** 423-439.

BENCHIMOL, E. I., TO, T., GRIFFITHS, A. M., RABENECK, L. & GUTTMANN, A. 2011b. Outcomes of Pediatric Inflammatory Bowel Disease: Socioeconomic Status Disparity in a Universal-Access Healthcare System. *The Journal of Pediatrics,* 158**,** 960-967.e4.

BÉRES, N. J., SZABÓ, D., KOCSIS, D., SZŰCS, D., KISS, Z., MÜLLER, K. E., LENDVAI, G., KISS, A., ARATÓ, A., SZIKSZ, E., VANNAY, Á., SZABÓ, A. J. & VERES, G. 2016. Role of Altered Expression of miR-146a, miR-155, and miR-122 in Pediatric Patients with Inflammatory Bowel Disease. *Inflammatory Bowel Diseases,* 22**,** 327-335.

BERINDAN-NEAGOE, I., MONROIG, P. D. C., PASCULLI, B. & CALIN, G. A. 2014. MicroRNAome genome: A treasure for cancer diagnosis and therapy. *CA: A Cancer Journal for Clinicians,* 64**,** 311-336.

BERKOWITZ, L., SCHULTZ, B. M., SALAZAR, G. A., PARDO-ROA, C., SEBASTIÁN, V. P., ÁLVAREZ-LOBOS, M. M. & BUENO, S. M. 2018. Impact of Cigarette Smoking on the Gastrointestinal Tract Inflammation: Opposing Effects in Crohn's Disease and Ulcerative Colitis. *Frontiers in Immunology,* 9.

BERNSTEIN, C. N., BURCHILL, C., TARGOWNIK, L. E., SINGH, H. & ROOS, L. L. 2019. Events Within the First Year of Life, but Not the Neonatal Period, Affect Risk for Later Development of Inflammatory Bowel Diseases. *Gastroenterology,* 156**,** 2190-2197.e10.

BHAT, A. A., NISAR, S., SINGH, M., ASHRAF, B., MASOODI, T., PRASAD, C. P., SHARMA, A., MAACHA, S., KAREDATH, T., HASHEM, S., YASIN, S. B., BAGGA, P., REDDY, R., FRENNAUX, M. P., UDDIN, S., DHAWAN, P., HARIS, M. & MACHA, M. A. 2022. Cytokine- and chemokine-induced inflammatory colorectal tumor microenvironment: Emerging avenue for targeted therapy. *Cancer Communications,* 42**,** 689-715.

BJERRUM, J. T., NIELSEN, O. H., RIIS, L. B., PITTET, V., MUELLER, C., ROGLER, G. & OLSEN, J. 2014. Transcriptional Analysis of Left-sided Colitis, Pancolitis, and Ulcerative Colitis-associated Dysplasia. *Inflammatory Bowel Diseases,* 20**,** 2340-2352.

BOCCHETTI, M., FERRARO, M. G., RICCIARDIELLO, F., OTTAIANO, A., LUCE, A., COSSU, A. M., SCRIMA, M., LEUNG, W.-Y., ABATE, M., STIUSO, P., CARAGLIA, M., ZAPPAVIGNA, S. & YAU, T. O. 2021. The Role of microRNAs in Development of Colitis-Associated Colorectal Cancer. *International Journal of Molecular Sciences,* 22**,** 3967.

BOLLRATH, J., PHESSE, T. J., VON BURSTIN, V. A., PUTOCZKI, T., BENNECKE, M., BATEMAN, T., NEBELSIEK, T., LUNDGREN-MAY, T., CANLI, Ö., SCHWITALLA, S., MATTHEWS, V., SCHMID, R. M., KIRCHNER, T., ARKAN, M. C., ERNST, M. & GRETEN, F. R. 2009. gp130-Mediated Stat3 Activation in Enterocytes Regulates Cell Survival and Cell-Cycle Progression during Colitis-Associated Tumorigenesis. *Cancer Cell,* 15**,** 91-102.

BOPANNA, S., ANANTHAKRISHNAN, A. N., KEDIA, S., YAJNIK, V. & AHUJA, V. 2017. Risk of colorectal cancer in Asian patients with ulcerative colitis: a systematic review and meta-analysis. *Lancet Gastroenterol Hepatol,* 2**,** 269-276.

BOWMAN, T., GARCIA, R., TURKSON, J. & JOVE, R. 2000. STATs in oncogenesis. *Oncogene,* 19**,** 2474-2488.

BOYAPATI, R. K., ROSSI, A. G., SATSANGI, J. & HO, G.-T. 2016. Gut mucosal DAMPs in IBD: from mechanisms to therapeutic implications. *Mucosal Immunology,* 9**,** 567-582.

BRESSLER, B., MARSHALL, J. K., BERNSTEIN, C. N., BITTON, A., JONES, J., LEONTIADIS, G. I., PANACCIONE, R., STEINHART, A. H., TSE, F. & FEAGAN, B. 2015. Clinical practice guidelines for the medical management of nonhospitalized ulcerative colitis: the Toronto consensus. *Gastroenterology,* 148**,** 1035-1058.e3.

BUI, T. M., YALOM, L. K., NING, E., URBANCZYK, J. M., REN, X., HERRNREITER, C. J., DISARIO, J. A., WRAY, B., SCHIPMA, M. J., VELICHKO, Y. S., SULLIVAN, D. P., ABE, K., LAUBERTH, S. M., YANG, G.-Y., DULAI, P. S., HANAUER, S. B. & SUMAGIN, R. 2024. Tissue-specific reprogramming leads to angiogenic neutrophil specialization and tumor vascularization in colorectal cancer. *Journal of Clinical Investigation,* 134.

CAI, H., CHEN, Y., CHEN, X., SUN, W. & LI, Y. 2023. Tumor-associated macrophages mediate gastrointestinal stromal tumor cell metastasis through CXCL2/CXCR2. *Cell Immunol,* 384**,** 104642.

CAIRNS, S. R., SCHOLEFIELD, J. H., STEELE, R. J., DUNLOP, M. G., THOMAS, H. J., EVANS, G. D., EADEN, J. A., RUTTER, M. D., ATKIN, W. P., SAUNDERS, B. P., LUCASSEN, A., JENKINS, P., FAIRCLOUGH, P. D. & WOODHOUSE, C. R. 2010. Guidelines for colorectal cancer screening and surveillance in moderate and high risk groups (update from 2002). *Gut,* 59**,** 666-89.

CAMPBELL, N. A., URRY, L. A., CAIN, M. L., WASSERMAN, S. A., MINORSKY, P. V. & REECE, J. B. 2017. *Biology: A Global Approach, Global Edition*, Pearson Education.

CARDOSO, M. H., MENEGUETTI, B. T., OLIVEIRA-JÚNIOR, N. G., MACEDO, M. L. R. & FRANCO, O. L. 2022. Antimicrobial peptide production in response to gut microbiota imbalance. *Peptides,* 157**,** 170865.

CASTRO-DOPICO, T., DENNISON, T. W., FERDINAND, J. R., MATHEWS, R. J., FLEMING, A., CLIFT, D., STEWART, B. J., JING, C., STRONGILI, K., LABZIN, L. I., MONK, E. J. M., SAEB-PARSY, K., BRYANT, C. E., CLARE, S., PARKES, M. & CLATWORTHY, M. R. 2019. Anti-commensal IgG Drives Intestinal Inflammation and Type 17 Immunity in Ulcerative Colitis. *Immunity,* 50**,** 1099-1114.e10.

CAVIGLIA, G. P., GARRONE, A., BERTOLINO, C., VANNI, R., BRETTO, E., POSHNJARI, A., TRIBOCCO, E., FRARA, S., ARMANDI, A., ASTEGIANO, M., SARACCO, G. M., BERTOLUSSO, L. & RIBALDONE, D. G. 2023. Epidemiology of Inflammatory Bowel

Diseases: A Population Study in a Healthcare District of North-West Italy. *Journal of Clinical Medicine,* 12**,** 641.

CHAI, B., GUO, Y., CUI, X., LIU, J., SUO, Y., DOU, Z. & LI, N. 2019. MiR-223-3p promotes the proliferation, invasion and migration of colon cancer cells by negative regulating PRDM1. *American journal of translational research,* 11**,** 4516-4523.

CHALUVALLY-RAGHAVAN, P., JEONG, K. J., PRADEEP, S., SILVA, A. M., YU, S., LIU, W., MOSS, T., RODRIGUEZ-AGUAYO, C., ZHANG, D., RAM, P., LIU, J., LU, Y., LOPEZ-BERESTEIN, G., CALIN, G. A., SOOD, A. K. & MILLS, G. B. 2016. Direct Upregulation of STAT3 by MicroRNA-551b-3p Deregulates Growth and Metastasis of Ovarian Cancer. *Cell Reports,* 15**,** 1493-1504.

CHEN, B., ZHANG, S., WANG, B., CHEN, H., LI, Y., CAO, Q., ZHONG, J., XIE, M., RAN, Z., TANG, T., YANG, M., GUO, T., XU, B., CAI, Z., MA, L., SCHREIBER, S. & CHEN, M. 2021a. 775b Olamkicept, an IL-6 Trans-Signaling Inhibitor, is Effective for Induction of Response and Remission in A Randomized, Placebo-Controlled Trial in Moderate to Severe Ulcerative Colitis. *Gastroenterology,* 161**,** e28-e29.

CHEN, G., FENG, Y., LI, X., JIANG, Z., BEI, B., ZHANG, L., HAN, Y., LI, Y. & LI, N. 2019. Post-transcriptional Gene Regulation in Colitis Associated Cancer. *Front Genet,* 10**,** 585.

CHEN, L., ZHU, X., HAN, B., JI, L., YAO, L. & WANG, Z. 2021b. High Expression of microRNA-223 Indicates a Good Prognosis in Triple-Negative Breast Cancer. *Front Oncol,* 11**,** 630432.

CHEN, Q., WANG, H., LIU, Y., SONG, Y., LAI, L., HAN, Q., CAO, X. & WANG, Q. 2012. Inducible MicroRNA-223 Down-Regulation Promotes TLR-Triggered IL-6 and IL-1β Production in Macrophages by Targeting STAT3. *PLoS ONE,* 7**,** e42971.

CHENG, R. Y. S., RIDNOUR, L. A., WINK, A. L., GONZALEZ, A. L., FEMINO, E. L., RITTSCHER, H., SOMASUNDARAM, V., HEINZ, W. F., COUTINHO, L., RANGEL, M. C., EDMONDSON, E. F., BUTCHER, D., KINDERS, R. J., LI, X., WONG, S. T. C., MCVICAR, D. W., ANDERSON, S. K., PORE, M., HEWITT, S. M., BILLIAR, T. R., GLYNN, S. A., CHANG, J. C., LOCKETT, S. J., AMBS, S. & WINK, D. A. 2023. Interferon-gamma is quintessential for NOS2 and COX2 expression in ER- breast tumors that lead to poor outcome. *Cell Death & Disease,* 14.

CHO, H. J., XIE, Q. W., CALAYCAY, J., MUMFORD, R. A., SWIDEREK, K. M., LEE, T. D. & NATHAN, C. 1992. Calmodulin is a subunit of nitric oxide synthase from macrophages. *The Journal of experimental medicine,* 176**,** 599-604.

CHOI, C. H., RUTTER, M. D., ASKARI, A., LEE, G. H., WARUSAVITARNE, J., MOORGHEN, M., THOMAS-GIBSON, S., SAUNDERS, B. P., GRAHAM, T. A. & HART, A. L. 2015. Forty-Year Analysis of Colonoscopic Surveillance Program for Neoplasia in Ulcerative Colitis: An Updated Overview. *Am J Gastroenterol,* 110**,** 1022-34.

CHOLAPRANEE, A. & ANANTHAKRISHNAN, A. N. 2016. Environmental Hygiene and Risk of Inflammatory Bowel Diseases. *Inflammatory Bowel Diseases,* 22**,** 2191-2199.

CHUNG, Y.-C. & CHANG, Y.-F. 2003. Serum interleukin-6 levels reflect the disease status of colorectal cancer. *Journal of Surgical Oncology,* 83**,** 222-226.

CLAPPER, M. L., GARY, M. A., COUDRY, R. A., LITWIN, S., CHANG, W.-C. L., DEVARAJAN, K., LUBET, R. A. & COOPER, H. S. 2008. 5-aminosalicylic acid inhibits colitis-associated colorectal dysplasias in the mouse model of azoxymethane/dextran sulfate sodium-induced colitis. *Inflammatory Bowel Diseases,* 14**,** 1341-1347.

COLANGELO, T., POLCARO, G., MUCCILLO, L., D'AGOSTINO, G., ROSATO, V., ZICCARDI, P., LUPO, A., MAZZOCCOLI, G., SABATINO, L. & COLANTUONI, V. 2017. Friend or foe? The tumour microenvironment dilemma in colorectal cancer. *Biochim Biophys Acta Rev Cancer,* 1867**,** 1-18.

COLOMBEL, J. F., SANDS, B. E., RUTGEERTS, P., SANDBORN, W., DANESE, S., D'HAENS, G., PANACCIONE, R., LOFTUS, E. V., JR., SANKOH, S., FOX, I., PARIKH, A., MILCH, C., ABHYANKAR, B. & FEAGAN, B. G. 2017. The safety of vedolizumab for ulcerative colitis and Crohn's disease. *Gut,* 66**,** 839-851.

COOKS, T., IOANNIS, TARCIC, O., SOLOMON, H., AARON, WILDER, S., LOZANO, G., PIKARSKY, E., FORSHEW, T., ROZENFELD, N., HARPAZ, N., ITZKOWITZ, S., CURTIS, ROTTER, V., VASSILIS & OREN, M. 2013. Mutant p53 Prolongs NF-κB Activation and Promotes Chronic Inflammation and Inflammation-Associated Colorectal Cancer. *Cancer Cell,* 23**,** 634-646.

COSKUN, M., BJERRUM, J. T., SEIDELIN, J. B., TROELSEN, J. T., OLSEN, J. & NIELSEN, O. H. 2013. miR-20b, miR-98, miR-125b-1*, and let-7e* as new potential diagnostic biomarkers in ulcerative colitis. *World J Gastroenterol,* 19**,** 4289-99.

CURIEL, T. J., COUKOS, G., ZOU, L., ALVAREZ, X., CHENG, P., MOTTRAM, P., EVDEMON-HOGAN, M., CONEJO-GARCIA, J. R., ZHANG, L., BUROW, M., ZHU, Y., WEI, S., KRYCZEK, I., DANIEL, B., GORDON, A., MYERS, L., LACKNER, A., DISIS, M. L., KNUTSON, K. L., CHEN, L. & ZOU, W. 2004. Specific recruitment of regulatory T cells in ovarian carcinoma fosters immune privilege and predicts reduced survival. *Nat Med,* 10**,** 942-9.

CUTLER, S. J., DOECKE, J. D., GHAZAWI, I., YANG, J., GRIFFITHS, L. R., SPRING, K. J., RALPH, S. J. & MELLICK, A. S. 2017. Novel STAT binding elements mediate IL-6 regulation of MMP-1 and MMP-3. *Scientific Reports,* 7.

CZARNEWSKI, P., PARIGI, S. M., SORINI, C., DIAZ, O. E., DAS, S., GAGLIANI, N. & VILLABLANCA, E. J. 2019. Conserved transcriptomic profile between mouse and human colitis allows unsupervised patient stratification. *Nature Communications,* 10.

DANG, C. P. & LEELAHAVANICHKUL, A. 2020. Over-expression of miR-223 induces M2 macrophage through glycolysis alteration and attenuates LPS-induced sepsis mouse model, the cell-based therapy in sepsis. *PLoS One,* 15**,** e0236038.

DANNE, C., SKERNISKYTE, J., MARTEYN, B. & SOKOL, H. 2024. Neutrophils: from IBD to the gut microbiota. *Nat Rev Gastroenterol Hepatol,* 21**,** 184-197.

DE CALISTO, J., VILLABLANCA, E. J. & MORA, J. R. 2012. <scp>F</scp>cγ<scp>RI</scp> (<scp>CD</scp>64): An identity card for intestinal macrophages. *European Journal of Immunology,* 42**,** 3136-3140.

DE DEO, D., DAL BUONO, A., GABBIADINI, R., SPAGGIARI, P., BUSACCA, A., MASONI, B., FERRETTI, S., BEZZIO, C. & ARMUZZI, A. 2024. Management of proctitis in ulcerative colitis and the place of biological therapies. *Expert Opinion on Biological Therapy,* 24**,** 443-453.

DE FILIPPO, K., DUDECK, A., HASENBERG, M., NYE, E., VAN ROOIJEN, N., HARTMANN, K., GUNZER, M., ROERS, A. & HOGG, N. 2013. Mast cell and macrophage chemokines CXCL1/CXCL2 control the early stage of neutrophil recruitment during tissue inflammation. *Blood,* 121**,** 4930-4937.

DE HENAU, O., RAUSCH, M., WINKLER, D., CAMPESATO, L. F., LIU, C., CYMERMAN, D. H., BUDHU, S., GHOSH, A., PINK, M., TCHAICHA, J., DOUGLAS, M., TIBBITTS, T., SHARMA, S., PROCTOR, J., KOSMIDER, N., WHITE, K., STERN, H., SOGLIA, J., ADAMS, J., PALOMBELLA, V. J., MCGOVERN, K., KUTOK, J. L., WOLCHOK, J. D. & MERGHOUB, T. 2016. Overcoming resistance to checkpoint blockade therapy by targeting PI3Kγ in myeloid cells. *Nature,* 539**,** 443-447.

DEHAAN, R. K., SARVESTANI, S. K. & HUANG, E. H. 2020. Organoid Models of Colorectal Pathology: Do They Hold the Key to Personalized Medicine? A Systematic Review. *Dis Colon Rectum,* 63**,** 1559-1569.

DEN BESTEN, G., VAN EUNEN, K., GROEN, A. K., VENEMA, K., REIJNGOUD, D.-J. & BAKKER, B. M. 2013. The role of short-chain fatty acids in the interplay between diet, gut microbiota, and host energy metabolism. *Journal of Lipid Research,* 54**,** 2325-2340.

DENG, J. & FLEMING, J. B. 2022. Inflammation and Myeloid Cells in Cancer Progression and Metastasis. *Frontiers in Cell and Developmental Biology,* 9.

DENG, Y., ZHENG, X., ZHANG, Y., XU, M., YE, C., LIN, M., PAN, J., XU, Z., LU, X. & CHI, P. 2020. High SPRR1A expression is associated with poor survival in patients with colon cancer. *Oncology Letters*.

DIGNASS, A., LINDSAY, J. O., STURM, A., WINDSOR, A., COLOMBEL, J.-F., ALLEZ, M., D'HAENS, G., D'HOORE, A., MANTZARIS, G. & NOVACEK, G. 2012. Second European evidence-based consensus on the diagnosis and management of ulcerative colitis part 2: current management. *Journal of Crohn's and Colitis,* 6**,** 991-1030.

DILILLO, D., ZUCCOTTI, G. V., GALLI, E., MENEGHIN, F., DELL'ERA, A., PENAGINI, F., COLELLA, G., LEWINDON, P., CARMAGNOLA, S., FARINA, E., ARDIZZONE, S. & MACONI, G. 2019. Noninvasive testing in the management of children with suspected inflammatory bowel disease. *Scandinavian Journal of Gastroenterology,* 54**,** 586-591.

DINALLO, V., MARAFINI, I., DI FUSCO, D., LAUDISI, F., FRANZÈ, E., DI GRAZIA, A., FIGLIUZZI, M. M., CAPRIOLI, F., STOLFI, C., MONTELEONE, I. & MONTELEONE, G. 2019. Neutrophil Extracellular Traps Sustain Inflammatory Signals in Ulcerative Colitis. *Journal of Crohn's and Colitis,* 13**,** 772-784.

DIVEU, C., LELIÈVRE, E., PERRET, D., LAK-HAL, A.-H. L., FROGER, J., GUILLET, C., CHEVALIER, S., ROUSSEAU, F., WESA, A., PREISSER, L., CHABBERT, M., GAUCHAT, J.-F., GALY, A., GASCAN, H. & MOREL, A. 2003. GPL, a Novel Cytokine Receptor Related to GP130 and Leukemia Inhibitory Factor Receptor. *Journal of Biological Chemistry,* 278**,** 49850-49859.

DIXON, S. W., COLLARD, T. J., MORTENSSON, E. M. H., LEGGE, D. N., CHAMBERS, A. C., GREENHOUGH, A., CREED, T. J. & WILLIAMS, A. C. 2021. 5-Aminosalicylic acid inhibits stem cell function in human adenoma-derived cells: implications for chemoprophylaxis in colorectal tumorigenesis. *British Journal of Cancer,* 124**,** 1959-1969.

DONG, J., CHENG, M. & SUN, H. 2014. Function of inducible nitric oxide synthase in the regulation of cervical cancer cell proliferation and the expression of vascular endothelial growth factor. *Molecular Medicine Reports,* 9**,** 583-589.

DONG, Z., QI, R., GUO, X., ZHAO, X., LI, Y., ZENG, Z., BAI, W., CHANG, X., HAO, L., CHEN, Y., LOU, M., LI, Z. & LU, Y. 2017. MiR-223 modulates hepatocellular carcinoma cell proliferation through promoting apoptosis via the Rab1-mediated mTOR activation. *Biochemical and Biophysical Research Communications,* 483**,** 630-637.

DORF, J., ZARĘBA, K., MATOWICKA-KARNA, J., PRYCZYNICZ, A., GUZIŃSKA-USTYMOWICZ, K., ZALEWSKA, A. & MACIEJCZYK, M. 2022. May the Nitrosative and Carbonyl Stress Promote Inflammation in Patients with Colorectal Cancer? *Journal of Inflammation Research,* Volume 15**,** 4585-4600.

DU, T., WANG, D., WAN, X., XU, J., XIAO, Q. & LIU, B. 2021. Regulatory effect of microRNA-223-3p on breast cancer cell processes via the Hippo/Yap signaling pathway. *Oncology Letters,* 22.

DUCKWORTH, C. A. 2021. Identifying key regulators of the intestinal stem cell niche. *Biochemical Society Transactions,* 49**,** 2163-2176.

ESQUELA-KERSCHER, A., TRANG, P., WIGGINS, J. F., PATRAWALA, L., CHENG, A., FORD, L., WEIDHAAS, J. B., BROWN, D., BADER, A. G. & SLACK, F. J. 2008. Thelet-7microRNA reduces tumor growth in mouse models of lung cancer. *Cell Cycle,* 7**,** 759-764.

FABRIS, L., BERTON, S., CITRON, F., D'ANDREA, S., SEGATTO, I., NICOLOSO, M. S., MASSARUT, S., ARMENIA, J., ZAFARANA, G., ROSSI, S., IVAN, C., PERIN, T., VAIDYA, J. S., AVANZO, M., RONCADIN, M., SCHIAPPACASSI, M., BRISTOW, R. G., CALIN, G., BALDASSARRE, G. & BELLETTI, B. 2016. Radiotherapy-induced miR-223 prevents relapse of breast cancer by targeting the EGF pathway. *Oncogene,* 35**,** 4914-4926.

FAZI, F., ROSA, A., FATICA, A., GELMETTI, V., DE MARCHIS, M. L., NERVI, C. & BOZZONI, I. 2005. A Minicircuitry Comprised of MicroRNA-223 and Transcription Factors NFI-A and C/EBPα Regulates Human Granulopoiesis. *Cell,* 123**,** 819-831.

FENG, J., ZHU, Y., CHEN, L. & WANG, M. 2020a. Clinical significance of microRNA-146a in patients with ulcerative colitis. *Annals of Clinical & Laboratory Science,* 50**,** 463-467.

FENG, J., ZHU, Y., CHEN, L. & WANG, M. 2020b. Clinical Significance of microRNA-146a in Patients with Ulcerative Colitis. *Ann Clin Lab Sci,* 50**,** 463-467.

FENG, Q., HE, P. & WANG, Y. 2018a. MicroRNA-223-3p regulates cell chemo-sensitivity by targeting FOXO3 in prostatic cancer. *Gene,* 658**,** 152-158.

FENG, W., ZHU, L., LIU, Y., XU, L. & SHEN, H. 2023. C-reactive protein/albumin ratio and <scp>IL</scp>-6 are associated with disease activity in patients with ulcerative colitis. *Journal of Clinical Laboratory Analysis,* 37.

FENG, X., WANG, H., YE, S., GUAN, J., TAN, W., CHENG, S., WEI, G., WU, W., WU, F. & ZHOU, Y. 2012. Up-Regulation of microRNA-126 May Contribute to Pathogenesis of Ulcerative Colitis via Regulating NF-kappaB Inhibitor IκBα. *PLOS ONE,* 7**,** e52782.

FENG, Y., DONG, Y. W., SONG, Y. N., XIAO, J. H., GUO, X. Y., JIANG, W. L. & LU, L. G. 2018b. MicroRNA-449a is a potential predictor of colitis-associated colorectal cancer progression. *Oncology Reports*.

FERNANDES, J. V., DE MEDEIROS FERNANDES, T. A. A., DE AZEVEDO, J. C. V., COBUCCI, R. N. O., DE CARVALHO, M. G. F., ANDRADE, V. S. & DE ARAÚJO, J. M. G. 2015. Link between chronic inflammation and human papillomavirus-induced carcinogenesis (Review). *Oncology Letters,* 9**,** 1015-1026.

FLYNN, C. L., MARKEY, G. E., NEUDECKER, V., FARRELLY, C., FURUTA, G. T., ELTZSCHIG, H. K., MASTERSON, J. C. & MCNAMEE, E. N. 2024. The MicroRNA miR-223 Constrains Colitis-associated Tumorigenesis by Limiting Myeloid Cell Infiltration and Chemokine Expression. *J Immunol,* 213**,** 1869-1883.

FU, Y., MACKOWIAK, B., FENG, D., LU, H., GUAN, Y., LEHNER, T., PAN, H., WANG, X. W., HE, Y. & GAO, B. 2023. MicroRNA-223 attenuates hepatocarcinogenesis by blocking hypoxia-driven angiogenesis and immunosuppression. *Gut*.

FUKAO, T., FUKUDA, Y., KIGA, K., SHARIF, J., HINO, K., ENOMOTO, Y., KAWAMURA, A., NAKAMURA, K., TAKEUCHI, T. & TANABE, M. 2007. An Evolutionarily Conserved

Mechanism for MicroRNA-223 Expression Revealed by MicroRNA Gene Profiling. *Cell,* 129**,** 617-631.

GAJENDRAN, M., LOGANATHAN, P., JIMENEZ, G., CATINELLA, A. P., NG, N., UMAPATHY, C., ZIADE, N. & HASHASH, J. G. 2019. A comprehensive review and update on ulcerative colitis. *Disease-a-Month,* 65**,** 100851.

GALLO, G., KOTZE, P. G. & SPINELLI, A. 2018. Surgery in ulcerative colitis: When? How? *Best Practice & Research Clinical Gastroenterology,* 32-33**,** 71-78.

GAO, Y., ZHOU, S., XU, Y., SHENG, S., QIAN, S. Y. & HUO, X. 2019. Nitric oxide synthase inhibitors 1400W and L-NIO inhibit angiogenesis pathway of colorectal cancer. *Nitric Oxide,* 83**,** 33-39.

GARO, L. P., AJAY, A. K., FUJIWARA, M., GABRIELY, G., RAHEJA, R., KUHN, C., KENYON, B., SKILLIN, N., KADOWAKI-SAGA, R., SAXENA, S. & MURUGAIYAN, G. 2021. MicroRNA-146a limits tumorigenic inflammation in colorectal cancer. *Nature Communications,* 12**,** 2419.

GELMEZ, E., LEHR, K., KERSHAW, O., FRENTZEL, S., VILCHEZ-VARGAS, R., BANK, U., LINK, A., SCHÜLER, T., JERON, A. & BRUDER, D. 2022. Characterization of Maladaptive Processes in Acute, Chronic and Remission Phases of Experimental Colitis in C57BL/6 Mice. *Biomedicines,* 10.

GIL-MARTÍNEZ, M., LORENTE-SOROLLA, C., NAHARRO, S., RODRIGO-MUÑOZ, J. M. & DEL POZO, V. 2023. Advances and Highlights of miRNAs in Asthma: Biomarkers for Diagnosis and Treatment. *International Journal of Molecular Sciences,* 24**,** 1628.

GIONCHETTI, P., RIZZELLO, F., VENTURI, A., FERRETTI, M., BRIGNOLA, C., MIGLIOLI, M. & CAMPIERI, M. 1998. Comparison of oral with rectal mesalazine in the treatment of ulcerative proctitis. *Dis Colon Rectum,* 41**,** 93-7.

GIRISH, N., LIU, C. Y., GADEOCK, S., GOMEZ, M. L., HUANG, Y., SHARIFKHODAEI, Z., WASHINGTON, M. K. & POLK, D. B. 2021. Persistence of Lgr5+ colonic epithelial stem cells in mouse models of inflammatory bowel disease. *American Journal of Physiology-Gastrointestinal and Liver Physiology,* 321**,** G308-G324.

GOCHMAN, E., MAHAJNA, J., SHENZER, P., DAHAN, A., BLATT, A., ELYAKIM, R. & REZNICK, A. Z. 2012. The expression of iNOS and nitrotyrosine in colitis and colon cancer in humans. *Acta Histochem,* 114**,** 827-35.

GOLOGORSKY, M. B., MECHLER, C. M., FORGÓ, E., CHARVILLE, G. W. & HOWITT, M. R. 2023. The abundance and morphology of human large intestinal goblet and tuft cells during chronic schistosomiasis. *Parasite Immunology,* 45**,** e12981.

GONG, B., HU, H., CHEN, J., CAO, S., YU, J., XUE, J., CHEN, F., CAI, Y., HE, H. & ZHANG, L. 2013. Caprin-1 is a novel microRNA-223 target for regulating the proliferation and invasion of human breast cancer cells. *Biomed Pharmacother,* 67**,** 629-36.

GOWER-ROUSSEAU, C., DAUCHET, L., VERNIER-MASSOUILLE, G., TILLOY, E., BRAZIER, F., MERLE, V., DUPAS, J. L., SAVOYE, G., BALDE, M., MARTI, R., LEREBOURS, E., CORTOT, A., SALOMEZ, J. L., TURCK, D. & COLOMBEL, J. F. 2009. The natural history of pediatric ulcerative colitis: a population-based cohort study. *Am J Gastroenterol,* 104**,** 2080-8.

GRANADOS-PRINCIPAL, S., LIU, Y., GUEVARA, M. L., BLANCO, E., CHOI, D. S., QIAN, W., PATEL, T., RODRIGUEZ, A. A., CUSIMANO, J., WEISS, H. L., ZHAO, H., LANDIS, M. D., DAVE, B., GROSS, S. S. & CHANG, J. C. 2015. Inhibition of iNOS as a novel effective targeted therapy against triple-negative breast cancer. *Breast Cancer Research,* 17.

GREENWOOD-VAN MEERVELD, B., JOHNSON, A. C. & GRUNDY, D. 2017. Gastrointestinal Physiology and Function. *In:* GREENWOOD-VAN MEERVELD, B. (ed.) *Gastrointestinal Pharmacology.* Cham: Springer International Publishing.

GREK, C. L., ZHANG, J., MANEVICH, Y., TOWNSEND, D. M. & TEW, K. D. 2013. Causes and Consequences of Cysteine S-Glutathionylation. *Journal of Biological Chemistry,* 288**,** 26497-26504.

GRILLO, T. G., QUAGLIO, A. E. V., BERALDO, R. F., LIMA, T. B., BAIMA, J. P., DI STASI, L. C. & SASSAKI, L. Y. 2021. MicroRNA expression in inflammatory bowel disease-associated colorectal cancer. *World J Gastrointest Oncol,* 13**,** 995-1016.

GRISWOLD-PRENNER, I., KASHYAP, A. K., MAZHAR, S., HALL, Z. W., FAZELINIA, H. & ISCHIROPOULOS, H. 2023. Unveiling the human nitroproteome: Protein tyrosine nitration in cell signaling and cancer. *Journal of Biological Chemistry,* 299**,** 105038.

GRIVENNIKOV, S., KARIN, E., TERZIC, J., MUCIDA, D., YU, G.-Y., VALLABHAPURAPU, S., SCHELLER, J., ROSE-JOHN, S., CHEROUTRE, H. & ECKMANN, L. 2009a. IL-6 and Stat3 are required for survival of intestinal epithelial cells and development of colitis-associated cancer. *Cancer cell,* 15**,** 103-113.

GRIVENNIKOV, S., KARIN, E., TERZIC, J., MUCIDA, D., YU, G. Y., VALLABHAPURAPU, S., SCHELLER, J., ROSE-JOHN, S., CHEROUTRE, H., ECKMANN, L. & KARIN, M. 2009b. IL-6 and Stat3 are required for survival of intestinal epithelial cells and development of colitis-associated cancer. *Cancer Cell,* 15**,** 103-13.

GRIVENNIKOV, S. I. & KARIN, M. 2011. Inflammatory cytokines in cancer: tumour necrosis factor and interleukin 6 take the stage. *Annals of the Rheumatic Diseases,* 70**,** i104-i108.

GU, J., REMZI, F. H., LIAN, L. & SHEN, B. 2016. Practice pattern of ileal pouch surveillance in academic medical centers in the United States. *Gastroenterology Report,* 4**,** 119-124.

GUAGNOZZI, D. 2012. Colorectal cancer surveillance in patients with inflammatory bowel disease: What ¡s new? *World Journal of Gastrointestinal Endoscopy,* 4**,** 108.

GUIMBAUD, R., ABITBOL, V., BERTRAND, V., QUARTIER, G., CHAUVELOT-MOACHON, L., GIROUD, J., COUTURIER, D. & CHAUSSADE, D. C. 1998. Leukemia inhibitory

factor involvement in human ulcerative colitis and its potential role in malignant course. *Eur Cytokine Netw,* 9**,** 607-12.

GUO, J., ZHANG, R., ZHAO, Y. & WANG, J. 2021. MiRNA-29c-3p Promotes Intestinal Inflammation via Targeting Leukemia Inhibitory Factor in Ulcerative Colitis. *Journal of Inflammation Research,* Volume 14**,** 2031-2043.

GUO, Z., SHAO, L., ZHENG, L., DU, Q., LI, P., JOHN, B. & GELLER, D. A. 2012. miRNA-939 regulates human inducible nitric oxide synthase posttranscriptional gene expression in human hepatocytes. *Proceedings of the National Academy of Sciences,* 109**,** 5826-5831.

HABERMAN, Y., KARNS, R., DEXHEIMER, P. J., SCHIRMER, M., SOMEKH, J., JURICKOVA, I., BRAUN, T., NOVAK, E., BAUMAN, L., COLLINS, M. H., MO, A., ROSEN, M. J., BONKOWSKI, E., GOTMAN, N., MARQUIS, A., NISTEL, M., RUFO, P. A., BAKER, S. S., SAUER, C. G., MARKOWITZ, J., PFEFFERKORN, M. D., ROSH, J. R., BOYLE, B. M., MACK, D. R., BALDASSANO, R. N., SHAH, S., LELEIKO, N. S., HEYMAN, M. B., GRIFITHS, A. M., PATEL, A. S., NOE, J. D., ARONOW, B. J., KUGATHASAN, S., WALTERS, T. D., GIBSON, G., THOMAS, S. D., MOLLEN, K., SHEN-ORR, S., HUTTENHOWER, C., XAVIER, R. J., HYAMS, J. S. & DENSON, L. A. 2019. Ulcerative colitis mucosal transcriptomes reveal mitochondriopathy and personalized mechanisms underlying disease severity and treatment response. *Nature Communications,* 10**,** 38.

HALAMA, N., ZOERNIG, I., BERTHEL, A., KAHLERT, C., KLUPP, F., SUAREZ-CARMONA, M., SUETTERLIN, T., BRAND, K., KRAUSS, J., LASITSCHKA, F., LERCHL, T., LUCKNER-MINDEN, C., ULRICH, A., KOCH, M., WEITZ, J., SCHNEIDER, M., BUECHLER, M. W., ZITVOGEL, L., HERRMANN, T., BENNER, A., KUNZ, C., LUECKE, S., SPRINGFELD, C., GRABE, N., FALK, C. S. & JAEGER, D. 2016. Tumoral Immune Cell Exploitation in Colorectal Cancer Metastases Can Be Targeted Effectively by Anti-CCR5 Therapy in Cancer Patients. *Cancer Cell,* 29**,** 587-601.

HALFVARSON, J., LUDVIGSSON, J. F., BRESSO, F., ASKLING, J., SACHS, M. C. & OLÉN, O. 2022. Age determines the risk of familial inflammatory bowel disease—A nationwide study. *Alimentary Pharmacology & Therapeutics,* 56**,** 491-500.

HAN, J., LI, Y., ZHANG, H., GUO, J., WANG, X., KANG, Y., LUO, Y., WU, M. & ZHANG, X. 2018. MicroRNA-142-5p facilitates the pathogenesis of ulcerative colitis by regulating SOCS1. *Int J Clin Exp Pathol,* 11**,** 5735-5744.

HAN, J., ZHAO, F., ZHANG, J., ZHU, H., MA, H., LI, X., PENG, L., SUN, J. & CHEN, Z. 2016. miR-223 reverses the resistance of EGFR-TKIs through IGF1R/PI3K/Akt signaling pathway. *International Journal of Oncology,* 48**,** 1855-1867.

HANAHAN, D. 2022. Hallmarks of Cancer: New Dimensions. *Cancer Discov,* 12**,** 31-46.

HANAHAN, D. & WEINBERG, R. A. 2011a. Hallmarks of cancer: the next generation. *Cell,* 144**,** 646-74.

HANAHAN, D. & WEINBERG, ROBERT A. 2011b. Hallmarks of Cancer: The Next Generation. *Cell,* 144**,** 646-674.

HE, C., YU, T., SHI, Y., MA, C., YANG, W., FANG, L., SUN, M., WU, W., XIAO, F., GUO, F., CHEN, M., YANG, H., QIAN, J., CONG, Y. & LIU, Z. 2017. MicroRNA 301A Promotes Intestinal Inflammation and Colitis-Associated Cancer Development by Inhibiting BTG1. *Gastroenterology,* 152**,** 1434-1448.e15.

HE, N., TAN, H., DENG, X., SHU, L., QING, B. & LIANG, H. 2022. MiR-223-3p-loaded exosomes from bronchoalveolar lavage fluid promote alveolar macrophage autophagy and reduce acute lung injury by inhibiting the expression of STK39. *Human Cell,* 35**,** 1736-1751.

HEICHLER, C., SCHEIBE, K., SCHMIED, A., GEPPERT, C. I., SCHMID, B., WIRTZ, S., THOMA, O.-M., KRAMER, V., WALDNER, M. J., BÜTTNER, C., FARIN, H. F., PEŠIĆ, M., KNIELING, F., MERKEL, S., GRÜNEBOOM, A., GUNZER, M., GRÜTZMANN, R., ROSE-JOHN, S., KORALOV, S. B., KOLLIAS, G., VIETH, M., HARTMANN, A., GRETEN, F. R., NEURATH, M. F. & NEUFERT, C. 2020. STAT3 activation through IL-6/IL-11 in cancer-associated fibroblasts promotes colorectal tumour development and correlates with poor prognosis. *Gut,* 69**,** 1269-1282.

HELLER, F., FROMM, A., GITTER, A. H., MANKERTZ, J. & SCHULZKE, J. D. 2008. Epithelial apoptosis is a prominent feature of the epithelial barrier disturbance in intestinal inflammation: effect of pro-inflammatory interleukin-13 on epithelial cell function. *Mucosal Immunology,* 1**,** S58-S61.

HENDEL, S. K., KELLERMANN, L., HAUSMANN, A., BINDSLEV, N., JENSEN, K. B. & NIELSEN, O. H. 2022. Tuft Cells and Their Role in Intestinal Diseases. *Frontiers in Immunology,* 13.

HENKE, E., NANDIGAMA, R. & ERGÜN, S. 2020. Extracellular Matrix in the Tumor Microenvironment and Its Impact on Cancer Therapy. *Frontiers in Molecular Biosciences,* 6.

HIGUCHI, L. M., KHALILI, H., CHAN, A. T., RICHTER, J. M., BOUSVAROS, A. & FUCHS, C. S. 2012. A prospective study of cigarette smoking and the risk of inflammatory bowel disease in women. *Official journal of the American College of Gastroenterology| ACG,* 107**,** 1399-1406.

HIRSCHBERGER, S., HINSKE, L. C. & KRETH, S. 2018. MiRNAs: dynamic regulators of immune cell functions in inflammation and cancer. *Cancer Letters,* 431**,** 11-21.

HOPE, B., SHAHDADPURI, R., DUNNE, C., BRODERICK, A. M., GRANT, T., HAMZAWI, M., O'DRISCOLL, K., QUINN, S., HUSSEY, S. & BOURKE, B. 2012. Rapid rise in incidence of Irish paediatric inflammatory bowel disease. *Archives of Disease in Childhood,* 97**,** 590-594.

HOSSAIN, M. S., KARUNIAWATI, H., JAIROUN, A. A., URBI, Z., OOI, D. J., JOHN, A., LIM, Y. C., KIBRIA, K. M. K., MOHIUDDIN, A. K. M., MING, L. C., GOH, K. W. & HADI, M. A. 2022. Colorectal Cancer: A Review of Carcinogenesis, Global Epidemiology, Current Challenges, Risk Factors, Preventive and Treatment Strategies. *Cancers,* 14**,** 1732.

HU, X. & IVASHKIV, L. B. 2009. Cross-regulation of Signaling Pathways by Interferon-γ: Implications for Immune Responses and Autoimmune Diseases. *Immunity,* 31**,** 539-550.

HU, Y., DONG, Z. & LIU, K. 2024a. Unraveling the complexity of STAT3 in cancer: molecular understanding and drug discovery. *Journal of Experimental & Clinical Cancer Research,* 43.

HU, Z., SUI, Q., JIN, X., SHAN, G., HUANG, Y., YI, Y., ZENG, D., ZHAO, M., ZHAN, C., WANG, Q., LIN, Z., LU, T. & CHEN, Z. 2024b. IL6-STAT3-C/EBPβ-IL6 positive feedback loop in tumor-associated macrophages promotes the EMT and metastasis of lung adenocarcinoma. *Journal of Experimental & Clinical Cancer Research,* 43.

HUANG, Y., LU, D., MA, W., LIU, J., NING, Q., TANG, F. & LI, L. 2022. miR-223 in exosomes from bone marrow mesenchymal stem cells ameliorates rheumatoid arthritis via downregulation of NLRP3 expression in macrophages. *Molecular Immunology,* 143**,** 68-76.

HUNTER, C. A. & JONES, S. A. 2015. IL-6 as a keystone cytokine in health and disease. *Nature Immunology,* 16**,** 448-457.

HYUN, Y. S., HAN, D. S., LEE, A. R., EUN, C. S., YOUN, J. & KIM, H.-Y. 2012. Role of IL-17A in the development of colitis-associated cancer. *Carcinogenesis,* 33**,** 931-936.

IBRAHIM, M. L., KLEMENT, J. D., LU, C., REDD, P. S., XIAO, W., YANG, D., BROWNING, D. D., SAVAGE, N. M., BUCKHAULTS, P. J., MORSE, H. C., 3RD & LIU, K. 2018. Myeloid-Derived Suppressor Cells Produce IL-10 to Elicit DNMT3b-Dependent IRF8 Silencing to Promote Colitis-Associated Colon Tumorigenesis. *Cell Rep,* 25**,** 3036-3046.e6.

INNOCENTI, T., BIGAGLI, E., LYNCH, E. N., GALLI, A. & DRAGONI, G. 2023. MiRNA-Based Therapies for the Treatment of Inflammatory Bowel Disease: What Are We Still Missing? *Inflammatory Bowel Diseases,* 29**,** 308-323.

ISCHIROPOULOS, H. 2003. Biological selectivity and functional aspects of protein tyrosine nitration. *Biochem Biophys Res Commun,* 305**,** 776-83.

JAMES, J. P., RIIS, L. B., MALHAM, M., HØGDALL, E., LANGHOLZ, E. & NIELSEN, B. S. 2020. MicroRNA Biomarkers in IBD—Differential Diagnosis and Prediction of Colitis-Associated Cancer. *International Journal of Molecular Sciences,* 21**,** 7893.

JANSSEN, H. L. A., REESINK, H. W., LAWITZ, E. J., ZEUZEM, S., RODRIGUEZ-TORRES, M., PATEL, K., MEER, A. J. V. D., PATICK, A. K., CHEN, A., ZHOU, Y., PERSSON, R., KING, B. D., KAUPPINEN, S., LEVIN, A. A. & HODGES, M. R. 2013. Treatment of HCV Infection by Targeting MicroRNA. *New England Journal of Medicine,* 368**,** 1685-1694.

JEFFRIES, J., ZHOU, W., HSU, A. Y. & DENG, Q. 2019. miRNA-223 at the crossroads of inflammation and cancer. *Cancer Letters,* 451**,** 136-141.

JHA, D., AL-TAIE, Z., KREK, A., ESHGHI, S. T., FANTOU, A., LAURENT, T., TANKELEVICH, M., CAO, X., MERINGER, H., LIVANOS, A. E., TOKUYAMA, M., COSSARINI, F., BOURREILLE, A., JOSIEN, R., HOU, R., CANALES-HERRERIAS, P., UNGARO, R. C., KAYAL, M., MARION, J., POLYDORIDES, A. D., KO, H. M., D'SOUZA, D., MERAND, R., KIM-SCHULZE, S., HACKNEY, J. A., NGUYEN, A., MCBRIDE, J. M., YUAN, G. C., COLOMBEL, J. F., MARTIN, J. C., ARGMANN, C., SUÁREZ-FARIÑAS, M., PETRALIA, F. & MEHANDRU, S. 2023. Myeloid cell influx into the colonic epithelium is associated with disease severity and non-response to anti-Tumor Necrosis Factor Therapy in patients with Ulcerative Colitis. *bioRxiv*.

JIANG, R., WANG, H., DENG, L., HOU, J., SHI, R., YAO, M., GAO, Y., YAO, A., WANG, X., YU, L. & SUN, B. 2013. IL-22 is related to development of human colon cancer by activation of STAT3. *BMC Cancer,* 13**,** 59.

JIMÉNEZ-CORTEGANA, C., PALOMARES, F., ALBA, G., SANTA-MARÍA, C., DE LA CRUZ-MERINO, L., SÁNCHEZ-MARGALET, V. & LÓPEZ-ENRÍQUEZ, S. 2024. Dendritic cells: the yin and yang in disease progression. *Frontiers in Immunology,* 14.

JIN, W. 2020. Role of JAK/STAT3 signaling in the regulation of metastasis, the transition of cancer stem cells, and chemoresistance of cancer by epithelial–mesenchymal transition. *Cells,* 9**,** 217.

JOHNNIDIS, J. B., HARRIS, M. H., WHEELER, R. T., STEHLING-SUN, S., LAM, M. H., KIRAK, O., BRUMMELKAMP, T. R., FLEMING, M. D. & CAMARGO, F. D. 2008. Regulation of progenitor cell proliferation and granulocyte function by microRNA-223. *Nature,* 451**,** 1125-1129.

JORDAN-ALEJANDRE, E., CAMPOS-PARRA, A. D., CASTRO-LÓPEZ, D. L. & SILVA-CÁZARES, M. B. 2023. Potential miRNA Use as a Biomarker: From Breast Cancer Diagnosis to Metastasis. *Cells,* 12**,** 525.

KAŁUŻNA, A., OLCZYK, P. & KOMOSIŃSKA-VASSEV, K. 2022a. The Role of Innate and Adaptive Immune Cells in the Pathogenesis and Development of the Inflammatory Response in Ulcerative Colitis. *Journal of Clinical Medicine,* 11**,** 400.

KAŁUŻNA, A., OLCZYK, P. & KOMOSIŃSKA-VASSEV, K. 2022b. The Role of Innate and Adaptive Immune Cells in the Pathogenesis and Development of the Inflammatory Response in Ulcerative Colitis. *J Clin Med,* 11.

KAMEYAMA, H., NAGAHASHI, M., SHIMADA, Y., TAJIMA, Y., ICHIKAWA, H., NAKANO, M., SAKATA, J., KOBAYASHI, T., NARAYANAN, S., TAKABE, K. & WAKAI, T. 2018. Genomic characterization of colitis-associated colorectal cancer. *World Journal of Surgical Oncology,* 16.

KANEDA, M. M., MESSER, K. S., RALAINIRINA, N., LI, H., LEEM, C. J., GORJESTANI, S., WOO, G., NGUYEN, A. V., FIGUEIREDO, C. C. & FOUBERT, P. 2016. PI3Kγ is a molecular switch that controls immune suppression. *Nature,* 539**,** 437-442.

KAO, N.-J., HU, J.-Y., WU, C.-S. & KONG, Z.-L. 2016. Curcumin represses the activity of inhibitor-κB kinase in dextran sulfate sodium-induced colitis by S-nitrosylation. *International Immunopharmacology,* 38**,** 1-7.

KAPLAN, G. G. 2015. The global burden of IBD: from 2015 to 2025. *Nature Reviews Gastroenterology & Hepatology,* 12**,** 720-727.

KASHFI, K., KANNIKAL, J. & NATH, N. 2021. Macrophage Reprogramming and Cancer Therapeutics: Role of iNOS-Derived NO. *Cells,* 10**,** 3194.

KE, Y., LIU, X., NIU, T., QIANG, Z. & GAO, F. 2024. MIR-21 regulating distribution of intestinal flora through TNF-α promotes progression of ulcerative colitis. *Journal of Medical Biochemistry,* 43**,** 299-305.

KELLERMANN, L. & RIIS, L. B. 2021. A close view on histopathological changes in inflammatory bowel disease, a narrative review. *Digestive Medicine Research,* 4.

KIESLER, P., FUSS, I. J. & STROBER, W. 2015. Experimental Models of Inflammatory Bowel Diseases. *Cellular and Molecular Gastroenterology and Hepatology,* 1**,** 154-170.

KILIC, T., ERDEM, A., OZSOZ, M. & CARRARA, S. 2018. microRNA biosensors: Opportunities and challenges among conventional and commercially available techniques. *Biosensors and Bioelectronics,* 99**,** 525-546.

KIM, H. S., LEE, C., KIM, W. H., MAENG, Y. H. & JANG, B. G. 2017. Expression profile of intestinal stem cell markers in colitis-associated carcinogenesis. *Scientific Reports,* 7.

KIM, J., YAO, F., XIAO, Z., SUN, Y. & MA, L. 2018. MicroRNAs and metastasis: small RNAs play big roles. *Cancer Metastasis Rev,* 37**,** 5-15.

KMIEĆ, Z., CYMAN, M. & ŚLEBIODA, T. J. 2017. Cells of the innate and adaptive immunity and their interactions in inflammatory bowel disease. *Advances in Medical Sciences,* 62**,** 1-16.

KMIOŁEK, T. & PARADOWSKA-GORYCKA, A. 2022. miRNAs as Biomarkers and Possible Therapeutic Strategies in Rheumatoid Arthritis. *Cells,* 11**,** 452.

KOBAYASHI, T., SIEGMUND, B., LE BERRE, C., WEI, S. C., FERRANTE, M., SHEN, B., BERNSTEIN, C. N., DANESE, S., PEYRIN-BIROULET, L. & HIBI, T. 2020. Ulcerative colitis. *Nature Reviews Disease Primers,* 6.

KOBELT, D., ZHANG, C., CLAYTON-LUCEY, I. A., GLAUBEN, R., VOSS, C., SIEGMUND, B. & STEIN, U. 2020. Pro-inflammatory TNF-α and IFN-γ Promote Tumor Growth and Metastasis via Induction of MACC1. *Frontiers in Immunology,* 11.

KORDE CHOUDHARI, S., CHAUDHARY, M., BAGDE, S., GADBAIL, A. R. & JOSHI, V. 2013. Nitric oxide and cancer: a review. *World Journal of Surgical Oncology,* 11**,** 118.

KORNBLUTH, A., SACHAR, D. B. & GASTROENTEROLOGY, P. P. C. O. T. A. C. O. 2010. Ulcerative colitis practice guidelines in adults: American college of gastroenterology, practice parameters committee. *Official journal of the American College of Gastroenterology| ACG,* 105**,** 501-523.

KOTA, J., CHIVUKULA, R. R., O'DONNELL, K. A., WENTZEL, E. A., MONTGOMERY, C. L., HWANG, H.-W., CHANG, T.-C., VIVEKANANDAN, P., TORBENSON, M., CLARK, K. R., MENDELL, J. R. & MENDELL, J. T. 2009. Therapeutic microRNA Delivery Suppresses Tumorigenesis in a Murine Liver Cancer Model. *Cell,* 137**,** 1005-1017.

KOUKOS, G., POLYTARCHOU, C., KAPLAN, J. L., MORLEY–FLETCHER, A., GRAS–MIRALLES, B., KOKKOTOU, E., BARIL–DORE, M., POTHOULAKIS, C., WINTER, H. S. & ILIOPOULOS, D. 2013. MicroRNA-124 Regulates STAT3 Expression and Is Down-regulated in Colon Tissues of Pediatric Patients With Ulcerative Colitis. *Gastroenterology,* 145**,** 842-852.e2.

KRAMMER, T. L., ZEIBIG, S., SCHROTTMAIER, W. C., PIRABE, A., GOEBEL, S., DIENDORFER, A. B., HOLTHOFF, H.-P., ASSINGER, A. & HACKL, M. 2022. Comprehensive Characterization of Platelet-Enriched MicroRNAs as Biomarkers of Platelet Activation. *Cells,* 11**,** 1254.

KRZYSTEK-KORPACKA, M., G. FLESZAR, M., BEDNARZ-MISA, I., LEWANDOWSKI, Ł., SZCZUKA, I., KEMPIŃSKI, R. & NEUBAUER, K. 2020. Transcriptional and Metabolomic Analysis of L-Arginine/Nitric Oxide Pathway in Inflammatory Bowel Disease and Its Association with Local Inflammatory and Angiogenic Response: Preliminary Findings. *International Journal of Molecular Sciences,* 21**,** 1641.

KUNWAR, A., ABLORDEPPEY, K. K., MIRESKANDARI, A., SHEINERMAN, K., KIEFER, M., UMANSKY, S. & KUMAR, G. 2023. Analytical Validation of a Novel MicroRNA Panel for Risk Stratification of Cognitive Impairment. *Diagnostics,* 13**,** 2170.

KUSHKEVYCH, I., DORDEVIĆ, D. & KOLLÁR, P. 2019. Analysis of physiological parameters of Desulfovibrio strains from individuals with colitis. *Open Life Sciences,* 13**,** 481-488.

LAINE, L., KALTENBACH, T., BARKUN, A., MCQUAID, K. R., SUBRAMANIAN, V., SOETIKNO, R., EAST, J. E., FARRAYE, F. A., FEAGAN, B., IOANNIDIS, J., KIESSLICH, R., KRIER, M., MATSUMOTO, T., MCCABE, R. P., MÖNKEMÜLLER, K., ODZE, R., PICCO, M., RUBIN, D. T., RUBIN, M., RUBIO, C. A., RUTTER, M. D., SANCHEZ-YAGUE, A., SANDULEANU, S., SHERGILL, A., ULLMAN, T., VELAYOS, F., YAKICH, D. & YANG, Y.-X. 2015. SCENIC International Consensus Statement on Surveillance and Management of Dysplasia in Inflammatory Bowel Disease. *Gastroenterology,* 148**,** 639-651.e28.

LALA, P. K. & CHAKRABORTY, C. 2001. Role of nitric oxide in carcinogenesis and tumour progression. *The Lancet Oncology,* 2**,** 149-156.

LAMPROU, E., SOTIRIOU, M., KALLIGOSFYRI, P. M., KALOGIANNI, D. P. & CHRISTOPOULOS, T. K. 2023. A universal lateral flow assay for microRNA visual detection in urine samples. *Talanta,* 262**,** 124682.

LANDSKRON, G., DE LA FUENTE, M., THUWAJIT, P., THUWAJIT, C. & HERMOSO, M. A. 2014. Chronic Inflammation and Cytokines in the Tumor Microenvironment. *Journal of Immunology Research,* 2014**,** 1-19.

LANGER, V., VIVI, E., REGENSBURGER, D., WINKLER, T. H., WALDNER, M. J., RATH, T., SCHMID, B., SKOTTKE, L., LEE, S., JEON, N. L., WOHLFAHRT, T., KRAMER, V., TRIPAL, P., SCHUMANN, M., KERSTING, S., HANDTRACK, C., GEPPERT, C. I., SUCHOWSKI, K., ADAMS, R. H., BECKER, C., RAMMING, A., NASCHBERGER, E., BRITZEN-LAURENT, N. & STÜRZL, M. 2019. IFN-γ drives inflammatory bowel disease pathogenesis through VE-cadherin–directed vascular barrier disruption. *Journal of Clinical Investigation,* 129**,** 4691-4707.

LARREA, E., SOLE, C., MANTEROLA, L., GOICOECHEA, I., ARMESTO, M., ARESTIN, M., CAFFAREL, M. M., ARAUJO, A. M., ARAIZ, M., FERNANDEZ-MERCADO, M. & LAWRIE, C. H. 2016. New Concepts in Cancer Biomarkers: Circulating miRNAs in Liquid Biopsies. *International Journal of Molecular Sciences,* 17**,** 627.

LE BERRE, C., HONAP, S. & PEYRIN-BIROULET, L. 2023. Ulcerative colitis. *The Lancet,* 402**,** 571-584.

LECHUGA, S., BRAGA-NETO, M. B., NAYDENOV, N. G., RIEDER, F. & IVANOV, A. I. 2023. Understanding disruption of the gut barrier during inflammation: Should we abandon traditional epithelial cell lines and switch to intestinal organoids? *Front Immunol,* 14**,** 1108289.

LEE, R. C., FEINBAUM, R. L. & AMBROS, V. 1993. The C. elegans heterochronic gene lin-4 encodes small RNAs with antisense complementarity to lin-14. *Cell,* 75**,** 843-54.

LESLIE, J. L., VENDROV, K. C., JENIOR, M. L. & YOUNG, V. B. 2019. The Gut Microbiota Is Associated with Clearance of Clostridium difficile Infection Independent of Adaptive Immunity. *mSphere,* 4.

LESLIE, K., LANG, C., DEVGAN, G., AZARE, J., BERISHAJ, M., GERALD, W., KIM, Y. B., PAZ, K., DARNELL, J. E., ALBANESE, C., SAKAMAKI, T., PESTELL, R. & BROMBERG, J. 2006. Cyclin D1 is transcriptionally regulated by and required for transformation by activated signal transducer and activator of transcription 3. *Cancer Res,* 66**,** 2544-52.

LEVINE, A., GRIFFITHS, A., MARKOWITZ, J., WILSON, D. C., TURNER, D., RUSSELL, R. K., FELL, J., RUEMMELE, F. M., WALTERS, T., SHERLOCK, M., DUBINSKY, M. & HYAMS, J. S. 2011. Pediatric modification of the Montreal classification for inflammatory bowel disease. *Inflammatory Bowel Diseases,* 17**,** 1314-1321.

LI, J., JI, Y., CHEN, N., DAI, L. & DENG, H. 2023. Colitis-associated carcinogenesis: crosstalk between tumors, immune cells and gut microbiota. *Cell & Bioscience,* 13.

LI, M., WANG, J., FANG, Y., GONG, S., LI, M., WU, M., LAI, X., ZENG, G., WANG, Y., YANG, K. & HUANG, X. 2016. microRNA-146a promotes mycobacterial survival in macrophages through suppressing nitric oxide production. *Scientific Reports,* 6**,** 23351.

LI, N., OUYANG, Y., XU, X., YUAN, Z., LIU, C. & ZHU, Z. 2021. MiR-155 promotes colitis-associated intestinal fibrosis by targeting HBP1/Wnt/β-catenin signalling pathway. *Journal of Cellular and Molecular Medicine,* 25**,** 4765-4775.

LI, S., FENG, Y., HUANG, Y., LIU, Y., WANG, Y., LIANG, Y., ZENG, H., QU, H. & WEI, L. 2020. MiR-223-3p regulates cell viability, migration, invasion, and apoptosis of non-small cell lung cancer cells by targeting RHOB. *Open Life Sciences,* 15**,** 389-399.

LI, W., HAN, W., MA, Y., CUI, L., TIAN, Y., ZHOU, Z. & WANG, H. 2015. P53-dependent miRNAs mediate nitric oxide-induced apoptosis in colonic carcinogenesis. *Free Radical Biology and Medicine,* 85**,** 105-113.

LI, X., ZHANG, Y., ZHANG, H., LIU, X., GONG, T., LI, M., SUN, L., JI, G., SHI, Y., HAN, Z., HAN, S., NIE, Y., CHEN, X., ZHAO, Q., DING, J., WU, K. & DAIMING, F. 2011. miRNA-223 Promotes Gastric Cancer Invasion and Metastasis by Targeting Tumor Suppressor EPB41L3. *Molecular Cancer Research,* 9**,** 824-833.

LI, Y., DE HAAR, C., CHEN, M., DEURING, J., GERRITS, M. M., SMITS, R., XIA, B., KUIPERS, E. J. & VAN DER WOUDE, C. J. 2010. Disease-related expression of the IL6/STAT3/SOCS3 signalling pathway in ulcerative colitis and ulcerative colitis-related carcinogenesis. *Gut,* 59**,** 227-35.

LI, Z.-W., YANG, Y.-M., DU, L.-T., DONG, Z., WANG, L.-L., ZHANG, X., ZHOU, X.-J., ZHENG, G.-X., QU, A.-L. & WANG, C.-X. 2014. Overexpression of miR-223 correlates with tumor metastasis and poor prognosis in patients with colorectal cancer. *Medical Oncology,* 31.

LIANG, F., WANG, S., GUO, Y., MU, Y., SHANG, F. & WANG, M. 2023. Proteome profiling of endogenous and potential S-nitrosylation in colorectal cancer. *Frontiers in Endocrinology,* 14.

LIANG, L., ZHU, J., ZAORSKY, N. G., DENG, Y., WU, X., LIU, Y., LIU, F., CAI, G., GU, W. & SHEN, L. 2014. MicroRNA-223 enhances radiation sensitivity of U87MG cells in vitro and in vivo by targeting ataxia telangiectasia mutated. *International Journal of Radiation Oncology* Biology* Physics,* 88**,** 955-960.

LIAO, X., LIU, J., GUO, X., MENG, R., ZHANG, W., ZHOU, J., XIE, X. & ZHOU, H. 2024. Origin and Function of Monocytes in Inflammatory Bowel Disease. *J Inflamm Res,* 17**,** 2897-2914.

LIN, Y., XU, J. & LAN, H. 2019. Tumor-associated macrophages in tumor metastasis: biological roles and clinical therapeutic applications. *Journal of Hematology & Oncology,* 12.

LIU, C., LIU, R., WANG, B., LIAN, J., YAO, Y., SUN, H., ZHANG, C., FANG, L., GUAN, X., SHI, J., HAN, S., ZHAN, F., LUO, S., YAO, Y., ZHENG, T. & ZHANG, Y. 2021. Blocking IL-17A enhances tumor response to anti-PD-1 immunotherapy in microsatellite stable colorectal cancer. *Journal for ImmunoTherapy of Cancer,* 9**,** e001895.

LIU, W. & RODGERS, G. P. 2022. Olfactomedin 4 Is Not a Precise Marker for Human Intestinal Stem Cells, But Is Involved in Intestinal Carcinogenesis. *Gastroenterology,* 162**,** 1001-1004.

LIU, Y., WANG, D., LUAN, Y., TAO, B., LI, Q., FENG, Q., ZHOU, H., MU, J. & YU, J. 2024. The application of organoids in colorectal diseases. *Front Pharmacol,* 15**,** 1412489.

LIU, Y., WANG, R., JIANG, J., YANG, B., CAO, Z. & CHENG, X. 2015. miR-223 is upregulated in monocytes from patients with tuberculosis and regulates function of monocyte-derived macrophages. *Molecular Immunology,* 67**,** 475-481.

LIU, Z., XIE, Y., XIONG, Y., LIU, S., QIU, C., ZHU, Z., MAO, H., YU, M. & WANG, X. 2020. TLR 7/8 agonist reverses oxaliplatin resistance in colorectal cancer via directing the myeloid-derived suppressor cells to tumoricidal M1-macrophages. *Cancer Lett,* 469**,** 173-185.

LOPETUSO, L. R., SCALDAFERRI, F., FRANCESCHI, F. & GASBARRINI, A. 2014. The gastrointestinal microbiome – Functional interference between stomach and intestine. *Best Practice & Research Clinical Gastroenterology,* 28**,** 995-1002.

LOW, D., MINO-KENUDSON, M. & MIZOGUCHI, E. 2014. Recent Advancement in Understanding Colitis-associated Tumorigenesis. *Inflammatory Bowel Diseases,* 20**,** 2115-2123.

LU, G., ZHANG, R., GENG, S., PENG, L., JAYARAMAN, P., CHEN, C., XU, F., YANG, J., LI, Q., ZHENG, H., SHEN, K., WANG, J., LIU, X., WANG, W., ZHENG, Z., QI, C.-F., SI, C., HE, J. C., LIU, K., LIRA, S. A., SIKORA, A. G., LI, L. & XIONG, H. 2015. Myeloid cell-derived inducible nitric oxide synthase suppresses M1 macrophage polarization. *Nature Communications,* 6**,** 6676.

LUNDBERG, J. O., WEITZBERG, E. & GLADWIN, M. T. 2008. The nitrate-nitrite-nitric oxide pathway in physiology and therapeutics. *Nat Rev Drug Discov,* 7**,** 156-67.

LUO, P., WANG, Q., YE, Y., ZHANG, J., LU, D., CHENG, L., ZHOU, H., XIE, M. & WANG, B. 2019. MiR-223-3p functions as a tumor suppressor in lung squamous cell carcinoma by miR-223-3p-mutant p53 regulatory feedback loop. *Journal of Experimental & Clinical Cancer Research,* 38.

MACFARLANE, L. A. & MURPHY, P. R. 2010. MicroRNA: Biogenesis, Function and Role in Cancer. *Curr Genomics,* 11**,** 537-61.

MALATY, H., ABRAHAM, MEHTA, S., GARNETT, E. & FERRY 2013. The natural history of ulcerative colitis in a pediatric population: a follow-up population- based cohort study. *Clinical and Experimental Gastroenterology***,** 77.

MANDAL, P. 2018. Molecular signature of nitric oxide on major cancer hallmarks of colorectal carcinoma. *Inflammopharmacology,* 26**,** 331-336.

MARTEAU, P., PROBERT, C., LINDGREN, S., GASSUL, M., TAN, T., DIGNASS, A., BEFRITS, R., MIDHAGEN, G., RADEMAKER, J. & FOLDAGER, M. 2005. Combined oral and enema treatment with Pentasa (mesalazine) is superior to oral therapy alone in patients with extensive mild/moderate active ulcerative colitis: a randomised, double blind, placebo controlled study. *Gut,* 54**,** 960-965.

MARTUCCI, G., ARCADIPANE, A., TUZZOLINO, F., OCCHIPINTI, G., PANARELLO, G., CARCIONE, C., BONICOLINI, E., VITIELLO, C., LORUSSO, R., CONALDI, P. G. & MICELI, V. 2020. Identification of a Circulating miRNA Signature to Stratify Acute Respiratory Distress Syndrome Patients. *Journal of Personalized Medicine,* 11**,** 15.

MARYŃCZAK, K., WŁODARCZYK, J., SABATOWSKA, Z., DZIKI, A., DZIKI, Ł. & WŁODARCZYK, M. 2022. Colitis-Associated Colorectal Cancer in Patients with Inflammatory Bowel Diseases in a Tertiary Referral Center: A Propensity Score Matching Analysis. *Journal of Clinical Medicine,* 11**,** 866.

MENON, A., ABD-AZIZ, N., KHALID, K., POH, C. L. & NAIDU, R. 2022. miRNA: A Promising Therapeutic Target in Cancer. *International Journal of Molecular Sciences,* 23**,** 11502.

MEYER, A. R., BROWN, M. E., MCGRATH, P. S. & DEMPSEY, P. J. 2022. Injury-Induced Cellular Plasticity Drives Intestinal Regeneration. *Cell Mol Gastroenterol Hepatol,* 13**,** 843-856.

MOLLER, F. T., ANDERSEN, V., WOHLFAHRT, J. & JESS, T. 2015. Familial risk of inflammatory bowel disease: a population-based cohort study 1977-2011. *Am J Gastroenterol,* 110**,** 564-71.

MOLODECKY, N. A., SOON, S., RABI, D. M., GHALI, W. A., FERRIS, M., CHERNOFF, G., BENCHIMOL, E. I., PANACCIONE, R., GHOSH, S. & BARKEMA, H. W. 2012. Increasing incidence and prevalence of the inflammatory bowel diseases with time, based on systematic review. *Gastroenterology,* 142**,** 46-54. e42.

MORGENSTERN-KAPLAN, D., KAREFF, S. A., TRABOLSI, A., RODRIGUEZ, E., KRAUSE, H., RIBEIRO, J. R., TAN, H., ANTONARAKIS, E. S., LOU, E., NAGASAKA, M., ALGAZE, S., LENZ, H.-J., LIU, S. V., HALMOS, B., HOON, D. S. B., SEEBER, A., MA, P. C., EL-DEIRY, W. S., VANDERWALDE, A. M. & LOPES, G. 2024. Genomic, immunologic, and prognostic associations of TROP2 (TACSTD2) expression in solid tumors. *The Oncologist*.

MOWAT, A. M. & AGACE, W. W. 2014. Regional specialization within the intestinal immune system. *Nat Rev Immunol,* 14**,** 667-85.

MU, K., YU, S. & KITTS, D. D. 2019. The Role of Nitric Oxide in Regulating Intestinal Redox Status and Intestinal Epithelial Cell Functionality. *International Journal of Molecular Sciences,* 20**,** 1755.

MULTHOFF, G., MOLLS, M. & RADONS, J. 2012. Chronic inflammation in cancer development. *Frontiers in immunology,* 2**,** 98.

MUTH, K. N., RECH, J., LOSCH, F. O. & HOERNING, A. 2023. Reversing the Inflammatory Process—25 Years of Tumor Necrosis Factor-α Inhibitors. *Journal of Clinical Medicine,* 12**,** 5039.

MUTHUPALANI, S., ANNAMALAI, D., FENG, Y., GANESAN, S. M., GE, Z., WHARY, M. T., NAKAGAWA, H., RUSTGI, A. K., WANG, T. C. & FOX, J. G. 2023. IL-1β transgenic mouse model of inflammation driven esophageal and oral squamous cell carcinoma. *Scientific Reports,* 13.

NAEGELI, A. N., HUNTER, T., DONG, Y., HOSKIN, B., MIDDLETON-DALBY, C., HETHERINGTON, J., STEFANI-HUNYADY, D. & CANAVAN, J. B. 2021. Full, Partial, and Modified Permutations of the Mayo Score: Characterizing Clinical and Patient-Reported Outcomes in Ulcerative Colitis Patients. *Crohn's & Colitis 360,* 3.

NAKASE, H., SATO, N., MIZUNO, N. & IKAWA, Y. 2022. The influence of cytokines on the complex pathology of ulcerative colitis. *Autoimmunity Reviews,* 21**,** 103017.

NARDONE, O. M., ZAMMARCHI, I., SANTACROCE, G., GHOSH, S. & IACUCCI, M. 2023. Inflammation-Driven Colorectal Cancer Associated with Colitis: From Pathogenesis to Changing Therapy. *Cancers (Basel),* 15.

NATA, T., FUJIYA, M., UENO, N., MORIICHI, K., KONISHI, H., TANABE, H., OHTAKE, T., IKUTA, K. & KOHGO, Y. 2013. MicroRNA-146b improves intestinal injury in mouse colitis by activating nuclear factor-κB and improving epithelial barrier function. *J Gene Med,* 15**,** 249-60.

NAUGLER, W. E. & KARIN, M. 2008. The wolf in sheep's clothing: the role of interleukin-6 in immunity, inflammation and cancer. *Trends Mol Med,* 14**,** 109-19.

NEUDECKER, V., BRODSKY, K. S., CLAMBEY, E. T., SCHMIDT, E. P., PACKARD, T. A., DAVENPORT, B., STANDIFORD, T. J., WENG, T., FLETCHER, A. A., BARTHEL, L., MASTERSON, J. C., FURUTA, G. T., CAI, C., BLACKBURN, M. R., GINDE, A. A., GRANER, M. W., JANSSEN, W. J., ZEMANS, R. L., EVANS, C. M., BURNHAM, E. L., HOMANN, D., MOSS, M., KRETH, S., ZACHAROWSKI, K., HENSON, P. M. & ELTZSCHIG, H. K. 2017a. Neutrophil transfer of miR-223 to lung epithelial cells dampens acute lung injury in mice. *Science Translational Medicine,* 9**,** eaah5360.

NEUDECKER, V., HANEKLAUS, M., JENSEN, O., KHAILOVA, L., MASTERSON, J. C., TYE, H., BIETTE, K., JEDLICKA, P., BRODSKY, K. S., GERICH, M. E., MACK, M., ROBERTSON, A. A. B., COOPER, M. A., FURUTA, G. T., DINARELLO, C. A.,

O'NEILL, L. A., ELTZSCHIG, H. K., MASTERS, S. L. & MCNAMEE, E. N. 2017b. Myeloid-derived miR-223 regulates intestinal inflammation via repression of the NLRP3 inflammasome. *Journal of Experimental Medicine,* 214**,** 1737-1752.

NG, A. Y., TU, C., SHEN, S., XU, D., OURSLER, M. J., QU, J. & YANG, S. 2018. Comparative Characterization of Osteoclasts Derived From Murine Bone Marrow Macrophages and RAW 264.7 Cells Using Quantitative Proteomics. *JBMR Plus,* 2**,** 328-340.

NGUYEN, L. H., GOEL, A. & CHUNG, D. C. 2020. Pathways of Colorectal Carcinogenesis. *Gastroenterology,* 158**,** 291-302.

NIAN, W., AO, X., WU, Y., HUANG, Y., SHAO, J., WANG, Y., CHEN, Z., CHEN, F. & WANG, D. 2013. miR-223 functions as a potent tumor suppressor of the Lewis lung carcinoma cell line by targeting insulin-like growth factor-1 receptor and cyclin-dependent kinase 2. *Oncology Letters,* 6**,** 359-366.

NISHIDA, A., INOUE, R., INATOMI, O., BAMBA, S., NAITO, Y. & ANDOH, A. 2018. Gut microbiota in the pathogenesis of inflammatory bowel disease. *Clinical Journal of Gastroenterology,* 11**,** 1-10.

O'REILLY, L. A., PUTOCZKI, T. L., MIELKE, L. A., LOW, J. T., LIN, A., PREAUDET, A., HEROLD, M. J., YAPRIANTO, K., TAI, L., KUEH, A., PACINI, G., FERRERO, R. L., GUGASYAN, R., HU, Y., CHRISTIE, M., WILCOX, S., GRUMONT, R., GRIFFIN, M. D. W., O'CONNOR, L., SMYTH, G. K., ERNST, M., WARING, P., GERONDAKIS, S. & STRASSER, A. 2018. Loss of NF-κB1 Causes Gastric Cancer with Aberrant Inflammation and Expression of Immune Checkpoint Regulators in a STAT-1-Dependent Manner. *Immunity,* 48**,** 570-583.e8.

OMRANI, O., KREPELOVA, A., RASA, S. M. M., SIRVINSKAS, D., LU, J., ANNUNZIATA, F., GARSIDE, G., BAJWA, S., REINHARDT, S., ADAM, L., KÄPPEL, S., DUCANO, N., DONNA, D., ORI, A., OLIVIERO, S., RUDOLPH, K. L. & NERI, F. 2023. IFNγ-Stat1 axis drives aging-associated loss of intestinal tissue homeostasis and regeneration. *Nature Communications,* 14**,** 6109.

ORDÁS, I., ECKMANN, L., TALAMINI, M., BAUMGART, D. C. & SANDBORN, W. J. 2012. Ulcerative colitis. *The Lancet,* 380**,** 1606-1619.

OTMANI, K. & LEWALLE, P. 2021. Tumor Suppressor miRNA in Cancer Cells and the Tumor Microenvironment: Mechanism of Deregulation and Clinical Implications. *Front Oncol,* 11**,** 708765.

OTTOSEN, S., PARSLEY, T. B., YANG, L., ZEH, K., VAN DOORN, L. J., VAN DER VEER, E., RANEY, A. K., HODGES, M. R. & PATICK, A. K. 2015. In vitro antiviral activity and preclinical and clinical resistance profile of miravirsen, a novel anti-hepatitis C virus therapeutic targeting the human factor miR-122. *Antimicrob Agents Chemother,* 59**,** 599-608.

PAKPOOR, J. & TRAVIS, S. 2023. Why Studying Urgency Is Urgent. *Gastroenterol Hepatol (N Y),* 19**,** 95-100.

PAN, Y., YU, Y., WANG, X. & ZHANG, T. 2020. Tumor-Associated Macrophages in Tumor Immunity. *Frontiers in Immunology,* 11.

PANELLI, S., EPIS, S., COCOCCIONI, L., PERINI, M., PARONI, M., BANDI, C., DRAGO, L. & ZUCCOTTI, G. V. 2020. Inflammatory bowel diseases, the hygiene hypothesis and the other side of the microbiota: Parasites and fungi. *Pharmacological Research,* 159**,** 104962.

PARANG, B., BARRETT, C. W. & WILLIAMS, C. S. 2016. AOM/DSS Model of Colitis-Associated Cancer. *Methods Mol Biol,* 1422**,** 297-307.

PARIAN, A., LIMKETKAI, B., KOH, J., BRANT, S. R., BITTON, A., CHO, J. H., DUERR, R. H., MCGOVERN, D. P., PROCTOR, D. D., REGUEIRO, M. D., RIOUX, J. D., SCHUMM, P., TAYLOR, K. D., SILVERBERG, M. S., STEINHART, A. H., HERNAEZ, R. & LAZAREV, M. 2017. Appendectomy does not decrease the risk of future colectomy in UC: results from a large cohort and meta-analysis. *Gut,* 66**,** 1390-1397.

PASCUAL-GARCÍA, M., BONFILL-TEIXIDOR, E., PLANAS-RIGOL, E., RUBIO-PEREZ, C., IURLARO, R., ARIAS, A., CUARTAS, I., SALA-HOJMAN, A., ESCUDERO, L., MARTÍNEZ-RICARTE, F., HUBER-RUANO, I., NUCIFORO, P., PEDROSA, L., MARQUES, C., BRAÑA, I., GARRALDA, E., VIEITO, M., SQUATRITO, M., PINEDA, E., GRAUS, F., ESPEJO, C., SAHUQUILLO, J., TABERNERO, J. & SEOANE, J. 2019. LIF regulates CXCL9 in tumor-associated macrophages and prevents CD8+ T cell tumor-infiltration impairing anti-PD1 therapy. *Nature Communications,* 10.

PEKOW, J. R., DOUGHERTY, U., MUSTAFI, R., ZHU, H., KOCHERGINSKY, M., RUBIN, D. T., HANAUER, S. B., HART, J., CHANG, E. B., FICHERA, A., JOSEPH, L. J. & BISSONNETTE, M. 2012. miR-143 and miR-145 are downregulated in ulcerative colitis: Putative regulators of inflammation and protooncogenes. *Inflammatory Bowel Diseases,* 18**,** 94-100.

PENG, Y. & CROCE, C. M. 2016. The role of MicroRNAs in human cancer. *Signal Transduction and Targeted Therapy,* 1**,** 15004.

PEPPERCORN, M. & DOHERTY 2009. Update on the role of modified release mesalamine in the management of ulcerative colitis and Crohn's disease. *Clinical and Experimental Gastroenterology***,** 139.

PIAZZA, M., GUILLEMETTE, J. G. & DIECKMANN, T. 2015. Dynamics of nitric oxide synthase-calmodulin interactions at physiological calcium concentrations. *Biochemistry,* 54**,** 1989-2000.

PIERDOMENICO, M., CESI, V., CUCCHIARA, S., VITALI, R., PRETE, E., COSTANZO, M., ALOI, M., OLIVA, S. & STRONATI, L. 2016. NOD2 Is Regulated By Mir-320 in

Physiological Conditions but this Control Is Altered in Inflamed Tissues of Patients with Inflammatory Bowel Disease. *Inflammatory Bowel Diseases,* 22**,** 315-326.

PIMPO, M. T., GALLETTI, B., PALUMBO, G., VISCIDO, A., GENTILE, P., CAPRILLI, R. & FRIERI, G. 2010. Mesalazine vanishing time from rectal mucosa following its topical administration. *Journal of Crohn's and Colitis,* 4**,** 102-105.

PINATEL, E. M., ORSO, F., PENNA, E., CIMINO, D., ELIA, A. R., CIRCOSTA, P., DENTELLI, P., BRIZZI, M. F., PROVERO, P. & TAVERNA, D. 2014. miR-223 Is a Coordinator of Breast Cancer Progression as Revealed by Bioinformatics Predictions. *PLoS ONE,* 9**,** e84859.

PITTAYANON, R., LAU, J. T., LEONTIADIS, G. I., TSE, F., YUAN, Y., SURETTE, M. & MOAYYEDI, P. 2020. Differences in Gut Microbiota in Patients With vs Without Inflammatory Bowel Diseases: A Systematic Review. *Gastroenterology,* 158**,** 930-946.e1.

PIVAC, I., JELICIC KADIC, A., DESPOT, R., ZITKO, V., TUDOR, D., RUNJIC, E. & MARKIC, J. 2023. Characteristics of the Inflammatory Bowel Disease in Children: A Croatian Single-Centre Retrospective Study. *Children,* 10**,** 1677.

POLYTARCHOU, C., HOMMES, D. W., PALUMBO, T., HATZIAPOSTOLOU, M., KOUTSIOUMPA, M., KOUKOS, G., VAN DER MEULEN-DE JONG, A. E., OIKONOMOPOULOS, A., VAN DEEN, W. K., VORVIS, C., SEREBRENNIKOVA, O. B., BIRLI, E., CHOI, J., CHANG, L., ANTON, P. A., TSICHLIS, P. N., POTHOULAKIS, C., VERSPAGET, H. W. & ILIOPOULOS, D. 2015. MicroRNA214 Is Associated With Progression of Ulcerative Colitis, and Inhibition Reduces Development of Colitis and Colitis-Associated Cancer in Mice. *Gastroenterology,* 149**,** 981-992.e11.

PUGLISI, M. A., CENCIARELLI, C., TESORI, V., CAPPELLARI, M., MARTINI, M., DI FRANCESCO, A. M., GIORDA, E., CARSETTI, R., RICCI-VITIANI, L. & GASBARRINI, A. 2015a. High nitric oxide production, secondary to inducible nitric oxide synthase expression, is essential for regulation of the tumour-initiating properties of colon cancer stem cells. *J Pathol,* 236**,** 479-90.

PUGLISI, M. A., CENCIARELLI, C., TESORI, V., CAPPELLARI, M., MARTINI, M., DI FRANCESCO, A. M., GIORDA, E., CARSETTI, R., RICCI-VITIANI, L. & GASBARRINI, A. 2015b. High nitric oxide production, secondary to inducible nitric oxide synthase expression, is essential for regulation of the tumour-initiating properties of colon cancer stem cells. *The Journal of Pathology,* 236**,** 479-490.

QIN, J.-Z., WANG, S.-J. & XIA, C. 2018. microRNAs regulate nitric oxide release from endothelial cells by targeting NOS3. *Journal of Thrombosis and Thrombolysis,* 46**,** 275-282.

QIU, X., MA, J., WANG, K. & ZHANG, H. 2017. Chemopreventive effects of 5-aminosalicylic acid on inflammatory bowel disease-associated colorectal cancer and dysplasia: a systematic review with meta-analysis. *Oncotarget,* 8**,** 1031-1045.

QU, T., WANG, E., JIN, B., LI, W., LIU, R. & ZHAO, Z.-B. 2017. 5-Aminosalicylic acid inhibits inflammatory responses by suppressing JNK and p38 activity in murine macrophages. *Immunopharmacology and Immunotoxicology,* 39**,** 45-53.

QUARANTA, V. & SCHMID, M. C. 2019. Macrophage-Mediated Subversion of Anti-Tumour Immunity. *Cells,* 8**,** 747.

RAFA, H., BENKHELIFA, S., AITYOUNES, S., SAOULA, H., BELHADEF, S., BELKHELFA, M., BOUKERCHA, A., TOUMI, R., SOUFLI, I., MORALÈS, O., DE LAUNOIT, Y., MAHFOUF, H., NAKMOUCHE, M. H., DELHEM, N. & TOUIL-BOUKOFFA, C. 2017. All-Trans Retinoic Acid Modulates TLR4/NF-κB Signaling Pathway Targeting TNF-αand Nitric Oxide Synthase 2 Expression in Colonic Mucosa during Ulcerative Colitis and Colitis Associated Cancer. *Mediators of Inflammation,* 2017**,** 1-16.

RAFA, H., SAOULA, H., BELKHELFA, M., MEDJEBER, O., SOUFLI, I., TOUMI, R., DE LAUNOIT, Y., MORALÈS, O., NAKMOUCHE, M. H., DELHEM, N. & TOUIL-BOUKOFFA, C. 2013. IL-23/IL-17A Axis Correlates with the Nitric Oxide Pathway in Inflammatory Bowel Disease: Immunomodulatory Effect of Retinoic Acid. *Journal of Interferon & Cytokine Research,* 33**,** 355-368.

RAJABIAN, Z., KALANI, F., TAGHILOO, S., TEHRANI, M., RAFIEI, A., HOSSEINI-KHAH, Z., HOSSEINI, V. & AJAMI, A. 2019. Over-Expression of Immunosuppressive Molecules, PD-L1 and PD-L2, in Ulcerative Colitis Patients. *Iran J Immunol,* 16**,** 62-70.

RANDALL, J. A., GUOBYTE, A., DELBECQUE, L., NEWTON, L., SYMONDS, T. & HUNTER, T. 2020. Qualitative research to explore the symptoms and impacts experienced by children with ulcerative colitis. *Journal of Patient-Reported Outcomes,* 4.

REINECKER, H.-C., STEFFEN, M., WITTHOEFT, T., PFLUEGER, I., SCHREIBER, S., MACDERMOTT, R. P. & RAEDLER, A. 2008. Enhand secretion of tumour necrosis factor-alpha, IL-6, and IL-1β by isolated lamina ropria monouclear cells from patients with ulcretive cilitis and Crohn's disease. *Clinical and Experimental Immunology,* 94**,** 174-181.

REVÉS, J., UNGARO, R. C. & TORRES, J. 2021. Unmet needs in inflammatory bowel disease. *Curr Res Pharmacol Drug Discov,* 2**,** 100070.

ROBLES, A. I., TRAVERSO, G., ZHANG, M., ROBERTS, N. J., KHAN, M. A., JOSEPH, C., LAUWERS, G. Y., SELARU, F. M., POPOLI, M., PITTMAN, M. E., KE, X., HRUBAN, R. H., MELTZER, S. J., KINZLER, K. W., VOGELSTEIN, B., HARRIS, C. C. & PAPADOPOULOS, N. 2016. Whole-Exome Sequencing Analyses of Inflammatory Bowel Disease-Associated Colorectal Cancers. *Gastroenterology,* 150**,** 931-43.

ROKAVEC, M., ÖNER, M. G., LI, H., JACKSTADT, R., JIANG, L., LODYGIN, D., KALLER, M., HORST, D., ZIEGLER, P. K., SCHWITALLA, S., SLOTTA-HUSPENINA, J., BADER, F. G., GRETEN, F. R. & HERMEKING, H. 2014. IL-6R/STAT3/miR-34a feedback loop

promotes EMT-mediated colorectal cancer invasion and metastasis. *Journal of Clinical Investigation,* 124**,** 1853-1867.

RUTGEERTS, P., SANDBORN, W. J., FEAGAN, B. G., REINISCH, W., OLSON, A., JOHANNS, J., TRAVERS, S., RACHMILEWITZ, D., HANAUER, S. B., LICHTENSTEIN, G. R., DE VILLIERS, W. J., PRESENT, D., SANDS, B. E. & COLOMBEL, J. F. 2005. Infliximab for induction and maintenance therapy for ulcerative colitis. *N Engl J Med,* 353**,** 2462-76.

SÆTERSTAD, S., ØSTVIK, A. E., RØYSET, E. S., BAKKE, I., SANDVIK, A. K. & GRANLUND, A. V. B. 2022. Profound gene expression changes in the epithelial monolayer of active ulcerative colitis and Crohn's disease. *PLOS ONE,* 17**,** e0265189.

SAEZ, A., HERRERO-FERNANDEZ, B., GOMEZ-BRIS, R., SANCHEZ-MARTINEZ, H. & GONZALEZ-GRANADO, J. M. 2023. Pathophysiology of Inflammatory Bowel Disease: Innate Immune System. *Int J Mol Sci,* 24.

SAISONGKORH, V., MAIUTHED, A. & CHANVORACHOTE, P. 2016. Nitric oxide increases the migratory activity of non-small cell lung cancer cells via AKT-mediated integrin αv and β1 upregulation. *Cellular Oncology,* 39**,** 449-462.

SALLA, M., GUO, J., JOSHI, H., GORDON, M., DOOKY, H., LAI, J., CAPICIO, S., ARMSTRONG, H., VALCHEVA, R., DYCK, J. R. B., THIESEN, A., WINE, E., DIELEMAN, L. A. & BAKSH, S. 2023. Novel Biomarkers for Inflammatory Bowel Disease and Colorectal Cancer: An Interplay between Metabolic Dysregulation and Excessive Inflammation. *International Journal of Molecular Sciences,* 24**,** 5967.

SAMADDER, N. J., VALENTINE, J. F., GUTHERY, S., SINGH, H., BERNSTEIN, C. N., LEIGHTON, J. A., WAN, Y., WONG, J., BOUCHER, K., PAPPAS, L., ROWE, K., BURT, R. W., CURTIN, K. & SMITH, K. R. 2019. Family History Associates With Increased Risk of Colorectal Cancer in Patients With Inflammatory Bowel Diseases. *Clinical Gastroenterology and Hepatology,* 17**,** 1807-1813.e1.

SARLOS, P., KOVESDI, E., MAGYARI, L., BANFAI, Z., SZABO, A., JAVORHAZY, A. & MELEGH, B. 2014. Genetic update on inflammatory factors in ulcerative colitis: Review of the current literature. *World J Gastrointest Pathophysiol,* 5**,** 304-21.

SCALAVINO, V., LISO, M., CAVALCANTI, E., GIGANTE, I., LIPPOLIS, A., MASTRONARDI, M., CHIEPPA, M. & SERINO, G. 2020. miR-369-3p modulates inducible nitric oxide synthase and is involved in regulation of chronic inflammatory response. *Scientific Reports,* 10.

SCHECHTER, A., GRIFFITHS, C., GANA, J. C., SHAOUL, R., SHAMIR, R., SHTEYER, E., BDOLAH-ABRAM, T., LEDDER, O. & TURNER, D. 2015. Early endoscopic, laboratory and clinical predictors of poor disease course in paediatric ulcerative colitis. *Gut,* 64**,** 580.

SCHMITT, M. & GRETEN, F. R. 2021. The inflammatory pathogenesis of colorectal cancer. *Nature Reviews Immunology,* 21**,** 653-667.

SCHÖNAUEN, K., LE, N., VON ARNIM, U., SCHULZ, C., MALFERTHEINER, P. & LINK, A. 2018. Circulating and Fecal microRNAs as Biomarkers for Inflammatory Bowel Diseases. *Inflammatory Bowel Diseases,* 24**,** 1547-1557.

SCHREIBER, S., ADEN, K., BERNARDES, J. P., CONRAD, C., TRAN, F., HÖPER, H., VOLK, V., MISHRA, N., BLASE, J. I. & NIKOLAUS, S. 2021. Therapeutic interleukin-6 trans-signaling inhibition by olamkicept (sgp130Fc) in patients with active inflammatory bowel disease. *Gastroenterology,* 160**,** 2354-2366. e11.

SEGAL, J. P., LEBLANC, J.-F. & HART, A. L. 2021. Ulcerative colitis: an update. *Clinical Medicine,* 21**,** 135-139.

SHAH, S. C. & ITZKOWITZ, S. H. 2022. Colorectal Cancer in Inflammatory Bowel Disease: Mechanisms and Management. *Gastroenterology,* 162**,** 715-730 e3.

SHARMA, V., FERNANDO, V., LETSON, J., WALIA, Y., ZHENG, X., FACKELMAN, D. & FURUTA, S. 2021. S-Nitrosylation in Tumor Microenvironment. *International Journal of Molecular Sciences,* 22**,** 4600.

SHEAHAN, B. J., FREEMAN, A. N., KEELEY, T. M., SAMUELSON, L. C., ROPER, J., HASAPIS, S., LEE, C.-L. & DEKANEY, C. M. 2021. Epithelial Regeneration After Doxorubicin Arises Primarily From Early Progeny of Active Intestinal Stem Cells. *Cellular and Molecular Gastroenterology and Hepatology,* 12**,** 119-140.

SHEEHAN, D., MORAN, C. & SHANAHAN, F. 2015. The microbiota in inflammatory bowel disease. *Journal of Gastroenterology,* 50**,** 495-507.

SHENG, Y. H., DAVIES, J. M., WANG, R., WONG, K. Y., GIRI, R., YANG, Y., BEGUN, J., FLORIN, T. H., HASNAIN, S. Z. & MCGUCKIN, M. A. 2022. MUC1-mediated macrophage activation promotes colitis-associated colorectal cancer via activating the interleukin-6/signal transducer and activator of transcription 3 axis. *Cellular and Molecular Gastroenterology and Hepatology,* 14**,** 789-811.

SHI, C., YANG, Y., XIA, Y., OKUGAWA, Y., YANG, J., LIANG, Y., CHEN, H., ZHANG, P., WANG, F., HAN, H., WU, W., GAO, R., GASCHE, C., QIN, H., MA, Y. & GOEL, A. 2016. Novel evidence for an oncogenic role of microRNA-21 in colitis-associated colorectal cancer. *Gut,* 65**,** 1470-1481.

SHI, T., XIE, Y., FU, Y., ZHOU, Q., MA, Z., MA, J., HUANG, Z., ZHANG, J. & CHEN, J. 2017. The signaling axis of microRNA-31/interleukin-25 regulates Th1/Th17-mediated inflammation response in colitis. *Mucosal Immunology,* 10**,** 983-995.

SINGH, S. B., CARROLL-PORTILLO, A. & LIN, H. C. 2023. Desulfovibrio in the Gut: The Enemy within? *Microorganisms,* 11.

SJÖBERG, F., BARKMAN, C., NOOKAEW, I., ÖSTMAN, S., ADLERBERTH, I., SAALMAN, R. & WOLD, A. E. 2017. Low-complexity microbiota in the duodenum of children with newly diagnosed ulcerative colitis. *PLOS ONE,* 12**,** e0186178.

SKAFI, N., FAYYAD-KAZAN, M. & BADRAN, B. 2020. Immunomodulatory role for MicroRNAs: Regulation of PD-1/PD-L1 and CTLA-4 immune checkpoints expression. *Gene,* 754**,** 144888.

SOLITANO, V., D'AMICO, F., ZACHAROPOULOU, E., PEYRIN-BIROULET, L. & DANESE, S. 2020. Early Intervention in Ulcerative Colitis: Ready for Prime Time? *Journal of Clinical Medicine,* 9**,** 2646.

SOON, I. S., MOLODECKY, N. A., RABI, D. M., GHALI, W. A., BARKEMA, H. W. & KAPLAN, G. G. 2012. The relationship between urban environment and the inflammatory bowel diseases: a systematic review and meta-analysis. *BMC Gastroenterology,* 12**,** 51.

SOUFLI, I., TOUMI, R., RAFA, H. & TOUIL-BOUKOFFA, C. 2016. Overview of cytokines and nitric oxide involvement in immuno-pathogenesis of inflammatory bowel diseases. *World J Gastrointest Pharmacol Ther,* 7**,** 353-60.

SPENCER, J. & BEMARK, M. 2023. Human intestinal B cells in inflammatory diseases. *Nature Reviews. Gastroenterology & Hepatology,* 20**,** 254-265.

STRACHAN, D. P. 1989. Hay fever, hygiene, and household size. *Bmj,* 299**,** 1259-60.

SU, X., YU, Y., ZHONG, Y., GIANNOPOULOU, E. G., HU, X., LIU, H., CROSS, J. R., RÄTSCH, G., RICE, C. M. & IVASHKIV, L. B. 2015. Interferon-γ regulates cellular metabolism and mRNA translation to potentiate macrophage activation. *Nat Immunol,* 16**,** 838-849.

SUN, D., WANG, C., LONG, S., MA, Y., GUO, Y., HUANG, Z., CHEN, X., ZHANG, C., CHEN, J. & ZHANG, J. 2015. C/EBP-β-activated microRNA-223 promotes tumour growth through targeting RASA1 in human colorectal cancer. *British Journal of Cancer,* 112**,** 1491-1500.

SUN, J., STEENBERGEN, C. & MURPHY, E. 2006. S-Nitrosylation: NO-Related Redox Signaling to Protect Against Oxidative Stress. *Antioxidants & Redox Signaling,* 8**,** 1693-1705.

SUN, W., GAO, J., YANG, B., CHEN, X., KANG, N. & LIU, W. 2023. Protocol for colitis-associated colorectal cancer murine model induced by AOM and DSS. *STAR Protocols,* 4**,** 102105.

SUN, W., SHEN, W., YANG, S., HU, F., LI, H. & ZHU, T.-H. 2010. miR-223 and miR-142 attenuate hematopoietic cell proliferation, and miR-223 positively regulates miR-142 through LMO2 isoforms and CEBP-β. *Cell Research,* 20**,** 1158-1169.

SUNG, H., FERLAY, J., SIEGEL, R. L., LAVERSANNE, M., SOERJOMATARAM, I., JEMAL, A. & BRAY, F. 2021. Global Cancer Statistics 2020: GLOBOCAN Estimates of Incidence and Mortality Worldwide for 36 Cancers in 185 Countries. *CA: A Cancer Journal for Clinicians,* 71**,** 209-249.

SUSZYNSKA, M., MACHOWSKA, M., FRASZCZYK, E., MICHALCZYK, M., PHILIPS, A., GALKA-MARCINIAK, P. & KOZLOWSKI, P. 2024. CMC: Cancer miRNA Census – a list of cancer-related miRNA genes. *Nucleic Acids Research,* 52**,** 1628-1644.

TAKASHIMA, S., MARTIN, M. L., JANSEN, S. A., FU, Y., BOS, J., CHANDRA, D., O'CONNOR, M. H., MERTELSMANN, A. M., VINCI, P., KUTTIYARA, J., DEVLIN, S. M., MIDDENDORP, S., CALAFIORE, M., EGOROVA, A., KLEPPE, M., LO, Y., SHROYER, N. F., CHENG, E. H., LEVINE, R. L., LIU, C., KOLESNICK, R., LINDEMANS, C. A. & HANASH, A. M. 2019a. T cell-derived interferon-γ programs stem cell death in immune-mediated intestinal damage. *Sci Immunol,* 4.

TAKASHIMA, S., MARTIN, M. L., JANSEN, S. A., FU, Y., BOS, J., CHANDRA, D., O'CONNOR, M. H., MERTELSMANN, A. M., VINCI, P., KUTTIYARA, J., DEVLIN, S. M., MIDDENDORP, S., CALAFIORE, M., EGOROVA, A., KLEPPE, M., LO, Y., SHROYER, N. F., CHENG, E. H., LEVINE, R. L., LIU, C., KOLESNICK, R., LINDEMANS, C. A. & HANASH, A. M. 2019b. T cell–derived interferon-γ programs stem cell death in immune-mediated intestinal damage. *Science Immunology,* 4**,** eaay8556.

TANG, B., ZHU, J., FANG, S., WANG, Y., VINOTHKUMAR, R., LI, M., WENG, Q., ZHENG, L., YANG, Y., QIU, R., XU, M., ZHAO, Z. & JI, J. 2021a. Pharmacological inhibition of MELK restricts ferroptosis and the inflammatory response in colitis and colitis-propelled carcinogenesis. *Free Radical Biology and Medicine,* 172**,** 312-329.

TANG, S., GUO, W., KANG, L. & LIANG, J. 2021b. MiRNA-182-5p aggravates experimental ulcerative colitis via sponging Claudin-2. *Journal of Molecular Histology,* 52**,** 1215-1224.

TEMBY, M., BOYE, T. L., HOANG, J., NIELSEN, O. H. & GUBATAN, J. 2023. Kinase Signaling in Colitis-Associated Colon Cancer and Inflammatory Bowel Disease. *Biomolecules,* 13**,** 1620.

THOMAS, D. D. & WINK, D. A. 2017. NOS2 as an Emergent Player in Progression of Cancer. *Antioxidants & Redox Signaling,* 26**,** 963-965.

THOMAS, T., ABRAMS, K. A., ROBINSON, R. J. & MAYBERRY, J. F. 2007. Meta-analysis: cancer risk of low-grade dysplasia in chronic ulcerative colitis. *Alimentary Pharmacology & Therapeutics,* 25**,** 657-668.

THOMPSON, A. I. & LEES, C. W. 2010. Genetics of ulcerative colitis. *Inflammatory Bowel Diseases,* 17**,** 831-848.

THOMSEN, L. L., SCOTT, J. M., TOPLEY, P., KNOWLES, R. G., KEERIE, A.-J. & FREND, A. J. 1997. Selective inhibition of inducible nitric oxide synthase inhibits tumor growth in vivo: studies with 1400W, a novel inhibitor. *Cancer research,* 57**,** 3300-3304.

TRAN, T.-H., KRISHNAN, S. & AMIJI, M. M. 2016. MicroRNA-223 Induced Repolarization of Peritoneal Macrophages Using CD44 Targeting Hyaluronic Acid Nanoparticles for Anti-Inflammatory Effects. *PLOS ONE,* 11**,** e0152024.

TRANG, P., WIGGINS, J. F., DAIGE, C. L., CHO, C., OMOTOLA, M., BROWN, D., WEIDHAAS, J. B., BADER, A. G. & SLACK, F. J. 2011. Systemic Delivery of Tumor Suppressor

microRNA Mimics Using a Neutral Lipid Emulsion Inhibits Lung Tumors in Mice. *Molecular Therapy,* 19**,** 1116-1122.

TURNER, D., HYAMS, J., MARKOWITZ, J., LERER, T., MACK, D. R., EVANS, J., PFEFFERKORN, M., ROSH, J., KAY, M., CRANDALL, W., KELJO, D., OTLEY, A. R., KUGATHASAN, S., CARVALHO, R., OLIVA-HEMKER, M., LANGTON, C., MAMULA, P., BOUSVAROS, A., LELEIKO, N. & GRIFFITHS, A. M. 2009. Appraisal of the pediatric ulcerative colitis activity index (PUCAI). *Inflammatory Bowel Diseases,* 15**,** 1218-1223.

TURNER, D., RUEMMELE, F. M., ORLANSKI-MEYER, E., GRIFFITHS, A. M., DE CARPI, J. M., BRONSKY, J., VERES, G., ALOI, M., STRISCIUGLIO, C., BRAEGGER, C. P., ASSA, A., ROMANO, C., HUSSEY, S., STANTON, M., PAKARINEN, M., DE RIDDER, L., KATSANOS, K. H., CROFT, N., NAVAS-LÓPEZ, V. M., WILSON, D. C., LAWRENCE, S. & RUSSELL, R. K. 2018. Management of Paediatric Ulcerative Colitis, Part 2. *Journal of Pediatric Gastroenterology and Nutrition,* 67**,** 292-310.

UNGARO, R., MEHANDRU, S., ALLEN, P. B., PEYRIN-BIROULET, L. & COLOMBEL, J. F. 2017. Ulcerative colitis. *Lancet,* 389**,** 1756-1770.

VAN LIMBERGEN, J., RUSSELL, R. K., DRUMMOND, H. E., ALDHOUS, M. C., ROUND, N. K., NIMMO, E. R., SMITH, L., GILLETT, P. M., MCGROGAN, P., WEAVER, L. T., BISSET, W. M., MAHDI, G., ARNOTT, I. D., SATSANGI, J. & WILSON, D. C. 2008. Definition of Phenotypic Characteristics of Childhood-Onset Inflammatory Bowel Disease. *Gastroenterology,* 135**,** 1114-1122.

VELTKAMP, C., ANSTAETT, M., WAHL, K., MÖLLER, S., GANGL, S., BACHMANN, O., HARDTKE-WOLENSKI, M., LÄNGER, F., STREMMEL, W., MANNS, M. P., SCHULZE-OSTHOFF, K. & BANTEL, H. 2011. Apoptosis of regulatory T lymphocytes is increased in chronic inflammatory bowel disease and reversed by anti-TNFα treatment. *Gut,* 60**,** 1345-1353.

VERSTOCKT, S., VERSTOCKT, B., MACHIELS, K., VANCAMELBEKE, M., FERRANTE, M., CLEYNEN, I., DE HERTOGH, G. & VERMEIRE, S. 2021. Oncostatin M Is a Biomarker of Diagnosis, Worse Disease Prognosis, and Therapeutic Nonresponse in Inflammatory Bowel Disease. *Inflammatory Bowel Diseases,* 27**,** 1564-1575.

VIENNOIS, E., CHEN, F. & MERLIN, D. 2013. NF-κB pathway in colitis-associated cancers. *Transl Gastrointest Cancer,* 2**,** 21-29.

VON LAMPE, B. 2000. Differential expression of matrix metalloproteinases and their tissue inhibitors in colon mucosa of patients with inflammatory bowel disease. *Gut,* 47**,** 63-73.

WALSH, K. T. & ZEMPER, A. E. 2019. The Enteric Nervous System for Epithelial Researchers: Basic Anatomy, Techniques, and Interactions With the Epithelium. *Cellular and Molecular Gastroenterology and Hepatology,* 8**,** 369-378.

WANG, F. F., ZHANG, X. J., YAN, Y. R., ZHU, X. H., YU, J., DING, Y., HU, J. L., ZHOU, W. J., ZENG, Z. C., LIAO, W. T., DING, Y. Q. & LIANG, L. 2017a. FBX8 is a metastasis suppressor downstream of miR-223 and targeting mTOR for degradation in colorectal carcinoma. *Cancer Lett,* 388**,** 85-95.

WANG, H., TIAN, T. & ZHANG, J. 2021a. Tumor-Associated Macrophages (TAMs) in Colorectal Cancer (CRC): From Mechanism to Therapy and Prognosis. *International Journal of Molecular Sciences,* 22**,** 8470.

WANG, H., WANG, D. H., YANG, X., SUN, Y. & YANG, C. S. 2021b. Colitis-induced IL11 promotes colon carcinogenesis. *Carcinogenesis,* 42**,** 557-569.

WANG, H., ZHANG, S., YU, Q., YANG, G., GUO, J., LI, M., ZENG, Z., HE, Y., CHEN, B. & CHEN, M. 2016a. Circulating MicroRNA223 is a New Biomarker for Inflammatory Bowel Disease. *Medicine (Baltimore),* 95**,** e2703.

WANG, J., HE, P., GAIDA, M., YANG, S., SCHETTER, A. J., GAEDCKE, J., GHADIMI, B. M., RIED, T., YFANTIS, H., LEE, D., WEISS, J. M., STAUFFER, J., HANNA, N., ALEXANDER, H. R. & HUSSAIN, S. P. 2016b. Inducible nitric oxide synthase enhances disease aggressiveness in pancreatic cancer. *Oncotarget,* 7**,** 52993-53004.

WANG, K., WANG, Y. & YIN, K. 2024. Role played by MDSC in colitis-associated colorectal cancer and potential therapeutic strategies. *Journal of Cancer Research and Clinical Oncology,* 150.

WANG, M., GUO, J., ZHAO, Y.-Q. & WANG, J.-P. 2020a. IL-21 mediates microRNA-423-5p /claudin-5 signal pathway and intestinal barrier function in inflammatory bowel disease. *Aging,* 12**,** 16099-16110.

WANG, M., ZHAO, J., ZHANG, L., WEI, F., LIAN, Y., WU, Y., GONG, Z., ZHANG, S., ZHOU, J., CAO, K., LI, X., XIONG, W., LI, G., ZENG, Z. & GUO, C. 2017b. Role of tumor microenvironment in tumorigenesis. *Journal of Cancer,* 8**,** 761-773.

WANG, M.-H., FIOCCHI, C., ZHU, X., RIPKE, S., KAMBOH, M. I., REBERT, N., DUERR, R. H. & ACHKAR, J.-P. 2014a. Gene–gene and gene–environment interactions in ulcerative colitis. *Human Genetics,* 133**,** 547-558.

WANG, T., FAHRMANN, J. F., LEE, H., LI, Y.-J., TRIPATHI, S. C., YUE, C., ZHANG, C., LIFSHITZ, V., SONG, J. & YUAN, Y. 2018a. JAK/STAT3-regulated fatty acid β-oxidation is critical for breast cancer stem cell self-renewal and chemoresistance. *Cell metabolism,* 27**,** 136-150. e5.

WANG, T., XU, X., XU, Q., REN, J., SHEN, S., FAN, C. & HOU, Y. 2017c. miR-19a promotes colitis-associated colorectal cancer by regulating tumor necrosis factor alpha-induced protein 3-NF-κB feedback loops. *Oncogene,* 36**,** 3240-3251.

WANG, X., ZHU, Y., ZHANG, M., WANG, H., JIANG, Y. & GAO, P. 2016c. Ulcerative Colitis Is Characterized by a Decrease in Regulatory B Cells. *Journal of Crohn's and Colitis,* 10**,** 1212-1223.

WANG, X.-J., ZHANG, D., YANG, Y.-T., LI, X.-Y., LI, H.-N., ZHANG, X.-P., LONG, J.-Y., LU, Y.-Q., LIU, L., YANG, G., LIU, J., HONG, J., WU, H.-G. & MA, X.-P. 2023. Suppression of microRNA-222-3p ameliorates ulcerative colitis and colitis-associated colorectal cancer to protect against oxidative stress via targeting BRG1 to activate Nrf2/HO-1 signaling pathway. *Frontiers in Immunology,* 14.

WANG, Y., DING, Y., DENG, Y., ZHENG, Y. & WANG, S. 2020b. Role of myeloid-derived suppressor cells in the promotion and immunotherapy of colitis-associated cancer. *Journal for ImmunoTherapy of Cancer,* 8**,** e000609.

WANG, Y., SHEN, Y., WANG, S., SHEN, Q. & ZHOU, X. 2018b. The role of STAT3 in leading the crosstalk between human cancers and the immune system. *Cancer letters,* 415**,** 117-128.

WANG, Y., SHI, S., WANG, Y., ZHANG, X., LIU, X., LI, J., LI, P., DU, L. & WANG, C. 2022. miR-223-3p targets FBXW7 to promote epithelial-mesenchymal transition and metastasis in breast cancer. *Thoracic Cancer,* 13**,** 474-482.

WANG, Y., WANG, K., HAN, G.-C., WANG, R.-X., XIAO, H., HOU, C.-M., GUO, R.-F., DOU, Y., SHEN, B.-F., LI, Y. & CHEN, G.-J. 2014b. Neutrophil infiltration favors colitis-associated tumorigenesis by activating the interleukin-1 (IL-1)/IL-6 axis. *Mucosal Immunology,* 7**,** 1106-1115.

WANG, Z., LI, S., CAO, Y., TIAN, X., ZENG, R., LIAO, D.-F. & CAO, D. 2016d. Oxidative Stress and Carbonyl Lesions in Ulcerative Colitis and Associated Colorectal Cancer. *Oxidative Medicine and Cellular Longevity,* 2016**,** 1-15.

WEBER, J. A., BAXTER, D. H., ZHANG, S., HUANG, D. Y., HUANG, K. H., LEE, M. J., GALAS, D. J. & WANG, K. 2010. The microRNA spectrum in 12 body fluids. *Clin Chem,* 56**,** 1733-41.

WEI, N., LI, J., FANG, C., CHANG, J., XIROU, V., SYRIGOS, N. K., MARKS, B. J., CHU, E. & SCHMITZ, J. C. 2019. Targeting colon cancer with the novel STAT3 inhibitor bruceantinol. *Oncogene,* 38**,** 1676-1687.

WEN, C., CHEN, D., ZHONG, R. & PENG, X. 2024. Animal models of inflammatory bowel disease: category and evaluation indexes. *Gastroenterol Rep (Oxf),* 12**,** goae021.

WÉRA, O., LANCELLOTTI, P. & OURY, C. 2016. The Dual Role of Neutrophils in Inflammatory Bowel Diseases. *Journal of Clinical Medicine,* 5**,** 118.

WEST, N. R., HEGAZY, A. N., OWENS, B. M. J., BULLERS, S. J., LINGGI, B., BUONOCORE, S., COCCIA, M., GÖRTZ, D., THIS, S., STOCKENHUBER, K., POTT, J., FRIEDRICH, M., RYZHAKOV, G., BARIBAUD, F., BRODMERKEL, C., CIELUCH, C., RAHMAN, N., MÜLLER-NEWEN, G., OWENS, R. J., KÜHL, A. A., MALOY, K. J., PLEVY, S. E.,

KESHAV, S., TRAVIS, S. P. L. & POWRIE, F. 2017. Oncostatin M drives intestinal inflammation and predicts response to tumor necrosis factor–neutralizing therapy in patients with inflammatory bowel disease. *Nature Medicine,* 23**,** 579-589.

WIGHTMAN, B., HA, I. & RUVKUN, G. 1993. Posttranscriptional regulation of the heterochronic gene lin-14 by lin-4 mediates temporal pattern formation in C. elegans. *Cell,* 75**,** 855-862.

WIJNANDS, A. M., DE JONG, M. E., LUTGENS, M. W. M. D., HOENTJEN, F., ELIAS, S. G. & OLDENBURG, B. 2021. Prognostic Factors for Advanced Colorectal Neoplasia in Inflammatory Bowel Disease: Systematic Review and Meta-analysis. *Gastroenterology,* 160**,** 1584-1598.

WINK, D. A., HINES, H. B., CHENG, R. Y., SWITZER, C. H., FLORES-SANTANA, W., VITEK, M. P., RIDNOUR, L. A. & COLTON, C. A. 2011. Nitric oxide and redox mechanisms in the immune response. *J Leukoc Biol,* 89**,** 873-91.

WONG, Q. W. L., LUNG, R. W. M., LAW, P. T. Y., LAI, P. B. S., CHAN, K. Y. Y., TO, K. F. & WONG, N. 2008. MicroRNA-223 Is Commonly Repressed in Hepatocellular Carcinoma and Potentiates Expression of Stathmin1. *Gastroenterology,* 135**,** 257-269.

WORKMAN, C. J., SZYMCZAK-WORKMAN, A. L., COLLISON, L. W., PILLAI, M. R. & VIGNALI, D. A. 2009. The development and function of regulatory T cells. *Cell Mol Life Sci,* 66**,** 2603-22.

WU, F., ZIKUSOKA, M., TRINDADE, A., DASSOPOULOS, T., HARRIS, M. L., BAYLESS, T. M., BRANT, S. R., CHAKRAVARTI, S. & KWON, J. H. 2008. MicroRNAs Are Differentially Expressed in Ulcerative Colitis and Alter Expression of Macrophage Inflammatory Peptide-2α. *Gastroenterology,* 135**,** 1624-1635.e24.

WU, M.-Y., LUO, Y.-X., JIA, W.-X., WANG, D.-D., SUN, D.-L., SONG, J., WANG, J., NIU, W.-W. & ZHANG, X.-L. 2022a. miRNA-320 inhibits colitis-associated colorectal cancer by regulating the IL-6R/STAT3 pathway in mice. *Journal of Gastrointestinal Oncology,* 13**,** 695.

WU, M. Y., LUO, Y. X., JIA, W. X., WANG, D. D., SUN, D. L., SONG, J., WANG, J., NIU, W. W. & ZHANG, X. L. 2022b. miRNA-320 inhibits colitis-associated colorectal cancer by regulating the IL-6R/STAT3 pathway in mice. *J Gastrointest Oncol,* 13**,** 695-709.

XIE, R., GU, Y., LI, M., LI, L., YANG, Y., SUN, Y., ZHOU, B., LIU, T., WANG, S., LIU, W., YANG, R., SU, X., ZHONG, W., WANG, B. & CAO, H. 2024. Desulfovibrio vulgaris interacts with novel gut epithelial immune receptor LRRC19 and exacerbates colitis. *Microbiome,* 12**,** 4.

XIONG, Y., UYS, J. D., TEW, K. D. & TOWNSEND, D. M. 2011. S-Glutathionylation: From Molecular Mechanisms to Health Outcomes. *Antioxidants & Redox Signaling,* 15**,** 233-270.

XU, L., LOCHHEAD, P., KO, Y., CLAGGETT, B., LEONG, R. W. & ANANTHAKRISHNAN, A. N. 2017. Systematic review with meta-analysis: breastfeeding and the risk of Crohn's disease and ulcerative colitis. *Alimentary Pharmacology & Therapeutics,* 46**,** 780-789.

YAGIHASHI, N., KASAJIMA, H., SUGAI, S., MATSUMOTO, K., EBINA, Y., MORITA, T., MURAKAMI, T. & YAGIHASHI, S. 2000. Increased in situ expression of nitric oxide synthase in human colorectal cancer. *Virchows Archiv,* 436**,** 109-114.

YAGIZ, K., RODRIGUEZ-AGUIRRE, M. E., LOPEZ ESPINOZA, F., MONTELLANO, T. T., MENDOZA, D., MITCHELL, L. A., IBANEZ, C. E., KASAHARA, N., GRUBER, H. E., JOLLY, D. J. & ROBBINS, J. M. 2018. A Retroviral Replicating Vector Encoding Cytosine Deaminase and 5-FC Induces Immune Memory in Metastatic Colorectal Cancer Models. *Mol Ther Oncolytics,* 8**,** 14-26.

YAHAYA, M. A. F., LILA, M. A. M., ISMAIL, S., ZAINOL, M. & AFIZAN, N. A. R. N. M. 2019. Tumour-Associated Macrophages (TAMs) in Colon Cancer and How to Reeducate Them. *Journal of Immunology Research,* 2019**,** 2368249.

YAN, Y., LU, K., YE, T. & ZHANG, Z. 2019. MicroRNA-223 attenuates LPS-induced inflammation in an acute lung injury model via the NLRP3 inflammasome and TLR4/NF-κB signaling pathway via RHOB. *International Journal of Molecular Medicine*.

YANG, J.-S. & LAI, E. C. 2011. Alternative miRNA biogenesis pathways and the interpretation of core miRNA pathway mutants. *Molecular cell,* 43**,** 892-903.

YANG, Y., DING, L., HU, Q., XIA, J., SUN, J., WANG, X., XIONG, H., GURBANI, D., LI, L., LIU, Y. & LIU, A. 2017. MicroRNA-218 functions as a tumor suppressor in lung cancer by targeting IL-6/STAT3 and negatively correlates with poor prognosis. *Molecular Cancer,* 16.

YANG, Y., FU, K. Z. & PAN, G. 2024. Role of Oncostatin M in the prognosis of inflammatory bowel disease: A meta-analysis. *World J Gastrointest Surg,* 16**,** 228-238.

YANG, Y., LI, L., XU, C., WANG, Y., WANG, Z., CHEN, M., JIANG, Z., PAN, J., YANG, C., LI, X., SONG, K., YAN, J., XIE, W., WU, X., CHEN, Z., YUAN, Y., ZHENG, S., YAN, J., HUANG, J. & QIU, F. 2021a. Cross-talk between the gut microbiota and monocyte-like macrophages mediates an inflammatory response to promote colitis-associated tumourigenesis. *Gut,* 70**,** 1495-1506.

YANG, Z., IJAZ, K. & ESEBUA, M. 2023. Molecular Testing Using ThyGeNEXT/ThyraMIR in Thyroid Nodules with Indeterminate Cytology: A Single Medical Institute Experience. *Journal of the American Society of Cytopathology,* 12**,** S58.

YANG, Z.-J., WANG, B.-Y., WANG, T.-T., WANG, F.-F., GUO, Y.-X., HUA, R.-X., SHANG, H.-W., LU, X. & XU, J.-D. 2021b. Functions of Dendritic Cells and Its Association with Intestinal Diseases. *Cells,* 10**,** 583.

YAO, D., DAI, W., DONG, M., DAI, C. & WU, S. 2021. MUC2 and related bacterial factors: Therapeutic targets for ulcerative colitis. *eBioMedicine,* 74**,** 103751.

YAO, D., DONG, M., DAI, C. & WU, S. 2019a. Inflammation and Inflammatory Cytokine Contribute to the Initiation and Development of Ulcerative Colitis and Its Associated Cancer. *Inflammatory Bowel Diseases,* 25**,** 1595-1602.

YAO, Y., XU, X.-H. & JIN, L. 2019b. Macrophage Polarization in Physiological and Pathological Pregnancy. *Frontiers in Immunology,* 10.

YARANI, R., SHOJAEIAN, A., PALASCA, O., DONCHEVA, N. T., JENSEN, L. J., GORODKIN, J. & POCIOT, F. 2022. Differentially Expressed miRNAs in Ulcerative Colitis and Crohn's Disease. *Frontiers in Immunology,* 13.

YASSIN, M., SADOWSKA, Z., DJURHUUS, D., NIELSEN, B., TOUGAARD, P., OLSEN, J. & PEDERSEN, A. E. 2019. Upregulation of PD-1 follows tumour development in the AOM/DSS model of inflammation-induced colorectal cancer in mice. *Immunology,* 158**,** 35-46.

YE, D., ZHANG, T., LOU, G. & LIU, Y. 2018. Role of miR-223 in the pathophysiology of liver diseases. *Experimental & Molecular Medicine,* 50**,** 1-12.

YE, J., XU, M., TIAN, X., CAI, S. & ZENG, S. 2019. Research advances in the detection of miRNA. *Journal of Pharmaceutical Analysis,* 9**,** 217-226.

YI, M., XU, L., JIAO, Y., LUO, S., LI, A. & WU, K. 2020. The role of cancer-derived microRNAs in cancer immune escape. *Journal of Hematology & Oncology,* 13.

YIN, N., QI, X., TSAI, S., LU, Y., BASIR, Z., OSHIMA, K., THOMAS, J. P., MYERS, C. R., STONER, G. & CHEN, G. 2016. p38γ MAPK is required for inflammation-associated colon tumorigenesis. *Oncogene,* 35**,** 1039-1048.

YIN, Y., WAN, J., YU, J. & WU, K. 2023. Molecular Pathogenesis of Colitis-associated Colorectal Cancer: Immunity, Genetics, and Intestinal Microecology. *Inflammatory Bowel Diseases,* 29**,** 1648-1657.

YING, L., DU, L., ZOU, R., SHI, L., ZHANG, N., JIN, J., XU, C., ZHANG, F., ZHU, C., WU, J., CHEN, K., HUANG, M., WU, Y., ZHANG, Y., ZHENG, W., PAN, X., CHEN, B., LIN, A., TAM, J. K. C., VAN DAM, R. M., LAI, D. T. M., CHIA, K. S., ZHOU, L., TOO, H.-P., YU, H., MAO, W. & SU, D. 2020. Development of a serum miRNA panel for detection of early stage non-small cell lung cancer. *Proceedings of the National Academy of Sciences,* 117**,** 25036-25042.

YU, H., YUE, X., ZHAO, Y., LI, X., WU, L., ZHANG, C., LIU, Z., LIN, K., XU-MONETTE, Z. Y., YOUNG, K. H., LIU, J., SHEN, Z., FENG, Z. & HU, W. 2014. LIF negatively regulates tumour-suppressor p53 through Stat3/ID1/MDM2 in colorectal cancers. *Nature Communications,* 5**,** 5218.

YU, L.-B. 2005. Effect of a nitric oxide synthase inhibitor NG-nitro-L-arginine methyl ester on invasion of human colorectal cancer cell line SL-174T. *World Journal of Gastroenterology,* 11**,** 6385.

YUAN, S., WU, Q., WANG, Z., CHE, Y., ZHENG, S., CHEN, Y., ZHONG, X. & SHI, F. 2021. miR-223: An Immune Regulator in Infectious Disorders. *Front Immunol,* 12**,** 781815.

YUAN, X., BERG, N., LEE, J. W., LE, T.-T., NEUDECKER, V., JING, N. & ELTZSCHIG, H. 2018. MicroRNA miR-223 as regulator of innate immunity. *Journal of Leukocyte Biology,* 104**,** 515-524.

YUKSEL, E. S., TOPAL, F., GÜR, Ö., TOPAL, F., KARAHANLÝ, C. & URAN, B. 2019. IL-17 and IL-22 in colitis associated colorectal cancer in mice. *Medical Science,* 23**,** 375-380.

ZAFIRELLIS, K., ZACHAKI, A., AGROGIANNIS, G. & GRAVANI, K. 2010. Inducible nitric oxide synthase expression and its prognostic significance in colorectal cancer. *APMIS,* 118**,** 115-24.

ZENG, J., TANG, Z. H., LIU, S. & GUO, S. S. 2017. Clinicopathological significance of overexpression of interleukin-6 in colorectal cancer. *World J Gastroenterol,* 23**,** 1780-1786.

ZENG, W. P. 2013. 'All things considered': transcriptional regulation of <scp>T</scp> helper type 2 cell differentiation from precursor to effector activation. *Immunology,* 140**,** 31-38.

ZENGIN, M., ZERGEROĞLU, S., OKCU, O. & BENEK, S. 2021. PD-1 and PD-L2 expression predict relapse risk and poor survival in patients with stage III colorectal cancer. *Cellular Oncology,* 44**,** 423-432.

ZEVE, D., STAS, E., DE SOUSA CASAL, J., MANNAM, P., QI, W., YIN, X., DUBOIS, S., SHAH, M. S., SYVERSON, E. P., HAFNER, S., KARP, J. M., CARLONE, D. L., ORDOVAS-MONTANES, J. & BREAULT, D. T. 2022. Robust differentiation of human enteroendocrine cells from intestinal stem cells. *Nature Communications,* 13.

ZHANG, B., PAN, X., COBB, G. P. & ANDERSON, T. A. 2007. microRNAs as oncogenes and tumor suppressors. *Developmental biology,* 302**,** 1-12.

ZHANG, H., WANG, X., ZHAO, L., ZHANG, K., CUI, J. & XU, G. 2024a. Biochanin a ameliorates DSS-induced ulcerative colitis by improving colonic barrier function and protects against the development of spontaneous colitis in the Muc2 deficient mice. *Chemico-Biological Interactions,* 395**,** 111014.

ZHANG, J., LUO, X., LI, H., YUE, X., DENG, L., CUI, Y. & LU, Y. 2014. MicroRNA-223 functions as an oncogene in human colorectal cancer cells. *Oncology Reports,* 32**,** 115-120.

ZHANG, J., WANG, C., GUO, Z., DA, B., ZHU, W. & LI, Q. 2021a. miR-223 improves intestinal inflammation through inhibiting the IL-6/STAT3 signaling pathway in dextran sodium sulfate-induced experimental colitis. *Immunity, Inflammation and Disease,* 9**,** 319-327.

ZHANG, K., ZAKERI, A., ALBAN, T., DONG, J., TA, H. M., ZALAVADIA, A. H., BRANICKY, A., ZHAO, H., JURIC, I., HUSIC, H., PARTHASARATHY, P. B., RUPANI, A., DRAZBA, J. A., CHAKRABORTY, A. A., CHING-CHENG HUANG, S., CHAN, T., AVRIL, S. & WANG, L. L. 2024b. VISTA promotes the metabolism and differentiation of myeloid-derived suppressor cells by STAT3 and polyamine-dependent mechanisms. *Cell Reports,* 43**,** 113661.

ZHANG, K. W., WANG, D., CAI, H., CAO, M. Q., ZHANG, Y. Y., ZHUANG, P. Y. & SHEN, J. 2021b. IL-6 plays a crucial role in epithelial-mesenchymal transition and pro-metastasis induced by sorafenib in liver cancer. *Oncology Reports,* 45**,** 1105-1117.

ZHANG, L.-Z., XUE, H., QIAO, C.-X., YOU, W.-L., DI, A.-T. & ZHAO, G. 2021c. MiR-223 promotes pyroptosis of enteritis cells through activating NF-κB signalling pathway by targeting SNIP1 in inflammatory bowel disease. *Autoimmunity,* 54**,** 362-372.

ZHANG, M., LI, X., ZHANG, Q., YANG, J. & LIU, G. 2023a. Roles of macrophages on ulcerative colitis and colitis-associated colorectal cancer. *Frontiers in Immunology,* 14.

ZHANG, M., LI, X., ZHANG, Q., YANG, J. & LIU, G. 2023b. Roles of macrophages on ulcerative colitis and colitis-associated colorectal cancer. *Front Immunol,* 14**,** 1103617.

ZHANG, M., ZHOU, L., XU, Y., YANG, M., XU, Y., KOMANIECKI, G. P., KOSCIUK, T., CHEN, X., LU, X., ZOU, X., LINDER, M. E. & LIN, H. 2020. A STAT3 palmitoylation cycle promotes TH17 differentiation and colitis. *Nature,* 586**,** 434-439.

ZHANG, Q., LIN, L., LI, W., LU, G. & LI, X. 2019a. MiR-223 inhibitor suppresses proliferation and induces apoptosis of thyroid cancer cells by down-regulating aquaporin-1. *Journal of Receptors and Signal Transduction,* 39**,** 146-153.

ZHANG, R.-F., LIU, S., WANG, Y.-W., LI, J., YIN, Y.-J. & HAO, X.-Y. 2021d. Potential molecular biomarkers used to predict the response to biological therapies in ulcerative colitis. *Chinese Medical Journal,* 134**,** 1058-1060.

ZHANG, T., MA, C., ZHANG, Z., ZHANG, H. & HU, H. 2021e. NF-κB signaling in inflammation and cancer. *MedComm,* 2**,** 618-653.

ZHANG, T., YANG, J., SUN, Y., SONG, J., GAO, D., HUANG, S., PANG, A., ZHANG, J., WANG, J., WANG, Y. & LI, Y. 2023c. Interleukin-6 and Hypoxia Synergistically Promote EMT-Mediated Invasion in Epithelial Ovarian Cancer via the IL-6/STAT3/HIF-1α Feedback Loop. *Analytical Cellular Pathology,* 2023**,** 1-14.

ZHANG, W., CHEN, L., MA, K., ZHAO, Y., LIU, X., WANG, Y., LIU, M., LIANG, S., ZHU, H. & XU, N. 2016. Polarization of macrophages in the tumor microenvironment is influenced by EGFR signaling within colon cancer cells. *Oncotarget,* 7**,** 75366-75378.

ZHANG, W., FU, X., XIE, J., PAN, H., HAN, W. & HUANG, W. 2021f. miR-26a attenuates colitis and colitis-associated cancer by targeting the multiple intestinal inflammatory pathways. *Molecular Therapy-Nucleic Acids,* 24**,** 264-273.

ZHANG, W., YAN, L., LI, Y., CHEN, W., HU, N., WANG, H. & OU, H. 2015. Roles of miRNA-24 in regulating endothelial nitric oxide synthase expression and vascular endothelial cell proliferation. *Molecular and Cellular Biochemistry,* 405**,** 281-289.

ZHANG, X., HU, F., LI, G., LI, G., YANG, X., LIU, L., ZHANG, R., ZHANG, B. & FENG, Y. 2018. Human colorectal cancer-derived mesenchymal stem cells promote colorectal cancer progression through IL-6/JAK2/STAT3 signaling. *Cell death & disease,* 9**,** 25.

ZHANG, Y. S., XIN, D. E., WANG, Z., SONG, X., SUN, Y., ZOU, Q. C., YUE, J., ZHANG, C., ZHANG, J. M., LIU, Z., ZHANG, X., ZHAO, T. C., SU, B. & CHIN, Y. E. 2019b. <scp>STAT</scp>

4 activation by leukemia inhibitory factor confers a therapeutic effect on intestinal inflammation. *The EMBO Journal,* 38**,** 1-20.

ZHAO, F.-Y., HAN, J., CHEN, X.-W., WANG, J., WANG, X.-D., SUN, J.-G. & CHEN, Z.-T. 2016. miR-223 enhances the sensitivity of non-small cell lung cancer cells to erlotinib by targeting the insulin-like growth factor-1 receptor. *International Journal of Molecular Medicine,* 38**,** 183-191.

ZHAO, H., MING, T., TANG, S., REN, S., YANG, H., LIU, M., TAO, Q. & XU, H. 2022a. Wnt signaling in colorectal cancer: pathogenic role and therapeutic target. *Molecular Cancer,* 21.

ZHAO, L., LIANG, X., WANG, L. & ZHANG, X. 2022b. The Role of miRNA in Ovarian Cancer: an Overview. *Reproductive Sciences,* 29**,** 2760-2767.

ZHAO, T., LI, Y., ZHANG, J. & ZHANG, B. 2020. PD-L1 expression increased by IFN-γ via JAK2-STAT1 signaling and predicts a poor survival in colorectal cancer. *Oncology Letters,* 20**,** 1127-1134.

ZHEN, Y., LUO, C. & ZHANG, H. 2018. Early detection of ulcerative colitis-associated colorectal cancer. *Gastroenterology Report,* 6**,** 83-92.

ZHOU, J., LIU, J., GAO, Y., SHEN, L., LI, S. & CHEN, S. 2021. miRNA-Based Potential Biomarkers and New Molecular Insights in Ulcerative Colitis. *Front Pharmacol,* 12**,** 707776.

ZHOU, L., YAN, Z., YANG, W., BUCKLEY, J. A., AL DIFFALHA, S., BENVENISTE, E. N. & QIN, H. 2023a. Socs3 expression in myeloid cells modulates the pathogenesis of dextran sulfate sodium (DSS)-induced colitis. *Frontiers in Immunology,* 14.

ZHOU, Q., SHEN, Z.-F., WU, B.-S., XU, C.-B., HE, Z.-Q., CHEN, T., SHANG, H.-T., XIE, C.-F., HUANG, S.-Y., CHEN, Y.-G., CHEN, H.-B. & HAN, S.-T. 2019. Risk of Colorectal Cancer in Ulcerative Colitis Patients: A Systematic Review and Meta-Analysis. *Gastroenterology Research and Practice,* 2019**,** 1-11.

ZHOU, R. W., HARPAZ, N., ITZKOWITZ, S. H. & PARSONS, R. E. 2023b. Molecular mechanisms in colitis-associated colorectal cancer. *Oncogenesis,* 12.

ZHOU, W., PAL, A. S., HSU, A. Y.-H., GUROL, T., ZHU, X., WIRBISKY-HERSHBERGER, S. E., FREEMAN, J. L., KASINSKI, A. L. & DENG, Q. 2018. MicroRNA-223 Suppresses the Canonical NF-κB Pathway in Basal Keratinocytes to Dampen Neutrophilic Inflammation. *Cell Reports,* 22**,** 1810-1823.

ZHOU, X., CHEN, B., ZHANG, Z., HUANG, Y., LI, J., WEI, Q., CAO, D. & AI, J. 2022. Crosstalk between Tumor-Associated Macrophages and MicroRNAs: A Key Role in Tumor Microenvironment. *International Journal of Molecular Sciences,* 23**,** 13258.

ZHU, F., LI, H., LIU, Y., TAN, C., LIU, X., FAN, H., WU, H., DONG, Y., YU, T. & CHU, S. 2020a. miR-155 antagomir protect against DSS-induced colitis in mice through regulating Th17/Treg cell balance by Jarid2/Wnt/β-catenin. *Biomedicine & Pharmacotherapy,* 126**,** 109909.

ZHU, Y., GU, L., LI, Y., LIN, X., SHEN, H., CUI, K., CHEN, L., ZHOU, F., ZHAO, Q., ZHANG, J., ZHONG, B., PROCHOWNIK, E. & LI, Y. 2017. miR-148a inhibits colitis and colitis-associated tumorigenesis in mice. *Cell Death & Differentiation,* 24**,** 2199-2209.

ZHU, Y., LI, K., YAN, L., HE, Y., WANG, L. & SHENG, L. 2020b. miR-223-3p promotes cell proliferation and invasion by targeting Arid1a in gastric cancer. *Acta Biochim Biophys Sin (Shanghai),* 52**,** 150-159.

ZIGMOND, E., VAROL, C., FARACHE, J., ELMALIAH, E., SATPATHY, ANSUMAN T., FRIEDLANDER, G., MACK, M., SHPIGEL, N., BONECA, IVO G., MURPHY, KENNETH M., SHAKHAR, G., HALPERN, Z. & JUNG, S. 2012. Ly6C^{hi} Monocytes in the Inflamed Colon Give Rise to Proinflammatory Effector Cells and Migratory Antigen-Presenting Cells. *Immunity,* 37**,** 1076-1090.